



UNIVERSITAT DE  
BARCELONA

## Effects and underlying mechanisms of bioactive compounds-enriched diets against obesity and associated pathologies

Hèctor Sanz Lamora



Aquesta tesi doctoral està subjecta a la llicència **Reconeixement- NoComercial – Compartir Igual 4.0. Espanya de Creative Commons.**

Esta tesis doctoral está sujeta a la licencia **Reconocimiento - NoComercial – Compartir Igual 4.0. España de Creative Commons.**

This doctoral thesis is licensed under the **Creative Commons Attribution-NonCommercial-ShareAlike 4.0. Spain License.**



UNIVERSITAT DE  
BARCELONA

UNIVERSITAT DE BARCELONA

FACULTAT DE FARMÀCIA I CIÈNCIES DE L'ALIMENTACIÓ

EFFECTS AND UNDERLYING MECHANISMS OF  
BIOACTIVE COMPOUNDS-ENRICHED DIETS AGAINST  
OBESITY AND ASSOCIATED PATHOLOGIES

Hèctor Sanz Lamora

2022







UNIVERSITAT DE  
BARCELONA

Programa de Doctorat en Biomedicina  
Facultat de Farmàcia i Ciències de l'Alimentació  
Departament de Nutrició, Ciències de l'Alimentació i Gastronomia

# Effects and underlying mechanisms of bioactive compounds-enriched diets against obesity and associated pathologies

Memòria presentada per Hèctor Sanz Lamora per optar al títol de  
Doctor per la Universitat de Barcelona

Dra. Joana Relat  
La Directora

Dr. Diego Haro  
El Director

Hèctor Sanz Lamora  
El Doctorand



*“Ser crítics és la condició fonamental  
per a poder viure junts sense ser governats.”*

Marina Garcés



## Summary

Bioactive compounds have long been proposed as a tool to help facing both obesity and its comorbidities pandemic. Knowledge on their properties, together with the discovery of new therapeutic targets in animals and humans, make then interesting proposals for the prevention and treatment of various metabolic diseases. One of the main parts of this thesis proposal was to evaluate the ability of a pure, isolated polyphenol supplementation to counteract the pernicious metabolic effects of a high-fat diet on a murine model. Contrary to expectations, the polyphenolic supplementation worsened the action of the high-fat diet and pointedly produced an aggression to the kidneys. The other main part of this thesis proposal had been to assess a natural source of bioactive compounds with a broad and diverse profile not only in phenolic species, on a diet-obesity model. Based on the experience of our research group and the positive results demonstrated in different studies on chronic diseases, the *Rosa canina* fruit was chosen. In this case it was demonstrated how the supplementation with *Rosa canina* flesh was able to slow down the pernicious effect of the high fat diet, and particularly how exhibited a strong anti-steatotic effect on liver by downregulating several key genes, and thus improving significantly the non-alcoholic fatty liver disease course on obese mice. Furthermore, through the flesh fractionation, bioactive compound characterization and in vitro analysis, it was possible to identify that the most lipophilic phases of the *Rosa canina* show an antagonistic role on the peroxisome proliferator activated receptor gamma and therefore were partly responsible for the observed anti-steatotic effect.



## **Resum**

Els compostos bioactius han estat proposats com a eina dietètica per a fer front a la pandèmica de l'obesitat i de les seves comorbiditats. El coneixement de les seves propietats, junt amb la cerca de noves dianes terapèutiques en animals i humans, els converteixen en una proposta interessant per a la prevenció i el tractament de diverses malalties metabòliques. Una de les principals parts d'aquesta proposta de tesi doctoral ha sigut avaluar la capacitat d'una suplementació de polifenols aïllats purs en front els efectes perniciosos d'una dieta d'alt greix en el metabolisme sobre un model murí. En contra a les expectatives, la suplementació amb la mescla de polifenols va empitjorar notòriament l'acció de la dieta alta en greix i va produir una clara agressió als ronyons. L'altra part principal d'aquesta proposta de tesi doctoral ha sigut avaluar una font natural de compostos bioactius però amb un ampli i divers perfil d'espècies. Basant-nos en l'experiència del nostre grup de recerca i en resultats previs positius demostrats en diversos estudis sobre malalties cròniques, es va triar el fruit de la *Rosa canina*. En aquest cas, es va demostrar com la suplementació amb la polpa de *Rosa canina* va ser capaç de frenar l'efecte pernicios de la dieta d'alt greix, i en particular com va exhibir un fort efecte antiestatòtic sobre el fetge mitjançant la regulació de diversos gens clau, i així millorant significativament el quadre de l'esteatosi hepàtica no alcohòlica. Paral·lelament, mitjançant el fraccionament de la polpa, la caracterització dels compostos bioactius i l'anàlisi in vitro, va ser possible identificar que les fases més lipòfiles de la *Rosa canina* exercien un paper antagonista del receptor PPAR $\gamma$  i que per tant, eren en part responsables de l'efecte antiestatòtic observat.





## Abbreviations

<b>AC</b>	Adenylyl Cyclase
<b>ACC or ACACA</b>	Acetyl-CoA Carboxylase 1
<b>ACLY</b>	ATP Citrate Synthase
<b>AD</b>	Alzheimer Disease
<b>AGE</b>	Advanced Glycation End-Product
<b>ALS</b>	Amyotrophic Lateral Sclerosis
<b>AMPK</b>	Adenosine Monophosphate-Activated Protein Kinase
<b>ANP</b>	Atrial Natriuretic Peptide
<b>AT</b>	Adipose Tissue
<b>ATGL</b>	Adipocyte Triglyceride Lipase
<b>AUC</b>	Area Under the Curve
<b>BAT</b>	Brown Adipose Tissue
<b>BMI</b>	Body Mass Index
<b>BSA</b>	Albumin
<b>C/EBP</b>	CCAATT/Enhancer Binding Proteins
<b>CAF</b>	Cafeteria Diet
<b>cAMP</b>	Cyclic Adenosine Monophosphate
<b>CD14</b>	Cluster of Differentiation 14
<b>CD36</b>	Fatty Acid Translocase or Cluster of Differentiation 36
<b>CEEA</b>	Comitè Ètic d'Experimentació Animal
<b>CHD</b>	Coronary Heart Disease
<b>ChoRE</b>	Carbohydrate Responsive Elements
<b>ChREBP</b>	Carbohydrate Response Element-Binding Protein
<b>Cide</b>	Cell Death-Inducing DNA Fragmentation Factor $\alpha$ (DFFA)-like Effector Protein
<b>CKD</b>	Chronic Kidney Disease
<b>COX-2</b>	Cytochrome C Oxidase Subunit 2,
<b>CPT</b>	Carnitine Palmitoyl-Transferase
<b>CVD</b>	Cardiovascular Diseases
<b>DAG</b>	Diacylglycerol
<b>DASH</b>	Dietary Approaches to Stop Hypertension
<b>DEX</b>	Dexamethasone
<b>DGAT</b>	Diacylglycerol Acyltransferase
<b>DIO</b>	Diet Induced Obesity
<b>DIO</b>	Diet Induced Obesity
<b>DKD</b>	Diabetic Kidney Disease
<b>DMEM</b>	Dulbecco's Modified Essential Medium
<b>DNL</b>	De Novo Lipogenesis
<b>EDTA</b>	Ethylenediaminetetraacetic Acid
<b>EGFR</b>	Epidermal Growth Factor Receptor
<b>ELISA</b>	Enzyme-Linked Immunosorbent Assay
<b>EMEM</b>	Eagle's Modified Essential Medium
<b>ER</b>	Endoplasmic Reticulum
<b>ESKD</b>	End Stage Kidney Disease
<b>ESLD</b>	End Stage Liver Disease
<b>eWAT</b>	Epydidymal White Adipose Tissue
<b>FABP4</b>	Fatty Acid-Binding Protein 4
<b>FASN</b>	Fatty Acid Synthase
<b>FATP</b>	Fatty Acid Transport Protein

<b>FBS</b>	Fetal Bovine Serum
<b>FFA</b>	Free Fatty Acids
<b>FGF21</b>	Fibroblast Growth Factor 21
<b>FGF21</b>	Fibroblast Growth Factor 21
<b>FGFR1</b>	Fibroblast Growth Factor Receptor 1
<b>FGFR4</b>	Fibroblast Growth Factor Receptor 4
<b>FKD</b>	Fatty Kidney Disease
<b>FSP27</b>	Fat-Specific Protein 27
<b>G3P</b>	Glycerol 3 Phosphate
<b>GAE</b>	Gallic Acid Equivalence
<b>GFR</b>	Glomerular Filtration Rate
<b>GH</b>	Growth Hormone
<b>GLP-1</b>	Glucagon-Like Peptide-1
<b>PKA</b>	Protein Kinase A
<b>GLUT4</b>	Facilitated Glucose Transporter 4
<b>GTT</b>	Glucose Tolerance Test
<b>GyK</b>	Glycerol Kinase
<b>HCC</b>	Hepato-Carcinoma
<b>HDL</b>	High Density Lipoprotein
<b>HFD</b>	High Fat Diet
<b>HSC</b>	Hepatic Stellate Cells
<b>HSL</b>	Hormone Sensitive Lipase
<b>IAPP</b>	Islet Amyloid Polypeptide
<b>IFG</b>	Impaired Fasting Glucose
<b>IGT</b>	Impaired Glucose Tolerance
<b>IL-1</b>	Interleukin 1
<b>IL-10</b>	Interleukin 10
<b>IL-6</b>	Interleukin 6
<b>IL-8</b>	Interleukin 8
<b>Insig-1</b>	Insulin-Induced Gene 1
<b>IR</b>	Insulin Resistance
<b>IRS</b>	Insulin Receptor Substrate
<b>ITT</b>	Insulin Tolerance Test
<b>IU</b>	Insulin Units
<b>JNK</b>	c-Jun N-terminal Kinase
<b>KDIGO</b>	Kidney Disease Improving Global Outcomes
<b>KIM-1</b>	Kidney Injury Molecule 1
<b>KLB</b>	Beta Klotho
<b>KO</b>	Knock Out
<b>LC-MS</b>	Liquid Chromatography and High-Resolution Mass Spectrometry
<b>LCN-2</b>	Neutrophil Gelatinase-Associated Lipocalin 2
<b>LD</b>	Lipid Droplet
<b>LDL</b>	Low Density Lipoprotein
<b>LOX</b>	Lysl Oxidase
<b>LPL</b>	Lipoprotein Lipase
<b>LXR</b>	Liver X Receptor
<b>MAG</b>	Monoacylglycerol
<b>MCP-1</b>	Monocyte Chemoattractant Protein-1
<b>MD</b>	Mediterranean Diet
<b>MDA</b>	Malonaldehyde

<b>MetS</b>	Metabolic Syndrome
<b>MGL</b>	Monoacylglycerol Lipase
<b>MHO</b>	Metabolic Healthy Obese
<b>MIND</b>	Mediterranean-DASH Intervention for Neurodegenerative Delay
<b>MSC</b>	Mesenchymal Stem Cells
<b>MTT</b>	Metabolic Tolerance Test
<b>MUFAs</b>	Monounsaturated Fatty Acids
<b>NA</b>	Noradrenaline
<b>NADPH</b>	Nicotinamide Adenine Dinucleotide Phosphate
<b>NAFL</b>	Non-Alcoholic Fatty Liver
<b>NAFLD</b>	Non-Alcoholic Fatty Liver Disease
<b>NASH</b>	Non-Alcoholic SteatoHepatitis
<b>NCBI</b>	National Center for Biotechnology Information
<b>NCD</b>	Non-Communicable Diseases
<b>NEFA</b>	Non-esterified Fatty Acids
<b>NF-<math>\kappa</math>B</b>	Nuclear Factor Kappa-light-chain Enhancer of Activated B cells
<b>Nrf2</b>	Nuclear Factor Erythroid 2-Related Factor 2
<b>OA</b>	Oleic Acid
<b>ORO</b>	Oil Red O
<b>PA</b>	Palmitic Acid
<b>PAI-1</b>	Plasminogen Activator Inhibitor-1
<b>PBS</b>	Phosphate Buffer Solution
<b>PCR</b>	Polymerase Chain Reaction
<b>PD</b>	Parkinson Disease
<b>PEPCK</b>	Phosphoenolpyruvate Carboxykinase
<b>PI3K</b>	Phosphoinositide 3 Kinase
<b>PKA</b>	Protein Kinase A
<b>PKC</b>	Protein Kinase C
<b>PNT</b>	Standardized Working Procedure
<b>Pol</b>	Polyphenols
<b>PPAR</b>	Peroxisome Proliferator Activated Receptors
<b>PPAR<math>\alpha</math></b>	Peroxisome Proliferator Activated Receptor Alpha
<b>PPAR<math>\beta/\delta</math></b>	Peroxisome Proliferator Activated Receptors Beta or Delta
<b>PPAR<math>\gamma</math></b>	Peroxisome Proliferator Activated Receptor Gamma
<b>PPP</b>	Pentose Phosphate Pathway
<b>PPRE</b>	PPAR $\gamma$ Response Element
<b>PREDIMED</b>	Prevención Con Dieta Mediterranea
<b>PUFAs</b>	Polyunsaturated Fatty Acids
<b>qPCR</b>	Quantitative Polymerase Chain Reaction
<b>RAAS</b>	Renin-Angiotensin-Aldosterone System
<b>RC</b>	<i>Rosa canina</i>
<b>ROS</b>	Reactive Oxygen Species
<b>RT-PCR</b>	Reverse Transcription Polymerase Chain Reaction
<b>RXR</b>	Retinoid X Receptor
<b>SCD</b>	Stearoyl-CoA desaturase
<b>scWAT</b>	Subcutaneous Adipose tissue
<b>SGLT2</b>	Sodium-Glucose Cotransporter Type 2
<b>SNS</b>	Sympathetic Nervous System
<b>SREBP1</b>	Sterol Regulatory Element-Binding Protein 1
<b>STATs</b>	Signal Transducer Activator Transcription Factor

<b>T2DM</b>	Type 2 Diabetes Mellitus
<b>TAG or TG</b>	Triglycerides
<b>TBARS</b>	Thiobarbituric Acid Reactive Substances
<b>TCA</b>	Tricarboxylic Acid Cycle or Krebs Cycle
<b>TGF-<math>\beta</math></b>	Transforming Growth Factor Beta
<b>TNF<math>\alpha</math></b>	Tumor Necrosis Alpha
<b>TRI</b>	Trizol
<b>TZDs</b>	Thiazolidinediones
<b>UCP1</b>	Uncoupling Protein 1
<b>UPR</b>	Unfolded Protein Response
<b>VAT</b>	Visceral Adipose tissue
<b>VCAM1</b>	Vascular Cell Adhesion Molecule 1
<b>VLDL</b>	Very Low-Density Lipoprotein
<b>WAT</b>	White Adipose Tissue
<b>WHO</b>	World Health Organization
<b><math>\beta</math>-AR</b>	Beta-Adrenergic Receptor

# Index

<b>SUMMARY</b>	<b>7</b>
<b>ABBREVIATIONS</b>	<b>11</b>
<b>1. INTRODUCTION</b>	<b>21</b>
<b>1.1. Perspectives on Metabolic Disorders</b>	<b>21</b>
1.1.1. Obesity As Central Pathological Axis	22
1.1.2. Non-Alcoholic Fatty Liver Disease	28
1.1.3. Chronic Kidney Disease	31
<b>1.2. Lipid Homeostasis</b>	<b>34</b>
1.2.1. Main Tissues	35
1.2.2. Fatty Acid Uptake	36
1.2.3. Lipolysis	37
1.2.4. Lipogenesis	39
1.2.5. Lipid Droplet Formation	42
1.2.6. Fatty Acid Oxidation	44
1.2.7. Thermogenesis	45
1.2.8. Adipokines and Hepatokines	47
<b>1.3. Metabolic Regulation</b>	<b>50</b>
1.3.1. The PPARs as Metabolic Regulators	51
1.3.2. PPAR $\alpha$	51
1.3.3. PPAR $\beta/\delta$	52
1.3.4. PPAR $\gamma$	53
<b>1.4. Diet and Health</b>	<b>57</b>
1.4.1. Dietary Proposals	58
1.4.2. Bioactive Compounds	59
1.4.2.1. Phenolic Compounds	61
1.4.2.2. Terpenoids	66
1.4.2.3. <i>Rosa canina</i>	70
<b>2. OBJECTIVES</b>	<b>75</b>
<b>3. METHODOLOGY</b>	<b>79</b>
<b>3.1. Cell Culture</b>	<b>79</b>
<b>3.3. Luciferase Assay</b>	<b>82</b>
<b>3.4. Gene Expression Analyses</b>	<b>83</b>
3.4.1. Total RNA Isolation	84

3.4.2.	mRNA Expression Analyses	84
3.4.3.	DNA Oligonucleotides	85
<b>3.5.</b>	<b>Animal Procedures</b>	<b>88</b>
3.5.1.	Animal Housing	89
3.5.2.	Ethical Committees	89
3.5.3.	Dietary Interventions	89
3.5.4.	Animal Monitoring	92
3.5.5.	Euthanasia and Tissue Harvesting	93
<b>3.6.</b>	<b>Glucose and Insulin Tolerance Tests</b>	<b>93</b>
3.6.1.	Glucose Tolerance Test (GTT)	94
3.6.2.	Insulin Tolerance Test (ITT)	95
3.6.3.	TBARS Assay	95
3.6.4.	LCN2 ELISA	96
3.6.5.	Total Iron Quantification	96
3.6.6.	Triglyceride Quantification	97
<b>3.7.</b>	<b>Histological Analyses</b>	<b>97</b>
<b>3.8.</b>	<b>Bioactive Compound Analyses</b>	<b>98</b>
3.8.1.	Folin-Ciocalteu Method Quantification	98
3.8.2.	<i>Rosa canina</i> Fractionation	99
3.8.3.	UPLC-LTQ-Orbitrap-MS	100
<b>3.9.</b>	<b>Statistics and Graphs</b>	<b>101</b>
<b>4.</b>	<b>RESULTS</b>	<b>105</b>
A)	Effects and molecular mechanisms underlying a pure, isolated polyphenol mixture supplementation against a high fat diet-induced obesity and NAFLD.	105
B)	Effects and molecular mechanisms underlying a <i>Rosa canina</i> flesh supplementation against a high fat diet-induced obesity and NAFLD.	123
C)	Characterization of the different <i>Rosa canina</i> flesh fractions and study of the anti-steatotic mechanisms underlying their different constituents.	140
<b>5.</b>	<b>DISCUSSION</b>	<b>151</b>
<b>6.</b>	<b>CONCLUSION</b>	<b>169</b>
<b>7.</b>	<b>BIBLIOGRAPHY</b>	<b>173</b>
<b>8.</b>	<b>ANNEXES</b>	<b>217</b>
	Review Article	217
	Scientific Article	273
	Other Scientific Publications	291







INTRODUCTION



## 1. Introduction

Under the global *Covid-19* pandemic situation, communicable infectious diseases have become the spotlight. However, according to the World Health Organization (WHO) the 71% of all deaths worldwide nowadays are caused by what we know as non-communicable diseases (NCDs). Within this group of pathologies are included heart diseases (CVD), stroke, cancer, diabetes, and chronic respiratory illnesses. At the same time the 80% of premature heart diseases, strokes and type 2 diabetes mellitus could be prevented(1). A big part of these type of illnesses are associated with unhealthy habits such as sedentary lifestyle, tobacco, alcohol, and unhealthy diets. Particularly, there is a group of risk factors directly related to the development of NCDs. Overweight or obesity, high sugar levels in blood, hyperlipidemia and hypertension change the proper function of metabolism and contribute to sickness(2). If we rely on the projections of WHO the total annual mortality from NCDs will increase worldwide to 55 million by 2030 which almost three quarters of these deaths will occur in low-middle income countries that already experience challenges in managing significant epidemics(3,4). Moreover, the economic burden of dealing with NCDs in EU is about 169€ billion a year in case of CVD and 170€ billion due to diabetes according to European Commission of Science data(5).

### 1.1. Perspectives on Metabolic Disorders

Nowadays the two most frequent metabolic disorders and major NCDs risk factors are obesity and type 2 diabetes mellitus (T2DM)(6). As it is already known, obesity has nearly tripled prevalence since 1975 and closely linked, the amount of people with T2DM has risen from 108 million in 1980 to 422million in 2014. Stated by WHO nearly 90% of diabetic patients develop T2DM due to excess body weight(7). Under the paradigm of these two associated diseases along with other NCDs, it also appears what is known as metabolic syndrome (MetS). Defined by WHO, MetS is as a pathologic condition characterized by abdominal obesity, insulin resistance, hypertension and hyperlipidemia(6). Although MetS is not a pathology *per se*, it helps to identify patients at an early stage, concretely to classify a specific group of patients with a shared pathophysiology. This allows medical staff to intervene and emphasize them the importance of having a healthy lifestyle and therefore reduce the risk of suffering these diseases(8). The umbrella of MetS and its risk factors often parallels the incidence of obesity and T2DM, however obesity is not always synonymous with MetS. As it's known, there are so-called metabolically healthy obese (MHO) individuals who have high level of insulin sensitivity and doesn't present hypertension,

hyperlipidemia or other features of MetS(9). All in all, actually there isn't a global data of MetS prevalence but can be estimated to be about one quarter of the world population, which means over a billion people in the world are now affected(6). Among this data, we can glimpse the real scourge worldwide and the need as a community to deal with this dangerous tandem of pathologies.

### 1.1.1. Obesity As Central Pathological Axis

Obesity is defined as a pathological state based on a peripheral accumulation of adiposity provoked by a calorie intake that is higher than the total energy expenditure(10). Humans consume carbohydrates, proteins, fats and non-nutritive bioactive compounds like fiber, polyphenols or terpenoids as part of the substrate required for life. When more macronutrients are ingested than expended, the excess is stored as energy in form of glycogen and fats. This storage fat is mainly formed by triglycerides (TAG), which are accumulated in aggregated adipocytes forming what is known as White Adipose Tissue (WAT)(11). Lipid depot function of WAT is to mobilize TAG for systemic utilization when other tissues require energy. The accumulation of fat turns pathogenic when the energy balance between the ingested and burnt become overly positive. This excess energy intake triggers several morphologic and metabolic changes such as hypertrophy and hyperplasia of the adipocytes, aside from fibrosis and inflammation processes(12).

First of all, hypertrophy (*Figure 11*) is an adaptive response to excess fat that maintains adipose tissue nutrient buffering capacity by increasing the size of the adipocyte(13). Hyperplasia (*Figure 11*) is known as the process of generating new mature adipocytes from preadipocytes. Moreover hyperplasia attempts to balance hypertrophy in order to maintain adipose tissues homeostasis(14). Peculiarly, the higher degree of hypertrophy, the lower rate of adipocyte formation occurs(15). Hence, in obesity the hypertrophic adipocytes reach the critical cell size becoming lipid-overloaded (*Figure 11*), undergoing less oxygenation and developing pro-inflammatory role, subsequent fibrosis, apoptosis, and insulin resistance(16). In contrast hyperplasia unsuccessfully attempts to repair metabolic alterations generated by the excess fat(16). Different cell types including endothelial cells, fibroblasts, various immune cells and mainly adipocytes form adipose tissue. Immune cells of adipose tissue are categorized into innate (macrophages, neutrophils, eosinophils and mast cells) and adaptive cells, whereas adaptive immune cells include various subtypes of T cells and B cells(17). While in lean adipose tissue anti-inflammatory immune cells such as

regulatory T cells, eosinophils and M2 type macrophages have a role in the maintenance of insulin sensitivity, in obese adipose tissue this role is reversed. Various immune cells, specially macrophages and its infiltration process, end up being responsible of the progression of insulin resistance *via* production of different pro-inflammatory mediators(17). In the WAT of lean mice, macrophages resemble M2 phenotype and constitute less than a 10% of the resident cells; however in obese mice WAT, macrophages become up the 50% of all cells and present an M1 phenotype(18). Therefore, macrophages can be classified in two major phenotypes: M1, classically activated “pro-inflammatory” macrophages, and M2, alternatively activated “anti-inflammatory” macrophages involved in the maintenance of WAT homeostasis(19). The general view in obesity is that there is an imbalance in the ratio of M1/M2 macrophages, with M1 type enhanced compared with M2 type being down-regulated, leading to chronic inflammation and the progression of metabolic dysfunction(20). Indeed, the increase of M1 macrophages correlates with the degree of obesity and is linked to systemic inflammation, insulin resistance and metabolic syndrome(21).

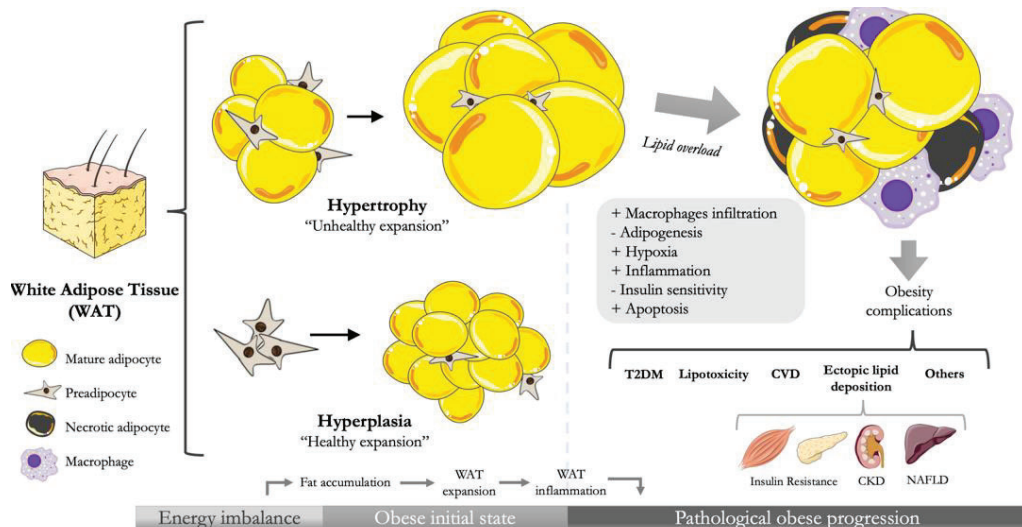


**Figure I1 – Comparative scheme between hypertrophy and hyperplasia processes in adipose tissue.** As it is shown in the image, once the energy imbalance is presented, fat accumulation begins in the adipose tissue. In this sense, the adipose tissue tries to manage this excess in two ways: in a healthy mode generating new adipocytes (hyperplasia) or in a pernicious manner with the enlargement of the existing ones (hypertrophy). In the case of hypertrophy, this happens because of an inability to manage such excess of lipids which leads to lipid overload and consequently to a pathological state. Thus, begins the infiltration of macrophages among other immune cells and the consequent inflammatory response of the adipose tissue.

Mechanistically, under energy imbalance and lipid overload presented in obesity, hypertrophic adipocytes produce greater amounts of tumor necrosis factor- $\alpha$  (TNF- $\alpha$ ), increase non-esterified fatty acids (NEFA) flow and chemokine ligand 2 (CCL2) previously known as monocyte chemoattractant protein-1 (MCP-1), which recruit monocytes to WAT where they polarize to M1 macrophages in response to TNF- $\alpha$  and NEFAs(22). Also hypoxia produced by the hypertrophy process and a mixture of insulin, glucose and palmitate can activate macrophages(23). In addition to macrophages, there are other types of immune cells that can be detected exacerbated in white adipose tissue of obese models, such as natural killer cells, mast cells, dendritic cells, B cells, CD4+ and cytotoxic CD8+ T cells(24).

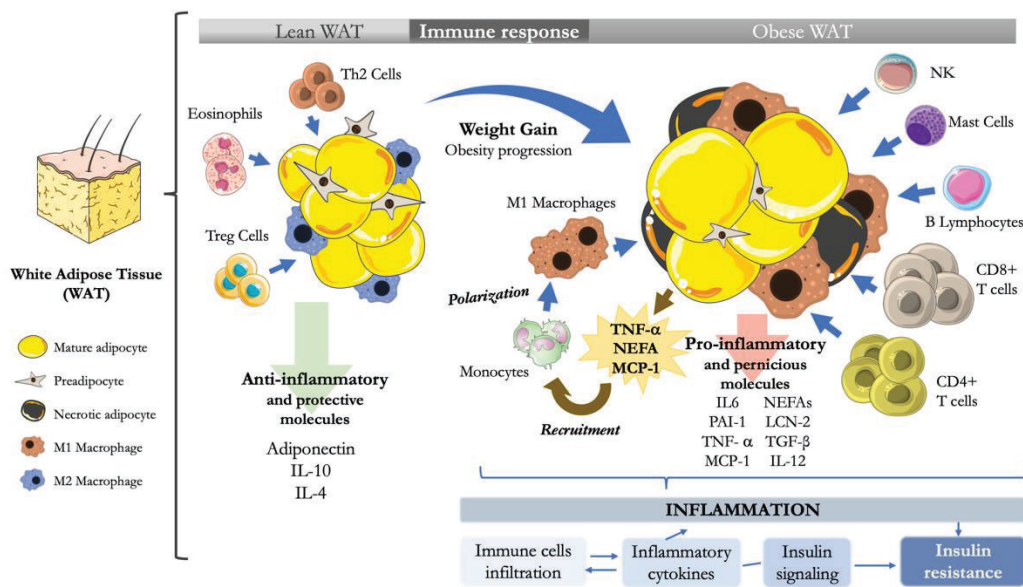


**Figure 12 – Comparative diagram of the immune and inflammatory status between lean and obese adipose tissue.** This image depicts the different type of immune cells found in adipose tissue along with the molecules they generate depending on the state of the adipose tissue. In lean WAT, alternatively activated M2 macrophages are native, and their phenotype is maintained by the presence of the T-regulatory cells (Treg), Th2 cells and eosinophils(25). In the opposite way, on obese WAT, M1 macrophages surround dying adipocytes and release different pro-inflammatory mediators. At the same time, obese WAT loses part of the Tregs, Th2 cells and eosinophils as the obesity progresses. Both facts facilitate the infiltration of other immune cells like Natural Killers, mast cells, lymphocytes, and T cells (cd8+ and cd4+). All this situation generates a series of-inflammatory and pernicious molecules that triggers an inflammatory response that can alter proper basic function such as insulin signaling, leading to insulins resistance(25).

As mentioned above, adipocytes produce a wide variety of molecules, fact that breaks the classical conception of adipose tissue being only a storage and lipid uptake. Now is known as a major endocrine actor due to its responsibility of synthesis and secretion of many molecules, hormones

and pro or anti-inflammatory cytokines that includes leptin, adiponectin, resistin, tumor necrosis factor- $\alpha$  (TNF- $\alpha$ ), monocyte chemoattractant protein-1 (MCP-1), plasminogen activator inhibitor-1 (PAI-1), interleukin 6 (IL-6), interleukin 1 (IL-1), non-esterified fatty acids (NEFA), transforming growth factor beta (TGF- $\beta$ ) and others(26). Concentrations of these biological substances change in obese adipose tissue, being increased the secretion of pro-inflammatory cytokines and decreased protective ones(27). This imbalance, also directly interferes negatively with insulin signaling, thus being one of the main causes of insulin resistance (*Figure I2*). On the other hand, the chronic low-grade inflammation related to obesity and subsequent metabolic disturbances produced by the infiltration of immune cells and cytokine secretion has been recently termed as “*metaflammation*”(28). Inflammation generally is an energy wasting process that enhances energy expenditure and reduces energy intake(29). Surprisingly, adipose tissue inflammation induced by over-nutrition is not associated with a significant increase in energy expenditure, which permits the coexistence of inflammation and weight gain in obese subjects(30). It should be noted that these inflammatory processes, both in adipose tissue and in its ectopic accumulation, are also directly related to a significant increase in oxidative stress(31).

Parallel to the immune response and to the inflammatory state, the accumulation and deleterious expansion of adiposity not only occurs at adipose tissue levels. In the progression of obesity fat ends up being deposited in skeletal-muscle and organs as liver or pancreas, located mainly within the chest, abdomen and pelvis, more known as visceral adipose tissue (VAT)(32). Kidneys were also surrounded by abdominal visceral adipose tissue and have the potential to accumulate and suffer deleterious effect of ectopic fat in the renal sinus(33). It is currently well established that obesity instigates a more complex and intense inflammatory reaction in VAT than in scWAT. Indeed, VAT contains more M1 macrophages and much higher degree of hypertrophy than scWAT(29). This visceral non-physiological displaced amount of fat also generates toxicity or recently named lipotoxicity. While lipids are pivotal for homeostatic processes they could as well become critical components of pathophysiological cascades that can involve a breakdown of homeostasis(34). Lipid toxicity depends primarily on two aspects: the quantitative amount of free fatty acids (FFA), cholesterol and TAG accumulated ectopically, and the quality of lipids, referring to the nature of specific lipid species. Some studies indicate that lipotoxicity may be more about quality than quantity(35). Thus, lipids such as long-chain non-esterified fatty acids and their derivatives ceramides and diacylglycerols (DAGs) have significantly more harmful effect than unsaturated and short chain-fatty acids(35).



One of the critical points of this adipose ectopic accumulation is when lipid-overload affects mitochondria function. Although there is certain controversy, mitochondrial dysfunction along with the pro-inflammatory cytokines have been proposed as the critical points in the development of insulin resistance. The fatty acid-overload directly effects mitochondria proper functioning, firstly through the increased production of reactive oxygen species (ROS) from the existing obese-inflammatory processes and secondly, by the increased ROS production from the overwhelmed Krebs cycle and mitochondrial respiratory chain itself due to the excess nutrient supply(36). Both mechanisms increase the overall oxidative stress which may exacerbate the inflammatory process, subsequently diminishing mitochondrial biogenesis and finally leading to cellular apoptosis(37).

Summarizing, the energy imbalance produced by the over-nutrition and the sedentary lifestyle leads to three major changes on the obese organism. Inflammation, produced by the infiltration of immune cells and their response with pro-inflammatory cytokines; mitochondrial dysfunction, and oxidative stress, which reportedly all-together lead to the development of insulin resistance and progressively to T2DM (*Figure 13*). Nevertheless, this sequence is still under debate. As Vidal-Puig et al. enounced, there is a strong correlation between obesity and T2DM; in fact, for every kilogram gained on a population level, diabetes rates increase linearly(38). However, while the link between obesity and T2DM is well established on a population level mechanistically, there are still many questions to be resolved(39). Even so, T2DM ends up being undoubtedly coetaneous to obesity in its worsening progress.

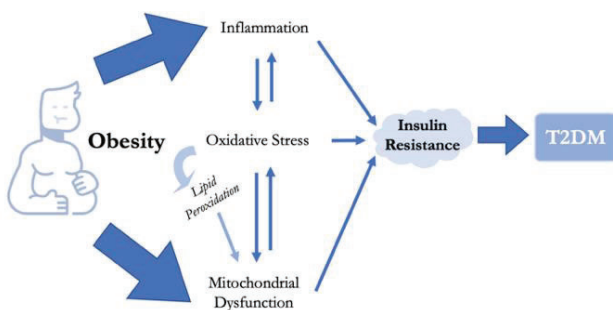


**Figure 13 – Diagram summarizing the progression of obesity and its consequences.** This image shows the three main alterations that follows obesity (inflammation, oxidative stress, and mitochondrial dysfunction) and how they are the principals responsible of trigger insulin resistance.

As we known, T2DM is a chronic disease characterized by the relative ineffective use of insulin, specifically it states an increased hyperinsulinemia, insulin resistance, hyperglycaemia and pancreatic  $\beta$ -cell dysfunction(40). Insulin is considered the main anabolic hormone whose role is to regulate the metabolism of carbohydrates, fats and proteins by allowing the glucose enter from

blood into cells and fuel the whole body (41). In a healthy state, insulin maintains body's normoglycaemia by the balance interplayed between insulin action and insulin secretion. In the progression of obesity, as stated above, insulin action gradually decreases but the system usually compensates the imbalance by increasing  $\beta$ -cell function at least for a period of time(42). However, over time pancreas loses this compensatory ability and basal blood glucose concentrations increase progressively. Subsequently, this significant glucose increases along with the elevated circulating NEFAs become damaging and trigger dysfunction of the pancreatic  $\beta$ -cells. When pancreatic  $\beta$ -cells become dysfunctional, insulin secretion begins to be reduced, limiting the physiological ability to maintain already elevated glucose levels, thereby generating a feedback loop(43). Thus, the combination of insulin resistance and pancreatic  $\beta$ -cell dysfunction in response to over-nutrition leads directly to the development of T2DM. There are four major stressors on pancreatic islets that arise in response to the progression of obesity compromising the functionality of the  $\beta$ -cells. Firstly endoplasmic reticulum (ER) stress, which appears as soon as there is a significant increase in insulin production to meet excessive metabolic demand. The second stressor is oxidative stress, which become critical in  $\beta$ -cell due to their limited ability to handle redox imbalance. In this way, obesity itself and hyperglycemia (glucotoxicity) generates an increase in ROS formation within the islet coupled with a decrease of endogenous antioxidant activity(44). Finally the two last major stressors are inflammation(45) and amyloid plaques, which characterize islets in T2DM. Amyloid plaques are made of islet amyloid polypeptide (IAPP), one of the major secretory products of  $\beta$ -cell with putative functions externally and locally where is able to inhibit insulin and glucagon secretion(46). Concurrently with hyperinsulinemia and increased IAPP secretion, IAPP deposition play a causative role in  $\beta$ -cell dysfunction and apoptosis in a similar manner to other diseases associated with amyloid depositions(47).

As obesity, T2DM is a multisystem disease with a strong correlation with a long list of other pathologies. Comorbidities such as non-alcoholic liver steatosis (NAFLD), renal pathologies like diabetic kidney disease (DKD) or chronic kidney disease (CKD), cardiovascular diseases (CVD), among others appear in the progression of T2DM. Most people with T2DM ends up having at least one other pathological condition that directly influence the self-management of diabetes and its progression. As demonstrated by cohort studies, high prevalence of T2DM is concordant with other pathologies such as NAFLD, CKD, CVD but also with other type of diseases like chronic obstructive pulmonary disease (COPD) or depression.

### 1.1.2. Non-Alcoholic Fatty Liver Disease

Non-alcoholic fatty liver disease (NAFLD) is an umbrella term used to describe a continuum of liver pathological conditions commonly ranging from steatosis to non-alcoholic steatohepatitis (NASH), cirrhosis and finally hepatocellular carcinoma(48). NAFLD currently has a global prevalence estimated to be over 25% and continues to rise worldwide in the setting of the obesity epidemic. Unfortunately, is also increasingly being diagnosed in the adolescent population with an estimated prevalence rates ranging from 3% to 18%(49). Furthermore, a growing general subpopulation with NAFLD in the absence of obesity has recently been described. This manifestation of lean-NALFD belong to the “metabolic obese, normal weight phenotype” and deserves a clinical attention due to its significant increase around the world(50).

The onset of NAFLD begins with the fat accumulation on liver (named steatosis), a condition associated with obesity, T2DM and dyslipidemia, being IR the key pathogenic element(51). IR makes adipose tissue resistant to the antilipolytic effect of insulin, leading to TAG breakdown with the consequent release of NEFAs and glycerol. This lack of lipolysis inhibition in the overloaded adipose tissue is therefore associated with massive release of circulating NEFAs that are absorbed by the liver where they are accumulated as TAG, which is the hallmark feature of steatosis(52). Moreover, in IR condition, the concomitant hyperinsulinemia also modulates hepatic lipid metabolism. Firstly by failing in the suppression of gluconeogenesis and thus increasing glucidic substrates, but at the same time increasing lipogenesis pathway (TAG synthesis) and promoting its accumulation(53). Thereby producing the deadly combination of hyperglycemia and hypertriglyceridemia(53).

In this way, metabolically, four misaligned pathways (*Figure I4*) contribute to fat accumulation in liver: **A**) Fatty acids newly synthesized in liver from dietary carbohydrates through *de novo* lipogenesis (DNL). **B**) Fatty acids uptake from intestinally derived chylomicrons remnants. **C**) The spillover of fatty acids into the plasma NEFAs pool. **D**) The flow of fatty acids stored in the overloaded adipose tissue as NEFAs(54). Using stable isotope-based flux techniques it has been possible to quantify the contribution of these pathways to the hepatic steatosis process(55). According to these techniques, the major contributor are the excessive NEFAs flux (59%) from the adipose tissue to the liver (**D** in *Figure I4*), followed by exacerbated DNL (26%) (**A** in *fig6*), and finally by the excess of direct calories and lipids from the diet (15%)(56).

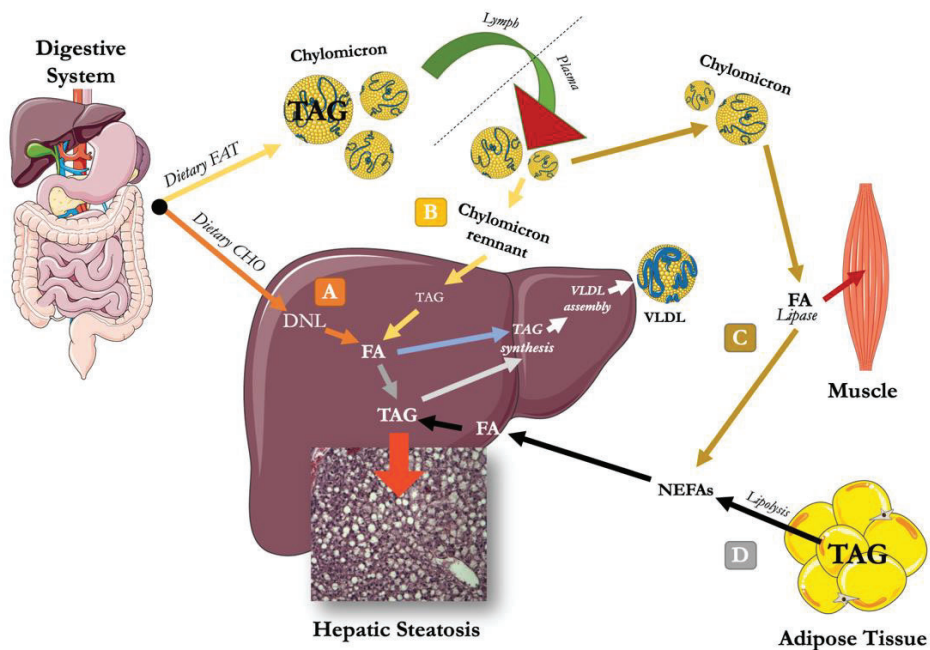


**Figure I4 – NAFLD hepatic lipid flux model.** This image shows the four main fat accumulation mechanism of liver steatosis. Letter **A** indicates the exacerbated pathway of hepatic *de novo* lipogenesis, which increases significantly with energy imbalance and insulin resistance. **B** indicates the remnant chylomicron route from intestinal absorption. **C** and **D** shows the spillover of fatty acids into the plasma, concretely **D** from the adipose tissue. Histological image of the hepatic steatosis from (H&E) stained liver section of an 18week-HFD45% fed mice.

Regarding the pathological progression of NAFLD (Figure I5), the initial steatotic state is also known as NAFL (Non-alcoholic Fatty Liver) and has a lower rate of progression, only about 20% of patients end up suffering NASH(57). NASH is defined as a more severe process with inflammation, hepatocyte injury (ballooning) and fibrosis that may progress to cirrhosis. There are three critical factors in the progression from NAFL to NASH: lipotoxicity, oxidative stress and mitochondrial dysfunction. Hepatic lipotoxicity occurs when the liver capacity to store, use and mobilize NEFAs as TGs is overwhelmed by a massive NEFAs flux from the adipose tissue or by the increased lipogenesis(58). As explained on the introductory obesity section, the lipid toxicity depends directly on its type, being the saturated NEFAs more toxic than unsaturated species. In agreement with this hypothesis, more saturated lipids and other toxic lipids like cholesterol, ceramides and DAGs are reported to be significantly elevated in NASH patients liver's(59). Toxic lipids are able to modify the biology and the function of intracellular organelles such as the endoplasmic reticulum (causing an increase of reticulum stress) or as mitochondria

(altering different metabolic pathways leading to mitochondrial dysfunction)(52). ER stress is also directly linked to chronic inflammation via the excessive production of ROS and the activation of nuclear factor kappa-light-chain enhancer of activated B cells (NF-κB) and JNK pathways(52). Furthermore, ER stress produced by the lipotoxic activity is also able to produce an imbalance in mitochondrial fluxes and induce an exacerbated oxidative stress(60). From this worsening situation, NASH becomes the fastest growing etiology for end-stage liver disease (ESLD) and have been established as the most common indication for liver transplantation in 2020(61).

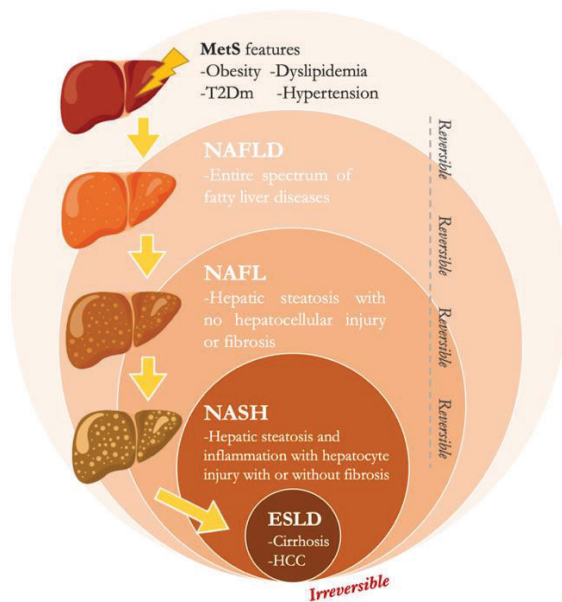


**Figure I5 –Diagram of the different NAFLD diseases states.** This picture briefly describes the different stages of NAFLD, from the onset of the pathology to the irreversible final stage. In this way three key phases can be identified; the first one known as NAFL, is characterized by the early stage of triglycerides accumulation. The next phase known as NASH differs from the previous phase by presenting exacerbated inflammation with cellular damage and possible fibrosis. Finally, the last phase known as ESLD, unlike the previous phases is irreversible. This final stage is characterized by an advanced cell damage and scar tissue known as cirrhosis. From this cirrhotic state, liver can develop hepatocarcinoma (HCC).

The gradual shift from NAFL to more severe stages along with the other obesity-related pathologies, lead a significantly increase on suffering other diseases such as kidney diseases. Concretely, mounting evidence connects NAFLD to chronic kidney disease (CKD). Several cross-sectional studies have reported a strong association between the presence and severity of NAFLD and the increased prevalence and incidence of CKD(62). Furthermore, mechanistically, a complex picture has been found in which NAFLD and CKD share common pathogenic factors but may also interact with each other, influencing each other, for example by the altered renin-angiotensin-aldosterone system (RAAS), the impaired antioxidant defense mediated by the nuclear factor

erythroid 2-related factor-2 (Nrf2), as well as through the altered lipogenesis, lipoprotein dysmetabolism and altered secretion of the hepatokines such as fibroblast growth factor-21 (FGF-21)(63,64).

### 1.1.3. Chronic Kidney Disease

Chronic kidney disease (CKD) is defined as a clinical syndrome secondary to the definitive change in function and structure of kidney. Patients are diagnosed with CKD when they present glomerular filtration rate (GFR) lower than  $60\text{ml}/1.73\text{m}^2$  or greater than  $60\text{ml}/1.73\text{m}^2$  but with an evidence of structural injury, in all cases for a period equal to or more than three months(65). Examples of structural damage include tumors, malformations, cysts, and atrophy. There are also different renal injury indicators that can help to detect signs of CKD such as albuminuria, hematuria, leukocyturia and persistent hydro-electrolytic disorders. Unlike the other pathologies associated with MetS, CKD is the only one characterized by its irreversibility from the beginning and by its slow progressive evolution(66). Its prevalence varies between 7-12% depending on the region and global mortality rises up to 1.2 million deaths per year being the 12<sup>th</sup> leading cause of death worldwide(67).

The two main causes of CKD are T2DM and hypertension. Moreover, obesity and hyperlipidemia, are considered the most prevalent independent risk factors on suffering CKD, proposing that lipid accumulation in kidney is also a key player on the physiopathology of the disease(68). Thus, we have three main actors in the development of the pathology: high glucose levels, lipid accumulation and high blood pressure. In this sense, CKD can be classified in different ways, by its own etiology or by its risk of progression. In the first case, there are two main groups: hypertensive CKD and diabetic CKD, later redefined as DKD(69). In the case of risk progression, the disease is categorized according to six GFR groups (from highest  $\geq 90\text{ml}/\text{min}/1.73\text{m}^2$  to lowest values  $<15\text{ ml}/\text{min}/1.73\text{m}^2$ ) and according to albuminuria levels separated into three categories, from  $<30\text{mg}/\text{g}$  to  $>300\text{mg}/\text{g}$  (tab1). This classification is the most widely used and was defined by the KDIGO organization (Kidney Disease Improving Global Outcomes)(70).

The pathophysiology of CKD involves two major sets of damage mechanisms: those that are specific to the underlying etiology and those related to hyperfiltration/hypertrophy of the remaining viable nephrons, which are the common consequence of a long-term reduction of renal mass (70). In the case of obesity, one of the first signs of CKD is the general hypertrophy of the nephrons, mainly comprising the enlargement of Bowman's capsule, proximal tubule and glomerular tuft, due to the significantly increased body mass and fat accumulation(66). At the same time, the increase of circulating fatty acids associated with obesity and NAFLD, makes them compiling to the different cell types of kidney from mesangial cells to podocytes and proximal tubule epithelial cells(68). In this last case, the ectopic accumulation of lipids in the tubular cells ends up causing what is known as fatty proximal tubules. Proximal tubule cells are more susceptible to lipotoxicity than other cells on kidney system; this could be due to an increased energy requirement that can only be supplied by oxidative phosphorylation on mitochondria. This fact makes them truly sensitive to lipid-induced mitochondrial damage(68). However, the pernicious action of lipids does not only affect the tubules. In obese high-fat diet-fed (HFD) animal models, lipotoxicity reaches the glomerulus, with a significant increase in ROS levels with an evident chronic inflammation and a marked increase of fibrotic processes(71). Podocytes are also affected by lipotoxicity, and its damage contributes to glomerulosclerosis and albuminuria. In parallel, multiple metabolic pathways are clearly altered, for example different fatty acid transport proteins like FATPs (Fatty Acid Transport Protein) and CD36 (Fatty Acid Translocase) are increased in this damaging process, thus increasing NEFAs uptake and feeding back whole progress(68). Lipid accumulation is also able to initiate ER stress with its consequent ROS production increase and direct toxic effects on the kidney.

Even though lipotoxicity plays a determining role in the onset of CKD, it is probably high glucose and diabetic pathogenesis the greatest factors on the development of CKD(66). Diabetes is a well-known actor associated with massive glomerular hyperfiltration and renomegaly(72). Half of all patients with T2DM will develop CKD, even though the percentage of the patients who can be considered to have CKD directly as a consequence of their T2DM is unclear(73). Accordingly, it is seldom possible to define precisely diabetic kidney disease (DKD) or diabetic nephropathy, particularly in T2DM patients(73). Thus, it is more appropriate to focus on the early identification and treatment of diabetic patients since DKD is the renal manifestation of the same diabetic glucose-driven pathological process. T2DM-associated renal damage has always been classified as a microvascular disorder, along with other diabetic related pathologies.



Mechanistically, chronic high glucose levels disable the ability of endothelial cells to downregulate their own glucose transport and leads to an overwhelming flux of intracellular glucose. This triggers the generation of pathogen mediators that contribute to the diabetic complications such as retinopathy, neuropathy or DKD(73). One of the main responsible toxic intermediates generated due to high glucose levels (and also NEFAs) are the ROS(74). The overproduction of superoxide as result of increased mitochondrial membrane potential from a raised substrate oxidation is one of the main origins of ROS. In parallel, increased glucose flux activates the NADPH oxidase and the uncoupling nitric oxide synthase(74). Accordingly, there are other four hypotheses about how hyperglycaemia cause diabetic complications: by increasing polyol pathway flux; via the activation of protein kinase K (PKC) isoforms; by increasing advanced glycation end-product (AGE) formation; and via increasing hexosamine pathway flux(75). Although there is a considerable amount of data on how hyperglycemia acts, there is no linking hypothesis of these mechanisms(76).

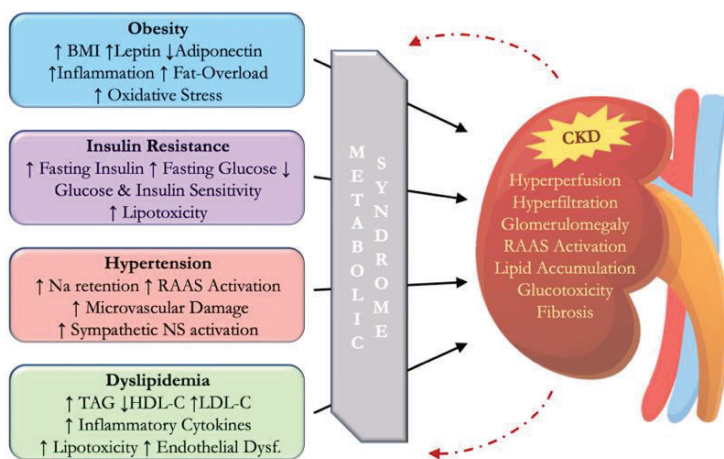


**Figure 16 – Summary diagram about the relationship between metabolic syndrome and CKD.** This picture briefly describes the principal implications of the four features of the MetS (obesity, IR, hypertension and dyslipidemia) with the primary consequences of CKD.

Apart from oxidative damage, there are other pathways by which hyperglycemia leads to renal damage. One of them is the alteration of the sodium-glucose cotransporter type 2 (SGLT2) of the proximal tubule whose function is to reabsorb approximately 90% of the filtered glucose(77). High glucose levels promotes SGLT2-driven reabsorption of sodium in the proximal tubule, a process that subsequently inactivates tubule-glomerular feedback and activates the renin-angiotensin-aldosterone system (RAAS)(66). RAAS is known to be the hormone system that regulates physiologically blood pressure, fluids and electrolyte balance as well as systemic vascular re-



sistance thought coordinated effects on the heart, blood vessels and kidney(78). Pathophysiologically, RAAS activation is directly associated with oxidative stress, hypertrophy, fibrosis and inflammation, being a key player in the pathogenesis of cardiovascular and renal diseases(79).

A couple of years ago a new clinical identity for kidney involvement in the setting of metabolic syndrome and T2DM was published. By using a comparison with fatty liver disease, this article proposed that kidney is not just a bystander and a victim of hypertension and T2DM. Authors suggests that the combination of systemic and direct local effects of ectopic fat renal deposition make kidney a major pathological contributor, deserving to be considered a distinct clinical entity that would be named “Fatty Kidney Disease” (FKD)(33). Although it has been extensively demonstrated that the accumulation of NEFAs and TG in the renal system directly contributes to hyperglycaemia and to hypertension due to the activation of RAAS, the consideration of FKD term has not generated sufficient consensus. However, kidney is increasingly being considered not only as a victim organ, but also as a pathological asset in obesity, MetS and T2DM (*Figure I6*).

## 1.2. Lipid Homeostasis

Within 10 years, one billion people approximately will suffer from disabling consequences of the metabolic disorders such as obesity, T2DM, NAFLD, or CKD making them the number one global health problem by 2030(80). Interestingly, these are mostly lifestyle-related diseases, being diet and physical activity the main axes for their development. In the last decade, both diet composition and life habits have made a radical turn, whereby a growing percentage of the population consume an excess of calories from high-fat and high-sugar diets without a corresponding physical energy expenditure(81). This energy imbalance over-time and the mismatched intake of macronutrients are responsible of homeostasis disruption, which leads to the pathological onset. Obesity arises as the main pathological axis from where, in its progression and worsening process, the different comorbidities emerge as explained above. In this section, it will be explained the key pathological changes on the metabolic homeostasis, specifically concerning the lipid metabolism role within the principal metabolic tissues.

### 1.2.1. Main Tissues

The adipose tissue and liver are the two major partners in the regulation of whole-body energy homeostasis. Particularly, WAT is the major site of energy storage on bony vertebrates, and liver is the non-adipose organ with the greatest capacity to accumulate fat(82). Both share different key processes due an evolutionary resembled origin in which metabolic cells are architecturally organized in close proximity with immune cells and blood vessels in order to coordinate the regulation of metabolic and immune responses(83). This was evidenced through fruit fly models of obesity and metabolic disease, since the *Drosophila* fat body performs many of the functions of the mammalian liver and adipose tissue in a single organ(84). Unfortunately, neither of the two organs on humans have evolved to cope with the continuous, chronic, nutrient surplus seen in obesity(83).

The main function of WAT has been described as storing and releasing fatty acids that supply fuel to the organism. Main metabolic functions include lipolysis, fatty acid oxidation and lipogenesis, and the endocrine function comprise the production of adipokines as explained above in the obesity section(82). Unlike WAT, Brown Adipose Tissue (BAT) the other type of adipose tissue, is conceived for maintaining the whole-body temperature significantly higher than ambient through producing heat via non-shivering thermogenesis using fat as a fuel. Initially, it was thought that BAT was only present in early infant humans, but imaging studies revealed metabolically active BAT in different regions of healthy adults contributing to fat oxidation and diet-induced thermogenesis(85). Regarding liver, it is probably one of the main hubs of physiological processes in our organism, specially being a major regulator of energy homeostasis sensing nutrient availability and altering energy and metabolite production needed for other tissues(86). Its ability to store glucose in glycogen form at feed states and raise glucose through gluconeogenesis in response to fasting, are principal live processes(87). At the same time, in terms of lipid metabolism, liver regulates the distribution of lipids within the body(86). In response to fasting and feeding, hepatocytes synthesize, store, and secrete lipids to maintain whole-body lipid homeostasis(88). In summary, the three tissues WAT, BAT, and liver, are essential actors in energy homeostasis and especially the alteration of their lipid-metabolic processes are determinant in the pathological development of obesity and its related diseases. Thus, in this section it will be analyzed the different shared metabolic processes involving lipid homeostasis and their regulation.

### 1.2.2. Fatty Acid Uptake

The first regulatory step in lipid homeostasis is cellular uptake at the plasma membrane. This is often highly regulated, involving specific membrane receptors with a downstream network of interacting proteins(89). The uptake of fatty acids firstly depends on the fatty acid delivery and the liver's capacity for their transport. In non-post digestive periods, mostly NEFAs delivered to the liver are released from the scWAT and to a lesser extent from VAT(90). On the other hand, after a meal dietary fat is digested mostly in the small intestine and then, they are absorbed into the enterocytes where fatty acids are resynthesized into TAG and secreted forming chylomicrons to the lymphatic system(91). Subsequently, these circulating chylomicrons reach the liver where the lipoprotein lipase enzyme (LPL) releases NEFAs. The released NEFAs, both from diet or WAT, enter to the hepatocytes through different fatty acid transporters, such as CD36, FATP2, FATP4 and FATP5, located in hepatocyte plasma membrane(91). Both LPL and the fatty acid transporters are key players in the steatosis process. For example in case of the LPL, it has been shown that its gene expression is significantly higher in NAFLD-obese subjects compared to non-NAFLD obese, suggesting that NEFAs released from circulating TAG also contribute to steatosis(92). At the same time, FATP transporters KO mice show a reduction of fatty acid uptake in hepatocytes, reduced hepatic TAG content and reversed steatosis indicating a key role for FATP-mediated lipid uptake as a facilitator of hepatic steatosis(93–95). This pattern is also observed with the peroxisome proliferator-activated receptor gamma (PPAR $\gamma$ ) regulated CD36 long-chain fatty acid transporter. Liver specific-KO of CD36 display a decreased hepatic lipid content in both genetic and DIO steatosis, while overexpression of CD36 enhances fat accumulation(96,97). Interestingly, CD36 expression in subjects with IR and intrahepatic TAGs is significantly lower in adipose tissue but higher in liver and skeletal muscle(98). Once inside the cells, fatty acids are transported to different organelles by the fatty acid binding protein 1 (FABP1), which facilitates the transport, storage and utilization of FAs as well as their acyl-CoA derivatives(99). Another function of this protein is to protect fatty acids from the environment by preventing interactions and promoting their functional oxidation or incorporation to TAGs. Although its main function is the protection of FAs against ROS and the promotion of their properly oxidation or TAG incorporation, in NAFLD context this is not always fulfilled due to lipid overload. Like the other transporters of the same family, FABP1 is increased in subjects with NAFLD and in turn, in KO liver specific animal models of this protein a significative reduction of TAGs is observed(99).

### 1.2.3. Lipolysis

Under physiological conditions when there is not enough metabolic fuel or when a greater energy requirement is need, such as in exercise, fasting and cold exposure, WAT mobilize their warehoused TAG via the catabolic process of lipolysis to provide fuel to peripheral tissues(100). Lipolysis process can occur in all tissues, mainly in the adipocytes of WAT and results in glycerol and NEFAs production from the enzymatic break-up of TAGs by lipases. Mechanistically, TAGs are broken down into diacylglycerols (DAGs) and subsequently into monoacylglycerols (MAGs) by the sequential action of the adipocyte triglyceride lipase (ATGL), hormone sensitive lipase (HSL), and the monoacylglycerol lipase (MGL)(*Figure I7*). At every step a single NEFA is released and in the final MGL-mediated step a glycerol and the last NEFA are liberated(101). These byproducts can have different destinations, being re-esterified within the adipocyte to reform TAGs or going to bloodstream to be used as fuel by other tissues. In this last case, released NEFAs could be consumed by oxidative tissues such as muscle, and glycerol could be used by the liver in the gluconeogenesis process(100). Activation of lipolysis is relayed by the sympathetic nervous system (SNS) as well as by a variety of hormones. Post-ganglionic sympathetic nerve fibers innervate adipose tissue depots, mainly scWAT and VAT, where they exert a master control on lipolysis by the release of noradrenaline (NA)(100). Noradrenaline stimulates  $\beta$ -adrenergic receptor, which at the same time stimulates protein kinase A (PKA) through the adenylyl cyclase (AC) mediated production of cyclic adenosine monophosphate (cAMP)(*Figure I7*). The PKA activates both ATGL and HSL lipolytic enzymes: ATGL indirectly via the phosphorylation of lipid droplet surface perilipin (PLIN1) which changes de conformation exposing the LD-stored lipids to the lipases, and HSL directly via its own phosphorylation(102). Other hormones secreted by peripheral tissues, such as glucagon-like peptide-1 (GLP-1) or leptin can regulate also fat metabolism via the central nervous system-SNS axis.

After a meal, the post-prandial plasmatic increase of insulin efficiently suppresses lipolysis to promote the storage of the dietary ingested lipids. On the contrary, in fasting state, NEFAs mobilization is enhanced by a release of adrenaline and noradrenaline accompanied with an increased  $\beta$ -adrenergic sensitivity and decrease of circulating insulin levels(103). In case of physical activity, lipolysis is also stimulated and involving the mutual action of several signaling pathways. Thereby, circulating levels of adrenaline, noradrenaline, atrial natriuretic peptide (ANP), growth hormone (GH) and cortisol increase as well as an insulin decrease in proportion to the

exercise intensity culminating to an overall lipolytic response(103). When WAT starts becoming insulin resistant, as it happens initially in obesity and T2DM due to WAT dysfunctionally, insulin loses the ability to inhibit adipocyte lipolysis and reduce the bloodstream dropped NEFAs and glycerol. This ineffectiveness results to a exacerbated lipolysis along with a dangerously increase of circulating NEFAs in both fasted and fed states(101). Constant exposure to these high levels, drive to a gradually deposition in non-adipose tissues like muscle, pancreas, liver, or kidney causing an ectopic fat accumulation with lipotoxic effects and exponentially increases the risk of suffering other related pathologies such as NAFLD or CKD as explained above. Clearly, this situation feeds back negatively whole process as these ectopic lipids impair insulin signaling, therefore adipocyte insulin resistance via increased lipolysis may be one of the major contributors to the obese insulin resistance states(104).

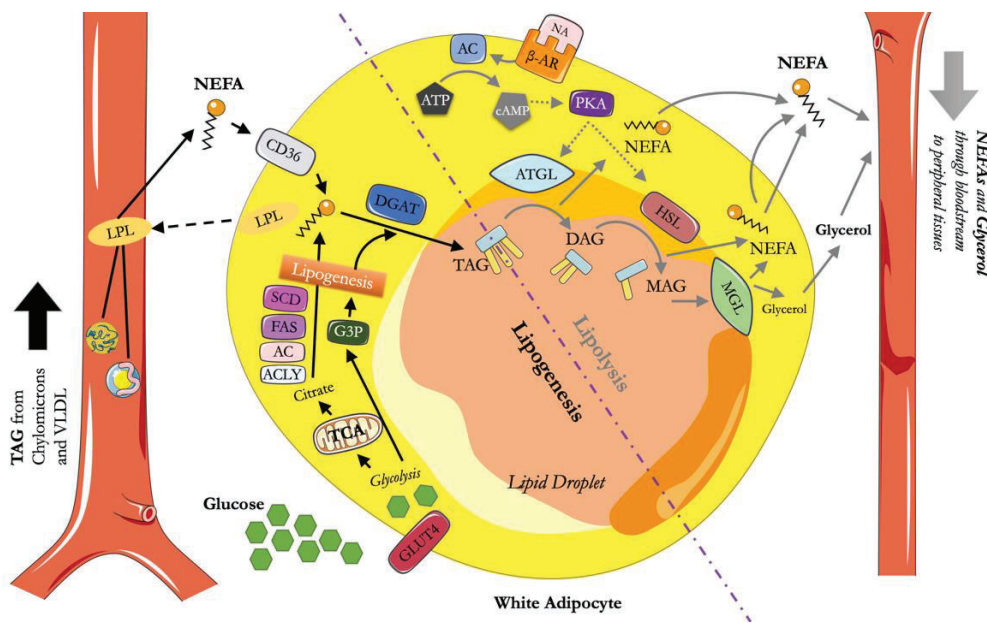


**Figure I7 – Summary of WAT lipogenesis and lipolysis metabolic pathways.** This figure shows the two main metabolic processes of the white adipocyte, separated by a purple dashed line. Lipogenesis is represented in the left side of the image by black arrows and lipolysis in the right side by gray arrows. In order to have a homeostatic energy balance and a good maintenance of whole-body insulin sensitivity, lipogenesis and lipolysis process must be balanced. Both processes are tightly regulated by different agents such as nutritional and hormonal cues. In case of pro-lipogenic actors, we found feed, and insulin, by the contrary fasting and growth hormone develop an anti-lipogenic role. In case of pro-lipolytic agents, it should be noted exercise, cold exposure, fasting and hormones such as catecholamines, natriuretic peptides, growth hormone, glucocorticoids, and TNF- $\alpha$ . Based on figure 4 of Richard AJ, White U, et al. Adipose Tissue: Physiology to Metabolic Dysfunction.

Regarding transcriptional control, regulation of lipases genes is a major mechanism controlling lipolysis. However, the transcriptional control elements in the promoters of lipolysis key genes such as *Atgl* or *Hsl*, have not been sufficiently characterized(105). Although, there is evidence suggesting that both genes are direct targets for Peroxisome Proliferator-Activated Receptors (PPAR) family of nuclear receptor transcription factors, which will be explained later. There are also other nuclear receptors like the originally described in the liver, Liver X Receptor (LXR) that are specific to the promoters of *Hsl* but that do not regulate *Atgl* promoter(105). LXR is a possible key regulator of lipid turnover in fat cells, concretely data suggests that activation of alpha LXR isoform up-regulates basal lipolysis implicating a role of LXR $\alpha$  in the development of IR(106). Subsequent trials with LXR agonists also had the ability to induce LXR expression and raised lipolysis levels on adipocytes(107). In addition, it is worth mentioning that LXR is not only involved in the transcriptional regulatory network of lipolysis, but also in the regulation of adipocyte differentiation, cholesterol transport, lipogenesis and glucose metabolism(108). In liver, contrary to what was expected, LXR activation promotes cholesterol elimination as well as the synthesis of fatty acids and TAG by up-regulating sterol regulatory-binding protein 1c (SREBP1c), the key regulator of hepatic lipogenesis(109). In that sense, LXR regulates lipid processes transcriptionally in a tissue specific manner: in liver inducing lipogenesis and TAG accumulation while in WAT, reducing lipogenesis and enhancing lipolysis(110).

#### 1.2.4. Lipogenesis

Adipocytes accumulate lipids via two different processes, the uptake of fatty acids from circulating lipoproteins and the synthesis of fatty acids from non-lipid precursors known DNL. Under normal daily feeding, adipocytes takes up the dietary lipids from the bloodstream circulation as NEFA liberated from circulating TAGs via the action of the LPL (*Figure 17*)(111). This lipase is secreted by the adipocytes themselves, and its principal function is to hydrolyze TAGs from the triglyceride-rich lipoproteins such as VLDL (synthesized by the liver) and chylomicrons (produced in the small intestine)(101). In parallel, adipocytes also capture glucose, which is converted to glycerol and later used as the backbone for the serial esterification of fatty acids to form TAG(101). The final step in TAG synthesis is performed by the diacylglycerol acyltransferase enzyme (DGAT) which catalyzes the covalent addition of a fatty acyl-CoA to diacylglycerol forming triglycerides(112). In eukaryotes there are two types of DGAT (DGAT1 and

DGAT2), both catalyzing the same reaction but evolutionarily unrelated and with different functions(113).

On its side DNL, comprises the synthesis of fatty acids from acetyl-CoA and the esterification of these fatty acids to a glycerol backbone producing TAGs (*Figure I7*)(101). DNL levels are relatively low in WAT compared to BAT and liver but can occur both in fasting and fed states. Interestingly in fed states, food composition also has dramatic effects on DNL, for example, high fructose or sucrose diets induce DNL in both liver and adipose tissue but HFD inhibits it. Mechanistically, after a rich-carbohydrate meal, excess glucose undergoes glycolysis and enters to the tricarboxylic (TCA) cycle to produce citrate in the mitochondria which is transported to cytosol and released to acetyl-CoA by the ATP-citrate lyase (ACLY)(114). Next, this acetyl-CoA is converted to malonyl-CoA by the acetyl-CoA carboxylase enzyme (ACC) and finally the fatty acid synthase (FAS), the key rate-limiting enzyme in the process, converts this malonyl-CoA into palmitate which is the first FA product in DNL (*Figure I7*)(114). The primary products of DNL are saturated fatty acids, which at certain levels confer adverse cellular effects, but then the stearoyl-CoA desaturase (SCD) converts the generated saturated fatty acid to a monounsaturated fatty acid (MUFA) for example from stearic acid to oleic acid(115). During fasting, DNL decreases due to increased glucagon and cellular cAMP levels that inhibits DNL through activating AMP-activated protein kinase (AMPK) and the cAMP-dependent protein kinase PKA(114).

In liver DNL has a particular value since it's the main organ where carbohydrates are transformed into lipids. Once converted into lipids, new fatty acids are then used for creating energy, phospholipids, ceramides, but also become esterified to cholesterol and finally for TAG synthesis, which will be used as storage or secreted on lipoproteins as VLDL to bloodstream where they reach the adipose tissue or other organs that need them(116). In obesity-insulin resistance state, parallelly to the TAG accumulation on liver from adipose tissue, the hepatic DNL is also increased, thus contributing to the formation of additional fatty acids from non-lipidic substrates that end up forming new TAG and rising the hepatic steatosis(57). The regulation of the DNL pathway is composed of two layers, first one relying on transcriptional regulation of key enzymes from fatty acid synthesis and finally the allosteric regulation of the ACC(117). At transcriptional level in both WAT and liver, there are two major regulators of the DNL, the carbohydrate response element-binding protein (ChREBP) and the sterol regulatory element-binding protein 1 (SREBP1), both activated by the high glucose and insulin concentrations characteristic of the



obesity and its related NAFLD onset. ChREBP, also known as MLXIPL, is a basic helix-loop-helix leucine zipper transcription factor that is mainly expressed in liver, WAT and BAT, intestine, muscle, and pancreatic  $\beta$ -cells(118). Replying to increased glucose levels, ChREBP suffers dephosphorylation and become translocate from the cytoplasm to the nucleus where it forms a heterodimer with its functional partner Max-like interacting protein (MLX). This heterodimer attaches to the carbohydrate responsive elements (ChoRE) of ChREBP target genes and thereby controls glucose and lipid metabolism(118). There are two isoforms of ChREBP, ChREBP- $\alpha$  (with a low glucose inhibitory domain) and ChREBP- $\beta$  which lacks most of the N-terminal low glucose-inhibitory domain(119). Alpha isoform is localized mainly in cytosol and beta remains in the nucleus. Under the activation conditions (high levels of glucose), ChREBP- $\alpha$  is translocated to the nucleus to induce ChREBP- $\beta$  transcription. This two-step activation mechanisms seems to be important to reach the glucose threshold for ChREBP-mediated gene expression(120). It has been demonstrated that the overexpression of ChREBP- $\beta$  in adipose tissue increases the of genes involving DNL such as *Fasn*, *Acy*, *Acc*, and *Scd*(121). On the contrary, the deficiency of ChREBP displays a significant impairment of lipogenic and DNL gene expression. Mice lacking adipose tissue ChREBP have decreased DNL and become IR(122).

The other major DNL regulator, SREBP1, belongs to the sterol regulatory element binding protein family of transcription factors that regulate lipid biosynthesis and adipogenesis by controlling the gene expression of several enzymes required for TAG, FA, and cholesterol synthesis(123). SREBP1c isoform is synthesized as a precursor in the ER membrane but requires a post-translational modification to generate its transcriptionally active nuclear form(124). Insulin activates the transcription and the maturation of SREBP1c which induces the expression of adipose cell genes involving glucose utilization and fatty acid synthesis such as *Fasn* and leptin, being both key genes and sensitive to nutritional alterations(125). Activation of SREBP1c downstream of the insulin receptor occurs through two pathways: first one involving PI3K/PKB pathway resulting with the direct phosphorylation and activation of the mature SREBP1c, and the other pathway involves the LXR transcription factor by heterodimerizing its alpha isoform with RXR which activates the transcription of SREBP1c(117). In this way, it has been observed that SREBP1c and all its subsequent enzymes of DNL are activated in the context of NAFLD, and thus contributing to the pathogenesis of the disease(126).



As already discussed in the introductory part of NAFLD, the main contributor to the steatosis hepatic process is the excessive NEFAs flux from the AT but secondly it is the exacerbation of DNL pathway(54). In this sense, modifying DNL, for example in *ob/ob* mice models with *Srebp1c* deletion, a reduction of 50% of TG accumulation in the liver has been observed(127). On the other hand, the increase in DNL not only results in an increase of steatosis. For example, a relationship has been observed between DNL and increased expression of ACC isoform 2, which has the capacity to inhibit fatty acid oxidation through indirect inhibition of the carnitine palmitoyl transferase 1 (CPT1)(128). Therefore, it can be concluded that although it is not the main NAFLD cause, hepatic DNL plays a major role in the development of this pathology.

#### 1.2.5. Lipid Droplet Formation

Within cells, lipids are stored in specialized organelles called lipid droplets (LD) which are the universal cellular warehouse for the lipid transient or long-term storage. The number, size and composition of LDs vary greatly within cells in a homogenous population as well as in different tissues and cell types(129). Its biogenesis starts with the generation of neutral lipids in the lipogenesis process, synthesizing species such as TAGs which are the most prevalent. These TAGs are transferred between the ER monolayers rising a critical lipid concentration, thereby when the neutral lipid concentration reaches a critical level, it becomes thermodynamically favorable that the molecules coalesce to nucleate to a lipid lens(*Figure I8*)(129). The nucleation process is controlled by energetic constraints in response to the increased accumulation of TAGs in the ER intermembrane, thus lipid nucleation needs to overcome an energy barrier. Different factors contribute to the energy barrier such as the interactions between molecules, the thermal energy, or the propensity to disperse TAG molecules between ER monolayers(130). In this sense, until necessary energy is not reached, TAGs will be accumulated in the ER intermembrane ultimately overcoming the barrier and resulting in the formation of big lipid droplets (LD)(129). Once stable and mature, LDs are distributed according to their cellular origin. In WAT, whose role is to warehouse excess energy in lipid form and rapidly hydrolyze, large unilocular LD with a minimum surface area become the ideal structure to store TAG. In this form, the contact area of LD with lipases is reduced, resulting in a physic restriction of lipolysis. Moreover, being unilocular, the LD of the white adipocyte remains close to the plasma membrane being able to efficiently flow out the NEFAs and glycerol to the bloodstream(131). Conversely, in BAT and beige adipose tissue this LD distribution change notably. Brown adipocytes possess small multilocular

LDs in order to increase the contact LD area with lipases, which efficiently promotes lipolysis and facilitates NEFA transport to the mitochondria for  $\beta$ -oxidation and heat production(131).

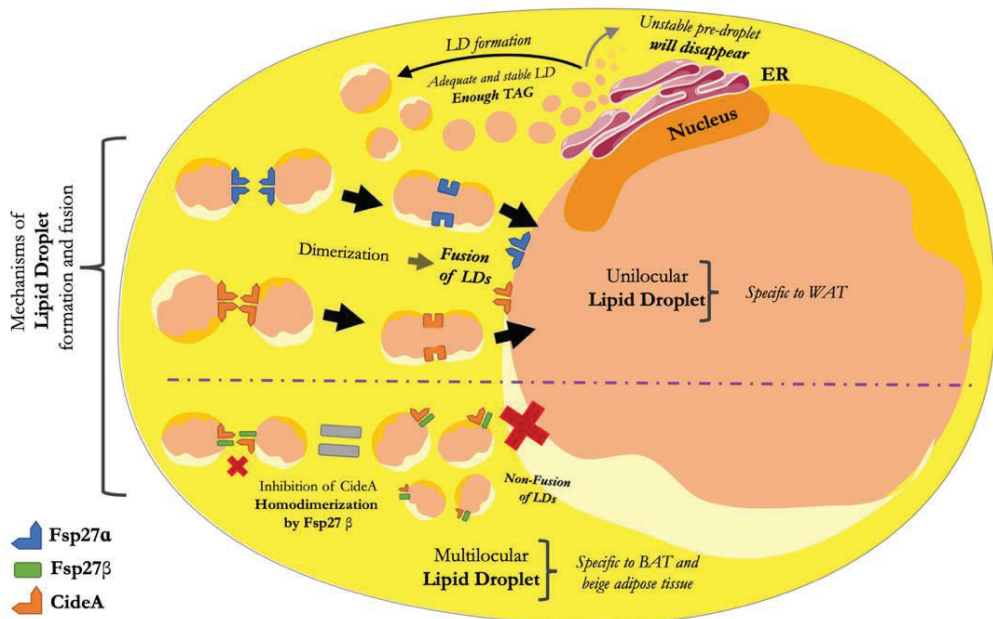


**Figure 18**—Figure explaining mechanisms of formation and subsequent fusion of adipose tissue lipid droplets. This diagram shows from the origin of LD in the ER to their possible fusion to reach unilocular LD or their non-fusion becoming multilocular LD. In the first case, the formation of LDs is limited by the amount of TAG and its energetic stability. On the other hand, the fusion and growth of these already stable LDs depends on the dimerization of CideA and FSP27 $\alpha$  proteins due to LD-LD contact. If FSP27 $\beta$  is present on the LD surface, it will form a complex with CideA and prevent its dimerization and therefore avoiding the LD fusion and growth.

The reasons of these aggregation differences are due to the cell death-inducing DNA fragmentation factor alpha (DFFA)-like effector (Cide) family proteins. There are three members in the Cide family: CideA, CideB, and CideC (132). The expression and distribution of the three Cide members demonstrate their tissue-specificity. CideA is abundantly expressed in the murine BAT and human WAT, whereas expression highly correlates with lipid storage and lipid secretion in these tissues(133). Meanwhile, CideB expression is poorly expressed in the intestine but primarily detected in the liver, where controls both insulin sensitivity and VLDL maturation(134,135). CideC, also known as fat-specific protein 27 (FSP27) in mouse, is highly expressed in fatty liver. Knock-down of its expression in NAFLD-liver ameliorates hepatic steatosis, and inversely, its overexpression enhances the triglyceride content of LDs(136). The two FSP27 $\alpha$  and  $\beta$  murine isoforms of FSP27, which differ in 10 amino acids, correspond to the human CideC1 and 2,

respectively(137). It is notable that Fsp27 $\alpha$  is highly expressed in WAT, whereas Fsp27 $\beta$  is highly expressed in BAT and the liver, which consume TAG for thermogenesis, ketogenesis, and VLDL production(138). In that sense, Xu-xu et al hypothesized that Fsp27 $\beta$  might be relevant for the short-term storage of TAG prior to oxidation or secretion in the liver and BAT, while Fsp27 $\alpha$  promotes long-term TG storage in WAT(138).

Initially these proteins were identified as apoptotic proteins, but some studies have changed the perception redefining them as crucial actors in lipid and energy metabolism, including lipolysis, lipid oxidation and LD formation(131). Each Cide proteins are localized to the surface of lipid droplets (*Figure I8*) in their respective tissues as well as in other cell types when they are expressed ectopically. Mechanistically, through the association between LDs, FSP27 $\alpha$  and CideA respectively form a homodimer between contacting lipid droplets and mediate LD fusion and growth (*Figure I8*). These fusions, due to FSP27 $\alpha$  and CideA dimerization, leads to a gradual formation of a single unilocular LD typical from WAT. On the contrary, when FSP27 $\beta$  is present on the LD surface, it forms a complex with CideA which prevents its homodimerization and therefore avoiding lipid droplet binding and fusion process(137). This inhibition of LD fusion results in a greater number of smaller lipid droplets typical from BAT or beige adipose tissue or liver.

#### 1.2.6. Fatty Acid Oxidation

The main energy source for adipose tissue and liver comes from fatty acid oxidation. In case of liver it accounts, along with amino acid oxidation, more than 90% of the fuel for basal hepatic requirements(139). Fatty acid oxidation takes place primarily within mitochondria and to a much lesser extent in peroxisomes and microsomes(90). Before  $\beta$ -oxidation occurs in mitochondria, fatty acids are activated by coenzyme A in the hepatocyte cytoplasm through the action of the fatty acyl-CoA synthetase and then subsequently the resulting fatty acyl-CoA is converted to fatty acyl carnitine by CPT1 in the outer mitochondrial membrane(140). Following, the fatty acyl carnitine is shuttled across the mitochondrial membrane by carnitine translocase and then, inside the mitochondrial matrix CPT2 regenerates the initial fatty acyl-CoA(140). Mitochondrial  $\beta$ -oxidation successively shortens the fatty acyl-CoA by two carbon units per cycle released as acetyl-CoA via different dehydrogenation, hydration and cleavage reactions that involve diverse enzymes transcriptionally regulated by PPAR $\alpha$ (141). Finally, the generated acetyl-CoA enters to the TCA and the electron transport chain, where it completes the oxidation to carbon dioxide

and generates energy for the liver. There are particular situations where FA oxidation is increased, such as in fasting states, which results in an excess of acetyl-CoA unable to be processed in the TCA(142). It is in these conditions where from the condensation of two acetyl-CoA molecules acetoacetate is originated which in turn can be converted into  $\beta$ -hydroxybutyrate or acetone. These species are known as ketone bodies and their function is to provide energy in starvation states to the extrahepatic tissues(142).

One of the main control points of  $\beta$ -oxidation is the flow rate of fatty acids into the mitochondrial matrix, which depends on both availability of FA and the activity of CPT1. Interestingly malonyl-CoA produced in DNL process is the major inhibitor of CPT1 activity(143). Conceptually and in practical terms, both main pathways of lipid metabolism in liver DNL and  $\beta$ -oxidation contemplate opposite directions. In deficient mitochondrial oxidative enzymes models, an increment in steatosis processes has been observed(144). On the other hand, if the expression of these enzymes is increased, a reduction of TG accumulation is proved. In the case of subjects suffering NAFLD, the existing data on DNL and  $\beta$ -oxidation relation is contradictory although it is clear that steatosis process is not produced by a deficit of  $\beta$ -oxidation(143).

#### 1.2.7. Thermogenesis

Thermogenesis is the metabolic process whereby heat is generated as energy lost through macronutrient metabolism in specialized fat cells or adipocytes(145). Adipose thermogenesis is activated by neuronal, hormonal, and metabolic cues in response to cold temperatures, dietary excess, and daytime(146). Thermogenic activity is mainly mediated by the expression of the tissue-specific uncoupling protein 1 (UCP1) within the numerous mitochondria that confers the distinctive brownish appearance of BAT or to lesser extent in beige adipose tissue. UCP1 is a proton transporter within the inner mitochondrial membrane that upon activation allows proton transfer from the membrane space to the matrix of the mitochondria effectively generating heat rather than ATP(147). Conversely to white adipocytes, brown ones contain multilocular LDs dispersed along with significantly larger mitochondria number through a more ellipsoidal and much smaller type cell(101).

BAT thermogenesis can be activated by two factors, the most effective is the cold temperature, and the other but less effective, is food intake. Exposure to cold activates thermogenic activity in BAT by increasing the mitochondrial content and the metabolic rate via sympathetic nervous system and thyroid activation(148). Norepinephrine acts as the primary transmitter and subsequently activates  $\beta$ -adrenergic signaling pathways within brown adipocytes. Therefore, lipolysis but also DNL are activated to generate NEFAs which in turn activate UCP1(149). On the other hand, there is the diet-induced thermogenesis which is associated with the increase of energy expenditure above the basal metabolic rate in response to food intake(150). Activation of BAT by the specific dynamic action of food seems partially related to a dissipation of the excess energy intake in form of heat rather than storage(151). Thermogenesis after a meal is usually divided into two components: obligatory thermogenesis linked to the digestion, absorption, and storage of food; and the facultative thermogenesis, which refers to the increase in the energy expenditure in response to dietary intake that varies with food composition as well as its volume. This is regulated by the hypothalamic centers (150,152).

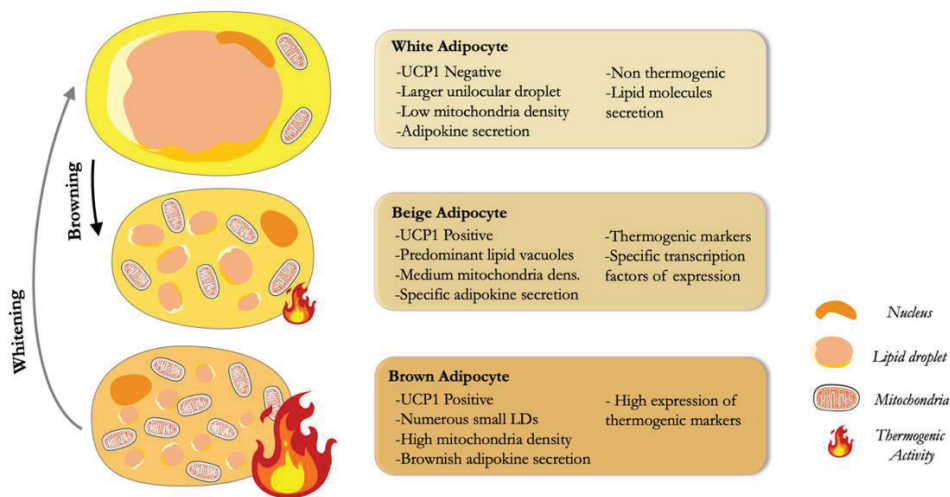


**Figure I9 – Graphic diagram with the main characteristics of the different types of adipocytes.** The image shows the three types of adipocytes, white, beige, and brown adipocytes, as well as their major characteristics. White adipocytes are notable for the presence of a large lipid droplet in addition to their ability to secrete obesogenic adipokines and their low ratio of FA oxidation and thermogenesis. In contrast, beige adipocytes, although derived from white adipocytes, they have a greater number of smaller lipid droplets and a higher capacity for AG oxidation and thermogenesis. Finally, brown adipocytes are characterized by their high presence of mitochondria, the large number of small lipid droplets and their strong thermogenic capacity.

Besides brown adipocytes characteristic from BAT, there are other closely related adipocytes, the beige adipocytes. Both possess thermogenic properties, common morphological and biochemical characteristics, including multilocular LDs and large number of mitochondria (*Figure 19*). However there are four major differences: they don't have the same cell origin, neither the same anatomical location and plasticity, and not even the same gene markers(151). Beige adipocytes, forming what is known as beige adipose tissue, were initially observed in rodents WAT in response to cold exposure(153). However, since then many studies have identified other “browning” or “beiging” factors such as exercise, drugs, diet and their bioactive compounds and even adipokines(101). Accordingly, both activation of BAT and induction of browning processes have been proposed as a therapeutic target for pathologies such as obesity. In fact, the capacity of increase energy expenditure, the potential of improving glucose metabolism, their insulin sensitizing role, and their capacity to burn fat, makes brown and beige adipose tissue interesting to all related obesity pathologies like T2DM, NAFLD and CKD.

#### 1.2.8. Adipokines and Hepatokines

It is widely described that WAT is not only an energy warehouse but also a potent endocrine actor. As explained in the introductory obesity section of this thesis proposal, adipocytes and other adipose tissue cells contribute to the release of metabolites, lipids, and bioactive peptides; so-called adipokines(154). Adipokines modulate the regulation of insulin secretion and sensitivity, fat distribution, energy expenditure, inflammation, endothelial function, blood pressure and regulation of appetite and satiety. This modulatory role is not only relayed within the WAT, but also at systemic level. Adipokines regulate different biological processes in target organs such as brain, liver, muscle, heart, pancreas, and others(101). Obviously, the type and role of these adipokines is determined by the state of the adipose tissue that secretes them. Individuals with hypertrophic larger adipocytes, exhibit elevated proinflammatory adipokines, including leptin, IL-6, IL-8 and MCP-1; in turn insulin sensitivity-related species like adiponectin and anti-inflammatory IL-10 have decreased levels(154). Similarly, the liver has also been recognized as an endocrine organ that secretes its own metabolites called hepatokines, which are liver-derived factors that can signal and communicate with other organs including the CNS, adipose tissues, and skeletal muscle(155). Hepatokines are proteins regulated via autocrine, paracrine, and endocrine both in liver and within other tissues. Its function is essential for the transmission of information

regarding the hepatic metabolic status, as it happens on WAT. In recent years, several hepatokines have been studied for their roles in the development of obesity, insulin resistance, and NAFLD tissue, showing an endocrine-dependent relationship, therefore acting through cross-talk with the cytokines released by the other disease-related tissues(156).

**Leptin** is probably the best known adipokine and the prototype for all adipocyte secreted hormones. Leptin is a 167-aminoacid peptide produced mainly in the adipose tissue but is also expressed in variety of other tissues such as placenta, ovaries, mammary epithelium, bone marrow and lymphoid tissues(157). Circulating levels of leptin reflect primarily the amount of energy stored in fat and secondarily acute changes in caloric intake, therefore its levels are positively correlated with the amount of body fat(158). Leptin principal role is to regulate satiety, appetite, food intake and energy expenditure but it has also growth and reproductive functions. In addition, leptin is able to exert insulin sensitizing effects and is now considered a key regulator of pancreatic  $\beta$ -cell mass and survival(154). Obesity promotes multiple cellular processes which attenuate leptin signaling and in turn amplify the extent of weight gain induced by genetic and nutritional factors. In that sense, leptin reduces food intake and body weight by central action on hypothalamus but the coexistence of elevated levels with obesity and worsened leptin signaling, reveals obesity as a leptin resistance state(159).

**Adiponectin** was discovered shortly after leptin and has been characterized by its remarkably high circulating levels on human plasma, reaching more than 1000-fold higher levels than other major secreted factors(154). It is mainly produced by adipocytes acting in an autocrine or paracrine manner in adipose tissue and other tissues. It has also gained a lot of interest due its anti-inflammatory, antiapoptotic and insulin sensitizing properties(154). Adiponectin enhances fatty acid oxidation through the activation of the AMPK which inhibits ACC (the rate limiting enzyme in DNL) and in turn, reduces malonyl-CoA production that enhances fatty acid oxidation(101). Adiponectin can also lower serum glucose through suppression of hepatic glucose production through multiple pathways and independently of AMPK(160). This suppression of hepatic gluconeogenesis is opposed to the adiponectin effect on whole-body glucose uptake and glycolysis since it increases glucose transporter-4 (GLUT-4) translocation and directly targets the IRS-1(161). There are many clinical trials showing that adiponectin levels inversely correlate with obesity, visceral fat distribution, T2DM, NAFLD progression and other related diseases(162). In the liver, it also promotes hepatocyte survival, inhibits fibrosis and inflammation,



simulate fatty acid oxidation and modulates fatty acid uptake(101). The antidiabetic TZDs drugs mentioned above, increase notably adiponectin levels which is thought to be the principal mechanism of action that improves insulin sensitivity and glucose tolerance(154). Even in muscle, adiponectin shows the capacity to promote fat oxidation as well as promoting glucose uptake(101). Adiponectin, analogue, its activators and signaling enhancers have become into the spotlight in the management of obesity-related metabolic diseases like NAFLD, T2DM and CKD.

Another major cytokine, being essentially an hepatokine, is the **fibroblast growth factor 21 (FGF21)**. FGF21 is an atypical member of the fibroblast growth factor family which its main function involves the metabolic homeostasis in healthy individuals. FGF21 primarily was conceived as a hepatokine because it is produced in liver, although nowadays it is known that is also synthesized by the adipose tissues and the skeletal muscle targeting to multiple organs(163). The biology of FGF21 is still partly unknown owing to its diverse effects and its ability to act as an autocrine, paracrine, and endocrine factor(164). In brief, via direct effects on FGF receptors, FGF21 has demonstrated to play glucose and lipid lowering role as well as thermogenic effects(165,166). In this way on animal models of metabolic diseases such as obesity and T2DM, FGF21 has showed the ability to increase energy expenditure, restore glycaemia and improve the lipid profile as well as recovering IR(165,167). Interestingly, in obesity and T2DM, serum levels of FGF21 increase significantly. However, this increase is not associated with an improvement of its signaling but with a state of resistance.

Finally, it is worth to highlight another relevant cytokine that recurs in obesity, T2DM and renal pathologies the **lipocalin 2 (LCN-2)**. Lipocalin-2 also known as neutrophil gelatinase-associated lipocalin, is a glycoprotein identified as a cytokine derived from adipose tissue. However it is also known as an iron carrier protein whose circulating levels are increased in different pathological states mainly by kidney injury, ageing, bacterial infection, and inflammatory status. In addition, it has been also designed as a mediator of insulin resistance associated with obesity(137)(138). Transcriptional activation of *Lcn2* gene in WAT has been proposed to be directly related to the inflammatory state of obesity(170). On the other hand, it has been demonstrated that adipose tissue-derived lipocalin-2 not only plays a critical role in causing both chronic and acute renal injury, but is essential for the progression of CKD in rodent and human models (171,172). Viau et al. concluded that *Lcn2* acts as a growth regulator by mediating the mitogenic



effect of EGFR signaling(172). The activation of epidermal growth factor receptor (EGFR) is linked to the regulation of several cellular responses involved in the progression of renal damage including cell proliferation, inflammatory processes, and extracellular matrix regulation(173). Curiously, it has been shown that overexpressed LCN2, widely used as a renal injury biomarker, possesses obesity-promoting and anti-thermogenic effects through the inhibition of BAT activity(169). In addition, LCN-2 deficiency was described to have a protective role from developing aging and obesity-induced IR by modulating 12-lipoxygenase and TNF- $\alpha$  levels in adipose tissue(174). At the same time the opposite was published, the disruption of LCN2 in mice significantly potentiate the diet-induced obesity, dyslipidemia, fatty liver disease, IR and an impaired adaptative thermogenesis(175). In this way, the importance of LCN2 is highlighted in both adipose tissue and kidneys relationship with obesity and its related pathologies but there are still gaps to fill.

	Leptin	Adiponectin	FGF21	Lipocalin 2
Expression in obesity, T2DM and related pathologies	+ (Resistance)	-	+ (Resistance)	+
Expressing Tissue	White Adipose Tissue	White Adipose Tissue	Liver, WAT, BAT, Muscle	WAT, Lymphoid Tissues, Liver, Kidney
Target Tissue	CNS, Brain, Hepatocytes, $\beta$ -Cells	Liver, Muscle, Heart, Adipose Tissues	Liver, Muscle, Heart, ATs, Kidney, Brain...	Systemic
Main Function and Metabolic Effects	Regulate Satiety -Food Intake +EE Modulate Lipid and Glucose Metabolism	+Insulin Sensitivity, +FAO, +EE in Muscle -Lipogenesis, -Glucose Output, -TAG accumulation	+Insulin Sensitivity, +Lipid Oxidation, +Glucose Uptake -Inflammation, -Oxidative Stress, -Fibrosis	Defense Against Bacterial Infection +CV and Renal Injury +Inflammation

**Table I2–Schematic table of the main characteristics of the adipokines studied in this thesis proposal.** This summary of the adipocyte-specific adipokines, shows where these species are expressed, which are their target tissues, their main functions, and other relevant functions. Based on figure 6 of Richard AJ, White U, et al. Adipose Tissue: Physiology to Metabolic Dysfunction.

### 1.3. Metabolic Regulation

The regulation of the above explained metabolic processes and pathways is necessary to balance the energetic balance in the different cell cycle and states. The presence of an excess of nutrients will stimulate nutrient storage pathways, while in periods of deficiency the cell will use previously accumulated reserves. Likewise, pathological processes will also have the capacity to alter this regulation of the energy homeostasis. Transcriptional regulation of gene expression is one of

the fundamental molecular mechanisms by which cells can control energy homeostasis(176). Thereby, modulation of the activity of transcription factors implicated in metabolic control has emerged as an important target for therapeutic intervention.

One of the main groups of transcription factors are the family of nuclear receptors. Nuclear receptors are ancient transcription factors present all along the animal kingdom and whose role is essential for the regulation of developmental and physiological processes, mainly related to basic metabolic functions(177). Nuclear receptors are activated by various lipophilic molecules, including steroid hormones, such as estrogen and progesterone, and various other lipid-soluble signals, like different nutrients and bioactive compounds. Once activated, most function as transcription factors to control gene expression for numerous biological processes.

### 1.3.1. The PPARs as Metabolic Regulators

The peroxisome proliferator-activated receptors (**PPARs**) are a group of nuclear receptor which regulate the expression of many genes involving lipid metabolism, energy production, and inflammation(178). They were firstly described as members of the steroid hormone receptor superfamily related with the proliferation of peroxisomes(179). Interestingly, their role not only involve peroxisomes but were found to be fundamental control elements for metabolism. PPARs have pleiotropic actions and they are critical regulators not only of fatty acid metabolism, but also of glucose metabolism, inflammation, oxidative damage, fibrosis processes and in general energy metabolism(180). Mechanistically, PPARs binds to DNA in a complex with the retinoid X receptor (RXR) altering the transcription of genes harboring PPAR response elements (PPREs). There are three PPAR isoforms: alpha ( $\alpha$ ), beta/delta ( $\beta/\delta$ ), and gamma ( $\gamma$ ), each one with a different expression and function profile depending on the expressing tissue.

### 1.3.2. PPAR $\alpha$

**PPAR $\alpha$**  is highly expressed in tissues with high catabolic rate of FAs such as muscle, intestine, BAT and mainly in liver(181). In hepatocytes PPAR $\alpha$  commands the fatty acid transport,  $\beta$ -oxidation, ketogenesis, lipolysis and also modulates the production of apolipoproteins, the gluconeogenesis pathway and the amino acid metabolism(182). In parallel also controls other processes like the inflammatory responses by directly inhibiting inflammatory genes related to NF-kb pathway such as *Vcam-1*, *Cox-2* and *IL-6*, proving a molecular basis for the anti-inflammatory

effects of PPAR $\alpha$  ligands(181,183). PPAR $\alpha$  controls fatty acid  $\beta$ -oxidation via regulation the expression of *Cpt-1* as well as other major  $\beta$ -oxidation enzymes such as *Acyl-CoA synthetase*, *very-long- and medium-chain acyl-CoA dehydrogenase* or *3-ketoacyl-CoA thiolase*(182). The peroxisomal FA oxidation also is controlled by PPAR $\alpha$  through the modulation of the expression of its main enzymes, like the *Acyl-CoA oxidase*. In parallel, PPAR $\alpha$  controls the ketogenesis through regulating the expression of *Hmg-CoA synthase*, which is responsible of transforming acetyl-CoA units into ketone bodies(184). Regarding fatty acid transport in hepatocytes, both expression of *Cd36* and other transporters from the FABP family are upregulated by PPAR $\alpha$ (182). Another of its critical points is the TAG and lipoprotein metabolism. PPAR $\alpha$  is able to mediate TG hydrolysis of VLDL and chylomicrons via upregulating the LPL enzyme(185). As it is already known, LPL is a TG hydrolase found in the capillary endothelium of the peripheral tissues responsible to release NEFAs from TG-rich lipoproteins and thus allowing them to entry to the corresponding cells. Inactivation of this enzyme leads to a severe hypertriglyceridemia and hypercholesterolemia state(182). All these aspects establish PPAR $\alpha$  as a general regulator of fatty acid processes, which in turn makes *de facto* PPAR $\alpha$  a relevant therapeutic target. Therefore, studying molecules capable of modulate the PPAR $\alpha$  activity has become medical relevant such as in the case of PPARs agonists. One example are fibrates, being synthetic ligands of the PPAR $\alpha$  nuclear receptor that they can lower circulating TG by 36% on average and raise levels of small HDL particles(186). On the other hand, there are some compounds in nature such as bioactive compounds, able to act also as agonists or antagonists and modulate the activity not only of PPAR $\alpha$  but also of the other isoforms as mentioned above.

### 1.3.3. PPAR $\beta/\delta$

**PPAR $\beta/\delta$**  also has a relevant role either in liver metabolism or in other metabolic active tissues such as muscle, where it has a higher expression level and the ability to modulate energy production from glycolysis to fatty oxidation during fed states and exercise(187). In liver its main function is to contribute to the maintenance of energy balance by regulating fatty acid uptake, its transport and the  $\beta$ -oxidation as well as managing insulin secretion and sensitivity(188). Targeting PPAR $\beta/\delta$  with tissue-specific modulators stimulated  $\beta$  cell survival and insulin release under conditions of sustained glucose levels as encountered in type 2 diabetes(189). Using KO rodent models of PPAR $\beta/\delta$ , has been demonstrated a positively regulation of genes related to lipoprotein metabolism and glucose utilization pathway in liver(190). Other studies reflex its

capacity to increase glucose catabolism by inducing glucose 6-phosphate dehydrogenase, inhibiting liver glucose output and suppressing fatty acid release from WAT(191). It should be noted that PPAR $\beta/\delta$ , like PPAR $\alpha$ , has the capacity to modulate inflammatory processes by inhibiting the NF-kb activity via its union to the NF-kb subunit p65 resulting in a strong anti-inflammatory role(192). Regarding lipid metabolism in liver, overexpression of PPAR $\beta/\delta$  show an increase of the *Insulin-induced gene-1 (Insig-1)*, which its encoded protein function is to stop the activation of SREBP thereby inhibiting the proteolytic processing of SREBP-1 with the subsequently suppression expression of the lipogenic genes *Fasn*, *Scd* and *Aca*(193). At the same time this research expose an upregulation of LPL by the overexpression of PPAR $\beta/\delta$  and a clearly improvement in the liver steatosis on their *db/db* mice models(193). Parallely, PPAR $\beta/\delta$  -agonist research not only led to the development of new therapeutic strategies but also to a better understanding of PPAR $\beta/\delta$  itself. In this way, treatment with PPAR $\beta/\delta$  agonists has verified the known regulation of the lipogenesis process in liver but also the capacity of enhancing FA oxidation via up-regulating *Cpt1*(194). In clinical trials with NASH patients, some PPAR $\delta$  agonists have demonstrated the ability to normalize serum insulin and TAG levels, decrease LDL levels while increasing HDL, and significantly decrease fibrotic processes(191). Unfortunately, treatment with synthetic agonists has also given contradictory results as there is a possible link between PPAR $\beta/\delta$  and carcinogenesis(195). However, the role of PPAR $\beta/\delta$  in carcinogenesis is controversial and partly unknown because there is data both demonstrating its ability to inhibit and to promote tumorigenesis. For this reason, as it happens with the other isoforms, the study of natural compounds as possible middle agonists or antagonists of the PPAR family is therapeutically relevant.

#### 1.3.4. PPAR $\gamma$

**PPAR $\gamma$**  isoform is mainly expressed in adipose tissue where it dominates the regulation of adipocyte differentiation, adipogenesis and lipid metabolism(191). PPAR $\gamma$  includes three isoforms regulated by alternative promoters with different 5' exons which results in three different mRNAs: PPAR $\gamma$ 1, PPAR $\gamma$ 2 and PPAR $\gamma$ 3. The resulting proteins of 1 and 3 are identical and expressed ubiquitously but in case of PPAR $\gamma$ 2 it contains an additional terminal region of 30 amino acids and is limited mainly to the adipose tissue(196). It is in adipose tissue where PPAR $\gamma$

aims to protect peripheral tissues from lipid excess and maintain proper functioning in homeostatic conditions. PPAR $\gamma$  activation in adipocytes ensures a balanced secretion of the main regulatory adipokines leptin and adiponectin (197).

The PPAR $\gamma$  is characterized as the master regulator of adipogenesis, because it is indispensable for adipocyte differentiation both in vitro and in vivo(198). White adipocytes are lipid-laden cells that acquire the ability to accumulate lipids. These types of cells are derived from multipotent mesenchymal stem cells (MSCs) which are first transformed into preadipocytes before suffering differentiation step to become mature adipocytes (199). This process of adipocyte origination is known as adipogenesis and involves two basic phases. First one the determination, which MSCs become preadipocyte and second one, which on the preadipocyte differentiate into a mature adipocyte capable of accumulate lipids. Adipogenesis is regulated by hundreds of factors, including nutrients, cellular signaling pathways, miRNAs and endocrine hormones like GH, GLP1, insulin, steroid hormones as well as cytokines(199). The discovery of PPAR $\gamma$  as a key regulator of adipogenesis significantly enhanced the understanding of the adipocyte and its role in metabolic diseases. For example, in a mice fat-specific PPAR $\gamma$  knockout model, the deletion result in a progressive lipodystrophy, steatosis and insulin resistance both in fat and liver(200). These observations clearly implicate defects of PPAR $\gamma$  in obesity and obesity-related pathologies. Another transcendental point was the discovery of PPAR $\gamma$  as the receptor for the insulin sensitizing drugs thiazolidinediones (TZDs) that have been described as PPAR $\gamma$  agonists. The activation of PPAR $\gamma$ -target genes results in an increase of the storage of FA in adipocytes, thus decreasing the amount of circulating ones improving metabolic outcomes such as insulin sensitivity(201). In addition, there are other associated beneficial effects such as an increase of glucose intake and a decrease on cardiac hypertrophy and systemic blood pressure(202). Unfortunately, the increase in fatty storage leads to a direct induction of weight gain especially in scWAT, being a negative side effect of TZDs treatment. Other safety problems emerged during TZDs prescriptions, include hepatic dysfunction, hypoglycemia, cardiac decompensation, bone fractures and edema(180,203,204). Thus, increased efforts have been made lately to find moderate activators of PPARs.

Obviously, there are endogenous and natural external PPAR $\gamma$  ligands with milder effects than the described TZDs. These compounds are also insulin sensitizers but without the detrimental

effects of TZDs. The list of endogenous ligands includes lipophilic species like free fatty acids, components of oxidized plasma lipoproteins, conjugated linoleic acid derivatives, products of phospholipase hydrolysis, platelet activating factors and eicosanoid derivatives(202). The main issue of this type of ligands is their intrinsically low binding affinities, which reduces the capacity to be relevant signaling mediators(205). On the other side, a large number of bioactive compounds have recently been described as potential agonists and, to a lesser extent, antagonists of PPAR $\gamma$ (206,207). This makes them an interesting object of study as they may become potent nutritional therapeutic agents against metabolic diseases such as obesity.

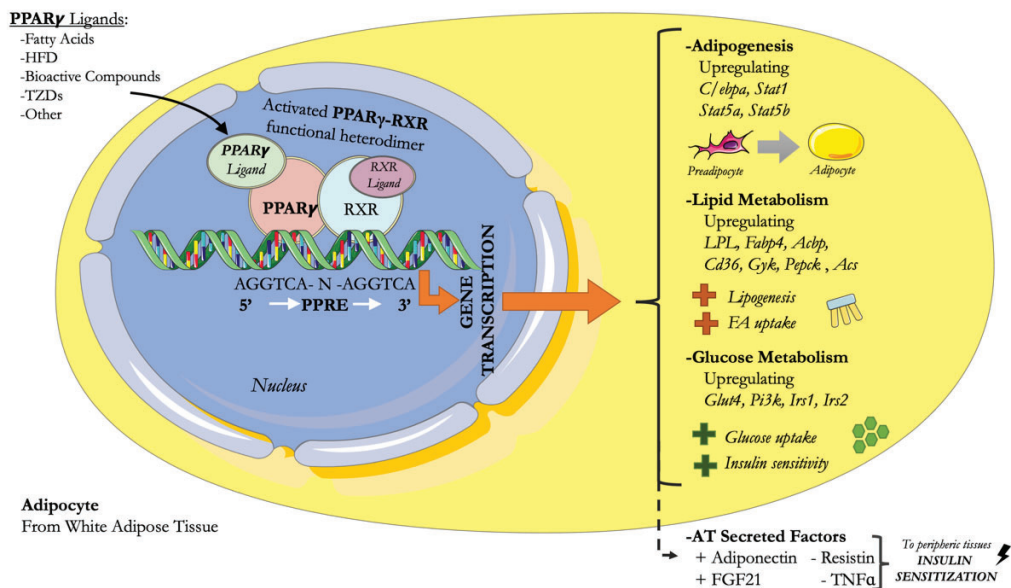


**Figure 19**–Schematic representation of PPAR $\gamma$ /RXR heterodimer binding to the PPRE and its gene transcription triggering effect of key genes on the white adipocyte. This diagram shows the PPAR $\gamma$  activation pathway and the transcriptional regulation of its target genes. When PPAR $\gamma$  is activated by ligand binding, it is able to heterodimerize with RXR and activate the target gene expression by binding to the PPRE element. The transcription of these key genes has different effects both on the adipogenesis process and on glucidic and lipidic metabolism. For example, the adipogenesis process is upregulated by the enhanced expression of *C/ebp $\alpha$* , and the signal transducers and activators of transcription genes *Stat1*, *Stat5a* and *Stat5b*. At the same time, the uptake of fatty acids is increased by the enhanced expression of genes encoding the LPL and fat transporters such as CD36 and FABP4. In turn, the gene expression of *GyK* and *Pepck* is also enhanced, thus increasing the useful intermediates for glycolysis and TAG synthesis. In case of glucidic metabolism, the glucose uptake is increased by the enhanced expression of *Glut4* as well as the insulin sensitivity by the expressed insulin receptor substrate genes *Irs1* and *Irs2*.

Focusing on the adipogenic role of PPAR $\gamma$ , one of the most important downstream effects is the activation of the CCAAT/enhancer binding protein transcription factor (C/EBP $\alpha$ )(208).

They mutually induce the expression of each other being the key adipogenic transcription factors and cooperating in the activation of adipocyte gene expression program(209). PPAR $\gamma$  besides being essential in adipogenesis and adipocyte differentiation, also is required for the proper mature adipocyte metabolic function, as revealed the finding that adipocytes only survive a few days after selective ablation of PPAR $\gamma$  in mice mature adipocytes(210).

Regarding liver, PPAR $\gamma$  hepatic expression is very low under healthy conditions but is robustly increased in rodent models suffering obesity and NAFLD(211). It has been shown that liver specific-KO animal models of PPAR $\gamma$  are resistant to the onset of HFD-induced steatosis and NAFLD(212). Since PPAR $\gamma$  upregulates genes involving lipogenesis and FA transport (such as *Aac*, *Cd36*, *Fabp4* and *Scd*), TAG synthesis (*Mgat*, *Dgat*), and lipid droplet formation (*Fsp27*, *Plin2* and *Cidea*) among others, it has been established PPAR $\gamma$  as a prosteatotic key factor in NAFLD(213). At physiological states the main role of PPAR $\gamma$  in liver is to modulate the lipogenesis pathway and the uptake of NEFAs. However, in response to a HFD, adipose tissue becomes dysfunctional and promotes a lipid overload which forces liver to act as a secondary lipidic reserve inducing the expression of adipogenic genes such as PPAR $\gamma$  that mediates an adipogenic transformation of hepatocytes(214). This driven-PPAR $\gamma$  change begins with a promotion of the expression of key genes of NEFAs transport into hepatocytes such as *Cd36* and *Fabp4*(215). Parallely, the expression of the battery genes related to hepatic DNL like *Fasn*, *Aac*, *Scd* or *Dgat* are also increased by PPAR $\gamma$ . Therefore, PPAR $\gamma$  mediates the steatosis process by promoting the lipid deposition and synthesis in liver and thus counteracting the hyperlipemia and hyperglycemia caused by the HFD consumption and the overloaded WAT. This compensatory act is not observed in liver PPAR $\gamma$ -specific KO animals, which do not develop steatosis but show a drastic increase in TAG deposition in muscle, a severe increase of circulating NEFAs and a clear IR(211,216). In the reverse direction is where PPAR $\gamma$  agonists such as TZDs come into play. The main effect of TZDs is to increase PPAR $\gamma$  activity in liver and thus decrease the number of circulating fatty acids, favoring carbohydrate oxidation in the rest of the body. Thereby decreasing IR, decreasing certain interleukins, and increasing adiponectin levels(217). Paradoxically in clinical trials with NAFLD patients treated with rosiglitazone a significative reduction in steatosis is manifested(215). However, this alleviation is caused by the effects of the agonist on adipose tissue where PPAR $\gamma$  activation promotes the expression of protective adipokines like Adiponectin and the formation of more adipocytes (increasing hyperplasia and avoiding hypertopia) which in turn prevents the deposition of excess lipids on liver(215).



Besides the explained steatotic action, PPAR $\gamma$  also plays a key role in the inflammatory and fibrotic processes in livers suffering NAFLD. In case of inflammation, it can be observed how the onset of lipid accumulation on HFD-induced NAFLD activates the resident liver macrophages, more commonly known as Kupffer cells, which in turn initiates the release of inflammatory cytokines driving to the recruitment of more immune cells encouraging the inflammatory cascade and worsening the NAFLD status(218). The induction of PPAR $\gamma$  as it happens with TZDs, exerts a counteracting role against inflammation by decreasing the number of M1 macrophages and thus achieving an anti-inflammatory effect(219). Thus, PPAR $\gamma$  activation has the capacity to modulate the inflammatory response by decreasing the number of M1 Kupffer cells and increasing M2-type. Parallely to this, PPAR $\gamma$  activation also has the ability to negatively interfere with NF-kB signaling, signaling transducers and transcriptional activators, exerting a potent anti-inflammatory role(220). Regarding fibrosis processes, in NAFLD progression growth factors like TGF $\beta$  induce the hepatic stellate cells (HSCs) which its extracellular matrix production of collagen plays a central role in fibrotic deposition. During the activation of HSCs PPAR $\gamma$  is downregulated but with the activation of PPAR $\gamma$  by agonists HSC activation is inhibited(221). This results to a reduction of alpha-actin and collagen presence, as well as reduced cell proliferation and TGF $\beta$  expression, thereby reducing the hepatic fibrosis process(221).

In summary, it can be observed that PPAR $\gamma$  has a vertebral role both in physiological and pathological states of liver due to its ability to regulate lipid metabolism by modulating lipogenesis, fatty acid uptake and the inflammatory and fibrotic responses. From this point of view, the study of agonists and antagonists that can modulate PPAR $\gamma$  activity without the pernicious consequences of TZDs seems to be a good therapeutic route against NAFLD and obesity. In this sense, bioactive compounds appear as a possible asset not only in the modulation of PPAR $\gamma$  but also of PPAR $\delta$  and PPAR $\alpha$ .

#### 1.4. Diet and Health

Diet and nutrition are major factors in promoting and maintaining good health throughout the entire life. In fact, diet is the environmental factor with the greatest impact on the expression of our genes. Its determinant role in the development of chronic NCDs but also its possible palliative power is well established on the scientific literature and therefore, they occupy a prominent



position in prevention activities. From the first governmental dietary recommendations dating back to the 18<sup>th</sup> century, through the progression of the obesogenic Western diets or the current *trending* Mediterranean diet studies, dietary patterns have always been a key on the origin but also on the proposal against pathological events. In case of Western diets containing high amounts of processed foods, red meat, high-fat dairy products, high-sugar foods, and pre-packaged foods, they have been directly associated with metabolic syndrome, obesity, NAFLD, insulin resistance and CVDs(222,223). Conversely, there have been different dietary recommendations many of them sharing certain features with powerful positive effects. A low intake of simple sugars, saturated fats, and animal proteins, along with an increase in polyunsaturated fats and vegetables intake, lead to a significant decrease in mortality risk and an improvement of health. In this way, the main modifications in the dietary proposals are related to the quantity but also to the nature of the edibles, prioritizing vegetable sources, with lower caloric value as well as higher fiber content and phytochemicals. Under these concepts there already exist different patterns coming from scientific consensus or from specific cultures and geographical areas with direct improvement effects on health. Therefore, it can be firmly established that there are dietary patterns that favor the onset or even are the origin of certain NCDs and at the same time there are dietary patterns with palliative and ameliorating effects.

#### 1.4.1. Dietary Proposals

In the current field of dietetics on NCDs, different nutritional proposals have been investigated such as Mediterranean Diet (MD), Dietary Approaches to Stop Hypertension (DASH), Mediterranean-DASH Intervention for Neurodegenerative Delay (MIND), Nordic Diet and Traditional Asian Diets, among others. In comparison with a Western diet these proposals are higher in plant-based foods, including fresh vegetables and fruits, legumes, seeds, whole grains, nuts and lower in animal-based foods, concretely on fatty and processed meats(224). Evidence from epidemiologic studies and clinical trials indicates that these types of dietary patterns reduce risks of NCDs ranging from cardiovascular disease to cancer(224). In parallel to the similarities in terms of origin and macronutrient intake, there is one repeated key factor due to their high vegetable presence, the amount and variety of bioactive compounds.

MD is probably the dietary pattern that stands out the most being one of the hot topics in the field of nutrition and biomedical research with more than 1300 related publications last year in

the NCBI-PubMed portal. Since PREDIMED (*Prevención Con Dieta Mediterranea*) study provided strong evidence of its cardioprotective effects, MD beneficial role has been investigated against different pathological states like obesity or T2DM. Better glycemic control, reduction of cardiovascular risk factors and a remission from the metabolic syndrome state have been associated with MD consumption in comparison with regular low-fat diets(225). In that sense, even if the beneficial effects are due to a synergy of the different elements of the MD, an attempt has been made to find out which compound or compounds exert a greater beneficial role. As mentioned above, the MD shares basic principles with other reference diets that could therapeutically relevant. One of these backbone elements is its content and variety of bioactive compounds. Although it is not one of the worldwide dietary patterns with the highest number of phytochemicals, the MD contains a very specific and interesting profile with compounds that have been attributed multiple beneficial effects.

#### 1.4.2. Bioactive Compounds

According to the recent published book *Bioactive Food Components Activity in Mechanistic* by Elsevier editorial, bioactive compounds are defined as molecules present in the food matrix that can produce physiological effects beyond their classical nutritional properties(226). This large compendium of molecules can be divided into two different blocks. The first would be for discerning those molecules with nutritional contribution, for example polyunsaturated fatty acids or probiotic oligosaccharides versus those that do not, such as vitamins, terpenoids, or phenolic compounds. Secondly, it would be necessary to emphasize their origin, highlighting in this case those belonging to the secondary metabolism of plants and which not.

Plants synthesize hundreds of thousands of organic compounds, which are from two main groups of metabolic pathways. The first one includes two main families, primary metabolites that are directly required for the plant growth along with the phytohormones molecules which perform a regulatory function in the plant body. The other main group are molecules from what is known as secondary metabolism, which are substances not always required for the plant basics and normally associated to the response in front of external agents such as biotic and abiotic environmental stress(227). The plant physiological processes impact on primary metabolism which in turn provides biosynthetic intermediates for the secondary metabolism(228). Albrecht

Kossel, Nobel laureate in physiology and medicine, firstly introduced the term secondary metabolite and defined them as organic substances with relative low molecular and high biological activity(227).

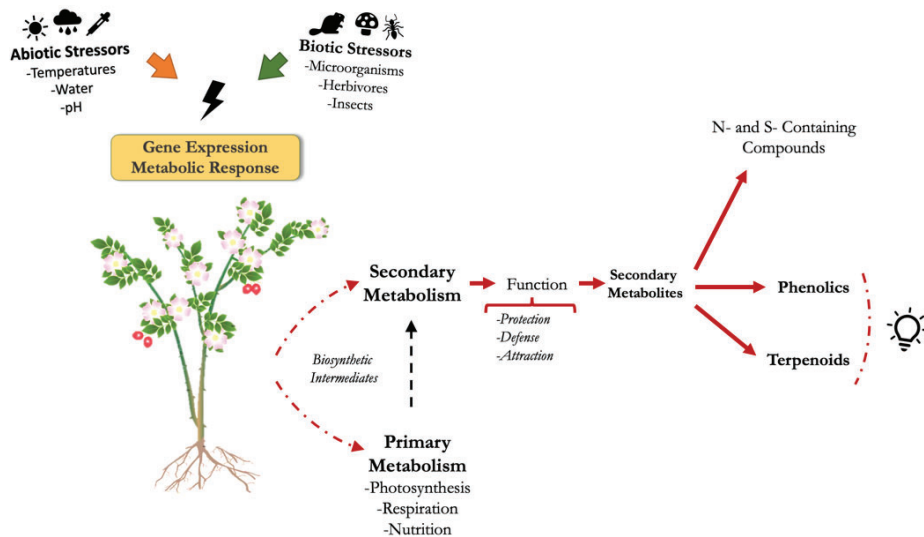


**Figure I16 – Plant secondary metabolites formation diagram.** This scheme illustrates how both biotic and abiotic agents modulate plant metabolic response. These changes influence the production of biosynthetic intermediates of the primary metabolism and therefore also modify the production of secondary metabolites. Usually these secondary metabolites have functions against external agents such as defense, attraction, or protection. As indicated, three major groups of secondary metabolites are classified, phenolic compounds, terpenoids and compounds containing nitrogen or sulfur.

There are three major classes of plant secondary metabolites (Figure I16) based on their composition and biosynthetic pathway(227). First one is the phenolic compounds group which species are composed basically of simple sugars and benzene rings. Second one is the terpene and steroid family, known as terpenoids, which spices are composed mainly of carbon and hydrogen. Finally, there are the nitrogen and sulfur containing species. Broadly, phenolic compounds and terpenoids represent a great interest due to their high protective effect, while N- and S-containing compounds have a disparity of effects. In this last group are found compounds such as alkaloids, including cocaine, nicotine, morphine, caffeine, and also poisonous species like cyanogenic glycosides and glucosinolates(229). In contrast, phenolic compounds and terpenoids have been associated with mostly positive effects.

### 1.4.2.1. Phenolic Compounds

Phenolic compounds, or more known as polyphenols, are the most prominent secondary metabolites produced by plants and they are primarily synthesized through the pentose phosphate pathway (PPP), shikimate and phenylpropanoid pathways(230). Forming species range from simple phenolic molecules to polymerized compounds both containing benzene rings with one or more hydroxyl substituents(231). Normally, these compounds are related to defense responses having antibacterial and antifungal activities, but they have also more complex roles like increase attractiveness to appeal pollinators. These polyphenols species can be distributed in different subfamilies according to the forming skeleton (*Figure I17*), finding phenolic acids, coumarins, simple and complex flavonoids, stilbenes, lignans and others like tyrosols or curcuminoids. These subfamilies contain approximately more than 8,000 identified compounds(232).

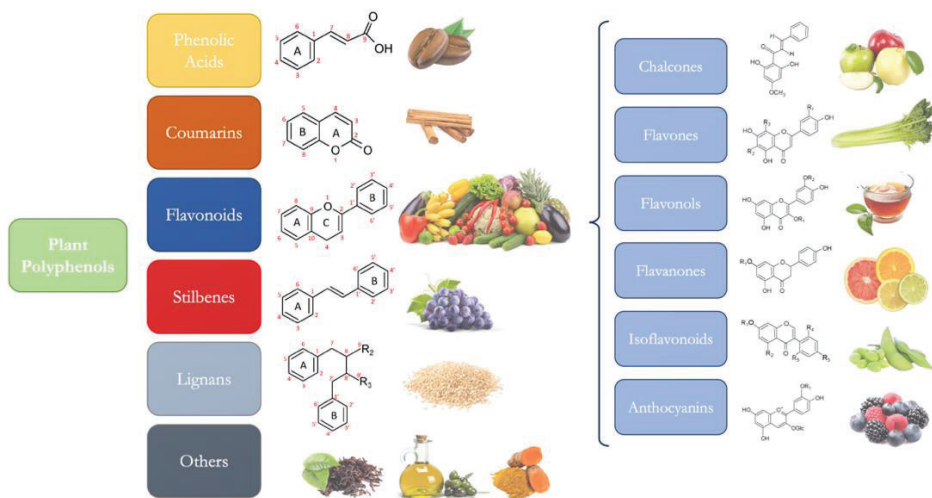


**Figure I17 – Diagram of the different forming polyphenol families, polyphenol structures and food sources.** In this scheme the 6 main groups of polyphenols are organized together with their basic structures and main plant sources. In case of flavonoids, the corresponding subfamilies with their structures and sources are also shown.

The evidence that polyphenols have a positive impact on health is growing, especially against pathological conditions such as chronic diseases. An increasing number of epidemiological, in vivo and in vitro studies, as well as meta-analyses or clinical studies support the health-enhancing role of polyphenols(233–236). These beneficial effects are based on the biological activity of polyphenols including antioxidant, anti-inflammatory, anticarcinogenic, antiviral, antidiabetic

and antiobesogenic. Primarily these effects are due to the ability of polyphenols and their metabolites to modulate multiple signalling transduction pathways involved in the pathophysiology of chronic diseases. A bibliographic review regarding the metabolic impact of the main group of polyphenols, the flavonoids, published in *Nutrients* journal and co-authored with Dr. Sandoval, is included in the annexes of this thesis proposal.

The first group of polyphenols are the phenolic acids, or phenolcarboxylic acids, which exhibit a simple structure based on an organic carboxylic acid function and a phenolic ring. Hydroxycinnamic acids and hydroxybenzoic acids are the two main forms of this subfamily but there are also other relevant species such as benzoic acids and more complex phenolic acids. Some authors also include curcuminoids in this category, although there are discrepancies, for this reason in this classification they have been placed in the group of other polyphenols. Phenolic acids are ubiquitously distributed through vegetable products but there are some foods rich in hydroxycinnamic acids and hydroxybenzoic acids like ferulic, caffeic and sinapic acids. Coffee beverage, wine, legumes, cocoa, nuts, vegetable oils, olives, herbs and spices have demonstrated elevated levels of these species (237–239). Regarding health effects, phenolic acids have demonstrated different range of benefits. The first effects described were the strong antioxidant character but more recently anticarcinogenic, antimicrobial, anti-inflammatory and significant cardioprotective effects have been demonstrated by decreasing vascular endothelial injury, fibrosis, apoptosis, and platelet aggregation (240–243). Finally, it should also be noted that phenolic acids have been described to have a great effect on the microbiota, but in this case there is still controversy about their impact since some compounds may be able to act as pro-inflammatory species (244).

The second relevant subfamily of polyphenols are the coumarins, which are characterized by being benzopyrones. The name coumarins comes from the species belonging to the *Fabaceae* family from which coumarin was first extracted (232). These species have been identified from different natural sources especially green plants but definitely the most relevant source of coumarins and derivatives is cinnamon due to coumarin biosynthesis occurring via cinnamic acid, through phenylalanine metabolism (245). As it happens on mostly polyphenol groups, coumarins exhibit wide range of effects including antimicrobial, anticoagulant, anti-inflammatory, neuroprotective, antidiabetic and antiproliferative (246). Finally, the coumarins have been recognized as a very

good platform not only for new drugs in medicinal chemistry but also in the agrochemical field as well as in the cosmetic and fragrances industry.

Regarding flavonoids group, they are probably the most relevant subfamily with the largest number of components and ubiquitously present. The basic structure of flavonoids consists of two phenyl rings and one heterocyclic ring. As indicated above, a literature review was performed on the effect of flavonoids mainly in the pathogenic context of obesity included on the annexes(247).

The stilbenes group is another remarkable subfamily of polyphenols and is characterized by its simple basis structure having a C6-C2-C6 skeleton, usually with two isomeric forms(248). The origin of stilbenes has been linked to one of the plant defense mechanisms against infections and UV radiation(249). One of the main known sources of stilbenes, specifically resveratrol, is grape and grape derivatives, although other foods such as peanuts, bilberries, blueberries, and cranberries, are described as a rich source, being Paonia plant the highest resveratrol source(250). Besides to their role on the defense plant system, stilbenes have demonstrated a wide range of pharmacological and biological activities(251). Recently a extensive bibliographic review was published about stilbenes on health, finding more than 100 studied compounds with ranging effects from anticancer, antimicrobial anti-osteoporosis, antidiabetic, neuroprotective, antifatigue, anti-aging, cardioprotective, anti-obesity, antioxidant, anti-inflammatory, and anti-atherosclerosis(248).

The polyphenols called lignans, are diphenolic compounds derived from the shikimic acid biosynthetic pathway being a combination of two phenylpropanoid C6–C3 units which can be linked to additional ether, lactone, or carbon bonds(252). Lignans have a great disparity of species due to the multiple structures possible found in nature and their biological also cover a wide range of functional properties. Linseed (*Linum usitatissimum*) is one of the richest sources of lignans followed by other seeds like sesame or cereals and legumes(253). Some of the notable species within the lignan group are secoisolariciresinol, lariciresinol, matairesinol, pinoresinol, medioresinol, and syringaresinol(252). Although they have multiple benefits associated with their consumption, there is not as much scientific literature on the effects of lignans compared to the other polyphenol subgroups. Even so, they have been described as having antiestrogenic, antiangiogenic, antioxidant mechanisms, and thus chemopreventive properties(254). On the

other hand, studies have also shown cardioprotective properties through its anti-inflammatory and antioxidant effect, as well as its lipid lowering role(255).

In addition, there are the remaining subcategories that are usually classified as other polyphenols. Even so, there are multiple types of categorizations and differences between authors. In the above classification, two subgroups stand out in the category of other polyphenols, the first would be the curcuminoids and the second would be the phenylethanoids or better known as tyrosols. Curcuminoids are sometimes grouped in the subfamily of phenolic acids although since their structure is based on a linear diarylheptanoid and not on an organic carboxylic acid function and a phenolic ring, some authors attribute a subfamily of their own. The main species are curcumin, demethoxycurcumin, bisdemethoxycurcumin, and also some of their derivative metabolites(256). These compounds are found mainly in the rhizomes of plants of the genus *Curcuma*, being the turmeric (*Curcuma longa*) the main source. Given the strong yellowish color associated with them and their characteristic taste, these rhizomes containing curcuminoids have been used extensively throughout history in both gastronomy and industry. In addition, their associated medicinal properties have also made their use date back to ancient times in the regions where they grow. Curcuminoids are probably one of the earliest known and tested groups of polyphenols, with clinical studies with curcumin dating back to the beginning of the 20th century(257). This fact has led to curcuminoids being studied for a long time and proving their multiple beneficial effects not only reduced to folkloric medicine. One of the first therapeutic attributions of curcuminoids, particularly curcumin, is its high antioxidant and anti-inflammatory power, being able to modulate key factors as the cyclooxygenase-2 (COX-2), the lipoxygenase (LOX) and the Nf-kB but also the advanced glycation end products (AGE), and the advanced lipoperoxidation end products (ALE)(258). This great anti-inflammatory power of curcuminoids has been demonstrated both in multiple inflammatory diseases. In fact an extensive review article collecting positive results on clinical trials over more than 30 pathologies, ranging from cancer, cardiovascular diseases, diabetes, renal diseases, to specific ones like prostatitis, lupus, arthritis was published recently(259). Another large group of diseases that improve with curcuminoid treatments are neurodegenerative diseases due to their inflammatory and oxidative nature. Preclinical and clinical studies have shown therapeutic efficacy of curcuminoids against Alzheimer's disease (AD), Parkinson's disease (PD), and amyotrophic lateral sclerosis (ALS), through the modulation of different metabolic pathways like the Akt/Nrf2 one(260). Specifically in Alzheimer's

disease, different biological activities implying different pathways with diverse efficacy and potency have been observed among the curcuminoid species treatments(261). In addition, a synergistic and cumulative effect was observed between its different constituents.

Finally tyrosols, or also named phenylethanoids, are a small as well as the most representative phenolic group of olive fruits and olive oil, where they occur as such, or in the form of esters of the secoiridoid elenolic acid(262). In some of the polyphenol family distributions, tyrosols are not categorized as a single subfamily, in this thesis proposal it has been decided to expose them as an independent group due to their relevance both on Mediterranean diet and at clinical relevance. The main characteristic of these compounds is the presence of a phenethyl alcohol structure consisting of a phenethyl group ( $C_6H_5CH_2CH_2$ ) attached to OH. In parallel, these compounds are also closely related to an independent group of more complex coumarins derivatives, known as secoiridoids whose presence is exclusive to the botanical family of *Oleaceae* where it is found the olive tree. Among these secoiridoids, three key compounds stand out: olacein, oleocanthal and oleopeurin. Unlike tyrosols, there are still few referential studies of their bioavailability and effects, although there is growing interest and positive results are increasing exponentially(263). Regarding specifically the phenylethanoids, the tyrosol and hydroxytyrosol are the most noteworthy species. Like other polyphenols, the first described effects were the antioxidant and anti-inflammatory capacity of both species and derivatives(264,265). Hydroxytyrosol for example, has shown to exert a wide range of biological effects like cardioprotective, anticancer, neuroprotective, antimicrobial, beneficial endocrine as well as other positive effects but the exact molecular mechanisms underlying these actions are yet to be fully clarified(266–271). In addition, tyrosol stands out as one of the most stable polyphenols compared to more active flavonoids, being less susceptible to auto-oxidation and thus having a greater capacity to maintain its antioxidant role in critical situations(266). For example, it has been observed that in presence of oxidized-LDL, when autooxidation is already present, tyrosol does not alter its antioxidant activity, while other more potent polyphenols significantly decrease their antioxidant role and may even act as pro-oxidants(272). In addition to its ability to decrease oxidative damage due to its high antioxidant stability, tyrosol is also able to drastically reduce the inflammatory response by modulating cluster of differentiation 14 (CD14) up-regulation(273,274). This may be one of the multiple mechanisms by which tyrosol exert its beneficial effects against hypertension, atherosclerosis, coronary heart disease, chronic heart failure, insulin resistance and obe-



sity. There are multiple studies that reinforce the protective effects of both tyrosol and hydroxytyrosol, and it should also be noted that both polyphenols have been subject of research for some time, being together with different flavonoids, probably the earliest bioactive compounds to be studied.

#### 1.4.2.2. Terpenoids

Terpenoids, also known as isoprenoids or terpenes, stand out for being the most numerous and structurally diverse group of secondary metabolites(275). Over 60.000 terpenoid structures have been identified, making them the largest bioactive compound class from natural sources(276). One of the relevant characteristics of terpenoids is their generally lipophilic nature as opposed to the hydrophilic character of polyphenols. This fact considerably changes the bioavailability and absorption of terpenoids. These species come from the mevalonate pathway in plant sources, while some terpenoids can be also found on marine organisms(277). In this thesis proposal, the term terpenoid and terpene have been used as synonyms, since their use in the scientific literature is widespread. Even so, there are authors who differ and distinguish the two groups, defining terpenes as simple hydrocarbons and terpenoids as modified terpenes containing a functional group and oxidized methyl groups(278). Due to their structural diversity, terpenoids have a simple unifying feature which is referred as the isoprene rule: all terpenes must have a fundamental repeating five-carbon isoprene unit(279). Therefore terpenoids are classified as hemiterpenes ( $C_5$ ), monoterpenes ( $C_{10}$ ), sesquiterpenes ( $C_{15}$ ), diterpenes ( $C_{20}$ ), sesterterpenes ( $C_{25}$ ), triterpenes ( $C_{30}$ ), and tetraterpenes/carotenoids ( $C_{40}$ )(275). Like polyphenols and other secondary metabolites, terpenoids are major mediators of plant ecological interactions. For example, they play a key role in defense against herbivores, disease resistance, attraction of mutualists such as pollinators but in their case they stand out as being powerful communicators among plants(280).

Regarding the applications of these compounds, the first subfamily, the monoterpenes, are characterized for being highly present in essential oils and distinguished for presenting a strong aroma(278). This makes them widely used in the pharmaceutical industry both in perfumery and cosmetics. In that way, this characteristic feature has identified monoterpenes as key actors of the complex plant ecosystem, being fundamental for the interaction with microorganisms, pollinators, or other plants(281). Therefore, most monoterpenes have a high biological activity. The

first biological property that emerges from monoterpenes is their high antioxidant capacity. This fact has been demonstrated both *in vitro* and *in vivo*. It has been described that, many of them mechanistically link their antioxidant effect to their ability not only to regulate endogenous sources of ROS and the defense system, but also to modify certain metabolic pathways responsible for regulating the antioxidant enzymes and the detoxifying processes such as Nrf2(281).

The second subfamily, the sesquiterpenes, are colorless, volatile, and also distinguished for being strong lipophilic compounds. Like so many other subfamilies of terpenes, sesquiterpenes have attracted a significant interest due to its protective role on the biological systems. One of the distinctive features of the sesquiterpene group is the large number of different species that have been identified. They biosynthesis and great diversity in plants come from the assembly of the 15-carbon skeleton and the layering of functional groups and substituents upon the structural scaffolds in distinct regions and stereospecific manners occurring via farnesyl pyrophosphate pathway, in the cell plant ER(282). The principal function of these compounds is to protect the plant against stressful environmental conditions, whether biotic or abiotic(283). One of the main consequences of stress on the plant is the accumulation of ROS, whose presence is ultimately deleterious to the vegetables. Interestingly, sesquiterpenes synthesized in response to this stress, can quench ROS by reacting with the unsaturated sesquiterpene hydrocarbon skeleton and thereby can serve as a potent antioxidant in plant protection(284). It is probably for this reason that one of the first reported effects of sesquiterpenes is their strong ability to inhibit inflammatory processes in humans. Targeting specific components of the nuclear NF- $\kappa$ B signaling pathway and nitric oxide generation as well as its capacity to inhibit the maturation and function of mast cells, monocytes and dendritic cells which are directly correlated to the inflammation regulation, are some of the described anti-inflammatory mechanisms of sesquiterpenes in humans(285). It should be noted that these compounds have not only been attributed anti-inflammatory capacity, further research has shown their ability to reduce tumorigenesis and some of the species are even being used against pathologies caused by parasites such as malaria due to their great antimicrobial power(284,286).

On the other hand, diterpenes are the third subfamily of terpenoids and they are defined by the molecular formula  $C_{20}H_{32}$ . Just as it happens with the other subgroups, diterpenes exhibit high biological activity for both plants and the organisms that consume them(287). Thousands of diterpenes have been described from plants, insects, and marine organisms but only few have

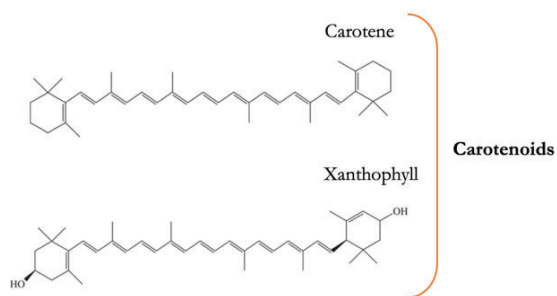
been proved and described as clinically effective. Besides the already described antioxidant and anti-inflammatory capacity characteristic of terpenoids, some of the diterpenes such as taxol or abietane derivatives have been used in therapies against ovarian, breast and lung cancers with very positive results for more than twenty years(288). On the other side, diterpenes derived from *Ginkgo* vegetal species, have shown a selective activity against toward platelet-activating factor increased in pathological conditions such as burns, ulceration, and inflammation skin diseases(289). In addition, there are many more species with other interesting effects such as the vanilloid resiniferatoxin that demonstrated potent restorative effects in clinical trials involving diabetic nephropathy(289)(290).

Unlike the previous terpenoid subfamilies, sesterterpenes have been found to a greater extent in aquatic organisms and fungi. In fact, their discovery and valorization are more recent than the other subgroups(291). In contrast, triterpenes, the penultimate terpenoid subgroup, are widely present in plants, fungi, animals, but also marine organisms. Triterpenes are defined with three or six isoprene units resulting on the formula  $C_{30}H_{48}$  which includes steroids and sterols with squalene being the biological precursor base(292). Triterpenoids, as the other terpenoids, can be found in a free state and in combination with sugars forming what is called glycosides. Within the glycosylated forms we find the saponins, which contain a sugar moiety (glycone) and a triterpenoid component (aglycone)(292). This form of triterpenoids stands out, firstly because are generally water soluble and characterized by their strong foam-forming and surfactant properties in aqueous solution (hence the name saponin, *sapo-* means soap in Latin)(293). Secondly, because they have a high structural and bioactive diversity which have become on the spotlight in the treatments of several chronic diseases. As compiled in different bibliographical reviews, there are multiple studies that report the ability of saponins, as well as other similar triterpenoids, to inhibit cancer formation and its progression by modulating multiple signalling pathways related to cellular proliferation, apoptosis, autophagy, metastasis, angiogenesis, inflammation, oxidative stress, cancer stem cells and microRNAs(293–296). Apart from being prominent in cancer treatments, triterpenoid glucosides have also been emerged as a possible treatment for diabetes, not only due to their ability to alter multiple metabolic pathways directly related to diabetes, but also for their ability to alleviate the damage caused by the pathology, such as the diabetic retinopathy, neuropathy or nephropathy(297–300). Against obesity, triterpenoids have also shown powerful effects involving many biochemical mechanisms. Species such as ursolic acid, oleanolic acid, among others, have shown anti-obesogenic effects, although the most successful

in vivo studies are those which used triterpenoid-rich extracts, not single compounds(301–303). As mentioned above, the metabolic pathways that could be modulated by these compounds are not fully described, but there are already some publications that propose the modulation of some key transcription factors like PPARs as possible underlying mechanisms(304–306).

Finally, the carotenoid subfamily is the most prominent tetraterpene group. It shares the basic molecular formula  $C_{40}H_{56}$  with a long carbon-chain rich in conjugated double bonds that makes them very hydrophobic and extremely difficult to isolate and purify(287). Carotenoids are natural pigments synthesized by autotroph organisms and some of them are precursors of vitamin A(307). In plants, carotenoids are closely related to the photosynthetic process and also to the protection against photo-damage absorbing wavelengths between 400 and 550 nanometers, and hence presenting red, orange or yellow colors(308). Regarding classification, there are two subgroups of carotenoids according to their chemical structure. First one, xanthophylls stand out for being oxygenated derivatives, while the second subgroup carotenes, are only carotenoid hydrocarbons (*Fig I18*)(309).

**Figure I18 – Diagram showing the two subgroups constituting the carotenoid category, the carotenes and the xanthophylls.** There are two major differences between groups, the first one, they show different ranges of colors at macroscopic level, being the carotenes more orange while the xanthophylls are more yellowish. This is because they absorb different wavelengths of light during the photosynthesis process. At micro level, the difference lies in their structure, xanthophylls contain oxygen, while carotenes are hydrocarbons and do not contain oxygen.



Approximately 600 carotenoids have been identified in nature but just around 50 have been identified in a standard human diet(309). They are the most frequently consumed liposoluble bioactive compound up rising an intake of several mg/d(310). As mentioned above, some carotenoids stand out for being precursors of vitamin A and for this reason, they have been subject to multiple studies, both at epidemiological, nutritional, and biochemical level. The enzyme  $\beta$ -carotene 15,15'-dioxygenase, encoded in humans by the *Bco1* gene, is the responsible of catalyzing the central cleavage of certain carotenoids to retinoids, thus converting pro-vitamin A to vitamin A species(311). This reaction is highly relevant, and it has been demonstrated that its

alteration can cause firstly a decrease on carotenoid plasma levels and thereby changing the ability to resist oxidative stress(312). In addition to their importance on vitamin A metabolism, carotenoids have demonstrated different beneficial roles, firstly as a potent antioxidants by quenching liposoluble radicals as well as singlet oxygen and peroxide radicals(313). At the same time, carotenoids can act as antioxidants indirectly by activating the gene expression of the body's own antioxidant defense system *Superoxide-dismutase (Sod)*, *Catalase (Cat)*, and *Glutathione-peroxidase, (GPX)*(314). However, negative effects have also been reported to carotenoids. Negative associations have been seen especially in studies with non-healthy subjects either in studies with smokers or in studies with high doses of carotenoids reporting DNA damage(314,315). However, there have been seen a distinction between direct pro-vitamin A carotenoids, and effects of non-vitamin A carotenoids. The non-vitamin A carotenoid group are almost invariably reported to protect against DNA damage while the pro-vitamin A carotenoids show a more varied spectrum sometimes protecting, sometimes enhancing DNA damage, but there are still gaps to fill(315). Back to the positive effects, carotenoids, and especially their metabolites, have shown the ability to interact with different nuclear receptors. First, interacting with the known RAR/RXR (retinoic acid receptor/retinoid X receptor) and also the RXR/PPARs through which they have been observed to exert immune-modulating effects but also other interesting anti-obesity roles such as the ability to regulate adipocyte differentiation, lipid metabolism, oxidative stress and the production of inflammatory signaling(316,317). In the case of inflammatory processes, it has been observed that more polar metabolites are able to interact with NF- $\kappa$ B, inhibiting its translocation to the nucleus and thus decreasing the expression of genes related to the inflammatory response and the expression of cytokines such as TNF- $\alpha$ (318,319). Also, it has been demonstrated the ability of certain carotenoids and their metabolites to foster the translocation of Nrf-2 to the nucleus thus stimulating the expression of antioxidant enzymes such as *Cat* or *Sod* and thereby lowering lipid peroxidation markers like MDA(319,320).

#### 1.4.2.3. *Rosa canina*

*Rosa canina* is one of the main species of the Rosaceae family that grows extensively in European mountainous zones like the Pyrenees but can also be found in northeast Africa and certain Asian zones. *Rosa canina* was first described as a medicinal plant by Pliny the Elder (23-79 BC), who discovered its use among French tribes for the treatment of dog bites, thereby this description generated the name of the specie(321). Also known as rosehip, as a reference to its fruit, *Rosa*

*canina* is characterized as a thorny perennial shrub with an identifying reddish fang-shaped pseudo-fruit (Fig I19) which has been used as a traditional and folklore remedy since ancient times due its medicinal properties(322). This type of aggregated pseudo-fruits, no unique to *Rosa canina* specie, consist of several achenes enclosed by an enlarged, red, fleshy floral cups, containing a large and varied number of micronutrients and bioactive compounds(323). Other Rosaceae species also present this type of fruit but *Rosa canina* present a larger amount of bibliography, more reported medicinal effects according to popular knowledge and, as will be discussed later, more concentration of certain bioactive compounds(324).



**Figure I19 – Images showing the false pyriform red-orange fruits called rosehip from the *Rosa canina*.** Commonly in areas of the Catalan Pyrenees, the fruit is known as *gratacul*, and in other areas of the Iberian Peninsula as *escaramujo*. The image on the right side shows the inside of the fruit cut longitudinally, where the fleshy area called hypanthium and the achenes containing the prismatic seeds can be seen. Image from Giuseppe Mazza of Monaco Nature Encyclopedia©.

Rosehips from *Rosa canina* contain vast and high diverse number of bioactive compounds. This rich and varied profile of compounds is related to the harsh climatic conditions from the areas where it grows and due the nature of its pseudo-fruit, since a great part of the fruit is formed by seeds (achenes) containing oils and therefore more liposoluble species, but also by a fleshy part (hypanthium) with more hydrophilic species(324). These two conditions favor not only the presence of many secondary metabolites in the fruit, but also a great variety from high hydrophilic to high liposoluble species, which makes *Rosa canina* truly interesting to study. Regarding phenolic compounds, there are different *Rosa canina* identifications in the bibliography describing many polyphenols, mainly flavonoids and from these, distinguishing flavonols subfamily(325–328). The flavonols are highlighted in *Rosa canina* for two main reasons: first one because they are the most concentrated phenolic compounds, especially species such as hyperoside, rutin, astragalol, tiliroside, quercetin and kaempferol; and secondly because there are studies reporting the effect of the flavonol tiliroside from *Rosa canina* as the main anti-obesogenic and anti-diabetic agent(329–331). At the same time, flavanols (catechin and epicatechin), flavanonols (taxifolin), flavanones (eriodictiol and isosakuranetin), isoflavones (genistein), but also other polyphenols like hydroxybenzoic acids (gallic acid, syringic acid and protocatechuic acid), hydroxycinnamic acids (caf-

feic acid and p-coumaric acid) and the chlorogenic acid are also present in significant concentrations (325). Apart from phenolic compounds, the literature also reports a high presence of terpenoids, particularly triterpenoids and carotenoids, that gives the fruit its orangish color (332,333). In the case of carotenoids, chromatographic studies (TLC and HPLC) on *Rosa canina* rosehips extractions have reported that the major species are  $\beta$ -carotene, lycopene, rubixanthin, lutein and zeaxanthin, all of them with demonstrated high biological activity(334). Finally, a significant presence of galactolipids, PUFAs, fiber and vitamins, both hydro-soluble and lipo-soluble, has also been described(324). Overall, the large number of bioactive compounds identified in *Rosa canina* have been reported to have multiple therapeutic properties, especially against chronic diseases, as explained above in the introduction. However, many of the pathways involved in these beneficial effects are still unknown.

OBJECTIVES





## 2. Objectives

The main objective of this thesis proposal is to evaluate the preventive effects and the molecular mechanisms of dietary supplementation with bioactive compounds against the pernicious action of a high fat diet and its induction of obesity, T2DM and NAFLD.

Three secondary aims are derived from the central objective:

- a) Study of the effects and molecular mechanisms underlying a pure, isolated polyphenol mixture supplementation against a high fat diet-induced obesity and NAFLD.
- b) Study of the effects and molecular mechanisms underlying a rich natural source of bioactive compounds, concretely *Rosa canina* flesh supplementation, against a high fat diet-induced obesity and NAFLD.
- c) Characterization of the different *Rosa canina* flesh fractions and study of the anti-obesogenic mechanisms underlying their different constituents.



METHODOLOGY



### **3. Methodology**

#### **3.1. Cell Culture**

In order to achieve the objectives set for this thesis proposal, a specific combination of materials and methodologies were employed. First, in the case of cell cultures, two specific types of secondary lines were used. Basically, a specific human liver cell model, the HepG2, and a mouse model of white adipose tissue, the 3T3L1. Both were purchased from the ATCC (American Type Culture Collection, Rockville, MD, USA) and their specific protocols for maintenance and proper care were followed.

#### **HepG2 – *Homo sapiens* Liver Carcinoma Cell Line (ATCC No. HB-8065)**

The HepG2 cell line exhibits epithelial-like morphology growing as monolayers in small aggregates. This cell line was firstly isolated from a hepatocellular carcinoma of a 15-year-old youth male with liver cancer by researchers at Wistar Institute (USA) on the 1980s and were entered into the ATCC repository as a human cell line (HB 8065). In this thesis proposal, the Hepg2 cell line was used both for transfection and for the NAFLD modelling. The suitable conditions tested for Hepg2 cells are firstly Eagle's Minimum Essential Medium (EMEM) supplemented with 10% (v/v) of Fetal Bovine Serum (FBS), 4mM of glutamine, 1x of non-essential amino acids, 100 units/ml of penicillin G, 100ug/ml of streptomycin sulfate and pH adjusted with sodium bicarbonate (7.0 to 7.6). Culture medium must be discarded and changed thrice a week. Regarding incubation, the optimal conditions are 37°C with 5% of CO<sub>2</sub> and saturated humidity. For sub-culture, cells at 80-90% of confluence were briefly rinsed twice with 1x PBS to remove all traces of serum that contains trypsin inhibitors. For trypsinization, 0.05% Trypsin-EDTA solution was added and incubated at least 5 minutes at 37°C. Once cell layer was dispersed, cells were resuspended in fresh growth medium and then split in a 1:2-1:4 dilution. The culture plates used for Hepg2 maintenance were 75 cm<sup>2</sup> T-flasks and for experimental procedures 24, 48 and 96 multi-wells.

Regarding steatosis induction in Hepg2, different protocols were tested. The protocol set up was initially based on the positive results of Dr. Matteo Ricchi et al studies, which compared PA and OA in different concentrations and cultures(335). The conclusion of this study was that induction with OA in hepatocytes produced greater steatosis but less associated apoptosis than with PA. Thus, a protocol was developed testing different concentrations of OA following also

other published studies. HepG2 cells were firstly seeded at  $5 \times 10^5$  cells/ml. After 24 hours of incubation under optimal conditions ( $37^\circ\text{C}$  with 5% of  $\text{CO}_2$  and saturated humidity), the maintenance culture medium was removed, and fresh medium was added with either 0.5mM OA or 0.25mM BSA. Since the OA used (Sigma ref. O3008) is complexed with bovine serum albumin (BSA) at a molar ratio of 2:1, a concentration of 0.25mM was used in negative controls. Parallel to the addition of OA and BSA, *Rosa canina* extracts were also added in the corresponding concentrations when indicated. Since the extracts were in a DMSO as vehicle, DMSO was also added to the control cells group. The extracts stock solutions were at of 10 mg/ml and therefore in any case the DMSO in cells exceeded 5%.

#### 3T3L1 – *Mus musculus* Embryo Cell Line (ATCC No. CL-173)

3T3L1 cells are a standard fibroblast cell line derived from the embryo tissue of a Swiss albino mice and developed through clonal isolation. The 3T3 cell line, abbreviation from label 3-day transfer inoculum  $3 \times 10^5$  cells referring to the used protocol, was originally established in 1962 by two scientist at New York University School of Medicine. 3T3L1 cells have a fibroblast-like morphology but are known as pre-adipocytes due to the capacity, under appropriate conditions, to differentiate into adipocytes. This cell line has not only been used for transfection but also for the study of basic cellular mechanisms associated with diabetes, obesity, and related disorders. The suitable conditions for 3T3L1 cell line growing and maintenance are Dulbecco's Modified Eagle's Medium (DMEM) supplemented with 10% (v/v) of Fetal Bovine Serum (FBS) (on experimental procedures) and Calf Serum (CS) (on maintenance), 4mM of glutamine, 100 units/ml of penicillin G, 100ug/ml of streptomycin sulfate and pH adjusted with sodium bicarbonate (7.0 to 7.6). Culture medium must be discarded and changed thrice a week. Regarding incubation, the optimal conditions are  $37^\circ\text{C}$  with 5% of  $\text{CO}_2$  and saturated humidity. For sub-culture, cells at 70-90% of confluence were briefly rinsed twice with 1x PBS to remove all traces of serum that contains trypsin inhibitors. For trypsinization, 0.05% Trypsin-EDTA solution was added and incubated about 5 minutes at  $37^\circ\text{C}$ . Once cell layer was dispersed, cells were resuspended in fresh growth medium, and then split in a 1:3 dilution. The culture plates used for 3T3L1 maintenance were  $75 \text{ cm}^2$  T-flasks and for experimental procedures 12, 24, and 48 multi-wells plates.

### 3T3L1 Differentiation

Regarding 3T3L1 differentiation, the Katarzyna Kowalska et al. protocol was used(227). 3T3L1 cells were seeded at  $5 \times 10^4$  cell/ml on multi-well plates to confluence. Two days post-confluence, the 3T3L1 pre-adipocytes were stimulated by a differentiation cocktail containing 0.25uM dexamethasone (DEX), 10uM rosiglitazone and  $1 \mu\text{M}$  insulin using the previous explained supplemented growth media. The nutritional treatments with *Rosa canina* fractionations were applied filter-sterilized at different concentrations simultaneously to the differentiation mix. Since the *Rosa canina* extractions tested on the cell cultures were in DMSO as vehicle, in the control points DMSO was added both with and without differentiating mix. After two days of differentiation, medium was replaced with DMEM/10% FBS  $1 \mu\text{M}$  insulin growth media. Cultures were incubated 2 more day and medium was replaced with the standard DMEM/10% FBS growth media.

### Cell Culture Reagents

The following reagents were used during the different assays involving cell cultures:

<i>Reagent</i>	<i>Company</i>	<i>Reference</i>	<i>Process</i>
Dulbecco's Modified Eagle's Medium (DMEM)	Gibco	12100-061	Culture Medium
Eagle's Minimal Essential Medium (EMEM)	Gibco	61100-087	Culture Medium
Fetal Bovine Serum (FBS)	Gibco	10270-106	Culture Medium
Penicillin-Streptomycin-Glutamine 100x	Gibco	10278-016	Culture Medium
Sodium Bicarbonate Solution 7.5%	Sigma	S8761	Culture Medium
Trypsin-EDTA	Gibco	15400-054	Culture Medium
3-Isobutyl-1-methylxanthine (IBMX)	Sigma	I5879	3T3L1 Differentiation
Dexamethasone	Sigma	D2915	3T3L1 Differentiation
Rosiglitazone	Sigma	R2408	3T3L1 Diff. and PPAR Assay
OPTI-MEM	Gibco	31985-047	HepG2 Transfection
Lipofectamine 2000	Invitrogen	11668027	HepG2 Transfection
Dimethyl sulfoxide (DMSO)	Panreac	A7248	Freezing and Cell Treatments

### 3.2. Oil Red Quantification

Oil Red O (ORO) is a fat-soluble dye used for staining different types of lipids. This staining is usually used prior to optical microscopic analyses as it enables to identify the lipid vacuoles of different tissues and cell cultures. In addition, ORO staining can provide semi-quantitative data on the amount of total lipids using regular spectrophotometry. Thus, this type of staining is very



useful due to its low cost on adiposity studies with cell cultures or histological sections. In the experimental processes of this thesis proposal, ORO staining has been used for both microscopic and semiquantitative lipid analysis. It has been mainly used in cultures of differentiated 3T3L1 adipocytes and in a HepG2-induced NAFLD cell culture model.

Two different types of ORO solutions were used to prepare the staining. The first was the stock solution, which was made by using Oil Red O reagent (Sigma ref. O0625) at 3mg/ml concentration in isopropanol and then allowed to stand for half an hour before being filtered through a filter paper (8-11 $\mu$ m pore). The second ORO solution, the working solution, was prepared from 3 parts of the stock solution and 2 parts of milli-Q water and filtered on 0,2 $\mu$ m syringe filter following the protocol established by Biovision in its ORO kit (K580-24). Prior to staining with working ORO solution, the cultures were first washed twice with PBS1x and fixed with formalin (Thermo Scientific ref.5701) for half an hour in gentle rotation. Once the cells were fixed, they were washed with milli-Q water twice and a 60% solution of isopropanol was added for 5 minutes. Once acclimated, the isopropanol solution was removed, and the working ORO solution was applied and incubated in gentle rotation for 20 minutes. Then, cells were washed 5 times with milli-Q water until the ORO excess was removed. At this point the lipid droplets were evident in a reddish color so cultures were visually analyzed by an optical microscope. To perform the semiquantitative analysis, starting from the previous step, 100% isopropanol was applied to obtain the dye from the inside of the vacuoles and its absorbance was read at 492nm by spectrophotometry on the Thermo Scientific™ Varioskan™ LUX multimode microplate reader. 100% isopropanol was used as background control. In case of 3T3L1 culture, this protocol was used with 24- and 48-well plates, whereas in Hepg2 cell culture, 96-well plates were used. All experiments performed with the ORO staining technique were repeated a minimum of three times and had a minimum of 8 replicates for each group.

### 3.3. Luciferase Reporter Assay

The luciferase assay is a very sensitive and convenient technique for analyzing the transcriptional activity of a specific gene. This type of assay examine whether a protein can activate or repress the expression of a target gene using luciferase as a reporter protein(336). In case of this thesis proposal, this technique has been used to study the possible ability of *Rosa canina* fractions to modulate PPAR gamma isoform activity. HepG2 cells were transfected with Lipofectamine

2000 kit (Invitrogen ref. 11668027) in 48 well-plates according to the manufacturer instructions (ratio 1:2,5 Lipofectaine:DNA). 24h before the transfection cell were seed at a density of  $5 \times 10^5$  cell/mL. To perform the luciferase reporter assay a 3xPPRETKluc reporter plasmid (includes 3 direct copies of the APoII PPRE) (2 ng/ $\mu$ L) (kindly provided by Dr. Villarroya's Lab) was co-transfected with the expression vectors of PPARg (pSV-SPORT-PPARg) and RXR $\alpha$  (pCDM8-RXR $\alpha$ ) (0.4 ng/ $\mu$ L each). The pRL-CMV vector (Promega, ref. E2261) (0.04 ng/ $\mu$ L) was used as an internal transfection control. Transfected cells were treated with *Rosa canina* or its fractions as indicated.

To analyze the luciferase activity the cells transfected, after the appropriate incubation times, were lysed with 200  $\mu$ L/per 48-well plates of a commercial passive lysis buffer (Passive Lysis Buffer, Promega, ref. E1941). The cell extracts obtained were assayed with the commercial kit Dual-Luciferase™ Reporter Assay System (Promega ref. E1910), following the instructions of the manufacturer. In general, 10 $\mu$ L of cell extract was incubated with 20 $\mu$ L of each of the reagents. The luciferase values of *Photinus pyralis* (representative of the activity of the promoter) and of *Renilla reniformis* (transfection internal control used to normalize the values of the former) were thus obtained. Luminescence measurements were performed on a Berthold Detection System Sirius luminometer.

#### *DNA's used on the Luciferase Assay*

Reporter Gene Construct	pPPRE3x-tk-Luc: <b>2 ng/<math>\mu</math>L</b>
Eukaryotic Expression Vector	pCDM8-RXR $\alpha$ : <b>0.4 ng/<math>\mu</math>L</b>
Internal Transfection Control	pRL-CMV: <b>0.04 ng/<math>\mu</math>L</b>
PPARg	pSV-SPORT-PPARg: <b>0.4 ng/<math>\mu</math>L</b>

### 3.4. Gene Expression Analyses

RNA expression analysis provides insight into the regulation of expression and stability of the RNA species under examination and can be extrapolated to the understanding of protein regulation derived from its RNA. Although proteins are effectors, RNA is a blueprint. Therefore this extrapolation should be done with care. As with any template, the existence of the template does not prove that the material for which it codes has been produced and, conversely, failure

to detect the template does not mean that the protein is not present(337). Nevertheless, RNA-based gene expression analysis provides a great advantage in terms of speed, reliability, and cost. In addition, the mapping of metabolic movements provided by these analyses gives us a better understanding of both pathological processes and their possible treatments.

#### 3.4.1. Total RNA Isolation

In order to carry out the gene expression analysis both in cell cultures and tissues from experimental animals, RNA was used as the starting point. Total RNA was extracted from previously washed cell culture or from previously snap-frozen and homogenized tissues using either TRIzol™ reagent (Invitrogen™ 15596026) or TRI reagent (Invitrogen™ AM9738). For homogenizations in TRIzol™ or TRI reagent in both cells and tissues, a pellet pestle machine (Sigma-Aldrich ref. Z359971) was used to minimize aggression. Extractions in limited and lipid-rich tissues, Phasemaker tubes™ (Invitrogen™ ref. A33248) were also used to optimize total RNA extraction. In all cases, the protocols established by the manufacturers were followed. After RNA extraction, all samples were pretreated with DNase I treatment (Thermo Scientific ref. K2981) to eliminate genomic DNA contamination and dissolved in DNase, RNase, protease free water. Both before and after DNase treatment, the concentration and purity (A260/A280 and A260/A230) of each sample was obtained using the BioDrop spectrophotometer (Harvard Bioscience™ BioDrop). Samples that did not achieve the quality standards for A260/A280 and A260/A230 ratios (>1.8) were discarded, or the RNA extraction was repeated.

#### 3.4.2. mRNA Expression Analyses

To measure relative mRNA levels, between 1µg (from adipose tissues, muscle, and cell cultures samples) and 1.5µg (from liver and kidney samples) of total RNA was synthesized by the RT-PCR technique using the kit High-Capacity cDNA Reverse Transcription Kit (Applied Biosystems™ ref. 10400745) following the manufacture's official protocol. Then, from a 1:50 dilution of the obtained cDNAs, a quantitative PCR (qPCR) was performed to obtain the relative mRNA levels. For the qPCR process a Bio-Rad, CFX96 Touch Real-Time PCR Detection System was used both with SYBR™ Select Master Mix for CFX (Applied Biosystems™ ref. 13226529) or TaqMan Gene Expression Master Mix (Applied Biosystems™ ref. 4461882) depending on the gene analyzed. Each mRNA from a single sample was measured in duplicate,

using *Anti-beta 2 microglobulin (B2m)*, *Ribosomal protein lateral stalk subunit P0 (M36b4)* and *Beta-Actin* as housekeeper genes and calculating the corresponding bestkeeper using the *BestKeeper.gene-quantification.info* website excel template. Results from the qPCR were obtained by the Relative Standard Curve Method and expressed as fold increase versus the experimental control.

### 3.4.3. DNA Oligonucleotides

DNA oligonucleotides used in this thesis proposal were designed internally or based on high quality sources and synthesized by Sigma-Aldrich with ultra-high base coupling efficiency technology, combined with optimized cartridge purification and quality control by mass spectrometry. The primer sequences are shown above.

<i>Gene</i>			<i>Sequence</i>	<i>Code</i>
<b><i>B-Actin</i></b>	Beta-Actin	SYBR	F-5'-GCTCTGGCTCCTAGCACCAT	NM_007393.5
		Green	R-5'-GCCACCGATCCACACAGAGT	
<b><i>B2M</i></b>	Beta-2 Microglobulin	SYBR	F-5'-ACTGATACATACGCTGCAGAGTT	NM_009735.3
		Green	R-5'-TCACATGTCTCGATCCCAGTAGA	
<b><i>M36B4</i></b>	Ribosomal protein, large, P0 (Rplp0)	SYBR	F-5'-AGATGCAGCAGATCCGCAT	NM_007475.5
		Green	R-5'-GTTCTTGCCCATCAGACC	
<i>Acaca</i>	Acetyl-Coenzyme A car- boxylase alpha	SYBR	F-5'-TGTACAAGCAGTGTGGGCTGGCT	NM_133360.2
		Green	R-5'-CCACATGGCCTGGCTTGGAGGG	
<i>Acox3</i>	Acyl-Coenzyme A oxi- dase 3, pristanoy	SYBR	F-5'-GCCTCCTCAACTCTGGGG	NM_030721.3
		Green	R-5'-TCAGTTCTTCGTAGCTTCTCTAGG	
<i>Adiponectin</i>	Adiponectin	SYBR	F-5'- CAGTGGATCTGACGACACCAA	NM_009605.5
		Green	R-5'- TGGGCAGGATTAAGAGGAACA	
<i>CrebH</i>	cAMP responsive ele- ment binding protein 3- like 3	SYBR	F-5'-GTGTCACACCAGGGAGCAAG	NM_001382818.1
		Green	R-5'-CAGTGAGGTTGAAGCGGGAG	
<i>Cris1</i>	Cardiolipin synthase 1	SYBR	F-5'-GGGCTACCTGATTCTTGAAGA	NM_001024385.1
		Green	R-5'-GGCCCAGTTTCGAGCAATAA	
<i>Cpt1a</i>	Carnitine Palmitoyl transferase 1a	SYBR	F-5'-AGAATCTCATTGGCCACCAG	NM_013495.2
		Green	R-5'-CAGGGTCTCACTCTCCTTGC	
<i>Cpt1b</i>	Carnitine Palmitoyl transferase 1b	SYBR	F-5'-GCGTGCCAGCCACAATTC	NM_009948.2
		Green	R-5'-TCCATGCGGTAATATGCTTCAT	
<i>Cpt2</i>	Carnitine Palmitoyl transferase 2	SYBR	F-5'-TGCTCGCTCAGGATAAACAG	NM_009949.2
		Green	R-5'-CGGATTGAATGCCATGAA	
<i>Cat</i>	Catalase	SYBR	F-5'-GTCACCTCAGGTGCGGACATT	NM_009804.2
		Green	R-5'-CAGGGTGGACGTCAGTGA	
<i>Cebpb</i>	CCAAT/enhancer bind- ing protein beta	SYBR	F-5'-GGGTTGTTGATGTTTTTGGTTT	NM_001287738.1
		Green	R-5'-GAAACGGAAAAGTTTCTCAAAA	
<i>Cd36</i>	Platelet glycoprotein 4, fatty acid translocase	SYBR	F-5'-GCCAAGCTATTGCGACATGA	NM_001159558.1
		Green	R-5'-TCTCAATGTCCGAGACTTTTCAAC	

<i>Fsp27</i>	Cell death-inducing DFFA-like effector C, Transcript variant ALL	SYBR Green	F-5'-AGGCCCTGTCGTGTTAGCAC R-5'-CATGATGCCTTTGCGAACCT	NM_178373.4
<i>Fsp27<math>\alpha</math></i>	Cell death-inducing DFFA-like effector c (Ci- dec), transcript 1 & 2	SYBR Green	F-5'-GCCACGCGGTATTGCCAGGA R-5'-GGGTCTCCCGGCTGGGCTTA	NM_178373.4
<i>Fsp27<math>\beta</math></i>	Cell death-inducing DFFA-like effector c (Ci- dec), transcript variant 3	SYBR Green	F-5'-GTGACCACAGCTTGGGTCGGA R-5'-GGGTCTCCCGGCTGGGCTTA	NM_001372264.1
<i>Cidea</i>	Cell death-inducing DNA fragmentation fac- tor, alpha subunit-like ef- factor A	SYBR Green	F-5'-GTGGACACAGAGGAGTTCTTT R-5'-GTCGAAGGTGACTCTGGCTATTC	NM_007702.2
<i>Dio2</i>	Deiodinase, iodothyro- nine, type II	SYBR Green	F-5'-TGCCTGTGTCTGGAACAG R-5'-CTGGAATTGGGAGCATCTCA	NM_010050.4
<i>Dgat1</i>	Diacylglycerol O-acyl- transferase 1	SYBR Green	F-5'-CGACGGCTACTGGGATCTGA R-5'-CTCAGGATCAGCATCACCACAC	NM_010046.3
<i>Dgat2</i>	Diacylglycerol O-acyl- transferase 2	SYBR Green	F-5'-GAACACGCCAAGAAAGGTGG R-5'-GGTGGTCAGCAGGTTGTGTG	NM_026384.3
<i>Chop</i>	DNA-damage inducible transcript 3	SYBR Green	F-5'-CTGCCTTTCACCTTGGAGAC R-5'-CGTTTCCITGGGATGAGATA	NM_007837.4
<i>Egr1</i>	Early growth response 1	SYBR Green	F-5'-GCCGAGCGAACAACCCTAT R-5'-ATAACTCGTCTCCACCATCGC	NM_007913.5
<i>Ehhadh</i>	Enoyl-Coenzyme A	SYBR Green	F-5'-AATACAGCGATACCAGAAGCC R-5'-ATTCCCAGCATCACTTCCG	NM_023737.3
<i>Fabp4</i>	Fatty acid binding pro- tein 4	SYBR Green	F-5'-GATGCCTTTGTGGGAACCTG R-5'-GAATTCCACGCCAGTTTGA	NM_024406.3
<i>Fasn</i>	Fatty acid synthase	SYBR Green	F-5'-GCTGCGGAAACTTCAGGAAAT R-5'-AGAGACGTGTCACCTCTGGACTT	NM_007988.3
<i>Fos</i>	FBJ osteosarcoma oncogene	SYBR Green	F-5'-CAGAAGGGGCAAAGTAGAGC R-5'-TCAAGTTGATCTGTCTCCGCTTG	NM_010234.3
<i>Fgf21</i>	Fibroblast growth factor 21	SYBR Green	F-5'-CCGCAGTCCAGAAAGTCTCC R-5'-CTGCAGGCCTCAGGATCAAA	NM_020013.4
<i>FgfR1</i>	Fibroblast growth factor receptor 1	SYBR Green	F-5'-CTGGCAGCGATACCACCTAC R-5'-CTGGGGATGTCCAGTAGGGA	NM_010206.3
<i>FgfR4</i>	Fibroblast growth factor receptor 4	SYBR Green	F-5'-CTGCTTGGGCAAGTGGTTC R-5'-TGCCAAATCCTTGTCGGAGG	NM_008011.2
<i>Fibronectin</i>	Fibronectin	SYBR Green	F-5'-GGAACCAGCAGAGTCCAAA R-5'-ACACCAGCTTGAAGCCAAT	NM_010233.2
<i>GluK</i>	Glucokinase	SYBR Green	F-5'-GGCGTGAACCGCTCCTT R-5'-GTGGATGGCTCCGTGTACAA	NM_010292.5
<i>G6pc</i>	Glucose-6-phosphatase, catalytic	SYBR Green	F-5'-CAGTGGTCCGAGACTGGTTC R-5'-GTCCAGGACCCACCAATACG	NM_008061.4
<i>Gsr</i>	Glutathione reductase	SYBR Green	F-5'-CAGTTGGCATGTATCAAGCA R-5'-CGAATGTTGCATAGCCGTGG	NM_010344.4

<i>Gk</i>	Glycerol kinase	SYBR Green	F-5'-TGGCAGCCGCGAAGAA R-5'-TGATGACTAAGAAGTTCAGCTGTT	NM_001331046.1
<i>Bip</i>	Heat shock protein 5	SYBR Green	F-5'-CATGGTTCTCACTAAAAATGAAGG R-5'-GCTGGTACAGTAACAACTG	NM_001163434.1
<i>Kim-1</i>	Hepatitis A virus cellular receptor 1	SYBR Green	F-5'-CTGCTGCTACTGCTCCTTGT R-5'-GGAAGGCAACCACGCCTAGA	NM_134248.2
<i>Hamp</i>	Hepcidin antimicrobial peptide	SYBR Green	F-5'-CTGAGCAGCACCACCTATCT R-5'-TCTTCTGCATTGGTATCGCA	NM_032541.2
<i>Hepb</i>	Hephaestin (Heph)	SYBR Green	F-5'-GCTGGCATGGAGACCATCTT R-5'-TCCCTTAGAATCACTGCTTTTCCA	NM_010417.2
<i>Itgb</i>	Integrin Beta 1 (Fibronectin receptor Beta)	SYBR Green	F-5'-GACGCTGCGAAAAGATGAATTT R-5'-CGCAAGATTTGGCATTTCCTTTT	NM_010578.2
<i>Klb</i>	Klotho Beta	SYBR Green	F-5'-TACACTGTGGGACACAACCTG R-5'-ATCCAATGGGACCCCAAGGT	NM_031180.2
<i>Lpr</i>	Leptin Receptor	SYBR Green	F-5'-TGTCCTACTGCTCGGAACAC R-5'-AGAGTGTCCGTCTCTTTTGG	NM_146146.3
<i>Lcn2</i>	Lipocalin 2	SYBR Green	F-5'-GGTGGCCACTGCACATTGT R-5'-GGACCAGGGCTGTCGCTACT	NM_008491.1
<i>Chrebp</i>	MLX interacting protein-like (Mlxipl), transcript variant 1 & 2	SYBR Green	F-5'-CACTCAGGGAATACACGCCTAC R-5'-ATCTTGGTCTTAGGGTCTTCAGG	NM_021455.5
<i>Chrebpa</i>	MLX interacting protein-like (transcript variant 1)	SYBR Green	F-5'-CGACACTCACCCACCTCTTC R-5'-TTGTTCAGCCGGATCTTGTTC	NM_021455.5
<i>Chrebpb</i>	MLX interacting protein-like transcript variant 2	SYBR Green	F-5'-TCTGCAGATCGCGTGGAG R-5'-CTTGTCCCGGCATAGCAAC	NM_001359237.1
<i>Nrf2</i>	Nuclear factor, erythroid derived 2, like 2	SYBR Green	F-5'-CAGTGGATCCGCCAGCTAC R-5'-GGCAAGCGACTCATGGTCATC	NM_010902.4
<i>Atgl</i>	Patatin-like phospholipase domain	SYBR Green	F-5'-CGCCTCTCGAAGGCTCTCT R-5'-TGTAGCCCTGTTTGCACATCTC	NM_001163689.1
<i>Pgc1a</i>	Peroxisome proliferative activated receptor, gamma, coactivator 1A	SYBR Green	F-5'-AACCACACCCACAGGATCAGA R-5'-CTCTTCGCTTTATTGCTCCATGA	NM_008904.2
<i>Ppara</i>	Peroxisome proliferator activated receptor alpha	SYBR Green	F-5'-GATTCAGAAGAAGAACCGBAACA R-5'-GCGAATTGCATTGTGTGACAT	NM_011144.6
<i>Pparb/d</i>	Peroxisome proliferator activator receptor delta	SYBR Green	F-5'-TGTGTGGAGACCGGCCA R-5'-CGCAGAAATGGTGTCTGGA	NM_011145.3
<i>Pparg</i>	Peroxisome proliferator activated receptor gamma	SYBR Green	F-5'-GCATCAGGCTTCCACTATGGA R-5'-AATCGGATGGTTCCTCGGAAA	NM_001127330.2
<i>Pepck</i>	Phosphoenolpyruvate carboxykinase 1	SYBR Green	F-5'-CTTTGGTGGCCGTAGACCTG R-5'-GATGATCTTGCCCTTGTGTCTG	NM_011044.3
<i>Pltp</i>	Phospholipid transfer protein	SYBR Green	F-5'-CATCCATCCCAGACGTGTA R-5'-CAGATCTTGGTCTGGCTGGAA	NM_011125.2
<i>Prdm16</i>	PR domain containing 16	SYBR Green	F-5'-CAGCACGGTGAAGCCATT R-5'-GCGTGCATCCGCTTGTG	NM_027504.3

<i>Lpk</i>	Pyruvate kinase liver and red blood cell	SYBR Green	F-5'-CATTGTGCTGACAAAGACTGG R-5'-AGCCTGTCACCACAATCACC	NM_013631.2
<i>Opn</i>	Osteopontin	SYBR Green	F-5'-TTCTCCTGGCTGAATTCTGAGG R-5'-AATCAGTCACITTCACCGGG	NM_001204201.1
<i>Glut1</i>	Solute carrier family 2 (facilitated glucose transporter), member 1	SYBR Green	F-5'-GCCCCCAGAAGGTTATTGA R-5'-CGTGGTGAGTGTGGTGGAT	NM_011400.3
<i>Glut4</i>	Solute carrier family 2 (facilitated glucose transporter), member 4	SYBR Green	F-5'-ACTCATTCTTGGACGGTTCCCTC R-5'-CACCCCGAAGATGAGTGGG	NM_001359114.1
<i>Scd1</i>	Stearoyl-Coenzyme A desaturase 1	SYBR Green	F-5'-CTTGCGGATCTTCCTTATCATT R-5'-GATCTCGGGCCCATTCG	NM_009127.4
<i>Srebp1c</i>	Sterol regulatory element binding transcription F1	SYBR Green	F-5'-GGAGCCATGGATTGCACATT R-5'-GGCCCGGAAGTCACTGT	NM_001358314.1
<i>Sod</i>	Superoxide dismutase 1	SYBR Green	F-5'-GGGTTCCACGTCCATCAGTA R-5'-CAGGTCTCCAACATGCCTCTC	NM_011434.2
<i>Txnip</i>	Thioredoxin interacting protein	SYBR Green	F-5'-GTCAGTGTCCCTGGCTCCAAGA R-5'-AGTCATCTCAGAGCTCGTCCG	NM_001009935.2
<i>Tfr2</i>	Transferrin receptor 2	SYBR Green	F-5'-CCTTCTCTTCCATGGTCAGCA R-5'-GCTGAGGTAGCCCTCCAACC	NM_001289507.2
<i>Tgfb</i>	Transforming growth factor, beta 1	SYBR Green	F-5'-ACGTCACTGGAGTTGTACGG R-5'-GGGCTGATCCCGTTGATTTTC	NM_011577.2
<i>Tnfa</i>	Tumor necrosis factor alpha	SYBR Green	F-5'-GGTGCCTATGTCTCAGCCTCTT R-5'-GCCATAGAAGTATGAGAGGGAG	NM_013693.3
<i>Ucp1</i>	Uncoupling protein 1	SYBR Green	F-5'-CCCGCTGGACACTGCC R-5'-ACCTAATGGTACTGGAAGCCTGG	NM_009463.3
<i>Atf4</i>	Activating transcription factor 4	Taqman	Mm00515325_g1	
<i>Hsl</i>	Lipase E, hormone sensitive	Taqman	Mm00495359_m1	
<i>Lpl</i>	Lipoprotein lipase	Taqman	Mm00434764_m1	
<i>Plin1</i>	Perilipin 1	Taqman	Mm00558672_m1	

### 3.5. Animal Procedures

Mice are primarily the preclinical model to study the underlying mechanisms of obesity as well as to evaluate new therapeutic approaches. The anatomical and physiological similarities between humans and mice facilitate a closer approximation on the study of metabolic changes in obesity and also permit the screening of potential bioactive compounds with therapeutic properties(338). In this thesis proposal, a diet-induced obesity (DIO) model has been used on the

C57BL/6J mouse strain. The C57BL/6 is an established subline of The Jackson Laboratory. It is one of the most sensitive strains to dietary changes, when fed HFD, these mice develop human-like characteristics with complex metabolic syndrome, such as obesity, high fat accumulation, insulin resistance, hyperglycemia, hyperlipidemia, hypertension, NAFLD, kidney damage and endothelial damage associated with cardiovascular disease (339–341).

### 3.5.1. Animal Housing

Mice were housed at the animal facility of the School of Pharmacy of the University of Barcelona. The animals were under the same conditions in a temperature-controlled room ( $22\pm 1^\circ\text{C}$ ) on a 12h/12h - light/dark cycle and provided free access to commercial rodent chow and filtered tap water prior to the nutritional interventions. At the beginning of the intervention, only their diet was switched to the corresponding ones, but they were subjected to the same prior ambient and ad libitum conditions.

### 3.5.2. Ethical Committees

Prior to perform the animal experimentation corresponding to this doctoral thesis, all the protocols were approved by the ethical committee of the University of Barcelona as an authorized institution of the Generalitat de Catalunya. The person responsible for the CEEA project was Dr. Joana Relat Pardo, the center where it was performed the UEA-Farmàcia B-9900030 and finally the evaluation date dated from 19/04/2018.

<i>Project Title</i>	<i>CEEA</i>	<i>Procedures</i>
Intervencions dietètiques basades en la suplementació de polifenols sobre la senyalització de FGF21 per a reduir l'esteatosi hepàtica, la resistència a la insulina i l'obesitat	137/18	<p><b>P2:</b> Obesitat induïda per la dieta més suplementació en paral·lel del pinso amb polifenols de l'estudi PREDIMED en ratolins C57BL/6J</p> <p><b>P3:</b> Obesitat induïda per la dieta més suplementació en paral·lel del pinso amb polpa de <i>Rosa canina</i> en ratolins C57BL/6J</p> <p><b>P4:</b> Processos associats al manteniment de les colònies de ratolins</p>

### 3.5.3. Dietary Interventions

According to the expertise of our research group on animal experimentation and supported by the bibliography, 4-week-old littermate male C57BL/6J mice were used to develop the different DIO models used in this thesis proposal. The nutritional interventions were maintained for 18



or 26 weeks (342)(343)(344). Litters used for these experimental approaches came from normoglycemic, and normal weight progenitors aged 6 to 8 weeks for males, and 8 to 10 weeks for females. Prior to the interventions, mice that were normoglycemic (fasting blood glucose healthy levels of 80-100 mg/dL and with a normal weight according to their age) were randomized according. In order to be identified, ear tagging was performed to experimental mice with a prior inhaled anesthetic isoflurane to minimize the animal's discomfort. The same ear-tag identification code was used for both nutritional interventions. In the first experiment, concerning pure isolated polyphenol supplementation, a total of 29 mice were used (Chow Diet n=8; HFD n=11; HFD+Pol n=10). In the second experiment, concerning *Rosa canina*, a total of 26 mice were used (HFD n=13; HFD+RC n=13). The same type of cages were used during all the interventions. All the processes applied to experimental animals were previously approved and always in accordance with quality and animal welfare guidelines.

One of the main axes of this thesis proposal has been the nutritional interventions. During this period, a total of 4 different diets were used depending on the experimental needs. For the DIO animal model, there are multiple types of diets such as western diet, cafeteria diet (CAF) or high-fat diet (HFD) which can induce obesity. In this work a 45% fat-derived-calories high-fat diet was chosen. The choice of the 45% HFD was made based on two reasons. First one, as several studies have shown, the 60% HFD is too aberrant and deviates from the dietary reality of most humans suffering from obesity(345). Nowadays, the two diets most in accordance with the human model and showing the best results in inducing obesity and its comorbidities are the CAF and the 45% HFD(346). Secondly, most of the studies in DIO and associated pathology models with bioactive compound treatments do not exceed half of the total caloric value in fat. The following table shows the different types of diets used in the interventions of this thesis proposal.

<i>Experiment Title</i>	<i>Groups</i>	<i>Nutritional Intervention</i>
Effects and molecular mechanisms underlying a pure, isolated polyphenol mixture supplementation against a high fat diet-induced obesity and NAFLD.	<b>Chow Diet</b>	2918, Envigo
	<b>HFD</b>	D12451, Research Diets
	<b>HFD+Pol</b>	D12451 - D18060501 Research Diets
Effects and molecular mechanisms underlying a <i>Rosa canina</i> flesh supplementation against a high fat diet-induced obesity and NAFLD.	<b>HFD</b>	D12451, Research Diets
	<b>HFD+RC</b>	D12451, Research Diets + <i>Rosa canina</i> flesh from Gratacool®

### Isolated Pure Polyphenol Mixture Intervention

In the first experiment, corresponding to the polyphenol intervention, there were three different diets. The first one consisted of a standard rodent stabling diet (Envigo ref. 2918) administered to the control animals (Chow Diet group). Secondly, to achieve the DIO model, HFD group were fed with a 45% fat-derived-calories diet (Research Diets, HFD, ref. D12451). Finally, the intervention group (HFD+Pol) were fed with an equal high-fat diet as HFD group but supplemented with a pure, isolated polyphenol mixture ensembled by the same Research Diets company. The HFD+Pol diet included a representative mixture of pure, isolated polyphenols acquired from Sigma-Aldrich. This diet contained traces of (S)-2-[(Diphenylphosphino)methyl]pyrrolidine (0.014 mg/g diet). The composition of the polyphenol mixture was designed according to the research of Tresserra-Rimbau et al. its detailed below(347). The dosage of the compounds included are in a similar and sometimes on a lower range compared to the dosages previously published for these pure, isolated compounds. The usual range in previous publications goes from 15 mg/kg(348–353). Considering a weight average of 35g BW and an intake of 4.5 g/day of HFD that means for 15 mg/kg-0.525 mg of polyphenol and for 100 mg/kg-3.5 mg in mice. Cis-stilbene has been just used in cell culture for studying the role of polyphenols in proliferation and apoptosis and dosages are not comparable(354,355). All of the compounds used, except for the cis-stilbene, have demonstrated previous beneficial effects in obesity and insulin resistance(247).

**Polyphenols on HFD+Pol**

<i>Family</i>	<i>% of total Polyphenols</i>	<i>Polyphenol (CAS Num)</i>	<i>Mg/ g Diet</i>
Flavanones	54,4%	Hesperidin (520-26-3)	0,738
		(±)-Naringenin (67604-48-2)	0,234
Phenolic Acids	35,3%	2-Hydroxycinnamic acid (614-60-8)	0,594
		Syringic acid (530-57-4)	0,036
Stilbenes	1,2%	cis-Stilbene (645-49-8)	0,022
Tyrosols	9,1%	Tyrosol (510-94-0)	0,162
<b>Total</b>	<b>100%</b>		<b>1,786</b>

During the HFD+Pol intervention, three quantifications of total polyphenols were performed using the Folin-Ciocalteu technique to ensure that there was no significant degradation of the bioactive compounds. In none of the three measurements carried out throughout the intervention showed a decrease of more than 20% in comparison to the total polyphenols from the beginning of the experiment. In addition, to prevent compound degradation, the diet was replaced three times a week, discarding the remainder that was not consumed.

#### Rosa canina Flesh Intervention

For the second experiment, concerning the *Rosa canina* intervention, two different diets were used both derived from the same 45% commercial HFD (D12451, Research Diets). Since *Rosa canina* flesh has a semi-liquid texture, it was added to the HFD using a manual rotary grinder. In turn, the HFD control was also processed through the manual grinder to avoid differences between them. The HFD texture was adjusted with milliQ water to get the same density as the HFD+RC. The dosage of *Rosa canina* flesh, provided by Gratacool®, was calculated according to the polyphenol intake recommended as a beneficial by the PREDIMED Study (820mg in a human diet of 2300). In this sense, flesh contains 15,89mg/g of total polyphenols, calculated by Folin-Ciocalteu technique, and mice needs 4,5mg/day of polyphenols (considering 5g/day intake of HFD)(356,357). Thereby, HFD was supplemented with 0.0708g of flesh for each gram of HFD. At the end of the intervention, the caloric gain associated with flesh consumption was calculated by summing it to the caloric contribution of the HFD (0.95kcal/g RC). The diet was prepared on the spot and as in the previous experiment, it was replaced three times a week, discarding the remainder that was not consumed. To ensure proper maintenance of the flesh, it was always kept frozen (-20°C) and a quantification of total polyphenols was carried out both at the beginning and at the end of the experiment without any significant change.

#### 3.5.4. Animal Monitoring

In both experiments, food intake, drinking, weight, and animal welfare were monitored. Tap filtered water was supplied in 50 ml sterile bottles which were changed three times a week and its consumption was recorded. In this case the data are not shown since there were no changes in any of the experiments. Regarding food intake, thrice a week, the respective diets were provided in excess (*ad libitum*) to the animals and weighted before and after the consumption. During the nutritional intervention, animals were weighed twice a week in the first 2/3 weeks to

ensure proper adherence but after this period they were weighted weekly. All manipulations were carried out as quickly as possible and at the same time of day, respecting the animal's cycles. For animal welfare, 2 facts were considered. First, whether the animals were barbered and/or injured. Secondly, if any of the mice showed abnormal or isolated behavior. In both cases those animals were dis-carded in the subsequent steps.

### 3.5.5. Euthanasia and Tissue Harvesting

In the first experiment, concerning pure isolated polyphenol supplementation, the euthanasia was performed on two contiguous days after 26 weeks of nutritional intervention. In case of the *Rosa canina* experiment, all animals were sacrificed on the same day after 18 weeks of nutritional intervention. Mice were euthanatized by cervical dislocation. Blood was extracted by intracardiac puncture, and serum was obtained using centrifugation (1500 rpm, 30 min). Liver; scWAT; BAT; epididymal WAT (eWAT); soleus; gastrocnemius; hypothalamus, pancreas and kidneys were isolated, weighted, immediately snap-frozen, homogenized with liquid nitrogen, and stored at  $-80^{\circ}\text{C}$  for subsequent analysis. In addition to mRNA analysis, different assays were also performed using commercial kits, which are explained below. Sections of different organs were freshly stored in 1ml of 10% buffered formalin (Thermo Scientific ref.5701) to perform subsequent histological sections and different stains.

### 3.6. Glucose and Insulin Tolerance Tests

Metabolic tolerance tests (MTT) have been helpful for years in the diagnosis of diabetes and other metabolic abnormalities. In both animal and human models, these tests represent a simple but powerful screening method to diagnose and monitor impaired carbohydrate metabolism, glucose intolerance and early IR. In this thesis proposal, several glucose and insulin tolerance tests have been performed on the two nutritional interventions. For both processes, standardized and persistent conditions were applied through the whole experimental period (time of fasting, route of administration, dosage of glucose and insulin, brand of glucometer) following the latest Guidelines and Considerations for Metabolic Tolerance Tests in Mice published on Diabetes, Metabolic Syndrome and Obesity journal(358). All material used for the glucose tolerance test (GTT) and insulin tolerance test (ITT) processes are listed in the table below.

<i>Material used in GTT and ITT</i>	<i>Company</i>	<i>Reference</i>	<i>Process</i>
High Precision #10 Style Scalpel Blade	Fisher	12-000-162	Tail Cutting
Glucometer and Strips Glucomen® Areo 2K	Menarini	48014	Glucose Measurement
Nano Timer	Fisher	15294006	Time Control
D-Glucose	Sigma-Aldrich	G7021	Glucose Solution
Actrapid Insulin (100IU/ml)	Novo Nordisk	775536	Insulin Solution
Phosphate Buffered Saline (PBS1x)	Fisher	10388739	Dilutions
Syringe 0,2 <sup>o</sup> m Filter	Merck	10462553	Sterilization
Medical Gauzes	-	-	Animal Care
20ml Medical Syringes	-	-	Sterilization
1ml Plastipak Syringe with 24G Needle	BD	010060	Injection

In both GTT and ITT, animals were firstly transferred to clean cages without food and with new water bottles prior to fasting. Mice were fasted for 6h [from 08:00h (Zeitgeber Time 0) to 14:00h (Zeitgeber Time 6)]. Body weight was measured after fasting process. Based on the data obtained from the weighing, the amount of glucose and insulin needed was calculated. Mice were located at the experimentation room 30 minutes before the beginning of the tolerance tests. A one-week interval between the GTT and ITT processes was always respected to minimize animal stress.

### 3.6.1. Glucose Tolerance Test (GTT)

Firstly, a 1,1M glucose solution was freshly prepared before the GTT procedure: 1981,7mg of D-glucose in 10ml of PBS1x. Once prepared, it was filtered with a 0.2 $\mu$ m sterilizing filter to avoid possible infections and glucose granules that were not correctly solubilized. Secondly, the basal glucose of mice was measured at the end of the fasting period. For the blood collection, a cut was made at the tail end of the mice using a new, previously sterilized scalpel blade. Every blood extraction was made by gently massaging the tail and sampling a small drop onto the glucometer strip. Once all the basal glucose levels were registered, the previous prepared glucose solution was injected intraperitoneally at 1.5 mg glucose/g body weight rate. Considering the glucose injection as the starting point per animal, blood glucose was sampled from the tail of

each mouse and dropped onto the glucometer strip at 30', 60', 90' and 120' minutes. The measurement times between mice were controlled with a stopwatch and in no case exceeded 3 minutes. Data was plotted as blood glucose concentration (mg/dl) over time (min) and the area under the curve (AUC) of the glucose levels was calculated using GraphPad Prism 9.02. In the first study, a total of 3 GTTs were performed at 7th, 14th, and 21th week of polyphenol intervention. In case of the *Rosa canina* intervention, only one GTT was performed at the 14th week since the experiment was shorter and in order to minimize human interference.

### 3.6.2. Insulin Tolerance Test (ITT)

Firstly, a 0,05UI/ml insulin solution was freshly prepared from the commercial Actrapid Insulin (100IU/ml) diluted in PBS1x before the ITT procedure. Once prepared, it was filtered with a 0.2µm sterilizing filter to avoid possible infections. Secondly, the basal glucose of mice was measured at the end of the fasting period (the same as the GTT). For the blood collection, a cut was made at the tail end of the mice using a new, previously sterilized scalpel blade. Every blood extraction was made by gently massaging the tail and sampling a small drop onto the glucometer strip. Once all the basal glucose levels were registered, the previous prepared insulin solution was injected intraperitoneally at 0,75 I.U insulin/kg body weight. Considering the insulin injection as the starting point per animal, blood glucose was sampled from the tail of each mouse and dropped onto the glucometer strip at 30', 60', 90' and 120' minutes. The measurement times between mice were controlled with a stopwatch and in no case exceeded 3 minutes. Data was plotted as blood glucose concentration (mg/dl) over time (min) and the area under the curve (AUC) of the glucose levels was calculated using GraphPad Prism 9.02. In the first study, a total of 3 ITTs were performed at 8th, 15th, and 22nd week of polyphenol intervention. In case of the *Rosa canina* intervention, only one ITT was performed during the 15th week since the experiment was shorter and in order to minimize human interference.

### 3.6.3. TBARS Assay

Thiobarbituric acid reactive substances (TBARS) are formed as a byproduct of lipid peroxidation reaction. Lipid peroxidation can be described as a process under which oxidants such as ROS attack lipids containing carbon-carbon double bond(s), especially PUFAs from the membrane, resulting in cell damage. Because ROS have extremely short half-lives as well as the high

price of their analysis kits, they become difficult to measure directly. Instead, there are several byproducts of the damage reaction produced by oxidative stress that can be analyzed easily and cheaper than ROS, such as TBARS. The TBARS assay detects the level of MDA (malondialdehyde), the major lipid oxidation product, and also some minor related compounds(359). However, there is some controversy within the scientific community on the use of these analyses since they not only quantify MDA but also other derived species. Nevertheless, since the major by-product of the reaction is MDA as well as its low cost compared to ROS activity assays, the TBARS test remains one of the most widely used assays for initial screening of oxidative damage. The kit used in the different analyses was the Abnova TBARS kit (Abnova, ref. KA1381). This assay can be performed colorimetrically or fluorometrically, depending on the sensitivity desired. In case of this thesis proposal, the fluorometrically method was used using 25 mg of sample for the different experiments at an excitation wavelength of 530 nm and an emission wavelength of 550 nm. The plates were read twice, and a MDA solution was used as a standard. The corrected fluorescence values of the standards were plotted as function of MDA concentration and the corresponding values for each sample were calculated from the standard curve using Graph Pad Prism 9.02. In all cases, the protocols established by the manufacturer were strictly followed.

#### 3.6.4. LCN2 ELISA

In order to determine circulating Lipocalin-2 serum levels on the polyphenol intervention experiment, an ELISA assay was used. ELISA (enzyme-linked immunosorbent assay) is a plate-based assay technique designed for detecting and quantifying soluble substances like peptides, proteins, antibodies, and hormones. In this case the specific EMLCN2 solid-phase sandwich enzyme-linked immunosorbent assay kit (Thermo Fisher Scientific, ref. EMLCN2) was used. From the very beginning, the manufacturer's instructions were strictly followed. Absorbance was read at 450 nm, and a four-parameter standard curve (4PL) was performed using Graph Pad Prism 9.02.

#### 3.6.5. Total Iron Quantification

Since the preliminary results of the first experiment suggested an alteration of Lipocalin-2 metabolism and renal damage, as well as a worsening of insulin and glucose response, circulating and hepatic iron were quantified. Total iron level was determined using the iron assay kit from

Sigma-Aldrich (MAK025). In this assay, iron is released by the addition of an acidic buffer and reacted with a chromogen resulting in colorimetric product (593nm), proportional to the iron present in the samples. Serum (40ul) was directly added to the wells and liver (10mg) was previously homogenized in the iron assay buffer and centrifuged to remove insoluble material before performing the kit. In all cases, the protocols established by the manufacturer were strictly followed. Values were obtained plotting the iron standards on a standard curve using Graph Pad Prism 9.02.

#### 3.6.6. Triglyceride Quantification

To determine total TAG, 100 mg of tissue per mouse was pulverized in liquid nitrogen and homogenized in 1 ml of Nonidet P40 at 5% (A1694, 0250, Panreac Applichem, Spain). The amount of TAG was determined by using and following the protocol of the Triglyceride Quantification Colorimetric Kit (MAK266, Sigma Aldrich, St. Louis, MO, USA). All data and standard curves were treated and calculated on Graph Pad Prism 9.02.

#### 3.7. Histological Analyses

For histological analysis, fresh tissues were first sectioned and placed in 1ml of 10% buffered formalin (Thermo Scientific ref.5701). After 5 days in formalin they were switched to a 50% ethanol solution, to prevent hardening, and within 48 hours they were sent to the Universitat de Barcelona School of Medicine histopathology service. From the samples provided several histological sections of the different organs were prepared and from those, various stains were performed. In both experimental approaches described a hematoxylin-eosin (H&E) staining were performed on liver, kidney, and scWAT on 4 µm-thick longitudinal and transversal sections. Concerning kidneys from the polyphenol experiment, a Sirius Red staining was also performed. Unfortunately, since kidneys were not supposed to be histologically analyzed initially, they were not properly stored in formalin. Nevertheless, correct histological sections were successfully obtained in more than half of the samples. The H&E stain was selected since it is very useful and reliable for an overall view, whereas Sirius Red was applied to the kidney sections to visualize whether there were regions affected by fibrosis. Sirius red stain with red color the connective tissue, concretely the collagen fibers being a useful tool to identify fibrotic regions The



first randomized screening was performed by the histology service technician. Based on his preliminary analysis, an exhaustive viewing of the samples was subsequently performed on the optical microscopy. Furthermore, the 8<sup>th</sup> edition of the Ross, Michael H. and Wojciech Pawlina histology manual was used as a guideline(360). Once fully examined, a minimum of 4 pictures per mice on different magnifications were taken and then were analyzed by 3 supervisors in a double-blinded mode. Images were acquired using a Digital Upright Microscope BA310 Digital and a Moticam 2500 camera. None of the pictures were subjected to any photographic treatment, although in case of lipid droplet quantification the free Gimp software was used to binarize the images and therefore allow the compiling.

### 3.8. Bioactive Compound Analyses

During the development of this doctoral thesis, not only molecular biology techniques from our research group have been used but also methods from the nutritional research area, concretely from the bioactive compound study field. In this sense, it has been possible to work closely with researchers from the Natural Antioxidants group of the Departament de Nutrició i Ciències de l'Alimentació from UB, led by Dr. Rosa Lamuela. Therefore, this methodology section has been followed according to the expertise of the mentioned research group, specifically with the support and guidance of the PhD candidate Julián Lozano Castellón.

#### 3.8.1. Folin-Ciocalteu Method Quantification

Folin-Ciocalteu method, also called the gallic acid equivalence method (GAE), is a colorimetric method based on the reduction in an alkaline medium of a mixture of phosphomolybdic and phospho-wolframic acid (Folin-Ciocalteu reagent) using gallic acid as a standard. This type of assay is widely used to quantify the total polyphenol content of food samples, but since the related reduction reaction can be produced not only by phenolic compounds but also by other compounds such as vitamins, it is used less and less and only to obtain orientative data as it is inexpensive and fast. In case of this thesis proposal, the Folin-Ciocalteu method was performed on several occasions, both as a screening test and to assess intervention dosage. Firstly to determine the polyphenol degradation rate during both nutritional interventions, with no significant changes, and in order to calculate de *Rosa canina* flesh dosage. The reagents used in the process were Folin-Ciocalteu Reagent (Sigma-Aldrich ref. 47641), Sodium Carbonate (Panreac ref. 141648-1211) and gallic acid as standard (Sigma-Aldrich ref. G-7384). Regarding procedures,

the standardized working procedure (PNT) based on the “*Changes in phenolic profile and antioxidant activity during production of diced tomatoes*” by the Natural Antioxidants research group and published on Food Chemistry journal was followed(361).

### 3.8.2. Rosa canina Fractionation

Preparation of plants or fruits for experimental purposes is an initial step in achieving quality research outcome. It involves extraction and determination of quality and quantity of bioactive constituents commonly before proceeding with biological testing(362). In case of this thesis proposal, the fractionation was done after the intervention with animals, since the aim was to discern which was the most active part, but also which species may be responsible of the effects of the *Rosa canina* flesh according to the mechanistic obtained results. Even so, these fractions were also evaluated in vitro afterwards.

Prior to fractionation, a literature screening was carried out on solvent methods used in similar experiments. In our case, different procedures were combined since the aim was to have a maximum range of solubilities and therefore be able to categorize and relate the effects with greater accuracy(363–366). Usually, in bioactive compound extractions, different solvents are used according to the species desired to be extracted, for example, in case of more water-soluble species, using polar solvents such as water or alcohol; in case of intermediate species, using intermediate polar solvents such as acetone or dichloromethane; and finally, in case of more liposoluble species, using non-polar solvents such as n-hexane, ether or chloroform. In our case, 5 different solvents were chosen to provide 5 different fractions to achieve the maximum range of extracted species. Following the bibliography, ranked from the most polar to the most non-polar: water (MiliQ-ultra Pure Water), 80% ethanol (Panreac ref. 361086), ethyl acetate (Panreac ref. 361318), chloroform (Biochemica ref. A3691) and n-hexane (Panreac ref. 362063) were chosen. Each of these solvents favors the extraction of specific groups of bioactive compounds. The methodology followed in the extraction processes was the same used by Lasse Saaby and colleagues from the University of Copenhagen in their study on the immunomodulatory role of the triterpene acids from *Rosa canina*(365). First, 50 grams of freshly thawed flesh were weighed for each solvent, thus a total of 250 grams of *Rosa canina* were used. To these 50 grams of flesh, 250 ml of solvent were added respectively and sonicated for 15 minutes on ice. After sonication, the mixture was blended with a glass stick for 10 minutes and then filtered with a standard paper filter.

This process was repeated 4 times but only with one sonication, resulting in a total of 1L of dissolution for each solvent. Each dilution was subsequently subjected to evaporation using a rotary evaporator (Resona Technics ref. Laborota 300). In no case the temperature exceeded 35 °C in order to avoid compound deterioration. Once the solvents were completely evaporated, the resulting dry extract were weighed, 10 mg/ml aliquots of each extract and one for fresh flesh were made in DMSO and quickly frozen in opaque microtubes at -80°C. When fractions were used on cell cultures, firstly were dissolved in the corresponding growth medium and then filtered by syringe with a 0.2µm filter.

### 3.8.3. UPLC-LTQ-Orbitrap-MS

Liquid chromatography analysis was carried out using an Accela chromatograph (Thermo Scientific, Hemel Hempstead, UK) equipped with a quaternary pump, a photodiode array detector (DAD), and a thermostated autosampler. Chromatographic separation was achieved using a BEH C18 (2.1x100mm, 1.7µm) analytical column (Waters ®, Dublin, Ireland) maintained at 40°C. The BEH C18 column provides the most universal generic column choice for UPLC separations and the trifunctionally bonded BEH particle gives the widest pH range (pH 1-12), superior low pH stability, and ultra-low column bleed for high sensitivity MS applications. The mobile phases were water and acetonitrile both with 0.1% of formic acid. A linear gradient water-acetonitrile from 6 to 94% of acetonitrile in 35min was used for the separation of the different compounds(367).

The detector used was a high-resolution mass spectrometer LTQ-Orbitrap Velos mass spectrometer (Thermo Scientific, Hemel Hempstead, UK) equipped with an ESI source operated in negative and positive modes. Operation parameters were as follows: source voltage, 4 kV; sheath gas, 20a.u. (arbitrary units); auxiliary gas, 10a.u.; sweep gas, 2a.u.; and capillary temperature, 275°C. Samples were analyzed in full scan mode at a resolving power of 30,000 (FWHM at m/z 400) and data-dependent MS/MS events acquired at a resolving power of 15,000. The most intense ions detected in the full scan spectrum were selected for the data-dependent scan. Parent ions were fragmented by high-energy C-trap dissociation (HCD) with normalized collision energy of 35V and an activation time of 10ms. The mass range in Fourier transformation mass spectrometry (FTMS) mode was from m/z 100 to 1000. Instrument control was performed with Xcalibur 3.0 software (Thermo Fisher Scientific)(368). The identification step was based on mass

accuracy, isotopic pattern, and spectral matching. Using the software MS-DIAL, the mentioned criteria were used to calculate a total identification score(369). The total identification score cut off was 75%, considering the most common ion adducts for the chromatographic solvents. Gap filling using peak finder algorithm was performed to fill in missing peaks, considering 5 ppm tolerance for m/z values. Finally, with the software MS-FINDER(370), in-silico fragmentation of the not annotated mass features was obtained and compared to *Food DB*, *Phytohub* and *Lipid-Maps* available in the same software. The compounds with an in-silico prediction score > 5 were chosen.

### 3.9. Statistics and Graphs

All statistical calculations were processed by using GraphPad Prism, version 9.02 (GraphPad, San Diego, CA, USA). The statistics applied at every point of result is indicated in the figure caption of each graph. Broadly, on the pure isolated polyphenol experiment, p-values were determined by using a one-way ANOVA with a follow-up Tukey's test. When ANOVA tests presented different variances, Brown–Forsythe, and Welch's corrections with a follow-up Dunnett's T3 tests were applied. On the *Rosa canina* experiments, p-values for each analysis were determined by using a two-tailed unpaired Student's T-test but when different variances were presented, Welch's corrections were applied. For repeated measures, on both experiments, the p-values were calculated by using a 2-way ANOVA with Geisser–Greenhouse correction. Then a Tukey's multiple comparison tests were performed between groups for each week.



RESULTS



## 4. Results

### A) Effects and molecular mechanisms underlying a pure, isolated polyphenol mixture supplementation against a high fat diet-induced obesity and NAFLD.

The literature on preventive effects of polyphenol supplementation in obesity and obesity-related chronic diseases is extensive and diverse both in terms of protective outcomes and action mechanisms. In most cases, the beneficial effects of polyphenols involve body weight control, anti-inflammatory action, improvement of insulin sensitivity, reduction of fat accumulation on the adipose tissue as well as on the ectopic depots and finally, a capacity to increase general energy expenditure(247). Target organs of polyphenol actions are mainly adipose tissues and liver, although beneficial actions are also observed in other organs such as kidney(371), pancreas(372), and muscle(373). Unfortunately, there is a great diversity in both phenolic chosen species, dosages, and supplementation format on polyphenol research. Moreover, the literature on adverse effects of polyphenols is quite limited and mostly related to toxicological in vitro studies at very high doses. This situation along with the low bioability and the heterogenous absorption rates of polyphenols, makes supplementation still under revision. In case of supplementation with pure synthetic polyphenol species not from lyophilized fruits nor plant extracts in DIO-animal models, the literature is almost inexistent.

To study the effects and molecular mechanisms underlying a pure, isolated polyphenol mixture supplementation against a high fat diet-induced obesity and NAFLD (*aim 1*), a dietary intervention with a polyphenol pure isolated mixture was performed on normoglycemic C57BL/6J 4-weeks old male mice fed for 26 weeks with a 45% HFD (see the nutritional intervention protocol in the Animal Procedures section on the Methodology chapter of this thesis proposal). Part of the findings of this study was published at *Antioxidants* journal in January 2022(374). The manuscript has been added in the 8.2 section of the annexes of this thesis proposal.



**A.1) Pure, isolated polyphenol mixture significantly enhanced the HFD-induced hyperphagia and showed an upward trend on animal body weight gain as well as significantly changes on tissues' weights.**

On diet-induced obesity models, HFD are mostly used due to their high energy density from fat and its capacity to increase food intake, as compared to standard normocaloric diets(375). During the performed intervention, a fluctuating raise (*Figure P1 A and C*) and an overall increase in weight gain and food intake in both HFD and HFD+Pol compared to chow diet-fed group (*Figure P1 B and D*) was detected. At the same time a significant increase in the kcal intake was observed between HFD-only and HFD+Pol fed mice. Conversely, the increase on kcal intake did not result in a significant shift on body weight gain, although there was an upward trend.

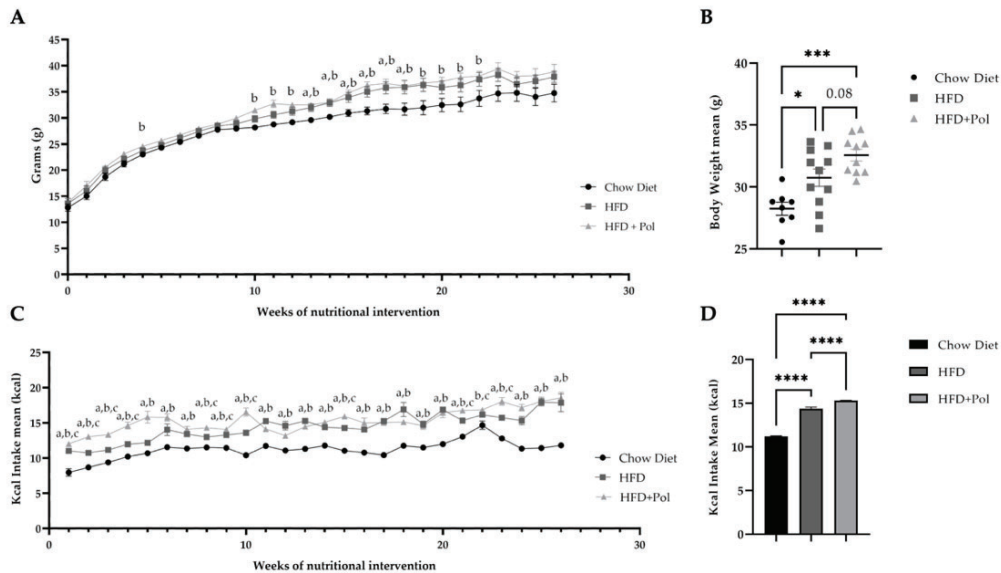


**Figure P1 – Polyphenol dietary supplementation increase the kcal intake of HFD-only mice and shows an upward trend on body weight gain.** (A) body weight means (g) per week along the whole nutritional intervention. (B) weight-gain mean between the beginning and the end of the intervention (26weeks). (C) food-intake means (kcal) per week. (D) average of food-intake (kcal) during the whole nutritional intervention. In (B) and (D) data are presented as means  $\pm$  SEM. \*  $p < 0.05$ ; \*\*\*  $p < 0.001$ ; \*\*\*\*  $p < 0.0001$  and p-values determined by using a one-way ANOVA test and a Tukey's multiple tests correction between the intervention groups (Chow Diet  $n=8$ ; HFD=11; HFD+Pol=10). In (A) and (C) data are presented as means  $\pm$  SEM. *a*  $p < 0.05$  (Chow Diet vs. HFD), *b*  $p < 0.05$  (Chow Diet vs. HFD+Pol) and *c*  $p < 0.05$  (HFD vs. HFD+Pol). The p-values on these graphs were determined by using two-way ANOVA test with Heisser-Greenhouse correction and Tukey's multiple comparison tests between the intervention groups (Chow Diet  $n=8$ ; HFD=11; HFD+Pol=10).

In addition, tissues weights were evaluated to determine if they exhibit differences due to the dietary interventions. A generalized weight gain was exhibited between organs from both HFD-fed animals and control ones. However, this increase is only a trend in scWAT, eWAT, BAT and kidneys in the HFD mice group (*Figure P2*). Interestingly in HFD+Pol mice the differences in those tissues reach statistical significance. At the same time, an upward trend in kidneys weight was showed between HFD and HFD+Pol, suggesting the presence of a change in kidney composition, functionality, or structure due to polyphenol supplementation.

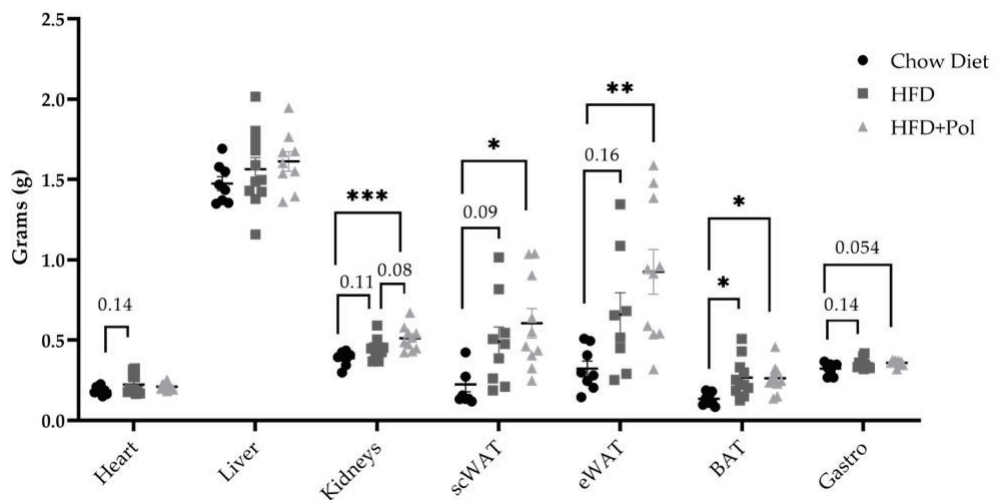


**Figure P2 – The polyphenol dietary supplementation produced an extra weight gain on kidneys of HFD+Pol fed mice compared to the HFD-only fed ones.** The graph represents the average weights of fresh tissues measured on the precision balance before snap-freezing process in liquid nitrogen. Data is presented as means  $\pm$  SEM. \*  $p < 0.05$ ; \*\*\*  $p < 0.001$ ; \*\*\*\*  $p < 0.0001$  and p-values were determined by using a one-way ANOVA test and a Tukey's multiple tests correction between the intervention groups (Chow Diet  $n=8$ ; HFD=11; HFD+Pol=10).

### **A.2) Mice supplemented with polyphenols showed an enhanced hyperglycemia and a worse response to glucose and insulin bolus than HFD-only fed mice.**

As extensively described in the literature, HFD consumption produced insulin resistance and glucose intolerance within few weeks of consumption. In this experimental model HFD-only mice starts showing an upward trend on glucose levels on the 7<sup>th</sup> week GTT or 8<sup>th</sup> week ITT (*Figure P3 A and D*). In the same tests HFD+Pol mice exhibited a significantly increased glucose levels compared to the control ones. On the subsequent tolerance tests corresponding to 14th

and 15th weeks of intervention, both HFD groups showed significantly worse response compared to the control group (*Figure P3. B and E*). Surprisingly, a worsened response in HFD+Pol compared with HFD fed mice was observed at 20<sup>th</sup> and 21<sup>th</sup> week of the intervention (*Figure P3. C and F*).

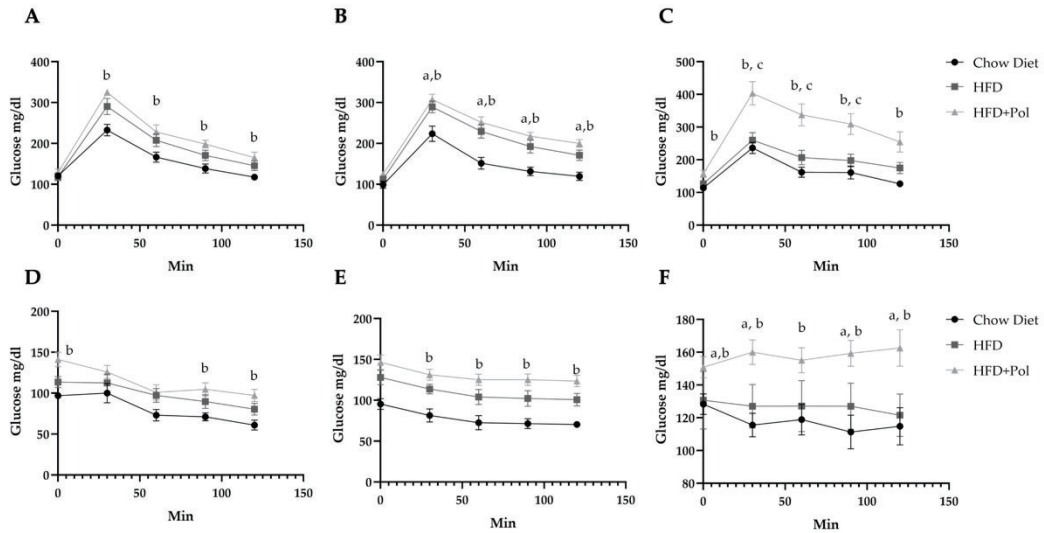


**Figure P3 – Throughout the different glucose and insulin tolerance tests performed during the dietary intervention, a gradually worse response can be observed on mice supplemented with polyphenols.** (A)(B)(C) plasma glucose levels after intraperitoneal administration of glucose (1.5 g/kg body weight) in the standard-chow-diet, HFD, and HFD+Pol corresponding to the GTTs performed at 7<sup>th</sup>, 14<sup>th</sup>, and 20<sup>th</sup> respectively weeks of nutritional intervention. (D)(E)(F) plasma glucose levels after intraperitoneal administration of insulin (0.75 UI/kg body weight) in the standard-chow-diet, HFD, and HFD+Pol corresponding to the ITTs performed at 8<sup>th</sup>, 15<sup>th</sup>, and 21<sup>th</sup> respectively weeks of nutritional intervention. Data are presented as means  $\pm$  SEM. *a*  $p < 0.05$  (Chow Diet vs. HFD), *b*  $p < 0.05$  (Chow Diet vs. HFD+Pol) and *c*  $p < 0.05$  (HFD vs. HFD+Pol). The *p*-values were determined by using two-way ANOVA test with Heisser-Greenhouse correction and Tukey's multiple comparison tests between the intervention groups (Chow Diet  $n=8$ ; HFD=11; HFD+Pol=10) for each tolerance test.

Our data indicated that the polyphenol supplementation worsened the insulin resistance and glucose intolerance caused by the HFD. Changes manifested in the tolerance tests curves are more clearly noticeable on the area under the curve graphs, where HFD+Pol not only show a worse response to glucose and insulin but also a significant worsening over time indicating a progressive aggravation of the response (*Figure P4 A and B*). On the other hand, the exposed worsening of supplemented mice is also observable in fasting basal glucose measurements where the deterioration over time is evident (*Figure P4 C*).

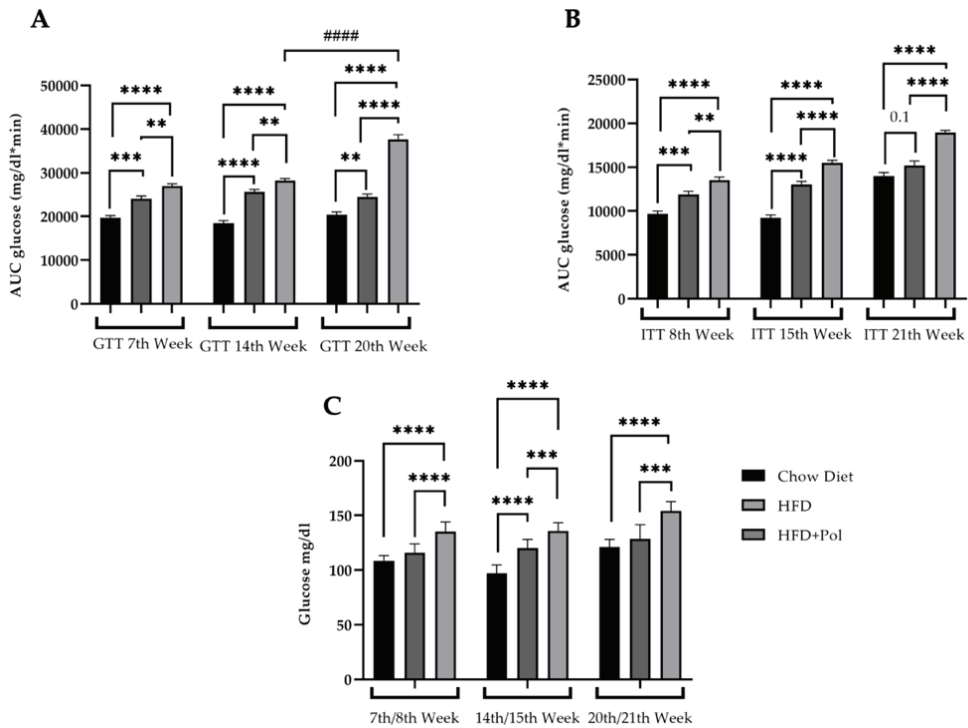


**Figure P4 –Both calculation of areas under the curve on performed tests and the measurements of basal glucose corroborate a worsening of the supplemented mice.** (A) AUCs of the plasma glucose levels after intraperitoneal administration of glucose (1.5 g/kg body weight) in the standard-chow-diet, HFD, and HFD+Pol corresponding to the GTTs performed at 7<sup>th</sup>, 14<sup>th</sup>, and 20<sup>th</sup> respectively week of nutritional intervention. (B) AUCs of the plasma glucose levels after intraperitoneal administration of insulin (0.75 UI/kg body weight) in the standard-chow-diet, HFD, and HFD+Pol corresponding to the ITTs performed at 8<sup>th</sup>, 15<sup>th</sup>, and 21<sup>th</sup> respectively week of nutritional intervention. AUCs were calculated using GraphPad Prism 9.1. (C) Fasting blood glucose levels after 6 hours of fasting in three fortnight periods of nutritional intervention. Data are presented as the mean  $\pm$  SEM. \*\*  $p < 0.01$ ; \*\*\*  $p < 0.001$ ; \*\*\*\*  $p < 0.0001$ . #####  $p < 0.0001$ . The  $p$ -values for each week were determined by using a one-way ANOVA test and a Tukey's multiple tests correction. Chow Diet  $n = 8$ ; HFD = 11; HFD + Pol = 10.

### A.3) Polyphenol supplementation increase the metabolic imbalance produced by HFD in subcutaneous WAT contributing to a worsened phenotype.

Through the analysis of different genes involving adipose tissue metabolism, some changes can be visualized on scWAT between the intervention groups (Figure P5). Firstly, *Lcn2* levels are significantly decreased between the HFD-only and HFD+Pol groups while *Fgf21* is significantly increased. Interestingly, a trend in the decrease of the *Fasn* gene expression can be seen in the

polyphenol-supplemented mice compared to the control. This same pattern is also exhibited in a downward trend in the expression of the *Chrs1* gene and significantly in the expression of the *Chrebbp* transcription factor. Regarding adipokine gene expression, a marked decrease on *Adiponectin* between control and HFD-only group but not among the HFDs, is observed. Finally, *Ucp1* expression exhibited a marked downward trend among the HFD groups. This expression pattern suggests several changes in the general scWAT metabolism state of HFD+Pol mice, albeit in a subtle way.

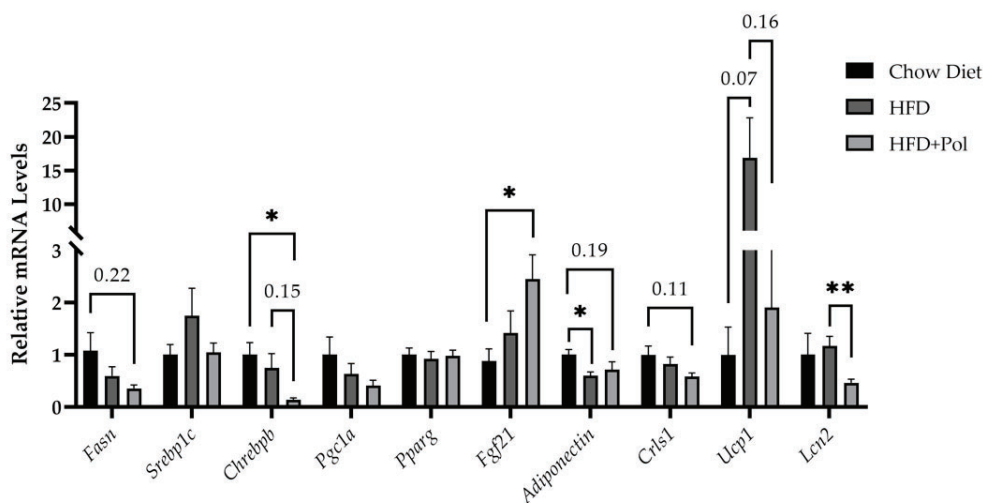


**Figure P5 – Relative mRNA levels of several genes related to DNL, adipokine synthesis, thermogenesis, and mitochondrial state.** *Fatty acid synthase (Fasn)*, *Sterol regulatory element-binding protein 1 isoform c (Srebp1c)*, *Carbohydrate-responsive element-binding protein β isoform (Chrebbp)*, *Peroxisome proliferator-activated receptor γ co-activator 1 a (Pgc1a)*, *Peroxisome Proliferator Activated Receptor Gamma (Pparγ)*, *Fibroblast growth factor 21 (Fgf21)*, *Adiponectin*, *Cardiolipin Synthase 1 (Crls1)*, *Uncoupling Protein 1 (Ucp1)* and *Lipocalin-2 (Lcn2)*. Data are presented as the mean ± SEM. \*  $p < 0.05$ ; \*\*  $p < 0.01$ . The  $p$ -values for *Pparγ*, *Crls1*, *Adiponectin*, and *Fgf21* genes were determined by using a one-way ANOVA test and Tukey’s multiple tests correction. For genes showing different variances like *Fasn*, *Srebp1c*, *Chrebbp*, *Pgc1a*, *Lcn2* and *Ucp1* a one-way ANOVA with Brown-Forsythe and Welch’s correction and a Dunnett’s comparisons tests were performed. Chow Diet  $n = 7$ ; HFD = 10; HFD + Pol = 9.

According to the histological analyses, the scWAT of both HFD-fed groups had significantly fewer and larger adipocytes (*Figure P6*). Therefore, the hypertrophic power of HFD on adipocytes is evident. However, there are no significant differences in the number of scWAT adipocytes between the supplemented group and the HFD-only even though a downward trend can be observed (*Figure P6 B*). In some histological samples, a slightly larger size is seen between supplemented and HFD-only mice, but this difference is not evident in all samples. Therefore, not clearly conclusions can be drawn.

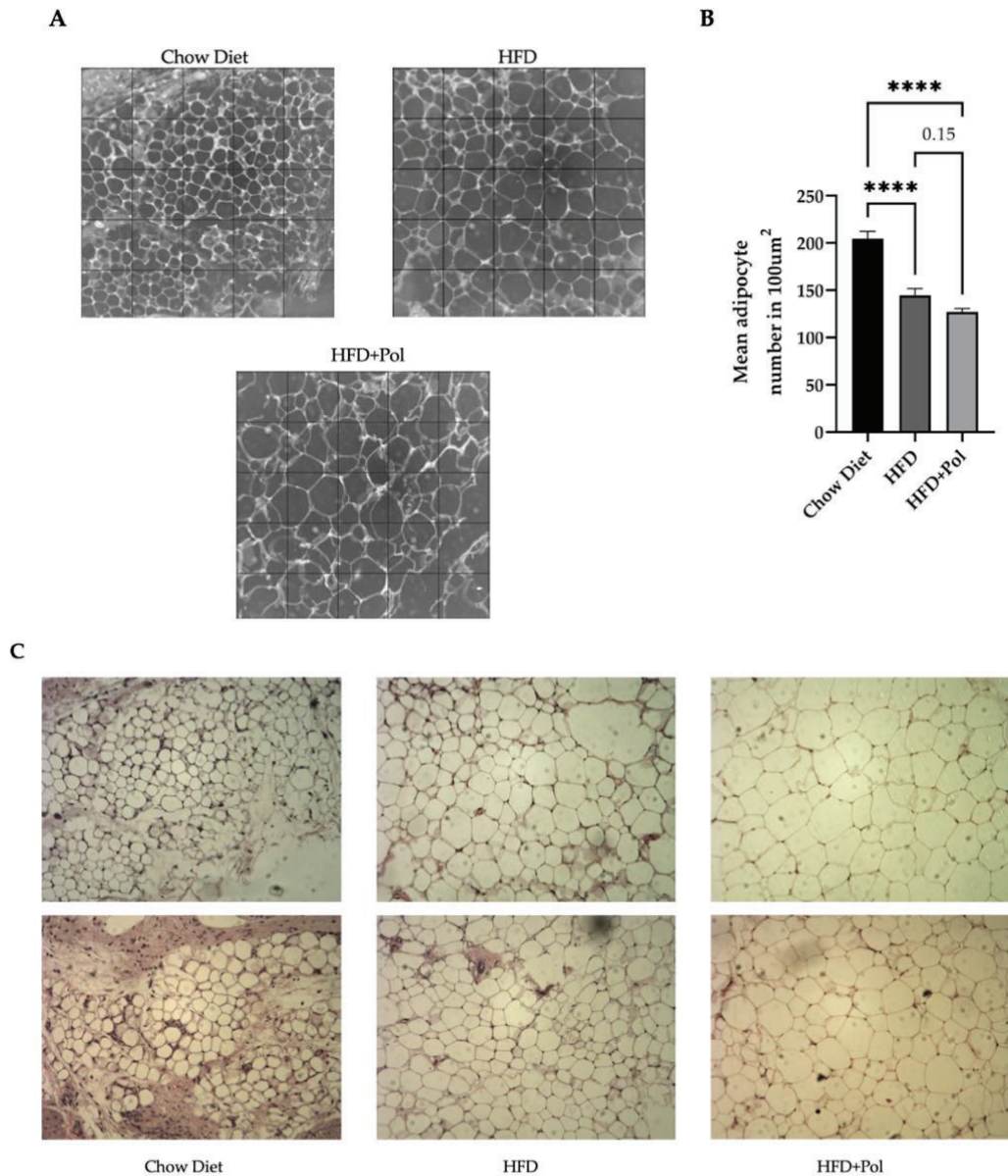


**Figure P6 – Histological analysis showed a noticeable hypertrophy of scWAT in both HFD groups.** (A) Hematoxylin eosin-stained scWAT sections of 100µm X 100µm converted into computer generated binary representations. Images captured at 10x magnification. (B) Adipocyte mean number in 100µm<sup>2</sup> of the H&E histological scWAT samples. (C) Hematoxylin eosin-stained scWAT sections captured at 10x magnification. A total of 8 duplicated and randomized photographs per group were analyzed. Data are presented as the mean ± SEM. \*\*\*\* p < 0.0001. The p-values for the adipocyte counting values were determined by using a one-way ANOVA test and Tukey's multiple tests correction.

**A.4) In liver, polyphenol supplementation significantly increased TAG content, worsened NAFLD gene expression profile, exhibited a more damaged tissue compared to HFD-only and produced an imbalance on iron levels.**

Although there were no significant differences between groups on liver's weight, an expression analysis of key genes of metabolism and liver status as well as the quantification of total hepatic triglyceride content were performed.

At gene expression level, there were three major changes. First, a clear decrease in the expression of the cytokine *Adiponectin* is exhibited by supplemented mice compared to the control group but this downregulation does not reach significance between the two HFD groups (*Figure P7 A*). On the other hand, a significant increase of *Fibronectin* gene expression is detected, both between the HFD+Pol group and control, as well as between HFD groups. Finally, the polyphenol-supplemented group displayed a significant upregulation in the expression of *Chop* gene, related to reticulum stress compared to control mice (*Figure P7 A*). The other hepatic reticulum stress referential gene, *Bip*, only shows a trend between these groups.

Due to variations on Lipocalin-2 levels, discussed below, and the described below kidney damage, we proceeded to analyze genes involved in iron metabolism on liver since a close relationship between the action of lipocalin, kidney damage and T2DM has been described(376). In this way, an upward trend on the mRNA levels of *Transferrin 2 (Trf2)* was detected between supplemented mice and control ones (*Figure P7 A*).

Even though no changes in genes related to hepatic lipid metabolism were manifested, the total content of triglycerides was analyzed (*Figure P7 B*). The supplemented group exhibited a significant increase in total triglyceride content compared to the control and an upward trend compared to the HFD-only group.



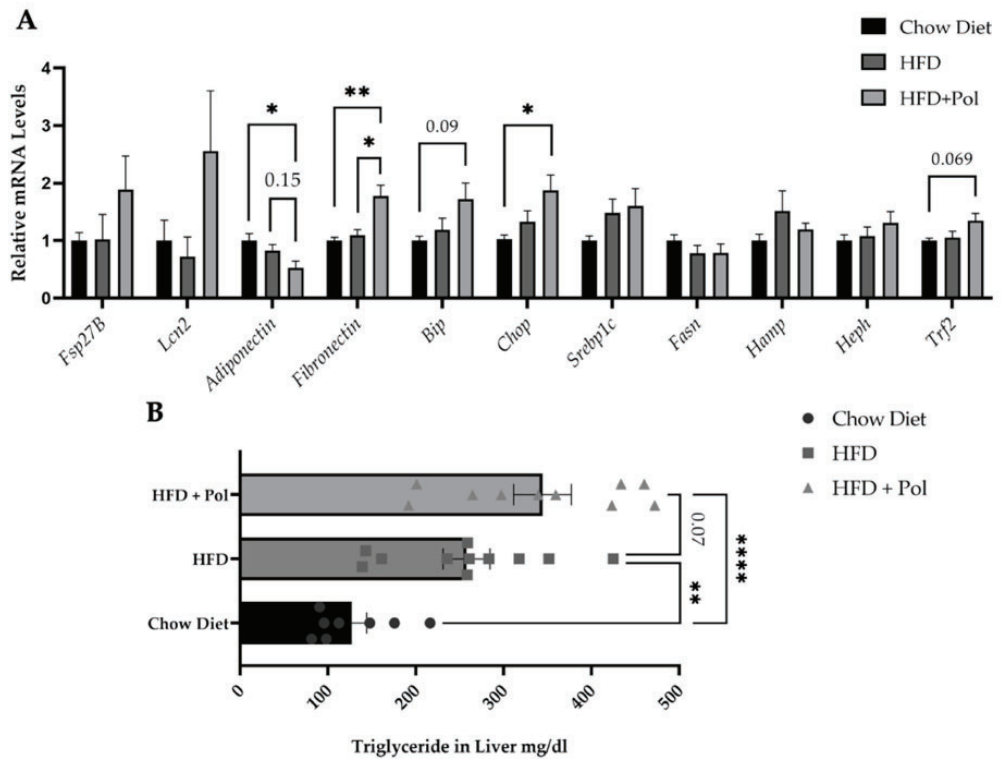


**Figure P7 – Polyphenol-supplemented HFD upregulates the expression of fibrosis markers and ER stress in the liver while increases the hepatic lipid content.** (A) Relative mRNA levels of several genes related to liver state. *Cell death activator CIDE-3 (Fsp27)*, *Lipocalin-2 (Lcn2)*, *Adiponectin*, *Fibronectin*, *Binding immunoglobulin protein (Bip)*, *C/EBP Homologous Protein (Chop)*, *Fatty acid synthase (Fasn)*, *Sterol regulatory element-binding protein 1 isoform c (Srebp1c)*, *Hepcidin (Hamp)*, *Hephaestin (Heph)* and *Transferrin 2 (Tfr2)*. (B) Hepatic TAG content. The concentration of TG (ng/uL) was measured in livers of chow, HFD and HFD+Pol mice. Data are presented as the mean  $\pm$  SEM. \*  $p < 0.05$ ; \*\*  $p < 0.01$ . TAG assay, *Fasn* and *Heph* genes were determined by using a one-way ANOVA test and a Tukey's multiple tests correction. For genes showing different variances like *Fsp27B*, *Fibronectin-1*, *Srebp1c*, *Hamp*, *Tfr2*, *Chop*, *Lcn2* and *Bip* a one-way ANOVA with Brown-Forsythe and Welch's correction and a Dunnett's comparisons tests were performed. Chow Diet  $n = 8$ ; HFD = 11; HFD + Pol = 10.



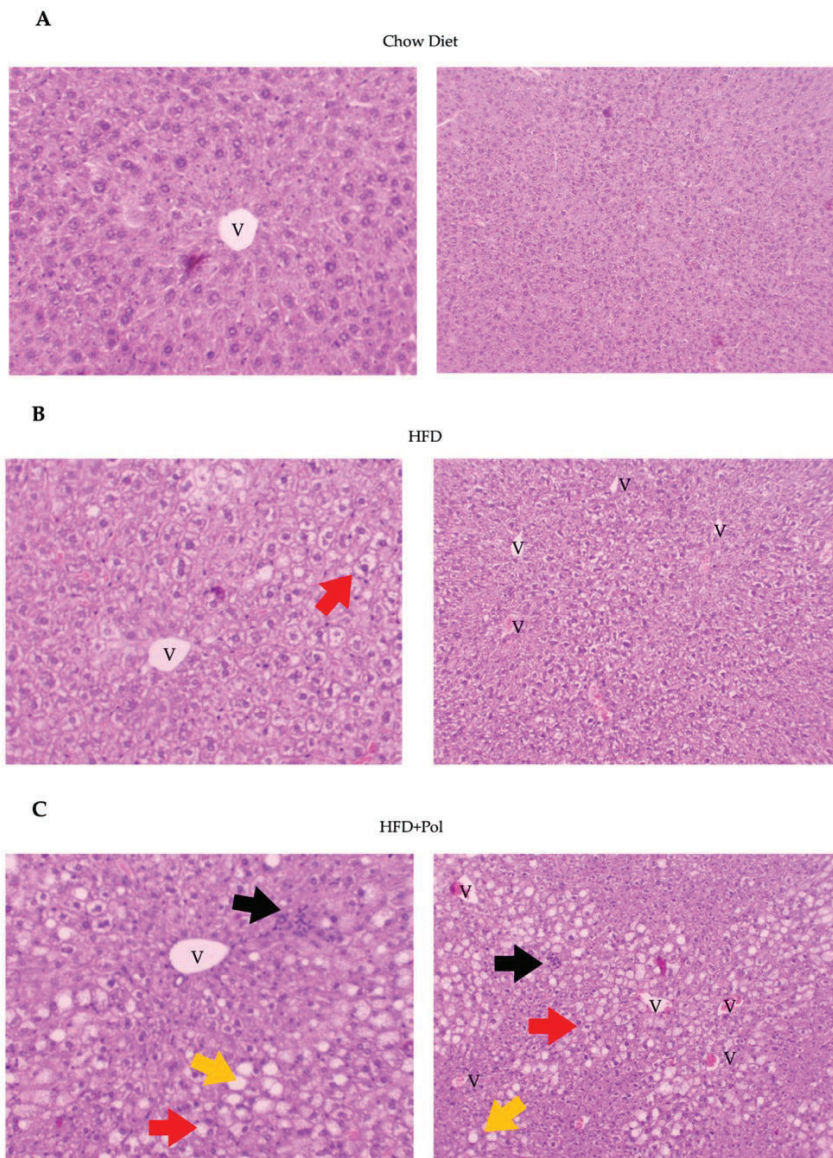


**Figure P8 – Polyphenol supplemented mice exhibit less hepatocellular ballooning but a clear immune cell infiltration and an increased heterogenic steatosis.** (A) Hematoxylin eosin-stained liver sections of Chow Diet animals left image captured at 20x magnification and right image at 10x magnification. Livers exhibit a normal architecture without fat accumulation or affected veins. (B) H&E-stained liver sections of HFD animals, left image captured at 20x magnification and right image at 10x magnification. A generalized ballooning process (ex. red arrow) and partial constricted veins (V) are shown. (C) H&E-stained liver sections of HFD+Pol animals left image captured at 20x magnification and right image at 10x magnification. A smaller and more distributed ballooning process is observed compared to the HFD-only samples. On the other hand, same constriction on veins but a greater infiltration of mononuclear immune cells (ex. black arrow) and a greater steatosis (ex. yellow arrow) are shown in supplemented mice. A total of 8 duplicated and randomized photographs per group were analyzed.

It is noteworthy the upward trend on total intrahepatic TAG in supplemented animals. As it is showed in (Figure P7 B), the hepatic lipid content is higher in both groups of HFD-fed mice compared to control mice and, despite no significance, a trend increase is observed in the HFD+Pol mice compared to HFD-only mice.

The hepatic histological analyses (Figure P8), shows that both HFD groups presented partial constriction on veins compared to the Chow Diet group. In HFD-only mice a generalized ballooning process is showed but not a clear steatosis (vacuolized fat) or immune cell infiltration. Conversely, livers of supplemented mice exhibit less ballooning but a more severe steatosis and immune cell infiltration as it shows (Figure P8 C). Somehow, it seems that supplemented animals show worse HFD-induced NAFLD management compared to the HFD-only mice.

In addition, since a relationship between iron metabolism, obesity, T2DM and renal damage has been described in the literature(377), total iron was quantified at both liver and circulating levels (Figure P9 A and B). A difference in total liver iron level was observed between control and HFD-supplemented mice. However, there was no difference between the HFD groups and neither any differences at serum circulating levels.

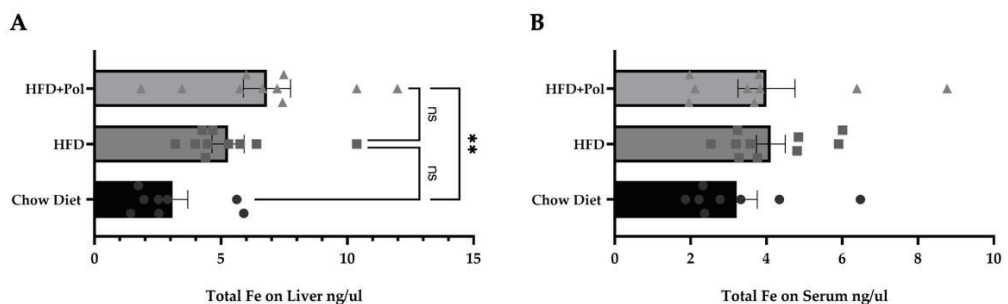


**Figure P9 – Polyphenol-supplemented HFD produced a misalignment on iron hepatic levels but only when compared to chow diet animals.** (A) Total iron levels measured in pulverized livers of chow diet, HFD and HFD+Pol mice. (B) Total iron levels measured in serum from chow diet, HFD and HFD+Pol mice. Data are presented as the mean  $\pm$  SEM. \*  $p < 0.05$ ; \*\*  $p < 0.01$ . P-values were determined by using a one-way ANOVA test and a Tukey’s multiple tests correction. Chow Diet  $n = 8$ ; HFD = 11; HFD + Pol = 10.

In summary, mice supplemented with polyphenols showed a worse response to the pernicious effect of HFD, resulting in a more prominent NAFLD compared to HFD-only mice. Changes such as higher TAG concentration, upregulation of *Fibronectin*, *Chop*, and downregulation of *Adiponectin* evidence a worsened pattern on the HFD+Pol liver. In parallel, variations in iron

metabolism were also displayed, although there were no significant differences between the HFD-only group and the polyphenol supplemented group.

#### **A.5) Polyphenol-supplemented HFD increases the oxidative stress markers in kidneys.**

The slight increase in the absolute weight of the kidneys between HFD-only mice and HFD+Pol mice along with the worsened glucose and insulin response, led to further testing kidneys of the HFD+Pol animals. As described in the introductory section, kidney is one of the tissues targeted by obesity and insulin resistance as well as being an actor of general pathological state. The involvement of kidney in these pathologies is a determining factor in the patients' prognosis. CKD and diabetic nephropathy are caused not just by high glucose circulating levels but also by lipid accumulation in the renal tissue that contributes to the development of glomerulitis, chronic inflammation, a high production of ROS, and fibrosis(33). In this situation, the damaged kidney responses activating the renin–angiotensin–aldosterone system (RAAS) and secreting specific cytokines that aggravate the systemic symptomatology associated to the CKD and diabetic nephropathy such as inflammation, hypertension and cardiovascular risk(71,378).

In this sense, one of the initial alterations described in CKD is the increase of ROS in the kidney. For this reason oxidative stress was evaluated through the thiobarbituric acid reactive substances (TBARS) assay. Oxidative stress on tissues leads the formation of highly unstable and reactive lipid peroxides which its decomposition from PUFAs results in the formation of malondialdehyde (MDA). The TBARS assay quantifies colorimetrically or fluorometrically the levels of MDA produced by these unstable peroxides and its usually used as a an indirectly measurement of oxidative stress damage. At the same time, the expression of antioxidant defense enzymes *Glutathione s-reductase (Gsr)*, *Catalase (Cat)*, and *Superoxide dismutase (Sod)* were measured to evaluate the kidney response to oxidative stress. TBARS assay showed an increased levels of MDA in kidneys of the HFD+Pol mice as it shows the *Figure 10 B*. Regarding the relative mRNA levels of antioxidant-defense genes, the data demonstrated a significant reduction in the relative down-regulation of *Gsr* expression and no significant changes in the expression of *Sod* and *Cat* in HFD-only mice (*Figure P10 A*). No significant changes neither with control mice nor HFD-only mice were detected in HFD + Pol mice.

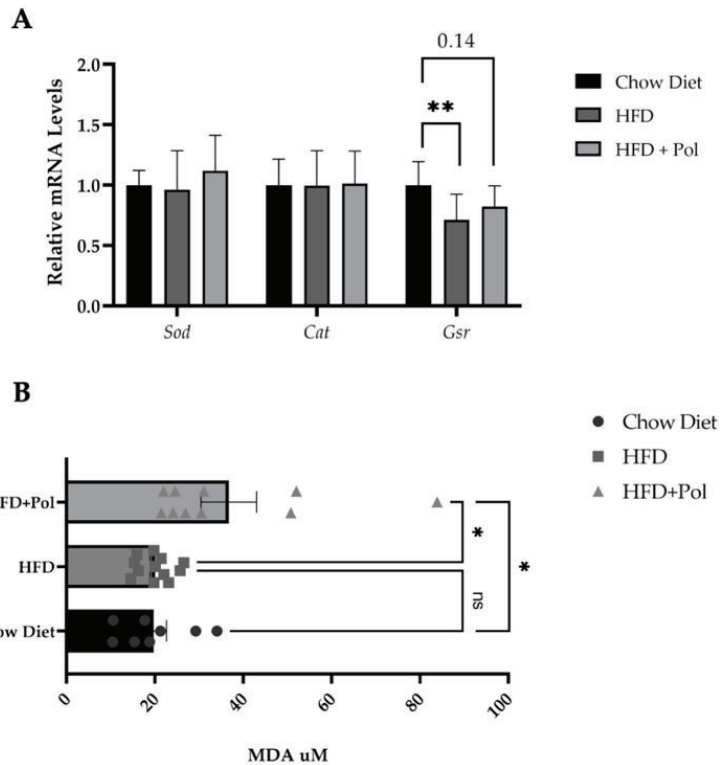


**Figure P10 –Polyphenol-supplemented HFD increases the oxidative stress markers but not modifies the gene expression of antioxidant defense enzymes.** (A) Relative mRNA levels of antioxidant defense enzymes. *Glutathione s-reductase (Gsr)*, *Catalase (Cat)*, and *Superoxide dismutase (Sod)*. (B) Malondialdehyde (MDA) levels in the kidneys of standard-chow-fed, HFD-only, and HFD+Pol mice measured fluorometrically by the TBARS assay. Data are presented as the mean  $\pm$  SEM. \*  $p < 0.05$ ; \*\*  $p < 0.01$ . The p-values were determined by using a one-way ANOVA test and a Tukey’s multiple tests correction. Chow Diet  $n = 8$ ; HFD = 11; HFD + Pol = 10.

### A.6) Polyphenol-supplemented HFD upregulates the expression of fibrosis and kidney damage markers.

The diagnosis of CKD implies certain parameters of involvement, such as certain levels glomerular filtration rate or structural kidney damage during a designed period as discussed in the introduction section. Prior to the development of CKD and the fulfillment of the diagnostic values, there are several key markers that assess the pathological onset and progression of kidney. In that sense, an expression profile of fibrosis and kidney injury markers were conducted on the kidneys of the different intervention groups. The results showed (Figure P11 A) an upregulation

on the HFD+Pol animals of the *Kidney injury molecule-1 (Kim-1)*, and an upregulation in the mRNA levels of the transcription factor *Carbohydrate-responsive element-binding protein  $\beta$  (ChREBP)*, the increase of which has been related to the progression of diabetic kidney(379). At the same time, an upward trend on the gene expression of the glycoprotein *Osteopontin (Opn)* was observed on supplemented mice. Osteopontin is a pleiotropic protein with multiple function also found in kidneys playing an important role in mineralization and bone resorption but in turn involves on the regulation of immunity and inflammation, angiogenesis, and apoptosis(380). Recent studies demonstrated the association of osteopontin and the pathogenesis of renal failure(381). Parallely, an upward trend was detected in the expression of *Fibronectin* gene, whose codified protein is related to the fibrotic processes(382,383).

Kidneys of the HFD+Pol mice also exhibited a significant upregulation of *Len2*. It is known that LCN2 circulating levels increase under different pathological states, particularly kidney injury, bacterial infection, and inflammation as well as on obesity and ageing(172,384,385). LCN2 is a biomarker for the development of renal injury, and it is considered an acute phase protein when upregulated in the kidney tubules. Circulating serum levels of LCN2 were also measured (*Figure P11 B*) and despite no significant results a clear upward trend was observed on HFD+Pol mice.

In summary, our results indicate that mice supplemented with polyphenols show a pathological kidney expression profile, with an increase in fibrosis and damage markers. To go deeper in the fibrotic profile of the kidneys histological analyses were performed. As the histological analysis was not previously planned, the samples were freeze and some of them were not able to be used. Even so, the most well-conserved were stained and analyzed. Kidney sections from polyphenol supplemented animals showed a larger size of glomerulus and a wider surface area of fibrotic tissue (*Figure P12 C*). Interestingly as discussed in the introduction section on HFD-pernicious role, a change was also observed in the glomerulus of the HFD-only animals (*Figure P12 B*), with some slight increase in the tuft area and a light increase in fibrosis areas but not as much as the evident glomerulonephritis of the supplemented mice.

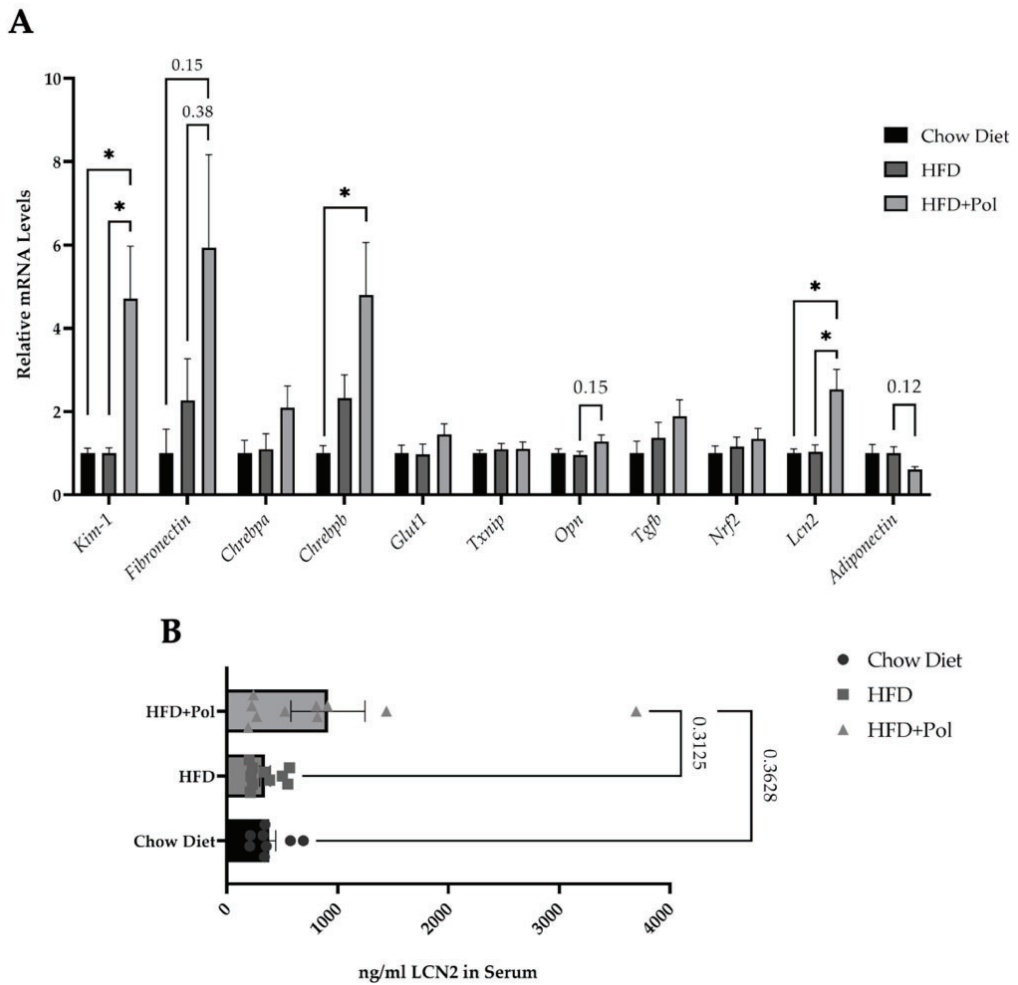


**Figure P11 – Polyphenol-supplemented HFD upregulates the expression of fibrosis and kidney-damage markers.** (A) Relative mRNA levels of several fibrosis, oxidative stress, and kidney damage markers. *Kidney injury molecule-1 (Kim-1)*, *Fibronectin*, *Carbohydrate-responsive element-binding protein b (Chrbpb)*, *Glucose transporter-1 (Glut1)*, *Thioredoxin-interacting protein (Txnip)*, *Osteopontin (Opn)*, *Transforming growth factor beta-1 (Tgfb)*, *Nuclear factor erythroid 2-related factor 2 (Nr2)*, *Lipocalin 2 (Lcn2)* and *Adiponectin*. (B) Protein circulating levels of LCN2 measured by an ELISA assay in serum. Data are presented as the mean  $\pm$  SEM. \*  $p < 0.05$ . The p-values for the ELISA assay and *Glut1*, *Txnip*, *Opn*, *Tgfb* and *Nr2* genes were determined by using a one-way ANOVA test and Tukey's multiple tests correction. For genes showing different variances like *Kim-1*, *Fibronectin-1*, *Chrbpa*, *Chrbpb*, *Lcn2* and *Adiponectin* a one-way ANOVA with Brown-Forsythe, Welch's correction and a Dunnett's comparisons tests were performed. Chow Diet  $n = 8$ ; HFD = 11; HFD + Pol = 10.



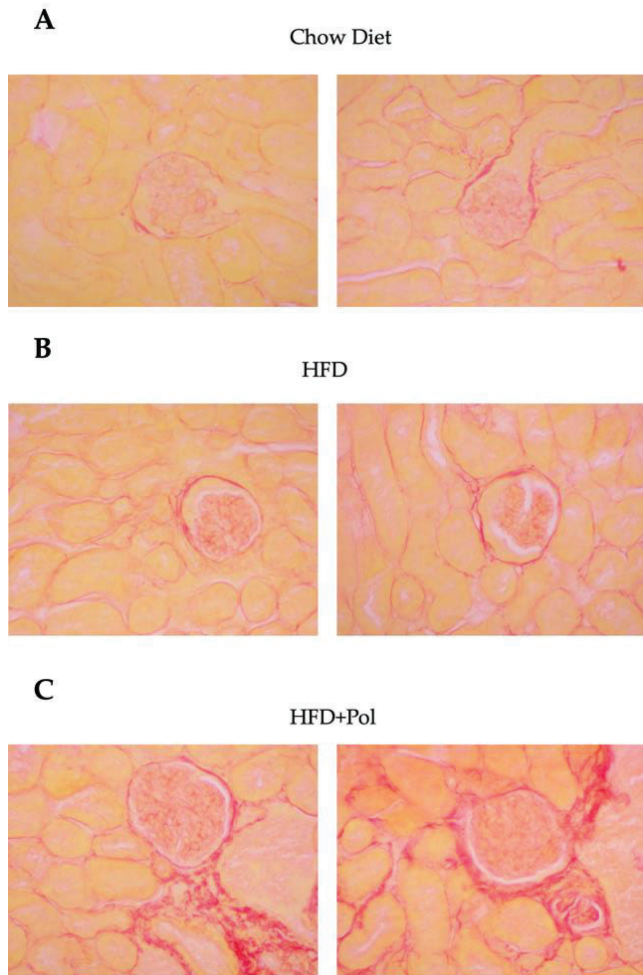
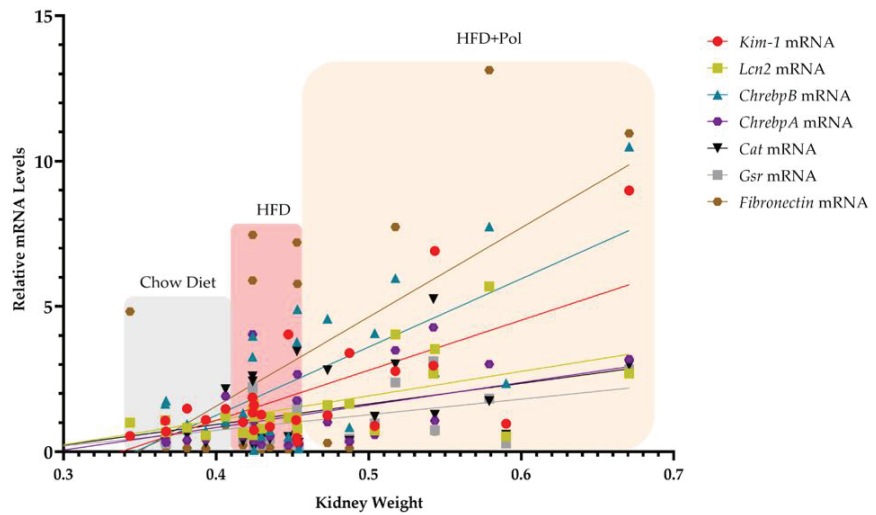


**Figure P12 – Polyphenol-supplemented HFD increased the size of glomerulus as well as the fibrosis process.** (A)(B)(C) Picrosirius red-stained images of kidney sections from chow diet, HFD and HFD+Pol mice respectively at 40x of magnification. In each image, a centrally delimited glomerulus is shown. In case of Chow Diet animals, no abnormalities in terms of fibrosis were observed. Although on animals fed with a HFD, a slight increase in fibrotic tissue and a larger size of the TUFT area could be observed. The increase in fibrosis is very subtle, since the increase of the red color is very weak. Concerning the TUFT area, which is the space between the interior of the glomerulus and its capsule, especially in the second image B it is more perceptible. Therefore, it is corroborated that HFD-consumption has an implication on damaging renal tissues. In case of supplemented mice these changes increase drastically leading to a larger glomerulus size and a much greater involvement of fibrotic tissue. A total of 8 duplicated and randomized photographs per group were analyzed.

As it showed (*Figure P2*), one of the initial signs of possible kidney impairment was the increase in tissue weight on the supplemented mice. As has been described in the literature, kidney weight gain may suggest a pathological involvement although this is not always the case. In HFD+Pol mice, the weight increase was accompanied by a fibrotic and kidney damaged gene expression profile. In this way, a Pearson correlation was performed between the actual renal damage expression profile and the tissue weight in order to verify if any linkage existed. Shown on *Figure P13* a clear and proportional relationship is found between kidney weight and expression of genes related to kidney injury. Interestingly, this relationship is not only seen on the supplemented mice. HFD-only mice kidneys also showed a proportional damaged gene expression profile according to the tissue weight but far less considerable. Therefore, there is a proportional correlation between tissue weight and the expression profile of renal damage markers.



	<i>Kim-1</i>	<i>Lcn-2</i>	<i>ChrebpB</i>	<i>ChrebpA</i>	<i>Cat</i>	<i>Gsr</i>	<i>Fibronectin</i>
<b>r</b>	0,6785	0,5659	0,7117	0,4751	0,4293	0,4810	0,4904
<b>R squared</b>	0,4604	0,3203	0,5066	0,2258	0,1843	0,2314	0,2405
<b>P-Value (two-tailed)</b>	0,001 (***)	0,0021 (**)	0,0001 (****)	0,0142 (*)	0,0254 (*)	0,0129 (*)	0,0081 (**)

**Figure P13– Correlation between kidney tissue weight and the expression profile of genes related to kidney damage.** Relative mRNA levels of several fibrosis, oxidative stress, and kidney damage markers. *Kidney injury molecule-1 (Kim-1)*, *Fibronectin*, *Carbohydrate-responsive element-binding protein b (Chrebpb)*, *Carbohydrate-responsive element-binding protein a (ChrebpA)*, *Catalase (Cat)*, *Glutathione s-reductase (Gsr)* and *Lipocalin 2 (Lcn2)* versus the kidney weight. The relative expression of these genes was plotted according to the corresponding animal kidney weight and its intervention group. A Pearson correlation was performed for kidney weight vs. each relative mRNA gene expression of all animals of the intervention groups (Chow Diet n=8; HFD=11; HFD+Pol=10). The p-values were determined by using Person correlation assuming Gaussian distribution with two tails and a confidence interval of 95%.





## **B) Effects and molecular mechanisms underlying a *Rosa canina* flesh supplementation against a high fat diet-induced obesity and NAFLD.**

From the earliest evidence written by the Sumerians about 5000 years ago, through the usage of Egyptians, ancient China, Roman Empire and even written in the Talmud scriptures, the connection between man and his search for medicine in nature is undoubted(386). Nowadays, modern science has recognized the active actions of plants and fruits and has included it in contemporary therapies, either by extracting the responsible bioactive compounds or by the nutritional supplementation of the vegetable itself. One of the plant families whose usage is repeated throughout time and across societies are the Rosaceae. As mentioned in the introduction section, its pseudo-fruit rosehip contains not only interesting bioactive compounds but also a wide variety and a highly concentrated profile. One of the main Rosaceae species, *Rosa canina*, has emerged as a major source of relevant compounds in the treatment of metabolic diseases such as obesity, T2DM and NAFLD. There is some bibliography supporting the therapeutic effect of the *Rosa canina* on different pathologies although the intervention format and the described underlying described mechanisms are variable. In addition, there is still no updated characterization of the different compounds that are the backbone of the beneficial effects of *Rosa canina*. At the same time there is still not enough bibliography covering all the multiple benefits and mechanisms of *Rosa canina* against metabolic diseases such as NAFLD.

To study the effects and molecular mechanisms underlying a rich natural source of bioactive compounds, concretely *Rosa canina* flesh supplementation, against a high fat diet-induced obesity and NAFLD (aim 2), a dietary intervention with *Rosa canina* flesh was performed on normoglycemic C57BL/6 4-weeks old male mice fed with a 45% HFD for 18 weeks (see the nutritional intervention protocol in the Methodology 3.5.3 section of this thesis proposal).

Furthermore, to characterize the *Rosa canina* flesh and its different fractions and study the anti-obesogenic potential of their different constituents (aim 3), different experiments have been performed in Hepg2 and 3T3L1 cell cultures as well as a characterization by HPLC-Orbitrap techniques of the different fractions of *Rosa canina* flesh in collaboration with Dr. Lamuela-Raventos' Natural Antioxidants research group. *Rosa canina* characterization and results from cell culture procedures are presented in results section C.

**B.1) *Rosa canina* flesh exerts a preventive effect on the HFD-induced obesity from the first week of nutritional treatment without causing any change in mice's food intake.**

The typical weight gain produced by a HFD consumption was progressively suppressed in the RC-supplemented mice from the first week of the flesh treatment (*Figure R1 A*). Already in the first 7 days of the intervention, a significant decrease in weight gain was observed on the RC-supplemented C57BL6/J mice (*Figure R1 B*). This significant weight difference between groups was maintained until the end of the experiment (*Figure R1 C and D*). During the intervention there were no changes in the food intake of the C57BL6/J mice; the caloric intake of both groups was practically identical (*Figure R1 E*). Moreover, the weight gain per kcal ingested was significantly lower in the flesh-supplemented mice (*Figure R1 F*).

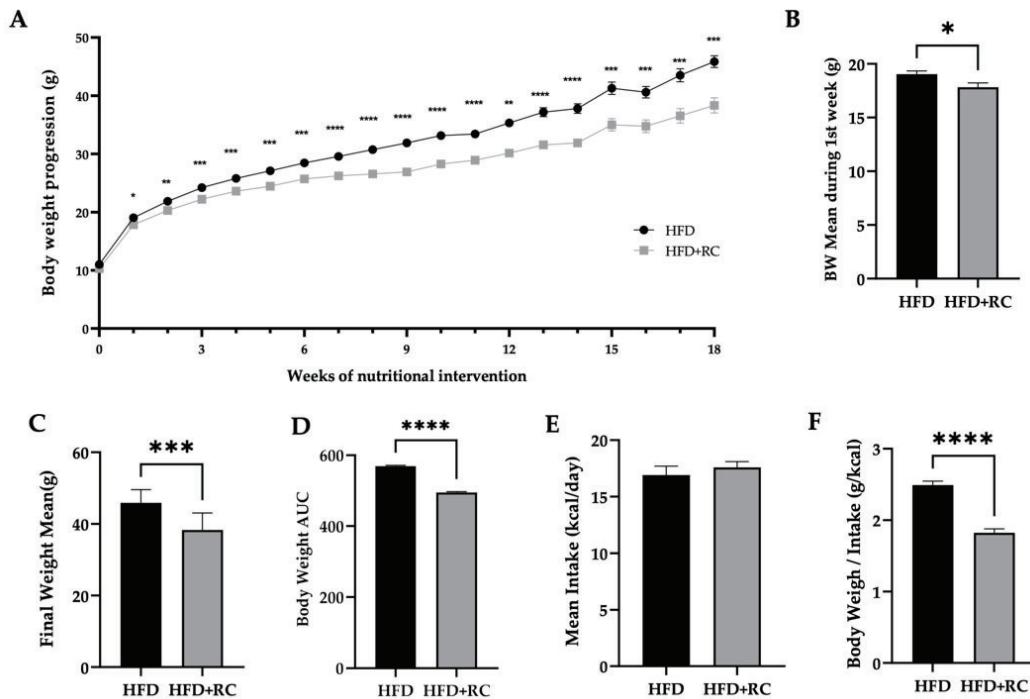


**Figure R1—*Rosa canina* dietary supplementation significantly reduces the weight gain produced by a HFD with no changes in food intake.** (A) Body weight progression (g) over the 18-week intervention based on twice-weekly weightings. The graph represents the mean  $\pm$  SEM of weekly weights in both experimental groups. (B) Body weights mean (g) on the first week of nutritional intervention. (C) Total body weight in grams after 18-week intervention. Both (B and C) graphs represent the mean  $\pm$  SEM of the total body weight in both experimental groups. (D) Area Under the Curve over the 18-week weight monitorization. The graph represents the mean  $\pm$  SEM of the AUC of weights in both experimental groups. (E) Mean daily

food intake (kcal/day) over the 18-week intervention. The graph represents the mean  $\pm$  SEM of the total kcal per day. (F) Final body weight (g) related to calorie intake (kcal). The graph represents the mean  $\pm$  SEM of the total body weight per kcal ingested. Calorie intake was calculated based on the energy density of the 45% HFD (D12451, Research Diets) plus the kcal from *Rosa canina* flesh and the amount of food consumed daily. Data are presented as means  $\pm$  SEM. \*  $p < 0.05$ ; \*\*  $p < 0.01$ ; \*\*\*  $p < 0.001$ ; \*\*\*\*  $p < 0.0001$  and  $p$ -values were determined by using a two-tailed unpaired Student's T-test. HFD=13, HFD+RC=13.

In this sense, the anti-obesogenic effect of *Rosa canina* is demonstrated by slowing down weight gain progression, as reported in the bibliography(331). It should be noted that the consumption of the supplemented animals is not altered even with the slight caloric increase provided by the flesh supplementation.

### **B.2) *Rosa canina* flesh supplementation significantly alleviates the hyperglycemia state caused by HFD consumption as well as its associated insulin resistance.**

Dietary intervention with a HFD produces a disruption in animals resulting in a glucose intolerance and an insulin resistance-state, both characteristics of obesity, since the first weeks of consumption. In *Rosa canina* supplemented mice, this typical obese imbalance occurs to a significantly lesser extent, resulting in a better response to glucose and insulin. Specifically, in either 14<sup>th</sup> week glucose tolerance test (GTT) (Figure R2 A) or 15<sup>th</sup> week insulin tolerance test (ITT) (Figure R2 C), the supplemented mice displayed a significantly better glucose curve with a significant difference in four of the five corresponding measurements and in both areas under the curves (AUC) (Figure R2 B and D). In both tolerance tests, a general proportional decrease of the whole glucose curve is observed, and specifically in the GTT, there was a clear improvement in the recovery phase with a marked accentuation of the final glucose curve slope (Figure R2 A).

Regarding basal glucose, a mouse is considered to be in a diabetic state within fasting blood glucose levels around 150-300mg/dl according to the bibliography(387). In *Rosa canina* intervention group these levels are significant lowered (Figure R2 E). Therefore, these results prove the relevant anti-diabetic role of the *Rosa canina* against the HFD-induced obesity progression.

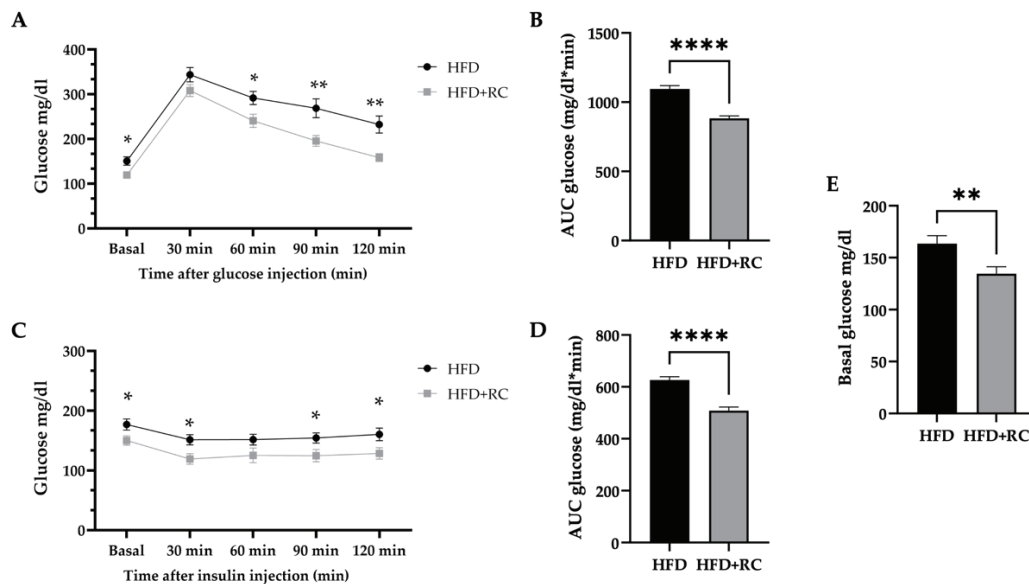


**Figure R2– *Rosa canina* flesh supplementation improves glucose and insulin response and reduces the hyperglycemic state associated with the consumption of an HFD.** (A) Plasma glucose levels after intraperitoneal administration of glucose (1.5 g/kg body weight) corresponding to a glucose tolerance test (GTT) at 14<sup>th</sup> week of nutritional intervention. (B) AUCs of the plasma glucose levels related to the 14<sup>th</sup> week GTT. (C) Plasma glucose levels after intraperitoneal administration of insulin (0.75 UI/kg body weight) at 15<sup>th</sup> week of nutritional intervention. (D) AUCs of the plasma glucose levels related to the 15<sup>th</sup> week IIT. (E) Fasting blood glucose levels after 6 hours of fasting in the two glucose and insulin tests. Data are presented as the mean  $\pm$  SEM. \*  $p < 0.05$ ; \*\*  $p < 0.01$ ; \*\*\*  $p < 0.001$ ; \*\*\*\*  $p < 0.0001$ . The  $p$ -values for each analysis were determined by using a two-tailed unpaired Student's T-test. HFD=13, HFD+RC=13.

### **B.3) WAT from *Rosa canina* flesh-supplemented mice is thinner and show smaller adipocytes in the scWAT compared to the HFD-fed ones.**

As stated in the introduction section, one of the first features of obesity is the WAT loss of functionality. Specifically, the process of hypertrophy firstly occurs in the fat-overloaded adipocytes such as it happens on the intervention mice fed with an HFD. Conversely to the HFD-only, WAT from mice supplemented with *Rosa canina* flesh exhibited a significant less tissue weight and in turn, scWAT showed smaller adipocytes (Figure R3 A and B). These results suggest that scWAT from supplemented mice displayed less hypertrophy and a more physiological hyperplasia. The difference in the number and size of adipocytes is evidenced in the histological sections of scWAT (Figure R3 D, E, F and G, H, I). This phenotypic change on adipocytes is also accompanied by a significant change in the expression of the lipid droplet fusion-related key

gene *Fsp27 $\alpha$* . As stated in the introduction, FSP27 $\alpha$  and CideA form a homodimer between contacting lipid droplets thereby mediating the fusion of a single unilocular LD. In scWAT of *Rosa canina* supplemented mice, *Fsp27 $\alpha$*  expression was significantly lower than on HFD-only mice, therefore matching the expression profile with the phenotypic shift (Figure R3 C, F, and I). No changes in *Fsp27 $\beta$*  expression were detected

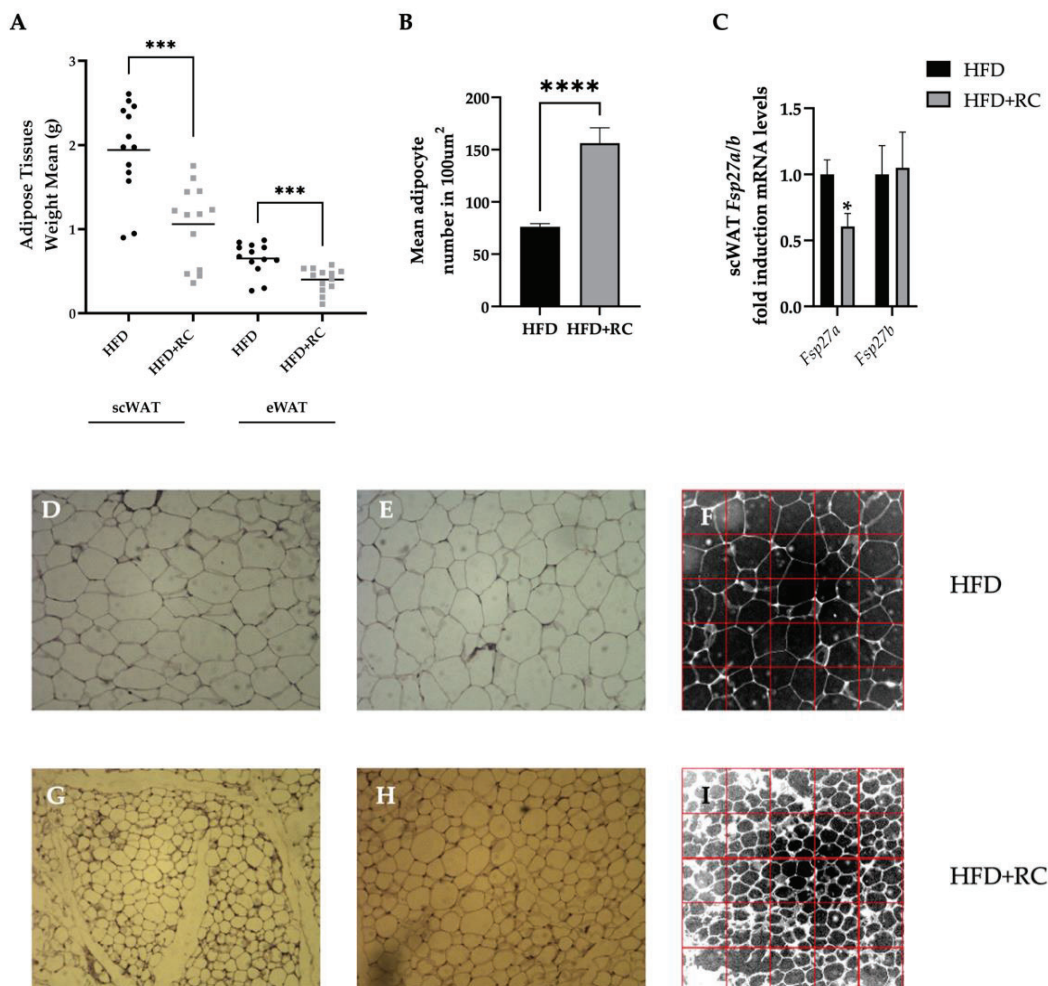


**Figure R3–** scWAT from *Rosa canina* flesh supplemented mice exhibited a significantly better response to a HFD than scWAT from mice fed with an HFD. (A) Average weight of scWAT and eWAT fresh tissue measured on the precision balance before snap-freezing process in liquid nitrogen. (B) Adipocyte mean number in 100µm<sup>2</sup> of the H&E histological scWAT samples. (C) Relative mRNA levels of *Fsp27 $\alpha$*  and *β*. Data are presented as the mean ± SEM. \* p < 0.05; \*\* p < 0.01. \*\*\* p < 0.001; \*\*\*\* p < 0.0001. The p-values for each analysis were determined by using a two-tailed unpaired Student's T-test. HFD=13, HFD+RC=13. (D)(E)(G)(H) Hematoxylin eosin-stained scWAT sections captured at 10x magnification. A

total of 8 duplicated and randomized photographs per group were analyzed. (F) Hematoxylin eosin-stained scWAT sections of 100um X 100um converted into computer generated binary representations. Images captured at 10x magnification

**B.4) A significantly decrease on lipid transport, lipogenesis, TG synthesis, and an upward trend of browning process is exhibited on scWAT of *Rosa canina* supplemented mice.**

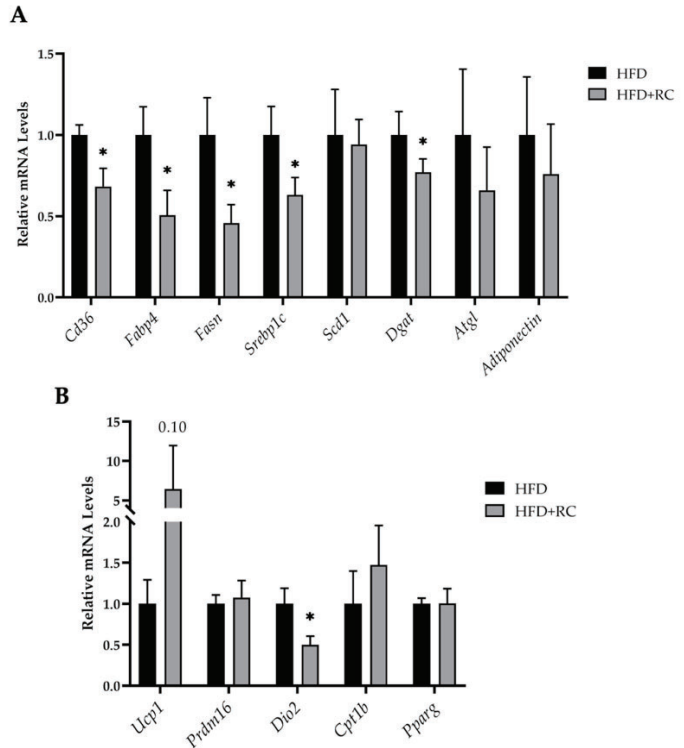
Regarding the gene expression profile of the scWAT, significant relevant differences were observed between supplemented and HFD-only animals. The scWAT of *Rosa canina* animals exhibited a lower fatty acids transport, with a significant decrease in the expression of both the *Cd36* and *Fabp4* transporter genes (Figure R4 A). At the same time, a reduction in the expression of the key gene in fatty acid synthesis *Fasn* was also observed in the scWAT of supplemented animals (Figure R4 A). Parallely, the transcription factor *Srebp1c* involved in the regulation of genes required for glucose metabolism and fatty acid and lipid production was also decreased significantly (Figure R4 A). Concerning triglyceride synthesis, animals supplemented with *Rosa canina* flesh had a significant decrease in the *Dgat* gene which is a key player in this pathway (Figure R4 A). However, no changes were observed in the expression of the *Scd1* gene, which limits the rate of FA formation of monounsaturated fatty acids, nor in the key lipolysis gene *Atgl*. Finally, the expression of the gene encoding the cytokine *adiponectin* was also assessed, and in this case no differences were observed in the scWAT (Figure R4 A).

Moreover, genes involved in the browning process were evaluated. A relevant marked trend on the overexpression of *Ucp1* was observed on the scWAT of supplemented mice. The large dispersion among animals influences the non resolutive statistics (Figure R4 B). From the other genes involved with the browning process that was analyzed, only a decrease in *Dio2* was observed (Figure R4 B). Therefore, gene expression profile of the scWAT of the supplemented animals, indicates a decrease in lipid transport, a decrease in fatty acid and triglyceride synthesis and a partial trend in the browning process.

**Figure R4 – scWAT from supplemented mice exhibit a significant decrease on lipid transport, lipogenesis, and an upward trend on browning process.** (A) Relative mRNA levels of different key genes of lipid metabolism of adipose tissue. *Cd36* (Platelet glycoprotein 4), *Fabp4* (Fatty acid binding protein 4), *Fasn* (Fatty acid synthase), *Srebp1c* (Sterol regulatory element-binding transcription factor 1), *Scd1* (Stearoyl-CoA desaturase), *Dgat* (Diacylglyceride acyltransferase), *Atgl* (Adipocyte triglyceride lipase) and *Adiponectin*. B) Relative mRNA levels of different key genes of thermogenesis, browning and fatty acid oxidation. *Ucp1* (Uncoupling protein 1), *Dio2* (Iodothyronine deiodinase 2), *Prdm16* (Histone-Lysine N-Methyltransferase), *Cpt1b* (Carnitine palmitoyl transferase 1B) and *Pparg* (Peroxisome Proliferator Activated Receptor Gamma). Data are presented as the mean  $\pm$  SEM. \*  $p < 0.05$ ; \*\*  $p < 0.01$ . \*\*\*  $p < 0.001$ ; \*\*\*\*  $p < 0.0001$ . The p-values for each analysis were determined by using a two-tailed unpaired Student's T-test. HFD=13, HFD+RC=13.

**B.5) *Rosa canina* supplementation enhances the thermogenic and mitochondrial biogenesis markers on BAT.**

One of the effects that have been attributed to some phytochemicals is the ability to stimulate the WAT browning process and activate BAT(388). Although the key *Ucp1* gene was not overexpressed significantly on *Rosa canina* supplemented mice, a clear upward trend was shown (Figure R5 B). Regarding other genes related to thermogenesis process, a significant increase on mRNA levels of *Dio2*, *Prdm16*, and the key regulator *Pparg* was observed (Figure R5 B). In addition, the results showed a significant overexpression of the *Pgc1a* gene that is related to mitochondria function and biogenesis. Therefore, even if there is no change on the lipid oxidation related gene *Cpt1a*, the other genes linked to thermogenic activity are increased. Finally, the results indicate there was no differences between BAT weights (Figure R5 A).





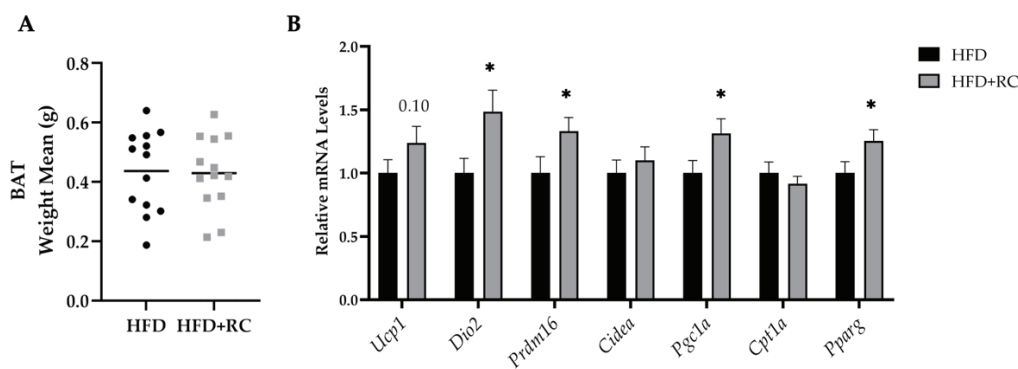


**Figure R5 – BAT from supplemented mice didn't exhibit any change on tissue weight but an activation of thermogenesis is showed on mRNA expression profile.** (A) Average weight of BAT fresh tissue measured on the precision balance before snap-freezing process in liquid nitrogen. (B) Relative mRNA levels of different key genes of thermogenesis, mitochondrial biogenesis, and fatty acid oxidation. *Ucp1* (Uncoupling protein 1), *Dio2* (Iodothyronine deiodinase 2), *Prdm16* (Histone-Lysine N-Methyltransferase), *Cidea* (Death-inducing DNA fragmentation factor-like effector A), *Pgc1a* (Peroxisome Proliferator-Activated Receptor Gamma Coactivator 1 Alpha), *Cpt1a* (Carnitine palmitoyl transferase 1A) and *Pparg* (Peroxisome Proliferator Activated Receptor Gamma). Data are presented as the mean  $\pm$  SEM. \*  $p < 0.05$ ; \*\*  $p < 0.01$ . \*\*\*  $p < 0.001$ ; \*\*\*\*  $p < 0.0001$ . The p-values for each analysis were determined by using a two-tailed unpaired Student's T-test. HFD=13, HFD+RC=13.

### B.6) Livers of the supplemented animals show a healthier condition exhibiting a lower tissue weight, a decreased amount of oxidative stress and a diminished gene expression of *Tnf $\alpha$* .

Liver is a key tissue in maintaining lipid and glucose homeostasis due to its crucial role in regulating metabolism. Prior to the gene expression profile study, different parameters were analyzed to determine the general hepatic state. Firstly, weights of fresh tissue were evaluated, showing a significant decrease in the supplemented animals (Figure R6 A). On the other hand, a quantification of the MDA by-product of lipid peroxidation produced by oxidative stress was also performed. In this case livers from supplemented mice showed a significative lower production of MDA (Figure R6 B). Finally, expression of the gene encoding major player of inflammatory processes TNF $\alpha$  was assessed also showing a significant decrease in the supplemented-mice livers (Figure R6 C). Thus, in general terms, the livers of mice supplemented with *Rosa canina* flesh exhibited a healthier status with a significantly lower tissue weight, a decrease in the oxidative stress marker MDA and finally a lower expression of the gene marker TNF $\alpha$  characteristic of inflammatory processes.

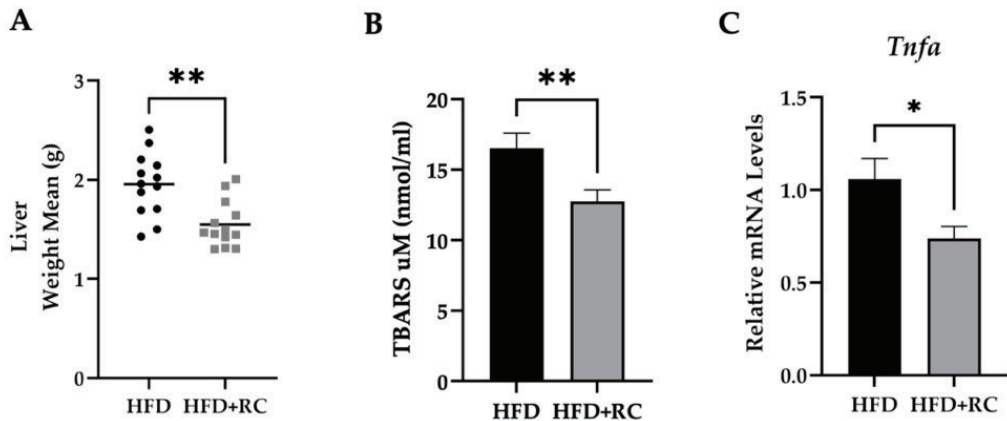


**Figure R6 – Livers from supplemented mice showed a lower tissue weight, a reduction of lipid peroxidation produced by oxidative stress and less gene expression of the inflammation marker *Tnfa*.** (A) Average weight of liver fresh tissue measured on the precision balance before snap-freezing process in liquid nitrogen. (B) MDA levels in pulverized livers of HFD, and HFD+RC mice measured fluorometrically by the TBARS assay. (C) Relative mRNA levels of *Tumor necrosis factor alpha* (*Tnfa*). Data are presented as the mean  $\pm$  SEM. \*  $p < 0.05$ ; \*\*  $p < 0.01$ . The p-values for each analysis were determined by using a two-tailed unpaired Student's T-test. HFD=13, HFD+RC=13.

**B.7) *Rosa canina* supplemented animals showed a significant shift in the hepatic expression of genes involved in lipid droplet formation.**

According to the introduction section, there are multiple genes that regulate the formation of lipid droplets. As discussed previously, the direct target gene of PPAR $\gamma$ , *Fsp27*, is highly involved in the promotion of lipid droplet growth and TAG storage. Specifically, *Fsp27* $\beta$  was found to be upregulated in the context of fatty liver and specifically reported in both rodent and human models of diet-induced obesity and steatohepatitis(138). In this sense, it has been corroborated that down-regulation of *Fsp27* $\beta$  in steatotic liver tissue resulted in lower accumulation of hepatic TAG and lipid droplets(389). Perilipin-1 (PLIN-1), another scaffold protein located on the surface of LDs, has also been shown to be of great relevance on NAFLD. Its main function is to control the access to stored TAGs by facilitating access of lipases to the LDs and orchestrating protein interactions(390). Depending on the state of the organism, PLIN-1 either limits the entry of lipases to stored TAGs or facilitates their entry and promotes lipolysis.

In case of livers from mice supplemented with *Rosa canina*, it was observed that beta isoform of *Fsp27* key gene of lipid droplet formation was significantly reduced compared to the HFD-only animals (Figure R7 A). In accordance with this previous data, the mRNA levels of *Plin-1* were increased significantly in the *Rosa canina* group (Figure R7 B). These changes were consistent with the observations of the histological hepatic sections. Based on the images collected from the hematoxylin-eosin staining and using binary computer processing it was possible to differentiate the lipidic droplet formations between groups. As can be clearly noticed in the inverted binary images, there are remarkable differences between the hepatic LDs of the two groups (Figure R7 C and D). In the case of Figure R7 C image corresponding to a HFD liver, large and delimited LDs are clearly observed with a major surface area. In contrast, in Figure R7 D corresponding to a liver supplemented with *Rosa canina*, the LDs are no longer perceptible and become blurred due to their large number and small size.

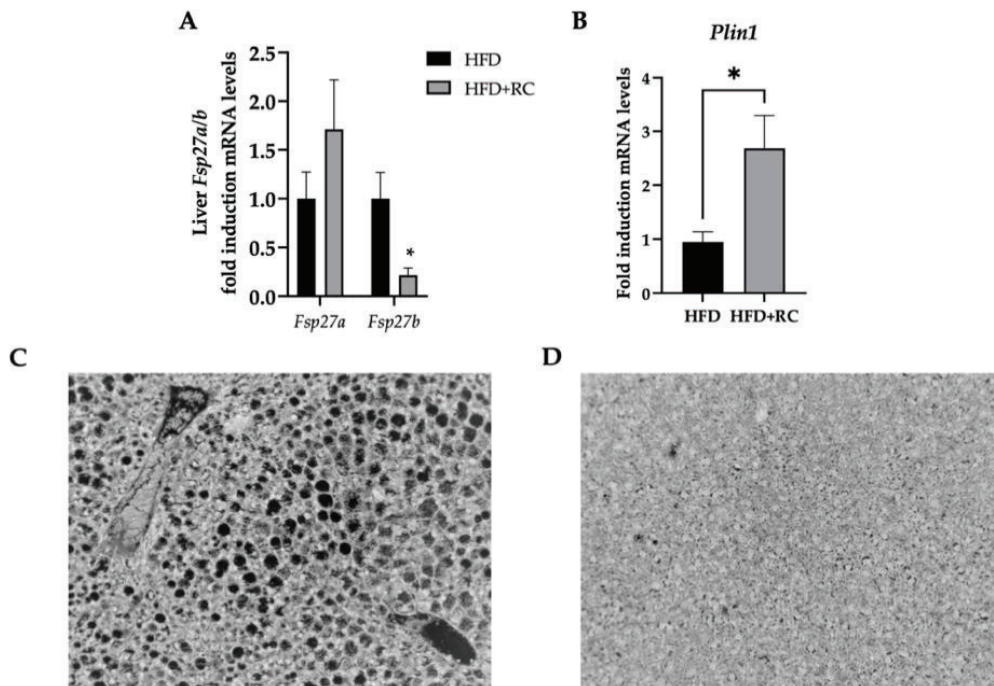
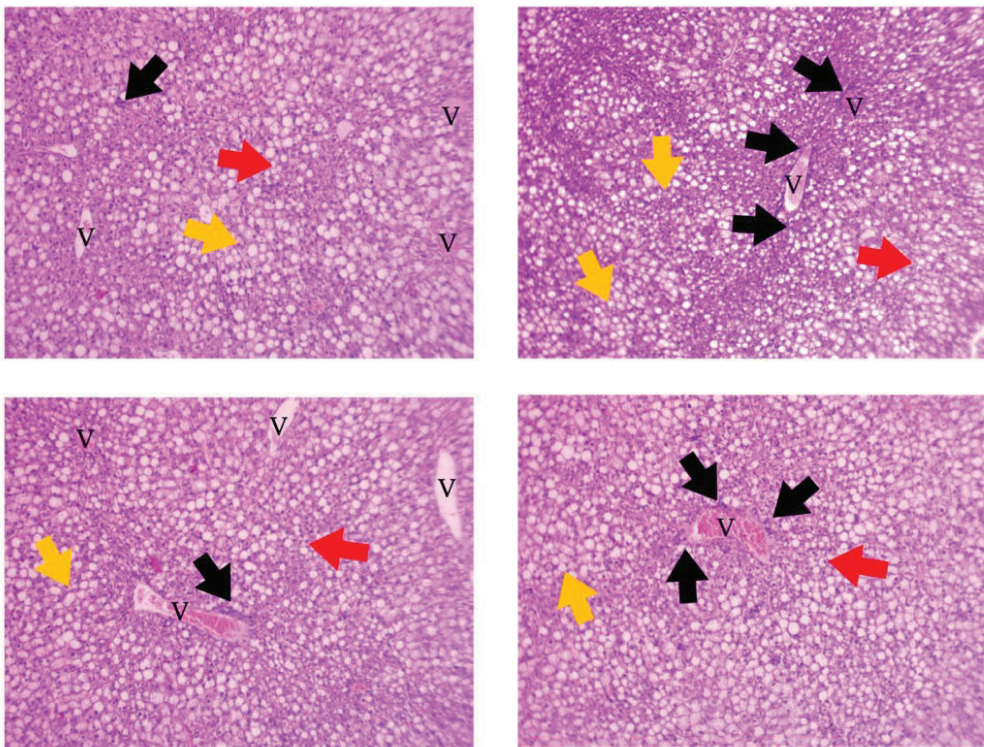


**Figure R7 – Livers from supplemented mice exhibited a lower amount of lipid droplets and lipid accumulation.** (A) Relative mRNA levels of levels of *Fsp27*  $\alpha$  and  $\beta$ . (B) Relative mRNA levels of *Perilipin-1* (*Plin1*). Data are presented as the mean  $\pm$  SEM. \*  $p < 0.05$ ; \*\*  $p < 0.01$ . The  $p$ -values for each analysis were determined by using a two-tailed unpaired Student's T-test. HFD=13, HFD+RC=13. (C)(D) Hematoxylin eosin stained HFD and HFD+RC respectively liver sections conversed into computer generated inverted binary representations. Black color indicates the lipidic parts of the cell and the white ones the rest. Randomized images captured at 10x magnification.

**B.8) Liver sections exhibited a prominent reduction on ballooning, steatosis, and infiltration of immune cells in the *Rosa canina* supplemented mice.**

As explained in the introductory section, NAFLD covers a compendium of different pathologic phases, which are easily differentiated in the histological analyses. After the *Rosa canina* intervention, it was observed that HFD-only animals suffered not only from severe steatosis but also from generalized ballooning, constriction of the hepatic veins and infiltration of immune cells in the areas near the blood vessels (*Figure R8 A*). Thus, it is evidenced the pernicious character of HFD in liver, capable of leading to hepatic disease. This severe HFD-associated NAFLD state was not observed in the supplemented mice. Livers from *Rosa canina* animals displayed only few isolated lipid vacuoles and slight ballooning process in some individuals on isolated liver regions (*Figure R7 B*). In addition, less constriction was observed at the venous level and no infiltration of immune cells (*Figure R7 B*). Hence, it is observed that the typical damage produced by HFD, which conforms the NAFLD state, was significantly mitigated in the supplemented mice.

**A**





**B**

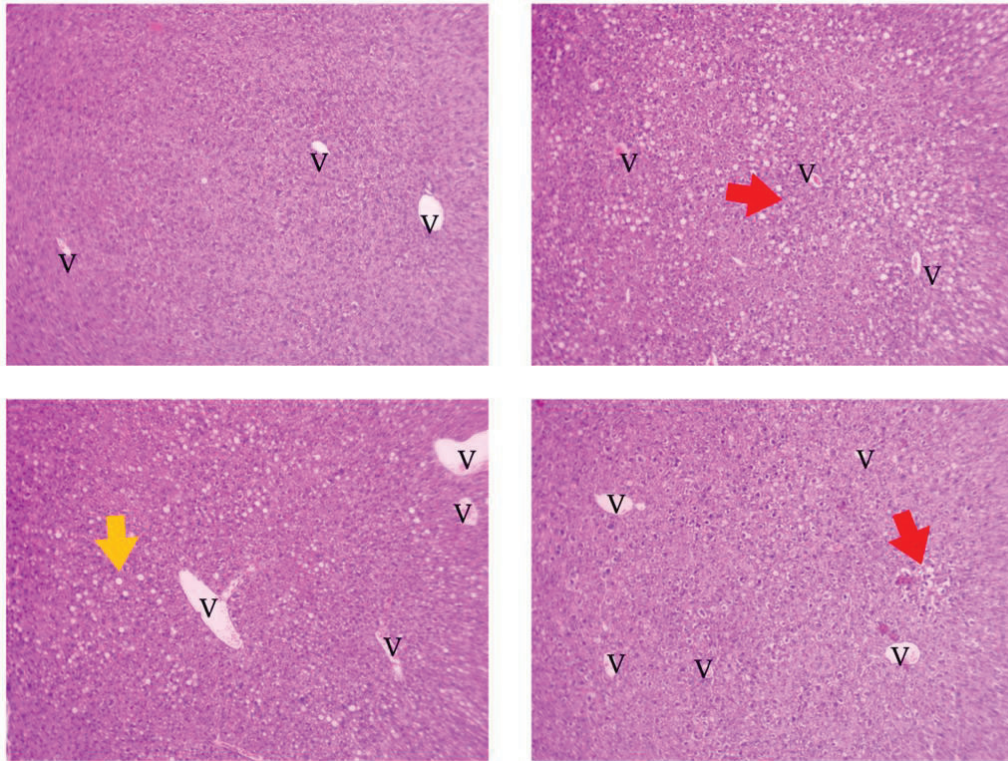


**Figure R8–** Livers from supplemented mice showed less steatotic hepatic tissue, with a reduction cellular and venous involvement and no immunity cell infiltration. (A) Hematoxylin eosin-stained liver sections of HFD-only animals images captured at 10x magnification. A generalized ballooning process (ex. red arrow), constricted veins (V), infiltration of mononuclear immune cells (ex. black arrow) and a severe steatosis (ex. yellow arrow) are exhibited. A total of 8 duplicated and randomized photographs were analyzed. (B) Hematoxylin eosin-stained liver sections of HFD+RC animals images captured at 10x magnification. Partial constriction of the veins is observed but to a lesser extent compared to HFD-only animals. Regarding steatosis and ballooning on supplemented mice, are markedly reduced and only in isolated manner. A total of 8 duplicated and randomized photographs were analyzed.

### **B.9) FGF21 signaling is enhanced in livers from supplemented mice.**

As explained in the introduction section, FGF21 has demonstrate to play a key role on glucose and lipid metabolism, having homeostatic regulatory properties as well as thermogenic effects(165,166). On metabolic diseases such as obesity and T2DM, FGF21 increased signaling show the ability to increase energy expenditure, restore glycaemia and lipidic profile and in turn improve insulin resistance(165). In the context of NAFLD, a clear resistance to FGF21 on liver

is observed which leads to an increase in the uptake of fatty acids and a decrease in their utilization. In contrast, when FGF21 signaling is enhanced, this resistance is substantially reduced, thus decreasing fat accumulation in hepatic tissue, and increasing its utilization as energetic substrate(167). In mice supplemented with *Rosa canina* flesh, an improvement in FGF21 signaling was observed, first through a significant reduction in the expression of the *Fgf21* gene itself (Figure R9). Subsequently, a significant overexpression of its two coreceptors *Fgfr1* and *Fgfr4* was observed (Figure R9). On the other hand, there was an upward trend in the expression of *Egr1*, a downstream key-gene in the *Fgf21* pathway (Figure R9). Finally, a significant increase in the gene expression of the regulatory cytokine *Adiponectin*, described as a mediator of the metabolic effects of FGF21, was also observed (Figure R9) (391).

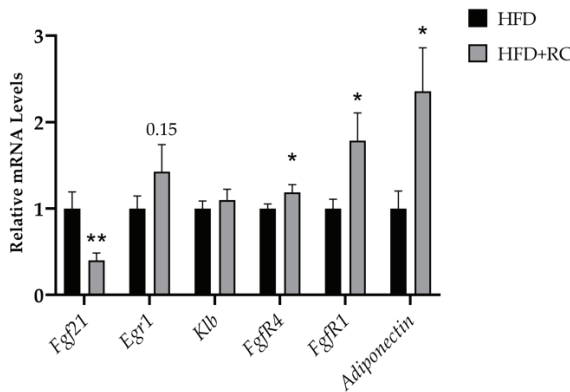


**Figure R9 – A significant improvement in FGF21 signaling and increased expression of the regulatory cytokine *Adiponectin* was observed in livers of supplemented animals.** mRNA levels of different key genes involved on FGF21 pathway. *Fgf21* (*Fibroblast growth factor 21*), *Egr1* (*Early growth response 1*), *Klb* (*Beta klotho*), *Fgfr1* (*Fibroblast growth factor receptor 1*), *Fgfr4* (*Fibroblast growth factor receptor 4*), *Adiponectin*. Data are presented as the mean  $\pm$  SEM. \*  $p < 0.05$ ; \*\*  $p < 0.01$ . The p-values for each analysis were determined by using a two-tailed unpaired Student's T-test. HFD=13, HFD+RC=13.

### B.10) Livers from supplemented mice, exhibited a decrease in the expression of genes such as *GluK*, *GlyK*, and *LpK*.

Although NAFLD is characterized by fat accumulation and an impairment in the hepatic lipid metabolism, glucose metabolism also plays a dramatic role in its pathophysiology. In case of mice supplemented with *Rosa canina* flesh, a significant decrease in limiting genes of the hepatic glycolysis process such as *GluK* (*Glucokinase*), *GlyK* (*Glycerol-kinase*) was detected (Figure R10). The function of *GlyK* is to convert glycerol to glycerol 3-phosphate and its isoform beta acts as a co-regulator of the hepatic glucose metabolism. At the same time *GlyK* up-regulates the expression of *Nr4a1* (*Nuclear receptor subfamily 4 group A1*) and thereby mediate *Nr4a1*-mediated expression of lipid metabolism related genes such as *Fasn*, *Acc*, *Srebp1c* and *Gpam*(392).

On the other hand, a significant decrease on *LpK* (*Pyruvate-kinase*) was also observed on *Rosa canina*-supplemented mice. High glucose/fat or insulin induce *LpK* and the other named genes, leading to direct stimulation of lipogenesis and thereby worsening the prognosis of the NALFD. Finally, a rising trend in the beta isoform of the transcription factor *Chrebp* was also observed on *Rosa canina*-supplemented animals. ChREBP mediates the glucose effect of both glycolytic and lipogenic gene expression and thus this transcription factor is a key determinant of lipid synthesis in the liver(393). Interestingly, no changes in the expression of genes involved in gluconeogenesis were observed.

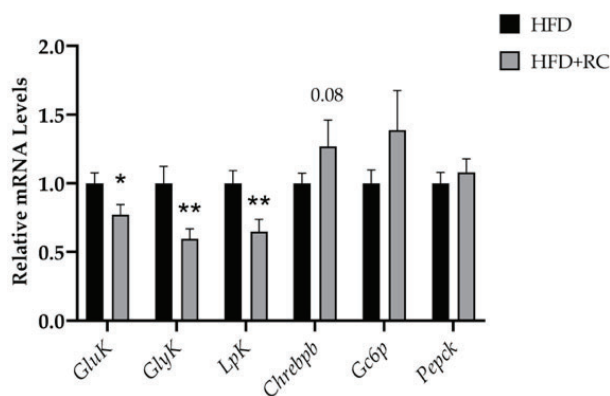


**Figure R10 – A reduction of gene expression related to hepatic glycolysis was observed in livers of supplemented animals.** Relative mRNA levels of different key genes involving glucose metabolism. *GluK* (*Glucokinase*), *GlyK* (*Glycerol-kinase*), *LpK* (*Pyruvate-Kinase*), *Chrebp* (*Carbohydrate response element binding protein b*), *G6p* (*Glucose 6-phosphatase*) and *Pepck* (*Phosphoenolpyruvate carboxykinase*). Data are presented as the mean  $\pm$  SEM. \*  $p < 0.05$ ; \*\*  $p < 0.01$ . The p-values for each analysis were determined by using a two-tailed unpaired Student's T-test. HFD=13, HFD+RC=13.

**B.11) Livers from supplemented mice displayed a decrease expression of genes involving lipid and cholesterol transport, lipogenesis, TAG synthesis, and an increase in peroxisomal oxidation ones.**

According to the bibliography, the main contributors to the NAFLD-related steatosis state on liver are firstly the excessive NEFAs flux from the overloaded adipose tissue and secondly the exacerbation of *de novo* lipogenesis. In this pathological scenario there is also a decrease in the hepatic oxidation of lipid substrates as well as an excess intake of fats from the diet. In the *Rosa canina* intervention study, both experimental groups were fed with an HFD for 18 weeks and therefore they suffered its pro-steatotic effects. However, in case of the supplemented mice, a generalized downregulation of genes related to fat accumulation in liver was observed. Firstly, a significant decrease in the gene expression related to fatty acid transport, such as *Cd36* and *Fabp4* was reported (*Figure R11 B*). Secondly, a downregulation in the expression of key genes of fatty

acid synthesis, such as *Fasn*, *Scd1* and *Acaca* was found (Figure R11 B). In parallel, livers from supplemented animals exhibited a significant decrease in the expression of the *Pltp* gene, related to cholesterol assembly and transport (Figure R11 B). On the other hand, triglyceride synthesis was also downregulated, with a significant drop in the expression of the key TG-synthesis gene *Dgat* (Figure R11 B). Interestingly, in the analysis of the hepatic gene expression profile, no changes in the transcription factor *Srebp1c* were found. In terms of oxidation processes, no changes were observed in the *Cpt1a* gene nor in the reference gene of mitochondrial biogenesis and oxidation *Pgc1a*. However, a significant increase in the expression of the gene related to peroxisomal lipid oxidation *Acox3* was observed in *Rosa canina* mice (Figure R11 A). Thus summarizing, livers from supplemented mice showed a slowing down NAFLD-state in comparison to HFD-only animals. Firstly, by a decrease in the transport of fatty acids, secondly by a reduction in *de novo* lipogenesis, thirdly by a decrease in the synthesis of triglycerides and finally by an increase in the peroxisomal oxidation of fatty acids. These substantial gene expression changes in the livers from supplemented mice are consistent with the phenotypes previously observed in histological analyses (Figure R7 C, D and R8 A, B).

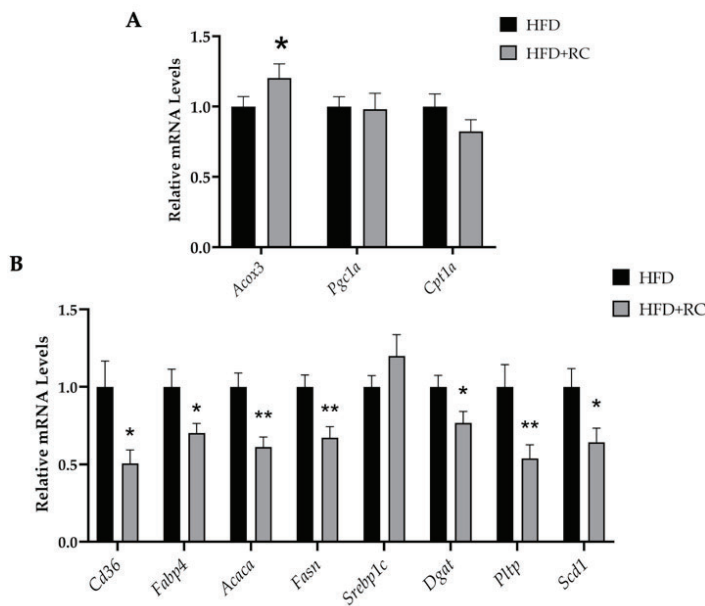


**Figure R11 – A reduction of gene expression related to lipid transport, FA, and TG synthesis as well as an increase of genes related to peroxisomal lipid oxidation was observed in livers from *Rosa canina* supplemented animals. (A) Relative mRNA levels of different key genes involving fatty acid oxidation and mitochondrial biogenesis. *Acox3* (*Acyl-Coenzyme A oxidase 3*), *Pgc1a* (*Peroxisome Proliferator-Activated Receptor Gamma Coactivator 1-Alpha*), and *Cpt1a* (*Carnitine palmitoyl transferase 1A*). (B) Relative mRNA levels of different key genes involving FA transport, lipogenesis process, triglyceride synthesis, and cholesterol transport and assembling. Data are presented as the mean  $\pm$  SEM. \*  $p < 0.05$ ; \*\*  $p < 0.01$ .**



**B.12) The expression of *Ppar delta* and *gamma* were regulated by *Rosa canina* flesh.**

As explained in the introduction, PPARs are nuclear receptors with pleiotropic actions. They are critical regulators not only of fatty acid metabolism, but also of glucose metabolism, inflammation, oxidative damage, fibrosis processes and in general energy metabolism(180). It is noteworthy to mention that the effects of *Rosa canina* against a HFD were similar to the outcomes of multiple *Ppara* $\alpha$ , *Ppar* $\beta/\delta$  and *Ppar* $\gamma$  agonistic/antagonistic studies. In addition, the observed modified gene profile of supplemented mice was in part downstream of the PPARs. In this way, gene expression of the three isoforms of the PPAR transcription factor were assessed. It was reported that in livers from supplemented mice there was an upregulation of *Ppar* $\beta/\delta$  and a downregulation of *Ppar* $\gamma$  (Figure R12). On the contrary, no modifications on the expression of the alpha isoform were observed

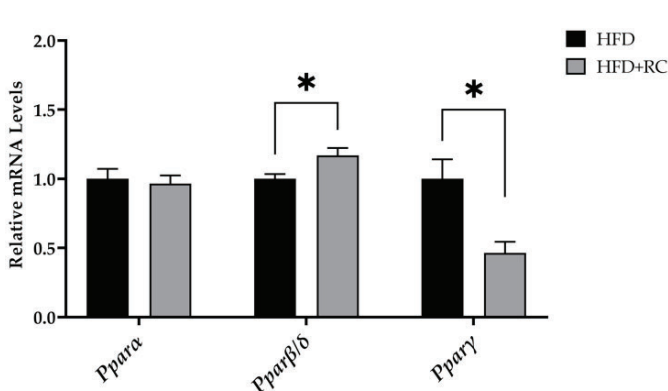


**Figure R12 – *Rosa canina* flesh upregulated the expression of *Ppar* $\beta/\delta$  and downregulated the *Ppar* $\gamma$ .** Relative mRNA levels of the three different peroxisome proliferator-activated receptors (PPARs) isoforms on liver. Data are presented as the mean  $\pm$  SEM. \*  $p < 0.05$ ; \*\*  $p < 0.01$ . The p-values for each analysis were determined by using a two-tailed unpaired Student's T-test. HFD=13, HFD+RC=13.

**B.13) Mice supplemented with *Rosa canina* flesh also exhibited a reduction of kidney and gastrocnemius muscle weight.**

As pointed out in the introduction and corroborated on the previous results, kidney plays a key role in chronic diseases prognosis. Just it happens in other ectopic organs such as liver, kidney also suffers fat accumulation in obesity(33). Parallely, it increases in size and weight due to the HFD-related damage and to the accumulated lipids. This process is also observed in muscles from patients suffering obesity, showing a muscular tissue with fat infiltration(394). In *Rosa canina* supplemented mice, a significant decrease in kidney weight (Figure R13 A) and a decrease in

the covering perirenal fat depot (Figure R13 B and C) were observed. At the same time, a significant decrease in the gastrocnemius muscle weight was detected. Although there is a significant difference between weights, an analysis of the genetic profile of the tissues is necessary to assess their involvement.

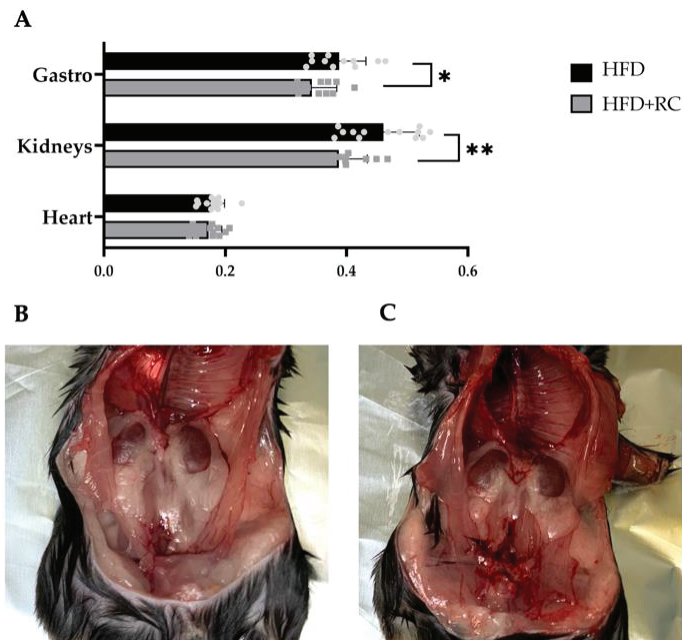


**Figure R13 – *Rosa canina* flesh also decreased the kidney and gastrocnemius tissue weight as well as the perirenal fat accumulation.** (A)The graph represents the average weights of fresh tissues measured on the precision balance before snap-freezing process in liquid nitrogen. Data is presented as means  $\pm$  SEM. \*  $p < 0.05$ ; \*\*  $p < 0.01$  and p-values were determined by using a two-tailed unpaired Student's T-test. HFD=13, HFD+RC=13. (B) Image of the thoracic cage of an HFD-only mouse prior to kidney removal. (C) Image of the thoracic cage of an HFD+RC mouse prior to kidney removal.

### **C) Characterization of the different *Rosa canina* flesh fractions and study of the anti-steatotic mechanisms underlying their different constituents.**

Based on the results of the nutritional *Rosa canina* against a HFD intervention as well as on the data from the literature, the powerful mitigating properties of the rosehip flesh are evident. As it happens in other studies of the same type, the next step is to be able to identify specifically which compounds form this pulp and which of them may be the main actors in its beneficial effect. There are previous identification studies on the phenolic compounds and on carotenoids from *Rosa canina*, but no characterization of a more concrete fractionation of the flesh has been carried out yet. In addition, no research of this type has been made on a liquid chromatography and high-resolution mass spectrometry (LC-MS). On the other hand, the biological effect of these flesh fractionations has not been studied either. Parallely, it must be highlighted that one of the remarkable actions of *Rosa canina* flesh was its great anti-steatosis role. Considering the gene expression profile of the supplemented liver, the data suggest a putative role of the PPARs transcriptionally activity as one of the putative molecular mechanisms of the *Rosa canina* effects. Thus, it could be possible that some of the bioactive compounds forming *Rosa canina* were agonist and/or antagonist molecules of the PPARs.

Taking these considerations, a fractionation of the flesh was performed according to the different solubility of the present compounds. By using LC-MS, the most relevant bioactive compounds of each fraction were identified. To evaluate the presence of PPARs agonists/antagonists, luciferase reporter assays were carried out in different cell types with the different fractions. These assays were specifically focus on finding PPAR $\gamma$  regulators.

#### **C.1) Screening of the phytochemical groups present in the different flesh fractions and relative species content.**

*Rosa canina* flesh was fractionated by different solvent extractions (water, ethanol, acetoethylene, chloroform and hexane). The compounds extracted from the different fractions were identified by comparing the exact mass and fragmentation pattern with the *Food DB*, *Phytohub* and *Lipid-Maps* libraries. On the other hand, using the peak areas resulting from the chromatography and the spectrometry, it was possible to determine which extract is rich in every identified compound.

Once the results were compared and checked together with the freely available databases, 106 total species from the major subfamilies of bioactive compounds were correctly identified (*Table C1*). The identified species were grouped in 13 families (*Table C2*). Species were quantified taking as a reference the aqueous phase and the presence of each one was expressed as the Log<sub>2</sub> fold change compared to water phase. Since we do not have the concentration of the compounds but instead the areas of each species provided by the chromatography, it is not possible to work linearly. For this reason, besides working with mainfolds, the results are expressed in Log<sub>2</sub> fold change thus indicating how many times certain species has been duplicated (positive values) or divided by 2 (negative values) compared to the aqueous fraction. Due to the wide solubility differences, some species are mostly present in the hydrophilic fractions but are less present in the lipophilic fractions and inversely. In addition, there are 4 compounds that were not identified in the aqueous fraction but appear in the other fractions (katatonic acid, coumaroylcorosolic acid, quercetin-glucoside and the platanic acid).

**Table C1.** This table shows the Log<sub>2</sub> fold change of the chromatographic areas of each specie, as well as the family sum of bioactive compounds from each extract in comparison to the aqueous fraction. The identification step was based on mass accuracy, isotopic pattern, and spectral matching. Using the software MS-DIAL, the mentioned criteria were used to calculate a total identification score(369). The total identification score cut off was 75%, considering the most common ion adducts for the chromatographic solvents. Gap filling using peak finder algorithm was performed to fill in missing peaks, considering 5 ppm tolerance for m/z values. Finally, with the software MS-FINDER(370), in-silico fragmentation of the not annotated mass features was obtained and compared to *Food DB*, *Phytohub* and *LipidMaps* available in the same software. The compounds with an in-silico prediction score > 5 were chosen. Once identified, the areas of each compound were compared between the different fractions using the aqueous fraction as reference by means of Log<sub>2</sub> fold change. At the final row of each family, a total sum of the areas from the identified compounds is shown. The *des.* code is for compounds that have disappeared, and the *gen.* code is for compounds that have been generated but were not originally in the aqueous fraction.

		Log <sub>2</sub> Fold EtOH	Log <sub>2</sub> Fold AcOEt	Log <sub>2</sub> Fold CHCl <sub>3</sub>	Log <sub>2</sub> Fold Hexane
Abscisic Acids	Abscisic acid	0,606	4,802	8,805	3,159
	Nigrospsydon A;(+) -Nigrospsydon A	0,360	3,278	8,183	des
	<b>Cumulative Total</b>	<b>0,966</b>	<b>8,080</b>	<b>16,988</b>	<b>3,159</b>
Catechins	Catechin	0,296	4,351	-3,035	-2,546
	Epicatechin	0,685	-0,217	-10,660	-10,880
	<b>Cumulative Total</b>	<b>0,981</b>	<b>4,133</b>	<b>-13,695</b>	<b>-13,426</b>
Fatty acyl glycosides of mono- and disaccharides	(3S,7E,9S)-9-Hydroxy-4,7-megastigmadien-3-one 9-glucoside	0,506	3,870	7,133	-7,715
	Ethyl 7-epi-12-hydroxyjasmonate glucoside	0,479	3,746	6,533	-9,623
	6-Acetoxy-7-hydroxymyrcene-7-O-beta-D-glucopyranoside-2'-O-acetate	0,409	4,136	7,293	-7,812
	Corchoionol C 9-glucoside	0,557	2,204	3,647	des
	<b>Cumulative Total</b>	<b>1,951</b>	<b>13,956</b>	<b>24,607</b>	<b>-25,150</b>

Flavanones	Naringenin	-1,865	4,331	6,440	-3,561
	Eriodictyol	-2,460	1,707	5,179	des
	Taxifolin	-1,307	2,269	1,730	-9,331
	<b>Cumulative Total</b>	<b>-5,632</b>	<b>8,307</b>	<b>13,349</b>	<b>-12,891</b>
Flavonoid O-glycosides	Phloridzin	0,545	4,248	-4,257	des
	3,4,2',4',6'-Pentahydroxychalcone 4'-glucoside	0,547	4,142	-4,589	des
	Spiraeoside	2,653	4,246	-3,815	des
	Neolucuroside	0,550	4,149	4,692	-6,568
	quercetin 3-O-glucuronide	5,903	9,318	-3,246	-4,378
	Avicularin	2,495	5,981	-0,879	des
	Taxifolin 3-arabinoside	1,332	4,670	-0,225	des
	(2R,3R)-Taxifolin 3-xyloside	0,559	4,119	-4,997	des
	(2R,3R)-Taxifolin 3-xyloside (taxifolin O-hexoside 1)	0,515	3,999	-4,662	des
	(2R,3R)-Taxifolin 3-xyloside (taxifolin O-hexoside 2)	1,254	4,931	0,230	des
	Kaempferol-3-O-glucoside	7,628	11,158	2,386	des
	Glucodistylin	1,873	5,864	-0,078	des
	Padmatin 3-glucoside	1,718	5,644	8,126	-6,879
	Eupatolin	2,845	6,701	2,041	des
	6- {[2-(3,4-dihydroxyphenyl)-5-hydroxy-4-oxo-4H-chromen-7-yl]oxy}-3,4,5-trihydroxyoxane-2-carboxylic acid	1,187	5,067	5,507	des
	Naringenin-7-O-glucoside	0,722	4,457	0,239	des
	Apigenin 7-xyloside	9,733	13,054	1,982	des
	Catechin 7-glucoside	1,552	5,242	6,484	des
	Trans-tiliroside	9,151	11,319	6,937	1,847
	<b>Cumulative Total</b>	<b>52,762</b>	<b>118,309</b>	<b>11,875</b>	<b>-15,978</b>
Flavonols	Kaempferol	1,343	4,328	9,385	0,038
	Quercetin	3,869	7,206	8,665	-4,800
	3-methylquercetin	3,236	6,925	12,057	2,951
	Myricetin	1,209	7,092	0,989	1,567
	<b>Cumulative Total</b>	<b>9,658</b>	<b>25,551</b>	<b>31,097</b>	<b>-0,243</b>
Tannins	Ellagic Acid	0,926	4,492	-0,634	-6,942
	3-O-Methylellagic acid	-0,636	3,791	6,117	-4,149
	Pseudolaroside B;(-)-Pseudolaroside B	0,448	3,583	-1,644	-8,909
	6-O-(3,4-dimethoxybenzoyl)-ajugol	0,958	5,016	6,286	des
<b>Cumulative Total</b>	<b>1,695</b>	<b>16,882</b>	<b>10,125</b>	<b>-19,999</b>	
Lignans	(-)-Isolariciresinol 4-O-beta-D-glucopyranoside	0,527	1,957	5,158	des
	(8R,8'R)-Secoisolariciresinol 9-glucoside	0,576	3,111	6,167	des
	Prupaside	0,504	3,154	4,901	des
	Alangilignoside D	0,545	3,630	6,677	des
	Sioriside	0,500	3,824	8,650	des
	Nymphaeoside A;(-)-Nymphaeoside A	0,417	2,012	8,080	des
	Lariciresinol 9-O-beta-D-glucoside	0,552	1,910	2,131	des
	(+)-7-epi-Syringaresinol 4'-glucoside	0,653	3,273	8,103	des
	Ehletianol C	0,124	3,328	8,911	des
	Buddlenol D	0,487	3,322	8,062	des
<b>Cumulative Total</b>	<b>5,586</b>	<b>33,331</b>	<b>82,901</b>	<b>0,000</b>	
Fatty Acids and Derivates	FA 18:3	1,354	4,068	6,357	10,439
	FA 18:2	1,446	4,629	6,591	9,375
	(9S,10E,12Z,15Z)-9-Hydroxy-10,12,15-octadecatrienoic acid	0,809	-0,745	6,857	9,825
	9-hydroxy-10,12-octadecadienoic acid	1,128	1,129	5,613	9,016
	Alpha-Linolenic acid	0,725	2,867	4,746	7,349
	Corchorifatty acid D	-0,574	-0,837	3,718	7,959
	13(S)-Hydroperoxylinolenic acid;(13S)-Hydroperoxy-cis-9,15-trans-11-octadecatrienoic acid;(13S)-HPLA	0,060	-1,347	6,514	9,492
	9(S)-HPODE	0,003	1,117	4,894	7,647
	13-L-Hydroperoxylinoleic acid	-0,070	3,189	7,228	8,296
	Corchorifatty acid F	-0,500	3,399	7,087	1,062
	Mayolene-14	3,459	5,965	9,344	1,750
	Oleic acid	0,187	1,459	3,045	5,328
	(S)-10,16-Dihydroxyhexadecanoic acid	0,697	3,802	8,727	4,614
	15(16)-EpODE	3,204	4,586	5,666	12,624
8,11,14-Eicosatrienoic acid	1,125	4,235	6,195	7,911	

	9,10-DHOME	-0,071	1,304	4,788	5,308
	9,12,13-TriHOME	-0,104	2,252	6,161	1,001
	(+)-Hexylitaconic acid	0,586	4,773	8,086	0,046
	9(10)-EpODE	0,460	2,812	6,073	9,064
	9,10-Epoxy-18-hydroxy-octadecanoic acid	0,218	1,597	4,970	6,596
	2-dehydro-3-deoxy-L-fuconic acid	0,306	4,555	6,826	-2,064
	FA 18:4;O	0,272	2,151	6,619	11,556
	FA 18:2;2O	-0,132	1,776	5,840	6,810
	FA 18:2;3O	-0,422	3,253	7,336	1,340
	FA 18:1;3O	-0,190	2,241	6,379	0,265
	<b>Cumulative Total</b>	<b>13,981</b>	<b>64,231</b>	<b>155,661</b>	<b>152,608</b>
	O-glycosyl Compounds	7-Hydroxyterpineol 8-glucoside	0,393	3,975	6,938
alpha-Morroniside		0,698	3,724	5,099	-6,642
Phenethyl rutinoside		0,552	4,094	-1,251	des
<b>Cumulative Total</b>		<b>1,642</b>	<b>11,793</b>	<b>10,785</b>	<b>-12,808</b>
Tetracarboxylic acids and derivatives	Sandoricin	1,274	2,526	9,536	des
	Cinercipadesin B;(+) -Cinercipadesin B	0,649	2,927	9,011	des
	<b>Cumulative Total</b>	<b>1,924</b>	<b>5,453</b>	<b>18,547</b>	<b>0,000</b>
Triterpene saponins	(20R)-Ginsenoside Rh2	2,210	3,501	4,163	-2,049
	Glucosyl passiflorate	0,856	4,531	7,496	des
	Arjunolic acid 3-glucoside	0,656	4,359	7,718	-8,282
	Quercilicoside A	0,597	3,706	4,315	des
	<b>Cumulative Total</b>	<b>4,320</b>	<b>16,097</b>	<b>23,693</b>	<b>-10,332</b>
Triterpenoids	Katononic acid	gen	gen	gen	gen
	Oleanolic acid	4,137	7,297	9,859	8,897
	Betulnic acid	4,685	7,765	10,053	8,154
	Glycyrrhetic acid	2,734	6,180	9,586	9,455
	Gypsogenin	5,392	8,076	13,123	10,365
	Pomolic acid	2,815	5,588	8,786	6,945
	Hederagenin	2,830	5,630	8,658	3,216
	Maslinic acid	3,074	5,678	8,888	2,054
	Esculentic acid (Diplazium)	1,796	4,094	7,040	3,332
	Euscaphic acid	1,669	4,210	6,749	4,167
	Ganolucidic acid A	1,132	4,918	8,993	6,578
	Medicagenic acid	0,741	4,539	8,846	4,728
	16alpha-hydroxygypsogenic acid	0,524	4,104	8,170	3,617
	Myrianthic acid	1,351	4,234	8,445	0,337
	Tomentosic acid	1,426	4,760	8,702	1,322
	6beta-Hydroxyasiatic acid	0,665	4,512	8,701	-2,985
	Ganoderic acid A	1,183	4,251	8,644	2,031
	Phytolaccatoxin	1,068	5,151	8,633	7,239
	Ganoderic acid C2	0,580	4,653	8,916	-2,014
	Ganolucidic acid C	0,895	4,423	8,777	-2,002
	cis-p-Coumaroylcorosolic acid	gen	gen	gen	des
	2-O-E-p-Coumaroylalphitolic acid	gen	gen	gen	gen
	Phytolaccasaponin G	0,755	4,140	6,913	des
<b>Cumulative Total</b>	<b>41,805</b>	<b>111,544</b>	<b>187,749</b>	<b>80,587</b>	

**Table C2. Summary of the Log<sub>2</sub> fold changes for each family of bioactive compounds and for each fraction of *Rosa canina*.** The identified compounds were divided into a total of 13 families. The range of families obtained comprises both polar and non-polar groups, since a generic C18 chromatographic column and a standard gradient water-acetonitrile as mobile phase has been used. However, as can be seen, it has not been possible to identify the highly non-polar families with larger species such as carotenoids. Even so, it has been possible to identify relevant families of phenolic compounds and their derivatives, as well as terpenoid compounds and derivatives. The Log<sub>2</sub> fold change values in bold correspond to the fraction with the highest presence of the indicated family.

	EtOH	AcOEt	CHCl <sub>3</sub>	Hexane
Abscisic acids and derivatives	0,966	8,080	<b>16,988</b>	3,159
Catechins	0,981	<b>4,133</b>	-13,695	-13,426
Fatty acyl glycosides of mono- and disaccharides	1,951	13,956	<b>24,607</b>	-25,150
Flavanones	-5,632	8,307	<b>13,349</b>	-12,891
Flavonoid O-glycosides	52,762	<b>118,309</b>	11,875	-15,978
Flavonols	9,658	25,551	<b>31,097</b>	-0,243
Hydrolyzable tannins	1,695	<b>16,882</b>	10,125	-19,999
Lignans and derivatives	5,586	33,331	<b>82,901</b>	0,000
FA and derivatives	13,981	64,231	<b>155,661</b>	152,608
O-glycosyl compounds	1,642	<b>11,793</b>	10,785	-12,808
Tetracarboxylic acids and derivatives	1,924	5,453	<b>18,547</b>	0,000
Triterpene saponins	4,320	16,097	<b>23,693</b>	-10,332
Triterpenoids	41,805	111,544	<b>187,749</b>	80,587
<b>Total Cumulative</b>	<b>131,639</b>	<b>437,668</b>	<b>573,682</b>	<b>125,527</b>

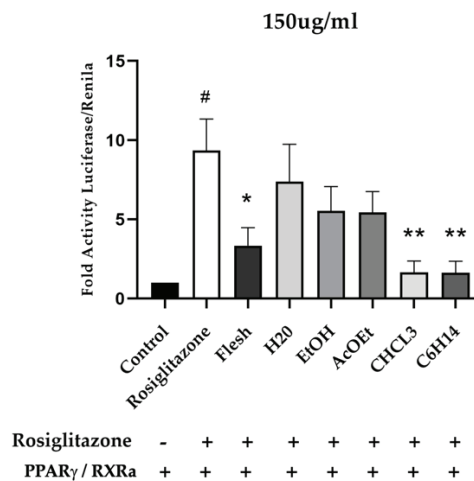
In general, the identification results in two large blocks of bioactive compounds. First, phenolic compounds, which are highlighted in *Table C2* with subfamilies such as catechins, flavonoids, flavonols, tannins, lignans and their corresponding derivatives, in many cases in glycosylated forms. Regarding polyphenolic specific species, as shown at *Table C1*, high active compounds not-bound such as catechin, epicatechin, naringenin, eriodictyol, taxifolin, kaempferol, quercetin, myricetin, ellagic acid, etc. was detected but also glycoside forms like, pohlridzin, spiraeoside, quercetin 3-O-glucuronide, taxifolin 3-arabinoside, kaempferol-3-O-glucoside, catechin 7-glucoside, tiliroside, secoisolariciresinol diglucoside. Most of the species of polyphenols identified have been attributed to health promoting effects. In the case of *Rosa canina*, tiliroside has been shown to be responsible, at least in part, of its beneficial effects(329) but other cannot be discarded. As expected, the bioactive compounds profile changes radically depending on the solvent used for the extraction, thus phenolic compounds are observed to lose their presence when moving towards to more non-polar solvents. Similarly, the second large block, the more lipophilic compounds such as abscisic acid, terpenoids and fatty acids increase their presence in non-polar solvents like chloroform and hexane. In this sense, species with high biological activity stand out, especially the derivatives of ursolic acid belonging to the triterpenoid category. Although it has not been possible to correctly identify the ursolic acid because it was not present as a standard, a high presence of similar compounds such as the katatonic acid, oleanolic acid, betulinic acid, euscaphic acid, myrianthic acid, tomentosic acid, pomolic acid among others, were

detected. In addition, numerous MUFAs and PUFAs both omega-3 and omega-6, as well as their derivatives, were also identified. Less common fatty acids were also observed, for example corchorifatty acids or more complex octadecenoic acid derivatives. Overall, as shown in *Table C2*, the chloroform and to lesser extent the ethyl acetate, are the two extracts with a significant major presence of relevant bioactive compounds.

### C.2) Chloroform and hexane fractions antagonize the PPAR $\gamma$ transcriptional activity on HepG2 cells.

Since one of the effects observed in the animal trial with *Rosa canina* was the potential modulation of the nuclear receptor PPAR $\gamma$  by the bioactive compounds of the flesh, a luciferase assay was performed on HepG2 cells. In this way, a first pre-test was carried out at different concentrations of the extracts (1 $\mu$ g/ml, 75 $\mu$ g/ml, 100 $\mu$ g/ml, 150 $\mu$ g/ml and 200 $\mu$ g/ml) (*data not shown*). Based on these previous results and the bibliographic support of the fractionation method, the concentration of 150 $\mu$ g/ml was chosen as it was consistent with other experiments of this type, as well as being innocuous for the cells and being the second minimum concentration where changes in PPAR $\gamma$  activity were observed. Luciferase assays were performed with a luciferase reporter plasmid containing 3xPPRE controlling the transcription of the gene luciferase and the expression plasmids of PPAR $\gamma$  and RXRa. Rosiglitazone (10 $\mu$ M) was used as a PPAR $\gamma$  agonist and the different extracts were added at a concentration of 150 $\mu$ g/ml. As shown in *Fig.C1*, both flesh and more liposoluble fractions such as chloroform and hexane, antagonized the rosiglitazone dependent PPAR $\gamma$  activity.

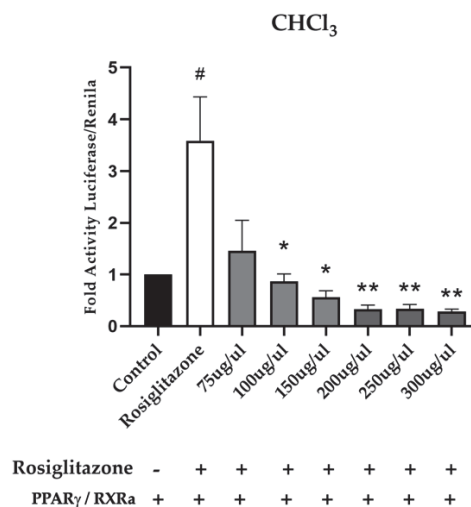
**Figure C1.** *Rosa canina* flesh, chloroform and hexane exerted an antagonistic effect to the Ppar $\gamma$  activity. The graph represents the fold induction of *Luciferase* activity compared to control cells normalized by *Renilla* activity. Data is presented as means  $\pm$  SEM of 4 independent assays. \* p < 0.05; \*\* p < 0.01 and p-values were determined by using a two-tailed unpaired Student's T-test with a Welch correction, between Rosiglitazone group and each extract. Rosiglitazone action was statistically significant using a two-tailed unpaired Student's T-test with a Welch correction # p < 0.05 compared to the control cells.





After these results, a dose-response curve was proposed using the luciferase assay for the two fractions with antagonist action, chloroform, and hexane (*Figure C2*) following the same procedures. In case of the hexane extract the dose-response curve it is not included in this thesis proposal. Both curves started at a concentration of 75µg/ml, followed by 100µg/ml, 150µg/ml, 200µg/ml, 250µg/ml and 300µg/ml. The minimum concentration of 75µg/ml was chosen since no trend or variation was observed at lower concentrations in the pre-tests. The action of the chloroform extract on PPAR $\gamma$  activity is increasing and proportionally to the concentration (*Figure C2*).

**Figure C2. Chloroform extract exerted an antagonistic effect to the Ppar $\gamma$  activity proportionally and increasingly to its concentration.** The graph represents the fold induction of *Luciferase* activity compared to control cells normalized by *Renilla* activity. Data is presented as means  $\pm$  SEM of 4 independent assays. \* p < 0.05; \*\* p < 0.01 and p-values were determined by using a two-tailed unpaired Student's T-test with a Welch correction, between Rosiglitazone group and each concentration of chloroform extract. Rosiglitazone action was statistically significant using a two-tailed unpaired Student's T-test with a Welch correction # p < 0.05 compared to the control cells.



### C.3) Chloroform and hexane fractions from *Rosa canina* flesh inhibited 3T3L1 differentiation and decrease lipid accumulation.

Once the PPAR $\gamma$  antagonistic action of the chloroform and hexane fractions of *Rosa canina* was demonstrated, an experiment in a different cell culture was proposed to verify if the same pattern was fulfilled. Therefore, the two extracts were administered at different concentrations in 3T3L1 cells undergoing differentiation. If these fractions had PPAR $\gamma$  antagonist action, they would alter the adipogenesis process, therefore, a significant decrease in lipid droplet formation would be observed(395). Through ORO staining, it was possible to semi-quantify the presence of lipids as well as the formation of lipid droplets by optical microscopy visualization. In this way, and as it is shown in (*Figure C3*) on the chloroform and (*Figure C4*) in case of hexane, both fractions significantly decreased the presence of lipids after its application. The bar graph shows the semi-

quantification by spectrophotometry and on the right side four images of the different groups at 10x of magnification are exposed.

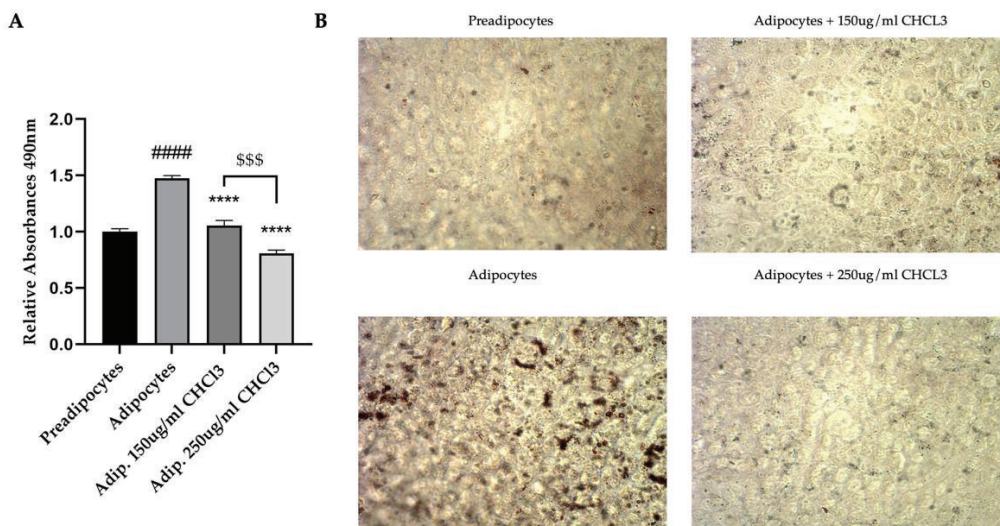


**Figure C3 – *Rosa canina* chloroform fraction modulates the preadipocyte differentiation.** (A) The bar graph shows the semi-quantification by spectrophotometry representing the means of relative absorbance levels at 490nm of the ORO stain on preadipocytes and differentiated adipocytes with different concentrations of *Rosa canina* chloroform extract. (B) Four images captured at 10x magnification of the different groups/cell states. The experimental procedure is indicated on the ORO methodology section. As explained above, ORO staining dyes lipid droplets in an intense reddish color. In this case it can be observed that in differentiated adipocytes the amount of lipid droplets increases significantly but decreases proportionally in the presence of chloroform extract. Data are presented as the mean  $\pm$  SEM. #####  $p < 0.0001$  (Preadipocytes vs. Adipocytes). \*\*\*\*  $p < 0.0001$  (Adipocytes vs. Adipocytes + Chloroform extract). \$\$\$  $p < 0.001$  (150ug/ml vs. 250ug/ml). The p-values for each analysis were determined by using a two-tailed unpaired Student's T-test.

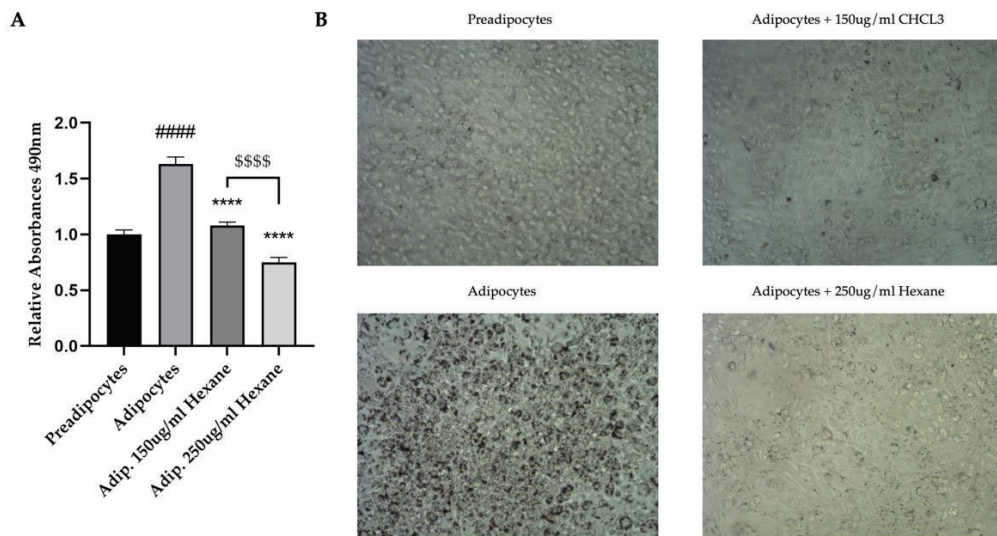


**Figure C4 – *Rosa canina* hexane fraction modulates the preadipocyte differentiation.** (A) The bar graph shows the semi-quantification by spectrophotometry representing the means of relative absorbance levels at 490nm of the ORO stain on preadipocytes and differentiated adipocytes with different concentrations of *Rosa canina* hexane extract. (B) Four images captured at 10x magnification of the different groups/cell states. The experimental procedure is indicated on the ORO methodology section. As explained above, ORO staining dyes lipid droplets in an intense reddish color. In this case it can be observed that in differentiated adipocytes the amount of lipid droplets increases significantly but decreases proportionally in the presence of hexane extract. Data are presented as the mean  $\pm$  SEM. #####  $p < 0.0001$  (Preadipocytes vs. Adipocytes). \*\*\*\*  $p < 0.0001$  (Adipocytes vs. Adipocytes + Hexane extract). \$\$\$  $p < 0.001$  (150ug/ml vs. 250ug/ml). The p-values for each analysis were determined by using a two-tailed unpaired Student's T-test.

In both experiments after applying the differentiation mix explained in the methodology section, a significant increase in the presence of lipids and in turn, an increase of lipid droplets, was observed. On the other hand, when the differentiation is accompanied by the extracts, both at a concentration of 150ug/ml and at 250ug/ml there was a severe decrease in the presence of lipids and in turn of lipid droplets. This difference increases significantly between doses, showing a greater decrease in the case of doses of 250ug/ml. On the other hand, at optical microscopy level, no drastic changes were observed between doses.

DISCUSSION



## 5. Discussion

Nowadays the scientific community is facing an unprecedented global problem, the massive growth of NCDs, as manifested by the large amount of epidemiological evidence. In the introduction of this thesis proposal, the mechanisms by which obesity and diabetes progress and end up being a substrate for the development of comorbidities such as NAFLD or CKD, leading to much adverse prognoses and causing an alarming health and economic impact have been described. In this sense, from different areas of the biomedical field, new treatments and therapeutic targets are being studied to improve the prognosis, alleviate the high mortality rate, and enhance the quality life of patients with these pathologies. In the present thesis proposal, based on the nutrigenomics research area, bioactive compounds with different presentations and characteristics have been studied as possible treatments against obesity and its comorbidities on an obese diet-induced animal model. At the same time, the way these compounds modified certain metabolic pathways and therefore how these pathways could be proposed as new therapeutic targets have also been explored.

The first set of results has demonstrated that supplementation of an HFD with pure, isolated polyphenols worsened the effects of the HFD by producing a homeostatic imbalance resulting in adipose tissue (*Figure P5 and P6*) and liver (*Figure P7 and P8*) metabolic impairment, as well as a clear kidney damage (*Figure P10, P11 and P12*). The HFD+Pol elicited a dysregulation in glucose and insulin metabolism (*Figure P3 and P4*) and an evident kidney damage, as demonstrated by the switch in the gene expression profile. In addition, the increase in MDA suggests an increase in oxidative stress and the histological analyses evidence unequivocal glomerular fibrosis (*Figure P10, P11 and P12*), all these changes being related to CKD and obesity(384,396–400).

The distinctive feature of these results is the kidney damage observed in HFD+Pol mice which was defined by the upregulation of *Kim-1* and *Lcn-2* but also contrasted by the Picrosirius red-stained histological images. KIM-1 is a transmembrane glycoprotein that has a low expression in the healthy kidney but becomes significantly up-regulated in pathological circumstances, for this reason it is widely used as a biomarker of renal damage(401). Up-regulation of KIM-1 has been associated with a hypoxic environment on CKD(400). A chronic hypoxia caused by structural and functional disorders such as alteration of the capillarity, excessive renin-angiotensin activity, oxidative stress, and others, has been described as the main pathogenic mechanism of

progressive CKD. In this sense, hypoxia is a powerful stimulus for KIM-1 expression on the proximal tubular cells and in turn, its upregulation increases the release of cytokines and chemokines which enhance inflammation, hypoxia, and fibrosis, thus aggravating CKD development(401,402). On the other hand, upregulation of KIM-1, as well as increased levels in blood and urine, are reported in early T2DM and can predict one of the main consequences of diabetes, DKD and also other diseases such as CVDs(403). KIM-1 has also been reported to mediate the uptake of palmitic acid on the proximal tubules, leading to enhanced tubule injury, interstitial inflammation, fibrosis, and glomerulosclerosis(404). Moreover, there are several studies where *Kim-1* expression in tubular epithelial cells correlated with the level of *Osteopontin* and  $\alpha$ -smooth muscle actin expression, both key markers of tubular fibrosis(405–407). Interestingly, in kidneys of HFD+Pol mice, this relationship between *Kim-1* and *Osteopontin* expression was also observed, although the increase in *Osteopontin* expression was only a trend. In one of the abovementioned studies, the researchers observed that the enhancement of KIM-1 on tubules in a murine polycystic kidney diseases model, increased proliferative activity and induced a higher presence of  $\alpha$ -smooth muscle actin which characterizes myofibroblasts. With these results, researchers proposed that KIM-1 expression in tubules was strongly associated with the development of interstitial fibrosis(406). Another interesting study in rodents, using an inhibitor of KIM-1 expression, demonstrated that KIM-1 was directly associated with the development of renin-angiotensin system (RAS)-mediated renal damage, being KIM-1 expression proportional to the tubulointerstitial fibrosis and interstitial collagen deposition(407,408).

In this first intervention with pure isolated polyphenols, the fibrotic process was evaluated by measuring the mRNA levels of *Fibronectin* both in kidney and liver and reinforced with Picrosirius red staining on kidney. Fibrosis is mainly caused by a pathological excess of extracellular matrix deposition which leads to a disruption of tissue structure that could finally provoke a loss of functionality. The fibrotic process involves a complex network of signal transduction pathways in which the transforming growth factor-beta (TGF $\beta$ ) has a central role(383). Fibrosis is determined, among other factors, by an increase in the expression of collagens, proteoglycans, glycoproteins, and fibronectins(382). In this sense, fibronectin is one of the main players of fibrosis development because it affects the TGF $\beta$  release and it is one of the responsible proteins for the accumulation of collagen and hence the development of this pathological process(409,410). Our results suggest that pure isolated polyphenol-supplementation within a HFD

drives the development of fibrosis in the liver and kidneys as shown by the significant enhancement of *Fibronectin* expression and in case of kidneys, as demonstrated the Picrosirius red staining.

Based on the literature, an alteration in the delicate balance of iron metabolism could be one of the possible links between renal damage and the observed progressive general decline in glucose and insulin metabolism. Iron is essential for multiple physiological processes ranging from oxygen transport to enzymatic activity and energy metabolism(376). Obesity itself has been found to influence every step of iron metabolism playing a pivotal role in the development of metabolic derangements(411). In parallel, several studies have shown a direct association between ferritin serum levels and increased risk of T2DM(412–414). Moreover, patients with hemochromatosis, a disease characterized by excess iron accumulation, suffer from insulin resistance and reduced insulin secretory capacity(415). Interestingly, Gabrielsen et al. went a step further and discovered an inverse association between human ferritin levels and adiponectin levels in serum(416). More specifically, they found that iron negatively regulated adiponectin transcription via FOXO1-mediated repression in mice adipocytes(416). Conversely, decreasing adipocyte iron levels involved an increase in adiponectin levels improving glucose tolerance and insulin sensitivity(416). Thus, adipocyte iron levels can modulate insulin sensitivity by regulating adiponectin transcription. Furthermore, hepcidin (*Hamp1*), which is considered the chief regulator of systemic iron homeostasis, undergoes drastic changes in the progression of insulin resistance and after a high fat diet consumption(417). On another note, it is worth mentioning that acquired and inherited disturbances in systemic iron homeostasis have been associated with kidney injury(376). Besides, renal disorders could reduce general iron levels as a result of enhanced urinary iron excretion and hepcidin-mediated reduction of iron transport(376). Altogether, the current knowledge evidences that iron has an important role in renal disorders being cause or effect, either as a critical initiator of oxidative stress and mitochondrial dysfunction or as a potent modulator of inflammation(376).

Interestingly, there is one key player that recurs in obesity, T2DM and renal pathologies which plays a major role in iron metabolism, LCN2, that together with KIM-1, is one of the main kidney injury biomarkers. Lipocalin-2 also known as Neutrophil gelatinase-associated lipocalin, is an iron carrier protein whose circulating levels are increased in different pathological states like kidney injury, ageing, bacterial infection, and inflammatory status. Nevertheless, it has also



been designated as an adipokine mediator of insulin resistance associated with obesity(168,169). Its biological activity depends mainly on its iron-load and on where it is produced (renal tubules or macrophages), which defines its dual role in the development of kidney damage (418–420). Iron-free LCN2 secreted by renal tubular epithelial cells has been associated with renal injury, and the expression and release of macrophage-derived iron-bound LCN2 has been linked to renal recovery. On the other hand, adipose tissue-derived LCN2 not only plays a critical role in causing both chronic and acute renal injury, but is essential for the progression of CKD in rodent and human models(171,172). Viau et al. concluded that LCN2 also acts as a growth regulator by mediating the mitogenic effect of EGFR signaling(172). The activation of EGFR is linked to the regulation of several cellular responses involved in the progression of renal damage including cell proliferation, inflammatory processes, and extracellular matrix regulation(173). Curiously, overexpressed LCN2 possesses obesity-promoting and anti-thermogenic effects through the inhibition of BAT activity(169). Lastly, LCN2 deficiency was described to have a protective role from developing aging and obesity-induced insulin resistance by modulating 12-lipoxygenase and TNF- $\alpha$  levels in adipose tissue(174).

There is strong evidence in the literature on the link between LCN2, iron metabolism, obesity/T2DM and kidney damage. Nevertheless, the results of our study only show a significant increase on *Lcn2* kidney expression levels between HFD+Pol and HFD-only. Other key expression markers on iron metabolism such as transferrin receptor 2 (*Trf2*), hephaestin (*Heph*), and hepcidin (*Hamp*) were also measured both on liver and kidneys, but no differences between the HFD+Pol and HFD-only mice were detected. Similarly, neither the circulating levels of iron were different in supplemented mice versus HFD-fed animals. Notwithstanding these nonsignificant results, when comparing the HFD+Pol values with the control group in liver, a significant enhancement in *Trf2* expression and an increase in total iron levels were exhibited. In addition, a decrease in *Adiponectin* expression was also observed in both liver and kidney of HFD+Pol mice compared to HFD-only, which according to the literature could appear since iron negatively regulated *Adiponectin* transcription(416). Moreover, a trend towards the decrease in the expression of *Ucp1* in HFD+Pol mice scWAT in comparison to HFD-only mice was observed, which could suggest the existence of an anti-thermogenic effect as reported in the scientific literature on LCN2(169).

Regarding metabolism of the scWAT, the first change that can be interpreted about its gene expression pattern is related to lipid metabolism. One of the effects of HFD consumption is the decrease on the DNL process and a proportionally decrease on glucose tolerance and insulin sensitivity(421). In this case it can be observed how one of the key genes in the DNL synthesis of fatty acids, *Fasn*, shows a greater tendency to decrease in the HFD-supplemented animals. In the same direction, the DNL and insulin-sensitivity key master *Chrebbp* transcription factor is significantly decreased in HFD-supplemented mice scWAT. This result fits with the aggravated glucose and insulin response patterns observed in supplemented mice since ChREBP is determinant on adipose tissue fatty acid synthesis and systemic insulin sensitivity(120). In contrast, no significant changes were observed on *Srebp1c* nor *Ppar $\gamma$* , the other major regulators of lipid metabolism. Concerning mitochondrial scWAT state, there are no changes in *Pgc1 $\alpha$*  although a decrease in its expression could be intuited but not with significance in HFD+Pol fed mice. Conversely, in these mice it can be observed a downward trend in the expression of *Chrs1*, whose encoded enzyme catalyzes the synthesis of cardiolipin critical for mitochondrial function.

In terms of cytokines, it is not surprising to see an increase on the *Fgf21* expression although this is not associated with an improvement but with a state of obese FGF21-resistance. This result is also corroborated by the downward trend in *Adiponectin* expression and the significantly decrease on *Lcn2*. While low plasma circulating LCN2 levels are associated with an improvement in the state of obesity and obesity-comorbidities, in WAT lower expression rates of *Lcn2* are directly associated with an impairment in thermogenesis and an aggravated state of insulin resistance(175). In case of thermogenesis process, no significant changes are observed due to the large dispersion between individuals, although a trend in the decrease of *Ucp1* expression can be observed in animals supplemented with polyphenols, which could indicate the existence of an anti-thermogenic effect as discussed above. Briefly, it can be seen how scWAT from HFD+Pol mice tend to present a more obesogenic tissue profile and therefore a worse condition than HFD-only fed animals. According to the histological analyses, the scWAT of both HFD-fed groups had significantly fewer and larger adipocytes (*Figure P6*). Therefore, the hypertrophic power of HFD on adipocytes is evident. However, there are no significant differences in the number of scWAT adipocytes between the supplemented group and the HFD-only even though a downward trend can be observed (*Figure P6 B*). In some histological samples, a slightly larger size is seen between supplemented and HFD-only mice, but this difference is not evident in all samples. Therefore, not clearly conclusions can be drawn.

As it happens on scWAT, one of the first changes in liver gene expression profile of the polyphenol supplemented mice is *Adiponectin* mRNA levels. Although its general hepatic expression is lower in comparison to adipose tissues, adiponectin regulates both glucose and lipid metabolism and exerts an insulin-sensitizing effect on liver. Its dysregulation is clearly observable in hepatic pathologies such as NAFLD or systemic pathologies such as obesity and T2DM(422). Another change of relevance in supplemented animals, is the significant increase in the fibrosis marker *Fibronectin*. One of the most important shifts in the pathological progression of NAFLD is the appearance of fibrosis. Although its presence is not necessary for the designation from NAFLD to NASH, it is a determining factor in the liver state being a clearly worsening on the pathology prognosis(423). Regarding reticulum stress, changes in the expression of two relevant genes on ER stress were observed in animals supplemented with polyphenols. Firstly and in a significant manner the *Chop* transcription factor, whose role involves essential response to a wide variety of cell stresses and the induction of cell cycle arrest and apoptosis in response to ER stress(424). *Bip* is the other induced gene but only showed an upward trend on the supplemented animals. The protein encoding *Bip* operates as a typical chaperone and at the same time as a regulator of ER homeostasis but during cellular stress plays a role in cellular apoptosis and cell senescence(424).

Although it has not been possible to conclusively clarify the link between the clear renal damage and the significative worsening of the obesogenic status presented by the supplemented mice, the pernicious effects of the pure, isolated polyphenols when administered under HFD conditions have been evidenced. These results may be controversial given the current and ongoing research, but we believe that all aspects of polyphenol supplementation should be discussed. In 2010, Bouayed and Torsten published a review suggesting the “double-edged sword” of the cellular redox state and exogenous antioxidants(425). Their report, as well as additional recent research, have indicated that it is essential to consider the type, the dosage, the combination, and the consumption matrices involved when using bioactive compounds because the administration of such molecules may alter the physiological balance between oxidation and antioxidant pathways, which may result in either beneficial or deleterious effects(426,427).

The inclusion of foods naturally rich in antioxidants (e.g., fruits and vegetables) has been widely recommended by health organizations and has been the basis of many “healthy eating” pro-

grams, such as the Mediterranean diet(428,429). Plenty of research has focused on the antioxidant effects of phenolic compounds when administered in isolation versus when ingested via their natural source, and increasing data has suggested that the beneficial properties of complete foods cannot be attributed to a single compound(247). Rather, it is the consumption of the food in its whole state (i.e., not extracted, or isolated compounds) that activates the additive, synergistic, and antagonistic effects of the phytochemicals and nutrients. The effects of polyphenols depend on their bioavailability, and it is assumed that only 5–10% of the total dietary polyphenol intake is absorbed directly through the stomach and/or small intestine(430). The rest of ingested polyphenols reach the colon where they are transformed by the gut microbiota(431–433). When absorbed, polyphenols undergo phase I and II metabolism (sulfation, glucuronidation, methylation, and glycine conjugation) in liver(434). The new-synthesized metabolites may then impact, among others, in the adipose tissue, pancreas, muscle, and liver, where they exert their bioactivity(247). In addition, not only natural food matrices are essential(435,436), but also the preparation process and the conditions under which they are ingested (e.g., cooking, juicing, etc.). Cooking has been widely demonstrated to affect the phytochemical content of foods as well as their chemical structures and the bioavailability of their bioactive compounds; in other words, how a food is processed before consumption may be directly related to its health effects(437–442).

Considering the first set of results, the second dietetic intervention against a diet induced obesity was based on two premises. The primary consideration was the inclusion of a non-artificial complex food matrix, so as described in the introduction a natural source rich in bioactive compounds was chosen, in this case the fruit of *Rosa canina*. This natural source was not altered or subjected to any freeze-drying or extraction process, unlike most animal intervention studies. The second consideration of this intervention was the profile of bioactive compounds, in this case the *Rosa canina* presents not only a high presence but also a wide and featured spectrum of bioactive compounds. The results of this second intervention demonstrated that supplementation of a HFD with *Rosa canina* flesh significantly slowed down the pernicious effects of the HFD through a general metabolic improvement and particularly, via a remarkable anti-steatotic action on liver. The HFD+RC mice exhibited a reduction in weight gain from the first week of treatment and throughout the whole intervention with no changes on food intake (*Figure R1*). In addition, as it shows (*Figure R2*), *Rosa canina* flesh supplementation not only significantly improved glucose and insulin response but also markedly reduced the hyperglycemic state associated with the consumption of an HFD by lowering fasting blood glucose levels to non-diabetic

values. On scWAT from supplemented mice, it was observed a significantly lower tissue weight, a greater number and smaller size of adipocytes (Figure R3) as well as a significant reduction on lipid transport, lipogenesis, TG synthesis, and an upward trend of browning process (Figure R4). Furthermore, the BAT of HFD+RC mice showed an enhancement of thermogenic and mitochondrial biogenesis markers (Figure R5). Nevertheless, as mentioned above, the most relevant changes observed among the supplemented mice were found in liver. Compared to HFD-only mice, livers from RC-supplemented mice showed a much healthier profile with lower tissue weight (Figure R6), lower lipid accumulation (Figure R7), a less structurally damaged hepatic tissue (Figure R8), lower values of oxidative and inflammation markers (Figure R6), as well as a significant improvement on FGF21 signaling (Figure R9). Regarding hepatic metabolism, the lipid-lowering action of *Rosa canina* flesh is evidenced, reducing drastically the expression of genes involving lipid and cholesterol transport, lipogenesis process, triglyceride synthesis, among other metabolic key processes (Figure R10 and R11).

The two main early findings of our *Rosa canina* flesh intervention were the marked decrease in weight gain and the substantial improvement in glucose and insulin response as discussed above. These two preliminary results are consistent with most of the published literature, both in treatments using *Rosa canina* and with other species of rosehip fruit-bearing *Rosaceae*. In case of its effect on body weight gain reduction, a remarkable study published by Nagatomo et al. presented for the first time in humans how the daily intake of an extract of rosehip decreases body weight by a reduction of abdominal visceral fat in pre-obese subjects(331). Similarly, the *Rosa canina* supplemented mice of our intervention showed this significant weight reduction in the WAT depots as well as on the ectopic tissues such as liver or kidneys. Sometime before, Nagatomo et al. had published an in vivo study in which they proposed the suppression of the expression of the PPAR $\gamma$  by *Rosa canina* as the responsible mechanism for the inhibition of lipid accumulation in the WAT(443). Parallel to Nagatomo's studies, other interventions with *Rosa canina* were performed on humans, but most of them focused on its effects against other pathologies such as osteoarthritis(444), urinary tract infections(445) and mental disorders such as attention-deficit/hyperactivity disorder(446) or depressive behavior(447), and only one on T2DM patients, exhibiting favorable effects in all trials. On the contrary, there are numerous studies both in vitro and with rodents about the anti-diabetic effects of *Rosa canina*, probably one of its most outstanding attributes. This antidiabetic role has been attributed to different mechanisms, one of them for example due to the high inhibitory activity against  $\alpha$ -amylase of *Rosa canina*(448)

but also to many others such as its potent action on pancreas acting as a protector and growth factor of  $\beta$ -cells and therefore helping the regeneration of damaged pancreatic islets(449–452). In addition on pancreas, is described its anti-diabetic role by exerting a protective effect against apoptosis by modulation of autophagy pathways(453), as well as modulating DNA methylation(454) and decreasing oxidative stress(455).

In our case we did not focus on the already explored mechanics in pancreas but rather we examined the metabolic processes involved in non-previously studied tissues such as scWAT or liver, since a metabolic improvement in these organs could also explain the *Rosa canina* antidiabetic and antiobesogenic effect. In that sense, the metabolic improvement of scWAT from flesh-supplemented mice compared to HFD-only mice is remarkable. As stated in the introduction, one of the first manifestations of obesity is the hypertrophy and lipid overload of WAT adipocytes, which is observed in HFD-only mice. In contrast, if we look at the scWAT of mice supplemented with *Rosa canina*, we can observe that there is a significant decrease in the size of adipocytes as well as a greater number of adipocytes, demonstrating less hypertrophy and more hyperplasia, therefore exhibiting a healthier response to HFD. This marked improvement could be explained by the capacity of the flesh to modify the expression for example the unilocular lipid droplet fusion-related key gene *Fsp27 $\alpha$*  but also the lipid metabolic pathways. As demonstrated by the performed analyses, exerting a decrease in the expression of genes involved in lipid transport such as *Cd36* or *Fabp4*, as well as genes involved in lipogenesis such as *Fasn* or *Dgat* and the decrease of the key transcriptional regulator of lipid metabolism *Srebp1c*. Although in liver *Srebp1c* role is clearly described and along with ChREBP necessary for the expression of lipogenic and glycolytic genes, in adipose tissue its role is still controversial(126). In other similar studies with natural sources of bioactive compounds or caloric restriction against a HFD, it has been shown that the expression of *Srebp1c* as well as its downstream genes in scWAT, are enhanced on the supplemented or caloric restricted animals. Thus, an increase in de novo lipogenesis was observed on those studies, but at the same time a beneficial and marked increase in lipid oxidation and thermogenesis process(344,456). In contrast, on the scWAT of our supplemented animals, we observed a decrease in *Srebp1c* as well as in the other DNL key genes; thereby *Rosa canina* supplementation resembles more the *Srebp1c*-inhibitory action and lipogenic gene repression of PUFAs(457) than the novo lipogenesis-enhancing effect described on high-flavonoid sources supplementation(458). This fact is also contrasted with the browning and increase on thermogenesis processes of scWAT, both reported together with an increase in DNL in this

type of interventions. In case of scWAT from mice supplemented with *Rosa canina*, no significant increase in browning and thermogenesis markers were observed, although there was an upward trend in the case of the *Ucp1* gene and, inversely to what might be expected, a decrease in *Dio2*. Contrary to scWAT, in the BAT of *Rosa canina*-supplemented animals, an upregulation of key thermogenesis genes and mitochondrial biogenesis markers was observed, thus leading to an increase in energy expenditure and consequently to a metabolic improvement against the obese state.

Even though the effects of *Rosa canina* were notable in adipose tissues, the main organ showing the greatest changes as a result of the flesh supplementation was the liver. In a first analysis, it was observed that livers from *Rosa canina* supplemented mice presented a lower tissue weight and a significant decrease in markers of oxidative stress and inflammation compared to HFD-only animals. These preliminary results, were consistent with the detailed performed histological analysis. As explained in the introductory section, NAFLD progresses through different states of deterioration, starting from an initial fat accumulation to inflammation, fibrosis, steatohepatitis, and cirrhosis, which are easily differentiated in the histological analyses. HFD-only animals suffered not only from severe steatosis but also from generalized ballooning, constriction of the hepatic veins and infiltration of pro-inflammatory immune cells in the areas near the blood vessels, thereby evidencing an advanced NAFLD-state and proving the pernicious character of HFD in liver. Interestingly this severe and advanced HFD-associated NAFLD state was not observed on livers from RC-supplemented mice. One of the first key genes involved in the exhibited improvement on livers of supplemented animals was *Fsp27*, whose role in the regulation of lipid droplet synthesis and hepatic lipid homeostasis is a major determinant in the progression of NAFLD. In livers from HFD-only mice, it is observed how *Fsp27β* is upregulated by the HFD and linked to the progression of NAFLD as it reported Xu et al., who first described the *FSP27β* isoform (138). On the contrary, in RC-supplemented mice livers, a marked decrease in the expression of *Fsp27β* and therefore a clear downregulation by the *Rosa canina* is exhibited. Interestingly, it has been reported that sustained downregulation of *Fsp27β* in the steatotic liver not only results in a significant reduction of lipid droplets but also diminish liver injury and inflammation both essential to the progression from steatosis to steatohepatitis, as observed in the histological sections of supplemented mouse livers(136). Evidently, this change in *Fsp27β* expression in livers from supplemented mice was also accompanied by other substantial changes in the expression of key genes.



Metabolically, there were 3 major changes on livers from supplemented mice compared to HFD-only ones. The first significant change was related to FGF21 signaling. As the literature on animal studies well exposes, aberrant FGF21 signaling is a key step in the development and progression of NAFLD(459). A recent phase II clinical study has shown that administration of an FGF21 analogue, improved the FGF21-resistance state and subsequently significantly reduced fat accumulation in advanced NASH subjects(460). In our intervention with *Rosa canina*, we observed a notably decrease in the expression of *Fgf21* in liver but also an enhancement in the expression of its co-receptors and an upward trend on its downstream genes as well as a significantly enhancement of *Adiponectin* expression was observed. Therefore, *Rosa canina* would be exerting an enhancement of FGF21 signaling and consequently contributing to alleviate the progression of NAFLD produced by HFD. The second major change on hepatic metabolism, was related to glucose metabolism. As explained on the results section, livers from supplemented mice exhibited a significantly decrease in key genes regulating glucose utilization which are linking glucose and lipogenesis processes, such as *GluK*, *Glyk*, *LpK* and the transcription factor *Chrebbp*. As it is known, liver plays a key role in glucose homeostasis increasing or decreasing glucose output through the different states, either fasting or feeding. *GluK* is central to this process by encoding the protein catalyzing glucose to glucose 6-phosphate, a step which is essential for glucose metabolism in liver as well as for the induction of glycolytic and lipogenic genes(461). In that sense, the *GluK* activity is the primary step of the hepatic DNL, which as discussed above is one of the main altered pathways on NAFLD. Andreas Peter et al suggested that increased *GluK* activity may induce fatty liver and its metabolic and hepatic consequences in humans by demonstrating for the first time that *GluK* expression is associated with markers of de DNL and liver TAG content in humans(462). Subsequently, other studies in humans have linked the overexpression of these kinases to the severity and progression of NAFLD, most recently in the case of *LpK* in patients with NASH(463). Regarding the ChREBP, it is known to be one of the main glucose-sensing transcription factors that potently activates the panel of the DNL upon excess glucose. *Chrebbp* expression increases in livers from NAFLD patients and inversely, a deficiency alleviates liver steatosis and improves glucose metabolism(464). As it can be seen, the *Rosa canina* flesh intervention drastically decreases *GluK*, *Glyk* and *LpK* genes which are directly associated with the pathological progression of the diet induced NAFLD by modulating the initiation of lipogenic pathway in the liver. However, as can be observed, the expression of *Chrebbp* present an upward trend on supplemented mice. This result differs from many studies



linking an improvement in NAFLD progression to a decrease in ChREBP expression. Thus, it could be that the improvement exerted by *Rosa canina* is not due to a modulation of ChREBP transcription factor and its upward trend of *Chrebbp* expression is a result of the dissociation capacity of ChREBP between hepatic steatosis and insulin resistance. The theory of ChREBP dissociation is based on the results of Fadila Benhamed et al. who exposed that mice fed with a HFD overexpressing ChREBP showed normal insulin levels and improved insulin signaling and glucose tolerance compared to HFD-controls non-overexpressed ChREBP, despite having increased hepatic steatosis(465). Finally, this research found that ChREBP expression in liver biopsies from patients with NASH increased when steatosis was greater than 50% and decreased in the presence of severe insulin resistance(465). Taken together, these results demonstrated that increased ChREBP can dissociate hepatic steatosis from insulin resistance, with beneficial effects on both glucose and lipid metabolism(465,466).

The third and the most relevant change on livers from supplemented mice was related directly to lipid metabolism. HFD+RC mice exhibited a generalized downregulation of genes linked to fat accumulation, firstly with a significant decrease in the gene expression tied to fatty acid transport, such as *Cd36* and *Fabp4*, and *Ptbp* gene, related to cholesterol assembly and transport; secondly with a decline in the expression of key genes of fatty acid synthesis, such as *Fasn*, *Scd1* and *Acaca*; and finally with a downregulation of the key TAG-synthesis gene *Dgat*. Thus summarizing, livers from supplemented mice showed a slowing down NAFLD-state in comparison to HFD-only animals by modulating expression genes linked to the two main contributors the NAFLD steatosis state: the excessive NEFAs flux transport from the overloaded adipose tissue and secondly the exacerbation of the hepatic novo lipogenesis metabolic pathway.

Interestingly, this complex set of results in liver but also on the global homeostatic improvement could be explained by the modulatory action of *Rosa canina* on the transcriptional regulation. Bioactive compounds regulate gene expression through different mechanisms, such as changes on chromatin structure, non-coding RNAs, and by modulating the expression of transcription factors or by direct ligand binding to nuclear receptors. The gene expression pattern on livers from supplemented animals showed that there was a strong decrease in the DNL process. This metabolic pathway, along with other modified pathways such as the lipid droplet formation, is controlled by the transcription factor SREBP1c which is involved in fatty acid synthesis, adipose tissue homeostasis and insulin-induced glucose metabolism mainly in the liver. Unfortunately,

no change in its expression was observed nor in the expression of the SMILE corepressor, which has been described to be strongly involved in the maintenance of lipid homeostasis regulated by SREBP1c and LXR in similar interventions with bioactive compound-rich sources(343). Likewise, a decrease in the transcription factor ChREBP was not observed, but an upward trend on its beta isoform, as discussed above. In contrast, a significant change in the expression of peroxisome proliferator-activated receptors (PPARs) was observed. As discussed in the introduction, PPARs have pleiotropic actions and they are critical regulators not only of fatty acid metabolism, but also of glucose metabolism, inflammation, oxidative damage, fibrosis processes and in general energy metabolism(180). Curiously, livers from *Rosa canina* supplemented mice exhibited a significant increase in  $\beta/\delta$  isoform and a marked decrease in the  $\gamma$  isoform. As discussed above, the study by Nagatomo et al. already attributed the effect of *Rosa canina* to its PPAR $\gamma$  modulating effect in WAT but not in liver. Thus, since the modification of the hepatic gene expression by *Rosa canina* is exhibited downstream of the PPARs, it could be that some of the compounds present in the flesh are acting as agonists or antagonists of these receptors. In fact, the results of the *Rosa canina* intervention largely resemble the results of studies conducted with PPAR $\gamma$  antagonists or with dual effect, PPAR $\gamma$  antagonists/PPAR $\beta/\delta$  agonists (395,467). In this sense, both the flesh and the different fractions into which the flesh was divided, were characterized, and tested in a reporter assay to see if they exhibited PPAR $\gamma$  antagonistic activity. Thereby, it was observed that the most liposoluble fractions of *Rosa canina* were those that exhibited the greatest PPAR $\gamma$  antagonist effect, in addition to demonstrating this effect both in a liver model using HepG2 cells and in a WAT model in the differentiation process of 3T3L1 cells.

Surprisingly, by analyzing the bioactive compound profile of the flesh fractions, large differences are exhibited. The two fractions with the highest presence of bioactive compounds and species with highest attributed biological activity are the chloroform and the ethyl acetate fractions. However, the ethyl acetate fraction does not show any PPAR $\gamma$ -antagonistic activity. In contrast, the hexane fraction as it can be observed, has a strong antagonistic activity but showed the lowest presence of bioactive compounds compared to the other fractions. By analyzing each characterized bioactive compound group and their presence in the different fractions, it is possible to hypothesize which might be the family responsible for the antagonistic activity of the flesh. Firstly, the families of phenolic compounds would be discarded, since although they are

present in the chloroform fraction and there is evidence in the literature that some polyphenols may act as antagonists, the hexane fraction their presence is severely decreased or absent. On the contrary, families like terpenoids or fatty acid derivatives are present in both chloroform and hexane fractions and thereby they could be the responsible of the PPAR $\gamma$  antagonistic action. In case of both FA derivatives and terpenoids, we note that some of the species identified already have effects on PPARs described in the literature. For example the betulinic acid, the oleanolic acid, the glycyrrhetic acid, the 9-hydroxy-10,12-octadecadienoic acid, as well as different PUFAs and other characterized lipidic species(395,468–470). Unfortunately, it can be observed that the ethyl acetate fraction also has the presence of these groups of compounds, but ethyl acetate fraction didn't show antagonistic activity. In this sense and based on the carried out analyses, it is not possible to elucidate with total certainty which group of bioactive compounds could be responsible for the PPAR $\gamma$  antagonist activity. However, there is another possibility in this perspective. As mentioned above, the identification process of compounds from the flesh and its fractions was performed using a BEH C18 (2.1x100mm, 1.7 $\mu$ m) analytical column in order to characterize as many compounds as possible. On the other hand, this separation column for chromatography analyses is incapable of retaining very long and highly non-polar compounds such as carotenoids or larger eicosanoids. Moreover, in the fractionation process of *Rosa canina* flesh, both chloroform and hexane are capable of extract carotenoids, but ethyl acetate does not do it so easily due its more polar character(471). It is for this reason why a possible scenario would be that the PPAR $\gamma$  antagonist effect exhibited was produced by a group of compounds which have not been possible to identify with the used technique.

Reviewing bibliography with other *Rosaceae* species treatments appears Abbas et al. postulating that the antidiabetic effect of *Rosa Damascena* extract in diabetic rats was due to the agonist effect of this extract on PPAR $\gamma$  and therefore to its similar action to TZDs(472). Thus, the mechanism described in that research is inverse to the one we have found. Interestingly, Abbas et al. intervention was not done with the fruit flesh but with a methanol extract. The Nagatomo study cited above, used an extract as well, but in his model, it was used an aqueous ethanol extract. In that sense, he observed a PPAR $\gamma$  antagonist effect but it was only described in the adipose tissue. On the other hand, and more recently, a very similar study to the one carried out in this thesis proposal was published, but instead of using rosehip flesh, they used *Rosa mosqueta* oil against a HFD of 60% on mice. The results of the intervention, in terms of scWAT profile, glucose and insulin metabolism, as well as liver status, were very similar to our research. In contrast, they

attributed the anti-inflammatory and antisteatotic effect to the ability of rosehip oil to upregulate PPAR $\alpha$  and Nrf2 in liver, without making any reference to PPAR $\gamma$ (473). This hypothesis about the modulatory effect on PPAR $\alpha$  is also reinforced by other studies. In particular there is a study regarding *Rosa canina* antioxidative role, that tested an aqueous acetone extract and its main constituents. In this study, they show that the species kaempferol 3-O- $\beta$ -d-glucopyranoside, p-coumaroyl and trans-tiliroside exert anti-obese effects. Furthermore, they exposed that a single oral administration of this last specie, the trans-tiliroside, at a dose of 10 mg/kg is able to increase the expression of hepatic PPAR $\alpha$  mRNA in mouse(474). Overall, it can be observed that even if the effects in all the studies involve a metabolic improvement, the underlying mechanisms are slightly different. However, no study alludes the antagonist role of the most lipophilic bioactive compound species of *Rosaceae* on PPAR $\gamma$ .

Our study reveals that *Rosa canina* slows down the steatotic effect of HFD and its more lipophilic fractions exert a modulating effect on the PPAR $\gamma$  transcription factor, thereby being partly responsible of the therapeutic effect. Concerning the responsible species for this effect, the identification of *Rosa canina* flesh and its fractions reveal a distributed large number of different compounds with beneficial effects that have been extensively demonstrated in the literature. Unfortunately, it was not possible to discern through our fractionation and characterization which of the families of bioactive compounds were responsible for the antagonistic effect observed. However, it has been observed that the most lipophilic fractions are responsible for the effect and therefore it is probably that the most lipophilic compounds, which in turn were the ones that could not be identified, were responsible for the effect.

On a global standpoint, the importance of the food matrix in nutritional interventions is evident. A mixture of pure isolated polyphenols against the action of a HFD can aggravate the damage caused by the HFD and lead to a severe aggression on the kidney. On the other hand, the study of bioactive compounds in their own matrix opens doors not only to new therapeutic targets but also to discover new compounds and synergistic effects against obesity and its comorbidities. Even so, we should not fall into reductionist arguments claiming that synthetic is worse than natural. In this case, in my opinion, it is necessary to value the whole of the source of the bioactive compounds, since it is probably this whole that is responsible for their effects.



CONCLUSION



## 6. Conclusion

On a global standpoint, the importance of the food matrix on bioactive compound nutritional interventions is evident. A mixture of pure isolated polyphenols against the action of a HFD can aggravate the damage caused by the HFD and lead to an aggression on kidney. Specifically:

- Supplementation with pure isolated polyphenols enhances hyperglycemia and worsens glucose and insulin response.
- Pure isolated polyphenols supplementation partially intensifies some changes inherent to HFD action related to general metabolism in scWAT and liver.
- On HFD-fed mice kidneys, pure isolated polyphenols increase oxidative stress and up-regulate fibrosis and kidney damage markers.

On the other hand, the study of bioactive compounds in their own matrix opens doors not only to new therapeutic targets but also to discover new compounds and synergistic effects against obesity and its comorbidities. In this sense *Rosa canina* flesh has shown a great potential in reducing the progression of NAFLD. In particular:

- Supplementation with *Rosa canina* slows down the pernicious action of HFD by down-regulating the metabolic pathways involved in lipid accumulation and by an overall metabolic improvement.
- More precisely, a downregulation of the transcription factor *Ppar $\gamma$*  was observed in the liver, which could be partly responsible for the anti-steatotic effects of the *Rosa canina* flesh.
- This regulatory action on PPAR $\gamma$  is characteristic of the liposoluble fractions of *Rosa canina* and therefore, specific to the more lipophilic groups of bioactive compounds.

Despite the results of this thesis, we should not fall into reductionist arguments claiming that synthetic is worse than natural. There is need for more research on the specific action of the individual polyphenols as well as on the synergies that bioactive compounds might have with other molecules and the food matrix to understand the actual role of these species against obesity and its associated pathologies.





## BIBLIOGRAPHY



## **Bibliography**

1. Dhital SM. Noncommunicable diseases. Vol. 369, *The New England journal of medicine*. 2013. p. 2562.
2. WHO | The world health report 2002 - Reducing Risks, Promoting Healthy Life. WHO. World Health Organization; 2013.
3. Sixty-sixth world health assembly provisional agenda item 13 Draft action plan for the prevention and control of noncommunicable diseases 2013-2020 Report by the Secretariat.
4. Gowshall M, Taylor-Robinson SD. The increasing prevalence of non-communicable diseases in low-middle income countries: the view from Malawi. *Int J Gen Med*. 2018 Jun 28;11:255–64.
5. Cost of Non-Communicable Diseases in the EU | EU Science Hub [Internet]. [cited 2020 Apr 24]. Available from: [https://ec.europa.eu/jrc/en/health-knowledge-gateway/societal-impacts/costs#\\_leal2006](https://ec.europa.eu/jrc/en/health-knowledge-gateway/societal-impacts/costs#_leal2006)
6. Saklayen MG. The Global Epidemic of the Metabolic Syndrome. *Curr Hypertens Rep*. 2018 Feb 26;20(2):12.
7. Wu Y, Ding Y, Tanaka Y, Zhang W. Risk factors contributing to type 2 diabetes and recent advances in the treatment and prevention. *Int J Med Sci*. 2014;11(11):1185–200.
8. Cornier M-A, Dabelea D, Hernandez TL, Lindstrom RC, Steig AJ, Stob NR, et al. The metabolic syndrome. *Endocr Rev*. 2008 Dec;29(7):777–822.
9. Wildman RP, Muntner P, Reynolds K, McGinn AP, Rajpathak S, Wylie-Rosett J, et al. The obese without cardiometabolic risk factor clustering and the normal weight with cardiometabolic risk factor clustering: prevalence and correlates of 2 phenotypes among the US population (NHANES 1999-2004). *Arch Intern Med*. 2008 Aug;168(15):1617–24.
10. De Lorenzo A, Romano L, Di Renzo L, Di Lorenzo N, Cennamo G, Gualtieri P. Obesity: a preventable, treatable, but relapsing disease. *Nutrition*. 2019;71:110615.
11. Malone JI, Hansen BC. Does obesity cause type 2 diabetes mellitus (T2DM)? Or is it the opposite? *Pediatr Diabetes*. 2019 Feb;20(1):5–9.
12. Yazıcı D, Sezer H. Insulin Resistance, Obesity and Lipotoxicity BT - Obesity and Lipotoxicity. In: Engin AB, Engin A, editors. Cham: Springer

International Publishing; 2017. p. 277–304.

13. Muir LA, Neeley CK, Meyer KA, Baker NA, Brosius AM, Washabaugh AR, et al. Adipose tissue fibrosis, hypertrophy, and hyperplasia: Correlations with diabetes in human obesity. *Obesity (Silver Spring)*. 2016 Mar;24(3):597–605.
14. Jo J, Gavrilova O, Pack S, Jou W, Mullen S, Sumner AE, et al. Hypertrophy and/or Hyperplasia: Dynamics of Adipose Tissue Growth. *PLoS Comput Biol*. 2009/03/27. 2009 Mar;5(3):e1000324–e1000324.
15. Arner E, Westermark PO, Spalding KL, Britton T, Rydén M, Frisén J, et al. Adipocyte turnover: relevance to human adipose tissue morphology. *Diabetes*. 2009/10/21. 2010 Jan;59(1):105–9.
16. Longo M, Zatterale F, Naderi J, Parrillo L, Formisano P, Raciti GA, et al. Adipose Tissue Dysfunction as Determinant of Obesity-Associated Metabolic Complications. *Int J Mol Sci*. 2019 May 13;20(9):2358.
17. Huh JY, Park YJ, Ham M, Kim JB. Crosstalk between adipocytes and immune cells in adipose tissue inflammation and metabolic dysregulation in obesity. *Mol Cells*. 2014/04/30. 2014 May;37(5):365–71.
18. Olefsky JM, Glass CK. Macrophages, Inflammation, and Insulin Resistance. *Annu Rev Physiol*. 2010 Feb 11;72(1):219–46.
19. Castoldi A, Naffah de Souza C, Câmara NOS, Moraes-Vieira PM. The Macrophage Switch in Obesity Development. *Front Immunol*. 2015;6:637.
20. Kraakman MJ, Murphy AJ, Jandeleit-Dahm K, Kammoun HL. Macrophage polarization in obesity and type 2 diabetes: weighing down our understanding of macrophage function? *Front Immunol*. 2014;5:470.
21. Esser N, Legrand-Poels S, Piette J, Scheen AJ, Paquot N. Inflammation as a link between obesity, metabolic syndrome and type 2 diabetes. *Diabetes Res Clin Pract*. 2014;105(2):141–50.
22. Mosser DM, Edwards JP. Exploring the full spectrum of macrophage activation. *Nat Rev Immunol*. 2008 Dec;8(12):958–69.
23. Kratz M, Coats BR, Hisert KB, Hagman D, Mutskov V, Peris E, et al. Metabolic dysfunction drives a mechanistically distinct proinflammatory phenotype in adipose tissue macrophages. *Cell Metab*. 2014 Oct;20(4):614–25.
24. Ren W, Xia Y, Chen S, Wu G, Bazer FW, Zhou B, et al. Glutamine Metabolism in Macrophages: A Novel Target for Obesity/Type 2 Diabetes.

- Adv Nutr. 2019 Mar 1;10(2):321–30.
25. Freerman AJ, Johnson AR, Sacks GN, Milner JJ, Kirk EL, Troester MA, et al. Metabolic reprogramming of macrophages: glucose transporter 1 (GLUT1)-mediated glucose metabolism drives a proinflammatory phenotype. *J Biol Chem*. 2014 Mar;289(11):7884–96.
  26. Shoelson SE, Herrero L, Naaz A. Obesity, Inflammation, and Insulin Resistance. *Gastroenterology*. 2007 May 1;132(6):2169–80.
  27. Mendez-Sanchez N, Cruz-Ramon VC, Ramirez-Perez OL, Hwang JP, Barranco-Fragoso B, Cordova-Gallardo J. New aspects of lipotoxicity in nonalcoholic steatohepatitis. *Int J Mol Sci*. 2018;19(7).
  28. Hotamisligil GS. Inflammation, metaflammation and immunometabolic disorders. *Nature*. 2017 Feb;542(7640):177–85.
  29. Kawai T, Autieri M V, Scalia R. Adipose tissue inflammation and metabolic dysfunction in obesity. *Am J Physiol Cell Physiol*. 2021 Mar;320(3):C375–91.
  30. Carneiro IP, Elliott SA, Siervo M, Padwal R, Bertoli S, Battezzati A, et al. Is Obesity Associated with Altered Energy Expenditure? *Adv Nutr*. 2016 May;7(3):476–87.
  31. Manna P, Jain SK. Obesity, Oxidative Stress, Adipose Tissue Dysfunction, and the Associated Health Risks: Causes and Therapeutic Strategies. *Metab Syndr Relat Disord*. 2015 Dec;13(10):423–44.
  32. Shen W, Wang Z, Punyanita M, Lei J, Sinav A, Kral JG, et al. Adipose tissue quantification by imaging methods: a proposed classification. *Obes Res*. 2003 Jan;11(1):5–16.
  33. Mende CW, Einhorn D. Fatty kidney disease: a new renal and endocrine clinical entity? describing the role of the kidney in obesity, metabolic syndrome, and type 2 diabetes. *Endocr Pract*. 2019 Aug;25(8):854–8.
  34. Ertunc ME, Hotamisligil GS. Lipid signaling and lipotoxicity in metaflammation: indications for metabolic disease pathogenesis and treatment. 2016;57:2099–114.
  35. Carobbio S, Rodriguez-Cuenca S, Vidal-Puig A. Origins of metabolic complications in obesity: ectopic fat accumulation. The importance of the qualitative aspect of lipotoxicity. *Curr Opin Clin Nutr Metab Care*. 2011 Nov;14(6):520–6.
  36. de Mello AH, Costa AB, Engel JDG, Rezin GT. Mitochondrial dysfunction

in obesity. *Life Sci.* 2018;192:26–32.

37. Engin AB. What Is Lipotoxicity? *Adv Exp Med Biol.* 2017;960:197–220.
38. Haffner SM. The Metabolic Syndrome: Inflammation, Diabetes Mellitus, and Cardiovascular Disease. *Am J Cardiol.* 2006;97(2, Supplement 1):3–11.
39. Virtue S, Vidal-Puig A. It's Not How Fat You Are, It's What You Do with It That Counts. *PLOS Biol.* 2008 Sep 23;6(9):e237.
40. Chatterjee S, Khunti K, Davies MJ. Type 2 diabetes. *Lancet (London, England).* 2017 Jun;389(10085):2239–51.
41. Jm B, Jl T, Biochemistry SL, York N. Berg JM, Tymoczko JL, Stryer L. *Biochemistry.* 5th edition. New York: W H Freeman; 2002. 2016;9–11.
42. Stumvoll M, Goldstein BJ, van Haeften TW. Type 2 diabetes: principles of pathogenesis and therapy. *Lancet (London, England).* 2005 Apr;365(9467):1333–46.
43. Galicia-Garcia U, Benito-Vicente A, Jebari S, Larrea-Sebal A, Siddiqi H, Uribe KB, et al. Pathophysiology of Type 2 Diabetes Mellitus. *Int J Mol Sci.* 2020 Aug;21(17).
44. Hayden MR, Sowers JR. Isletopathy in Type 2 diabetes mellitus: implications of islet RAS, islet fibrosis, islet amyloid, remodeling, and oxidative stress. *Antioxid Redox Signal.* 2007 Jul;9(7):891–910.
45. Ying W, Fu W, Lee YS, Olefsky JM. The role of macrophages in obesity-associated islet inflammation and  $\beta$ -cell abnormalities. *Nat Rev Endocrinol.* 2020 Feb;16(2):81–90.
46. Westermark P, Andersson A, Westermark GT. Islet Amyloid Polypeptide, Islet Amyloid, and Diabetes Mellitus. *Physiol Rev.* 2011 Jul 1;91(3):795–826.
47. Guardado-Mendoza R, Davalli AM, Chavez AO, Hubbard GB, Dick EJ, Majluf-Cruz A, et al. Pancreatic islet amyloidosis, beta-cell apoptosis, and alpha-cell proliferation are determinants of islet remodeling in type-2 diabetic baboons. *Proc Natl Acad Sci U S A.* 2009 Aug;106(33):13992–7.
48. Mundi MS, Velapati S, Patel J, Kellogg TA, Abu Dayyeh BK, Hurt RT. Evolution of NAFLD and Its Management. *Nutr Clin Pract.* 2020 Feb 1;35(1):72–84.
49. Lindenmeyer CC, McCullough AJ. The Natural History of Nonalcoholic Fatty Liver Disease—An Evolving View. *Clin Liver Dis.* 2018;22(1):11–21.

50. Younossi Z, Anstee QM, Marietti M, Hardy T, Henry L, Eslam M, et al. Global burden of NAFLD and NASH: trends, predictions, risk factors and prevention. *Nat Rev Gastroenterol Hepatol*. 2018 Jan;15(1):11–20.
51. Younossi ZM, Koenig AB, Abdelatif D, Fazel Y, Henry L, Wymer M. Global epidemiology of nonalcoholic fatty liver disease—Meta-analytic assessment of prevalence, incidence, and outcomes. *Hepatology*. 2016 Jul;64(1):73–84.
52. Pierantonelli I, Svegliati-Baroni G. Nonalcoholic Fatty Liver Disease: Basic Pathogenetic Mechanisms in the Progression From NAFLD to NASH. *Transplantation*. 2019;103(1).
53. Brown MS, Goldstein JL. Selective versus total insulin resistance: a pathogenic paradox. *Cell Metab*. 2008 Feb;7(2):95–6.
54. Donnelly KL, Smith CI, Schwarzenberg SJ, Jessurun J, Boldt MD, Parks EJ. Sources of fatty acids stored in liver and secreted via lipoproteins in patients with nonalcoholic fatty liver disease. *J Clin Invest*. 2005 May 2;115(5):1343–51.
55. Green CJ, Parry SA, Gunn PJ, Ceresa CDL, Rosqvist F, Piché M-E, et al. Studying non-alcoholic fatty liver disease: the ins and outs of in vivo, ex vivo and in vitro human models. *Horm Mol Biol Clin Investig*. 2020;41(1).
56. Santos-López JA, Garcimartín A, Bastida S, Bautista-ávila M, González-Muñoz MJ, Benedí J, et al. Lipoprotein profile in aged rats fed chia oil-or hydroxytyrosol-enriched pork in high cholesterol/high saturated fat diets. *Nutrients*. 2018;10(12):1–17.
57. Friedman SL, Neuschwander-Tetri BA, Rinella M, Sanyal AJ. Mechanisms of NAFLD development and therapeutic strategies. *Nat Med*. 2018/07/02. 2018 Jul;24(7):908–22.
58. Rada P, González-Rodríguez Á, García-Monzón C, Valverde ÁM. Understanding lipotoxicity in NAFLD pathogenesis: is CD36 a key driver? *Cell Death Dis*. 2020;11(9):802.
59. Peng C, Stewart AG, Woodman OL, Ritchie RH, Qin CX. Non-Alcoholic Steatohepatitis: A Review of Its Mechanism, Models and Medical Treatments . Vol. 11, *Frontiers in Pharmacology* . 2020. p. 1864.
60. Egnatchik RA, Leamy AK, Noguchi Y, Shiota M, Young JD. Palmitate-induced activation of mitochondrial metabolism promotes oxidative stress and apoptosis in H4IIEC3 rat hepatocytes. *Metabolism*. 2014 Feb;63(2):283–95.



61. Zarrinpar A, Busuttill RW. Liver transplantation: past, present and future. *Nat Rev Gastroenterol Hepatol*. 2013;10(7):434–40.
62. Byrne CD, Targher G. NAFLD as a driver of chronic kidney disease. *J Hepatol*. 2020 Apr 1;72(4):785–801.
63. Musso G, Cassader M, Cohney S, Pinach S, Saba F, Gambino R. Emerging Liver-Kidney Interactions in Nonalcoholic Fatty Liver Disease. *Trends Mol Med*. 2015 Oct;21(10):645–62.
64. Marcuccilli M, Chonchol M. NAFLD and Chronic Kidney Disease. *Int J Mol Sci*. 2016 Apr;17(4):562.
65. Ammirati AL. Chronic Kidney Disease. *Rev Assoc Med Bras*. 2020 Jan;66Suppl 1(Suppl 1):s03–9.
66. Romagnani P, Remuzzi G, Glassock R, Levin A, Jager KJ, Tonelli M, et al. Chronic kidney disease. *Nat Rev Dis Prim*. 2017;3(1):17088.
67. Carney EF. The impact of chronic kidney disease on global health. *Nat Rev Nephrol*. 2020;16(5):251.
68. Gai Z, Wang T, Visentin M, Kullak-Ublick GA, Fu X, Wang Z. Lipid Accumulation and Chronic Kidney Disease. *Nutrients*. 2019 Mar 28;11(4):722.
69. Anders H-J, Huber TB, Isermann B, Schiffer M. CKD in diabetes: diabetic kidney disease versus nondiabetic kidney disease. *Nat Rev Nephrol*. 2018;14(6):361–77.
70. Bargman JM, Skorecki KL. Chronic Kidney Disease. In: Jameson JL, Fauci AS, Kasper DL, Hauser SL, Longo DL, Loscalzo J, editors. *Harrison's Principles of Internal Medicine*, 20e. New York, NY: McGraw-Hill Education; 2018.
71. Yang P, Xiao Y, Luo X, Zhao Y, Zhao L, Wang Y, et al. Inflammatory stress promotes the development of obesity-related chronic kidney disease via CD36 in mice. *J Lipid Res*. 2017 Jul;58(7):1417–27.
72. Tonneijck L, Muskiet MHA, Smits MM, van Bommel EJ, Heerspink HJL, van Raalte DH, et al. Glomerular Hyperfiltration in Diabetes: Mechanisms, Clinical Significance, and Treatment. *J Am Soc Nephrol*. 2017 Apr 1;28(4):1023 LP – 1039.
73. Thomas MC, Brownlee M, Susztak K, Sharma K, Jandeleit-Dahm KAM, Zoungas S, et al. Diabetic kidney disease. *Nat Rev Dis Prim*. 2015;1(1):15018.

74. Inoguchi T, Li P, Umeda F, Yu HY, Kakimoto M, Imamura M, et al. High glucose level and free fatty acid stimulate reactive oxygen species production through protein kinase C--dependent activation of NAD(P)H oxidase in cultured vascular cells. *Diabetes*. 2000 Nov 1;49(11):1939 LP – 1945.
75. Brownlee M. Biochemistry and molecular cell biology of diabetic complications. *Nature*. 2001;414(6865):813–20.
76. Schaffer SW, Jong CJ, Mozaffari M. Role of oxidative stress in diabetes-mediated vascular dysfunction: Unifying hypothesis of diabetes revisited. *Vascul Pharmacol*. 2012;57(5):139–49.
77. van Bommel EJM, Muskiet MHA, Tonneijck L, Kramer MHH, Nieuwdorp M, van Raalte DH. SGLT2 Inhibition in the Diabetic Kidney—From Mechanisms to Clinical Outcome. *Clin J Am Soc Nephrol*. 2017 Apr 3;12(4):700 LP – 710.
78. Santos RAS, Oudit GY, Verano-Braga T, Canta G, Steckelings UM, Bader M. The renin-angiotensin system: going beyond the classical paradigms. *Am J Physiol Heart Circ Physiol*. 2019 May;316(5):H958–70.
79. Remuzzi G, Perico N, Macia M, Ruggenenti P. The role of renin-angiotensin-aldosterone system in the progression of chronic kidney disease. *Kidney Int Suppl*. 2005 Dec;(99):S57-65.
80. Tzika E, Dreker T, Imhof A. Epigenetics and Metabolism in Health and Disease . Vol. 9, *Frontiers in Genetics* . 2018. p. 361.
81. Zhang L, Bruce-Keller AJ, Dasuri K, Nguyen A, Liu Y, Keller JN. Diet-induced metabolic disturbances as modulators of brain homeostasis. *Biochim Biophys Acta - Mol Basis Dis*. 2009;1792(5):417–22.
82. Torres N, Vargas-Castillo AE, Tovar AR. Adipose Tissue: White Adipose Tissue Structure and Function. In: Caballero B, Finglas PM, Toldrá FBT-E of F and H, editors. Oxford: Academic Press; 2016. p. 35–42.
83. Azzu V, Vacca M, Virtue S, Allison M, Vidal-Puig A. Adipose Tissue-Liver Cross Talk in the Control of Whole-Body Metabolism: Implications in Nonalcoholic Fatty Liver Disease. *Gastroenterology*. 2020 May 1;158(7):1899–912.
84. Hotamisligil GS. Inflammation and metabolic disorders. *Nature*. 2006;444(7121):860–7.
85. Nedergaard J, Bengtsson T, Cannon B. Unexpected evidence for active brown adipose tissue in adult humans. *Am J Physiol Endocrinol Metab*. 2007

Aug;293(2):E444-52.

86. Trefts E, Gannon M, Wasserman DH. The liver. *Curr Biol*. 2017 Nov;27(21):R1147–51.
87. Malarkey DE, Johnson K, Ryan L, Boorman G, Maronpot RR. New insights into functional aspects of liver morphology. *Toxicol Pathol*. 2005;33(1):27–34.
88. Seebacher F, Zeigerer A, Kory N, Krahmer N. Hepatic lipid droplet homeostasis and fatty liver disease. *Semin Cell Dev Biol*. 2020;108:72–81.
89. Su X, Abumrad NA. Cellular fatty acid uptake: a pathway under construction. *Trends Endocrinol Metab*. 2009 Mar;20(2):72–7.
90. Fabbrini E, Sullivan S, Klein S. Obesity and nonalcoholic fatty liver disease: biochemical, metabolic, and clinical implications. *Hepatology*. 2010 Feb;51(2):679–89.
91. Rui L. Energy metabolism in the liver. *Compr Physiol*. 2014 Jan;4(1):177–97.
92. Pardina E, Baena-Fustegueras JA, Catalán R, Galard R, Lecube A, Fort JM, et al. Increased expression and activity of hepatic lipase in the liver of morbidly obese adult patients in relation to lipid content. *Obes Surg*. 2009 Jul;19(7):894–904.
93. Doege H, Grimm D, Falcon A, Tsang B, Storm TA, Xu H, et al. Silencing of hepatic fatty acid transporter protein 5 in vivo reverses diet-induced non-alcoholic fatty liver disease and improves hyperglycemia. *J Biol Chem*. 2008 Aug;283(32):22186–92.
94. Falcon A, Doege H, Fluitt A, Tsang B, Watson N, Kay MA, et al. FATP2 is a hepatic fatty acid transporter and peroxisomal very long-chain acyl-CoA synthetase. *Am J Physiol Endocrinol Metab*. 2010 Sep;299(3):E384-93.
95. Doege H, Baillie RA, Ortegon AM, Tsang B, Wu Q, Punreddy S, et al. Targeted deletion of FATP5 reveals multiple functions in liver metabolism: alterations in hepatic lipid homeostasis. *Gastroenterology*. 2006 Apr;130(4):1245–58.
96. Wilson CG, Tran JL, Erion DM, Vera NB, Febbraio M, Weiss EJ. Hepatocyte-Specific Disruption of CD36 Attenuates Fatty Liver and Improves Insulin Sensitivity in HFD-Fed Mice. *Endocrinology*. 2016 Feb;157(2):570–85.
97. Koonen DPY, Jacobs RL, Febbraio M, Young ME, Soltys C-LM, Ong H, et

- al. Increased hepatic CD36 expression contributes to dyslipidemia associated with diet-induced obesity. *Diabetes*. 2007 Dec;56(12):2863–71.
98. Greco D, Kotronen A, Westerbacka J, Puig O, Arkkila P, Kiviluoto T, et al. Gene expression in human NAFLD. *Am J Physiol Gastrointest Liver Physiol*. 2008 May;294(5):G1281-7.
99. Ipsen DH, Lykkesfeldt J, Tveden-Nyborg P. Molecular mechanisms of hepatic lipid accumulation in non-alcoholic fatty liver disease. *Cell Mol Life Sci*. 2018 Sep;75(18):3313–27.
100. Braun K, Oeckl J, Westermeier J, Li Y, Klingenspor M. Non-adrenergic control of lipolysis and thermogenesis in adipose tissues. *J Exp Biol*. 2018 Mar;221(Pt Suppl 1).
101. Richard AJ, White U, Elks CM, Stephens JM. Adipose Tissue: Physiology to Metabolic Dysfunction. In: Feingold KR, Anawalt B, Boyce A, Chrousos G, de Herder WW, Dhatariya K, et al., editors. South Dartmouth (MA); 2000.
102. Martinez-Botas J, Anderson JB, Tessier D, Lapillonne A, Chang BH-J, Quast MJ, et al. Absence of perilipin results in leanness and reverses obesity in *Lepr<sup>db/db</sup>* mice. *Nat Genet*. 2000;26(4):474–9.
103. Nielsen TS, Jessen N, Jørgensen JOL, Møller N, Lund S. Dissecting adipose tissue lipolysis: molecular regulation and implications for metabolic disease. *J Mol Endocrinol*. 2014;52(3):R199–222.
104. Czech MP. Mechanisms of insulin resistance related to white, beige, and brown adipocytes. *Mol Metab*. 2020 Apr;34:27–42.
105. Grabner GF, Xie H, Schweiger M, Zechner R. Lipolysis: cellular mechanisms for lipid mobilization from fat stores. *Nat Metab*. 2021;3(11):1445–65.
106. Stenson BM, Rydén M, Venteclef N, Dahlman I, Pettersson AML, Mairal A, et al. Liver X Receptor (LXR) Regulates Human Adipocyte Lipolysis\*. *J Biol Chem*. 2011;286(1):370–9.
107. Cruz-Garcia L, Sánchez-Gurmaches J, Gutiérrez J, Navarro I. Role of LXR in trout adipocytes: Target genes, hormonal regulation, adipocyte differentiation and relation to lipolysis. *Comp Biochem Physiol Part A Mol Integr Physiol*. 2012;163(1):120–6.
108. Korach-André M, Gustafsson J-Å. Liver X receptors as regulators of metabolism. *Biomol Concepts*. 2015;6(3):177–90.
109. Schultz JR, Tu H, Luk A, Repa JJ, Medina JC, Li L, et al. Role of LXRs in

- control of lipogenesis. *Genes Dev.* 2000 Nov;14(22):2831–8.
110. Korach-André M, Archer A, Gabbi C, Barros RP, Pedrelli M, Steffensen KR, et al. Liver X receptors regulate de novo lipogenesis in a tissue-specific manner in C57BL/6 female mice. *Am J Physiol Metab.* 2011 Apr 26;301(1):E210–22.
  111. Kersten S. Physiological regulation of lipoprotein lipase. *Biochim Biophys Acta.* 2014 Jul;1841(7):919–33.
  112. Harris CA, Haas JT, Streeper RS, Stone SJ, Kumari M, Yang K, et al. DGAT enzymes are required for triacylglycerol synthesis and lipid droplets in adipocytes. *J Lipid Res.* 2011 Apr;52(4):657–67.
  113. Chitraju C, Walther TC, Farese RVJ. The triglyceride synthesis enzymes DGAT1 and DGAT2 have distinct and overlapping functions in adipocytes. *J Lipid Res.* 2019 Jun;60(6):1112–20.
  114. Song Z, Xiaoli AM, Yang F. Regulation and Metabolic Significance of De Novo Lipogenesis in Adipose Tissues. Vol. 10, *Nutrients* . 2018.
  115. Collins JM, Neville MJ, Hoppa MB, Frayn KN. *De Novo* Lipogenesis and Stearoyl-CoA Desaturase Are Coordinately Regulated in the Human Adipocyte and Protect against Palmitate-induced Cell Injury\*. *J Biol Chem.* 2010 Feb 26;285(9):6044–52.
  116. Baykal AP, Parks EJ, Shamburek R, Syed-Abdul MM, Chacko S, Cochran E, et al. Leptin decreases de novo lipogenesis in patients with lipodystrophy. *JCI insight.* 2020 Jul;5(14).
  117. Sanders FWB, Griffin JL. De novo lipogenesis in the liver in health and disease: more than just a shunting yard for glucose. *Biol Rev.* 2016 May 1;91(2):452–68.
  118. Lei Y, Zhou S, Hu Q, Chen X, Gu J. Carbohydrate response element binding protein (ChREBP) correlates with colon cancer progression and contributes to cell proliferation. *Sci Rep.* 2020;10(1):4233.
  119. Iizuka K. The transcription factor carbohydrate-response element-binding protein (ChREBP): A possible link between metabolic disease and cancer. *Biochim Biophys Acta - Mol Basis Dis.* 2017;1863(2):474–85.
  120. Herman MA, Peroni OD, Villoria J, Schön MR, Abumrad NA, Blüher M, et al. A novel ChREBP isoform in adipose tissue regulates systemic glucose metabolism. *Nature.* 2012;484(7394):333–8.

121. Nuotio-Antar AM, Pongvarin N, Li M, Schupp M, Mohammad M, Gerard S, et al. FABP4-Cre Mediated Expression of Constitutively Active ChREBP Protects Against Obesity, Fatty Liver, and Insulin Resistance. *Endocrinology*. 2015;156(11):4020–32.
122. Iizuka K, Bruick RK, Liang G, Horton JD, Uyeda K. Deficiency of carbohydrate response element-binding protein (ChREBP) reduces lipogenesis as well as glycolysis. *Proc Natl Acad Sci U S A*. 2004/04/26. 2004 May 11;101(19):7281–6.
123. Bertolio R, Napoletano F, Mano M, Maurer-Stroh S, Fantuz M, Zannini A, et al. Sterol regulatory element binding protein 1 couples mechanical cues and lipid metabolism. *Nat Commun*. 2019;10(1):1326.
124. Ferré P, Foufelle F. SREBP-1c Transcription Factor and Lipid Homeostasis: Clinical Perspective. *Horm Res Paediatr*. 2007;68(2):72–82.
125. Kim JB, Sarraf P, Wright M, Yao KM, Mueller E, Solanes G, et al. Nutritional and insulin regulation of fatty acid synthetase and leptin gene expression through ADD1/SREBP1. *J Clin Invest*. 1998 Jan;101(1):1–9.
126. Linden AG, Li S, Choi HY, Fang F, Fukasawa M, Uyeda K, et al. Interplay between ChREBP and SREBP-1c coordinates postprandial glycolysis and lipogenesis in livers of mice. *J Lipid Res*. 2018 Mar;59(3):475–87.
127. Moon Y-A, Liang G, Xie X, Frank-Kamenetsky M, Fitzgerald K, Koteliensky V, et al. The Scap/SREBP pathway is essential for developing diabetic fatty liver and carbohydrate-induced hypertriglyceridemia in animals. *Cell Metab*. 2012 Feb;15(2):240–6.
128. Ruderman NB, Saha AK, Kraegen EW. Minireview: malonyl CoA, AMP-activated protein kinase, and adiposity. *Endocrinology*. 2003 Dec;144(12):5166–71.
129. Thiam AR, Beller M. The why, when and how of lipid droplet diversity. *J Cell Sci*. 2017 Jan;130(2):315–24.
130. Thiam AR, Forêt L. The physics of lipid droplet nucleation, growth and budding. *Biochim Biophys Acta - Mol Cell Biol Lipids*. 2016;1861(8, Part A):715–22.
131. Nishimoto Y, Tamori Y. CIDE Family-Mediated Unique Lipid Droplet Morphology in White Adipose Tissue and Brown Adipose Tissue Determines the Adipocyte Energy Metabolism. *J Atheroscler Thromb*. 2017 Oct;24(10):989–98.

132. Slayton M, Gupta A, Balakrishnan B, Puri V. CIDE Proteins in Human Health and Disease. *Cells*. 2019 Mar 13;8(3):238.
133. Chen F-J, Yin Y, Chua BT, Li P. CIDE family proteins control lipid homeostasis and the development of metabolic diseases. *Traffic*. 2020 Jan 1;21(1):94–105.
134. Li JZ, Ye J, Xue B, Qi J, Zhang J, Zhou Z, et al. Cideb regulates diet-induced obesity, liver steatosis, and insulin sensitivity by controlling lipogenesis and fatty acid oxidation. *Diabetes*. 2007 Oct;56(10):2523–32.
135. Zhang L-J, Wang C, Yuan Y, Wang H, Wu J, Liu F, et al. Cideb facilitates the lipidation of chylomicrons in the small intestine. *J Lipid Res*. 2014 Jul;55(7):1279–87.
136. Sans A, Bonnafe S, Rousseau D, Patouraux S, Canivet CM, Leclere PS, et al. The Differential Expression of Cide Family Members is Associated with Nafld Progression from Steatosis to Steatohepatitis. *Sci Rep*. 2019;9(1):7501.
137. Nishimoto Y, Nakajima S, Tateya S, Saito M, Ogawa W, Tamori Y. Cell death-inducing DNA fragmentation factor A-like effector A and fat-specific protein 27 $\beta$  coordinately control lipid droplet size in brown adipocytes. *J Biol Chem*. 2017 Jun;292(26):10824–34.
138. Xu X, Park J-G, So J-S, Lee A-H. Transcriptional activation of Fsp27 by the liver-enriched transcription factor CREBH promotes lipid droplet growth and hepatic steatosis. *Hepatology*. 2015 Mar 1;61(3):857–69.
139. Müller MJ. Hepatic Energy and Substrate Metabolism: A Possible Metabolic Basis for Early Nutritional Support in Cirrhotic Patients. *Nutrition*. 1998;14(1):30–8.
140. McGarry JD, Woeltje KF, Kuwajima M, Foster DW. Regulation of ketogenesis and the renaissance of carnitine palmitoyltransferase. *Diabetes Metab Rev*. 1989 May;5(3):271–84.
141. Desvergne B, Wahli W. Peroxisome proliferator-activated receptors: nuclear control of metabolism. *Endocr Rev*. 1999 Oct;20(5):649–88.
142. McGarry JD, Foster DW. Regulation of hepatic fatty acid oxidation and ketone body production. *Annu Rev Biochem*. 1980;49:395–420.
143. Fabbrini E, Magkos F. Hepatic Steatosis as a Marker of Metabolic Dysfunction. Vol. 7, *Nutrients* . 2015.
144. Ibdah JA, Perlegas P, Zhao Y, Angdisen J, Borgerink H, Shadoan MK, et al.



- Mice heterozygous for a defect in mitochondrial trifunctional protein develop hepatic steatosis and insulin resistance. *Gastroenterology*. 2005 May;128(5):1381–90.
145. Cannon B, Nedergaard J. Brown adipose tissue: function and physiological significance. *Physiol Rev*. 2004 Jan;84(1):277–359.
  146. Christian W, Zachary G-H. Fueling the fire of adipose thermogenesis. *Science* (80- ). 2022 Mar 18;375(6586):1229–31.
  147. Porter C. Quantification of UCP1 function in human brown adipose tissue. *Adipocyte*. 2017/04/14. 2017 Apr 3;6(2):167–74.
  148. Virtanen KA. Activation of Human Brown Adipose Tissue (BAT): Focus on Nutrition and Eating BT - Brown Adipose Tissue. In: Pfeifer A, Klingenspor M, Herzig S, editors. Cham: Springer International Publishing; 2019. p. 349–57.
  149. Lidell ME, Betz MJ, Enerbäck S. Brown adipose tissue and its therapeutic potential. *J Intern Med*. 2014 Oct 1;276(4):364–77.
  150. Suchacki KJ, Stimson RH. Nutritional Regulation of Human Brown Adipose Tissue. *Nutrients*. 2021 May;13(6).
  151. Marlatt KL, Ravussin E. Brown Adipose Tissue: an Update on Recent Findings. *Curr Obes Rep*. 2017 Dec;6(4):389–96.
  152. Saito M, Matsushita M, Yoneshiro T, Okamatsu-Ogura Y. Brown Adipose Tissue, Diet-Induced Thermogenesis, and Thermogenic Food Ingredients: From Mice to Men . Vol. 11, *Frontiers in Endocrinology* . 2020.
  153. Loncar D, Afzelius BA, Cannon B. Epididymal white adipose tissue after cold stress in rats. I. Nonmitochondrial changes. *J Ultrastruct Mol Struct Res*. 1988;101(2–3):109–22.
  154. Fasshauer M, Blüher M. Adipokines in health and disease. *Trends Pharmacol Sci*. 2015 Jul;36(7):461–70.
  155. de Oliveira dos Santos AR, de Oliveira Zanuso B, Miola VF, Barbalho SM, Santos Bueno PC, Flato UA, et al. Adipokines, Myokines, and Hepatokines: Crosstalk and Metabolic Repercussions. Vol. 22, *International Journal of Molecular Sciences* . 2021.
  156. Jensen-Cody SO, Potthoff MJ. Hepatokines and metabolism: Deciphering communication from the liver. *Mol Metab*. 2021;44:101138.
  157. Mantzoros CS, Magkos F, Brinkoetter M, Sienkiewicz E, Dardeno TA, Kim



- S-Y, et al. Leptin in human physiology and pathophysiology. *Am J Physiol Endocrinol Metab.* 2011 Oct;301(4):E567-84.
158. Kelesidis T, Kelesidis I, Chou S, Mantzoros CS. Narrative review: the role of leptin in human physiology: emerging clinical applications. *Ann Intern Med.* 2010 Jan 19;152(2):93–100.
  159. Myers Jr MG, Leibel RL, Seeley RJ, Schwartz MW. Obesity and leptin resistance: distinguishing cause from effect. *Trends Endocrinol Metab.* 2010/09/16. 2010 Nov;21(11):643–51.
  160. Miller RA, Chu Q, Le Lay J, Scherer PE, Ahima RS, Kaestner KH, et al. Adiponectin suppresses gluconeogenic gene expression in mouse hepatocytes independent of LKB1-AMPK signaling. *J Clin Invest.* 2011 Jun;121(6):2518–28.
  161. Yanai H, Yoshida H. Beneficial Effects of Adiponectin on Glucose and Lipid Metabolism and Atherosclerotic Progression: Mechanisms and Perspectives. *Int J Mol Sci.* 2019 Mar;20(5).
  162. Fasshauer M, Blüher M, Stumvoll M. Adipokines in gestational diabetes. *lancet Diabetes Endocrinol.* 2014 Jun;2(6):488–99.
  163. Itoh N. FGF21 as a Hepatokine, Adipokine, and Myokine in Metabolism and Diseases. *Front Endocrinol (Lausanne).* 2014;5:107.
  164. Fisher FM, Maratos-Flier E. Understanding the Physiology of FGF21. *Annu Rev Physiol.* 2016;78:223–41.
  165. Kharitonov A, Shiyanova TL, Koester A, Ford AM, Micanovic R, Galbreath EJ, et al. FGF-21 as a novel metabolic regulator. *J Clin Invest.* 2005;115(6):1627–35.
  166. Fisher FM, Kleiner S, Douris N, Fox EC, Mepani RJ, Verdeguer F, et al. FGF21 regulates PGC-1alpha and browning of white adipose tissues in adaptive thermogenesis. *Genes Dev.* 2012 Feb;26(3):271–81.
  167. Kharitonov A, Shanafelt AB. FGF21: a novel prospect for the treatment of metabolic diseases. *Curr Opin Investig Drugs.* 2009 Apr;10(4):359–64.
  168. Yan Q, Yang Q, Mody N, Graham TE, Hsu C, Xu Z, et al. Promotes Insulin Resistance. *October.* 2007;56(October):2533–40.
  169. Ishii A, Katsuura G, Imamaki H, Kimura H, Mori KP, Kuwabara T, et al. Obesity-promoting and anti-thermogenic effects of neutrophil gelatinase-associated lipocalin in mice. *Sci Rep.* 2017 Nov;7(1):15501.

170. Shen F, Hu Z, Goswami J, Gaffen SL. Identification of common transcriptional regulatory elements in interleukin-17 target genes. *J Biol Chem*. 2006 Aug;281(34):24138–48.
171. Sun WY, Bai B, Luo C, Yang K, Li D, Wu D, et al. Lipocalin-2 derived from adipose tissue mediates aldosterone-induced renal injury. *JCI insight*. 2018 Sep;3(17).
172. Viau A, El Karoui K, Laouari D, Burtin M, Nguyen C, Mori K, et al. Lipocalin 2 is essential for chronic kidney disease progression in mice and humans. *J Clin Invest*. 2010 Nov;120(11):4065–76.
173. Rayego-Mateos S, Rodrigues-Diez R, Morgado-Pascual JL, Valentijn F, Valdivielso JM, Goldschmeding R, et al. Role of Epidermal Growth Factor Receptor (EGFR) and Its Ligands in Kidney Inflammation and Damage. *Mediators Inflamm*. 2018 Dec 23;2018:8739473.
174. Law IKM, Xu A, Lam KSL, Berger T, Mak TW, Vanhoutte PM, et al. Lipocalin-2 deficiency attenuates insulin resistance associated with aging and obesity. *Diabetes*. 2010/01/12. 2010 Apr;59(4):872–82.
175. Guo H, Jin D, Zhang Y, Wright W, Bazuine M, Brockman DA, et al. Lipocalin-2 deficiency impairs thermogenesis and potentiates diet-induced insulin resistance in mice. *Diabetes*. 2010/03/23. 2010 Jun;59(6):1376–85.
176. Scholtes C, Giguère V. Transcriptional control of energy metabolism by nuclear receptors. *Nat Rev Mol Cell Biol*. 2022;
177. Sever R, Glass CK. Signaling by nuclear receptors. *Cold Spring Harb Perspect Biol*. 2013 Mar;5(3):a016709.
178. Michalik L, Auwerx J, Berger JP, Chatterjee VK, Glass CK, Gonzalez FJ, et al. International Union of Pharmacology. LXI. Peroxisome Proliferator-Activated Receptors. *Pharmacol Rev*. 2006 Dec 1;58(4):726 LP – 741.
179. Issemann I, Green S. Activation of a member of the steroid hormone receptor superfamily by peroxisome proliferators. *Nature*. 1990 Oct;347(6294):645–50.
180. Francque S, Szabo G, Abdelmalek MF, Byrne CD, Cusi K, Dufour J-F, et al. Nonalcoholic steatohepatitis: the role of peroxisome proliferator-activated receptors. *Nat Rev Gastroenterol Hepatol*. 2021 Jan;18(1):24–39.
181. Tailleux A, Wouters K, Staels B. Roles of PPARs in NAFLD: Potential therapeutic targets. *Biochim Biophys Acta - Mol Cell Biol Lipids*. 2012;1821(5):809–18.

182. Lefebvre P, Chinetti G, Fruchart J-C, Staels B. Sorting out the roles of PPAR $\alpha$  in energy metabolism and vascular homeostasis. *J Clin Invest*. 2006 Mar 1;116(3):571–80.
183. Marx N, Sukhova GK, Collins T, Libby P, Plutzky J. PPAR $\alpha$  activators inhibit cytokine-induced vascular cell adhesion molecule-1 expression in human endothelial cells. *Circulation*. 1999 Jun;99(24):3125–31.
184. Rodríguez JC, Gil-Gómez G, Hegardt FG, Haro D. Peroxisome proliferator-activated receptor mediates induction of the mitochondrial 3-hydroxy-3-methylglutaryl-CoA synthase gene by fatty acids. *J Biol Chem*. 1994 Jul;269(29):18767–72.
185. Schoonjans K, Peinado-Onsurbe J, Lefebvre AM, Heyman RA, Briggs M, Deeb S, et al. PPAR $\alpha$  and PPAR $\gamma$  activators direct a distinct tissue-specific transcriptional response via a PPRE in the lipoprotein lipase gene. *EMBO J*. 1996 Oct;15(19):5336–48.
186. Birjmohun RS, Hutten BA, Kastelein JJP, Stroes ESG. Efficacy and safety of high-density lipoprotein cholesterol-increasing compounds: A meta-analysis of randomized controlled trials. *J Am Coll Cardiol*. 2005;45(2):185–97.
187. Manickam R, Wahli W. Roles of Peroxisome Proliferator-Activated Receptor  $\beta/\delta$  in skeletal muscle physiology. *Biochimie*. 2017 May;136:42–8.
188. Liu Y, Colby JK, Zuo X, Jaoude J, Wei D, Shureiqi I. The Role of PPAR- $\delta$  in Metabolism, Inflammation, and Cancer: Many Characters of a Critical Transcription Factor. *Int J Mol Sci*. 2018 Oct 26;19(11):3339.
189. Iglesias J, Barg S, Vallois D, Lahiri S, Roger C, Yessoufou A, et al. PPAR $\beta/\delta$  affects pancreatic  $\beta$  cell mass and insulin secretion in mice. *J Clin Invest*. 2012 Nov;122(11):4105–17.
190. Sanderson LM, Boekschoten M V, Desvergne B, Müller M, Kersten S. Transcriptional profiling reveals divergent roles of PPAR $\alpha$  and PPAR $\beta/\delta$  in regulation of gene expression in mouse liver. *Physiol Genomics*. 2010;41(1):42–52.
191. Wang Y, Nakajima T, Gonzalez FJ, Tanaka N. PPARs as Metabolic Regulators in the Liver: Lessons from Liver-Specific PPAR-Null Mice. *Int J Mol Sci*. 2020 Mar 17;21(6):2061.
192. Zingarelli B, Piraino G, Hake PW, O'Connor M, Denenberg A, Fan H, et al. Peroxisome Proliferator-Activated Receptor Alpha; Regulates Inflammation via NF- $\kappa$ B Signaling in Polymicrobial Sepsis. *Am J Pathol*. 2010 Oct 1;177(4):1834–47.

193. Qin X, Xie X, Fan Y, Tian J, Guan Y, Wang X, et al. Peroxisome proliferator-activated receptor- $\delta$  induces insulin-induced gene-1 and suppresses hepatic lipogenesis in obese diabetic mice. *Hepatology*. 2008;48(2):432–41.
194. Bojic LA, Telford DE, Fullerton MD, Ford RJ, Sutherland BG, Edwards JY, et al. PPAR $\gamma$  activation attenuates hepatic steatosis in Ldlrmice by enhanced fat oxidation, reduced lipogenesis, and improved insulin sensitivity. *J Lipid Res*. 2014 Jul 1;55(7):1254–66.
195. Gupta RA, Wang D, Katkuri S, Wang H, Dey SK, DuBois RN. Activation of nuclear hormone receptor peroxisome proliferator-activated receptor- $\delta$  accelerates intestinal adenoma growth. *Nat Med*. 2004;10(3):245–7.
196. Feige JN, Gelman L, Michalik L, Desvergne B, Wahli W. From molecular action to physiological outputs: peroxisome proliferator-activated receptors are nuclear receptors at the crossroads of key cellular functions. *Prog Lipid Res*. 2006 Mar;45(2):120–59.
197. Grygiel-Górniak B. Peroxisome proliferator-activated receptors and their ligands: nutritional and clinical implications - a review. *Nutr J*. 2014;13(1):17.
198. Ghaben AL, Scherer PE. Adipogenesis and metabolic health. *Nat Rev Mol Cell Biol*. 2019;20(4):242–58.
199. Ahmad B, Serpell CJ, Fong IL, Wong EH. Molecular Mechanisms of Adipogenesis: The Anti-adipogenic Role of AMP-Activated Protein Kinase . Vol. 7, *Frontiers in Molecular Biosciences* . 2020. p. 76.
200. He W, Barak Y, Hevener A, Olson P, Liao D, Le J, et al. Adipose-specific peroxisome proliferator-activated receptor gamma knockout causes insulin resistance in fat and liver but not in muscle. *Proc Natl Acad Sci U S A*. 2003/12/05. 2003 Dec 23;100(26):15712–7.
201. Ahmadian M, Suh JM, Hah N, Liddle C, Atkins AR, Downes M, et al. PPAR $\gamma$  signaling and metabolism: the good, the bad and the future. *Nat Med*. 2013;19(5):557–66.
202. Villacorta L, Schopfer FJ, Zhang J, Freeman BA, Chen YE. PPAR $\gamma$  and its ligands: therapeutic implications in cardiovascular disease. *Clin Sci (Lond)*. 2009 Feb;116(3):205–18.
203. Rubenstrunk A, Hanf R, Hum DW, Fruchart J-C, Staels B. Safety issues and prospects for future generations of PPAR modulators. *Biochim Biophys Acta*. 2007 Aug;1771(8):1065–81.
204. Watkins PB, Whitcomb RW. Hepatic dysfunction associated with

- troglitazone. Vol. 338, The New England journal of medicine. United States; 1998. p. 916–7.
205. Schupp M, Clemenz M, Gineste R, Witt H, Janke J, Helleboid S, et al. Molecular characterization of new selective peroxisome proliferator-activated receptor gamma modulators with angiotensin receptor blocking activity. *Diabetes*. 2005 Dec;54(12):3442–52.
  206. Wang L, Waltenberger B, Pferschy-Wenzig E-M, Blunder M, Liu X, Malainer C, et al. Natural product agonists of peroxisome proliferator-activated receptor gamma (PPAR $\gamma$ ): a review. *Biochem Pharmacol*. 2014 Nov;92(1):73–89.
  207. Ammazalorso A, Amoroso R. Inhibition of PPAR $\gamma$  by Natural Compounds as a Promising Strategy in Obesity and Diabetes. *Open Med Chem J*. 2019 Feb 28;13:7–15.
  208. Wu Z, Rosen ED, Brun R, Hauser S, Adelmant G, Troy AE, et al. Cross-Regulation of C/EBP $\alpha$  and PPAR $\gamma$  Controls the Transcriptional Pathway of Adipogenesis and Insulin Sensitivity. *Mol Cell*. 1999;3(2):151–8.
  209. Madsen MS, Siersbæk R, Boergesen M, Nielsen R, Mandrup S. Peroxisome proliferator-activated receptor  $\gamma$  and C/EBP $\alpha$  synergistically activate key metabolic adipocyte genes by assisted loading. *Mol Cell Biol*. 2013/12/30. 2014 Mar;34(6):939–54.
  210. Imai T, Takakuwa R, Marchand S, Dentz E, Bornert J-M, Messaddeq N, et al. Peroxisome proliferator-activated receptor gamma is required in mature white and brown adipocytes for their survival in the mouse. *Proc Natl Acad Sci U S A*. 2004 Mar;101(13):4543–7.
  211. Gavrilova O, Haluzik M, Matsusue K, Cutson JJ, Johnson L, Dietz KR, et al. Liver peroxisome proliferator-activated receptor gamma contributes to hepatic steatosis, triglyceride clearance, and regulation of body fat mass. *J Biol Chem*. 2003 Sep;278(36):34268–76.
  212. Lee YJ, Ko EH, Kim JE, Kim E, Lee H, Choi H, et al. Nuclear receptor PPAR $\gamma$ -regulated monoacylglycerol O-acyltransferase 1 (MGAT1) expression is responsible for the lipid accumulation in diet-induced hepatic steatosis. *Proc Natl Acad Sci U S A*. 2012 Aug;109(34):13656–61.
  213. Morán-Salvador E, López-Parra M, García-Alonso V, Titos E, Martínez-Clemente M, González-Pérez A, et al. Role for PPAR $\gamma$  in obesity-induced hepatic steatosis as determined by hepatocyte- and macrophage-specific conditional knockouts. *FASEB J Off Publ Fed Am Soc Exp Biol*. 2011 Aug;25(8):2538–50.

214. Pan X, Wang P, Luo J, Wang Z, Song Y, Ye J, et al. Adipogenic changes of hepatocytes in a high-fat diet-induced fatty liver mice model and non-alcoholic fatty liver disease patients. *Endocrine*. 2015;48(3):834–47.
215. Skat-Rørdam J, Højland Ipsen D, Lykkesfeldt J, Tveden-Nyborg P. A role of peroxisome proliferator-activated receptor  $\gamma$  in non-alcoholic fatty liver disease. *Basic Clin Pharmacol Toxicol*. 2019 May 1;124(5):528–37.
216. Matsusue K, Haluzik M, Lambert G, Yim S-H, Gavrilova O, Ward JM, et al. Liver-specific disruption of PPAR $\gamma$  in leptin-deficient mice improves fatty liver but aggravates diabetic phenotypes. *J Clin Invest*. 2003 Mar 1;111(5):737–47.
217. Evans RM, Barish GD, Wang Y-X. PPARs and the complex journey to obesity. *Nat Med*. 2004;10(4):355–61.
218. Baffy G. Kupffer cells in non-alcoholic fatty liver disease: the emerging view. *J Hepatol*. 2009;51(1):212–23.
219. Wan J, Benkdane M, Teixeira-Clerc F, Bonnafous S, Louvet A, Lafdil F, et al. M2 Kupffer cells promote M1 Kupffer cell apoptosis: A protective mechanism against alcoholic and nonalcoholic fatty liver disease. *Hepatology*. 2014;59(1):130–42.
220. Konstantinopoulos PA, Vantoros GP, Sotiropoulou-Bonikou G, Kominea A, Papavassiliou AG. NF- $\kappa$ B/PPAR $\gamma$  and/or AP-1/PPAR $\gamma$  ‘on/off’ switches and induction of CBP in colon adenocarcinomas: correlation with COX-2 expression. *Int J Colorectal Dis*. 2007;22(1):57–68.
221. Wang Z, Xu J-P, Zheng Y-C, Chen W, Sun Y-W, Wu Z-Y, et al. Peroxisome proliferator-activated receptor gamma inhibits hepatic fibrosis in rats. *Hepatobiliary Pancreat Dis Int*. 2011 Feb;10(1):64–71.
222. Roth GA, Abate D, Abate KH, Abay SM, Abbafati C, Abbasi N, et al. Global, regional, and national age-sex-specific mortality for 282 causes of death in 195 countries and territories, 1980–2017: a systematic analysis for the Global Burden of Disease Study 2017. *Lancet*. 2018 Nov 10;392(10159):1736–88.
223. Arisawa K, Uemura H, Yamaguchi M, Nakamoto M, Hiyoshi M, Sawachika F, et al. Associations of dietary patterns with metabolic syndrome and insulin resistance: a cross-sectional study in a Japanese population. *J Med Investig*. 2014;61(3.4):333–44.
224. Cena H, Calder PC. Defining a Healthy Diet: Evidence for the Role of Contemporary Dietary Patterns in Health and Disease. *Nutrients*. 2020;12(2).

225. Esposito K, Maiorino MI, Bellastella G, Chiodini P, Panagiotakos D, Giugliano D. A journey into a Mediterranean diet and type 2 diabetes: A systematic review with meta-analyses. *BMJ Open*. 2015;5(8).
226. Cazarin CBB, Bicas JL, Pastore GM, Marostica Junior MR. Chapter 1 - Introduction. In: Cazarin CBB, Bicas JL, Pastore GM, Marostica Junior MRBT-BFCA in MA, editors. Academic Press; 2022. p. 1–3.
227. Revutska A, Belava V, Golubenko A, Taran N, Chen M. Plant secondary metabolites as bioactive substances for innovative biotechnologies. *E3S Web Conf*. 2021;280.
228. Isah T. Stress and defense responses in plant secondary metabolites production. *Biol Res*. 2019;52(1):39.
229. Ali B. Salicylic acid: An efficient elicitor of secondary metabolite production in plants. *Biocatal Agric Biotechnol*. 2021;31:101884.
230. Randhir R, Lin Y-T, Shetty K. Stimulation of phenolics, antioxidant and antimicrobial activities in dark germinated mung bean sprouts in response to peptide and phytochemical elicitors. *Process Biochem*. 2004;39(5):637–46.
231. Lin D, Xiao M, Zhao J, Li Z, Xing B, Li X, et al. An Overview of Plant Phenolic Compounds and Their Importance in Human Nutrition and Management of Type 2 Diabetes. *Molecules*. 2016 Oct 15;21(10):1374.
232. Hano C, Tungmunnithum D. Plant Polyphenols, More than Just Simple Natural Antioxidants: Oxidative Stress, Aging and Age-Related Diseases. Vol. 7, *Medicines* . 2020.
233. Costa C, Tsatsakis A, Mamoulakis C, Teodoro M, Briguglio G, Caruso E, et al. Current evidence on the effect of dietary polyphenols intake on chronic diseases. *Food Chem Toxicol*. 2017;110:286–99.
234. Bahadoran Z, Mirmiran P, Azizi F. Dietary polyphenols as potential nutraceuticals in management of diabetes: a review. *J Diabetes Metab Disord*. 2013;12(1):43.
235. D'Archivio M, Filesi C, Di Benedetto R, Gargiulo R, Giovannini C, Masella R. Polyphenols, dietary sources and bioavailability. *Ann Super di Sanita*. 2007;43(4):348.
236. Goutzourelas N, Stagos D, Spanidis Y, Liosi M, Apostolou A, Priftis A, et al. Polyphenolic composition of grape stem extracts affects antioxidant activity in endothelial and muscle cells. *Mol Med Rep*. 2015;12(4):5846–56.



237. Talcott ST, Passeretti S, Duncan CE, Gorbet DW. Polyphenolic content and sensory properties of normal and high oleic acid peanuts. *Food Chem.* 2005;90(3):379–88.
238. Bianco A, Uccella N. Biophenolic components of olives. *Food Res Int.* 2000;33(6):475–85.
239. Mattila P, Kumpulainen J. Determination of Free and Total Phenolic Acids in Plant-Derived Foods by HPLC with Diode-Array Detection. *J Agric Food Chem.* 2002 Jun 1;50(13):3660–7.
240. Gupta A, Singh AK, Loka M, Pandey AK, Bishayee A. Ferulic acid-mediated modulation of apoptotic signaling pathways in cancer. *Adv Protein Chem Struct Biol.* 2021;125:215–57.
241. Neto-Neves EM, da Silva Maia Bezerra Filho C, Dejana NN, de Sousa DP. Ferulic Acid and Cardiovascular Health: Therapeutic and Preventive Potential. *Mini Rev Med Chem.* 2021;21(13):1625–37.
242. Khan F, Bamunuarachchi NI, Tabassum N, Kim Y-M. Caffeic Acid and Its Derivatives: Antimicrobial Drugs toward Microbial Pathogens. *J Agric Food Chem.* 2021 Mar;69(10):2979–3004.
243. Li D, Rui Y-X, Guo S-D, Luan F, Liu R, Zeng N. Ferulic acid: A review of its pharmacology, pharmacokinetics and derivatives. *Life Sci.* 2021 Nov;284:119921.
244. Russell W, Duthie G. Plant secondary metabolites and gut health: the case for phenolic acids. *Proc Nutr Soc.* 2011/05/09. 2011;70(3):389–96.
245. Annunziata F, Pinna C, Dallavalle S, Tamborini L, Pinto A. An Overview of Coumarin as a Versatile and Readily Accessible Scaffold with Broad-Ranging Biological Activities. Vol. 21, *International Journal of Molecular Sciences* . 2020.
246. Srikrishna D, Godugu C, Dubey PK. A Review on Pharmacological Properties of Coumarins. *Mini Rev Med Chem.* 2018;18(2):113–41.
247. Sandoval V, Sanz-Lamora H, Arias G, Marrero PF, Haro D, Relat J. Metabolic Impact of Flavonoids Consumption in Obesity: From Central to Peripheral. *Nutrients.* 2020 Aug;12(8).
248. Teka T, Zhang L, Ge X, Li Y, Han L, Yan X. Stilbenes: Source plants, chemistry, biosynthesis, pharmacology, application and problems related to their clinical Application-A comprehensive review. *Phytochemistry.* 2022 May;197:113128.



249. Hapeshi A, Benarroch JM, Clarke DJ, Waterfield NR. Iso-propyl stilbene: a life cycle signal? *Microbiology*. 2019;165(5):516–26.
250. Tian B, Liu J. Resveratrol: a review of plant sources, synthesis, stability, modification and food application. *J Sci Food Agric*. 2020 Mar 15;100(4):1392–404.
251. Chan EWC, Wong CW, Tan YH, Foo JPY, Wong SK, Chan HT. Resveratrol and pterostilbene: A comparative overview of their chemistry, biosynthesis, plant sources and pharmacological properties. *J Appl Pharm Sci*. 2019;9(7):124–9.
252. Durazzo A, Lucarini M, Camilli E, Marconi S, Gabrielli P, Lisciani S, et al. Dietary Lignans: Definition, Description and Research Trends in Databases Development. Vol. 23, *Molecules* . 2018.
253. Chhillar H, Chopra P, Ashfaq MA. Lignans from linseed (*Linum usitatissimum* L.) and its allied species: Retrospect, introspect and prospect. *Crit Rev Food Sci Nutr*. 2021 Sep 8;61(16):2719–41.
254. Webb AL, McCullough ML. Dietary lignans: potential role in cancer prevention. *Nutr Cancer*. 2005;51(2):117–31.
255. Peterson J, Dwyer J, Adlercreutz H, Scalbert A, Jacques P, McCullough ML. Dietary lignans: physiology and potential for cardiovascular disease risk reduction. *Nutr Rev*. 2010 Oct;68(10):571–603.
256. Bengmark S, Mesa D, Gil A. Plant-derived health-the effects of turmeric and curcuminoids EFECTOS SALUDABLES DE LA CÚRCUMA Y DE LOS CURCUMINOIDES Resumen. *Nutr Hosp*. 2009;24(3):273–81.
257. Oppenheimer A. Turmeric (curcumin) in biliary diseases. *Lancet*. 1937;229(5924):619–21.
258. Bengmark S, Mesa MD, Gil A. Plant-derived health: the effects of turmeric and curcuminoids. *Nutr Hosp*. 2009;24(3):273–81.
259. Gupta SC, Patchva S, Aggarwal BB. Therapeutic Roles of Curcumin: Lessons Learned from Clinical Trials. *AAPS J*. 2013;15(1):195–218.
260. Silvestro S, Sindona C, Bramanti P, Mazzon E. A State of the Art of Antioxidant Properties of Curcuminoids in Neurodegenerative Diseases. Vol. 22, *International Journal of Molecular Sciences* . 2021.
261. Ahmed T, Gilani A-H. Therapeutic Potential of Turmeric in Alzheimer's Disease: Curcumin or Curcuminoids? *Phyther Res*. 2014 Apr 1;28(4):517–25.

262. Segura-Carretero A, Menéndez-Menéndez J, Fernández-Gutiérrez A. Chapter 19 - Polyphenols in Olive Oil: The Importance of Phenolic Compounds in the Chemical Composition of Olive Oil. In: Preedy VR, Watson RRBT-O and OO in H and DP, editors. San Diego: Academic Press; 2010. p. 167–75.
263. Lozano-Castellón J, López-Yerena A, Rinaldi de Alvarenga JF, Romero del Castillo-Alba J, Vallverdú-Queralt A, Escribano-Ferrer E, et al. Health-promoting properties of oleocanthal and oleacein: Two secoiridoids from extra-virgin olive oil. *Crit Rev Food Sci Nutr.* 2020 Aug 21;60(15):2532–48.
264. Xiong Q, Hase K, Tezuka Y, Tani T, Namba T, Kadota S. Hepatoprotective activity of phenylethanoids from *Cistanche deserticola*. *Planta Med.* 1998 Mar;64(2):120–5.
265. Xiong Q, Tezuka Y, Kaneko T, Li H, Tran LQ, Hase K, et al. Inhibition of nitric oxide by phenylethanoids in activated macrophages. *Eur J Pharmacol.* 2000 Jul;400(1):137–44.
266. Karković Marković A, Torić J, Barbarić M, Jakobušić Brala C. Hydroxytyrosol, Tyrosol and Derivatives and Their Potential Effects on Human Health. Vol. 24, *Molecules* . 2019.
267. Robles-Almazan M, Pulido-Moran M, Moreno-Fernandez J, Ramirez-Tortosa C, Rodriguez-Garcia C, Quiles JL, et al. Hydroxytyrosol: Bioavailability, toxicity, and clinical applications. *Food Res Int.* 2018;105:654–67.
268. Echeverría F, Ortiz M, Valenzuela R, Videla LA. Hydroxytyrosol and Cytoprotection: A Projection for Clinical Interventions. Vol. 18, *International Journal of Molecular Sciences* . 2017.
269. Tomé-Carneiro J, Crespo MC, Iglesias-Gutierrez E, Martín R, Gil-Zamorano J, Tomas-Zapico C, et al. Hydroxytyrosol supplementation modulates the expression of miRNAs in rodents and in humans. *J Nutr Biochem.* 2016;34:146–55.
270. Visioli F, Poli A, Gall C. Antioxidant and other biological activities of phenols from olives and olive oil. *Med Res Rev.* 2002 Jan 1;22(1):65–75.
271. Rodríguez-Morató J, Xicota L, Fitó M, Farré M, Dierssen M, De la Torre R. Potential Role of Olive Oil Phenolic Compounds in the Prevention of Neurodegenerative Diseases. Vol. 20, *Molecules* . 2015.
272. Perona JS, Cabello-Moruno R, Ruiz-Gutierrez V. The role of virgin olive oil components in the modulation of endothelial function. *J Nutr Biochem.*

- 2006;17(7):429–45.
273. Lee KM, Hur J, Lee Y, Yoon B-R, Choi SY. Protective Effects of Tyrosol Against Oxidative Damage in L6 Muscle Cells. *Food Sci Technol Res.* 2018;24(5):943–7.
  274. Chang C-Y, Huang I-T, Shih H-J, Chang Y-Y, Kao M-C, Shih P-C, et al. Cluster of differentiation 14 and toll-like receptor 4 are involved in the anti-inflammatory effects of tyrosol. *J Funct Foods.* 2019;53:93–104.
  275. Berthelot K, Estevez Y, Deffieux A, Peruch F. Isopentenyl diphosphate isomerase: A checkpoint to isoprenoid biosynthesis. *Biochimie.* 2012;94(8):1621–34.
  276. Köksal M, Hu H, Coates RM, Peters RJ, Christianson DW. Structure and mechanism of the diterpene cyclase ent-copalyl diphosphate synthase. *Nat Chem Biol.* 2011;7(7):431–3.
  277. Ghani U. Chapter four - Terpenoids and steroids. In: Ghani UBT-A-GI, editor. Elsevier; 2020. p. 101–17.
  278. Al-Taweel SPE-SPE-A. Introductory Chapter: Terpenes and Terpenoids. In Rijeka: IntechOpen; 2018. p. Ch. 1.
  279. Adefegha SA, Oboh G, Oluokun OO. Chapter 11 - Food bioactives: the food image behind the curtain of health promotion and prevention against several degenerative diseases. In: Atta-ur-Rahman BT-S in NPC, editor. *Studies in Natural Products Chemistry.* Elsevier; 2022. p. 391–421.
  280. Yang J, Xian M, Su S, Zhao G, Nie Q, Jiang X, et al. Enhancing Production of Bio-Isoprene Using Hybrid MVA Pathway and Isoprene Synthase in *E. coli*. *PLoS One.* 2012 Apr 27;7(4):e33509.
  281. Wojtunik-Kulesza KA, Kasprzak K, Oniszczyk T, Oniszczyk A. Natural Monoterpenes: Much More than Only a Scent. *Chem Biodivers.* 2019 Dec;16(12):e1900434.
  282. Chappell J, Coates RM. 1.16 - Sesquiterpenes. In: Liu H-W (Ben), Mander LBT-CNPII, editors. Oxford: Elsevier; 2010. p. 609–41.
  283. Chadwick M, Trewin H, Gawthrop F, Wagstaff C. Sesquiterpenoids lactones: benefits to plants and people. *Int J Mol Sci.* 2013 Jun;14(6):12780–805.
  284. Vickers CE, Gershenzon J, Lerdau MT, Loreto F. A unified mechanism of action for volatile isoprenoids in plant abiotic stress. *Nat Chem Biol.* 2009;5(5):283–91.

285. Arizmendi N, Alam SB, Azyat K, Makeiff D, Befus AD, Kulka M. The Complexity of Sesquiterpene Chemistry Dictates Its Pleiotropic Biologic Effects on Inflammation. *Molecules*. 2022 Apr;27(8).
286. Amorim MHR, Gil da Costa RM, Lopes C, Bastos MMSM. Sesquiterpene lactones: adverse health effects and toxicity mechanisms. *Crit Rev Toxicol*. 2013 Aug;43(7):559–79.
287. Cox-Georgian D, Ramadoss N, Dona C, Basu C. Therapeutic and Medicinal Uses of Terpenes. Joshee N, Dhekney SA, Parajuli P, editors. *Med Plants From Farm to Pharm*. 2019 Nov 12;333–59.
288. Long HJ. Paclitaxel (Taxol): a novel anticancer chemotherapeutic drug. *Mayo Clin Proc*. 1994 Apr;69(4):341–5.
289. Lanzotti V. Diterpenes for Therapeutic Use. In 2013.
290. Appendino G, Ech-Chahad A, Minassi A, De Petrocellis L, Di Marzo V. Structure-activity relationships of the ultrapotent vanilloid resiniferatoxin (RTX): The side chain benzylic methylene. *Bioorg Med Chem Lett*. 2010 Jan;20(1):97–9.
291. Crews P, Naylor S. Sesterterpenes: An Emerging Group of Metabolites from Marine and Terrestrial Organisms BT - Fortschritte der Chemie organischer Naturstoffe / Progress in the Chemistry of Organic Natural Products. In: Crews P, Moore RE, Naylor S, Steyn PS, Vleggaar R, Herz W, et al., editors. Vienna: Springer Vienna; 1985. p. 203–69.
292. Du J-R, Long F-Y, Chen C. Chapter Six - Research Progress on Natural Triterpenoid Saponins in the Chemoprevention and Chemotherapy of Cancer. In: Bathaie SZ, Tamanoi FBT-TE, editors. *Natural Products and Cancer Signaling: Isoprenoids, Polyphenols and Flavonoids*. Academic Press; 2014. p. 95–130.
293. Ali R, Mirza Z, Ashraf GMD, Kamal MA, Ansari SA, Damanhoury GA, et al. New anticancer agents: recent developments in tumor therapy. *Anticancer Res*. 2012 Jul;32(7):2999–3005.
294. Ateba SB, Mvondo MA, Ngeu ST, Tchoumtchoua J, Awounfack CF, Njamen D, et al. Natural Terpenoids Against Female Breast Cancer: A 5-year Recent Research. *Curr Med Chem*. 2018;25(27):3162–213.
295. Chopra B, Dhingra AK, Dhar KL, Nepali K. Emerging Role of Terpenoids for the Treatment of Cancer: A Review. *Mini Rev Med Chem*. 2021;21(16):2300–36.

296. El-Baba C, Baassiri A, Kiriako G, Dia B, Fadlallah S, Moodad S, et al. Terpenoids' anti-cancer effects: focus on autophagy. *Apoptosis*. 2021 Oct;26(9–10):491–511.
297. Nazaruk J, Borzym-Kluczyk M. The role of triterpenes in the management of diabetes mellitus and its complications. *Phytochem Rev*. 2014/06/24. 2015;14(4):675–90.
298. Putta S, Yarla NS, Kilari EK, Surekha C, Aliev G, Divakara MB, et al. Therapeutic Potentials of Triterpenes in Diabetes and its Associated Complications. *Curr Top Med Chem*. 2016;16(23):2532–42.
299. Sun H, Tan J, Lv W, Li J, Wu J, Xu J, et al. Hypoglycemic triterpenoid glycosides from *Cyclocarya paliurus* (Sweet Tea Tree). *Bioorg Chem*. 2020 Jan;95:103493.
300. Zhao Y, Li W, Zhang D. Gycyrrhizic acid alleviates atherosclerotic lesions in rats with diabetes mellitus. *Mol Med Rep*. 2021 Nov;24(5).
301. Mancha-Ramirez AM, Slaga TJ. Ursolic Acid and Chronic Disease: An Overview of UA's Effects On Prevention and Treatment of Obesity and Cancer. *Adv Exp Med Biol*. 2016;928:75–96.
302. Li W, Zeng H, Xu M, Huang C, Tao L, Li J, et al. Oleanolic Acid Improves Obesity-Related Inflammation and Insulin Resistance by Regulating Macrophages Activation. *Front Pharmacol*. 2021;12:697483.
303. Chen J, Leong PK, Leung HY, Chan WM, Wong HS, Ko KM. Biochemical mechanisms of the anti-obesity effect of a triterpenoid-enriched extract of *Cynomorium songaricum* in mice with high-fat-diet-induced obesity. *Phytomedicine*. 2020 Jul;73:153038.
304. Mannino G, Iovino P, Lauria A, Genova T, Asteggiano A, Notarbartolo M, et al. Bioactive Triterpenes of *Protium heptaphyllum* Gum Resin Extract Display Cholesterol-Lowering Potential. *Int J Mol Sci*. 2021 Mar;22(5).
305. Zhang Y, Li X, Ciric B, Curtis MT, Chen W-J, Rostami A, et al. A dual effect of ursolic acid to the treatment of multiple sclerosis through both immunomodulation and direct remyelination. *Proc Natl Acad Sci U S A*. 2020 Apr;117(16):9082–93.
306. O'Sullivan SE. An update on PPAR activation by cannabinoids. *Br J Pharmacol*. 2016 Jun;173(12):1899–910.
307. Marhuenda-Muñoz M, Hurtado-Barroso S, Tresserra-Rimbau A, Lamuela-Raventós RM. A review of factors that affect carotenoid concentrations in

- human plasma: differences between Mediterranean and Northern diets. *Eur J Clin Nutr.* 2019 Jul;72(S1):18–25.
308. Singh G, Sahota HK. Impact of benzimidazole and dithiocarbamate fungicides on the photosynthetic machinery, sugar content and various antioxidative enzymes in chickpea. *Plant Physiol Biochem PPB.* 2018 Nov;132:166–73.
309. Tan BL, Norhaizan ME. Carotenoids: How Effective Are They to Prevent Age-Related Diseases? *Molecules.* 2019 May 9;24(9):1801.
310. Böhm V, Lietz G, Olmedilla-Alonso B, Phelan D, Reboul E, Bánati D, et al. From carotenoid intake to carotenoid blood and tissue concentrations – implications for dietary intake recommendations. *Nutr Rev.* 2021 May 1;79(5):544–73.
311. During A, Smith MK, Piper JB, Smith JC.  $\beta$ -Carotene 15,15'-Dioxygenase activity in human tissues and cells: evidence of an iron dependency. *J Nutr Biochem.* 2001;12(11):640–7.
312. Cai X, Lian F, Kong Y, Huang L, Xu L, Wu Y, et al. Carotenoid metabolic (BCO1) polymorphisms and personal behaviors modify the risk of coronary atherosclerosis: a nested case-control study in Han Chinese with dyslipidaemia (2013-2016). *Asia Pac J Clin Nutr.* 2019;28(1):192–202.
313. Kancheva VD, Kasaikina OT. Bio-antioxidants - a chemical base of their antioxidant activity and beneficial effect on human health. *Curr Med Chem.* 2013;20(37):4784–805.
314. Bohn T. Carotenoids and Markers of Oxidative Stress in Human Observational Studies and Intervention Trials: Implications for Chronic Diseases. *Antioxidants (Basel, Switzerland).* 2019 Jun 17;8(6):179.
315. Azqueta A, Collins AR. Carotenoids and DNA damage. *Mutat Res Mol Mech Mutagen.* 2012;733(1):4–13.
316. Bonet ML, Canas JA, Ribot J, Palou A. Carotenoids in Adipose Tissue Biology and Obesity. *Subcell Biochem.* 2016;79:377–414.
317. Rühl R. Effects of dietary retinoids and carotenoids on immune development. *Proc Nutr Soc.* 2007 Aug;66(3):458–69.
318. Linnewiel-Hermoni K, Motro Y, Miller Y, Levy J, Sharoni Y. Carotenoid derivatives inhibit nuclear factor kappa B activity in bone and cancer cells by targeting key thiol groups. *Free Radic Biol Med.* 2014;75:105–20.

319. Linnewiel K, Ernst H, Caris-Veyrat C, Ben-Dor A, Kampf A, Salman H, et al. Structure activity relationship of carotenoid derivatives in activation of the electrophile/antioxidant response element transcription system. *Free Radic Biol Med.* 2009;47(5):659–67.
320. Kaulmann A, Bohn T. Carotenoids, inflammation, and oxidative stress—implications of cellular signaling pathways and relation to chronic disease prevention. *Nutr Res.* 2014;34(11):907–29.
321. Albu E. Pliny the Elder, Natural History. In: Mittman AS, Hensel M, editors. ARC, Amsterdam University Press; 2018. p. 43–8.
322. Garcés A, Torres E. El Escaramujo . Propiedades y uso terapeutico. *Med Natur.* 2010;4(1):44–52.
323. Ahmad N, Anwar F, Gilani A-H. Chapter 76 - Rose Hip (*Rosa canina* L.) Oils. In: Preedy Flavor and Safety VRBT-EO in FP, editor. San Diego: Academic Press; 2016. p. 667–75.
324. Winther K, Campbell-Tofte J, Hansen A. Bioactive ingredients of rose hips (*Rosa canina* L) with special reference to antioxidative and anti-inflammatory properties: in vitro studies. *Bot Targets Ther.* 2016 Feb 1;2016:11.
325. Kerasiotti E, Apostolou A, Kafantaris I, Chronis K, Kokka E, Dimitriadou C, et al. Polyphenolic Composition of *Rosa canina*, *Rosa sempervivens* and *Pyrocantha coccinea* Extracts and Assessment of Their Antioxidant Activity in Human Endothelial Cells. *Antioxidants* (Basel, Switzerland). 2019 Apr;8(4).
326. Fetni S, Bertella N, Ouahab A. LC-DAD/ESI-MS/MS characterization of phenolic constituents in *Rosa canina* L. and its protective effect in cells. *Biomed Chromatogr.* 2020 Dec;34(12):e4961.
327. Rovná K, Ivanišová E, Žiarovská J, Ferus P, Terentjeva M, Kowalczewski PŁ, et al. Characterization of *Rosa canina* Fruits Collected in Urban Areas of Slovakia. Genome Size, iPBS Profiles and Antioxidant and Antimicrobial Activities. *Molecules.* 2020 Apr;25(8).
328. Fecka I. Qualitative and quantitative determination of hydrolysable tannins and other polyphenols in herbal products from meadowsweet and dog rose. *Phytochem Anal.* 2009;20(3):177–90.
329. Bahrami G, Izadi B, Miraghaee SS, Mohammadi B, Hatami R, Sajadimajd S, et al. Antidiabetic potential of the isolated fractions from the plants of Rosaceae family in streptozotocin-induced diabetic rats. *Res Pharm Sci.* 2021 Oct;16(5):505–15.



330. Ninomiya K, Matsuda H, Kubo M, Morikawa T, Nishida N, Yoshikawa M. Potent anti-obese principle from *Rosa canina*: Structural requirements and mode of action of trans-tiliroside. *Bioorganic Med Chem Lett*. 2007;17(11):3059–64.
331. Nagatomo A, Nishida N, Fukuhara I, Noro A, Kozai Y, Sato H, et al. Daily intake of rosehip extract decreases abdominal visceral fat in preobese subjects: A randomized, double-blind, placebo-controlled clinical trial. *Diabetes, Metab Syndr Obes Targets Ther*. 2015;8:147–56.
332. Gruenwald J, Uebelhack R, Moré MI. *Rosa canina* – Rose hip pharmacological ingredients and molecular mechanics counteracting osteoarthritis – A systematic review. *Phytomedicine*. 2019;60:152958.
333. Al-Yafeai A, Malarski A, Böhm V. Characterization of carotenoids and vitamin E in *R. rugosa* and *R. canina*: Comparative analysis. *Food Chem*. 2018 Mar;242:435–42.
334. Hodisan T, Socaciu C, Ropan I, Neamtu G. Carotenoid composition of *Rosa canina* fruits determined by thin-layer chromatography and high-performance liquid chromatography. *J Pharm Biomed Anal*. 1997;16(3):521–8.
335. Ricchi M, Odoardi MR, Carulli L, Anzivino C, Ballestri S, Pinetti A, et al. Differential effect of oleic and palmitic acid on lipid accumulation and apoptosis in cultured hepatocytes. *J Gastroenterol Hepatol*. 2009;24(5):830–40.
336. Brasier AR, Ron DBT-M in E. [34] Luciferase reporter gene assay in mammalian cells. In: *Recombinant DNA Part G*. Academic Press; 1992. p. 386–97.
337. Bartlett JMS. mRNA Analyses BT - Ovarian Cancer: Methods and Protocols. In: Bartlett JMS, editor. Totowa, NJ: Humana Press; 2001. p. 399–409.
338. Martins T, Ferreira T, Nascimento-Gonçalves E, Castro-Ribeiro C, Lemos S, Rosa E, et al. Obesity Rodent Models Applied to Research with Food Products and Natural Compounds. *Obesities*. 2022;2(2):171–204.
339. Yang Y, Smith Jr. DL, Keating KD, Allison DB, Nagy TR. Variations in body weight, food intake and body composition after long-term high-fat diet feeding in C57BL/6J mice. *Obesity*. 2014 Oct 1;22(10):2147–55.
340. Kleinert M, Clemmensen C, Hofmann SM, Moore MC, Renner S, Woods SC, et al. Animal models of obesity and diabetes mellitus. *Nat Rev Endocrinol*. 2018;14(3):140–62.



341. Kanasaki K, Koya D. Biology of Obesity: Lessons from Animal Models of Obesity. Fedele M, editor. *J Biomed Biotechnol*. 2011;2011:197636.
342. Martí AP. The role of FGF21 in the metabolic response to amino acid restriction.
343. Sandoval V, Sanz-Lamora H, Marrero PF, Relat J, Haro D. Lyophilized Maqui (*Aristotelia chilensis*) Berry Administration Suppresses High-Fat Diet-Induced Liver Lipogenesis through the Induction of the Nuclear Corepressor SMILE. *Antioxidants* (Basel, Switzerland). 2021 Apr;10(5).
344. Sandoval V, Femenias A, Martinez-Garza U, Sanz-Lamora H, Castagnini JM, Quifer-Rada P, et al. Lyophilized Maqui (*Aristotelia chilensis*) Berry Induces Browning in the Subcutaneous White Adipose Tissue and Ameliorates the Insulin Resistance in High Fat Diet-Induced Obese Mice. *Antioxidants* (Basel, Switzerland). 2019 Sep;8(9).
345. Siersbæk MS, Ditzel N, Hejbøl EK, Præstholt SM, Markussen LK, Avolio F, et al. C57BL/6J substrain differences in response to high-fat diet intervention. *Sci Rep*. 2020 Aug;10(1):14052.
346. Lang P, Hasselwander S, Li H, Xia N. Effects of different diets used in diet-induced obesity models on insulin resistance and vascular dysfunction in C57BL/6 mice. *Sci Rep*. 2019;9(1):19556.
347. Tresserra-Rimbau A, Medina-Rejon A, Perez-Jimenez J, Martinez-Gonzalez MA, Covas MI, Corella D, et al. Dietary intake and major food sources of polyphenols in a Spanish population at high cardiovascular risk: the PREDIMED study. *Nutr Metab Cardiovasc Dis*. 2013 Oct;23(10):953–9.
348. Li S, Zhang Y, Sun Y, Zhang G, Bai J, Guo J, et al. Naringenin improves insulin sensitivity in gestational diabetes mellitus mice through AMPK. *Nutr Diabetes*. 2019;9(1):28.
349. Prasatthong P, Meeapat S, Rattanakanokchai S, Bunbupha S, Prachaney P, Maneesai P, et al. Hesperidin ameliorates signs of the metabolic syndrome and cardiac dysfunction via IRS/Akt/GLUT4 signaling pathway in a rat model of diet-induced metabolic syndrome. *Eur J Nutr*. 2021;60(2):833–48.
350. Peng P, Jin J, Zou G, Sui Y, Han Y, Zhao D, et al. Hesperidin prevents hyperglycemia in diabetic rats by activating the insulin receptor pathway. *Exp Ther Med*. 2021;21(1):53.
351. Tanaka T, Iwamoto K, Wada M, Yano E, Suzuki T, Kawaguchi N, et al. Dietary syringic acid reduces fat mass in an ovariectomy-induced mouse

- model of obesity. *Menopause*. 2021;28(12).
352. Chandramohan R, Pari L. Antihyperlipidemic effect of tyrosol, a phenolic compound in streptozotocin-induced diabetic rats. *Toxicol Mech Methods*. 2021 Sep 2;31(7):507–16.
  353. Hsu C-L, Wu C-H, Huang S-L, Yen G-C. Phenolic compounds rutin and o-coumaric acid ameliorate obesity induced by high-fat diet in rats. *J Agric Food Chem*. 2009 Jan;57(2):425–31.
  354. Mahbub AA, Le Maitre CL, Haywood-Small SL, Cross NA, Jordan-Mahy N. Polyphenols act synergistically with doxorubicin and etoposide in leukaemia cell lines. *Cell death Discov*. 2015;1:15043.
  355. Mahbub A, Le Maitre C, Haywood-Small S, Cross N, Jordan-Mahy N. Dietary polyphenols influence antimetabolite agents: methotrexate, 6-mercaptopurine and 5-fluorouracil in leukemia cell lines. *Oncotarget*. 2017 Aug 24;8(62):104877–93.
  356. Tresserra-Rimbau A, Medina-Reimon A, Perez-Jimenez J, Martinez-Gonzalez MA, Covas MI, Corella D, et al. Dietary intake and major food sources of polyphenols in a Spanish population at high cardiovascular risk: The PREDIMED study. *Nutr Metab Cardiovasc Dis*. 2013 Oct;23(10):953–9.
  357. Intake of Total Polyphenols and Some Classes of Polyphenols Is Inversely Associated with Diabetes in Elderly People at High Cardiovascular Disease Risk. *J Nutr*. 2016 Apr 1;146(4):767–77.
  358. Benedé-Ubieto R, Estévez-Vázquez O, Ramadori P, Cubero FJ, Nevzorova YA. Guidelines and Considerations for Metabolic Tolerance Tests in Mice. *Diabetes Metab Syndr Obes*. 2020 Feb 18;13:439–50.
  359. Pryor WA. The antioxidant nutrients and disease prevention--what do we know and what do we need to find out? *Am J Clin Nutr*. 1991 Jan;53(1):391S-393S.
  360. Pawlina W, Ross MH. *Ross histología : texto y atlas : correlación con biología molecular y celular* . 8ª ed. *Histología : texto y atlas : correlación con biología molecular y celular*. L'Hospitalet de Llobregat (Barcelona): Wolters Kluwer; 2019.
  361. Vallverdú-Queralt A, Medina-Remón A, Andres-Lacueva C, Lamuela-Raventos RM. Changes in phenolic profile and antioxidant activity during production of diced tomatoes. *Food Chem*. 2011 Jun;126(4):1700–7.

362. Abubakar AR, Haque M. Preparation of Medicinal Plants: Basic Extraction and Fractionation Procedures for Experimental Purposes. *J Pharm Bioallied Sci.* 2020/01/29. 2020;12(1):1–10.
363. Harman-Ware AE, Sykes R, Peter GF, Davis M. Determination of terpenoid content in pine by organic solvent extraction and fast-GC analysis. *Front Energy Res.* 2016;4(JAN):1–9.
364. Kotowska D, El-Houri RB, Borkowski K, Petersen RK, Fretté XC, Wolber G, et al. Isomeric C12-alkamides from the roots of *Echinacea purpurea* improve basal and insulin-dependent glucose uptake in 3T3-L1 adipocytes. *Planta Med.* 2014;80(18):1712–20.
365. Saaby L, Moesby L, Hansen EW, Christensen SB. Isolation of immunomodulatory triterpene acids from a standardized rose hip powder (*Rosa canina* L.). *Phyther Res.* 2011 Feb;25(2):195–201.
366. Porskjær Christensen L, Bahij El-Houri R. Development of an In Vitro Screening Platform for the Identification of Partial PPAR $\gamma$  Agonists as a Source for Antidiabetic Lead Compounds. *Molecules.* 2018;23(10).
367. Lozano-Castellón J, Rocchetti G, Vallverdú-Queralt A, Illán M, Torrado-Prat X, Lamuela-Raventós RM, et al. New vacuum cooking techniques with extra-virgin olive oil show a better phytochemical profile than traditional cooking methods: A foodomics study. *Food Chem.* 2021;362:130194.
368. Fayeulle N, Vallverdu-Queralt A, Meudec E, Hue C, Boulanger R, Cheynier V, et al. Characterization of new flavan-3-ol derivatives in fermented cocoa beans. *Food Chem.* 2018;259:207–12.
369. Tsugawa H, Ikeda K, Takahashi M, Satoh A, Mori Y, Uchino H, et al. A lipidome atlas in MS-DIAL 4. *Nat Biotechnol.* 2020;38(10):1159–63.
370. Tsugawa H, Kind T, Nakabayashi R, Yukihiro D, Tanaka W, Cajka T, et al. Hydrogen Rearrangement Rules: Computational MS/MS Fragmentation and Structure Elucidation Using MS-FINDER Software. *Anal Chem.* 2016 Aug 16;88(16):7946–58.
371. Liu H-W, Wei C-C, Chang S-J. Low-molecular-weight polyphenols protect kidney damage through suppressing NF- $\kappa$ B and modulating mitochondrial biogenesis in diabetic db/db mice. *Food Funct.* 2016;7(4):1941–9.
372. Gašić U, Ćirić I, Pejčić T, Radenković D, Djordjević V, Radulović S, et al. Polyphenols as Possible Agents for Pancreatic Diseases. *Antioxidants* (Basel, Switzerland). 2020 Jun 23;9(6):547.

373. Nikawa T, Ulla A, Sakakibara I. Polyphenols and Their Effects on Muscle Atrophy and Muscle Health. *Molecules*. 2021 Aug 12;26(16):4887.
374. Sanz-Lamora H, Marrero PF, Haro D, Relat J. A Mixture of Pure, Isolated Polyphenols Worsens the Insulin Resistance and Induces Kidney and Liver Fibrosis Markers in Diet-Induced Obese Mice. Vol. 11, *Antioxidants* . 2022.
375. Hariri N, Thibault L. High-fat diet-induced obesity in animal models. *Nutr Res Rev*. 2010/10/27. 2010;23(2):270–99.
376. van Swelm RPL, Wetzels JFM, Swinkels DW. The multifaceted role of iron in renal health and disease. *Nat Rev Nephrol*. 2020 Feb;16(2):77–98.
377. Fernández-Real JM, McClain D, Manco M. Mechanisms Linking Glucose Homeostasis and Iron Metabolism Toward the Onset and Progression of Type 2 Diabetes. *Diabetes Care*. 2015 Nov;38(11):2169–76.
378. Zhu Q, Scherer PE. Immunologic and endocrine functions of adipose tissue: implications for kidney disease. *Nat Rev Nephrol*. 2018;14(2):105–20.
379. Zhang W, Li X, Zhou S-G. Ablation of carbohydrate-responsive element-binding protein improves kidney injury in streptozotocin-induced diabetic mice. *Eur Rev Med Pharmacol Sci*. 2017 Jan;21(1):42–7.
380. Kaleta B. The role of osteopontin in kidney diseases. *Inflamm Res*. 2019;68(2):93–102.
381. Vianello E, Kalousová M, Dozio E, Tacchini L, Zima T, Corsi Romanelli MM. Osteopontin: The Molecular Bridge between Fat and Cardiac-Renal Disorders. *Int J Mol Sci*. 2020 Aug;21(15).
382. Masuzaki R, Kanda T, Sasaki R, Matsumoto N, Ogawa M, Matsuoka S, et al. Noninvasive Assessment of Liver Fibrosis: Current and Future Clinical and Molecular Perspectives. *Int J Mol Sci*. 2020 Jul;21(14).
383. Jiménez-Urbe AP, Gómez-Sierra T, Aparicio-Trejo OE, Orozco-Ibarra M, Pedraza-Chaverri J. Backstage players of fibrosis: NOX4, mTOR, HDAC, and S1P; companions of TGF- $\beta$ . *Cell Signal*. 2021;87:110123.
384. Jiang W, Wang X, Geng X, Gu Y, Guo M, Ding X, et al. Novel predictive biomarkers for acute injury superimposed on chronic kidney disease. *Nefrologia*. 2021;41(2):165–73.
385. Viau A, El Karoui K, Laouari D, Burtin M, Nguyen C, Mori K, et al. Identification of neutrophil gelatinase-associated lipocalin as a novel early urinary biomarker for ischemic renal injury. *J Am Soc Nephrol*. 2003

- Oct;120(10):2534–43.
386. Petrovska BB. Historical review of medicinal plants' usage. *Pharmacogn Rev.* 2012 Jan;6(11):1–5.
  387. King AJF. The use of animal models in diabetes research. *Br J Pharmacol.* 2012 Jun;166(3):877–94.
  388. Silvester AJ, Aseer KR, Yun JW. Dietary polyphenols and their roles in fat browning. *J Nutr Biochem.* 2019;64:1–12.
  389. Matsusue K, Kusakabe T, Noguchi T, Takiguchi S, Suzuki T, Yamano S, et al. Hepatic steatosis in leptin-deficient mice is promoted by the PPAR $\gamma$  target gene *Fsp27*. *Cell Metab.* 2008 Apr;7(4):302–11.
  390. Ordovas JM. Chapter 38 - Nutritional Genomics and Biological Sex. In: Legato MJB-T-P of G-SM (Third E, editor. San Diego: Academic Press; 2017. p. 557–68.
  391. Lin Z, Tian H, Lam KSL, Lin S, Hoo RCL, Konishi M, et al. Adiponectin mediates the metabolic effects of FGF21 on glucose homeostasis and insulin sensitivity in mice. *Cell Metab.* 2013 May;17(5):779–89.
  392. Miao L, Su F, Yang Y, Liu Y, Wang L, Zhan Y, et al. Glycerol kinase enhances hepatic lipid metabolism by repressing nuclear receptor subfamily 4 group A1 in the nucleus. *Biochem Cell Biol.* 2020 Jun;98(3):370–7.
  393. Dentin R, Girard J, Postic C. Carbohydrate responsive element binding protein (ChREBP) and sterol regulatory element binding protein-1c (SREBP-1c): two key regulators of glucose metabolism and lipid synthesis in liver. *Biochimie.* 2005;87(1):81–6.
  394. Walters J. Muscle hypertrophy and pseudohypertrophy. *Pract Neurol.* 2017 Oct;17(5):369–79.
  395. Brusotti G, Montanari R, Capelli D, Cattaneo G, Laghezza A, Tortorella P, et al. Betulinic acid is a PPAR $\gamma$  antagonist that improves glucose uptake, promotes osteogenesis and inhibits adipogenesis. *Sci Rep.* 2017;7(1):5777.
  396. Przybyciński J, Dziejczko V, Puchalowicz K, Domański L, Pawlik A. Adiponectin in chronic kidney disease. Vol. 21, *International Journal of Molecular Sciences.* 2020. p. 1–17.
  397. Zha D, Wu X, Gao P. Adiponectin and Its Receptors in Diabetic Kidney Disease: Molecular Mechanisms and Clinical Potential. *Endocrinology.* 2017 Jul;158(7):2022–34.

398. Schena FP, Gesualdo L. Pathogenetic mechanisms of diabetic nephropathy. *J Am Soc Nephrol.* 2005;16(3 suppl 1):S30–3.
399. Lousa I, Reis F, Beirão I, Alves R, Belo L, Santos-Silva A. New potential biomarkers for chronic kidney disease management—a review of the literature. *Int J Mol Sci.* 2020;22(1):43.
400. Lin Q, Chen Y, Lv J, Zhang H, Tang J, Gunaratnam L, et al. Kidney injury molecule-1 expression in IgA nephropathy and its correlation with hypoxia and tubulointerstitial inflammation. *Am J Physiol Physiol.* 2014;306(8):F885–95.
401. Karmakova TA, Sergeeva NS, Kanukoev KY, Alekseev BY, Kaprin AD. Kidney Injury Molecule 1 (KIM-1): a Multifunctional Glycoprotein and Biological Marker (Review). *Sovrem tekhnologii v meditsine.* 2021;13(3):64–78.
402. Humphreys BD, Xu F, Sabbisetti V, Grgic I, Naini SM, Wang N, et al. Chronic epithelial kidney injury molecule-1 expression causes murine kidney fibrosis. *J Clin Invest.* 2013;123(9):4023–35.
403. Medić B, Rovčanin B, Basta Jovanović G, Radojević-Škodrić S, Prostran M. Kidney Injury Molecule-1 and Cardiovascular Diseases: From Basic Science to Clinical Practice. *Biomed Res Int.* 2015;2015:854070.
404. Mori Y, Ajay AK, Chang J-H, Mou S, Zhao H, Kishi S, et al. KIM-1 mediates fatty acid uptake by renal tubular cells to promote progressive diabetic kidney disease. *Cell Metab.* 2021 May 4;33(5):1042-1061.e7.
405. Han WK, Alinani A, Wu C-L, Michaelson D, Loda M, McGovern FJ, et al. Human Kidney Injury Molecule-1 Is a Tissue and Urinary Tumor Marker of Renal Cell Carcinoma. *J Am Soc Nephrol.* 2005 Apr 1;16(4):1126 LP – 1134.
406. Kuehn EW, Park KM, Somlo S, Bonventre J V. Kidney injury molecule-1 expression in murine polycystic kidney disease. *Am J Physiol Physiol.* 2002 Dec 1;283(6):F1326–36.
407. Kramer AB, van Timmeren MM, Schuurs TA, Vaidya VS, Bonventre J V, van Goor H, et al. Reduction of proteinuria in adriamycin-induced nephropathy is associated with reduction of renal kidney injury molecule (Kim-1) over time. *Am J Physiol Physiol.* 2009 May 1;296(5):F1136–45.
408. De Borst MH, van Timmeren MM, Vaidya VS, de Boer RA, van Dalen MBA, Kramer AB, et al. Induction of kidney injury molecule-1 in homozygous Ren2 rats is attenuated by blockade of the renin-angiotensin system or p38 MAP kinase. *Am J Physiol Physiol.* 2007;292(1):F313–20.

409. Shi F, Harman J, Fujiwara K, Sottile J. Collagen I matrix turnover is regulated by fibronectin polymerization. *Am J Physiol Physiol*. 2010;298(5):C1265–75.
410. Kawelke N, Vasel M, Sens C, Au A von, Dooley S, Nakchbandi IA. Fibronectin protects from excessive liver fibrosis by modulating the availability of and responsiveness of stellate cells to active TGF- $\beta$ . *PLoS One*. 2011;6(11):e28181.
411. González-Domínguez Á, Visiedo-García FM, Domínguez-Riscart J, González-Domínguez R, Mateos RM, Lechuga-Sancho AM. Iron Metabolism in Obesity and Metabolic Syndrome. *Int J Mol Sci*. 2020 Aug;21(15).
412. Acton RT, Barton JC, Passmore L V, Adams PC, Speechley MR, Dawkins FW, et al. Relationships of serum ferritin, transferrin saturation, and HFE mutations and self-reported diabetes in the Hemochromatosis and Iron Overload Screening (HEIRS) study. *Diabetes Care*. 2006 Sep;29(9):2084–9.
413. Forouhi NG, Harding AH, Allison M, Sandhu MS, Welch A, Luben R, et al. Elevated serum ferritin levels predict new-onset type 2 diabetes: results from the EPIC-Norfolk prospective study. *Diabetologia*. 2007 May;50(5):949–56.
414. Jiang R, Manson JE, Meigs JB, Ma J, Rifai N, Hu FB. Body iron stores in relation to risk of type 2 diabetes in apparently healthy women. *JAMA*. 2004 Feb;291(6):711–7.
415. Fernández-Real JM, López-Bermejo A, Ricart W. Cross-talk between iron metabolism and diabetes. *Diabetes*. 2002 Aug;51(8):2348–54.
416. Gabrielsen JS, Gao Y, Simcox JA, Huang J, Thorup D, Jones D, et al. Adipocyte iron regulates adiponectin and insulin sensitivity. *J Clin Invest*. 2012/09/10. 2012 Oct;122(10):3529–40.
417. Varghese J, James J V, Anand R, Narayanasamy M, Rebekah G, Ramakrishna B, et al. Development of insulin resistance preceded major changes in iron homeostasis in mice fed a high-fat diet. *J Nutr Biochem*. 2020 Oct;84:108441.
418. Mori K, Lee HT, Rapoport D, Drexler IR, Foster K, Yang J, et al. Endocytic delivery of lipocalin-siderophore-iron complex rescues the kidney from ischemia-reperfusion injury. *J Clin Invest*. 2005 Mar;115(3):610–21.
419. Mishra J, Mori K, Ma Q, Kelly C, Yang J, Mitsnefes M, et al. Amelioration of ischemic acute renal injury by neutrophil gelatinase-associated lipocalin. *J Am Soc Nephrol*. 2004 Dec;15(12):3073–82.



420. Urbschat A, Thiemens A-K, Mertens C, Rehwald C, Meier JK, Baer PC, et al. Macrophage-Secreted Lipocalin-2 Promotes Regeneration of Injured Primary Murine Renal Tubular Epithelial Cells. Vol. 21, *International Journal of Molecular Sciences* . 2020.
421. Duarte JAG, Carvalho F, Pearson M, Horton JD, Browning JD, Jones JG, et al. A high-fat diet suppresses de novo lipogenesis and desaturation but not elongation and triglyceride synthesis in mice. *J Lipid Res*. 2014/09/30. 2014 Dec;55(12):2541–53.
422. Gamberi T, Magherini F, Modesti A, Fiaschi T. Adiponectin Signaling Pathways in Liver Diseases. *Biomedicines*. 2018 May 7;6(2):52.
423. Treeprasertsuk S, Björnsson E, Enders F, Suwanwalaikorn S, Lindor KD. NAFLD fibrosis score: a prognostic predictor for mortality and liver complications among NAFLD patients. *World J Gastroenterol*. 2013 Feb;19(8):1219–29.
424. Zhang X-Q, Xu C-F, Yu C-H, Chen W-X, Li Y-M. Role of endoplasmic reticulum stress in the pathogenesis of nonalcoholic fatty liver disease. *World J Gastroenterol*. 2014 Feb 21;20(7):1768–76.
425. Bouayed J, Bohn T. Exogenous antioxidants - Double-edged swords in cellular redox state: Health beneficial effects at physiologic doses versus deleterious effects at high doses. *Oxid Med Cell Longev*. 2010;3(4):228–37.
426. Valko M, Leibfritz D, Moncol J, Cronin MTD, Mazur M, Telser J. Free radicals and antioxidants in normal physiological functions and human disease. *Int J Biochem Cell Biol*. 2007;39(1):44–84.
427. Pandey KB, Rizvi SI. Plant polyphenols as dietary antioxidants in human health and disease. *Oxid Med Cell Longev*. 2009;2(5):270–8.
428. Santos L. The impact of nutrition and lifestyle modification on health. *Eur J Intern Med*. 2021 Oct;
429. Tüccar TB, Akbulut G. Mediterranean meal favorably effects postprandial oxidative stress response compared with a western meal in healthy women. *Int J Vitam Nutr Res Int Zeitschrift für Vitamin- und Ernährungsforschung J Int Vitaminol Nutr*. 2021 Oct;
430. Bohn T. Dietary factors affecting polyphenol bioavailability. *Nutr Rev*. 2014;72(7):429–52.
431. Eker ME, Aaby K, Budic-Leto I, Rimac Brnčić S, El SN, Karakaya S, et al. A review of factors affecting anthocyanin bioavailability: Possible implications



- for the inter-individual variability. *Foods*. 2019;9(1):2.
432. Lavefve L, Howard LR, Carbonero F. Berry polyphenols metabolism and impact on human gut microbiota and health. *Food Funct*. 2020;11(1):45–65.
  433. Marhuenda-Muñoz M, Laveriano-Santos EP, Tresserra-Rimbau A, Lamuela-Raventós RM, Martínez-Huélamo M, Vallverdú-Queralt A. Microbial Phenolic Metabolites: Which Molecules Actually Have an Effect on Human Health? Vol. 11, *Nutrients* . 2019.
  434. Manach C, Scalbert A, Morand C, Rémésy C, Jiménez L. Polyphenols: food sources and bioavailability. *Am J Clin Nutr*. 2004 May 1;79(5):727–47.
  435. Jakobek L, Matic P. Non-covalent dietary fiber - Polyphenol interactions and their influence on polyphenol bioaccessibility. *Trends Food Sci Technol*. 2019;83:235–47.
  436. Tang R, Yu H, Ruan Z, Zhang L, Xue Y, Yuan X, et al. Effects of food matrix elements (dietary fibres) on grapefruit peel flavanone profile and on faecal microbiota during in vitro fermentation. *Food Chem*. 2021 Sep;371:131065.
  437. Monari S, Ferri M, Montecchi B, Salinitro M, Tassoni A. Phytochemical characterization of raw and cooked traditionally consumed alimurgic plants. *PLoS One*. 2021;16(8):e0256703.
  438. Samaniego-Sánchez C, Martín-del-Campo ST, Castañeda-Saucedo MC, Blanca-Herrera RM, Quesada-Granados JJ, Ramírez-Anaya JD. Migration of Avocado Virgin Oil Functional Compounds during Domestic Cooking of Eggplant. Vol. 10, *Foods* . 2021.
  439. Sun Q, Du M, Navarre DA, Zhu M. Effect of Cooking Methods on Bioactivity of Polyphenols in Purple Potatoes. Vol. 10, *Antioxidants* . 2021.
  440. Rinaldi de Alvarenga JF, Quifer-Rada P, Francetto Juliano F, Hurtado-Barroso S, Illan M, Torrado-Prat X, et al. Using Extra Virgin Olive Oil to Cook Vegetables Enhances Polyphenol and Carotenoid Extractability: A Study Applying the sofrito Technique. *Molecules*. 2019 Apr;24(8).
  441. Rinaldi de Alvarenga JF, Quifer-Rada P, Westrin V, Hurtado-Barroso S, Torrado-Prat X, Lamuela-Raventós RM. Mediterranean sofrito home-cooking technique enhances polyphenol content in tomato sauce. *J Sci Food Agric*. 2019 Nov;99(14):6535–45.
  442. Beltrán Sanahuja A, De Pablo Gallego SL, Maestre Pérez SE, Valdés García A, Prats Moya MS. Influence of Cooking and Ingredients on the Antioxidant Activity, Phenolic Content and Volatile Profile of Different Variants of the

- Mediterranean Typical Tomato Sofrito. *Antioxidants* (Basel, Switzerland). 2019 Nov;8(11).
443. Nagatomo A, Nishida N, Matsuura Y, Shibata N. Rosehip Extract Inhibits Lipid Accumulation in White Adipose Tissue by Suppressing the Expression of Peroxisome Proliferator-activated Receptor Gamma. *Prev Nutr food Sci*. 2013 Jun;18(2):85–91.
  444. Winther K, Apel K, Thamsborg G. A powder made from seeds and shells of a rose-hip subspecies (*Rosa canina*) reduces symptoms of knee and hip osteoarthritis: a randomized, double-blind, placebo-controlled clinical trial. *Scand J Rheumatol*. 2005;34(4):302–8.
  445. Seifi M, Abbasalizadeh S, Mohammad-Alizadeh-Charandabi S, Khodaie L, Mirghafourvand M. The effect of *Rosa* (*L. Rosa canina*) on the incidence of urinary tract infection in the puerperium: A randomized placebo-controlled trial. *Phytother Res*. 2018 Jan;32(1):76–83.
  446. Golsorkhi H, Qorbani M, Kamalinejad M, Sabbaghzadegan S, Bahrami M, Vafae-Shahi M, et al. The effect of *Rosa canina* L. and a polyherbal formulation syrup in patients with attention-deficit/hyperactivity disorder: a study protocol for a multicenter randomized controlled trial. *Trials*. 2022 May;23(1):434.
  447. Farajpour R, Sadigh-Eteghad S, Ahmadian N, Farzipour M, Mahmoudi J, Majdi A. Chronic Administration of *Rosa canina* Hydro-Alcoholic Extract Attenuates Depressive-Like Behavior and Recognition Memory Impairment in Diabetic Mice: A Possible Role of Oxidative Stress. *Med Princ Pract Int J Kuwait Univ Heal Sci Cent*. 2017;26(3):245–50.
  448. Jemaa H Ben, Jemia A Ben, Khlifi S, Ahmed H Ben, Slama F Ben, Benzarti A, et al. Antioxidant activity and  $\alpha$ -amylase inhibitory potential of *rosa canina* l. african j tradit complement altern med ajtcam. 2017;14(2):1–8.
  449. Fattahi A, Niyazi F, Shahbazi B, Farzaei MH, Bahrami G. Antidiabetic Mechanisms of *Rosa canina* Fruits: An In Vitro Evaluation. *J Evid Based Complementary Altern Med*. 2017 Jan;22(1):127–33.
  450. Taghizadeh M, Rashidi AA, Taherian AA, Vakili Z, Sajad Sajadian M, Ghardashi M. Antidiabetic and Antihyperlipidemic Effects of Ethanol Extract of *Rosa canina* L. fruit on Diabetic Rats: An Experimental Study With Histopathological Evaluations. *J Evid Based Complementary Altern Med*. 2016 Oct;21(4):NP25-30.
  451. Rahimi M, Sajadimajd S, Mahdian Z, Hemmati M, Malekkhatabi P, Bahrami G, et al. Characterization and anti-diabetic effects of the oligosaccharide

- fraction isolated from *Rosa canina* in STZ-Induced diabetic rats. *Carbohydr Res*. 2020 Mar;489:107927.
452. Bahrami G, Miraghaee SS, Mohammadi B, Bahrami MT, Taheripak G, Keshavarzi S, et al. Molecular mechanism of the anti-diabetic activity of an identified oligosaccharide from *Rosa canina*. *Res Pharm Sci*. 2020 Feb;15(1):36–47.
  453. Sajadimajd S, Bahrami G, Mohammadi B, Nouri Z, Farzaei MH, Chen J-T. Protective effect of the isolated oligosaccharide from *Rosa canina* in STZ-treated cells through modulation of the autophagy pathway. *J Food Biochem*. 2020 Oct 1;44(10):e13404.
  454. Bahrami G, Sajadimajd S, Mohammadi B, Hatami R, Miraghaee S, Keshavarzi S, et al. Anti-diabetic effect of a novel oligosaccharide isolated from *Rosa canina* via modulation of DNA methylation in Streptozotocin-diabetic rats. *Daru*. 2020 Dec;28(2):581–90.
  455. Chen SJ, Aikawa C, Yoshida R, Kawaguchi T, Matsui T. Anti-prediabetic effect of rose hip (*Rosa canina*) extract in spontaneously diabetic Torii rats. *J Sci Food Agric*. 2017 Sep;97(12):3923–8.
  456. Kobayashi M, Fujii N, Narita T, Higami Y. SREBP-1c-Dependent Metabolic Remodeling of White Adipose Tissue by Caloric Restriction. Vol. 19, *International Journal of Molecular Sciences* . 2018.
  457. Yoshikawa T, Shimano H, Yahagi N, Ide T, Amemiya-Kudo M, Matsuzaka T, et al. Polyunsaturated Fatty Acids Suppress Sterol Regulatory Element-binding Protein 1c Promoter Activity by Inhibition of Liver X Receptor (LXR) Binding to LXR Response Elements\*. *J Biol Chem*. 2002;277(3):1705–11.
  458. Kang HW, Lee SG, Otieno D, Ha K. Flavonoids, Potential Bioactive Compounds, and Non-Shivering Thermogenesis. *Nutrients*. 2018 Aug;10(9).
  459. Tucker B, Li H, Long X, Rye K-A, Ong KL. Fibroblast growth factor 21 in non-alcoholic fatty liver disease. *Metabolism*. 2019 Dec;101:153994.
  460. Henriksson E, Andersen B. FGF19 and FGF21 for the Treatment of NASH- Two Sides of the Same Coin? Differential and Overlapping Effects of FGF19 and FGF21 From Mice to Human. *Front Endocrinol (Lausanne)*. 2020;11:601349.
  461. Massa ML, Gagliardino JJ, Francini F. Liver glucokinase: An overview on the regulatory mechanisms of its activity. *IUBMB Life*. 2011 Jan 1;63(1):1–6.

462. Peter A, Stefan N, Cegan A, Walenta M, Wagner S, Königsrainer A, et al. Hepatic Glucokinase Expression Is Associated with Lipogenesis and Fatty Liver in Humans. *J Clin Endocrinol Metab.* 2011 Jul 1;96(7):E1126–30.
463. Chella Krishnan K, Floyd RR, Sabir S, Jayasekera DW, Leon-Mimila P V, Jones AE, et al. Liver Pyruvate Kinase Promotes NAFLD/NASH in Both Mice and Humans in a Sex-Specific Manner. *Cell Mol Gastroenterol Hepatol.* 2021;11(2):389–406.
464. Zhang D, Tong X, VanDommelen K, Gupta N, Stamper K, Brady GF, et al. Lipogenic transcription factor ChREBP mediates fructose-induced metabolic adaptations to prevent hepatotoxicity. *J Clin Invest.* 2017 Jun;127(7):2855–67.
465. Benhamed F, Denechaud P-D, Lemoine M, Robichon C, Moldes M, Bertrand-Michel J, et al. The lipogenic transcription factor ChREBP dissociates hepatic steatosis from insulin resistance in mice and humans. *J Clin Invest.* 2012 Jun 1;122(6):2176–94.
466. Wang Y, Viscarra J, Kim S-J, Sul HS. Transcriptional regulation of hepatic lipogenesis. *Nat Rev Mol Cell Biol.* 2015;16(11):678–89.
467. Samuel VT, Shulman GI. Nonalcoholic Fatty Liver Disease as a Nexus of Metabolic and Hepatic Diseases. *Cell Metab.* 2018 Jan;27(1):22–41.
468. Loza-Rodríguez H, Estrada-Soto S, Alarcón-Aguilar FJ, Huang F, Aquino-Jarquín G, Fortis-Barrera Á, et al. Oleanolic acid induces a dual agonist action on PPAR $\gamma$ / $\alpha$  and GLUT4 translocation: A pentacyclic triterpene for dyslipidemia and type 2 diabetes. *Eur J Pharmacol.* 2020 Sep;883:173252.
469. Desouky HE, Jiang G-Z, Zhang D-D, Abasubong KP, Yuan X, Li X-F, et al. Influences of glycyrrhetic acid (GA) dietary supplementation on growth, feed utilization, and expression of lipid metabolism genes in channel catfish (*Ictalurus punctatus*) fed a high-fat diet. *Fish Physiol Biochem.* 2020 Apr;46(2):653–63.
470. Marion-Letellier R, Savoye G, Ghosh S. Fatty acids, eicosanoids and PPAR gamma. *Eur J Pharmacol.* 2016 Aug;785:44–9.
471. Paradiso VM, Castellino M, Renna M, Santamaria P, Caponio F. Setup of an Extraction Method for the Analysis of Carotenoids in Microgreens. *Foods* (Basel, Switzerland). 2020 Apr;9(4).
472. Mohammadi A, Fallah H, Gholamhosseinian A. Antihyperglycemic Effect of Rosa Damascena is Mediated by PPAR $\gamma$  Gene Expression in Animal Model of Insulin Resistance. *Iran J Pharm Res IJPR.* 2017;16(3):1080–8.

473. González-Mañán D, D'Espessailles A, Dossi CG, San Martín M, Mancilla RA, Tapia GS. Rosa Mosqueta Oil Prevents Oxidative Stress and Inflammation through the Upregulation of PPAR- $\alpha$  and NRF2 in C57BL/6J Mice Fed a High-Fat Diet. *J Nutr.* 2017 Apr;147(4):579–88.
474. Ninomiya K, Matsuda H, Kubo M, Morikawa T, Nishida N, Yoshikawa M. Potent anti-obese principle from *Rosa canina*: Structural requirements and mode of action of trans-tiliroside. *Bioorg Med Chem Lett.* 2007;17(11):3059–64.

ANNEXES



## 7. Annexes

### 7.1. Review Article

Sandoval V\*, Sanz-Lamora H\*, Arias G, Marrero PF, Haro D, Relat J. Metabolic Impact of Flavonoids Consumption in Obesity: From Central to Peripheral. *Nutrients*. 2020 Aug;12(8).  
*\*Equal Contribution*





Review

## Metabolic Impact of Flavonoids Consumption in Obesity: From Central to Peripheral

Viviana Sandoval <sup>1,†</sup>, Hèctor Sanz-Lamora <sup>1,2,†</sup>, Giselle Arias <sup>1</sup>, Pedro F. Marrero <sup>1,3,4</sup>,  
Diego Haro <sup>1,3,4,\*</sup> and Joana Relat <sup>1,2,4,\*</sup> 

<sup>1</sup> Department of Nutrition, Food Sciences and Gastronomy, School of Pharmacy and Food Sciences, Food Torribera Campus, University of Barcelona, E-08921 Santa Coloma de Gramenet, Spain; vivianapazsandovals@gmail.com (V.S.); h.sanz.lamora@gmail.com (H.S.-L.); giselle.arias@upr.edu (G.A.); pedromarrero@ub.edu (P.F.M.)

<sup>2</sup> Institute of Nutrition and Food Safety of the University of Barcelona (INSA-UB), E-08921 Santa Coloma de Gramenet, Spain

<sup>3</sup> Institute of Biomedicine of the University of Barcelona (IBUB), E-08028 Barcelona, Spain

<sup>4</sup> CIBER Physiopathology of Obesity and Nutrition (CIBER-OBN), Instituto de Salud Carlos III, E-28029 Madrid, Spain

\* Correspondence: dharo@ub.edu (D.H.); jrelat@ub.edu (J.R.); Tel.: +93-0403-3690 (D.H.); +34-9340-20862 (J.R.)

† Both authors contributed equally to this work.

Received: 21 July 2020; Accepted: 5 August 2020; Published: 10 August 2020



**Abstract:** The prevention and treatment of obesity is primary based on the follow-up of a healthy lifestyle, which includes a healthy diet with an important presence of bioactive compounds such as polyphenols. For many years, the health benefits of polyphenols have been attributed to their anti-oxidant capacity as free radical scavengers. More recently it has been described that polyphenols activate other cell-signaling pathways that are not related to ROS production but rather involved in metabolic regulation. In this review, we have summarized the current knowledge in this field by focusing on the metabolic effects of flavonoids. Flavonoids are widely distributed in the plant kingdom where they are used for growing and defending. They are structurally characterized by two benzene rings and a heterocyclic pyrone ring and based on the oxidation and saturation status of the heterocyclic ring flavonoids are grouped in seven different subclasses. The present work is focused on describing the molecular mechanisms underlying the metabolic impact of flavonoids in obesity and obesity-related diseases. We described the effects of each group of flavonoids in liver, white and brown adipose tissue and central nervous system and the metabolic and signaling pathways involved on them.

**Keywords:** non-alcoholic fatty liver disease; obesity; flavonoids; lipid metabolism; metabolic regulation; adipose tissue; brain

### 1. Introduction

Overnutrition and unhealthy diets together with physical inactivity cause an impairment in the metabolic homeostasis that lead to the development of pathologies such as obesity, type 2 diabetes, cardiovascular diseases (CVD) and more recently this kind of lifestyle has also been linked to neuroinflammation and neurodegenerative diseases [1–5].

The metabolic syndrome (MetS) is the medical term used to define the concomitance in an individual of some of the following alterations: hyperglycemia and/or insulin resistance, arterial hypertension, dyslipidemia and central or abdominal obesity [6]. It is currently one of the main public health problems worldwide and its incidence increases significantly each year,

affecting almost 25% of the adult population today and has been directly associated to a greater risk of suffering from CVD or type 2 diabetes among others [3].

Obesity is one of the most important trigger for many of the other alterations include in the MetS. Obesity is essentially caused by an imbalance between energy intake and energy expenditure that initially causes an expansion of the white adipose tissue (WAT) to store the overfeed as triglycerides (TG). Some evidences indicate that at some point, WAT fails to adequately keep the surplus of nutrients and together with an insufficient differentiation of new adipocytes lead to an off-WAT accumulation of lipids in peripheral relevant organs. This ectopic accumulation of lipids causes lipotoxicity that may be, at least in part, responsible of the metabolic obesity-related metabolic dysfunctions [7]. It seems obvious that defects in WAT functionality together with peripheral lipotoxicity are the key points in the onset of metabolic syndrome (MetS) [8]. Looking for a way to restore lipid homeostasis and reduce lipotoxicity but also to diminish adipose tissue inflammation and macrophage infiltration many research groups are focused on identifying specific dietary patterns or foods capable to counteract these effects to finally revert obesity and its comorbidities.

Furthermore, it has been described that long-term hyperglycemia and diabetes complications induce impairments in the hippocampal synaptic plasticity as well as cognitive deficits [9] and increase the risk for Alzheimer disease [10,11] and depressive illness [12]. On the other side, diet-induced hypothalamic inflammation and mitochondrial dysfunction result in the onset and development of obesity and related metabolic diseases. It has been shown that, in rats, high fat diet (HFD) induces metabolic inflammation in the central nervous system (CNS), particularly in the hypothalamus [13].

The prevention of MetS and obesity is primary based on the follow-up of a healthy lifestyle, which includes, among other recommendations, a healthy diet. In this context, the Mediterranean Diet (DietMed) has shown beneficial effects on the prevention and treatment of MetS and obesity by reducing chronic low-grade inflammation, improving endothelial function and reducing cardiovascular risk [14–16]. The study of Prevention with Mediterranean Diet (Predimed) has shown that high adherence to this nutritional profile is effective in the primary and secondary prevention of CVD, diabetes and obesity [17–24]. DietMed is characterized by a high consumption of foods rich in bioactive compounds such as polyphenols to whose have been attributed a large part of the health effects of this diet [18,23,25–28].

In this review, we have summarized the current knowledge on the metabolic effects of a specific group of polyphenols, the flavonoids, and the molecular mechanisms underlying these effects.

Concretely, the main goal of the present work is to describe the molecular mechanisms underlying the anti-obesity effects of flavonoids in three target organs/tissues: liver, adipose tissues (WAT and brown adipose tissue (BAT)) and central nervous system (CNS).

We choose a high variety of obesity models, sources and doses of flavonoids to identify the metabolic and signaling pathways involved in the effects of each subclass of flavonoids (anthocyanins, flavanols, flavanones, flavonols, isoflavones, flavones and chalcones) in these tissues/organs. Only studies in humans and experimental approaches whit animal models from the last years have been included, thus avoiding cell culture experimental approaches except when relevant.

## 2. Polyphenols and Metabolism

Polyphenols are the most abundant phytochemicals in nature. They are widely distributed in fruits, vegetables, and highly present in foods like legumes, cocoa, some cereals as well as in some beverages, such as tea, coffee and wine [29]. Polyphenols are not essential nutrients for humans but research in nutrition, including epidemiological studies, randomized controlled trials, in vivo and in vitro assays with animal models and cell lines, has shown that long-term and acute intakes can have beneficial effects on weight management and chronic diseases such as CVD, obesity, type 2 diabetes, the onset and development of some cancers and cognitive function [13,30–37].

The effects of polyphenols are directly related to their bioavailability. It is assumed that just the 5%-10% of the total dietary polyphenol intake is absorbed directly through the stomach and/or

small intestine, the rest reaches the colon where they are transformed by the microbiota [38–40]. After being absorbed, polyphenols undergo phase I and II metabolism (sulfation, glucuronidation, methylation, and glycine conjugation) in the liver [29]. Polyphenol metabolites derived from liver metabolism may interact, among others, with adipose tissue, pancreas, muscle, and liver, where they exert their bioactivity.

Polyphenols have been divided in two main families: flavonoids and non-flavonoids, that are subdivided into several subclasses. For many years, the health benefits of polyphenols have been attributed to their anti-oxidant capacity as free radical scavengers. More recently it has been described that polyphenols activate other cell-signaling pathways that are not related to ROS production but rather involved in metabolic regulation [23,41].

*Flavonoids*

Flavonoids are widely distributed in the plant kingdom when are used for vegetables for growing and defending. They are structurally characterized by two benzene rings and a heterocyclic pyrone ring and based on the oxidation and saturation status of the heterocyclic ring flavonoids are grouped in seven different subfamilies (Table 1).

**Table 1.** Flavonoids classes, compounds, representative food sources and chemical structures.

Class	Compounds	Representative Food Sources	Chemical Structure
Anthocyanins	Cyanidin, Delphinidin, Malvidin, Peonidin, Petunidin	Raspberries, Blackberries, Blueberries	
Flavanols	(+)-Catechin, (-)-Epigallocatechin gallate, (-)-Epigallocatechin, Procyanidin	Tea, Cocoa	
Flavanones	Hesperidin, Hesperetin, Narirutin, Naringin, Eriodictyol	Oranges, Lemons	
Flavonols	Kaempferol, Myricetin, Quercetin, Isoquercetin	Onions, Apples, Berries	
Isoflavones	Daidzein, Genistein	Soybeans	
Flavones	Chrysin, Fisetin, Quercetin, Xanthone	Onions, Apples, Berries	
Chalcones	Chalcone	Onions	



(NASH), fibrosis, cirrhosis and in some cases hepatocarcinoma. Anthocyanins and anthocyanin-rich foods extracts or juices have demonstrated in several studies their ability to reduce the hepatic content of TG and lipids [85,86] and their capacity to modulate hepatic metabolism to protect against NAFLD [62,87–89]. Although in most of the published approaches performed with rodent models of obesity or NAFLD, anthocyanins or anthocyanin-rich fruits or extracts significantly reduced the hepatic lipid content and ameliorated the hepatic steatosis profile of these animals [88,90–92] some ineffective approaches have also been described [93–95].

The beneficial effects of anthocyanins in the liver have been linked to the activation of the AMPK, the upregulation of glycolytic and FAO genes and the downregulation of the gluconeogenic and lipogenic genes among others [70–72,96,97].

Mulberry anthocyanin extract administration to type 2 diabetic mice increased the activity of AMPK/peroxisome proliferator-activated receptor gamma coactivator 1 alpha (PGC1 $\alpha$ )/p38 mitogen-activated protein kinase (MAPK) and reduced the activity of the acetyl-CoA carboxylase enzyme (ACC), a rate-limiting enzyme of fatty acid synthesis, and of the mammalian target of rapamycin (mTOR) that is involved in protein synthesis regulation and insulin signaling [96]. Similar effects were described in HFD-fed hamsters, where Mulberry water extracts exerted anti-obesity effects by inhibiting lipogenesis (downregulation of fatty acid synthase (FASN) and 3-hydroxy-3-methylglutaryl-coenzyme A (HMG-CoA) reductase) and upregulating PPAR $\alpha$  and CPT1A [81]. On its side, honeyberry (*Lonicera caerulea*) extract (HBE) also decreased lipid accumulation in the liver of HFD-obese mice. HBE downregulated the hepatic expression of lipogenic genes such as *sterol regulatory element-binding protein-1* (*Srebp-1c*), *CCAAT/enhancer-binding protein alpha* (*Cebpa*), *Ppar $\gamma$* , and *Fasn* as well as upregulated the mRNA and protein levels of CPT1a and PPAR $\alpha$ , thus enhancing FAO. As mulberry anthocyanin extract, HBE treatment also increased the phosphorylation of AMPK and ACC thus activating and inhibiting these enzymes respectively [98]. On the other hand, in NAFLD-induced rats, blackberry extracts improved insulin sensitivity and dyslipidemia, ameliorated triglyceride and lipid peroxide accumulation and suppressed the mRNA expression of genes involved in fatty-acid synthesis (*Fasn* and *Srebp-1c*) [88]. Finally, purple sweet potato reduced the protein levels of FASN and of the cluster of differentiation 36 (CD36), inactivated the C/EBP $\beta$ , restored AMPK activity and increased the protein levels of CPT1a in livers of HFD-fed mice, thus indicating decreased lipogenesis and fatty acid uptake and enhanced FAO [62].

Regarding glucose metabolism, protein-bound anthocyanin compounds of purple sweet potato ameliorate hyperglycemia in obese and diabetic mice by regulating hepatic glucose metabolism. Anthocyanin compounds of purple sweet potato induced the hepatic protein levels of p-AMPK, glucose transporter type 2 (GLUT2), insulin receptor  $\alpha$  (IR $\alpha$ ), glucokinase (GK), as well as the expression of *phosphofructokinase* (*Pfk*) and *pyruvate kinase* (*Pk*), while gluconeogenic genes, *glucose-6-phosphatase* (*G6Pase*) and *phosphoenolpyruvate carboxykinase* (*Pepck*) were downregulated [99]. Further, Saskatoon berry normalized liver expression of *Gk* and *glycogen phosphorylase* and increased *G6Pase* in diet-induced MetS rats, thus suggesting that Saskatoon berry regulated glycolysis, gluconeogenesis and glycogenesis to improve MetS [100].

Although most of the experimental approaches have been done using anthocyanins-rich extracts, pure compounds have been also analyzed. Cyanidin-3-glucoside (C3G) administration to C57BL/6J obese mice fed a HFD and db/db mice diminished the triglyceride hepatic content and steatosis [73,101], through the blockade of the c-Jun N-terminal kinase activation (JNK) and the promotion of the phosphorylation and nuclear exclusion of the transcription factor Forkhead box protein O1 (FoxO1) [101].

All these data confirm the impact of anthocyanins and even in a more significative way of the anthocyanin-rich foods on metabolism. These effects can be added to their anti-inflammatory, antiapoptotic, pro-autophagic and antioxidant properties in steatotic livers [59,62,102–104].

### 3.2. Anthocyanins in Adipose Tissue: The Activation of BAT and the Browning of WAT

The impairment of adipose tissue function is strongly associated with the development of obesity and insulin resistance (IR). The activation of BAT and the browning in WAT are considered potential strategies to counteract the metabolic alterations linked to the obese phenotype. Both actions are mechanisms to increase the energy expenditure (EE) through the induction of lipolysis, FAO and thermogenesis and consequently efficient ways to reduce the ectopic lipid accumulation and the lipotoxicity [105–108].

Part of the beneficial effects of anthocyanins on diet-induced obesity are due to their impact on adipose depots. Anthocyanidins regulate lipolysis, FAO, lipogenesis and adipose tissue development [76,109–111]. They affected the adipokines secretion [112], modified the adipocytes-gene expression [33,113,114]. Moreover, anthocyanins are able to improve WAT functionality, to induce browning in WAT [33,57,82,115] or to increase the BAT mass or its activity [57,109,115], thus regulating energy expenditure [59,73]. Moreover, in WAT, anthocyanins ameliorate the obesity-associated inflammation [57,59,116].

In WAT, an anthocyanin-rich bilberry extract ameliorated hyperglycemia and insulin sensitivity through the activation of AMPK that resulted in an increase of the glucose transporter 4 (GLUT4) [72]. On its side, C3G-enriched *Aronia melanocarpa* extract reduced food intake and WAT weight in HFD-fed mice but also suppressed adipogenesis. These animals showed a downregulating in the expression levels of *C/ebp $\alpha$* , *Srebp1c*, *Acc*, *ATP-citrate lyase*, *Pgc1 $\alpha$* , *Fasn*, and *adipocyte protein 2 (Ap2)* as well as in the circulating levels of leptin [111]. In the same way, in HFD-induced obese mice model, the dietary supplementation with maqui (*Aristotelia chilensis*) improved the body weight gain and glucose metabolism at least in part by modifying the expression of the *carbohydrate responsive element binding protein  $\beta$  (ChREBP $\beta$ )*, the *fibroblast growth factor 21 (Fgf21)* and *adiponectin* as well as of the lipogenic and FAO genes [82]. Globally, the maqui supplementation induced the browning of the subcutaneous WAT (scWAT) [82].

The induction of browning is a common phenotype in obese rodent models treated with anthocyanins or anthocyanin-rich foods. The thermogenic and mitochondrial markers were also increased in the inguinal WAT (iWAT) of high fat-high fructose (HF/HFD)-fed mice treated with C3G, thus indicating the browning of this adipose tissue depot and suggesting an increased heat production and energy expenditure (EE) [117]. In db/db mice, C3G and vanillic acid exerted similar effects: increased EE, limited weight gain and upregulated expression of *Ucp1* and other thermogenic and mitochondrial markers, thus indicating the induction of brown-like adipocytes development in the scWAT [73] or iWAT [115]. Freeze dried raspberry decreased WAT hypertrophy induced by HFD and promoted the browning of WAT as it is showed by a higher expression of beige markers such as *Ucp1*, *PR-Domain zinc finger protein 16 (Prdm16)*, *Cytochrome C*, *Cell death inducing DFFA like effector A (Cidea)*, and *Fatty acid elongase 3 (Elovl3)*, elevated levels of PGC-1 $\alpha$  and Fibronectin type III domain-containing protein 5 (FNDC5)/irisin, and an activation of the AMPK/Sirtuin 1 (SIRT1) pathway [33]. AMPK and Sirt1 are important sensors of the energy status that together with PGC-1 $\alpha$  regulate energy homeostasis and stimulate FNDC5/irisin expression, thus inducing beige adipogenesis [118]. The regulation of adipogenesis through the AMPK/SIRT1 pathway has also been described in HFD fed mice treated with maize extract rich in ferulic acid and anthocyanins [119].

In WAT, anthocyanins and anthocyanin-rich foods also improve the inflammatory profile. The administration of a black soybean testa extracts (BBT) to diet-induced obese mice decreased fat accumulation, and the expression of *Acc* and *C/ebp $\alpha$*  and increased the levels of lipolysis proteins such as lipoprotein lipase (LPL), hormone-sensitive lipase (HSL) in mesenteric fat but also showed anti-inflammatory effects [109]. Similar effects were observed in humans where the administration of BBT to overweight or obese individuals decreased the abdominal fat measured as waist and hip circumference and improved the lipid profile [110]. The anti-inflammatory effects have been also achieved with sweet cherry anthocyanins and blueberry (*Vaccinium ashei*) anthocyanins. These anthocyanins reduced the body weight gain, the size of adipocytes and the leptin secretion



in HFD-fed mice but also expression of *Il-6* and *Tnfa* genes, thus indicating an amelioration of the deleterious effects of a HFD [114,120].

Besides their effects on WAT, anthocyanins and anthocyanins-rich food also impact on BAT where they promote its activity. In high fructose/HFD-fed animals, besides inducing the browning of WAT, C3G attenuated the development of obesity by promoting the thermogenic capacity of BAT. C3G upregulated the expression of thermogenic markers such as *Ucp1*, induced the mitochondrial biogenesis and function and finally increased the EE [117]. In db/db mice, C3G and vanillic improved cold tolerance and enhanced BAT activity and induced mitochondrial biogenesis. In BAT, anthocyanin and anthocyanin-rich foods upregulated the expression of thermogenic markers (*Ucp1*, *Prdm16*, *Cidea*...), lipid metabolism (*Cpt1a*, *Hsl*, *adipose triglyceride lipase (Atgl)*), mitochondrial markers (*mitochondrial transcription factor A (Tfam)*, *Nuclear Respiratory Factor 1* and *2 (Nrf1* and *Nrf2)*...) and transcriptional regulators or coactivators of these processes (*Ppara*, *Pgc1β*, *Pgc1α*...) [73,115].

### 3.3. In the Central Nervous System (CNS) Anthocyanins Have Been Related to Neuroprotective Effects as Well as in Feeding Behavior

The neuroprotective activity of anthocyanins has been widely evidenced in several epidemiological studies and their potential for the prevention of many neurodegenerative diseases such as Parkinson's disease (PD) and Alzheimer's disease (AD) has been suggested [77,78]. The neuroprotective effects of anthocyanins and C3G correlate with the regulation of molecules upstream of nitric oxide (NO) production, neuroinflammatory response and oxidative stress [79,121–123].

It has been demonstrated that C3G and malvidin 3-O-glucoside (M3G) inhibited the hyperphosphorylation of Tau protein in Alzheimer's disease [124] and berries supplementation have shown neurocognitive benefits in older adults at risk for dementia with mild cognitive impairment [125]. Recent studies highlighted an anti-depressive effect of a maqui-berry extract in a mouse model of a post-stroke depression. In this case the maqui effects were associated to its antioxidant capacity [126]. Otherwise, anthocyanins extracted from dried fruits of *Lycium ruthenicum* Murr have demonstrated a protective role in cerebral ischemia/reperfusion injury in rats [127] by inhibiting cell apoptosis and reducing edema and inflammation.

Besides their role in neuroprotection, anthocyanins modulate the feeding behavior. In rats, anthocyanins from black soybean increase the expression of the gamma-aminobutyric acid B1 receptor (GABAB1R) and decrease the expression of neuropeptide Y (NPY) in the hypothalamus, thus modulating the food intake behavior/body weight control. The upregulation of GABAB1R is followed by a decrease of the activated protein kinase A (PKA) and the phosphorylated cAMP-response element binding protein (CREB), both located downstream of GABAR1 [83]. In a similar way, the administration of an anthocyanin-rich black soybean testa (*Glycine max* (L.) Merr.) to diet-induced obese mice decreased food intake [109].

## 4. Flavanols

Flavanols are present in cocoa, tea, red wine, beer and several fruits such as grapes, apricots, apples where they are responsible for their astringency [128]. Flavanols exist as monomers named catechins or as polymers named proanthocyanins. The monomeric forms include: catechin (–)-epicatechin (EC), (–)-epigallocatechin gallate (EGCG), (–)-epigallocatechin (EGC), and (–)-epicatechin gallate (ECC). The proanthocyanins, also known as tannins, are more complex structures (dimers, oligomers, and polymers of catechins) and can be transformed to anthocyanins [29]. Like other flavonoids, flavanols are absorbed between the small intestine and the colon depending on their physicochemical properties and structure [129].

Flavanols possess a health claim related to their role in maintaining the elasticity of blood vessels that was approved in 2014 by the European Food Safety Authority (EFSA) [130].

In humans and animal models, flavanols or flavanols-rich foods (mainly, cocoa or tea derivatives) have demonstrated the ability to reduce body weight, decrease waist circumference and fat percentages,



improve glucose metabolism in individuals with type 2 diabetes, obesity or MetS and increase energy expenditure [75,131–139]. One of the most described molecular mechanism underlying these effects are the activation of the AMPK enzyme [140].

Due to the high amount of publications including flavanols and metabolism we just included a representative group of the most recently published and the ones that deepen more on the molecular mechanisms underlying the beneficial effects of flavanols.

#### 4.1. Flavanols Improve Hepatic Steatosis and Glucose/Lipid Metabolism in Obesity Models

In humans and several rodent models of obesity, flavanols have been able to improve blood lipid profile and protect liver from excessive fat deposition and hepatic steatosis [136,141–146]. These effects have been related mostly with an activation of the AMPK and the protein kinase B (PKB/Akt) pathways that finally lead to the suppression of lipogenesis by modulating the expression of *Srebp1c*, *cAMP-response element-binding protein regulated transcription coactivator 2 (Crtc2)*, and *stearyl coenzyme A dehydrogenase-1 (Scd1)* or the activity of ACC, the inhibition of gluconeogenesis by affecting the levels of *Peck* and *G6pase* and the increment of FAO by increasing the *Cpt1a* levels. Moreover, flavanols are able to improve cholesterol homeostasis through the regulation of several enzymes from the cholesterol synthesis and bile acids metabolism apart from the modulation of the mRNA expression of apolipoprotein B100 and ATP-binding cassette transporter A1. Most of the approaches included have been done using tea extracts or cocoa flavanols but other extracts with a more diverse composition of flavonoids have been also described in this section [137,143,147–151].

Theabrownin from Pu-erh tea in combination with swinging improved serum lipid profile and prevented development of obesity and insulin resistance in rats fed a high-fat-sugar-salt diet and subjected to a 30-min daily swinging. A transcriptomic analysis in the liver indicated that theabrownin together with exercise activated circadian rhythm, PKA, AMPK, and insulin signaling pathway, increased the levels of cAMP and accelerated the consumption of sugar and fat [142]. Similar results were obtained with HFD-fed mice supplemented with Yunkang green tea and subjected to treadmill exercise. These animals showed a reduction in the body weight gain and liver weight, a lower level of blood glucose, serum total cholesterol (TC), TG, insulin and ALT and an improvement in the fatty liver and hepatic pro-inflammatory profile compared to HFD group. Supplemented and exercised-animals showed a downregulation of the lipid synthesis genes (*Srebp1c*, *Fasn*, *Acc*), and an improvement of the hepatic insulin signaling [143].

Furthermore, in obese Zucker rats fed with a HFD and treated with green tea polyphenols a significant reduction on fasting insulin, glucose and lipids and an improvement of the NAFLD were observed. Livers of treated rats had lower levels of alanine aminotransferase (ALT) and aspartate aminotransferase (AST), of inflammatory markers and of TG content and exhibited less lipid droplets. These improvements have been related to an activation of the AMPK pathway and the inhibition of the hepatic lipogenesis (higher levels of the inactive p-ACC and lower levels of SREBP1c) [152]. These effects on lipid metabolism were also observed after the administration of Benifuuki (a tea that contains methylated catechins such as epigallocatechin-3-O-(3-O-methyl) gallate (EGCG3'Me) to high fat/high sucrose diet-fed mice. Benifuuki treatment lowered the levels of TG and NEFA in serum and liver and reduced the expression of hepatic lipogenic genes (*Srebp-1c*, *Acc1*, *Fasn* and *Stearoyl-CoA desaturase 1(Scd1)*) [153]. In parallel the use of *Euterpe oleracea* Mart.-derived polyphenols, known by the popular name of açai and rich in catechin and polymeric proanthocyanins, when administered to HFD-fed mice [154] or a pistachio-diet supplementation to diet-induced obese mice exhibited similar impact on lipid metabolism and gene expression modulation [150].

Finally, Oliogonol, a flavanol-rich lychee fruit extract, significantly reduced hepatic lipid content (less lipid droplets and ballooning by downregulating the *Ppar $\gamma$*  and, *Srebp1c* mRNA levels [155] probably via the inhibition of the mTOR activity promoted by the activation of the AMPK enzyme [156]. Moreover, oligonol improved hepatic insulin sensitivity by reducing the phosphorylation of glycogen synthase kinase 3 $\alpha$  (GSK3 $\alpha$ ) and the phosphatase and tension homologue (PTEN) in HFD-induced

obese mice [155] as well as inhibiting the mTOR/S6K cascade. The activation of the mTOR/S6K phosphorylates and desensitizes the insulin receptor substrate 1 (IRS1) [157]. In a similar way, GC-(4→8)-GCG, a proanthocyanidin dimer from *Camellia ptilophylla* improved hepatic steatosis and hyperlipidemia in HFD-induced obese mice [158].

Besides on hepatic lipogenesis, tea extracts also impact in FAO. The administration of tea water extracts from green tea, yellow tea, white tea, black tea, raw pu-erh tea and oolong tea decreased TG and total cholesterol levels in serum and liver as well as the hepatic lipid content. Supplemented animals displayed less lipid droplets, the activation of the AMPK and the upregulation of the *Cpt1a* together with the inhibition of the FASN enzyme. These treatments also reduced the inflammation profile linked to HFD [149]. Similar results were obtained with grape seed procyanidin B2 (GSPB2) and a polyphenol extract from *Solanum nigrum* that contains among other different catechins. In db/db mice, GSPB2 decreased body weight and improved the lipid profile in serum (TG, total cholesterol and free fatty acids (FFA)) but also reduced hepatic lipid droplets and TG accumulation. The proposed mechanism implied the AMPK activation, the ACC phosphorylation and *Cpt1a* overexpression, thus inhibiting FA synthesis and increasing FAO [159]. In a similar way, the *Solanum nigrum* polyphenol extract inhibited lipogenesis and enhanced FAO (upregulation of *Cpt1a* and *Ppara*) through the AMPK cascade [151].

In different animal models of obesity and insulin resistance, EGCG has shown the capacity to improve glucose homeostasis, to inhibit gluconeogenesis, FA and cholesterol synthesis and to increase FAO [147,148]. In HFD and STZ-induced type 2 diabetes, EGCG downregulated *Pepck* and *G6Pase* and inhibited SREBP1c, FASN and ACC1. The mechanism underlying these effects is not yet well understood but it has been suggested that EGCG would activate the PXR/CAR-mediated phase II metabolism that through a direct or indirect mechanism would suppress gluconeogenesis and lipogenesis [147]. Moreover, in HFD Wistar rats, EGCG diminished the liver weight, the hepatic hyperlipidemia, animals showed less lipid droplets, reduced serum levels of ALT and AST, TG, total cholesterol and better profile of LDL/HDL but also an ameliorated oxidative stress. In this case, EGCG activated SIRT1, FoXO1 and regulate SREBP2 activity to suppress hepatic cholesterol synthesis. These data point out the downregulation of SREBP2 expression under the SIRT1/FOXO1 signaling pathway as a mechanism to reduce the cholesterol content [148]. Furthermore, EGCG also decreased bile acid reabsorption, which decreased the intestinal absorption of lipids [160]. In the same way, EC administered to a high-fat high cholesterol diet rats reduced serum levels of total cholesterol, LDL and TG while increased HDL [161]. Moreover, EC intake also reduced serum levels of ALT and AST enzymes, the lipid peroxidation and the pro-inflammatory cytokines levels, thus indicating an improvement in the liver functionality. The proposed mechanism of EC included the downregulation of the nuclear receptor liver-X-receptor (LXR), the FASN enzyme and the SIRT1 protein but also the blockade of the Insig-1-SREBP-SCAP pathway that drives the SREBP2 maturation [161].

#### 4.2. Flavanols in Adipose Tissue: Less Adiposity and More Energy Expenditure: The Browning Effect

In humans, some studies described the capacity of green tea to reduce body weight and abdominal fat accumulation [162,163], influence on the body fat mass index, waist circumference, total fat mass and energy expenditure through the induction of browning or BAT activity [164–166] but also to regulate ghrelin secretion and adiponectin levels, to control appetite and decrease nutrient absorption [135,167].

In rodents, the administration of grape seed-derived proanthocyanins to Wistar rats reduced the body weight by limiting food intake and activating EE in scWAT [168] and it has been widely described that in rodent models of obesity, flavanols are able to affect the lipid metabolism of WAT and BAT. Global effects of flavanols in adipose tissues lead to a decrease in adiposity, specially of the WAT depots and in adipocyte size by reducing adipogenesis, the release of adipokines such as leptin and resistin, the modulation of lipid metabolism and the induction of browning [153,155,158,169–174]. In BAT, flavanols caused the activation of thermogenesis and FAO [172–176].

As has been mentioned before, in WAT, flavanols modified lipid metabolism. EGCG reduced the expression of genes related with *de novo* lipogenesis (*Acc1*, *Fasn*, *Scd1*, *Cebpb*, *Pparγ* and *Sreb1c*),

increased the expression of genes involved in lipolysis (*Hsl*) and lipid oxidation (*Ppara*, *Acetyl-CoA oxidase (Acox)2*, and medium-chain acyl-CoA dehydrogenase (*Mcad*) in epididymal (eWAT) and scWAT and highly upregulated the expression of delta-9 desaturase, the enzyme responsible to convert saturated fatty acids to monounsaturated [177]. The activation of the AMPK in HFD-EGCG-treated mice indicated that at least in part the changes in lipid metabolism observed were due to the AMPK phosphorylation [177]. In scWAT, although EGCG increased lipolysis (*Hsl*) and FAO (*Cpt1a*) [168,178], some lipogenic genes (*Acc1*, *Fasn*, *Scd1*, *Pparγ*, and *Srebp1*) has been detected upregulated at the mRNA level but no at protein level [178]. These data suggested that EGCG might have different effects in scWAT and eWAT. Finally, pistachio-diet supplementation to diet-induced obese mice also ameliorated the HFD-induced expression of *Srebp1c*, *Pparγ*, and *Fatp* [150].

Besides its effects in the liver, the GC-(4→8)-GCG inhibited the expansion of all WAT depots in HFD fed mice. Adipocytes from eWAT were smaller and some of the main adipocyte-associated transcription markers were downregulated (*Srebp1c*, *Cebpa* and *Pparγ*), thus indicating a better WAT functionality [158]. The GC-(4→8)-GCG-supplemented mice showed an upregulation of the adiponectin and a downregulation of the leptin mRNA levels as well as an improved inflammatory profile with less macrophage infiltration [158].

Regarding the browning effect of flavanols it has been published that EC increased mitochondrial biogenesis, fatty acid metabolism and upregulated the expression of BAT-specific markers (*Prdm16*, *Dio2*, *Ucp1* and *Ucp2*) in WAT in a way that depends on phosphorylation and deacetylation cascades [170]. The authors demonstrated that EC supplementation upregulated the mitochondrial related proteins p-SIRT1, SIRT1, SIRT3, PGC1α, PPARγ, TFAM, NRF1, NRF2, complex II, IV and V and mitofilin [170]. In a similar way, a polyphenolic extract from green tea leaves (GTE) ameliorated the body weight gain caused by a HFD with no changes in calorie intake but reducing the adiposity and the adipocyte size in WAT and BAT. GTE supplementation induced BAT markers in scWAT (higher mRNA levels of *Pgc1α*, *Cbipp300-interacting transactivator 1 (Cited1)* and *Prdm16* and of UCP1 protein) and reduced HFD-induced whitening in BAT (lower expression of adipogenic markers *Cebpa* and *Ap2* and upregulation of *Pgc1α* and *vascular endothelial growth factor-A(165) (Vegfa165)*) [171]. These animals also showed an improvement in the inflammatory profile in scWAT and BAT. Finally, a Grape pomace extract (GPE) showed the capacity to induce browning (upregulation of *Pgc1α*, *Pparγ*, *Prdm16* and *Ucp1*) in the eWAT of HFD-fed rats [179,180].

Besides tea extracts also cacao components are able to induce browning and BAT activation. Concretely, theobromine alleviated diet-induced obesity in mice by inducing a brown-like phenotype in the iWAT and activated lipolysis and thermogenesis in BAT. In HFD fed mice theobromine inhibited phosphodiesterase-4 (PDE4D) activity in adipose tissue, thus increasing β3-adrenergic receptor (AR) signaling pathway and EE [172]. The inhibition of PDE increases the cellular levels of cAMP levels thus activating the β-AR cascade and finally PKA and UCP1 activity [181].

The capacity of flavanols on activating BAT has been described even with a single dose of a flavanol mixture that included catechins and B type procyanidins or by administering individual components by itself [182]. In these animals, *Ucp1* mRNA expression in BAT and levels of catecholamines in plasma were significantly increased via SNS stimulation but with varying efficacy depending on the stereochemical structure of flavanols [182]. It should be noted that prolonged ingestion of a catechin-rich beverage increased the BAT density with a decrease in extramyocellular lipids in humans [183]. EGCG-supplemented diet-induced obese mice exhibited higher body temperature and more mitochondrial DNA (mtDNA) content in BAT together with an upregulation of the genes related to fatty acid metabolism, thermogenesis and mitochondrial biogenesis (*Ucp1*, *Ucp2*, *Prdm16*, *Cpt1β*, *Pgc-1α*, *Nrf1*, and *Tfam*) [184,185] and a downregulation of *Acc*. These effects have been related to an increased activity of the AMPK in BAT [184].

Thermogenesis can also be induced by a polyphenol-rich green tea extract (PGTE) through a mechanism that depends on adiponectin signaling. The treatment with this extract reversed part of the obesity phenotype in WT mice but no in adiponectin KO mice (AdipoKO). PGTE treatment

increased EE, BAT thermogenesis, and promoted browning phenotype in the scWAT of WT mice but these effects were blunted in AdipoKO mice [176].

Some data regarding BAT activation by catechins in humans have also been described. Different approaches have been done to demonstrate the effects of green tea extract and caffeine over thermogenesis and body weight [186,187]. Short- and long-term effects have been studied with different results and effectiveness but suggesting that catechins and caffeine may act synergistically to control body weight and induce thermogenesis [175,188]. It has been proposed that the thermogenic response to green tea extracts or its components would be mediated, in BAT, by the direct stimulation of the  $\beta$ -adrenergic receptor ( $\beta$ -AR) cascade through the inhibition of the enzyme catechol-O-methyl transferase (COMT), which degrades catecholamines. On its side, caffeine inhibited PDE, thus inducing a sustained activation of the PKA and its downstream cascade [175].

#### 4.3. Flavanols Consumption Induces Energy Expenditure in Peripheral Organs through the Sympathetic Nervous System Activation

Part of the anti-obesity effects of flavanols have been also related to their influence on sympathetic nervous system (SNS) activity. The SNS activation by green tea catechins (GTC) has been associated to their capacity to inhibit COMT. The inhibition of COMT leads to a prolonged activation of the sympathetically-response and of the  $\beta$ -adrenergic cascade that produces cAMP and the activation of the PKA. Caffeine, in turn, is able to inhibit the PDE activity which drives to a sustained activation of the PKA and its downstream response [175]. Then, both effects act synergistically to increase EE, lipolysis and FAO as has been described in the above sections. Some other mechanisms to describe the anti-obesity effects of flavanols include the modulation of food intake. It has been demonstrated that grape-seed proanthocyanins extract (GSPE) reduced food intake in rats fed a cafeteria diet. These animals showed an activation of the STAT3 protein which upregulated the *pro-opiomelanocortin* (*Pomc*) expression, thus improving the leptin resistance [189].

Moreover, GSPE supplementation reduced the neuroinflammation and increased the expression of SIRT1 [189]. Flavanols has been described as active molecules against diet-induced neuroinflammation. The induction of neuroinflammation and cognitive impairment in rats by feeding them with a high salt and cholesterol diet (HSCD) could be in part reversed by the treatment with different doses of an enriched-tannins fraction of the Indian fruit *Emblica officinalis*. Treatment with this tannin-enriched gooseberry reversed the HSCD-induced behavioral and memory disturbances, neuronal cell death and reduced the levels of cognitive impairment markers. [190]. In the same way, it has been published that, in mice, EGCG attenuated the neuronal damage and insulin resistance caused by a high fat/high fructose diet (HF/HFD). In this case, EGCG upregulated the IRS-1/AKT and the extracellular-signal-regulated kinase (ERK)/CREB/Brain-derived neurotrophic factor (BDNF) signaling pathways. In longer nutritional interventions with the HF/HFD, EGCG was capable to inhibit the MAPK and NF- $\kappa$ B pathways, as well as the expression of inflammatory mediators, such as TNF- $\alpha$  to reverse the neuroinflammation [191]. Similar results were obtained with EGCG-HFD dietary supplementation. The authors demonstrated that EGCG ameliorated the HFD-induced obesity in part by attenuating hypothalamic inflammation through the inhibition of NF- $\kappa$ B and Signal transducer and activator of transcription 3 (STAT3) phosphorylation, as well as the expression and release of inflammatory cytokines, such as TNF- $\alpha$ , IL-6, and IL-1 $\beta$  [185].

Finally, EGCG alleviated part of the cognitive deficits in a mixed model of familial Alzheimer's disease (AD) and type 2 diabetes mellitus (T2DM). The AD mice model APP/PS1 fed with a HFD showed an improvement in peripheral parameters such as insulin sensitivity but also in central memory deficits when treated with EGCG. Synaptic markers and CREB phosphorylation were increased because of an amelioration in the unfolded protein response (UPR) activity via a downregulation of the activation factor 4 (ATF4) levels. Moreover, EGCG decreased brain amyloid  $\beta$  ( $A\beta$ ) production and plaque burden by increasing the levels of  $\alpha$ -secretase (ADAM10) and reduced the neuroinflammation

in these animals [192]. Finally, green tea extracts can modulate the redox status of the CNS in obese and lean rats [193].

## 5. Flavanones

Flavanones are a subfamily of flavonoids widely distributed in *citrus* fruits such as grape, tomatoes, and oranges and are the responsible of the bitter taste of their peel and of their juice. As other flavonoids, flavanones show strong health benefits due to its antioxidant activity but also exhibit antiviral, antimicrobial, antiatherogenic, anti-inflammatory antidiabetic and anti-obesity properties [45,48,75,194,195]. Flavanones are mainly found as aglycones or as glycosylated derivatives [196]. The most studied flavanones are hesperidin, naringenin but also eriodictiol, isosakuranetin and taxifolin.

Hesperidin and its aglycone, hesperetin are found in citrus fruits, such as limes and lemons, tomatoes and cherries and have demonstrated antidiabetic, neuroprotective, anti-allergic, anti-inflammatory anticarcinogenic besides their well-established antioxidant capacity [45,197]. Naringenin and its aglycone naringin are found to be more abundant in citrus fruits such as grapefruit orange, lemon but also in tomatoes. Naringenin and derivatives have been associated with beneficial effects in cardiovascular diseases, osteoporosis, cancer and have showed anti-inflammatory, antiatherogenic, lipid-lowering, neuroprotective, nephroprotective, hepatoprotective and antidiabetic properties [198,199].

### 5.1. Flavanones-Dietary Supplementation Ameliorates the NAFLD in Humans

Frequently, liver diseases are initiated by oxidative stress, inflammation and lipid accumulation that lead to an excessive production of extracellular matrix followed by a progression to fibrosis, cirrhosis and hepatocellular carcinoma [200]. In the last years, several studies have demonstrated the capacity of different flavanones to ameliorate liver diseases.

To analyze the positive effects of flavanones in liver different approaches have been used. Some authors worked with hepatic chemical-induced damage being the most used the streptozotocin injection to mice or rats [199,201]. Other authors induced liver damage with diet [199] or worked with genetically obese models. Although flavanones demonstrated positive effects in the different approaches, in this review we focused on the experimental approaches where the liver disease has been induced by diet or where genetically obese-models has been used. Experiments with naringenin, hesperidin and eriodictiol has been done to evaluate the impact of this flavanones' consumption in NAFLD or liver steatosis.

Naringenin has showed the capacity to restore the activities of liver hexokinase, PK, G6Pase and Fructose 1,6-bisphosphatase from rats fed a high fructose diet to levels similar to healthy non-diabetic animals [202]. In this animal model, naringenin also enhanced liver protein tyrosine kinase (PTK), while reduced protein tyrosine phosphatase (PTP) activity [202]. In addition, administration of naringenin to HF/HSD-fed rats increased the protein levels of PPAR $\alpha$ , CPT1a and UCP2 [203]. In a similar way, naringenin increased FAO and the AMPK activity in HFD fed mice where ameliorated the metabolic alterations caused by diet [204]. Similar results were obtained in high-fat/high-cholesterol (HFHC) fed Ldlr  $-/-$  mice. In lean Ldlr  $-/-$  mice, naringenin induced weight loss and reduce calorie intake, enhanced EE and increased hepatic FAO by upregulating *Pgc1 $\alpha$* , *Cpt1a* and *Hsl*, thus indicating that naringenin is also effective in non-obese models [195]. In HFD fed Ldlr  $-/-$ , naringenin increased FAO and reduced lipogenesis. Hepatic *Srebp1c* and *Acox1* mRNA levels were downregulated, while *Fgf21*, *Pgc1 $\alpha$* , and *Cpt1a* were upregulated by naringenin [205]. Later on, it was published that naringenin prevented obesity, hepatic steatosis, and glucose intolerance in an FGF21-independent way [206]. More recently, it has been described that in obese-mice naringin decreased hepatic liver content (TG and total cholesterol) and activated the AMPK enzyme resulting in reduced expression and protein levels of liver SREBP1C, SREBP2, but increased LDLR. Moreover, these mice showed reduced plasma

levels of proprotein convertase subtilisin/kexin type 9 (PCSK9), leptin, insulin, and LDL-C compared to obese non-treated mice [207].

Besides naringenin, naringin and hesperidin effects in liver have also been evaluated. Hesperidin and naringin supplementation in *db/db* and *ob/ob* mice regulated hepatic gluconeogenesis and glycolysis, as well as lipid metabolism [208]. Hesperidin stimulated PPAR $\gamma$ , increased the hepatic GK activity and glycogen concentration and reduced the hepatic levels of *Glut2* as well as increased the expression of *Glut4* in WAT [46,208,209]. Moreover, hesperidin prevented hepatic steatosis in western diet-fed rats by preventing the upregulation of lipogenesis-related genes *Srebp1*, and *Scd1* caused by Western diet and the downregulation of *Ppar $\alpha$*  and *Cpt1a* expression and CPT1a protein levels [210]. Most of these effects were blunted when hesperidin is combined with capsaicin [210].

In diet-induced obese mice treated with neohesperidin the expression and secretion of FGF21 and the activity of the AMPK/SIRT1/PGC-1 $\alpha$  axis were improved [211]. Treatment with neohesperidin improved the steatotic state (less and smaller lipid droplets), reversed the downregulation of hepatic *Ppar $\alpha$*  levels while increased the levels of the hepatic *Fgf21* expression and its plasma levels. Finally, neohesperidin treatment phosphorylated AMPK, resulting in a rise of the HFD-downregulated proteins SIRT1 and PGC1 $\alpha$  [211]. On its side, eriodyctiol has also demonstrated effects on diet-induced obesity. Diet-induced obese mice supplemented with eriodyctiol showed a reduction of hepatic TG, fatty acids and the size and number of lipid droplets accompanied with an increased fecal excretion of cholesterol and fatty acids [212]. It is worth to mention that eriodyctiol decreased the enzymatic activity of malic enzyme (ME), FASN, phosphatide phosphohydrolase (PAP) and downregulated the expression of *Srebp1c*, *Acc* and *Fasn* [212]. These data indicate that eriodyctiol improved the hepatic steatosis caused by a HFD by decreasing hepatic lipogenesis and increasing the hepatic FAO. On the other hand, alpinetin, an O-methylated flavanone, improved HFD-induced NAFLD via ameliorating oxidative stress, inflammatory response and lipid metabolism. Alpinetin decreased *Scd1*, *Fasn*, *Srebp1c*, *Lxra*, *Elovl2* and *Irs1* expressions, and increased PPAR $\alpha$  levels [213].

In humans a randomized placebo-controlled, double-blind clinical trial with NAFLD patients shown the effect of hesperidin supplementation [214]. Patients who follow healthy lifestyle habits and supplemented their diet with hesperidin have a significant reduction of ALT, glutamyl-transferase, total cholesterol, hepatic steatosis, C reactive protein and TNF $\alpha$ , proving the scope of hesperidin [214]. One of the possible mechanisms underlying the effects of flavanones on metabolism goes through the FGF21 and AMPK/Sirt1/PGC1 $\alpha$  signaling axis.

## 5.2. Flavanones Induce Browning in Adipose Tissue

As other flavonoids, flavanones can also modulate lipid metabolism in adipose tissue as well as induce browning in WAT, and activate in BAT [166] as well as reduce the characteristic obese-macrophage infiltration in adipose tissue [215].

In HFD fed mice, hesperetin supplementation on its side showed metabolic health effects in adipose tissue, concretely is able to reduce mesenteric adipose weight and decrease leptin levels [216]. In this case, lipid metabolism was not changed nor in liver nor in WAT. On the other hand, a characteristic of obesity is the recruitment of immune cells by adipose tissue that leads to metabolic disorders such as insulin resistance. In a short-term HFD mice model, naringenin can suppress neutrophil and macrophage infiltration into adipose tissue [215]. Concretely it can inhibit the expression of several chemokines like MCP-1 and MCP-3 [217]. Eriodyctiol (ED) supplementation on its side lowered the adiposity in diet-induced obese mice by regulating gene expression. ED-supplemented mice showed reduced weight of all the WAT depots but also a downregulated expression of adipocyte genes involved in lipid uptake (*Cd36*, and *Lpl*) and lipogenesis (*Srebp1*, *Acc*, and *Scd1*), an upregulation of the *Ucp1*, with no changes in FAO genes such as *Adrb3*, *Cpt2*, *Pgc1 $\alpha$* , *Pgc1 $\beta$* , and *Cox8b* genes [212].

Another beneficial effect of flavanones in adipose tissue is related to EE and thermogenesis. It has been demonstrated that in human white adipocytes and in scWAT a treatment with naringenin increased the expression of genes associated with thermogenesis and FAO, including *Atgl* and *Ucp1* as



well as *Pgc1 $\alpha$*  and *Pgc1 $\beta$*  that can mediate the PPAR $\delta$ -dependent transcriptional responses involved in mitochondrial biogenesis and uncoupling phenotype. Moreover, naringenin administration increased the expression of insulin sensitivity-related proteins such as *Glut4*, *adiponectin*, and *Ctneb1* [218]. These data indicate that naringenin may promote the conversion of human WAT to a brown/beige adipose tissue. Similarly, in HFD-obese mouse model, the induction of brown-like adipocyte formation on WAT was described by supplementing the diet with a flavanones-rich extract from *Citrus reticulata* [219]. The main phytochemical components of a water extraction of *Citrus reticulata* in were synephrine, narirutin, hesperidin, nobiletin, and tangeretin. Among flavanones, citrus also contain synephrine that is an alkaloid which binds to  $\beta_3$ AR in adipose tissue promoting lipolysis and thermogenesis [220]. Dietary supplementation with this citrus extract reduced body weight gain, epididymal fat weight, fasting blood glucose, serum levels of TG and total cholesterol, and lipid accumulation in liver and WAT as well as activated FAO and induced the browning phenotype [219]. These animals showed increased levels of *Ucp1* in the iWAT and an upregulation of *Prdm16*, *transmembrane protein 26 (Tmem26)*, *cluster of differentiation 137 (CD137)*, and *Cidea* [219].

In the same way it has been published that hesperidin induced browning in retroperitoneal WAT (rWAT) but not in iWAT of Western diet-fed rats. Hesperidin decreased the size of adipocytes and induced the formation of multilocular and positive-UCP1 and CIDEA brown-like adipocytes. Besides the induction browning, hesperidin also enhanced the expression of *Ucp1* in BAT [221]. In contrast, it has been recently published a study where not hesperidin but its monoglycosyl has the capacity to induce brown-like adipocyte formation in HFD-fed mice [222]. In this case,  $\alpha$ -monoglucosyl hesperidin increased EE and reduced body fat accumulation by stimulating the browning phenotype in the iWAT. iWAT adipocytes of supplemented mice exhibited a multilocular phenotype and were UCP1-positive cells. The iWAT of these animals also showed increased levels of COXIV. No effects were observed in BAT nor in other WAT depots [222].

In a human randomized double-blind placebo-controlled trial with moderate high BMI subjects, it's shown that glycosylated hesperidin decreased significantly abdominal and subcutaneous fat area when is supplemented with caffeine [223].

### 5.3. Flavanones Are Neuroprotective against Several CNS Injuries

There is low information about the effects of flavanones on CNS to combat obesity. It has been demonstrated that quercetin, naringenin and berberine can modulate glucose homeostasis in the brain of STZ-induced diabetic rats through the regulation of glucose transporters and other key components of insulin signaling pathway [224].

Most of the studies that show the neuroprotective role of flavanones have been performed using animal with CNS-induced injuries. In a rat model of global cerebral ischemia reperfusion (I/R), pinocembrin (a honey flavanone) exerted antioxidant, anti-inflammatory and anti-apoptotic effects. [225] as well as inhibited autophagy on the hippocampus [226]. Moreover, naringenin and eriodictiol exert effects in ischemic stroke, promoting cortical cell proliferation, inhibiting apoptosis and reducing oxidative stress in rodent models [227,228]. In a similar way, the induction of neurotoxicity by lipopolysaccharide (LPS) administration in mice can be ameliorated by the coadministration of hesperetin or naringenin that reduced the expression of inflammatory cytokines, attenuated the generation of reactive oxygen species/lipid peroxidation and enhanced the antioxidant capacity in CNS [229,230]. Furthermore, hesperetin enhanced synaptic integrity, cognition and memory processes by increasing the levels p-CREB, postsynaptic density protein-95 (PSD-95) and syntaxin proteins [229] and naringenin decreased the acetylcholinesterase (AChE) activity [230]. Other mental stresses such as social defeat stress, depression and autistic-like behaviors can also be counteract with flavanones in rodent models [231–233]. Hesperidin and naringenin have demonstrated positive effects by increasing the resilience through a reduction in the levels of interleukins and corticosterone thus suppressing the chronic inflammation caused by kynurenine pathway related to depression [234] and inhibiting the AChE activity, the oxidative stress as well as neuroinflammation [235].

## 6. Flavonols

Flavonols are widely distributed in plants and are present as minor compound in many polyphenol-rich foods. Their synthesis is stimulated by light and they accumulate in the skin of fruits and vegetables being absent in the flesh. The main dietetic flavonols are quercetin, kaempferol, isorhamnetin, fisetin, and myricetin [48,236,237].

Quercetin is found in capers, lovage (*Levisticum officinale*) apples, seeds of tomatoes, berries, red onions, grapes, cherries, broccoli, pepper, coriander, citrus fruits, fennel, flowers, leaves pepper and teas (*Camellia sinensis*) and it is the skeleton of other flavonoids, such as hesperidin, naringenin, and rutin. Rutin, rutoside or sophorin are the glycosylated form of quercetin and can be extracted from buckwheat, oranges, grapes, lemons, limes, peaches, and berries [238]. Kaempferol is abundant in apples, grapes, onions, tomatoes, teas, potatoes, beans, broccoli, spinaches, and some edible berries. Isorhamnetin is commonly found in medicinal plants such as ginko (*Ginkgo biloba*), sea-buckthorn (*Hippophae rhamnoides*) and *Oenanthe javanica*. Myricetin is found in teas, wines, berries, fruits and vegetables. Fisetin is abundant in apples, grapes, persimmon, cucumber, onions and strawberries. Finally, morin is present in *Prunus dulcis*, *Chlorophora tinctoria L.*, and fruits such as guava and figs [45].

As other groups of flavonoids, flavonols have shown healthy effects. They exhibit anticarcinogenic, anti-inflammatory, and antioxidant activities but also anti-obesity and antidiabetic properties in animal models and in humans where flavonols consumption has been associated to a lower risk of type 2 diabetes [43,236–243]. Some flavonols inhibited carbohydrate absorption thus lowering postprandial blood glucose mainly through the inhibition of the  $\alpha$ -glucosidase activity but also by inhibiting glucose transporters (GLUT2, SGLT1) or other enzymes such as maltase or saccharase [236]. Finally, a combination of quercetin and resveratrol have shown the capacity to reduce obesity in HFD-fed rats by modulating gut microbiota [244].

Due to the high number of publications and previous reviews [45,48,238], in the present work only the most recent data have been included.

### 6.1. Flavonols Exert Beneficial Effects on Lipid Steatosis by Regulating Lipid Metabolism, Inflammation and Oxidative Stress

Quercetin enhanced hepatic insulin sensitivity and reduced liver fat content and ameliorated hepatic steatosis [245]. Quercetin diminished the mRNA and protein levels of CD36 and MSR1, upregulated the levels of LC3II and downregulated p62 and mTOR thus suggesting an autophagy lysosomal degradation as the potential hepatoprotective mechanism of quercetin [245]. From another point of view the effects and mechanisms of quercetin against NAFLD were analyzed through a metabolomic approach [246]. Treatment with quercetin decreased AST and ALT levels in serum and reduced lipid droplets and hepatocyte swelling in rats fed a high fat/high sucrose diet. A metabolomic analysis indicated that quercetin modified fatty acid- inflammation- and oxidative stress-related metabolites among others. In this case, the effects of quercetin were more evident in 30-day NAFLD induction than in 50 days, thus indicating that dietary quercetin may be beneficial in early stages of NAFLD development [246]. Besides the effects of quercetin alone there are several studies where quercetin is used in combination with other compounds. The beneficial effects of quercetin in NAFLD development increased synergistically when quercetin is administered within benifuuki, a tea that contains EGCG. Both compounds administered to rats fed high fat/high cholesterol diet were more effective to downregulate *Fasn* and *Scd1* showing higher effects on their lipid-lowering effects alone [247]. In a similar way, the combination of quercetin with resveratrol ameliorated fatty liver in rats by improving the antioxidant capacity of the liver [248]. Finally, a combination of borage seed oil (as a source of linoleic (18:2n-6; LA) and gamma-linolenic (18:3n-6; GLA) acids and quercetin improved liver steatosis in obese rats [249].

On its side, isoquercetin (IQ), a glucoside derivative of quercetin has demonstrated beneficial effects in NAFLD by improving hepatic lipid accumulation via an AMPK dependent way in HFD-induced NAFLD rats [250]. Concretely, IQ treatment enhanced the phosphorylation of AMPK and ACC and



reversed the downregulation of liver kinase  $\beta$ 1 (LKB1) and Calcium/calmodulin-dependent protein kinase kinase-1 (CaMKK1) caused by HFD. The activation of AMPK modulated the expression of lipogenic and lipolytic genes, such as *Fasn*, *Srebp1c*, *Ppar $\gamma$*  and *Cpt1a*. Moreover, IQ supplementation upregulated PPAR $\alpha$  and downregulated nuclear factor- $\kappa$ B (NF- $\kappa$ B) protein levels [250].

As quercetin, kaempferol is also able to reduce lipid accumulation in liver of obese rodent models. In dyslipidemia-induced mice, kaempferol inhibited PKB (Akt) and SREBP-1 activities and blocked the Akt/mTOR pathway, thus inducing hepatic autophagy and decreasing hepatic lipid content [251]. Similarly, in ApoE deficient mice fed with a HFD, kaempferol attenuated metabolic syndrome via interacting with LXR receptors and inhibiting posttranslational activation of SREBP-1. Both effects contributed to the reduction of plasma and serum TG [252].

Other flavonols with positive effect in the liver are fisetin, dihydromyricetin or rutin. Obese rats fed with a high fat/high sucrose diet and supplemented with fisetin showed a decreased in body weight and hepatic lipid content as well as an improvement in the lipid profile (low levels of TG, total cholesterol, LDL) and liver functionality (reduced levels of ALT and AST). The hepatic nuclear receptor 4 $\alpha$  (HNF4 $\alpha$ ) has been pointed out as the key factor in the hepatic effects of fisetin. Fisetin upregulated *Hnf4a* gene expression, increased nuclear lipin-1 levels. Moreover, fisetin promoted FAO, diminished FASN activity, enhanced hepatic antioxidant capacity and decreased the hepatic poly (ADP-ribose) polymerase 1 (PARP1) activity, a DNA repair enzyme, and thioredoxin-interacting protein (TXNIP) that is important for maintaining the redox status [253]. Through the regulation of SIRT3 signaling, dihydromyricetin has shown the ability to ameliorate NAFLD in HFD-fed mice. Dihydromyricetin increased *Sirt3* expression via activation of the AMPK/PGC1 $\alpha$ /estrogen-related receptor  $\alpha$  (ERR $\alpha$ ) cascade thus improving mitochondrial capacity and restored redox homeostasis [254]. In a similar way, rutin lowered TG content and the abundance of lipid droplets in NAFLD-induced HFD fed mice. Rutin treatment restored the expression of *Ppara* and *Cpt1a* and *Cpt2*, while downregulated *Srebp-1c*, *diglyceride acyltransferase 1 and 2 (Dgat-1 and 2)* and *Acc*. These effects enhanced FAO and diminished lipid synthesis. In addition, rutin repressed the autophagy in the liver [255]. On its side, the rutin derivate, troxerutin (TRX), has also demonstrated effectiveness against metabolic disorders in a rat model of hereditary hypertriglyceridemia (HHTg) non-obese model of MetS [256]. The treatment with TRX lowered the levels of hepatic cholesterol and reduced the expression of cholesterol and lipid synthesis genes (*Hydroxymethylglutaryl-CoA reductase (Hmgcr)*, *Srebp2* and *Scd1*) as well as decreased lipoperoxidation and increased the activity of antioxidant enzymes [256]. Moreover, these animals exhibited higher levels of adiponectin in serum [256].

Besides the effects of flavonols by itself, flavonols-rich extracts have also been tested in fatty liver-associated diseases. A *Sicyos angulatus* extract that contains kaempferol as the main flavonol administered to a HFD-induced obese mice lowered plasma levels of ALT and AST and the hepatic lipid content. The *Sicyos angulatus* extract impacted on lipid metabolism by repressing the expression of genes related to fatty acid and TG synthesis (*Acc1*, *Fasn* *Scd1* and *Dgat*) and of the key transcription factors that regulate lipogenesis (*Srebp-1c* and *Ppar $\gamma$* ) [257]. Another source of kaempferol, quercetin and derivatives is Sanglan Tea (SLT), a Chinese medicine-based formulation consumed for the effective management of obesity-associated complications. It has been demonstrated that dietary SLT supplementation prevented body weight gain and fatty liver and ameliorated insulin resistance in HFD-induced obese mice. SLT improved the serum lipid profile (lower levels of TG, Total cholesterol and LDL) and reduced the ALT and AST circulating levels. The liver of these animals displayed less lipid droplets and a downregulation of the lipogenic genes (*Lxra*, *Fasn*, *Acacb*, *Srebf-1*, and *Scd1*) and the adipogenesis-related genes (*Ppar $\gamma$* , *Clebp $\alpha$*  and *Ap2*) that are induced under HFD [258].

In a similar way, the flower of *Prunus persica* commonly known as peach blossom has demonstrated that capacity to reduce body weight, abdominal fat mass, serum glucose, ALT, AST, and liver and spleen weights compared to a HFD fed mice. This flower is rich in flavonoids and phenolic phytochemicals with chlorogenic acid, kaempferol, quercetin and its derivatives as its major compounds. The supplementation with this flower suppressed hepatic expression of lipogenic genes (*Scd1*, *Scd2*,

*Fasn*) and increased the mRNA levels of FAO genes (*Cpt1a*), thus modifying the lipid metabolism in HFD-fed mice [259]. Furthermore, a mulberry leaf powder also showed effects on liver gene expression in a mice model of hepatic steatosis induced by a western diet. Liver weight, plasma TG and liver enzymes ALT and AST were reduced in treated-animals. A global hepatic gene expression analysis revealed that supplemented mice displayed a downregulation in inflammation-related genes and an upregulation in liver regeneration-related genes [260]. Finally, a 70% ethanol extract from leaves of *Moringa oleifera* (MO) that contains different flavonols and flavones such as quercetin and kaempferol and their derivatives, reduced glucose and insulin but also the total cholesterol, TG and LDL serum and increased the HDL in high-fat diet obese rats as well as downregulated hepatic expression of *Fasn* and *Hmgcr* [261].

Through a network pharmacological approach Nie et al. [262] highlighted that Chaihu shugan powder (CSP) may exert its beneficial effects against NAFLD through the interaction of its main compounds with nuclear receptors. Through a molecular docking approach, they screened PPAR $\gamma$ , FXR, PPAR $\alpha$ , RAR $\alpha$  and PPAR $\delta$  and quercetin, kaempferol, naringenin, isorhamnetin and nobiletin interactions. To confirm the results of docking, an in vivo approach was done using NAFLD-induced rats. The NAFLD-induced rats treated with CSP exhibited ameliorated effects in body weight, hepatic histopathology and serum and liver lipids. Moreover, the mRNA levels of *Ppar $\gamma$* , *FXR*, *Ppara* and *Rara* were modified suggesting nuclear receptors regulation as a potential molecular mechanism underlying the effects of CSP [262].

Adiponectin signaling and AMPK activation have been also pointed out as possible mechanisms underlying the effects of flavonols in the liver. An extract of black soybean leaves (EBL), which mainly contains quercetin glycosides and isorhamnetin glycosides was administered to HFD-fed mice. EBL supplementation reduced body weight, fasting glucose, TG, total cholesterol and non-esterified fatty acid levels as well as hepatic steatosis. EBL supplementation increased the levels of adiponectin and the expression of adiponectin-receptors in the liver (AdipoR1 and AdipoR2) thus restoring adiponectin signaling pathway [263]. Downstream of the adiponectin signaling there is the activation of AMPK and FAO, the suppression of fatty acid synthesis and the improvement of insulin signaling [264]. Moreover, the mRNA levels of *Pgc1*, *Ppara*, *Ppar $\delta$* , *Ppar $\gamma$* , *Acc*, *Fasn*, *Cpt1a*, *Glut2*, *FoxO1* and *Irs1* were partially or totally normalized in HFD-EBL-supplemented animals [263].

Finally, it has been described that part of the mechanisms involving the hepatic beneficial effects of flavonols may be mediated by gut microbiota. An experimental approach of gut microbiota transplantation revealed a gut–liver axis where the *Akkermansia* genus have a key role on the quercetin protecting effects against obesity-associated NAFLD development. [247]. In a similar way, kaempferol blunted part of the effects of HFD in gut microbiota diversity. HFD fed mice displayed a reduced microbial diversity that it is mostly reversed by kaempferol [265]. Furthermore, IQ combined with inulin attenuated weight gain, improved glucose tolerance and insulin sensitivity and reduced lipid accumulation in the liver, adipocyte hypertrophy in WAT and diminished the circulating levels of leptin in HFD-fed mice probably through the modulation of gut microbiota [266].

## 6.2. Flavonols Impact on WAT Where They Modulate Lipid Metabolism and Induce Browning

Several studies with animal models showed that flavonols can protect mice or rats from HFD obesity by reducing body weight gain and lipid accumulation in WAT via reducing inflammation, modifying lipid metabolism, increasing EE, inducing browning of WAT and activating BAT [174,242,267–269].

Quercetin and quercetin-rich red onion (ROE) ameliorated diet-induced WAT expansion and inflammation in HFD-fed mice [270]. Quercetin and ROE ameliorated adipocyte size and number compared to HFD fed mice in WAT depots and induced a multilocular phenotype typical of BAT [270]. Moreover, quercetin and ROE diminished the HFD-increased levels of leptin. Besides its impact on adipose tissue phenotype, quercetin and ROE supplementation also attenuated the inflammatory profile induced by HFD in WAT [270]. Similarly, a quercetin-rich supplement administered to diet-induced obese rats decreased body fat and adipocyte size of the perirenal WAT as well as increased adiponectin

circulating levels [271]. Quercetin-rich supplement attenuated the upregulation of genes related to lipid synthesis such as *Acc*, *Fasn*, *HMG-CoA reductase*, *Lpl*, *Ap2*, and *Fatty acid transporter protein 1 (Fatp1)* caused by HFD; and upregulated the HFD-downregulated genes such as *Atgl*, *Hsl*, *Ampk*, *Acox*, *Ppara*, and *Cpt1a* [271]. In diet-induced obese mice quercetin administration decreased plasma TG levels without affecting food intake, body composition, or EE [272]. Quercetin enhanced the uptake of [<sup>3</sup>H]-oleate derived from labeled lipoprotein-like particles in the scWAT [272]. On the other side Perdicaro et al. demonstrated that quercetin attenuated adipose tissue hypertrophy, reduced the adipocyte size but activated the adipogenesis in HFD-fed rats. Quercetin supplemented rats showed increased levels of angiogenic (*Vascular endothelial growth factor 1 and 2 (Vegf1, Vegf2)*) and adipogenic (*Pparg* and *C/ebpa*) markers but also mitigated inflammation, and reticulum stress [273].

Together with their capacity to modulate lipid metabolism, flavonols are also able to induce browning in WAT depots. Quercetin treatment increased the expression of *Ucp1*, *Pgc1α* and *Elovl3* in WAT [272,274]. In a similar way, the administration of onion peel extract (rich in quercetin) to HFD-fed mice upregulated markers of BAT (*Prdm16*, *Pgc1α*, *Ucp1*, *Fgf21*, *Cidea*) in perirenal and scWAT [275]. It has been described that the induction of browning was mediated at least in part through the activation of the AMPK and the SIRT1 or via sympathetic stimulation. The quercetin-supplemented HFD-fed mice displayed higher levels of plasma norepinephrine and of PKA protein levels in scWAT [274]. Besides the activation of PKA signaling, it has been described that quercetin also increased SIRT1 protein levels and pAMPK in visceral WAT [276]. Although most of the studies showed positive effects of quercetin, this flavonol did not induce significant effects on the adipose tissue weights of rats fed an obesogenic diet except when combined with resveratrol (RSV). The treatment with quercetin and RSV but not with just quercetin or RSV promoted multilocular UCP1-positive adipocytes that also displayed increased levels of browning markers (*Cidea*, *bone morphogenic protein 4 (Bmp4)*, *Homeobox C9 (Hoxc9)*, *Solute Carrier Family 27 Member 1 (Slc27a1)*, *Tmem26* and *proton/amino acid symporter (Pat2)*) and genes related to catabolic pathways (*Atgl* and *ATP synthase subunit delta (Atp5d)*) in perirenal WAT. Regarding BAT, the supplementation with RSV and quercetin upregulated *Cidea* and *Ucp1* expression, thus indicating more thermogenic capacity in this tissue [277].

It is worth to mention that quercetin effectiveness is specie dependent. Studies in rats usually showed more effects than in mice whilst in humans the results are still unclear. In rodent models the levels of quercetin reached after its administration are higher than in humans [269]. Similar to quercetin, isoquercetin (IQ), a quercetin glycoside with greater bioavailability than quercetin, also exerts positive effects in WAT. In normal diet-fed mice IQ supplementation decreased WAT weight and increased pAMPK levels in WAT as well as in liver and muscle. Moreover, IQ reduced the expression of *Pparγ*, *C/ebpa*, *C/ebpβ* and *Srebp1* whilst increased the expression of *Ucp2*, *Pgc1α*, *Prdm16*, *Sirt1* and *Cpt1a* in WAT, suggesting less adipogenesis, enhanced FAO and browning [278].

On its side, rutin administration to db/db mice and diet-induced mice reduced body weight gain and improved adiposity (smaller lipid droplets) mainly by increasing EE [279]. These animals exhibited higher core temperature when submitted to a cold environment indicating enhanced BAT activity. Rutin-treated animals overexpressed BAT markers (*Ucp1*, *Cidea*, *Prdm16*), FAO-related genes (*Cpt1a*, *Mcad*, *Pparα* and *Pgc1α*), mitochondrial biogenic transcription factors (*tfam*, *Nrf1*, *Nrf2*) and more copies of mitochondrial DNA in BAT [279]. Besides BAT, rutin also affected scWAT, where induces browning (upregulation of BAT-specific genes, including *Ucp1*, *Pgc1α*, *Pgc1β*, *Cpt1a*, *Ppara*, *Tfam*, *Nrf1* and *Nrf2*...) [279]. The molecular mechanism underlying these effects may go through the Sirt1 activation. It has been demonstrated that rutin was able to directly bind to Sirt1 protein and activate the SIRT/PGC1α/NRF2/Tfam signaling pathway [279]. On the other hand, rutin combined with exercise (treadmill running) in diet-induced obese mice increased the mRNA levels of *adiponectin*, the protein levels of PPARγ, the binding immunoglobulin protein (BIP), and the phosphorylated form of c-Jun terminal kinase (JNK) and reduced disulfide-bond A oxidoreductase-like protein (DsbA-L). These profile indicated an improvement on the ER stress and on adipose tissue functionality [280].

When instead of flavonols, plant extracts were used similar effects were observed. A 70% ethanol extract of *Moringa oleifera* (MO) that mainly contains quercetin, kaempferol and their derivatives induced the expression of *Glut4*, *adiponectin*, *omentin* and upregulated *Ppara* and *melanocortin-4 receptor* (MC4R) on the WAT of diet-induced obese rats. [261]. *Cuscuta pedicellata* and some of its isolated compounds, including kaempferol, quercetin and some derivatives were suggested to have an anti-obesity effect in HFD-fed rats. Supplemented animals showed a reduction in HOMA-IR and oxidative stress as well as exhibited an upregulation of *Ucp1* and *Cpt1a* expression in BAT [281]. Finally, through a high-throughput metabolomic approach it has been described that the consumption of a hawthorn ethanol extract that contains chlorogenic acid, hyperoside, isoquercetin, rutin, vitexin, quercetin, and apigenin affected several metabolic pathways including: fatty acid biosynthesis, galactose metabolism, biosynthesis of unsaturated fatty acids, arginine and proline metabolism, alanine, aspartate and glutamate metabolism, glycerolipid metabolism and steroid biosynthesis [282].

### 6.3. Flavonols: Neuroprotection in Neurodegenerative Diseases

Flavonols have shown neuroprotective effects in neurodegenerative diseases. Quercetin, rutin and some other flavonols have exhibited positive effects against pathologies such as Alzheimer's Disease (AD), Parkinson's disease, Huntington's Disease, multiple sclerosis, brain ischemic injury, epilepsy neurotoxins but also for aging cognitive alterations [238,283–288]. Furthermore, flavonols have also demonstrated beneficial effects in the CNS alterations caused by HFD.

It is well-known that HFD induces oxidative stress in brain that may lead to neurodegenerative diseases. In HFD-fed mice, quercetin ameliorated the cognitive and memory impairment and enhanced the expression of *phosphatidylinositol-4,5-bisphosphate 3-kinase* (PI3K), *PKB/Akt*, *Creb*, and *brain-derived neurotrophic factor* (*Bdnf*) [289]. In a similar way, in HFD-fed mice, *Acer okamotoanum* and its main bioactive compound isoquercetin improved cognitive function by inhibiting the ROS production, the lipid peroxidation and nitric oxide formation, thus reducing oxidative stress [290]. Furthermore, it has been described that obesity induces hypothalamic inflammation and activates microglia. In diet-induced obese mice, quercetin supplementation reduced the levels of inflammatory cytokines and microglia activation markers in the hypothalamus [291]. Quercetin has also showed positive effects in streptozotocin (STZ)-induced AD rats where improved memory impairment and the anxiogenic-like behavior induced by STZ. In these rats, quercetin prevented the acetylcholinesterase (AChE) overactivity and the increased malondialdehyde levels caused by STZ [292]. Finally, quercetin showed capacity to modulate several kinases signaling cascades involved in synaptic plasticity such as the PI3K/Akt, protein kinase C (PKC) and mitogen-activated protein kinase (MAPK) [293].

## 7. Isoflavones

Isoflavones, also known as phytoestrogens, are flavonoids with a limited distribution in plant kingdom. They are found in leguminous plants such as soybean, kudzu, red clover, fava beans, alfalfa, chickpeas or peanuts but also soy-based foods (tofu, soymilk, miso . . . ) and some pants such the *Puerariae* genus [42,294]. Genistein and daidzein are the most representative dietary isoflavones.

Although there are several human clinical studies studying soy isoflavone consumption and diabetes the data obtained are not conclusive. Some evidence suggests that long-term intake of isoflavones may improve insulin resistance in type 2 diabetic patients and have anti-obesity effects [295–299]. In animal studies, isoflavones have showed antidiabetic and anti-obesity activities [45,236,297,300]. The beneficial effects of isoflavones include the improvement of insulin sensitivity, lipid profile and adiposity [45,49,301–303].

### 7.1. Isoflavones Reduced H Steatosis by Modulating Lipid Metabolism

Like many of the other flavonoids, isoflavones also exert an hepatoprotective action [49]. A recent publication using data of the National Health and Nutrition Examination Survey from 1999 to 2010 in

the USA describes an inverse correlation between urinary genistein levels and serum ALT levels in males but not in females [304]. On the other hand, in NAFLD-rodent models, genistein supplementation decreased fat accumulation, inflammation, hepatic steatosis and liver fibrosis in animal models and in humans [302]. These effects on hepatic steatosis have been described both in short- and long-term interventions [305].

One of the mechanisms proposed is the blockade of aldose reductase (AR)/polyol pathway. It has been described that some isoflavones are AR inhibitors. The inhibition of the AR/polyol pathway reduces fructose production and hepatic fat accumulation in high glucose diets as well as improved PPAR $\alpha$  activity and enhanced FAO, thus attenuating liver steatosis in HFD-obese models [306]. Moreover, the blockade of AR/polyol pathway reduced the CYP2E1-mediated oxidative stress [306]. Other mechanism suggested for isoflavones is the downregulation of PPAR $\gamma$  and fat-specific protein 27 (FSP27) together with a reduction of fatty acid synthesis and increased lipolysis [307]. This mechanism was described in female rats fed with a 20% casein-diet and supplemented with soy isoflavones [307].

Effects via the activation of AMPK has been also described for genistein [308,309]. Hepatic activation of AMPK drives to an inhibition of cholesterol and fatty acid synthesis and an enhancement of FAO [310]. In high fat/high sucrose-fed rats, genistein improved lipid metabolism and ameliorated hepatic lipid accumulation. P-AMPK and p-ACC were increased while SREBP1 protein levels were decreased. Moreover, genistein downregulated the expression of *Fasn*, *glycerol-3-phosphate acyltransferase (Gpat)* as well as upregulated *Ppara*, *Cpi1a* and *Acox* [309]. A similar effect on NAFLD has been described with Puerarin, a major bioactive isoflavone compound isolated from the roots of the *Pueraria lobata*. Puerarin attenuated NAFLD development in high fat/high sucrose-fed mice via the activation of the Poly(ADP-ribose) polymerase 1 (PARP-1)/PI3K/Akt signaling pathway and lately the improvement of the mitochondrial function [311]. In HFD-obese mice, puerarin reduced TG, total cholesterol and leptin serum levels as well as decreased the hepatic lipid content. Puerarin inactivated FASN and activated AMPK, CPT and HSL as well as increased the protein levels of PPAR $\gamma$ . These data indicated that puerarin regulated lipid metabolism by reducing lipid synthesis and enhancing lipid consumption [312].

Positive effects on NAFLD has been also observed by combining soluble soybean polysaccharides and genistein. This combination increased the bioavailability of genistein and administered to HFD-fed mice prevented weight gain, oxidative stress inflammation and dyslipidemia. These effects on lipid profile have been related to an activation of AMPK and PPAR $\alpha$ /PPAR $\gamma$  pathways and changes in the mRNA levels of *Fasn*, *Acc*, *Srebp1c* and *adipose differentiation-related protein (Adrp)* [313].

Besides genistein some of its derivatives are also active. Sophoricoside, a genistein derivate isolated from the *Sophora japonica* L, has been tested in high fructose-fed mice. Administration of sophoricoside diminished body and liver weight as well as reduced hepatic cholesterol and TG and serum levels of ALT, AST and LDL whilst increased the levels of circulating HDL. Moreover, the livers of treated-mice displayed a better inflammatory profile and an increased antioxidant capacity [314]. Calycosin, an o-methylated isoflavone showed positive effects against NAFLD-induced in HFD-fed mice. Calycosin improved insulin sensitivity, decreased the levels of ALT and AST and increased the levels of adiponectin. In the liver, calycosin blocked gluconeogenesis and lipogenesis by suppressing PEPCK G6Pase, SREBP1c and FASN, as well as induced the expression of *Gsk3 $\beta$* , *Glut4*, increased the phosphorylation of Irs1 and Irs2 and activated farnesoid X receptor (FXR) [315].

Similar to isolated compounds, soy isoflavones (that includes genistein, daidzein and glycitein) or a soy protein preparation also reverted hepatic steatosis when administered to obese female Zucker or HFD-obese rats. Soy isoflavones reduced hepatic lipid accumulation, improved serum levels of ALT and downregulated *Srebp1c* and *Fasn* levels as well as increased the protein levels of PPAR $\alpha$  indicating less lipogenesis and more FAO [316]. In a similar way, the intake of soy protein with isoflavones decreased the liver steatosis, reduced the levels of AST and ALT and increased the levels of leptin in female Zucker obese rats [305].

Apart from the effects of isoflavones on lipid metabolism they also exhibit anti-inflammatory properties. Genistein protected against NAFLD by targeting the arachidonic acid cascade that is responsible for the chronic inflammation [317]. Genistein supplementation to HFD-fed mice blocked the synthesis of cyclooxygenase-1 activity and thromboxane A2 [317]. Other mechanism to explain the anti-inflammatory effect of genistein is the promotion of miR-451 [318]. In humans a randomized controlled trial described that genistein supplementation improved the inflammatory state in NAFLD patients [319].

### 7.2. Isoflavones Ameliorate the Weight Gain in Diet-Induced Obesity Models and Improve Lipid Metabolism in Adipose Tissue

It has been widely described that isoflavones are able to control food satiety and appetite, to ameliorate the body weight gain and fat accumulation in rodent models of obesity, to modulate fatty acid metabolism and to induce browning and BAT activation which make its use in nutritional interventions as a promising approach for weight management therapies [269]. Isoflavones reach and affect adipose tissue as it was demonstrated through a whole-transcriptome microarray analysis of the perigonadal WAT from mice fed either control diet or a soybean extract diet containing a genistein/daidzein mix. This study described the impact of soy isoflavones on adipose tissue describing 437 downregulated genes and 546 upregulated [320].

In HFD-fed rats, soy isoflavones attenuated diet-induced obesity mainly by reducing the visceral WAT depot (lower hypertrophy and less lipid accumulation). Soy isoflavones supplementation downregulated fat synthesis (reduced SREBP1 protein levels) and upregulated lipolysis (increased ATGL protein levels) in visceral WAT via the activation of AMPK and the inhibition of SREBP1 [321]. In a similar way, 6,8-diprenylgenistein (DPG), a major isoflavone of *Cudrania tricuspidata* fruits decreased the body weight of HFD-induced obese mice at least in part by the suppression of de novo lipogenesis via the AMPK activation [322]. This isoflavone reduced the expression of lipogenic genes by regulating Ppar $\gamma$  and C/EBP $\alpha$  transcriptional activity as well as leptin and adiponectin levels. DPG also regulated ACC and HMGCR [322].

Isoflavones are also present in fermented soy products. The healthy properties of these products have been also evaluated. Fermented soybean meal (SBM) administered to HFD-fed rats showed positive effects on the obese profile of these animals. The body weight gain, as well as weights of abdominal and epididymal fat were reduced. Also, the lipid profile was improved. Supplemented rats exhibited lower levels of TG, total cholesterol and LDL and higher levels of HDL compared to HFD-non supplemented rats. Moreover, in WAT, there were a decrease on the hepatic lipogenesis (downregulation of *Fasn* and *Acc*) and an increase on lipolysis (upregulation of *Lpl*) [323].

Besides their effects on lipid metabolism, isoflavones also induce browning and BAT activation [166]. Genistein administration to HFD-fed mice reduced body weight gain and scWAT mass and induced the expression of *Ucp1* and *Cidea* in WAT, indicating a browning phenotype [324]. Genistein may induce the browning phenotype by a direct upregulation of *Ucp1* expression or through an indirect pathway that would imply irisin signaling. Irisin is a myokine that induces the expression of *Ucp1* and *Tmem26* in preadipocytes [325]. This indirect mechanism describes an induction of the PGC-1 $\alpha$ /FNDC5 pathway in skeletal muscle that lead to an increase of irisin production and secretion [325].

Formononetin and puerarin also modulate adipogenesis and thermogenesis. Formononetin attenuated visceral fat accumulation and increased EE in HFD-fed mice [326,327]. In vitro, this isoflavone downregulated Ppar $\gamma$ , C/ebp $\alpha$  and Srebp1 probably via AMPK/ $\beta$ -catenin signal transduction pathway that drove its antiadipogenic effect [326]. Moreover, formononetin induced *Ucp1* expression in primary culture of mouse adipocytes [327]. In a similar way, *Puerariae lobata* root extracts (PLR) activated browning in iWAT and regulated BAT activity [328]. PLR treatment caused weight loss and improved glucose metabolism in diet-induced obese mice as well as increased EE. In BAT, PLR upregulated *Ucp1* expression (but no other thermogenic markers) and in iWAT



induced the expression of BAT markers (*Ucp1*, *Ppary1*, *Ppary2* and *Ppara*), thus indicating a brown-like phenotype [328].

Several studies focused on describing the mechanisms underlying the isoflavones' effects have been performed in ovariectomized mice or rats. These models mimic menopausal stage in humans and are useful to analyze the potential role of isoflavones to counteract the increase of the adipose tissue that takes place during this period of life. In these rodent models, isoflavones exert positive effects on body weight gain and food intake as well as in fat pads enlargement [297]. In HFD-fed ovariectomized rats the administration of genistein decreased the body weight gain, improved insulin sensitivity and reduced plasma TG and cholesterol [329]. In liver, genistein blocked the lipogenic pathway by inhibiting p-ACC, SREBP-1, FASN and CD36 proteins. In retroperitoneal WAT, genistein diminished adiposity and adipocyte hypertrophy, inflammatory phenotype and induced browning. In iWAT, genistein-supplemented rats exhibited higher levels of UCPI, PRDM16, PGC-1 $\alpha$  and CIDEA proteins and *Ppargc1a* and *Ucp-1* mRNAs [329]. Furthermore, isoflavones supplementation can modulate the metabolic effects of estradiol treatments in ovariectomized rats [330]. Finally, calycosin has demonstrated positive effects perivascular adipose tissue of obese mice. Through the adiponectin/AMPK/endothelial nitric oxide synthase (eNOS) pathway, calycosin is able to restore at least in part the perivascular adipose tissue functionality [331].

### 7.3. Isoflavones Have Become Engaging Flavonoids in Neuronal Diseases due to Their Estrogenic-Like Structure and Its High Antioxidant Capacity

Obesity is a risk factor for neurodegenerative diseases essentially because it causes the neuroinflammation and oxidative stress. Isoflavones can ameliorate part of these effects as well as affect food intake and feeding behavior.

It has been described that daidzein administered to HFD-fed rats reduced food intake and attenuated body weight gain as well as improved glucose tolerance, adiponectin and leptin levels and increased the 17 $\beta$ -estradiol. In rat hippocampus, daidzein enhanced cell proliferation and reduced apoptosis and gliosis, thus exerting a neuroprotective effect against the brain injuries caused by diet [332]. On the other side, doenjang, a Korean traditional fermented soybean pastry alleviated hippocampal neuronal loss and enhanced cell proliferation in HFD-fed mice as well as reduced oxidative stress markers (less oxidative metabolites and lower levels of oxidative stress- and neuroinflammation-related genes). Dietary doenjang reduced A $\beta$  and tau phosphorylation [333]. Furthermore, genistein has shown the capacity to improve metabolism and induce browning via hypothalamus gene expression regulation. Through a transcriptome analysis it was identified that the hypothalamic expression of *urocortin 3 (Ucn3)*, *decidual protein induced by progesterone (Depp)*, and *stanniocalcin1 (Stc1)* correlated with the browning markers in WAT and with insulin sensitivity [324].

Regarding neurodegenerative diseases isoflavones have shown protective properties. An extract of soybean isoflavone reduced the elevated oxidative stress parameters and reversed the overproduction of A $\beta$  in rats with colchicine-induced neuronal damage [334]. In the same way, daidzein alone or mixed with genistein and glycitin isoflavones could reverse the cognitive impairments produced by scopolamine injection by activating the cholinergic system and the BDNF/ERK/CREB signaling pathway in mice [335,336], thus reinforcing the idea that soy isoflavones may be a good candidate for the treatment of neurodegenerative diseases. Besides the BDNF/ERK/CREB signaling pathway, it has been postulated that the Nrf2 signaling pathway can also be underlying the neuroprotective effects of isoflavones [337].

## 8. Flavones

Flavones is one of the largest groups of flavonoids with a high degree of chemical diversity. Some of the richest sources of flavones are parsley, celery, peppermint, and sage, which predominantly contain apigenin and luteolin as well as maize and citrus fruits. In general, flavones are found as glucosides in citrus fruits, vegetables, herbs and grains and although they represent a small fraction of

the total flavonoid intake, they have shown health effects and anti-obesity properties [338,339]. As it is going to be described later, most of the studies that investigate the beneficial effects of flavones use them as aglycone and a scarce number of approaches deepen on the effects of flavones when consumed within the whole food and a feasible doses or in combination with other bioactive compounds.

### 8.1. Flavones Improved Liver Steatosis and Hepatic Inflammation

Flavones such as apigenin, luteolin, baicalin, vitexin, nobiletin among others prevented NAFLD and hepatic steatosis mainly by modulating lipid metabolism (increasing FAO and decreasing lipogenesis) and reducing oxidative stress and inflammation [340–345].

As many other flavonoids, some flavones also exert their hepatic effects by activating the AMPK enzyme. Vitexin, an apigenin flavone glucoside, for instance, when administered to HFD-fed mice reduced body and liver weight, triglyceride and cholesterol content in serum and liver and circulating levels of ALT and AST. Moreover, vitexin regulated lipid metabolism suppressing de novo lipogenesis by downregulating the expression of *Ppar $\gamma$* , *Cletpa*, *Srebp1c*, *Fasn*, and *Acc* and enhancing FAO and lipolysis by increasing the expression of *Ppara*, *Cpt1a* and *Atgl* in an AMPK-dependent way that has been suggested may be activated by the binding of vitexin to the Leptin receptor [345].

In a similar way, luteolin, the principal yellow dye compound from *Reseda luteola*, or luteolin-enriched artichoke leaf extract alleviated hepatic alterations caused by a HFD by exerting anti-inflammatory activities and modulating lipid metabolism. Luteolin treatment of HFD-fed mice reduced hepatic lipotoxicity by improving the inflammatory profile, decreasing the extracellular matrix, enhancing the antioxidant capacity of the liver and increasing the FFA flux between liver and WAT [346]. A crosstalk between adipose tissue and liver has been suggested to explain the effects of luteolin on hepatic steatosis [347]. Moreover, luteolin and luteolin-enriched artichoke leaf extract administered to HFD-fed mice prevented hepatic steatosis (less and smaller lipid droplets, lower levels of *Cidea*) and insulin resistance by suppressing lipogenesis and gluconeogenesis (suppression of PEPCCK and G6Pase activities) and increasing FAO (more CPT1a activity and higher expression of *Ppara*, *Pgc1 $\alpha$*  and *Pgc1 $\beta$* ) [342]. The repression of hepatocyte nuclear factor 4 $\alpha$  and of LXR/SREBP1c signaling pathway has been described as putative molecular mechanisms for luteolin improvement of liver steatosis and NAFLD [348,349].

Regarding the capacity of flavones to modulate FAO, it has been described through a quantitative proteomic study that baicalin may act as an allosteric activator of CPT1a enzyme thus increasing the FA entrance to the mitochondria to undergo the  $\beta$ -oxidation in the liver [343]. Moreover, baicalin attenuated liver alterations by regulating the AMPK/ACC pathway in diet-induced obese mice [350]. Finally, baicalin is also a potent anti-inflammatory and antioxidant compound in a way that as other flavones also implied the nuclear erythroid 2-related factor 2 (Nrf2) activity in a cholestatic mice model [351].

It has been described that some flavones exert their hepatoprotective effects via the activation of the Nrf2 transcription factor. Nrf2 is a positive regulator of the expression of genes involved in the protection against oxidative stress as well as a negative regulator of genes that promote hepatic steatosis [352,353]. In this context, apigenin and scutellarin exerted their hepatoprotective activity via the activation of Nrf2. Scutellarin is a natural compound of *Erigeron breviscapus* (vant.) that in a HFD-fed mice attenuated obesity. It repressed lipogenesis and promoted FAO and cholesterol output besides its anti-inflammatory activity [340]. Moreover it has been described that scutellarin increased mRNA and/or protein levels of PPAR $\gamma$ , PGC1 $\alpha$ , Nrf2, haem oxygenase-1 (HO-1), glutathione S-transferase (GST), NAD(P)H quinone dehydrogenase 1 (NQO1) and PI3K and AKT, whilst reduced nuclear factor kappa B (NF- $\kappa$ B), Kelch-like ECH-associated protein 1 (Keap1) [354,355]. By contrast, apigenin administration to HFD-fed mice inhibited the expression of PPAR $\gamma$  target genes via the translocation to the nucleus and activation of the Nrf2 transcription factor that seems to block PPAR $\gamma$  activity. Apigenin treatment downregulated the expression of genes related to lipid droplet formation (*Cidea*, *Plin2*, *fat storage inducing transmembrane protein 1 and 2*) as well as genes involved in FA uptake



(*Fabp1* and *Lpl*), FAO (*Cpt1a*, *Pdk4*, *Acox1*, *Acaa2*) and lipogenesis (*Fasn*, *Scd11*, *Acaca*) [341]. On the other side, apigenin may act as a PPAR $\gamma$  modulator in a mouse model of obesity where it activated the p65/PPAR $\gamma$  complex translocation into the nucleus, thereby decreasing the NF- $\kappa$ B activation and favoring the M2 macrophage polarization [356] or blocking NLRP3 inflammasome assembly and the ROS production [357]. The capacity of flavones to modulate PPAR $\gamma$  activity and induce macrophage polarization to M2 phenotype has also been described for Chrysin in a HFD-fed mice model [358].

Finally, wogonin have shown beneficial effects on the liver steatosis development in a mice NAFLD model [359]. Concretely wogonin administration to HFD fed mice ameliorated the NAFLD progression via enhancing the PPAR $\alpha$ /Adiponectin receptor R2 (AdipoR2) pathway. Wogonin induced the hepatic activity of PPAR $\alpha$  and upregulated the levels of the AdipoR2. Moreover, wogonin also reduced the inflammatory profile and alleviated the hepatic oxidative stress [359].

Besides their effects alone, the combination of flavones with other bioactive compounds or polyphenols-rich extracts have also shown positive effects against hepatic steatosis [360].

### 8.2. Flavones Improved the Adipose Tissue Inflammation and Reduced the Macrophages Infiltration as Well as Enhanced the Thermogenic Capacity

Although flavones have been widely studied for their antioxidant and anti-inflammatory properties [338] their capacity to impact on adipose tissue metabolism and functionality cannot be underestimated.

Besides its reduction of the inflammatory phenotype in adipose tissue, apigenin administration to diet-induced obese mice ameliorated the body weight increment, reduced the visceral adiposity by inhibiting the adipogenesis via a STAT3/CD36 signaling pathway [361], decreased leptin and increased adiponectin [362] and induced energy expenditure mainly by promoting lipolysis and FAO as well as browning of WAT [363]. In scWAT, apigenin-treated mice exhibited a downregulation of adipogenic genes (*Ppar $\gamma$* , *Lpl* and *aP2*) and of genes involved in lipogenesis (*Fasn* and *Scd1*) and a promotion of lipolysis by increasing the mRNA levels of *Atgl*, *Hsl*, *Forkhead box protein O1 (FoxO1)* and *Sirt1*. In BAT there is an increment of the p-AMPK and p-ACC levels, thus indicating that FAO is enhanced in this fat depot after apigenin administration. Finally, apigenin activated the thermogenesis in BAT (upregulation of *Ucp1* and *Pgc1 $\alpha$* ) and induced the browning phenotype in scWAT (upregulation of *Ucp1*, *Pgc1 $\alpha$* , *Tmem26*, *Cited1*) [363]. Similar results were obtained with vitexin. Vitexin administration reduced the adipocyte size of HFD-fed mice and increased the p-AMPK levels in eWAT followed by a downregulation of C/EBP $\alpha$  and FASN protein levels [364].

In the case of nobiletin and luteolin, their administration to HFD-fed mice improved the fibrotic and inflammatory profile in adipose tissue and reduced the macrophage infiltration and polarization [344,346,365,366]; but in contrast with other flavones they increased the mRNA expression of FAO- (*Ppara $\alpha$* , *Cox8b*, and *Cpt1a*) and lipogenic (*Ppar $\gamma$* , *Srebp1c*, *Fasn* and *Scd1*) -related genes simultaneously [342,344] as well as CPT1 and FASN activity [344] in WAT. The simultaneously activation of both metabolic pathways in adipose tissues has been demonstrated as a way to maintain thermogenesis in BAT [367,368] and as a marker of browning in WAT [82]. In the case of luteolin, its administration either in HFD-fed or low-fat-fed mice activated browning and thermogenesis in mice via the AMPK/PGC1 $\alpha$  cascade. Under the AMPK/PGC1 $\alpha$  signal, luteolin increased energy expenditure in HFD-fed mice and upregulated the mRNA levels of *Pgc1 $\alpha$* , *PPAR $\alpha$* , *Cidea* and *Sirt1* in BAT as well as *Ucp1*, *Pgc1 $\alpha$* , *Tmem26*, *Cidea*, *PPAR $\alpha$* , *Sirt1*, *Elovl3* and *Cited1* in scWAT [369]. Moreover, the increased of PPAR $\gamma$  protein levels in WAT has been linked to an alleviation of the hepatic lipotoxicity in HFD-fed mice [347]. Similar effects were observed with baicalein that administered to HFD-fed mice decreased p38MAPK, pERK and PPAR $\gamma$  levels and increased pAKT, PGC1 $\alpha$  and UCP1 as well as the presence of GLUT4 in cell membranes of the eWAT. Globally, baicalein reversed the glucose intolerance and insulin resistance produced by HFD [370].

Besides the effects of each compound by itself some flavones-rich extracts or foods or combinations of different bioactive compounds have been evaluated regarding their potential therapeutic role against obesity and its metabolic and inflammatory features [371,372].

### 8.3. Flavones and Obesity in the CNS: No Clear Evidences

There are few studies describing the potential role of flavones in obesity-related central alterations. Just luteolin has been demonstrated a protective effect against HFD-induced cognitive effects in obese mice. Luteolin administration alleviated neuroinflammation, oxidative stress and neuronal insulin resistance as well as improved the Morris water maze (MWM) and step-through task and increased the levels of BDNF [373]. Other effects of flavones described recently are anxiolytic-like activity [374], neuroprotection against gamma-radiation [375] treatment of glioblastoma [376], amelioration of the hypoxia-reoxygenation injury [377] or inhibition of the neuroinflammation caused by LPS [378].

## 9. Chalcones

Chalcones is a group of polyphenolic compounds with a broad structural diversity. Chalcones are precursors of other flavonoids and responsible for the golden yellow pigments found in flowers, fruits, vegetables, spices, teas and different plant tissues. Although their metabolism in the gastrointestinal tract and their rate of absorption are not still completely known, chalcones have shown a wide variety of biological activities. Several studies have demonstrated that, either from natural sources or synthetic, chalcones can impact on glucose and lipid metabolism and their health benefits have been studied in relation to type 2 diabetes [379]. Chalcones have shown hypoglycemic capacity, the ability to modulate food intake and activate AMPK, as well as antioxidant, anti-inflammatory, anticancer, anti-obesity, hepatoprotective and neuroprotective properties [380–392]. Although there are no many studies in humans the effects of chalcones in the obese phenotype in animal models are similar to the ones described for other flavonoids, thus suggesting a potential therapeutic role of these group of bioactive compounds.

### 9.1. The Hepatoprotective Role of Chalcones

Chalcones have hepatoprotective properties in NAFLD, alcoholic fatty liver, drug- and toxicant-induced liver injury, and liver cancer [381]. It has been described that chalcones are able to inhibit the synthesis of triglycerides and the lipogenesis, to increase FAO, and to modulate adiponectin production and signaling.

Licochalcone F, a novel synthetic retrochalcone, has shown anti-inflammatory properties when administered to diet-induced obese mice. Licochalcone F inhibited TNF $\alpha$ -induced NF- $\kappa$ B activation and the mRNA expression of several pro-inflammatory markers. In the liver licochalcone F alleviated hepatic steatosis, by decreasing lipid droplets and glycogen deposition [380]. On its side, Licochalcone A, a chalcone isolated from *Glycyrrhiza uralensis*, administered to HFD-fed mice, reduced body weight, decreased serum triglycerides, LDL free fatty acids and fasting blood glucose, ameliorated hepatic steatosis, reduced lipid droplet accumulation [393]. In the liver, licochalcone A downregulated the protein levels of SREBP1c, PPAR $\gamma$ , and FASN as well as increased the phosphorylation of HSL, ATGL and ACC enzymes [393]. Moreover, licochalcone A increase the protein levels of CPT1A and stimulated SIRT1 and AMPK activity [393]. Taken together, licochalcone A ameliorated obesity and NAFLD in mice at least in part by reducing the fatty acid synthesis and increasing lipolysis and FAO via the activation of the SIRT1/AMPK pathway.

In a mouse model of HFD-induced obesity, *trans*-chalcone reduced the ALT levels and increased the HDL [394]. Similarly, in a mouse model of non-alcoholic steatohepatitis KK-Ay mice, xanthohumol, the chalcone from beer hops (*Humulus lupulus* L.), diminished hepatic inflammation and prevented from the expression of profibrogenic genes in the liver [395] as well as lowered hepatic fatty acid synthesis through the downregulation of *Srebp1c* expression and promoted FAO by upregulating the mRNA expression of *Ppara* in KK-Ay mice [396]. Moreover, in HFD-fed mice, xanthohumol prevented

body weight gain; decreased glycemia, triglyceride and cholesterol, and improved insulin sensitivity. Xanthohumol activated the hepatic and skeletal muscle AMPK, downregulated the expression of *Srebp1c* and *Fasn* and inhibited the activity of ACC, thus reducing the lipogenic pathway [386,397].

According to these data, aspalathin a C-glucosyl dihydrochalcone present in rooibos tea from *Aspalathus linearis*, also activated AMPK and reduced the expression of hepatic enzymes and transcriptional regulators that are associated with either gluconeogenesis and/or lipogenesis (*Acc*, *Fasn*, *Scd1*) in diabetic *ob/ob* mice [388,398]. Furthermore, Aspalathin-enriched green rooibos extract (GRE) improved hepatic insulin resistance via the regulation of the PI3K/AKT and AMPK Pathways [399]. In obese insulin resistant rats GRE upregulated the expression of *Glut2*, *insulin receptor (Insr)*, *Irs1* and *Irs2*, as well as *Cpt1a* [399]. Finally, Isoliquiritigenin at a low dose ameliorated insulin resistance and NAFLD in diet-induced obese mice. Isoliquiritigenin administration to HFD-fed mice decreased body fat mass and plasma cholesterol as well as alleviated hepatic steatosis (smaller lipid droplets) with no changes in TG and FFA serum levels [400]. It has been described that isoliquiritigenin suppressed the expression of lipogenic genes (*Fasn* and *Scd1*) and increased FAO activity. Moreover, isoliquiritigenin improved the insulin signaling in the liver and muscle [400].

Besides chalcones, chalcones-enriched products like Safflower yellow or ashitaba have demonstrated hepatoprotective properties. In mice fed with HFD, Safflower yellow improved lipid profile and alleviated fatty liver in a mechanism that has been associated to a reduction of the biosynthesis of intracellular cholesterol. Safflower yellow significantly reduced the levels of total cholesterol, triglycerides, LDL-cholesterol and the LDL/HDL ratio [401]. On its side, ashitaba (*Angelica keiskei*) extract showed hepatoprotective activity in fructose-induced dyslipidemia due to increased expression of FAO genes in the liver. Treatment with this extract upregulated the expression of the *Acox1*, *Mead*, *ATP-binding membrane cassette transporter A1 (ABCA1)* and *apolipoprotein A1 (Apo-A1)* [402]. In a similar way, this extract exerted hepatoprotective effects in HFD-fed mice. Ashitaba extract reduced plasma levels of cholesterol, glucose, and insulin, lowered triglyceride and cholesterol content in the liver, inhibited hepatic lipogenesis by downregulating *Srebp1* and *Fasn* and activated FAO by upregulating the expression of *Cpt1A* and *Ppara* [403]. The proposed mechanism underlying this hepatic metabolic effects is an activation of the AMPK enzyme in the liver [403].

In some of the studies the hepatoprotective role of chalcones has been linked to the adiponectin production. Concretely, trans-chalcone administration to high cholesterol diet-induced liver fibrosis increased the serum levels of adiponectin and the hepatic antioxidant enzymes, thus alleviating liver damage [404]. Similarly, xanthohumol and ashitaba extract or licochalcone A also increased the adiponectin expression and secretion [393,403,405].

#### 9.2. Chalcones in the Adipose Tissue, Upregulation of Adiponectin, Induction of Browning and Enhancement of Energy Expenditure

As has been mentioned above, chalcones induce adiponectin expression and secretion but also improve adipocytes function and reduce fat depots. Different molecular mechanisms underlying these effects has been described.

The treatment of obese mice with licochalcone F to reduced adipocyte size and ameliorated macrophage infiltration in WAT depots as well as enhanced Akt signaling and reduced p38 MAPK pathway [380]. On its side, the administration of Licochalcone A, isoliquiritigenin or a *Glycyrrhiza uralensis* extract containing licochalcone A, isoliquiritigenin, and liquiritigenin to diet-induced obese mice reduced body weight gain and adipose tissues depots [393,400,406]. In this case, Licochalcone A and *Glycyrrhiza uralensis* extract induced the browning phenotype in the iWAT this fat depot [393,406] as it is demonstrated by the enhanced expression of brown fat markers such as *Ucp1*, *Prdm16* and *Pgc1a* [406]. By contrast, isoliquiritigenin elevated energy expenditure by increasing the expression of thermogenic genes (*Ucp1* and *Prdm16*) as well as *Sirt1* that is linked to mitochondrial biogenesis [407] in interscapular BAT [400].

Finally, butein, besides its anti-inflammatory activity via the p38 MAPK/Nrf2/HO-1 pathway that leads to a reduction of the adipocyte hypertrophy [408] is also capable to enhance energy expenditure and increase thermogenesis. Butein induced the browning phenotype in the iWAT (upregulation of *Ucp1*, *Prdm16*, *cytochrome C oxidase 8b*, and *Cidea*) and increased the UCP1 protein levels in BAT in HFD-fed mice as well as in lean mice. The proposed molecular mechanism underlying these effects is the induction of the PR domain containing 4 (*Prdm4*) and the activation of the PI3K $\alpha$ /Akt1/PR domain containing 4 (*Prdm4*) axis [409,410]. The browning effect of butein was not observed in other mice models such as ThermoMouse strain nor in methionine- and choline-deficient diet-fed mice [411]. Butein actions have also been linked to its capacity to downregulate PPAR $\gamma$  expression [387,410].

Finally, chalcone-rich extracts such as Safflower yellow or Ashitaba extract have also demonstrated effects in adipose tissues. Concretely, in mice fed with HFD, Safflower yellow administration exerts anti-obesity and insulin-sensitizing effects by upregulating the expression of *Pgc1 $\alpha$*  that may indicate a browning phenotype of the scWAT as well as activating the protein levels of AKT and GSK3 $\beta$  in visceral WAT [412]. On its side, Ashitaba extract suppressed the HF diet-induced body weight gain and fat deposition in WAT, increased the adiponectin level and the phosphorylation AMPK, inhibited lipogenesis by downregulating *Ppar $\gamma$* , *CCAAT/enhancer-binding protein  $\alpha$*  (*Cebpa*) and *Srebp1* [403].

### 9.3. Chalcones in CNS: A Potential Neuroprotective Role

The antioxidant and anti-inflammatory properties of chalcones has been linked to some of their neuroprotective effects [382,383,389] but no studies with obesity-related neuronal damage has been found. Further studies are needed to identify the potential therapeutic role of chalcones on this obesity side effect.

## 10. Concluding Remarks

Undoubtedly flavonoids are potential therapeutic agents against metabolic disorders such as obesity, type 2 diabetes or NAFLD. Their impact in CNS, liver, and adipose tissue has been extensively studied and the results let us to be optimistic. Several metabolic effects and signaling pathways have been described underlying the anti-obesity effects of flavonoids specially in liver, EAT and BAT but also in CNS. Globally these effects go to control body weight, improve insulin sensitivity, reduce fat accumulation in adipose tissues as well in ectopic depots and to increase energy expenditure (Figure 1). Furthermore, the data presented in this review highlight that:

- Flavonoids are effective over a high variety of obesity and obesity-related diseases models.
- The anti-obesity effects of flavonoids are robust and consistent as they can be achieved using different sources, ways of administration and doses.
- Most of the molecular mechanisms underlying the anti-obesity effects of flavonoids are shared for the different subclasses of flavonoids (Tables 2 and 3).

expenditure (Figure 1). Furthermore, the data presented in this review highlight that:

- Flavonoids are effective over a high variety of obesity and obesity-related diseases models.
- The anti-obesity effects of flavonoids are robust and consistent as they can be achieved using different sources, ways of administration and doses.

Nutrients 2020, 12, 2333  
 28 of 42

Figure 1 illustrates the molecular mechanisms underlying the anti-obesity effects of flavonoids for the different subclasses of flavonoids (Tables 2 and 3).

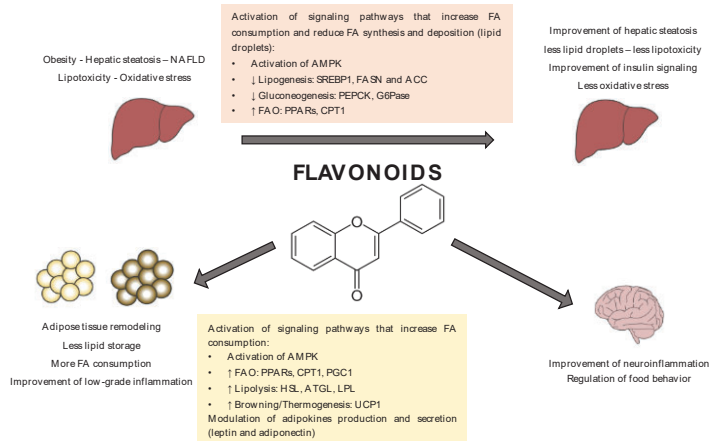


**Figure 1.** Summary of the metabolic and signaling pathways underlying the anti-obesity effects of flavonoids. Most of the mechanisms underlying the beneficial effects of flavonoids have been widely studied and, in many cases, involved the activation of the AMP-activated protein kinase (AMPK). AMPK is a key enzyme for the control of lipid metabolism and energy balance. AMPK is involved in and activation of more catabolic processes such as FA O, lipolysis, and glycolysis, as well as inhibition of the pathways such as fatty acid synthesis or gluconeogenesis.

Even so, more research is needed to confirm their therapeutic utility in humans, and to see the anti-obesity effects of the better combination of bioactive compounds. Now a days, it is still difficult to establish in some cases, the question is: what is the effective dose of polyphenols, and if for polyphenols we need to intake them to get positive effects? It is obvious that different diets might experimental diets to experimentally validate doses of bioactive compounds, as well as the presence of other food components on the use of isolated or extracted polyphenols obtained in vitro or in vivo. Furthermore, the use of flavonoids as a preventive food treatment also shows different results. Usually, the doses used in published papers are much higher than the doses reached from fruits and vegetables consumed as a whole.

The Predimed study determined that Spanish adults should intake around  $820 \pm 323$  mg of polyphenols/day in a 2000 Kcal diet to get their beneficial effects [25,27] but probably these effects at this dose are closely related to the MedDiet lifestyle. It is evident that, as MedDiet, some other dietary patterns include high amounts of fruits, vegetables or polyphenols-rich beverages that make possible to reach the optimal doses of polyphenols and by extension of flavonoids. Then, the question is: Are the effects of polyphenols linked to the dietary pattern where they are included? Two recent systematic reviews analyzed if there are enough evidence to define a health promoting polyphenol-rich dietary pattern and concluded that the high variability in the experimental approaches and methods used to evaluate polyphenols intake and health outcomes make difficult to establish specific polyphenol intake recommendations and to clarify whether total flavonoids or rather individual subclasses may exert beneficial effects [30,36].

Moreover, low is known about the effects of combining different bioactive compounds from different families. Are they going to have synergic, additive or antagonic effects? And not less important is the need to identify the role of the food matrix on polyphenols and flavonoid effects.

**Table 2.** Metabolic effects and signaling pathways underlying the anti-obesity effects of flavonoids in the liver.

Liver	Anthocyanins	Flavanols	Flavanones	Flavonols
<b>Signaling pathways</b>	Activation of the AMPK Inactivation of mTOR pathway	Activation of the AMPK Activation of SIRT and SIRT1/FoxO1 pathway Activation of the PKB/AKT—p-GSK3 $\alpha$ and p-PTEN Activation of PKA Inactivation of mTOR pathway Activation of the PXR/CAR-mediated phase II metabolism	Activation of the AMPK Activation of AMPK/SIRT1/PCCL1 $\alpha$ axis Activation of FGF21 signaling	Activation of the AMPK Activation of AMPK/PGC1 $\alpha$ /ERR $\alpha$ axis Inactivation of LXR/SREBP1c axis Inactivation of mTOR pathway Inhibition of the PKB/AKT—downregulation of SREBP1 $\uparrow$ Adiponectin signaling
<b>Lipid metabolism</b>	$\downarrow$ Lipogenesis and TG synthesis $\uparrow$ FA consumption (FAO) $\downarrow$ Lipid droplets	$\downarrow$ Lipogenesis and TG synthesis $\uparrow$ FA consumption (FAO) $\downarrow$ Lipid droplets $\downarrow$ Cholesterol synthesis and bile acids reabsorption	$\downarrow$ Lipogenesis and TG synthesis $\uparrow$ FA consumption (FAO) $\downarrow$ Lipid droplets	$\downarrow$ Lipogenesis and TG synthesis $\uparrow$ FA consumption (FAO) $\downarrow$ Lipid droplets $\downarrow$ Cholesterol synthesis
<b>Glucose metabolism</b>	$\downarrow$ Gluconeogenesis $\uparrow$ Glucose transport $\uparrow$ Glycolysis $\uparrow$ Insulin signaling	$\downarrow$ Gluconeogenesis	$\downarrow$ Gluconeogenesis $\downarrow$ Glucose transport $\uparrow$ Glycolysis	$\uparrow$ Glucose transport $\uparrow$ Insulin signaling
LIVER	Isoflavones	Flavones	Flavones	Chalcones
<b>Signaling pathways</b>	Activation of the AMPK Blockade of aldose reductase (AR)/polyol pathway Activation of the PKB/AKT	Activation of the AMPK Inactivation of LXR/SREBP1c axis. Nuclear erythroid 2-related factor 2 (Nrf2) and PPAR $\gamma$ activity $\uparrow$ Adiponectin signaling	Activation of the AMPK Activation of AMPK/SIRT pathway Activation of FIKK/AKT/PRDM4 signaling	
<b>Lipid metabolism</b>	$\downarrow$ Lipogenesis and TG synthesis $\uparrow$ FA consumption (FAO) $\downarrow$ Cholesterol synthesis	$\downarrow$ Lipogenesis and TG synthesis $\uparrow$ FA consumption (FAO)	$\downarrow$ Lipogenesis and TG synthesis $\uparrow$ FA consumption (FAO) $\downarrow$ Lipid droplets $\downarrow$ Cholesterol synthesis	
<b>Glucose metabolism</b>	$\downarrow$ Gluconeogenesis $\uparrow$ Glucose transport $\uparrow$ Insulin signaling	$\downarrow$ Gluconeogenesis	$\downarrow$ Gluconeogenesis $\uparrow$ Glucose transport $\uparrow$ Insulin signaling	

**Table 3.** Metabolic effects and signaling pathways underlying the anti-obesity effects of flavonoids in the adipose tissues.

Adipose Tissue	Anthocyanins	Flavanols	Flavanones	Flavonols
<b>Signaling pathways</b>	Activation of the AMPK Activation of SIRT and SIRT1/FoxO1 pathway Activation of the FDNCS/irisin pathway $\uparrow$ FGF21 signaling	Activation of b-adrenergic receptor— $\uparrow$ cAMP/PKA Inhibition of the PDE $\uparrow$ Adiponectin signaling		Activation of b-adrenergic receptor— $\uparrow$ cAMP/PKA Activation of the AMPK/SIRT1 pathway Activation of SIRT1/PGC1 $\alpha$ axis
<b>Adipokines</b>	$\downarrow$ Leptin $\uparrow$ Adiponectin		$\downarrow$ Leptin $\uparrow$ Adiponectin	$\uparrow$ Adiponectin
<b>Adipose tissue profile</b>	$\uparrow$ Browning and Thermogenesis $\downarrow$ Adipogenesis	$\uparrow$ Browning and Thermogenesis $\downarrow$ Adipogenesis	$\uparrow$ Browning and Thermogenesis	$\uparrow$ Browning and Thermogenesis $\downarrow$ Adipogenesis
<b>Lipid metabolism</b>	$\uparrow$ FA consumption (lipolysis and FAO) $\downarrow$ Lipogenesis and TG synthesis $\downarrow$ Lipid droplets	$\uparrow$ FA consumption (lipolysis and FAO) $\downarrow$ Lipogenesis and TG synthesis	$\uparrow$ FA consumption (lipolysis and FAO) $\downarrow$ Lipogenesis and TG synthesis	$\uparrow$ FA consumption (lipolysis and FAO) $\downarrow$ Lipogenesis and TG synthesis
<b>Glucose metabolism</b>	$\uparrow$ Glucose transport		$\uparrow$ Glucose transport	$\uparrow$ Glucose transport
ADIPOSE TISSUE	Isoflavones	Flavones	Flavones	Chalcones
<b>Signaling pathways</b>	Activation of the AMPK Activation of the FDNCS/irisin pathway	Activation of the AMPK Activation of the AMPK/PGC1 $\alpha$ axis Activation of the STAT3/CD36 signaling pathway	Activation of the AMPK Activation of PDK/AKT signaling	
<b>Adipokines</b>	$\downarrow$ Leptin $\uparrow$ Adiponectin		$\uparrow$ Adiponectin	
<b>Adipose tissue profile</b>	$\uparrow$ Browning and Thermogenesis	$\uparrow$ Browning and Thermogenesis $\downarrow$ Adipogenesis	$\uparrow$ Browning and Thermogenesis	
<b>Lipid metabolism</b>	$\uparrow$ FA consumption (lipolysis and FAO) $\downarrow$ Lipid droplets $\downarrow$ Lipogenesis and TG synthesis	$\uparrow$ FA consumption (lipolysis and FAO) $\downarrow$ Lipid droplets $\downarrow$ Lipogenesis and TG synthesis	$\uparrow$ FA consumption (lipolysis and FAO) $\downarrow$ Lipid droplets $\downarrow$ Lipogenesis and TG synthesis	
<b>Glucose metabolism</b>		$\uparrow$ Glucose transport		

The bioavailability of polyphenols is low and not just their basic chemical structures (aglycons) are key but also the attachment of additional groups. There are described around 8000 structures of polyphenols with different physiological impact and several chemical structures, but all of them with at least one phenolic ring with one or more hydroxyl groups attached [38,413,414]. The polyphenols absorption in human body is dose- and type-dependent and their effects are related to their bioavailability and pharmacokinetics. They show a low absorption rate and limited stability during pass through the intestinal tract where microbiome may contribute to their absorption. Once absorbed, polyphenols enter portal circulation and are metabolized in the liver. This first pass metabolism modifies the polyphenol structure and in consequence its bioavailability and bioactivity [415,416]. Finally, the conjugate metabolites reach the bloodstream and the target tissues [415–418].

Several studies have demonstrated that the bioavailability and safety of polyphenols changed when they are included in a food matrix [419–421]. Although most of the assays has been done with in vitro models of digestion [422] it seems that the food matrices protect bioactive compounds from intestinal degradation [420,423]. Finally, also cooking processes would have an impact in the polyphenols content and bioavailability of some preparations [424–426]. On the other side, it has been described that bioactive compounds with antioxidant properties are safe and beneficial but that exogenous supplementation with isolated compounds can be toxic [427].

The role of intestinal digestion and microbiota impact on polyphenols' effects must be also considered. Besides their direct action in the liver, some flavonoids may exert their metabolic effects through the gut microbiota modulation. An experimental approach with rabbits described that procyanidin b2 may downregulated fatty acid synthesis genes and protected against obesity and NAFLD by increasing the ratio of *Bacteroidetes* and *Akkermansia* [159]. Similar results were obtained with green tea oolong tea and black tea water extracts that administered to HFD-fed mice improved the glucose tolerance and reduced the weight gained caused by the HFD. Moreover, these animals showed a better hepatic lipid profile and a reduced mass of the WAT. These effects were accompanied by a reduction in plasma LPS, thus indicating less production and a significant increase in the production of short-chain fatty acids (SCFAs). A metagenomic analysis indicated that the tea extracts changed the gut microbiota's composition [428]. In the same way also flavones' effects on obesity has been linked to gut microbiota modifications [338]. Oral hydroxysafflor yellow A (HSYA) reversed the HFD-induced gut microbiota dysbiosis and reduced the obese phenotype [429].

**Author Contributions:** V.S., H.S.-L., G.A. and J.R. performed the literature research and wrote the first draft of the manuscript; P.F.M., D.H. and J.R. evaluated the information, reviewed and edited the manuscript to define its last version. All authors have read and agreed to the published version of the manuscript.

**Funding:** This study was supported by the Ministerio de Economía y Competitividad [grants AGL2017-82417-R to PFM and DH, by the Generalitat de Catalunya [grants 2017SGR683, VS was supported by Conicyt's fellowship from the Government of Chile. The APC was funded by the University of Barcelona.

**Acknowledgments:** We acknowledge Jacques Truffert for the images used in Table 1 and Ursula Martínez-Garza for the images used in Figure 1. Chemical structures of flavonoids' subclasses from Table 1 have been done with Chemdraw®.

**Conflicts of Interest:** The authors declare no conflict of interest.

## References

1. Romieu, I.; Dossus, L.; Barquera, S.; Blottiere, H.M.; Franks, P.W.; Gunter, M.; Hwalla, N.; Hursting, S.D.; Leitzmann, M.; Margets, B.; et al. Energy balance and obesity: What are the main drivers? *Cancer Causes Control* **2017**, *28*, 247–258. [PubMed]
2. Eckel, R.H.; Kahn, S.E.; Ferrannini, E.; Goldfine, A.B.; Nathan, D.M.; Schwartz, M.W.; Smith, R.J.; Smith, S.R. Obesity and type 2 diabetes: What can be unified and what needs to be individualized? *J. Clin. Endocrinol. Metab.* **2011**, *96*, 1654–1663. [CrossRef] [PubMed]
3. O'Neill, S.; O'Driscoll, L. Metabolic syndrome: A closer look at the growing epidemic and its associated pathologies. *Obes. Rev.* **2015**, *16*, 1–12. [CrossRef] [PubMed]



4. Picone, P.; Di Carlo, M.; Nuzzo, D. Obesity and Alzheimer disease: Molecular bases. *Eur. J. Neurosci.* **2020**, *1–7*. [[CrossRef](#)]
5. Mazon, J.N.; de Mello, A.H.; Ferreira, G.K.; Rezin, G.T. The impact of obesity on neurodegenerative diseases. *Life Sci.* **2017**, *182*, 22–28. [[CrossRef](#)] [[PubMed](#)]
6. Samson, S.L.; Garber, A.J. Metabolic syndrome. *Endocrinol. Metab. Clin. N. Am.* **2014**, *43*, 1–23. [[CrossRef](#)]
7. Peirce, V.; Carobbio, S.; Vidal-Puig, A. The different shades of fat. *Nature* **2014**, *510*, 76–83. [[CrossRef](#)]
8. Carobbio, S.; Pellegrinelli, V.; Vidal-Puig, A. Adipose Tissue Function and Expandability as Determinants of Lipotoxicity and the Metabolic Syndrome. *Adv. Exp. Med. Biol.* **2017**, *960*, 161–196.
9. Reagan, L.P. Insulin signaling effects on memory and mood. *Curr. Opin. Pharmacol.* **2007**, *7*, 633–637. [[CrossRef](#)]
10. Craft, S. Insulin Resistance and Alzheimers Disease Pathogenesis: Potential Mechanisms and Implications for Treatment. *Curr. Alzheimer Res.* **2007**, *4*, 147–152. [[CrossRef](#)]
11. Pugazhenth, S.; Qin, L.; Reddy, P.H. Common neurodegenerative pathways in obesity, diabetes, and Alzheimer's disease. *Biochim. Biophys. Acta Mol. Basis Dis.* **2017**, *1863*, 1037–1045. [[CrossRef](#)] [[PubMed](#)]
12. Lustman, P.J.; Clouse, R.E. Depression in diabetic patients: The relationship between mood and glycemic control. *J. Diabetes Complicat.* **2005**, *19*, 113–122. [[PubMed](#)]
13. Samodien, E.; Johnson, R.; Pfeiffer, C.; Mabasa, L.; Erasmus, M.; Louw, J.; Chellan, N. Diet-induced hypothalamic dysfunction and metabolic disease, and the therapeutic potential of polyphenols. *Mol. Metab.* **2019**, *27*, 1–10. [[CrossRef](#)] [[PubMed](#)]
14. Serra-Majem, L.; Roman, B.; Estruch, R. Scientific evidence of interventions using the Mediterranean diet: A systematic review. *Nutr. Rev.* **2006**, *64*, S27–S47. [[CrossRef](#)] [[PubMed](#)]
15. Bendall, C.L.; Mayr, H.L.; Opie, R.S.; Bes-Rastrollo, M.; Itsiopoulos, C.; Thomas, C.J. Central obesity and the Mediterranean diet: A systematic review of intervention trials. *Crit. Rev. Food Sci. Nutr.* **2018**, *58*, 3070–3084. [[CrossRef](#)]
16. Sofi, F.; Macchi, C.; Abbate, R.; Gensini, G.F.; Casini, A. Mediterranean diet and health. *BioFactors* **2013**, *39*, 335–342. [[CrossRef](#)]
17. Estruch, R.; Martínez-González, M.A.; Corella, D.; Salas-Salvado, J.; Fito, M.; Chiva-Blanch, G.; Fiol, M.; Gomez-Gracia, E.; Aros, F.; Lapetra, J.; et al. Effect of a high-fat Mediterranean diet on bodyweight and waist circumference: A prespecified secondary outcomes analysis of the PREDIMED randomised controlled trial. *Lancet Diabetes Endocrinol.* **2019**, *7*, e6–e17. [[CrossRef](#)]
18. Tresserra-Rimbau, A.; Guasch-Ferre, M.; Salas-Salvado, J.; Toledo, E.; Corella, D.; Castaner, O.; Guo, X.; Gomez-Gracia, E.; Lapetra, J.; Aros, F.; et al. Intake of Total Polyphenols and Some Classes of Polyphenols Is Inversely Associated with Diabetes in Elderly People at High Cardiovascular Disease Risk. *J. Nutr.* **2016**, *146*, 767–777.
19. Chiva-Blanch, G.; Badimon, L.; Estruch, R. Latest evidence of the effects of the Mediterranean diet in prevention of cardiovascular disease. *Curr. Atheroscler. Rep.* **2014**, *16*, 446. [[CrossRef](#)]
20. Martínez-González, M.A.; Salas-Salvado, J.; Estruch, R.; Corella, D.; Fitó, M.; Ros, E. Benefits of the Mediterranean Diet: Insights from the PREDIMED Study. *Prog. Cardiovasc. Dis.* **2015**, *58*, 50–60. [[CrossRef](#)]
21. Casas, R.; Sacanella, E.; Urpi-Sarda, M.; Chiva-Blanch, G.; Ros, E.; Martínez-González, M.-A.; Covas, M.-I.; Salas-Salvado, J.; Fiol, M.; Aros, F.; et al. The effects of the mediterranean diet on biomarkers of vascular wall inflammation and plaque vulnerability in subjects with high risk for cardiovascular disease. A randomized trial. *PLoS ONE* **2014**, *9*, e100084. [[CrossRef](#)] [[PubMed](#)]
22. Amiot, M.J.; Riva, C.; Vinet, A. Effects of dietary polyphenols on metabolic syndrome features in humans: A systematic review. *Obes. Rev.* **2016**, *17*, 573–586. [[CrossRef](#)] [[PubMed](#)]
23. Castro-Barquero, S.; Lamuela-Raventós, R.M.; Doménech, M.; Estruch, R. Relationship between mediterranean dietary polyphenol intake and obesity. *Nutrients* **2018**, *10*, 1523. [[CrossRef](#)] [[PubMed](#)]
24. Schwingshackl, L.; Morze, J.; Hoffmann, G. Mediterranean diet and health status: Active ingredients and pharmacological mechanisms. *Br. J. Pharmacol.* **2019**, *177*, 1241–1257. [[CrossRef](#)] [[PubMed](#)]
25. Tresserra-Rimbau, A.; Rimm, E.B.; Medina-Remón, A.; Martínez-González, M.A.; López-Sabater, M.C.; Covas, M.I.; Corella, D.; Salas-Salvado, J.; Gómez-Gracia, E.; Lapetra, J.; et al. Polyphenol intake and mortality risk: A re-analysis of the PREDIMED trial. *BMC Med.* **2014**, *12*, 77. [[CrossRef](#)] [[PubMed](#)]
26. Tresserra-Rimbau, A.; Rimm, E.B.; Medina-Remón, A.; Martínez-González, M.A.; de la Torre, R.; Corella, D.; Salas-Salvado, J.; Gómez-Gracia, E.; Lapetra, J.; Arós, F.; et al. Inverse association between habitual polyphenol



- intake and incidence of cardiovascular events in the PREDIMED study. *Nutr. Metab. Cardiovasc. Dis.* **2014**, *24*, 639–647. [[CrossRef](#)] [[PubMed](#)]
27. Tresserra-Rimbau, A.; Medina-Remón, A.; Pérez-Jiménez, J.; Martínez-González, M.A.; Covas, M.I.; Corella, D.; Salas-Salvadó, J.; Gómez-Gracia, E.; Lapetra, J.; Arós, F.; et al. Dietary intake and major food sources of polyphenols in a Spanish population at high cardiovascular risk: The PREDIMED study. *Nutr. Metab. Cardiovasc. Dis.* **2013**, *23*, 953–959. [[CrossRef](#)]
  28. Medina-Remón, A.; Tresserra-Rimbau, A.; Pons, A.; Tur, J.A.; Martorell, M.; Ros, E.; Buil-Cosiales, P.; Sacanella, E.; Covas, M.I.; Corella, D.; et al. Effects of total dietary polyphenols on plasma nitric oxide and blood pressure in a high cardiovascular risk cohort. The PREDIMED randomized trial. *Nutr. Metab. Cardiovasc. Dis.* **2015**, *25*, 60–67. [[CrossRef](#)]
  29. Manach, C.; Scalbert, A.; Morand, C.; Rémésy, C.; Jiménez, L. Polyphenols: Food sources and bioavailability. *Am. J. Clin. Nutr.* **2004**, *79*, 727–747. [[CrossRef](#)]
  30. Godos, J.; Vitale, M.; Micek, A.; Ray, S.; Martini, D.; Del Rio, D.; Riccardi, G.; Galvano, F.; Grosso, G. Dietary Polyphenol Intake, Blood Pressure, and Hypertension: A Systematic Review and Meta-Analysis of Observational Studies. *Antioxidants* **2019**, *8*, 152. [[CrossRef](#)]
  31. Williamson, G. The role of polyphenols in modern nutrition. *Nutr. Bull.* **2017**, *42*, 226–235. [[CrossRef](#)] [[PubMed](#)]
  32. Vauzour, D.; Rodriguez-Mateos, A.; Corona, G.; Oruna-Concha, M.J.; Spencer, J.P.E. Polyphenols and human health: Prevention of disease and mechanisms of action. *Nutrients* **2010**, *2*, 1106–1131. [[CrossRef](#)] [[PubMed](#)]
  33. Xing, T.; Kang, Y.; Xu, X.; Wang, B.; Du, M.; Zhu, M.J. Raspberry Supplementation Improves Insulin Signaling and Promotes Brown-Like Adipocyte Development in White Adipose Tissue of Obese Mice. *Mol. Nutr. Food Res.* **2018**, *62*, 1701035. [[CrossRef](#)] [[PubMed](#)]
  34. Saibandith, B.; Spencer, J.P.E.; Rowland, I.R.; Commane, D.M. Olive Polyphenols and the Metabolic Syndrome. *Molecules* **2017**, *22*, 1082. [[CrossRef](#)]
  35. Castelli, V.; Grassi, D.; Bocale, R.; d’Angelo, M.; Antonosante, A.; Cimini, A.; Ferri, C.; Desideri, G. Diet and Brain Health: Which Role for Polyphenols? *Curr. Pharm. Des.* **2018**, *24*, 227–238. [[CrossRef](#)] [[PubMed](#)]
  36. Del Bo, C.; Bernardi, S.; Marino, M.; Porrini, M.; Tucci, M.; Guglielmetti, S.; Cherubini, A.; Carrieri, B.; Kirkup, B.; Kroon, P.; et al. Systematic Review on Polyphenol Intake and Health Outcomes: Is there Sufficient Evidence to Define a Health-Promoting Polyphenol-Rich Dietary Pattern? *Nutrients* **2019**, *11*, 1355.
  37. Konstantinidi, M.; Koutelidakis, A.E. Functional Foods and Bioactive Compounds: A Review of Its Possible Role on Weight Management and Obesity’s Metabolic Consequences. *Medicines* **2019**, *6*, 94. [[CrossRef](#)]
  38. Bohn, T. Dietary factors affecting polyphenol bioavailability. *Nutr. Rev.* **2014**, *72*, 429–452. [[CrossRef](#)]
  39. Lavefve, L.; Howard, L.R.; Carbonero, F. Berry polyphenols metabolism and impact on human gut microbiota and health. *Food Funct.* **2020**, *11*, 45–65. [[CrossRef](#)]
  40. Eker, M.E.; Aaby, K.; Budic-Leto, I.; Brncic, S.R.; El, S.N.; Karakaya, S.; Simsek, S.; Manach, C.; Wiczowski, W.; de Pascual-Teresa, S. A Review of Factors Affecting Anthocyanin Bioavailability: Possible Implications for the Inter-Individual Variability. *Foods* **2019**, *9*, 2. [[CrossRef](#)]
  41. Xiao, J.B.; Högger, P. Dietary polyphenols and type 2 diabetes: Current insights and future perspectives. *Curr. Med. Chem.* **2015**, *22*, 23–38. [[CrossRef](#)] [[PubMed](#)]
  42. Panche, A.N.; Diwan, A.D.; Chandra, S.R. Flavonoids: An overview. *J. Nutr. Sci.* **2016**, *5*, e47. [[CrossRef](#)] [[PubMed](#)]
  43. Caro-Ordieres, T.; Marín-Royo, G.; Opazo-Ríos, L.; Jiménez-Castilla, L.; Moreno, J.A.; Gómez-Guerrero, C.; Egido, J. The Coming Age of Flavonoids in the Treatment of Diabetic Complications. *J. Clin. Med.* **2020**, *9*, 346. [[CrossRef](#)] [[PubMed](#)]
  44. Xu, H.; Luo, J.; Huang, J.; Wen, Q. Flavonoids intake and risk of type 2 diabetes mellitus: A meta-analysis of prospective cohort studies. *Medicine* **2018**, *97*, e0686. [[CrossRef](#)]
  45. Al-Ishaq, R.K.; Abotaleb, M.; Kubatka, P.; Kajo, K.; Busselberg, D. Flavonoids and Their Anti-Diabetic Effects: Cellular Mechanisms and Effects to Improve Blood Sugar Levels. *Biomolecules* **2019**, *9*, 430. [[CrossRef](#)]
  46. Hussain, T.; Tan, B.; Murtaza, G.; Liu, G.; Rahu, N.; Saleem Kalhor, M.; Hussain Kalhor, D.; Adebawale, T.O.; Usman Mazhar, M.; Rehman, Z.U.; et al. Flavonoids and type 2 diabetes: Evidence of efficacy in clinical and animal studies and delivery strategies to enhance their therapeutic efficacy. *Pharmacol. Res.* **2020**, *152*, 104629. [[CrossRef](#)]

47. Rees, A.; Dodd, G.F.; Spencer, J.P.E. The effects of flavonoids on cardiovascular health: A review of human intervention trials and implications for cerebrovascular function. *Nutrients* **2018**, *10*, 1852. [[CrossRef](#)]
48. Kawser Hossain, M.; Abdal Dayem, A.; Han, J.; Yin, Y.; Kim, K.; Kumar Saha, S.; Yang, G.-M.; Choi, H.Y.; Cho, S.-G. Molecular Mechanisms of the Anti-Obesity and Anti-Diabetic Properties of Flavonoids. *Int. J. Mol. Sci.* **2016**, *17*, 569. [[CrossRef](#)]
49. Shin, J.H.; Jung, J.H. Non-alcoholic fatty liver disease and flavonoids: Current perspectives. *Clin. Res. Hepatol. Gastroenterol.* **2017**, *41*, 17–24. [[CrossRef](#)]
50. Salomone, F.; Godos, J.; Zelber-Sagi, S. Natural antioxidants for non-alcoholic fatty liver disease: Molecular targets and clinical perspectives. *Liver Int.* **2016**, *36*, 5–20. [[CrossRef](#)]
51. Khan, M.S.; Ikram, M.; Park, J.S.; Park, T.J.; Kim, M.O. Gut Microbiota, Its Role in Induction of Alzheimer's Disease Pathology, and Possible Therapeutic Interventions: Special Focus on Anthocyanins. *Cells* **2020**, *9*, 853. [[CrossRef](#)]
52. Reddy, V.P.; Aryal, P.; Robinson, S.; Rafiu, R.; Obrenovich, M.; Perry, G. Polyphenols in Alzheimer's Disease and in the Gut–Brain Axis. *Microorganisms* **2020**, *8*, 199. [[CrossRef](#)] [[PubMed](#)]
53. Garcia, D.; Shaw, R.J. AMPK: Mechanisms of Cellular Energy Sensing and Restoration of Metabolic Balance. *Mol. Cell* **2017**, *66*, 789–800. [[CrossRef](#)] [[PubMed](#)]
54. Petropoulos, S.A.; Sampaio, S.L.; Di Gioia, F.; Tzortzakis, N.; Roupheal, Y.; Kyriacou, M.C.; Ferreira, I. Grown to be Blue-Antioxidant Properties and Health Effects of Colored Vegetables. Part I: Root Vegetables. *Antioxidants* **2019**, *8*, 617. [[CrossRef](#)] [[PubMed](#)]
55. Di Gioia, F.; Tzortzakis, N.; Roupheal, Y.; Kyriacou, M.C.; Sampaio, S.L.; Ferreira, I.C.F.R.; Petropoulos, S.A. Grown to be Blue-Antioxidant Properties and Health Effects of Colored Vegetables. Part II: Leafy, Fruit, and Other Vegetables. *Antioxidants* **2020**, *9*, 97. [[CrossRef](#)] [[PubMed](#)]
56. Bendokas, V.; Skemiene, K.; Trumbeckaite, S.; Stanys, V.; Passamonti, S.; Borutaite, V.; Liobikas, J. Anthocyanins: From plant pigments to health benefits at mitochondrial level. *Crit. Rev. Food Sci. Nutr.* **2019**, *1*–14. [[CrossRef](#)]
57. Gomes, J.V.P.; Rigolon, T.C.B.; da Silveira Souza, M.S.; Alvarez-Leite, J.I.; Della Lucia, C.M.; Martino, H.S.D.; Rosa, C.D.O.B. Antiobesity effects of anthocyanins on mitochondrial biogenesis, inflammation, and oxidative stress: A systematic review. *Nutrition* **2019**, *66*, 192–202. [[CrossRef](#)]
58. Bhaswant, M.; Shafie, S.R.; Mathai, M.L.; Mouatt, P.; Brown, L. Anthocyanins in chokeberry and purple maize attenuate diet-induced metabolic syndrome in rats. *Nutrition* **2017**, *41*, 24–31. [[CrossRef](#)]
59. Wu, T.; Gao, Y.; Guo, X.; Zhang, M.; Gong, L. Blackberry and blueberry anthocyanin supplementation counteract high-fat-diet-induced obesity by alleviating oxidative stress and inflammation and accelerating energy expenditure. *Oxid. Med. Cell. Longev.* **2018**, *2018*, 4051232. [[CrossRef](#)]
60. Wu, T.; Yu, Z.; Tang, Q.; Song, H.; Gao, Z.; Chen, W.; Zheng, X. Honeysuckle anthocyanin supplementation prevents diet-induced obesity in C57BL/6 mice. *Food Funct.* **2013**, *4*, 1654–1661. [[CrossRef](#)]
61. Huang, H.; Chen, G.; Liao, D.; Zhu, Y.; Xue, X. Effects of Berries Consumption on Cardiovascular Risk Factors: A Meta-analysis with Trial Sequential Analysis of Randomized Controlled Trials. *Sci. Rep.* **2016**, *6*, 23625. [[CrossRef](#)]
62. Wang, X.; Zhang, Z.F.; Zheng, G.H.; Wang, A.M.; Sun, C.H.; Qin, S.P.; Zhuang, J.; Lu, J.; Ma, D.F.; Zheng, Y.L. Attenuation of hepatic steatosis by purple sweet potato colour is associated with blocking Src/ERK/C/EBP $\beta$  signalling in high-fat-diet-treated mice. *Appl. Physiol. Nutr. Metab.* **2017**, *42*, 1082–1091. [[CrossRef](#)] [[PubMed](#)]
63. Tsuda, T. Recent Progress in Anti-Obesity and Anti-Diabetes Effect of Berries. *Antioxidants* **2016**, *5*, 13. [[CrossRef](#)] [[PubMed](#)]
64. Calvano, A.; Izuora, K.; Oh, E.C.; Ebersole, J.L.; Lyons, T.J.; Basu, A. Dietary berries, insulin resistance and type 2 diabetes: An overview of human feeding trials. *Food Funct.* **2019**, *10*, 6227–6243. [[CrossRef](#)] [[PubMed](#)]
65. de Pascual-Teresa, S.; Moreno, D.A.; García-Viguera, C. Flavanols and anthocyanins in cardiovascular health: A review of current evidence. *Int. J. Mol. Sci.* **2010**, *11*, 1479–1703. [[CrossRef](#)]
66. He, J.; Giusti, M.M. Anthocyanins: Natural Colorants with Health-Promoting Properties. *Annu. Rev. Food Sci. Technol.* **2010**, *1*, 163–187. [[CrossRef](#)]
67. Wood, E.; Hein, S.; Heiss, C.; Williams, C.; Rodriguez-Mateos, A. Blueberries and cardiovascular disease prevention. *Food Funct.* **2019**, *10*, 7621–7633. [[CrossRef](#)]

68. Salamone, F.; Volti, G.L.; Titta, L.; Puzzo, L.; Barbagallo, I.; La Delia, F.; Zelber-Sagi, S.; Malaguarnera, M.; Pelicci, P.G.; Giorgio, M.; et al. Moro orange juice prevents fatty liver in mice. *World J. Gastroenterol.* **2012**, *18*, 3862–3868. [CrossRef]
69. Esposito, D.; Damsud, T.; Wilson, M.; Grace, M.H.; Strauch, R.; Li, X.; Lila, M.A.; Komarnytsky, S. Black Currant Anthocyanins Attenuate Weight Gain and Improve Glucose Metabolism in Diet-Induced Obese Mice with Intact, but Not Disrupted, Gut Microbiome. *J. Agric. Food Chem.* **2015**, *63*, 6172–6180. [CrossRef]
70. Iizuka, Y.; Ozeki, A.; Tani, T.; Tsuda, T. Blackcurrant extract ameliorates hyperglycemia in type 2 diabetic mice in association with increased basal secretion of glucagon-like peptide-1 and activation of AMP-activated protein kinase. *J. Nutr. Sci. Vitaminol.* **2018**, *64*, 258–264. [CrossRef]
71. Choi, K.H.; Lee, H.A.; Park, M.H.; Han, J.-S. Mulberry (*Morus alba* L.) Fruit Extract Containing Anthocyanins Improves Glycemic Control and Insulin Sensitivity via Activation of AMP-Activated Protein Kinase in Diabetic C57BL/KsJ-db Mice. *J. Med. Food* **2016**, *19*, 737–745. [CrossRef]
72. Takikawa, M.; Inoue, S.; Horio, F.; Tsuda, T. Dietary Anthocyanin-Rich Bilberry Extract Ameliorates Hyperglycemia and Insulin Sensitivity via Activation of AMP-Activated Protein Kinase in Diabetic Mice. *J. Nutr.* **2010**, *140*, 527–533. [CrossRef]
73. You, Y.; Yuan, X.; Liu, X.; Liang, C.; Meng, M.; Huang, Y.; Han, X.; Guo, J.; Guo, Y.; Ren, C.; et al. Cyanidin-3-glucoside increases whole body energy metabolism by upregulating brown adipose tissue mitochondrial function. *Mol. Nutr. Food Res.* **2017**, *61*, 1700261. [CrossRef] [PubMed]
74. Nieman, D.C.; Simonson, A.; Sakaguchi, C.A.; Sha, W.; Blevins, T.; Hattabaugh, J.; Kohlmeier, M. Acute Ingestion of a Mixed Flavonoid and Caffeine Supplement Increases Energy Expenditure and Fat Oxidation in Adult Women: A Randomized, Crossover Clinical Trial. *Nutrients* **2019**, *11*, 2665. [CrossRef] [PubMed]
75. Rupasinghe, H.P.V.; Sekhon-Loodu, S.; Mantso, T.; Panayiotidis, M.I. Phytochemicals in regulating fatty acid beta-oxidation: Potential underlying mechanisms and their involvement in obesity and weight loss. *Pharmacol. Ther.* **2016**, *165*, 153–163. [CrossRef] [PubMed]
76. Solverson, P.M.; Rumpfer, W.V.; Leger, J.L.; Redan, B.W.; Ferruzzi, M.G.; Baer, D.J.; Castonguay, T.W.; Novotny, J.A. Blackberry Feeding Increases Fat Oxidation and Improves Insulin Sensitivity in Overweight and Obese Males. *Nutrients* **2018**, *10*, 1048. [CrossRef] [PubMed]
77. Afzal, M.; Redha, A.; AlHasan, R. Anthocyanins Potentially Contribute to Defense against Alzheimer's Disease. *Molecules* **2019**, *24*, 4255. [CrossRef] [PubMed]
78. Burton-Freeman, B.M.; Sandhu, A.K.; Edirisinghe, I. Red Raspberries and Their Bioactive Polyphenols: Cardiometabolic and Neuronal Health Links. *Adv. Nutr.* **2016**, *7*, 44–65. [CrossRef] [PubMed]
79. Zhang, J.; Wu, J.; Liu, F.; Tong, L.; Chen, Z.; Chen, J.; He, H.; Xu, R.; Ma, Y.; Huang, C. Neuroprotective effects of anthocyanins and its major component cyanidin-3-O-glucoside (C3G) in the central nervous system: An outlined review. *Eur. J. Pharmacol.* **2019**, *858*, 172500. [CrossRef]
80. Jiang, X.; Li, X.; Zhu, C.; Sun, J.; Tian, L.; Chen, W.; Bai, W. The target cells of anthocyanins in metabolic syndrome. *Crit. Rev. Food Sci. Nutr.* **2019**, *59*, 921–946. [CrossRef]
81. Peng, C.-H.; Liu, L.-K.; Chuang, C.-M.; Chyau, C.-C.; Huang, C.-N.; Wang, C.-J. Mulberry Water Extracts Possess an Anti-obesity Effect and Ability to Inhibit Hepatic Lipogenesis and Promote Lipolysis. *J. Agric. Food Chem.* **2011**, *59*, 2663–2671. [CrossRef]
82. Sandoval, V.; Femenias, A.; Martínez-Garza, U.; Sanz-Lamora, H.; Castagnini, J.M.; Quifer-Rada, P.; Lamuela-Raventós, R.M.; Marrero, P.F.; Haro, D.; Relat, J. Lyophilized Maqui (*Aristotelia chilensis*) Berry Induces Browning in the Subcutaneous White Adipose Tissue and Ameliorates the Insulin Resistance in High Fat Diet-Induced Obese Mice. *Antioxidants* **2019**, *8*, 360. [CrossRef] [PubMed]
83. Badshah, H.; Ullah, I.; Kim, S.E.; Kim, T.H.; Lee, H.Y.; Kim, M.O. Anthocyanins attenuate body weight gain via modulating neuropeptide Y and GABAB1 receptor in rats hypothalamus. *Neuropeptides* **2013**, *47*, 347–353. [CrossRef] [PubMed]
84. Alvarez-Suarez, J.M.; Giampieri, F.; Tulipani, S.; Casoli, T.; Di Stefano, G.; González-Paramás, A.M.; Santos-Buelga, C.; Busco, F.; Quiles, J.L.; Cordero, M.D.; et al. One-month strawberry-rich anthocyanin supplementation ameliorates cardiovascular risk, oxidative stress markers and platelet activation in humans. *J. Nutr. Biochem.* **2014**, *25*, 289–294. [CrossRef] [PubMed]
85. Novotny, J.A.; Baer, D.J.; Khoo, C.; Gebauer, S.K.; Charron, C.S. Cranberry Juice Consumption Lowers Markers of Cardiometabolic Risk, Including Blood Pressure and Circulating C-Reactive Protein, Triglyceride, and Glucose Concentrations in Adults. *J. Nutr.* **2015**, *145*, 1185–1193. [CrossRef] [PubMed]

86. Yang, L.; Ling, W.; Yang, Y.; Chen, Y.; Tian, Z.; Du, Z.; Chen, J.; Xie, Y.; Liu, Z.; Yang, L. Role of Purified Anthocyanins in Improving Cardiometabolic Risk Factors in Chinese Men and Women with Prediabetes or Early Untreated Diabetes—A Randomized Controlled Trial. *Nutrients* **2017**, *9*, 1104. [[CrossRef](#)] [[PubMed](#)]
87. Valenti, L.; Riso, P.; Mazzocchi, A.; Porrini, M.; Fargion, S.; Agostoni, C. Dietary anthocyanins as nutritional therapy for nonalcoholic fatty liver disease. *Oxid. Med. Cell. Longev.* **2013**, *2013*, 145421. [[CrossRef](#)]
88. Park, S.; Cho, S.M.; Jin, B.R.; Yang, H.J.; Yi, Q.J. Mixture of blackberry leaf and fruit extracts alleviates non-alcoholic steatosis, enhances intestinal integrity, and increases Lactobacillus and Akkermansia in rats. *Exp. Biol. Med.* **2019**, *244*, 1629–1641. [[CrossRef](#)]
89. Huang, T.-W.; Chang, C.-L.; Kao, E.-S.; Lin, J.-H. Effect of Hibiscus sabdariffa extract on high fat diet-induced obesity and liver damage in hamsters. *Food Nutr. Res.* **2015**, *59*, 29018. [[CrossRef](#)]
90. Wu, T.; Qi, X.; Liu, Y.; Guo, J.; Zhu, R.; Chen, W.; Zheng, X.; Yu, T. Dietary supplementation with purified mulberry (Morus australis Poir) anthocyanins suppresses body weight gain in high-fat diet fed C57BL/6 mice. *Food Chem.* **2013**, *141*, 482–487. [[CrossRef](#)]
91. Pei, L.; Wan, T.; Wang, S.; Ye, M.; Qiu, Y.; Jiang, R.; Pang, N.; Huang, Y.; Zhou, Y.; Jiang, X.; et al. Cyanidin-3-O- $\beta$ -glucoside regulates the activation and the secretion of adipokines from brown adipose tissue and alleviates diet induced fatty liver. *Biomed. Pharmacother.* **2018**, *105*, 625–632. [[CrossRef](#)]
92. Franklin, R.; Bispo, R.F.M.; Sousa-Rodrigues, C.F.; Pires, L.A.S.; Fonseca, A.J.; Babinski, M.A. Grape Leucoanthocyanidin Protects Liver Tissue in Albino Rabbits with Nonalcoholic Hepatic Steatosis. *Cells Tissues Organs* **2018**, *205*, 129–136. [[CrossRef](#)] [[PubMed](#)]
93. Overall, J.; Bonney, S.A.; Wilson, M.; Beermann, A.; Grace, M.H.; Esposito, D.; Lila, M.A.; Komarnytsky, S. Metabolic effects of berries with structurally diverse anthocyanins. *Int. J. Mol. Sci.* **2017**, *18*, 422. [[CrossRef](#)] [[PubMed](#)]
94. van der Heijden, R.A.; Morrison, M.C.; Sheedfar, F.; Mulder, P.; Schreurs, M.; Hommelberg, P.P.H.; Hofker, M.H.; Schalkwijk, C.; Kleemann, R.; Tietge, U.J.F.; et al. Effects of Anthocyanin and Flavanol Compounds on Lipid Metabolism and Adipose Tissue Associated Systemic Inflammation in Diet-Induced Obesity. *Mediat. Inflamm.* **2016**, *2016*, 2042107. [[CrossRef](#)] [[PubMed](#)]
95. Parra-Vargas, M.; Sandoval-Rodriguez, A.; Rodriguez-Echevarria, R.; Dominguez-Rosales, J.A.; Santos-Garcia, A.; Armendariz-Borunda, J. Delphinidin Ameliorates Hepatic Triglyceride Accumulation in High-Fat Diet/Streptozotocin-Induced Obese Mice. *Nutrients* **2018**, *10*, 1060. [[CrossRef](#)] [[PubMed](#)]
96. Yan, F.; Zheng, X. Anthocyanin-rich mulberry fruit improves insulin resistance and protects hepatocytes against oxidative stress during hyperglycemia by regulating AMPK/ACC/mTOR pathway. *J. Funct. Foods* **2017**, *30*, 270–281. [[CrossRef](#)]
97. Chang, J.-J.; Hsu, M.-J.; Huang, H.-P.; Chung, D.-J.; Chang, Y.-C.; Wang, C.-J. Mulberry Anthocyanins Inhibit Oleic Acid Induced Lipid Accumulation by Reduction of Lipogenesis and Promotion of Hepatic Lipid Clearance. *J. Agric. Food Chem.* **2013**, *61*, 6069–6076. [[CrossRef](#)]
98. Park, M.; Yoo, J.-H.; Lee, Y.-S.; Lee, H.-J. Lonicera caerulea Extract Attenuates Non-Alcoholic Fatty Liver Disease in Free Fatty Acid-Induced HepG2 Hepatocytes and in High Fat Diet-Fed Mice. *Nutrients* **2019**, *11*, 494. [[CrossRef](#)]
99. Jiang, T.; Shuai, X.; Li, J.; Yang, N.; Deng, L.; Li, S.; He, Y.; Guo, H.; Li, Y.; He, J. Protein-Bound Anthocyanin Compounds of Purple Sweet Potato Ameliorate Hyperglycemia by Regulating Hepatic Glucose Metabolism in High-Fat Diet/Streptozotocin-Induced Diabetic Mice. *J. Agric. Food Chem.* **2020**, *68*, 1596–1608. [[CrossRef](#)]
100. du Preez, R.; Wanyonyi, S.; Mouatt, P.; Panchal, S.K.; Brown, L. Saskatoon Berry Amelanchier alnifolia Regulates Glucose Metabolism and Improves Cardiovascular and Liver Signs of Diet-Induced Metabolic Syndrome in Rats. *Nutrients* **2020**, *12*, 931. [[CrossRef](#)]
101. Guo, H.; Xia, M.; Zou, T.; Ling, W.; Zhong, R.; Zhang, W. Cyanidin 3-glucoside attenuates obesity-associated insulin resistance and hepatic steatosis in high-fat diet-fed and db/db mice via the transcription factor FoxO1. *J. Nutr. Biochem.* **2012**, *23*, 349–360. [[CrossRef](#)] [[PubMed](#)]
102. Su, W.; Zhang, C.; Chen, F.; Sui, J.; Lu, J.; Wang, Q.; Shan, Q.; Zheng, G.; Lu, J.; Sun, C.; et al. Purple sweet potato color protects against hepatocyte apoptosis through Sirt1 activation in high-fat-diet-treated mice. *Food Nutr. Res.* **2020**, *64*. [[CrossRef](#)] [[PubMed](#)]
103. Li, A.; Xiao, R.; He, S.; An, X.; He, Y.; Wang, C.; Yin, S.; Wang, B.; Shi, X.; He, J. Research Advances of Purple Sweet Potato Anthocyanins: Extraction, Identification, Stability, Bioactivity, Application, and Biotransformation. *Molecules* **2019**, *24*, 3816. [[CrossRef](#)] [[PubMed](#)]

104. Chu, Q.; Zhang, S.; Chen, M.; Han, W.; Jia, R.; Chen, W.; Zheng, X. Cherry Anthocyanins Regulate NAFLD by Promoting Autophagy Pathway. *Oxid. Med. Cell. Longev.* **2019**, *2019*, 4825949. [[CrossRef](#)]
105. Ishibashi, J.; Seale, P. Beige can be slimming. *Science* **2010**, *328*, 1113–1114. [[CrossRef](#)]
106. Bartelt, A.; Heeren, J. Adipose tissue browning and metabolic health. *Nat. Rev. Endocrinol.* **2014**, *10*, 24–36. [[CrossRef](#)]
107. Barbatelli, G.; Murano, I.; Madsen, L.; Hao, Q.; Jimenez, M.; Kristiansen, K.; Giacobino, J.P.; De Matteis, R.; Cinti, S. The emergence of cold-induced brown adipocytes in mouse white fat depots is determined predominantly by white to brown adipocyte transdifferentiation. *AJP Endocrinol. Metab.* **2010**, *298*, E1244–E1253. [[CrossRef](#)]
108. Whittle, A.; Relat-Pardo, J.; Vidal-Puig, A. Pharmacological strategies for targeting BAT thermogenesis. *Trends Pharmacol. Sci.* **2013**, *34*, 347–355. [[CrossRef](#)]
109. Kim, S.Y.; Wi, H.-R.; Choi, S.; Ha, T.J.; Lee, B.W.; Lee, M. Inhibitory effect of anthocyanin-rich black soybean testa (*Glycine max* (L.) Merr.) on the inflammation-induced adipogenesis in a DIO mouse model. *J. Funct. Foods* **2015**, *14*, 623–633. [[CrossRef](#)]
110. Lee, M.; Sorn, S.R.; Park, Y.; Park, H.-K. Anthocyanin Rich-Black Soybean Testa Improved Visceral Fat and Plasma Lipid Profiles in Overweight/Obese Korean Adults: A Randomized Controlled Trial. *J. Med. Food* **2016**, *19*, 995–1003. [[CrossRef](#)]
111. Lim, S.-M.; Lee, H.S.; Jung, J.I.; Kim, S.M.; Kim, N.Y.; Seo, T.S.; Bae, J.-S.; Kim, E.J. Cyanidin-3-O-galactoside-enriched Aronia melanocarpa extract attenuates weight gain and adipogenic pathways in high-fat diet-induced obese C57BL/6 mice. *Nutrients* **2019**, *11*, 1190. [[CrossRef](#)] [[PubMed](#)]
112. Tsuda, T.; Ueno, Y.; Aoki, H.; Koda, T.; Horio, F.; Takahashi, N.; Kawada, T.; Osawa, T. Anthocyanin enhances adipocytokine secretion and adipocyte-specific gene expression in isolated rat adipocytes. *Biochem. Biophys. Res. Commun.* **2004**, *316*, 149–157. [[CrossRef](#)] [[PubMed](#)]
113. Tsuda, T.; Ueno, Y.; Yoshikawa, T.; Kojo, H.; Osawa, T. Microarray profiling of gene expression in human adipocytes in response to anthocyanins. *Biochem. Pharmacol.* **2006**, *71*, 1184–1197. [[CrossRef](#)] [[PubMed](#)]
114. Wu, T.; Jiang, Z.; Yin, J.; Long, H.; Zheng, X. Anti-obesity effects of artificial planting blueberry (*Vaccinium ashei*) anthocyanin in high-fat diet-treated mice. *Int. J. Food Sci. Nutr.* **2016**, *67*, 257–264. [[CrossRef](#)] [[PubMed](#)]
115. Han, X.; Guo, J.; You, Y.; Yin, M.; Liang, J.; Ren, C.; Zhan, J.; Huang, W. Vanillic acid activates thermogenesis in brown and white adipose tissue. *Food Funct.* **2018**, *9*, 4366–4375. [[CrossRef](#)] [[PubMed](#)]
116. Jayarathne, S.; Stull, A.J.; Park, O.-H.; Kim, J.H.; Thompson, L.; Moustaid-Moussa, N. Protective Effects of Anthocyanins in Obesity-Associated Inflammation and Changes in Gut Microbiome. *Mol. Nutr. Food Res.* **2019**, *63*, e1900149. [[CrossRef](#)]
117. You, Y.; Han, X.; Guo, J.; Guo, Y.; Yin, M.; Liu, G.; Huang, W.; Zhan, J. Cyanidin-3-glucoside attenuates high-fat and high-fructose diet-induced obesity by promoting the thermogenic capacity of brown adipose tissue. *J. Funct. Foods* **2018**, *41*, 62–71. [[CrossRef](#)]
118. Rocha-Rodrigues, S.; Rodriguez, A.; Gouveia, A.M.; Goncalves, I.O.; Becerril, S.; Ramirez, B.; Belezca, J.; Fruhbeck, G.; Ascensao, A.; Magalhaes, J. Effects of physical exercise on myokines expression and brown adipose-like phenotype modulation in rats fed a high-fat diet. *Life Sci.* **2016**, *165*, 100–108. [[CrossRef](#)]
119. Luna-Vital, D.; Luzardo-Ocampo, I.; Cuellar-Nunez, M.L.; Loarca-Pina, G.; Gonzalez de Mejia, E. Maize extract rich in ferulic acid and anthocyanins prevents high-fat-induced obesity in mice by modulating SIRT1, AMPK and IL-6 associated metabolic and inflammatory pathways. *J. Nutr. Biochem.* **2020**, *79*, 108343. [[CrossRef](#)]
120. Wu, T.; Tang, Q.; Yu, Z.; Gao, Z.; Hu, H.; Chen, W.; Zheng, X.; Yu, T. Inhibitory effects of sweet cherry anthocyanins on the obesity development in C57BL/6 mice. *Int. J. Food Sci. Nutr.* **2014**, *65*, 351–359. [[CrossRef](#)]
121. Fan, D.; Alamri, Y.; Liu, K.; Macaskill, M.; Harris, P.; Brimble, M.; Dalrymple-Alford, J.; Prickett, T.; Menzies, O.; Laurenson, A.; et al. Supplementation of blackcurrant anthocyanins increased cyclic glycine-proline in the cerebrospinal fluid of parkinson patients: Potential treatment to improve insulin-like growth factor-1 function. *Nutrients* **2018**, *10*, 714. [[CrossRef](#)] [[PubMed](#)]
122. Rehman, S.U.; Shah, S.A.; Ali, T.; Chung, J., II; Kim, M.O. Anthocyanins Reversed D-Galactose-Induced Oxidative Stress and Neuroinflammation Mediated Cognitive Impairment in Adult Rats. *Mol. Neurobiol.* **2017**, *54*, 255–271. [[CrossRef](#)] [[PubMed](#)]

123. Wei, J.; Zhang, G.; Zhang, X.; Xu, D.; Gao, J.; Fan, J.; Zhou, Z. Anthocyanins from Black Chokeberry (*Aroniamelanocarpa* Elliot) Delayed Aging-Related Degenerative Changes of Brain. *J. Agric. Food Chem.* **2017**, *65*, 5973–5984. [[CrossRef](#)] [[PubMed](#)]
124. Li, D.; Wang, P.; Luo, Y.; Zhao, M.; Chen, F. Health benefits of anthocyanins and molecular mechanisms: Update from recent decade. *Crit. Rev. Food Sci. Nutr.* **2017**, *57*, 1729–1741. [[CrossRef](#)] [[PubMed](#)]
125. Boespflug, E.L.; Eliassen, J.C.; Dudley, J.A.; Shidler, M.D.; Kalt, W.; Summer, S.S.; Stein, A.L.; Stover, A.N.; Krikorian, R. Enhanced neural activation with blueberry supplementation in mild cognitive impairment. *Nutr. Neurosci.* **2018**, *21*, 297–305. [[CrossRef](#)] [[PubMed](#)]
126. Di Lorenzo, A.; Sobolev, A.P.; Nabavi, S.F.; Sureda, A.; Moghaddam, A.H.; Khanjani, S.; Di Giovanni, C.; Xiao, J.; Shirooie, S.; Tsetegho Sokeng, A.J.; et al. Antidepressive effects of a chemically characterized maqui berry extract (*Aristotelia chilensis* (molina) stuntz) in a mouse model of Post-stroke depression. *Food Chem. Toxicol.* **2019**, *129*, 434–443. [[CrossRef](#)]
127. Pan, Z.; Cui, M.; Dai, G.; Yuan, T.; Li, Y.; Ji, T.; Pan, Y. Protective Effect of Anthocyanin on Neurovascular Unit in Cerebral Ischemia/Reperfusion Injury in Rats. *Front. Neurosci.* **2018**, *12*, 947. [[CrossRef](#)]
128. Rasmussen, S.E.; Frederiksen, H.; Struntze Krogholm, K.; Poulsen, L. Dietary proanthocyanidins: Occurrence, dietary intake, bioavailability, and protection against cardiovascular disease. *Mol. Nutr. Food Res.* **2005**, *49*, 159–174. [[CrossRef](#)]
129. Kumar, S.; Pandey, A.K. Chemistry and biological activities of flavonoids: An overview. *Sci. World J.* **2013**, *2013*, 162750. [[CrossRef](#)]
130. Scientific Opinion on the modification of the authorisation of a health claim related to cocoa flavanols and maintenance of normal endothelium-dependent vasodilation pursuant to Article 13(5) of Regulation (EC) No 1924/2006 following a request in accordance. *EFSA J.* **2016**, *12*, 3654.
131. Yu, J.; Song, P.; Perry, R.; Penfold, C.; Cooper, A.R. The effectiveness of green tea or green tea extract on insulin resistance and glycemic control in type 2 diabetes mellitus: A meta-analysis. *Diabetes Metab. J.* **2017**, *41*, 251–262. [[CrossRef](#)] [[PubMed](#)]
132. Li, X.; Wang, W.; Hou, L.; Wu, H.; Wu, Y.; Xu, R.; Xiao, Y.; Wang, X. Does tea extract supplementation benefit metabolic syndrome and obesity? A systematic review and meta-analysis. *Clin. Nutr.* **2020**, *39*, 1049–1058. [[CrossRef](#)] [[PubMed](#)]
133. Martin, M.A.; Goya, L.; Ramos, S. Protective effects of tea, red wine and cocoa in diabetes. Evidences from human studies. *Food Chem. Toxicol.* **2017**, *109*, 302–314. [[CrossRef](#)] [[PubMed](#)]
134. Akhlaghi, M.; Ghobadi, S.; Mohammad Hosseini, M.; Gholami, Z.; Mohammadian, F. Flavanols are potential anti-obesity agents, a systematic review and meta-analysis of controlled clinical trials. *Nutr. Metab. Cardiovasc. Dis.* **2018**, *28*, 675–690. [[CrossRef](#)]
135. Lin, Y.; Shi, D.; Su, B.; Wei, J.; Gaman, M.-A.; Sedanur Macit, M.; Borges do Nascimento, I.J.; Guimaraes, N.S. The effect of green tea supplementation on obesity: A systematic review and dose-response meta-analysis of randomized controlled trials. *Phytother. Res.* **2020**, 1–12. [[CrossRef](#)]
136. Payab, M.; Hasani-Ranjbar, S.; Shahbal, N.; Qorbani, M.; Aletaha, A.; Haghi-Aminjan, H.; Soltani, A.; Khatami, F.; Nikfar, S.; Hassani, S.; et al. Effect of the herbal medicines in obesity and metabolic syndrome: A systematic review and meta-analysis of clinical trials. *Phytother. Res.* **2020**, *34*, 526–545. [[CrossRef](#)]
137. Tang, G.-Y.; Meng, X.; Gan, R.-Y.; Zhao, C.-N.; Liu, Q.; Feng, Y.-B.; Li, S.; Wei, X.-L.; Atanasov, A.G.; Corke, H.; et al. Health Functions and Related Molecular Mechanisms of Tea Components: An Update Review. *Int. J. Mol. Sci.* **2019**, *20*, 6196. [[CrossRef](#)]
138. Oh, J.; Jo, S.-H.; Kim, J.S.; Ha, K.-S.; Lee, J.-Y.; Choi, H.-Y.; Yu, S.-Y.; Kwon, Y.-I.; Kim, Y.-C. Selected tea and tea pomace extracts inhibit intestinal alpha-glucosidase activity in vitro and postprandial hyperglycemia in vivo. *Int. J. Mol. Sci.* **2015**, *16*, 8811–8825. [[CrossRef](#)]
139. Ramos, S.; Martin, M.A.; Goya, L. Effects of Cocoa Antioxidants in Type 2 Diabetes Mellitus. *Antioxidants* **2017**, *6*, 84. [[CrossRef](#)]
140. Yang, C.S.; Zhang, J.; Zhang, L.; Huang, J.; Wang, Y. Mechanisms of body weight reduction and metabolic syndrome alleviation by tea. *Mol. Nutr. Food Res.* **2016**, *60*, 160–174. [[CrossRef](#)]
141. Leon-Flores, P.; Najera, N.; Perez, E.; Pardo, B.; Jimenez, F.; Diaz-Chiguer, D.; Villarreal, F.; Hidalgo, I.; Ceballos, G.; Meaney, E. Effects of Cacao By-Products and a Modest Weight Loss Intervention on the Concentration of Serum Triglycerides in Overweight Subjects: Proof of Concept. *J. Med. Food* **2020**, *23*, 745–749. [[CrossRef](#)] [[PubMed](#)]

142. Wu, E.; Zhang, T.; Tan, C.; Peng, C.; Chisti, Y.; Wang, Q.; Gong, J. Theabrownin from Pu-erh tea together with swinging exercise synergistically ameliorates obesity and insulin resistance in rats. *Eur. J. Nutr.* **2019**, *59*, 1937–1950. [[CrossRef](#)] [[PubMed](#)]
143. Zhang, Y.; Gu, M.; Wang, R.; Li, M.; Li, D.; Xie, Z. Dietary supplement of Yunkang 10 green tea and treadmill exercise ameliorate high fat diet induced metabolic syndrome of C57BL/6 J mice. *Nutr. Metab.* **2020**, *17*, 14.
144. Pezeshki, A.; Safi, S.; Feizi, A.; Askari, G.; Karami, F. The Effect of Green Tea Extract Supplementation on Liver Enzymes in Patients with Nonalcoholic Fatty Liver Disease. *Int. J. Prev. Med.* **2016**, *7*, 28.
145. Braud, L.; Battault, S.; Meyer, G.; Nascimento, A.; Gaillard, S.; de Sousa, G.; Rahmani, R.; Riva, C.; Armand, M.; Maixent, J.-M.; et al. Antioxidant properties of tea blunt ROS-dependent lipogenesis: Beneficial effect on hepatic steatosis in a high fat-high sucrose diet NAFLD obese rat model. *J. Nutr. Biochem.* **2017**, *40*, 95–104. [[CrossRef](#)]
146. Venkatakrishnan, K.; Chiu, H.-F.; Cheng, J.-C.; Chang, Y.-H.; Lu, Y.-Y.; Han, Y.-C.; Shen, Y.-C.; Tsai, K.-S.; Wang, C.-K. Comparative studies on the hypolipidemic, antioxidant and hepatoprotective activities of catechin-enriched green and oolong tea in a double-blind clinical trial. *Food Funct.* **2018**, *9*, 1205–1213. [[CrossRef](#)]
147. Li, X.; Li, S.; Chen, M.; Wang, J.; Xie, B.; Sun, Z. (-)-Epigallocatechin-3-gallate (EGCG) inhibits starch digestion and improves glucose homeostasis through direct or indirect activation of PXR/CAR-mediated phase II metabolism in diabetic mice. *Food Funct.* **2018**, *9*, 4651–4663. [[CrossRef](#)]
148. Li, Y.; Wu, S. Epigallocatechin gallate suppresses hepatic cholesterol synthesis by targeting SREBP-2 through SIRT1/FOXO1 signaling pathway. *Mol. Cell. Biochem.* **2018**, *448*, 175–185. [[CrossRef](#)]
149. Liu, C.; Guo, Y.; Sun, L.; Lai, X.; Li, Q.; Zhang, W.; Xiang, L.; Sun, S.; Cao, F. Six types of tea reduce high-fat-diet-induced fat accumulation in mice by increasing lipid metabolism and suppressing inflammation. *Food Funct.* **2019**, *10*, 2061–2074. [[CrossRef](#)]
150. Terzo, S.; Caldara, G.F.; Ferrantelli, V.; Puleio, R.; Cassata, G.; Mulè, F.; Amato, A. Pistachio Consumption Prevents and Improves Lipid Dysmetabolism by Reducing the Lipid Metabolizing Gene Expression in Diet-Induced Obese Mice. *Nutrients* **2018**, *10*, 1857. [[CrossRef](#)]
151. Chang, J.-J.; Chung, D.-J.; Lee, Y.-J.; Wen, B.-H.; Jao, H.-Y.; Wang, C.-J. Solanum nigrum Polyphenol Extracts Inhibit Hepatic Inflammation, Oxidative Stress, and Lipogenesis in High-Fat-Diet-Treated Mice. *J. Agric. Food Chem.* **2017**, *65*, 9255–9265. [[CrossRef](#)] [[PubMed](#)]
152. Tan, Y.; Kim, J.; Cheng, J.; Ong, M.; Lao, W.G.; Jin, X.L.; Lin, Y.G.; Xiao, L.; Zhu, X.Q.; Qu, X.Q. Green tea polyphenols ameliorate non-alcoholic fatty liver disease through upregulating AMPK activation in high fat fed Zucker fatty rats. *World J. Gastroenterol.* **2017**, *23*, 3805–3814. [[CrossRef](#)] [[PubMed](#)]
153. Suzuki, T.; Kumazoe, M.; Kim, Y.; Yamashita, S.; Nakahara, K.; Tsukamoto, S.; Sasaki, M.; Hagihara, T.; Tsurudome, Y.; Huang, Y.; et al. Green tea extract containing a highly absorbent catechin prevents diet-induced lipid metabolism disorder. *Sci. Rep.* **2013**, *3*, 2749. [[CrossRef](#)] [[PubMed](#)]
154. de Oliveira, P.R.B.; da Costa, C.A.; de Bem, G.F.; Cordeiro, V.S.C.; Santos, I.B.; de Carvalho, L.C.R.M.; da Conceição, E.P.S.; Lisboa, P.C.; Ognibene, D.T.; Sousa, P.J.C.; et al. Euterpe oleracea Mart.-Derived Polyphenols Protect Mice from Diet-Induced Obesity and Fatty Liver by Regulating Hepatic Lipogenesis and Cholesterol Excretion. *PLoS ONE* **2015**, *10*, e0143721. [[CrossRef](#)] [[PubMed](#)]
155. Liu, H.W.; Wei, C.C.; Chen, Y.J.; Chen, Y.A.; Chang, S.J. Flavanol-rich lychee fruit extract alleviates diet-induced insulin resistance via suppressing mTOR/SREBP-1 mediated lipogenesis in liver and restoring insulin signaling in skeletal muscle. *Mol. Nutr. Food Res.* **2016**, *60*, 2288–2296. [[CrossRef](#)] [[PubMed](#)]
156. Laplante, M.; Sabatini, D.M. An emerging role of mTOR in lipid biosynthesis. *Curr. Biol.* **2009**, *19*, R1046–R1052. [[CrossRef](#)]
157. Um, S.H.; Frigerio, F.; Watanabe, M.; Picard, F.; Joaquin, M.; Sticker, M.; Fumagalli, S.; Allegrini, P.R.; Kozma, S.C.; Auwerx, J.; et al. Absence of S6K1 protects against age- and diet-induced obesity while enhancing insulin sensitivity. *Nature* **2004**, *431*, 200–205. [[CrossRef](#)]
158. Peng, J.; Jia, Y.; Hu, T.; Du, J.; Wang, Y.; Cheng, B.; Li, K. GC-(4→8)-GCC, A Proanthocyanidin Dimer from Camellia ptilophylla, Modulates Obesity and Adipose Tissue Inflammation in High-Fat Diet Induced Obese Mice. *Mol. Nutr. Food Res.* **2019**, *63*, e1900082. [[CrossRef](#)]
159. Yin, M.; Zhang, P.; Yu, F.; Zhang, Z.; Cai, Q.; Lu, W.; Li, B.; Qin, W.; Cheng, M.; Wang, H.; et al. Grape seed procyanidin B2 ameliorates hepatic lipid metabolism disorders in db/db mice. *Mol. Med. Rep.* **2017**, *16*, 2844–2850. [[CrossRef](#)]



160. Huang, J.; Feng, S.; Liu, A.; Dai, Z.; Wang, H.; Reuhl, K.; Lu, W.; Yang, C.S. Green Tea Polyphenol EGCG Alleviates Metabolic Abnormality and Fatty Liver by Decreasing Bile Acid and Lipid Absorption in Mice. *Mol. Nutr. Food Res.* **2018**, *62*, 1700696. [[CrossRef](#)]
161. Cheng, H.; Xu, N.; Zhao, W.; Su, J.; Liang, M.; Xie, Z.; Wu, X.; Li, Q. (-)-Epicatechin regulates blood lipids and attenuates hepatic steatosis in rats fed high-fat diet. *Mol. Nutr. Food Res.* **2017**, *61*, 1–11. [[CrossRef](#)] [[PubMed](#)]
162. Chen, I.-J.; Liu, C.-Y.; Chiu, J.-P.; Hsu, C.-H. Therapeutic effect of high-dose green tea extract on weight reduction: A randomized, double-blind, placebo-controlled clinical trial. *Clin. Nutr.* **2015**, *35*, 592–599. [[CrossRef](#)] [[PubMed](#)]
163. Hibi, M.; Takase, H.; Iwasaki, M.; Osaki, N.; Katsuragi, Y. Efficacy of tea catechin-rich beverages to reduce abdominal adiposity and metabolic syndrome risks in obese and overweight subjects: A pooled analysis of 6 human trials. *Nutr. Res.* **2018**, *55*, 1–10. [[CrossRef](#)] [[PubMed](#)]
164. Kapoor, M.P.; Sugita, M.; Fukuzawa, Y.; Okubo, T. Physiological effects of epigallocatechin-3-gallate (EGCG) on energy expenditure for prospective fat oxidation in humans: A systematic review and meta-analysis. *J. Nutr. Biochem.* **2017**, *43*, 1–10. [[CrossRef](#)] [[PubMed](#)]
165. Yoneshiro, T.; Aita, S.; Kawai, Y.; Iwanaga, T.; Saito, M. Nonpungent capsaicin analogs (capsinoids) increase energy expenditure through the activation of brown adipose tissue in humans. *Am. J. Clin. Nutr.* **2012**, *95*, 845–850. [[CrossRef](#)] [[PubMed](#)]
166. Mele, L.; Bidault, G.; Mena, P.; Crozier, A.; Brighenti, F.; Vidal-Puig, A.; Del Rio, D. Dietary (Poly)phenols, Brown Adipose Tissue Activation, and Energy Expenditure: A Narrative Review. *Adv. Nutr.* **2017**, *8*, 694–704. [[CrossRef](#)]
167. Huang, J.; Wang, Y.; Xie, Z.; Zhou, Y.; Zhang, Y.; Wan, X. The anti-obesity effects of green tea in human intervention and basic molecular studies. *Eur. J. Clin. Nutr.* **2014**, *68*, 1075–1087. [[CrossRef](#)]
168. Serrano, J.; Casanova-Marti, A.; Gual, A.; Perez-Vendrell, A.M.; Blay, M.T.; Terra, X.; Ardevol, A.; Pinent, M. A specific dose of grape seed-derived proanthocyanidins to inhibit body weight gain limits food intake and increases energy expenditure in rats. *Eur. J. Nutr.* **2017**, *56*, 1629–1636. [[CrossRef](#)]
169. Yamashita, Y.; Wang, L.; Wang, L.; Tanaka, Y.; Zhang, T.; Ashida, H. Oolong, black and pu-erh tea suppresses adiposity in mice via activation of AMP-activated protein kinase. *Food Funct.* **2014**, *5*, 2420–2429. [[CrossRef](#)]
170. Varela, C.E.; Rodriguez, A.; Romero-Valdovinos, M.; Mendoza-Lorenzo, P.; Mansour, C.; Ceballos, G.; Villarreal, F.; Ramirez-Sanchez, I. Browning effects of (-)-epicatechin on adipocytes and white adipose tissue. *Eur. J. Pharmacol.* **2017**, *811*, 48–59. [[CrossRef](#)]
171. Neyrinck, A.M.; Bindels, L.B.; Geurts, L.; Van Hul, M.; Cani, P.D.; Delzenne, N.M. A polyphenolic extract from green tea leaves activates fat browning in high-fat-diet-induced obese mice. *J. Nutr. Biochem.* **2017**, *49*, 15–21. [[CrossRef](#)] [[PubMed](#)]
172. Jang, M.H.; Mukherjee, S.; Choi, M.J.; Kang, N.H.; Pham, H.G.; Yun, J.W. Theobromine alleviates diet-induced obesity in mice via phosphodiesterase-4 inhibition. *Eur. J. Nutr.* **2020**. [[CrossRef](#)] [[PubMed](#)]
173. Okla, M.; Kim, J.; Koehler, K.; Chung, S. Dietary Factors Promoting Brown and Beige Fat Development and Thermogenesis. *Adv. Nutr.* **2017**, *8*, 473–483. [[CrossRef](#)] [[PubMed](#)]
174. Silvester, A.J.; Aseer, K.R.; Yun, J.W. Dietary polyphenols and their roles in fat browning. *J. Nutr. Biochem.* **2019**, *64*, 1–12. [[CrossRef](#)] [[PubMed](#)]
175. Saito, M.; Matsushita, M.; Yoneshiro, T.; Okamatsu-Ogura, Y. Brown Adipose Tissue, Diet-Induced Thermogenesis, and Thermogenic Food Ingredients: From Mice to Men. *Front. Endocrinol.* **2020**, *11*, 222. [[CrossRef](#)]
176. Bolin, A.P.; Sousa-Filho, C.P.B.; Marinovic, M.P.; Rodrigues, A.C.; Otton, R. Polyphenol-rich green tea extract induces thermogenesis in mice by a mechanism dependent on adiponectin signaling. *J. Nutr. Biochem.* **2020**, *78*, 108322. [[CrossRef](#)]
177. Li, F.; Gao, C.; Yan, P.; Zhang, M.; Wang, Y.; Hu, Y.; Wu, X.; Wang, X.; Sheng, J. EGCG reduces obesity and white adipose tissue gain partly through AMPK activation in mice. *Front. Pharmacol.* **2018**, *9*, 1–9. [[CrossRef](#)]
178. Wang, Q.; Liu, S.; Zhai, A.; Zhang, B.; Tian, G. AMPK-Mediated Regulation of Lipid Metabolism by Phosphorylation. *Biol. Pharm. Bull.* **2018**, *41*, 985–993. [[CrossRef](#)]
179. Rodriguez Lanzi, C.; Perdicaro, D.J.; Landa, M.S.; Fontana, A.; Antonioli, A.; Miatello, R.M.; Oteiza, P.L.; Vazquez Prieto, M.A. Grape pomace extract induced beige cells in white adipose tissue from rats and in 3T3-L1 adipocytes. *J. Nutr. Biochem.* **2018**, *56*, 224–233. [[CrossRef](#)]



180. Rodríguez Lanzi, C.; Perdicaro, D.J.; Gambarte Tudela, J.; Muscia, V.; Fontana, A.R.; Oteiza, P.I.; Vazquez Prieto, M.A. Grape pomace extract supplementation activates FNDC5/irisin in muscle and promotes white adipose browning in rats fed a high-fat diet. *Food Funct.* **2020**, *11*, 1537–1546. [\[CrossRef\]](#)
181. Jang, M.H.; Kang, N.H.; Mukherjee, S.; Yun, J.W. Theobromine, a Methylxanthine in Cocoa Bean, Stimulates Thermogenesis by Inducing White Fat Browning and Activating Brown Adipocytes. *Biotechnol. Bioprocess Eng.* **2018**, *23*, 617–626. [\[CrossRef\]](#)
182. Nakagawa, Y.; Ishimura, K.; Oya, S.; Kamino, M.; Fujii, Y.; Nanba, F.; Toda, T.; Ishii, T.; Adachi, T.; Suhara, Y.; et al. Comparison of the sympathetic stimulatory abilities of B-type procyanidins based on induction of uncoupling protein-1 in brown adipose tissue (BAT) and increased plasma catecholamine (CA) in mice. *PLoS ONE* **2018**, *13*, e0201203. [\[CrossRef\]](#) [\[PubMed\]](#)
183. Nirengi, S.; Amagasa, S.; Homma, T.; Yoneshiro, T.; Matsumiya, S.; Kurosawa, Y.; Sakane, N.; Ebi, K.; Saito, M.; Hamaoka, T. Daily ingestion of catechin-rich beverage increases brown adipose tissue density and decreases extramyocellular lipids in healthy young women. *Springerplus* **2016**, *5*, 1363. [\[CrossRef\]](#) [\[PubMed\]](#)
184. Lee, M.-S.; Shin, Y.; Jung, S.; Kim, Y. Effects of epigallocatechin-3-gallate on thermogenesis and mitochondrial biogenesis in brown adipose tissues of diet-induced obese mice. *Food Nutr. Res.* **2017**, *61*, 1325307. [\[CrossRef\]](#)
185. Zhou, J.; Mao, L.; Xu, P.; Wang, Y. Effects of (–)-epigallocatechin gallate (EGCG) on energy expenditure and microglia-mediated hypothalamic inflammation in mice fed a high-fat diet. *Nutrients* **2018**, *10*, 1681. [\[CrossRef\]](#)
186. Hursel, R.; Westerterp-Plantenga, M.S. Catechin- and caffeine-rich teas for control of body weight in humans. *Am. J. Clin. Nutr.* **2013**, *98*, 1682S–1693S. [\[CrossRef\]](#)
187. Dulloo, A.G.; Seydoux, J.; Girardier, L.; Chantre, P.; Vandermander, J. Green tea and thermogenesis: Interactions between catechin-polyphenols, caffeine and sympathetic activity. *Int. J. Obes. Relat. Metab. Disord. J. Int. Assoc. Study Obes.* **2000**, *24*, 252–258. [\[CrossRef\]](#)
188. Yoneshiro, T.; Matsushita, M.; Hibi, M.; Tone, H.; Takeshita, M.; Yasunaga, K.; Katsuragi, Y.; Kameya, T.; Sugie, H.; Saito, M. Tea catechin and caffeine activate brown adipose tissue and increase cold-induced thermogenic capacity in humans. *Am. J. Clin. Nutr.* **2017**, *105*, 873–881. [\[CrossRef\]](#)
189. Ibars, M.; Ardid-Ruiz, A.; Suárez, M.; Muguerza, B.; Bladé, C.; Aragonés, G. Proanthocyanidins potentiate hypothalamic leptin/STAT3 signalling and Pomc gene expression in rats with diet-induced obesity. *Int. J. Obes.* **2017**, *41*, 129–136. [\[CrossRef\]](#)
190. Husain, I.; Akhtar, M.; Shaharyar, M.; Islamuddin, M.; Abdin, M.Z.; Akhtar, M.J.; Najmi, A.K. High-salt and cholesterol diet-associated cognitive impairment attenuated by tannins-enriched fraction of *Emblica officinalis* via inhibiting NF-kB pathway. *Inflammopharmacology* **2018**, *26*, 147–156. [\[CrossRef\]](#)
191. Mi, Y.; Qi, G.; Fan, R.; Qiao, Q.; Sun, Y.; Gao, Y.; Liu, X. EGCG ameliorates high-fat- and high-fructose-induced cognitive defects by regulating the IRS/AKT and ERK/CREB/BDNF signaling pathways in the CNS. *FASEB J.* **2017**, *31*, 4998–5011. [\[CrossRef\]](#)
192. Ettchetto, M.; Cano, A.; Manzine, P.R.; Busquets, O.; Verdaguer, E.; Castro-Torres, R.D.; Garcia, M.L.; Beas-Zarate, C.; Olloquequi, J.; Auladell, C.; et al. Epigallocatechin-3-Gallate (EGCG) Improves Cognitive Deficits Aggravated by an Obesogenic Diet Through Modulation of Unfolded Protein Response in APP<sup>swe</sup>/PS1<sup>dE9</sup> Mice. *Mol. Neurobiol.* **2020**, *57*, 1814–1827. [\[CrossRef\]](#) [\[PubMed\]](#)
193. Macedo, R.C.; Bondan, E.F.; Otton, R. Redox status on different regions of the central nervous system of obese and lean rats treated with green tea extract. *Nutr. Neurosci.* **2019**, *22*, 119–131. [\[CrossRef\]](#) [\[PubMed\]](#)
194. Xiong, H.; Wang, J.; Ran, Q.; Lou, G.; Peng, C.; Gan, Q.; Hu, J.; Sun, J.; Yao, R.; Huang, Q. Hesperidin: A Therapeutic Agent For Obesity. *Drug Des. Devel. Ther.* **2019**, *13*, 3855–3866. [\[CrossRef\]](#) [\[PubMed\]](#)
195. Burke, A.C.; Telford, D.E.; Edwards, J.Y.; Sutherland, B.G.; Sawyez, C.G.; Huff, M.W. Naringenin Supplementation to a Chow Diet Enhances Energy Expenditure and Fatty Acid Oxidation, and Reduces Adiposity in Lean, Pair-Fed Ldlr <sup>-/-</sup> Mice. *Mol. Nutr. Food Res.* **2019**, *63*, 1–9. [\[CrossRef\]](#) [\[PubMed\]](#)
196. Barreca, D.; Gattuso, G.; Bellocco, E.; Calderaro, A.; Trombetta, D.; Smeriglio, A.; Laganà, G.; Daglia, M.; Meneghini, S.; Nabavi, S.M. Flavanones: Citrus phytochemical with health-promoting properties. *BioFactors* **2017**, *43*, 495–506. [\[CrossRef\]](#)
197. Li, C.; Schluessener, H. Health-promoting effects of the citrus flavanone hesperidin. *Crit. Rev. Food Sci. Nutr.* **2017**, *57*, 613–631. [\[CrossRef\]](#)
198. Patel, K.; Singh, G.K.; Patel, D.K. A Review on Pharmacological and Analytical Aspects of Naringenin. *Chin. J. Integr. Med.* **2018**, *24*, 551–560. [\[CrossRef\]](#)

199. Den Hartogh, D.J.; Tsiani, E. Antidiabetic Properties of Naringenin: A Citrus Fruit Polyphenol. *Biomolecules* **2019**, *9*, 99. [[CrossRef](#)]
200. Hernández-Aquino, E.; Muriel, P. Beneficial effects of naringenin in liver diseases: Molecular mechanisms. *World J. Gastroenterol.* **2018**, *24*, 1679–1707. [[CrossRef](#)]
201. Shirani, K.; Yousefsani, B.S.; Shirani, M.; Karimi, G. Protective effects of naringin against drugs and chemical toxins induced hepatotoxicity: A review. *Phytother. Res.* **2020**. [[CrossRef](#)] [[PubMed](#)]
202. Kannappan, S.; Anuradha, C.V. Naringenin enhances insulin-stimulated tyrosine phosphorylation and improves the cellular actions of insulin in a dietary model of metabolic syndrome. *Eur. J. Nutr.* **2010**, *49*, 101–109. [[CrossRef](#)] [[PubMed](#)]
203. Cho, K.W.; Kim, Y.O.; Andrade, J.E.; Burgess, J.R.; Kim, Y.-C. Dietary naringenin increases hepatic peroxisome proliferator-activated receptor alpha protein expression and decreases plasma triglyceride and adiposity in rats. *Eur. J. Nutr.* **2011**, *50*, 81–88. [[CrossRef](#)] [[PubMed](#)]
204. Pu, P.; Gao, D.-M.; Mohamed, S.; Chen, J.; Zhang, J.; Zhou, X.-Y.; Zhou, N.-J.; Xie, J.; Jiang, H. Naringin ameliorates metabolic syndrome by activating AMP-activated protein kinase in mice fed a high-fat diet. *Arch. Biochem. Biophys.* **2012**, *518*, 61–70. [[CrossRef](#)]
205. Assini, J.M.; Mulvihill, E.E.; Sutherland, B.G.; Telford, D.E.; Sawyez, C.G.; Felder, S.L.; Chhoker, S.; Edwards, J.Y.; Gros, R.; Huff, M.W. Naringenin prevents cholesterol-induced systemic inflammation, metabolic dysregulation, and atherosclerosis in Ldlr(-)/(-) mice. *J. Lipid Res.* **2013**, *54*, 711–724. [[CrossRef](#)]
206. Assini, J.M.; Mulvihill, E.E.; Burke, A.C.; Sutherland, B.G.; Telford, D.E.; Chhoker, S.S.; Sawyez, C.G.; Drangova, M.; Adams, A.C.; Kharitonov, A.; et al. Naringenin prevents obesity, hepatic steatosis, and glucose intolerance in male mice independent of fibroblast growth factor 21. *Endocrinology* **2015**, *156*, 2087–2102. [[CrossRef](#)]
207. Sui, G.-G.; Xiao, H.-B.; Lu, X.-Y.; Sun, Z.-L. Naringin Activates AMPK Resulting in Altered Expression of SREBPs, PCSK9, and LDLR to Reduce Body Weight in Obese C57BL/6j Mice. *J. Agric. Food Chem.* **2018**, *66*, 8983–8990. [[CrossRef](#)]
208. Jung, U.J.; Lee, M.-K.; Jeong, K.-S.; Choi, M.-S. The hypoglycemic effects of hesperidin and naringin are partly mediated by hepatic glucose-regulating enzymes in C57BL/KsJ-db/db mice. *J. Nutr.* **2004**, *134*, 2499–2503. [[CrossRef](#)]
209. Jung, U.J.; Lee, M.-K.; Park, Y.B.; Kang, M.A.; Choi, M.-S. Effect of citrus flavonoids on lipid metabolism and glucose-regulating enzyme mRNA levels in type-2 diabetic mice. *Int. J. Biochem. Cell Biol.* **2006**, *38*, 1134–1145. [[CrossRef](#)]
210. Mosqueda-Solis, A.; Sanchez, J.; Reynes, B.; Palou, M.; Portillo, M.P.; Palou, A.; Pico, C. Hesperidin and capsaicin, but not the combination, prevent hepatic steatosis and other metabolic syndrome-related alterations in western diet-fed rats. *Sci. Rep.* **2018**, *8*, 15100. [[CrossRef](#)]
211. Wu, H.; Liu, Y.; Chen, X.; Zhu, D.; Ma, J.; Yan, Y.; Si, M.; Li, X.; Sun, C.; Yang, B.; et al. Neohesperidin exerts lipid-regulating effects in vitro and in vivo via fibroblast growth factor 21 and AMP-activated protein kinase/sirtuin type 1/peroxisome proliferator-activated receptor gamma coactivator 1 $\alpha$  signaling axis. *Pharmacology* **2017**, *100*, 115–126. [[CrossRef](#)] [[PubMed](#)]
212. Kwon, E.Y.; Choi, M.S. Dietary eriodictyol alleviates adiposity, hepatic steatosis, insulin resistance, and inflammation in diet-induced obese mice. *Int. J. Mol. Sci.* **2019**, *20*, 1227. [[CrossRef](#)] [[PubMed](#)]
213. Zhou, Y.; Ding, Y.-L.; Zhang, J.-L.; Zhang, P.; Wang, J.-Q.; Li, Z.-H. Alpinetin improved high fat diet-induced non-alcoholic fatty liver disease (NAFLD) through improving oxidative stress, inflammatory response and lipid metabolism. *Biomed. Pharmacother.* **2018**, *97*, 1397–1408. [[CrossRef](#)] [[PubMed](#)]
214. Cheraghpour, M.; Imani, H.; Ommi, S.; Alavian, S.M.; Karimi-Shahrbabak, E.; Hedayati, M.; Yari, Z.; Hekmatdoost, A. Hesperidin improves hepatic steatosis, hepatic enzymes, and metabolic and inflammatory parameters in patients with nonalcoholic fatty liver disease: A randomized, placebo-controlled, double-blind clinical trial. *Phyther. Res.* **2019**, *33*, 2118–2125. [[CrossRef](#)]
215. Yoshida, H.; Watanabe, H.; Ishida, A.; Watanabe, W.; Narumi, K.; Atsumi, T.; Sugita, C.; Kurokawa, M. Naringenin suppresses macrophage infiltration into adipose tissue in an early phase of high-fat diet-induced obesity. *Biochem. Biophys. Res. Commun.* **2014**, *454*, 95–101. [[CrossRef](#)]
216. Hoek-van den Hil, E.F.; van Schothorst, E.M.; van der Stelt, I.; Swarts, H.J.M.; van Vliet, M.; Amolo, T.; Vervoort, J.J.M.; Venema, D.; Hollman, P.C.H.; Rietjens, I.M.C.M.; et al. Direct comparison of metabolic health

- effects of the flavonoids quercetin, hesperetin, epicatechin, apigenin and anthocyanins in high-fat-diet-fed mice. *Genes Nutr.* **2015**, *10*, 1–13. [[CrossRef](#)]
217. Tsuchioka, R.; Yoshida, H.; Sugita, C.; Kurokawa, M. Naringenin suppresses neutrophil infiltration into adipose tissue in high-fat diet-induced obese mice. *J. Nat. Med.* **2020**, *74*, 229–237. [[CrossRef](#)]
  218. Rebello, C.J.; Greenway, F.L.; Lau, F.H.; Lin, Y.; Stephens, J.M.; Johnson, W.D.; Coulter, A.A. Naringenin Promotes Thermogenic Gene Expression in Human White Adipose Tissue. *Obesity* **2019**, *27*, 103–111. [[CrossRef](#)]
  219. Chou, Y.C.; Ho, C.T.; Pan, M.H. Immature citrus reticulata extract promotes browning of beige adipocytes in high-fat diet-induced C57BL/6 mice. *J. Agric. Food Chem.* **2018**, *66*, 9697–9703. [[CrossRef](#)]
  220. Stohs, S.J.; Badmaev, V. A Review of Natural Stimulant and Non-stimulant Thermogenic Agents. *Phytother. Res.* **2016**, *30*, 732–740. [[CrossRef](#)]
  221. Mosqueda-Solis, A.; Sánchez, J.; Portillo, M.P.; Palou, A.; Picó, C. Combination of capsaicin and hesperidin reduces the effectiveness of each compound to decrease the adipocyte size and to induce browning features in adipose tissue of western diet fed rats. *J. Agric. Food Chem.* **2018**, *66*, 9679–9689. [[CrossRef](#)] [[PubMed](#)]
  222. Nishikawa, S.; Hyodo, T.; Nagao, T.; Nakanishi, A.; Tandia, M.; Tsuda, T.  $\alpha$ -Monoglucosyl Hesperidin but Not Hesperidin Induces Brown-Like Adipocyte Formation and Suppresses White Adipose Tissue Accumulation in Mice. *J. Agric. Food Chem.* **2019**, *67*, 1948–1954. [[CrossRef](#)] [[PubMed](#)]
  223. Ohara, T.; Muroyama, K.; Yamamoto, Y.; Murosaki, S. Oral intake of a combination of glucosyl hesperidin and caffeine elicits an anti-obesity effect in healthy, moderately obese subjects: A randomized double-blind placebo-controlled trial. *Nutr. J.* **2016**, *15*, 1–11. [[CrossRef](#)] [[PubMed](#)]
  224. Sandeep, M.S.; Nandini, C.D. Influence of quercetin, naringenin and berberine on glucose transporters and insulin signalling molecules in brain of streptozotocin-induced diabetic rats. *Biomed. Pharmacother.* **2017**, *94*, 605–611.
  225. Saad, M.A.; Abdel Salam, R.M.; Kenawy, S.A.; Attia, A.S. Pinocembrin attenuates hippocampal inflammation, oxidative perturbations and apoptosis in a rat model of global cerebral ischemia reperfusion. *Pharmacol. Rep.* **2015**, *67*, 115–122. [[CrossRef](#)] [[PubMed](#)]
  226. Tao, J.; Shen, C.; Sun, Y.; Chen, W.; Yan, G. Neuroprotective effects of pinocembrin on ischemia/reperfusion-induced brain injury by inhibiting autophagy. *Biomed. Pharmacother.* **2018**, *106*, 1003–1010. [[CrossRef](#)] [[PubMed](#)]
  227. Wang, K.; Chen, Z.; Huang, J.; Huang, L.; Luo, N.; Liang, X.; Liang, M.; Xie, W. Naringenin prevents ischaemic stroke damage via anti-apoptotic and anti-oxidant effects. *Clin. Exp. Pharmacol. Physiol.* **2017**, *44*, 862–871. [[CrossRef](#)]
  228. De Lima, N.M.R.; Ferreira, E.D.O.; Fernandes, M.Y.S.D.; Lima, F.A.V.; Neves, K.R.T.; Do Carmo, M.R.S.; De Andrade, G.M. Neuroinflammatory response to experimental stroke is inhibited by boldine. *Behav. Pharmacol.* **2016**, *28*, 223–227. [[CrossRef](#)]
  229. Muhammad, T.; Ikram, M.; Ullah, R.; Rehman, S.U.; Kim, M.O. Hesperetin, a citrus flavonoid, attenuates LPS-induced neuroinflammation, apoptosis and memory impairments by modulating TLR4/NF- $\kappa$ B signaling. *Nutrients* **2019**, *11*, 648. [[CrossRef](#)]
  230. Afshin-Majd, S.; Motevalizadeh, S.-A.; Khajevand-Khazaei, M.-R.; Roghani, M.; Baluchnejadmojarad, T.; Rohani, M.; Ziaee, P. Naringenin ameliorates learning and memory impairment following systemic lipopolysaccharide challenge in the rat. *Eur. J. Pharmacol.* **2018**, *826*, 114–122.
  231. Khalaj, R.; Hajizadeh Moghaddam, A.; Zare, M. Hesperetin and its nanocrystals ameliorate social behavior deficits and oxido-inflammatory stress in rat model of autism. *Int. J. Dev. Neurosci.* **2018**, *69*, 80–87. [[CrossRef](#)] [[PubMed](#)]
  232. Kosari-Nasab, M.; Shokouhi, G.; Ghorbanhaghjo, A.; Abbasi, M.M.; Salari, A.A. Hesperidin attenuates depression-related symptoms in mice with mild traumatic brain injury. *Life Sci.* **2018**, *213*, 198–205. [[CrossRef](#)] [[PubMed](#)]
  233. Fu, H.; Liu, L.; Tong, Y.; Li, Y.; Zhang, X.; Gao, X.; Yong, J.; Zhao, J.; Xiao, D.; Wen, K.; et al. The antidepressant effects of hesperidin on chronic unpredictable mild stress-induced mice. *Eur. J. Pharmacol.* **2019**, *853*, 236–246. [[CrossRef](#)] [[PubMed](#)]
  234. Sato, M.; Okuno, A.; Suzuki, K.; Ohsawa, N.; Inoue, E.; Miyaguchi, Y.; Toyoda, A. Dietary intake of the citrus flavonoid hesperidin affects stress-resilience and brain kynurenine levels in a subchronic and mild social defeat stress model in mice. *Biosci. Biotechnol. Biochem.* **2019**, *83*, 1756–1765. [[CrossRef](#)] [[PubMed](#)]

235. Umukoro, S.; Kalejaye, H.A.; Ben-Azu, B.; Ajayi, A.M. Naringenin attenuates behavioral derangements induced by social defeat stress in mice via inhibition of acetylcholinesterase activity, oxidative stress and release of pro-inflammatory cytokines. *Biomed. Pharmacother.* **2018**, *105*, 714–723. [[CrossRef](#)]
236. Alkhalidi, H.; Wang, Y.; Liu, D. Dietary flavonoids in the prevention of T2D: An overview. *Nutrients* **2018**, *10*, 438. [[CrossRef](#)]
237. Dabeek, W.M.; Marra, M.V. Dietary quercetin and kaempferol: Bioavailability and potential cardiovascular-related bioactivity in humans. *Nutrients* **2019**, *11*, 2288. [[CrossRef](#)]
238. Batiha, G.E.-S.; Beshbishy, A.M.; Ikram, M.; Mulla, Z.S.; El-Hack, M.E.A.; Taha, A.E.; Algamal, A.M.; Elewa, Y.H.A. The Pharmacological Activity, Biochemical Properties, and Pharmacokinetics of the Major Natural Polyphenolic Flavonoid: Quercetin. *Foods* **2020**, *9*, 374. [[CrossRef](#)]
239. Hoek-van den Hil, E.F.; van Schothorst, E.M.; van der Stelt, I.; Swarts, H.J.M.; Venema, D.; Sailer, M.; Vervoort, J.J.M.; Hollman, P.C.H.; Rietjens, I.M.; Keijer, J. Quercetin decreases high-fat diet induced body weight gain and accumulation of hepatic and circulating lipids in mice. *Genes Nutr.* **2014**, *9*, 418. [[CrossRef](#)]
240. Zamora-Ros, R.; Forouhi, N.G.; Sharp, S.J.; Gonzalez, C.A.; Buijse, B.; Guevara, M.; van der Schouw, Y.T.; Amiano, P.; Boeing, H.; Bredsdorff, L.; et al. Dietary intakes of individual flavanols and flavonols are inversely associated with incident type 2 diabetes in European populations. *J. Nutr.* **2014**, *144*, 335–343. [[CrossRef](#)]
241. Eid, H.M.; Haddad, P.S. The Antidiabetic Potential of Quercetin: Underlying Mechanisms. *Curr. Med. Chem.* **2017**, *24*, 355–364. [[CrossRef](#)] [[PubMed](#)]
242. Carrasco-Pozo, C.; Cires, M.J.; Gotteland, M. Quercetin and Epigallocatechin Gallate in the Prevention and Treatment of Obesity: From Molecular to Clinical Studies. *J. Med. Food* **2019**, *22*, 753–770. [[CrossRef](#)] [[PubMed](#)]
243. Bule, M.; Abdurahman, A.; Nikfar, S.; Abdollahi, M.; Amini, M. Antidiabetic effect of quercetin: A systematic review and meta-analysis of animal studies. *Food Chem. Toxicol.* **2019**, *125*, 494–502. [[CrossRef](#)]
244. Zhao, L.; Zhang, Q.; Ma, W.; Tian, F.; Shen, H.; Zhou, M. A combination of quercetin and resveratrol reduces obesity in high-fat diet-fed rats by modulation of gut microbiota. *Food Funct.* **2017**, *8*, 4644–4656. [[CrossRef](#)]
245. Liu, L.; Gao, C.; Yao, P.; Gong, Z. Quercetin Alleviates High-Fat Diet-Induced Oxidized Low-Density Lipoprotein Accumulation in the Liver: Implication for Autophagy Regulation. *Biomed Res. Int.* **2015**, *2015*, 607531. [[CrossRef](#)] [[PubMed](#)]
246. Xu, Y.; Han, J.; Dong, J.; Fan, X.; Cai, Y.; Li, J.; Wang, T.; Zhou, J.; Shang, J. Metabolomics Characterizes the Effects and Mechanisms of Quercetin in Nonalcoholic Fatty Liver Disease Development. *Int. J. Mol. Sci.* **2019**, *20*, 1220. [[CrossRef](#)]
247. Porras, D.; Nistal, E.; Martinez-Florez, S.; Olcoz, J.L.; Jover, R.; Jorquera, F.; Gonzalez-Gallego, J.; Garcia-Mediavilla, M.V.; Sanchez-Campos, S. Functional Interactions between Gut Microbiota Transplantation, Quercetin, and High-Fat Diet Determine Non-Alcoholic Fatty Liver Disease Development in Germ-Free Mice. *Mol. Nutr. Food Res.* **2019**, *63*, e1800930. [[CrossRef](#)]
248. Rubio-Ruiz, M.E.; Guarner-Lans, V.; Cano-Martinez, A.; Diaz-Diaz, E.; Manzano-Pech, L.; Gamam-Magana, A.; Castrejon-Tellez, V.; Tapia-Cortina, C.; Perez-Torres, I. Resveratrol and Quercetin Administration Improves Antioxidant DEFENSES and reduces Fatty Liver in Metabolic Syndrome Rats. *Molecules* **2019**, *24*, 1297. [[CrossRef](#)]
249. Aranaz, P.; Zabala, M.; Romo-Hualde, A.; Navarro-Herrera, D.; Lopez-Yoldi, M.; Vizmanos, J.L.; Martinez, J.A.; Milagro, F.I.; Gonzalez-Navarro, C.J. A combination of borage seed oil and quercetin reduces fat accumulation and improves insulin sensitivity in obese rats. *Food Funct.* **2020**. [[CrossRef](#)]
250. Qin, G.; Ma, J.; Huang, Q.; Yin, H.; Han, J.; Li, M.; Deng, Y.; Wang, B.; Hassan, W.; Shang, J. Isoquercetin Improves Hepatic Lipid Accumulation by Activating AMPK Pathway and Suppressing TGF-beta Signaling on an HFD-Induced Nonalcoholic Fatty Liver Disease Rat Model. *Int. J. Mol. Sci.* **2018**, *19*, 4126. [[CrossRef](#)]
251. Hoang, M.-H.; Jia, Y.; Lee, J.H.; Kim, Y.; Lee, S.-J. Kaempferol reduces hepatic triglyceride accumulation by inhibiting Akt. *J. Food Biochem.* **2019**, *43*, e13034. [[CrossRef](#)] [[PubMed](#)]
252. Hoang, M.H.; Jia, Y.; Mok, B.; Jun, H.J.; Hwang, K.Y.; Lee, S.J. Kaempferol ameliorates symptoms of metabolic syndrome by regulating activities of liver X receptor- $\beta$ . *J. Nutr. Biochem.* **2015**, *26*, 868–875. [[CrossRef](#)] [[PubMed](#)]
253. Gaballah, H.H.; El-Horany, H.E.; Helal, D.S. Mitigative effects of the bioactive flavonol fisetin on high-fat/high-sucrose induced nonalcoholic fatty liver disease in rats. *J. Cell. Biochem.* **2019**, *120*, 12762–12774. [[CrossRef](#)] [[PubMed](#)]

254. Zeng, X.; Yang, J.; Hu, O.; Huang, J.; Ran, L.; Chen, M.; Zhang, Y.; Zhou, X.; Zhu, J.; Zhang, Q.; et al. Dihydropyridinyl Ameliorates Nonalcoholic Fatty Liver Disease by Improving Mitochondrial Respiratory Capacity and Redox Homeostasis Through Modulation of SIRT3 Signaling. *Antioxid. Redox Signal.* **2019**, *30*, 163–183. [\[CrossRef\]](#)
255. Liu, Q.; Pan, R.; Ding, L.; Zhang, F.; Hu, L.; Ding, B.; Zhu, L.; Xia, Y.; Dou, X. Rutin exhibits hepatoprotective effects in a mouse model of non-alcoholic fatty liver disease by reducing hepatic lipid levels and mitigating lipid-induced oxidative injuries. *Int. Immunopharmacol.* **2017**, *49*, 132–141. [\[CrossRef\]](#)
256. Malinska, H.; Huttli, M.; Oliyarnyk, O.; Markova, I.; Poruba, M.; Racova, Z.; Kazdova, L.; Vecera, R. Beneficial effects of trolox on metabolic disorders in non-obese model of metabolic syndrome. *PLoS ONE* **2019**, *14*, e0220377. [\[CrossRef\]](#)
257. An, J.-P.; Choi, J.H.; Huh, J.; Lee, H.J.; Han, S.; Noh, J.-R.; Kim, Y.-H.; Lee, C.-H.; Oh, W.-K. Anti-hepatic steatosis activity of *Sicyos angulatus* extract in high-fat diet-fed mice and chemical profiling study using UHPLC-qTOF-MS/MS spectrometry. *Phytomedicine* **2019**, *63*, 152999. [\[CrossRef\]](#)
258. Guruvaiiah, P.; Guo, H.; Li, D.; Xie, Z. Preventive Effect of Flavonol Derivatives Abundant Sanglan Tea on Long-Term High-Fat-Diet-Induced Obesity Complications in C57BL/6 Mice. *Nutrients* **2018**, *10*, 1276. [\[CrossRef\]](#)
259. Song, J.; Kim, Y.-S.; Kim, L.; Park, H.J.; Lee, D.; Kim, H. Anti-Obesity Effects of the Flower of *Prunus persica* in High-Fat Diet-Induced Obese Mice. *Nutrients* **2019**, *11*, 2176. [\[CrossRef\]](#)
260. Omatsu, K.-I.; Nakata, A.; Sato, K.; Mihara, Y.; Takaguri, A.; Nagashima, T.; Wakame, K. Global Liver Gene Expression Analysis on a Murine Hepatic Steatosis Model Treated with Mulberry (*Morus alba* L.) Leaf Powder. *Anticancer Res.* **2018**, *38*, 4305–4311.
261. Ezzat, S.M.; El Bishbishy, M.H.; Aborehab, N.M.; Salama, M.M.; Hasheesh, A.; Motaal, A.A.; Rashad, H.; Metwally, F.M. Upregulation of MC4R and PPAR- $\alpha$  expression mediates the anti-obesity activity of *Moringa oleifera* Lam. in high-fat diet-induced obesity in rats. *J. Ethnopharmacol.* **2020**, *251*, 112541. [\[CrossRef\]](#) [\[PubMed\]](#)
262. Nie, H.; Deng, Y.; Zheng, C.; Pan, M.; Xie, J.; Zhang, Y.; Yang, Q. A network pharmacology-based approach to explore the effects of Chaihu Shugan powder on a non-alcoholic fatty liver rat model through nuclear receptors. *J. Cell. Mol. Med.* **2020**, *24*, 5168–5184. [\[CrossRef\]](#) [\[PubMed\]](#)
263. Li, H.; Kim, U.-H.; Yoon, J.-H.; Ji, H.-S.; Park, H.-M.; Park, H.-Y.; Jeong, T.-S. Suppression of Hyperglycemia and Hepatic Steatosis by Black-Soybean-Leaf Extract via Enhanced Adiponectin-Receptor Signaling and AMPK Activation. *J. Agric. Food Chem.* **2019**, *67*, 90–101. [\[CrossRef\]](#) [\[PubMed\]](#)
264. Yamauchi, T.; Iwabu, M.; Okada-Iwabu, M.; Kadowaki, T. Adiponectin receptors: A review of their structure, function and how they work. *Best Pract. Res. Clin. Endocrinol. Metab.* **2014**, *28*, 15–23. [\[CrossRef\]](#)
265. Wang, T.; Wu, Q.; Zhao, T. Preventive Effects of Kaempferol on High-Fat Diet-Induced Obesity Complications in C57BL/6 Mice. *Biomed Res. Int.* **2020**, *2020*, 4532482. [\[CrossRef\]](#)
266. Tan, S.; Caparros-Martin, J.A.; Matthews, V.B.; Koch, H.; O’Gara, F.; Croft, K.D.; Ward, N.C. Isoquercetin and inulin synergistically modulate the gut microbiome to prevent development of the metabolic syndrome in mice fed a high fat diet. *Sci. Rep.* **2018**, *8*, 10100. [\[CrossRef\]](#)
267. Zhao, Y.; Chen, B.; Shen, J.; Wan, L.; Zhu, Y.; Yi, T.; Xiao, Z. The Beneficial Effects of Quercetin, Curcumin, and Resveratrol in Obesity. *Oxid. Med. Cell. Longev.* **2017**, *2017*, 1459497. [\[CrossRef\]](#)
268. Li, H.; Qi, J.; Li, L. Phytochemicals as potential candidates to combat obesity via adipose non-shivering thermogenesis. *Pharmacol. Res.* **2019**, *147*, 104393. [\[CrossRef\]](#)
269. Horvath, C.; Wolfrum, C. Feeding brown fat: Dietary phytochemicals targeting non-shivering thermogenesis to control body weight. *Proc. Nutr. Soc.* **2020**, 1–19. [\[CrossRef\]](#)
270. Forney, L.A.; Lenard, N.R.; Stewart, L.K.; Henagan, T.M. Dietary Quercetin Attenuates Adipose Tissue Expansion and Inflammation and Alters Adipocyte Morphology in a Tissue-Specific Manner. *Int. J. Mol. Sci.* **2018**, *19*, 895. [\[CrossRef\]](#)
271. Ting, Y.; Chang, W.-T.; Shiau, D.-K.; Chou, P.-H.; Wu, M.-F.; Hsu, C.-L. Antiobesity Efficacy of Quercetin-Rich Supplement on Diet-Induced Obese Rats: Effects on Body Composition, Serum Lipid Profile, and Gene Expression. *J. Agric. Food Chem.* **2018**, *66*, 70–80. [\[CrossRef\]](#) [\[PubMed\]](#)
272. Kuipers, E.N.; van Dam, A.D.; Held, N.M.; Mol, I.M.; Houtkooper, R.H.; Rensen, P.C.N.; Boon, M.R. Quercetin Lowers Plasma Triglycerides Accompanied by White Adipose Tissue Browning in Diet-Induced Obese Mice. *Int. J. Mol. Sci.* **2018**, *19*, 1786. [\[CrossRef\]](#) [\[PubMed\]](#)

273. Perdicaro, D.J.; Rodriguez Lanzi, C.; Gambarte Tudela, J.; Miatello, R.M.; Oteiza, P.I.; Vazquez Prieto, M.A. Quercetin attenuates adipose hypertrophy, in part through activation of adipogenesis in rats fed a high-fat diet. *J. Nutr. Biochem.* **2020**, *79*, 108352. [[CrossRef](#)]
274. Choi, H.; Kim, C.-S.; Yu, R. Quercetin Upregulates Uncoupling Protein 1 in White/Brown Adipose Tissues through Sympathetic Stimulation. *J. Obes. Metab. Syndr.* **2018**, *27*, 102–109. [[CrossRef](#)] [[PubMed](#)]
275. Lee, S.G.; Parks, J.S.; Kang, H.W. Quercetin, a functional compound of onion peel, remodels white adipocytes to brown-like adipocytes. *J. Nutr. Biochem.* **2017**, *42*, 62–71. [[CrossRef](#)]
276. Dong, J.; Zhang, X.; Zhang, L.; Bian, H.-X.; Xu, N.; Bao, B.; Liu, J. Quercetin reduces obesity-associated ATM infiltration and inflammation in mice: A mechanism including AMPK $\alpha$ /SIRT1. *J. Lipid Res.* **2014**, *55*, 363–374. [[CrossRef](#)]
277. Arias, N.; Picó, C.; Teresa Macarulla, M.; Oliver, P.; Miranda, J.; Palou, A.; Portillo, M.P. A combination of resveratrol and quercetin induces browning in white adipose tissue of rats fed an obesogenic diet. *Obesity* **2017**, *25*, 111–121. [[CrossRef](#)]
278. Jiang, H.; Yoshioka, Y.; Yuan, S.; Horiuchi, Y.; Yamashita, Y.; Croft, K.D.; Ashida, H. Enzymatically modified isoquercitrin promotes energy metabolism through activating AMPK $\alpha$  in male C57BL/6 mice. *Food Funct.* **2019**, *10*, 5188–5202. [[CrossRef](#)]
279. Yuan, X.; Wei, G.; You, Y.; Huang, Y.; Lee, H.J.; Dong, M.; Lin, J.; Hu, T.; Zhang, H.; Zhang, C.; et al. Rutin ameliorates obesity through brown fat activation. *FASEB J.* **2017**, *31*, 333–345. [[CrossRef](#)]
280. Chen, N.; Lei, T.; Xin, L.; Zhou, L.; Cheng, J.; Qin, L.; Han, S.; Wan, Z. Depot-specific effects of treadmill running and rutin on white adipose tissue function in diet-induced obese mice. *J. Physiol. Biochem.* **2016**, *72*, 453–467. [[CrossRef](#)]
281. Mehanna, E.T.; El-Sayed, N.M.; Ibrahim, A.K.; Ahmed, S.A.; Abo-Elmatty, D.M. Isolated compounds from *Cuscuta pedicellata* ameliorate oxidative stress and upregulate expression of some energy regulatory genes in high fat diet induced obesity in rats. *Biomed. Pharmacother.* **2018**, *108*, 1253–1258. [[CrossRef](#)] [[PubMed](#)]
282. Hu, C.; Zhang, Y.; Liu, G.; Liu, Y.; Wang, J.; Sun, B. Untargeted Metabolite Profiling of Adipose Tissue in Hyperlipidemia Rats Exposed to Hawthorn Ethanol Extracts. *J. Food Sci.* **2019**, *84*, 717–725. [[CrossRef](#)] [[PubMed](#)]
283. Suganthi, N.; Devi, K.P.; Nabavi, S.F.; Braidy, N.; Nabavi, S.M. Bioactive effects of quercetin in the central nervous system: Focusing on the mechanisms of actions. *Biomed. Pharmacother.* **2016**, *84*, 892–908. [[CrossRef](#)] [[PubMed](#)]
284. Babaei, F.; Mirzababaei, M.; Nassiri-Asl, M. Quercetin in Food: Possible Mechanisms of Its Effect on Memory. *J. Food Sci.* **2018**, *83*, 2280–2287. [[CrossRef](#)]
285. Li, Y.; Tian, Q.; Li, Z.; Dang, M.; Lin, Y.; Hou, X. Activation of Nrf2 signaling by sitagliptin and quercetin combination against  $\beta$ -amyloid induced Alzheimer's disease in rats. *Drug Dev. Res.* **2019**, *80*, 837–845. [[CrossRef](#)]
286. Paula, P.-C.; Angelica Maria, S.-G.; Luis, C.-H.; Gloria Patricia, C.-G. Preventive Effect of Quercetin in a Triple Transgenic Alzheimer's Disease Mice Model. *Molecules* **2019**, *24*, 2287. [[CrossRef](#)]
287. Hayakawa, M.; Itoh, M.; Ohta, K.; Li, S.; Ueda, M.; Wang, M.; Nishida, E.; Islam, S.; Suzuki, C.; Ohzawa, K.; et al. Quercetin reduces eIF2 $\alpha$  phosphorylation by GADD34 induction. *Neurobiol. Aging* **2015**, *36*, 2509–2518. [[CrossRef](#)]
288. Budzynska, B.; Faggio, C.; Kruk-Slomka, M.; Samec, D.; Nabavi, S.F.; Sureda, A.; Devi, K.P.; Nabavi, S.M. Rutin as Neuroprotective Agent: From Bench to Bedside. *Curr. Med. Chem.* **2019**, *26*, 5152–5164. [[CrossRef](#)]
289. Xia, S.-F.; Xie, Z.-X.; Qiao, Y.; Li, L.-R.; Cheng, X.-R.; Tang, X.; Shi, Y.-H.; Le, G.-W. Differential effects of quercetin on hippocampus-dependent learning and memory in mice fed with different diets related with oxidative stress. *Physiol. Behav.* **2015**, *138*, 325–331. [[CrossRef](#)]
290. Kim, J.H.; Lee, S.; Cho, E.J. Acer okamotoanum and isoquercitrin improve cognitive function via attenuation of oxidative stress in high fat diet- and amyloid beta-induced mice. *Food Funct.* **2019**, *10*, 6803–6814. [[CrossRef](#)]
291. Yang, J.; Kim, C.-S.; Tu, T.H.; Kim, M.-S.; Goto, T.; Kawada, T.; Choi, M.-S.; Park, T.; Sung, M.-K.; Yun, J.W.; et al. Quercetin Protects Obesity-Induced Hypothalamic Inflammation by Reducing Microglia-Mediated Inflammatory Responses via HO-1 Induction. *Nutrients* **2017**, *9*, 650. [[CrossRef](#)] [[PubMed](#)]
292. Maciel, R.M.; Carvalho, F.B.; Olabiya, A.A.; Schmatz, R.; Gutierrez, J.M.; Stefanello, N.; Zanini, D.; Rosa, M.M.; Andrade, C.M.; Rubin, M.A.; et al. Neuroprotective effects of quercetin on memory and anxiogenic-like

- behavior in diabetic rats: Role of ectonucleotidases and acetylcholinesterase activities. *Biomed. Pharmacother.* **2016**, *84*, 559–568. [[CrossRef](#)] [[PubMed](#)]
293. Dajas, F.; Juan Andres, A.-C.; Florencia, A.; Carolina, E.; Felicia, R.-M. Neuroprotective Actions of Flavones and Flavonols: Mechanisms and Relationship to Flavonoid Structural Features. *Cent. Nerv. Syst. Agents Med. Chem.* **2013**, *13*, 30–35. [[CrossRef](#)] [[PubMed](#)]
  294. McCue, P.; Shetty, K. Health benefits of soy isoflavonoids and strategies for enhancement: A review. *Crit. Rev. Food Sci. Nutr.* **2004**, *44*, 361–367. [[CrossRef](#)]
  295. Dixon, R.A.; Pasinetti, G.M. Flavonoids and isoflavonoids: From plant biology to agriculture and neuroscience. *Plant Physiol.* **2010**, *154*, 453–457. [[CrossRef](#)]
  296. Curtis, P.J.; Sampson, M.; Potter, J.; Dhatariya, K.; Kroon, P.A.; Cassidy, A. Chronic ingestion of flavan-3-ols and isoflavones improves insulin sensitivity and lipoprotein status and attenuates estimated 10-year CVD risk in medicated postmenopausal women with type 2 diabetes: A 1-year, double-blind, randomized, controlled trial. *Diabetes Care* **2012**, *35*, 226–232. [[CrossRef](#)]
  297. Wang, S.; Wang, Y.; Pan, M.-H.; Ho, C.-T. Anti-obesity molecular mechanism of soy isoflavones: Weaving the way to new therapeutic routes. *Food Funct.* **2017**, *8*, 3831–3846. [[CrossRef](#)]
  298. Cao, H.; Ou, J.; Chen, L.; Zhang, Y.; Szkudelski, T.; Delmas, D.; Daglia, M.; Xiao, J. Dietary polyphenols and type 2 diabetes: Human Study and Clinical Trial. *Crit. Rev. Food Sci. Nutr.* **2019**, *59*, 3371–3379. [[CrossRef](#)]
  299. Akhlaghi, M.; Zare, M.; Nouripour, F. Effect of Soy and Soy Isoflavones on Obesity-Related Anthropometric Measures: A Systematic Review and Meta-analysis of Randomized Controlled Clinical Trials. *Adv. Nutr.* **2017**, *8*, 705–717. [[CrossRef](#)]
  300. Zhou, Y.-X.; Zhang, H.; Peng, C. Puerarin: A review of pharmacological effects. *Phytother. Res.* **2014**, *28*, 961–975. [[CrossRef](#)]
  301. Ganai, A.A.; Farooqi, H. Bioactivity of genistein: A review of in vitro and in vivo studies. *Biomed. Pharmacother.* **2015**, *76*, 30–38. [[CrossRef](#)] [[PubMed](#)]
  302. Xin, X.; Chen, C.; Hu, Y.Y.; Feng, Q. Protective effect of genistein on nonalcoholic fatty liver disease (NAFLD). *Biomed. Pharmacother.* **2019**, *117*, 109047. [[CrossRef](#)] [[PubMed](#)]
  303. Rockwood, S.; Mason, D.; Lord, R.; Lamar, P.; Prozialeck, W.; Al-Nakkash, L. Genistein diet improves body weight, serum glucose and triglyceride levels in both male and female ob/ob mice. *Diabetes. Metab. Syndr. Obes.* **2019**, *12*, 2011–2021. [[CrossRef](#)] [[PubMed](#)]
  304. Marcelo, C.; Warwick, M.; Marcelo, C.; Malik, M.; Qayyum, R. The relationship between urinary genistein levels and serum alanine aminotransferase levels in adults in the USA: National Health and Nutrition Examination Survey 1999–2010. *Eur. J. Gastroenterol. Hepatol.* **2018**, *30*, 904–909. [[CrossRef](#)]
  305. Hakkak, R.; Gauss, C.H.; Bell, A.; Korourian, S. Short-term soy protein isolate feeding prevents liver steatosis and reduces serum ALT and AST levels in obese female zucker rats. *Biomedicines* **2018**, *6*, 55. [[CrossRef](#)]
  306. Qiu, L.-X.; Chen, T. Novel insights into the mechanisms whereby isoflavones protect against fatty liver disease. *World J. Gastroenterol.* **2015**, *21*, 1099–1107. [[CrossRef](#)]
  307. Xiao, C.W.; Wood, C.M.; Weber, D.; Aziz, S.A.; Mehta, R.; Griffin, P.; Cockell, K.A. Dietary supplementation with soy isoflavones or replacement with soy proteins prevents hepatic lipid droplet accumulation and alters expression of genes involved in lipid metabolism in rats. *Genes Nutr.* **2014**, *9*, 373. [[CrossRef](#)]
  308. Arunkumar, E.; Karthik, D.; Anuradha, C.V. Genistein sensitizes hepatic insulin signaling and modulates lipid regulatory genes through p70 ribosomal S6 kinase-1 inhibition in high-fat-high-fructose diet-fed mice. *Pharm. Biol.* **2013**, *51*, 815–824. [[CrossRef](#)]
  309. Liu, H.; Zhong, H.; Yin, Y.; Jiang, Z. Genistein has beneficial effects on hepatic steatosis in high fat-high sucrose diet-treated rats. *Biomed. Pharmacother.* **2017**, *91*, 964–969. [[CrossRef](#)]
  310. Lyons, C.L.; Roche, H.M. Nutritional Modulation of AMPK-Impact upon Metabolic-Inflammation. *Int. J. Mol. Sci.* **2018**, *19*, 3092. [[CrossRef](#)]
  311. Wang, S.; Yang, F.-J.; Shang, L.-C.; Zhang, Y.-H.; Zhou, Y.; Shi, X.-L. Puerarin protects against high-fat high-sucrose diet-induced non-alcoholic fatty liver disease by modulating PARP-1/PI3K/AKT signaling pathway and facilitating mitochondrial homeostasis. *Phytother. Res.* **2019**, *33*, 2347–2359. [[CrossRef](#)] [[PubMed](#)]
  312. Zheng, G.; Lin, L.; Zhong, S.; Zhang, Q.; Li, D. Effects of puerarin on lipid accumulation and metabolism in high-fat diet-fed mice. *PLoS ONE* **2015**, *10*, e0122925. [[CrossRef](#)] [[PubMed](#)]



313. Lu, Y.; Zhao, A.; Wu, Y.; Zhao, Y.; Yang, X. Soybean soluble polysaccharides enhance bioavailability of genistein and its prevention against obesity and metabolic syndrome of mice with chronic high fat consumption. *Food Funct.* **2019**, *10*, 4153–4165. [[CrossRef](#)] [[PubMed](#)]
314. Li, W.; Lu, Y. Hepatoprotective Effects of Sophoricoside against Fructose-Induced Liver Injury via Regulating Lipid Metabolism, Oxidation, and Inflammation in Mice. *J. Food Sci.* **2018**, *83*, 552–558. [[CrossRef](#)] [[PubMed](#)]
315. Duan, X.; Meng, Q.; Wang, C.; Liu, Z.; Sun, H.; Huo, X.; Sun, P.; Ma, X.; Peng, J.; Liu, K. Effects of calycosin against high-fat diet-induced nonalcoholic fatty liver disease in mice. *J. Gastroenterol. Hepatol.* **2018**, *33*, 533–542. [[CrossRef](#)] [[PubMed](#)]
316. Liu, H.; Zhong, H.; Leng, L.; Jiang, Z. Effects of soy isoflavone on hepatic steatosis in high fat-induced rats. *J. Clin. Biochem. Nutr.* **2017**, *61*, 85–90. [[CrossRef](#)]
317. Wang, W.; Chen, J.; Mao, J.; Li, H.; Wang, M.; Zhang, H.; Li, H.; Chen, W. Genistein Ameliorates Non-alcoholic Fatty Liver Disease by Targeting the Thromboxane A2 Pathway. *J. Agric. Food Chem.* **2018**, *66*, 5853–5859. [[CrossRef](#)]
318. Gan, M.; Shen, L.; Fan, Y.; Tan, Y.; Zheng, T.; Tang, G.; Niu, L.; Zhao, Y.; Chen, L.; Jiang, D.; et al. MicroRNA-451 and Genistein Ameliorate Nonalcoholic Steatohepatitis in Mice. *Int. J. Mol. Sci.* **2019**, *20*, 6084. [[CrossRef](#)]
319. Amanat, S.; Eftekhari, M.H.; Fararouei, M.; Bagheri Lankarani, K.; Massoumi, S.J. Genistein supplementation improves insulin resistance and inflammatory state in non-alcoholic fatty liver patients: A randomized, controlled trial. *Clin. Nutr.* **2018**, *37*, 1210–1215. [[CrossRef](#)]
320. Giordano, E.; Dávalos, A.; Crespo, M.C.; Tomé-Carneiro, J.; Gómez-Coronado, D.; Visioli, F. Soy isoflavones in nutritionally relevant amounts have varied nutrigenomic effects on adipose tissue. *Molecules* **2015**, *20*, 2310–2322. [[CrossRef](#)]
321. Tan, J.; Huang, C.; Luo, Q.; Liu, W.; Cheng, D.; Li, Y.; Xia, Y.; Li, C.; Tang, L.; Fang, J.; et al. Soy Isoflavones Ameliorate Fatty Acid Metabolism of Visceral Adipose Tissue by Increasing the AMPK Activity in Male Rats with Diet-Induced Obesity (DIO). *Molecules* **2019**, *24*, 2809. [[CrossRef](#)] [[PubMed](#)]
322. Jo, Y.H.; Choi, K.M.; Liu, Q.; Kim, S.B.; Ji, H.J.; Kim, M.; Shin, S.K.; Do, S.G.; Shin, E.; Jung, G.; et al. Anti-obesity effect of 6,8-diprenylgenistein, an isoflavonoid of *Cudrania tricuspidata* fruits in high-fat diet-induced obese mice. *Nutrients* **2015**, *7*, 10480–10490. [[CrossRef](#)] [[PubMed](#)]
323. Huang, C.-H.; Chen, C.-L.; Chang, S.-H.; Tsai, G.-J. Evaluation of Antiobesity Activity of Soybean Meal Products Fermented by *Lactobacillus plantarum* FPS 2520 and *Bacillus subtilis* N1 in Rats Fed with High-Fat Diet. *J. Med. Food* **2020**, *23*, 667–675. [[CrossRef](#)] [[PubMed](#)]
324. Zhou, L.; Xiao, X.; Zhang, Q.; Zheng, J.; Li, M.; Deng, M. A Possible Mechanism: Genistein Improves Metabolism and Induces White Fat Browning through Modulating Hypothalamic Expression of Ucn3, Depp, and Stc1. *Front. Endocrinol.* **2019**, *10*, 478. [[CrossRef](#)]
325. Palacios-González, B.; Vargas-Castillo, A.; Velázquez-Villegas, L.A.; Vázquez-Reyes, S.; López, P.; Noriega, L.G.; Aleman, G.; Tovar-Palacio, C.; Torre-Villalvazo, I.; Yang, L.J.; et al. Genistein increases the thermogenic program of subcutaneous WAT and increases energy expenditure in mice. *J. Nutr. Biochem.* **2019**, *68*, 59–68. [[CrossRef](#)]
326. Gautam, J.; Khedgikar, V.; Kushwaha, P.; Choudhary, D.; Nagar, G.K.; Dev, K.; Dixit, P.; Singh, D.; Maurya, R.; Trivedi, R. Formononetin, an isoflavone, activates AMP-activated protein kinase  $\beta$ -catenin signalling to inhibit adipogenesis and rescues C57BL/6 mice from high-fat diet-induced obesity and bone loss. *Br. J. Nutr.* **2017**, *117*, 645–661. [[CrossRef](#)]
327. Nie, T.; Zhao, S.; Mao, L.; Yang, Y.; Sun, W.; Lin, X.; Liu, S.; Li, K.; Sun, Y.; Li, P.; et al. The natural compound, formononetin, extracted from *Astragalus membranaceus* increases adipocyte thermogenesis by modulating PPAR $\gamma$  activity. *Br. J. Pharmacol.* **2018**, *175*, 1439–1450. [[CrossRef](#)]
328. Buhlmann, E.; Horváth, C.; Houriet, J.; Kiehlmann, E.; Radtke, J.; Marcourt, L.; Wolfender, J.-L.; Wolfrum, C.; Schröder, S. *Puerariae lobatae* root extracts and the regulation of brown fat activity. *Phytomedicine* **2019**, *64*, 153075. [[CrossRef](#)]
329. Shen, H.-H.; Huang, S.-Y.; Kung, C.-W.; Chen, S.-Y.; Chen, Y.-F.; Cheng, P.-Y.; Lam, K.-K.; Lee, Y.-M. Genistein ameliorated obesity accompanied with adipose tissue browning and attenuation of hepatic lipogenesis in ovariectomized rats with high-fat diet. *J. Nutr. Biochem.* **2019**, *67*, 111–122. [[CrossRef](#)]
330. Russell, A.L.; Grimes, J.M.; Cruthirds, D.F.; Westerfield, J.; Wooten, L.; Keil, M.; Weiser, M.J.; Landauer, M.R.; Handa, R.J.; Wu, T.J.; et al. Dietary Isoflavone-Dependent and Estradiol Replacement Effects on Body Weight in the Ovariectomized (OVX) Rat. *Horm. Metab. Res.* **2017**, *49*, 457–465. [[CrossRef](#)]



331. Han, F.; Li, K.; Pan, R.; Xu, W.; Han, X.; Hou, N.; Sun, X. Calycosin directly improves perivascular adipose tissue dysfunction by upregulating the adiponectin/AMPK/eNOS pathway in obese mice. *Food Funct.* **2018**, *9*, 2409–2415. [[CrossRef](#)] [[PubMed](#)]
332. Rivera, P.; Pérez-Martin, M.; Pavón, F.J.; Serrano, A.; Crespillo, A.; Cifuentes, M.; López-Ávalos, M.-D.; Grondona, J.M.; Vida, M.; Fernández-Llebrez, P.; et al. Pharmacological administration of the isoflavone daidzein enhances cell proliferation and reduces high fat diet-induced apoptosis and gliosis in the rat hippocampus. *PLoS ONE* **2013**, *8*, e64750. [[CrossRef](#)] [[PubMed](#)]
333. Ko, J.W.; Chung, Y.-S.; Kwak, C.S.; Kwon, Y.H. Doenjang, A Korean Traditional Fermented Soybean Paste, Ameliorates Neuroinflammation and Neurodegeneration in Mice Fed a High-Fat Diet. *Nutrients* **2019**, *11*, 1702. [[CrossRef](#)] [[PubMed](#)]
334. Essawy, A.E.; Abdou, H.M.; Ibrahim, H.M.; Bouthahab, N.M. Soybean isoflavone ameliorates cognitive impairment, neuroinflammation, and amyloid  $\beta$  accumulation in a rat model of Alzheimer's disease. *Environ. Sci. Pollut. Res.* **2019**, *26*, 26060–26070. [[CrossRef](#)]
335. Ko, Y.H.; Kwon, S.H.; Ma, S.X.; Seo, J.Y.; Lee, B.R.; Kim, K.; Kim, S.Y.; Lee, S.Y.; Jang, C.G. The memory-enhancing effects of 7,8,4'-trihydroxyisoflavone, a major metabolite of daidzein, are associated with activation of the cholinergic system and BDNF signaling pathway in mice. *Brain Res. Bull.* **2018**, *142*, 197–206. [[CrossRef](#)]
336. Lu, C.; Wang, Y.; Wang, D.; Zhang, L.; Lv, J.; Jiang, N.; Fan, B.; Liu, X.; Wang, F. Neuroprotective effects of soy isoflavones on scopolamine-induced amnesia in mice. *Nutrients* **2018**, *10*, 853. [[CrossRef](#)]
337. Seo, J.Y.; Kim, B.R.; Oh, J.; Kim, J.S. Soybean-derived phytoalexins improve cognitive function through activation of Nrf2/HO-1 signaling pathway. *Int. J. Mol. Sci.* **2018**, *19*, 268. [[CrossRef](#)]
338. Sudhakaran, M.; Doseff, A.I. The Targeted Impact of Flavones on Obesity-Induced Inflammation and the Potential Synergistic Role in Cancer and the Gut Microbiota. *Molecules* **2020**, *25*, 2477. [[CrossRef](#)]
339. Jiang, N.; Doseff, A.I.; Grotewold, E. Flavones: From Biosynthesis to Health Benefits. *Plants* **2016**, *5*, 27. [[CrossRef](#)]
340. Lin, Y.; Ren, N.; Li, S.; Chen, M.; Pu, P. Novel anti-obesity effect of scutellarein and potential underlying mechanism of actions. *Biomed. Pharmacother.* **2019**, *117*, 109042. [[CrossRef](#)]
341. Feng, X.; Yu, W.; Li, X.; Zhou, F.; Zhang, W.; Shen, Q.; Li, J.; Zhang, C.; Shen, P. Apigenin, a modulator of PPAR $\gamma$ , attenuates HFD-induced NAFLD by regulating hepatocyte lipid metabolism and oxidative stress via Nrf2 activation. *Biochem. Pharmacol.* **2017**, *136*, 136–149. [[CrossRef](#)]
342. Kwon, E.-Y.; Kim, S.Y.; Choi, M.-S. Luteolin-Enriched Artichoke Leaf Extract Alleviates the Metabolic Syndrome in Mice with High-Fat Diet-Induced Obesity. *Nutrients* **2018**, *10*, 979. [[CrossRef](#)]
343. Dai, J.; Liang, K.; Zhao, S.; Jia, W.; Liu, Y.; Wu, H.; Lv, J.; Cao, C.; Chen, T.; Zhuang, S.; et al. Chemoproteomics reveals baicalin activates hepatic CPT1 to ameliorate diet-induced obesity and hepatic steatosis. *Proc. Natl. Acad. Sci. USA* **2018**, *115*, E5896–E5905. [[CrossRef](#)]
344. Kim, Y.-J.; Choi, M.-S.; Woo, J.T.; Jeong, M.J.; Kim, S.R.; Jung, U.J. Long-term dietary supplementation with low-dose nobilletin ameliorates hepatic steatosis, insulin resistance, and inflammation without altering fat mass in diet-induced obesity. *Mol. Nutr. Food Res.* **2017**, *61*, 1600889. [[CrossRef](#)]
345. Inamdar, S.; Joshi, A.; Malik, S.; Boppana, R.; Ghaskadbi, S. Vitexin alleviates non-alcoholic fatty liver disease by activating AMPK in high fat diet fed mice. *Biochem. Biophys. Res. Commun.* **2019**, *519*, 106–112. [[CrossRef](#)]
346. Kwon, E.-Y.; Choi, M.-S. Luteolin Targets the Toll-Like Receptor Signaling Pathway in Prevention of Hepatic and Adipocyte Fibrosis and Insulin Resistance in Diet-Induced Obese Mice. *Nutrients* **2018**, *10*, 1415. [[CrossRef](#)]
347. Kwon, E.-Y.; Jung, U.J.; Park, T.; Yun, J.W.; Choi, M.-S. Luteolin Attenuates Hepatic Steatosis and Insulin Resistance Through the Interplay Between the Liver and Adipose Tissue in Mice with Diet-Induced Obesity. *Diabetes* **2015**, *64*, 1658–1669. [[CrossRef](#)]
348. Li, J.; Inoue, J.; Choi, J.-M.; Nakamura, S.; Yan, Z.; Fushinobu, S.; Kamada, H.; Kato, H.; Hashidume, T.; Shimizu, M.; et al. Identification of the Flavonoid Luteolin as a Repressor of the Transcription Factor Hepatocyte Nuclear Factor 4 $\alpha$ . *J. Biol. Chem.* **2015**, *290*, 24021–24035. [[CrossRef](#)]
349. Yin, Y.; Gao, L.; Lin, H.; Wu, Y.; Han, X.; Zhu, Y.; Li, J. Luteolin improves non-alcoholic fatty liver disease in db/db mice by inhibition of liver X receptor activation to down-regulate expression of sterol regulatory element binding protein 1c. *Biochem. Biophys. Res. Commun.* **2017**, *482*, 720–726. [[CrossRef](#)]

350. Xi, Y.; Wu, M.; Li, H.; Dong, S.; Luo, E.; Gu, M.; Shen, X.; Jiang, Y.; Liu, Y.; Liu, H. Baicalin Attenuates High Fat Diet-Induced Obesity and Liver Dysfunction: Dose-Response and Potential Role of CaMKK $\beta$ /AMPK/ACC Pathway. *Cell. Physiol. Biochem.* **2015**, *35*, 2349–2359. [[CrossRef](#)]
351. Shen, K.; Feng, X.; Pan, H.; Zhang, F.; Xie, H.; Zheng, S. Baicalin Ameliorates Experimental Liver Cholestasis in Mice by Modulation of Oxidative Stress, Inflammation, and NRF2 Transcription Factor. *Oxid. Med. Cell. Longev.* **2017**, *2017*, 6169128. [[CrossRef](#)]
352. Chambel, S.S.; Santos-Gonçalves, A.; Duarte, T.L. The Dual Role of Nrf2 in Nonalcoholic Fatty Liver Disease: Regulation of Antioxidant Defenses and Hepatic Lipid Metabolism. *Biomed Res. Int.* **2015**, *2015*, 597134. [[CrossRef](#)]
353. Xu, D.; Xu, M.; Jeong, S.; Qian, Y.; Wu, H.; Xia, Q.; Kong, X. The Role of Nrf2 in Liver Disease: Novel Molecular Mechanisms and Therapeutic Approaches. *Front. Pharmacol.* **2019**, *9*, 1428. [[CrossRef](#)]
354. Zhang, X.; Ji, R.; Sun, H.; Peng, J.; Ma, X.; Wang, C.; Fu, Y.; Bao, L.; Jin, Y. Scutellarin ameliorates nonalcoholic fatty liver disease through the PPAR $\gamma$ /PGC-1 $\alpha$ -Nrf2 pathway. *Free Radic. Res.* **2018**, *52*, 198–211. [[CrossRef](#)]
355. Fan, H.; Ma, X.; Lin, P.; Kang, Q.; Zhao, Z.; Wang, L.; Sun, D.; Cheng, J.; Li, Y. Scutellarin Prevents Nonalcoholic Fatty Liver Disease (NAFLD) and Hyperlipidemia via PI3K/AKT-Dependent Activation of Nuclear Factor (Erythroid-Derived 2)-Like 2 (Nrf2) in Rats. *Med. Sci. Monit.* **2017**, *23*, 5599–5612. [[CrossRef](#)]
356. Feng, X.; Weng, D.; Zhou, F.; Owen, Y.D.; Qin, H.; Zhao, J.; Huang, Y.; Chen, J.; Fu, H.; Yang, N.; et al. Activation of PPAR $\gamma$  by a Natural Flavonoid Modulator, Apigenin Ameliorates Obesity-Related Inflammation Via Regulation of Macrophage Polarization. *EBioMedicine* **2016**, *9*, 61–76. [[CrossRef](#)]
357. Lv, Y.; Gao, X.; Luo, Y.; Fan, W.; Shen, T.; Ding, C.; Yao, M.; Song, S.; Yan, L. Apigenin ameliorates HFD-induced NAFLD through regulation of the XO/NLRP3 pathways. *J. Nutr. Biochem.* **2019**, *71*, 110–121. [[CrossRef](#)]
358. Feng, X.; Qin, H.; Shi, Q.; Zhang, Y.; Zhou, F.; Wu, H.; Ding, S.; Niu, Z.; Lu, Y.; Shen, P. Chrysin attenuates inflammation by regulating M1/M2 status via activating PPAR $\gamma$ . *Biochem. Pharmacol.* **2014**, *89*, 503–514. [[CrossRef](#)]
359. Chen, J.; Liu, J.; Wang, Y.; Hu, X.; Zhou, F.; Hu, Y.; Yuan, Y.; Xu, Y. Wogonin mitigates nonalcoholic fatty liver disease via enhancing PPAR $\alpha$ /AdipoR2, in vivo and in vitro. *Biomed. Pharmacother.* **2017**, *91*, 621–631. [[CrossRef](#)]
360. Pan, M.-H.; Yang, G.; Li, S.; Li, M.-Y.; Tsai, M.-L.; Wu, J.-C.; Badmaev, V.; Ho, C.-T.; Lai, C.-S. Combination of citrus polymethoxyflavones, green tea polyphenols, and Lychee extracts suppresses obesity and hepatic steatosis in high-fat diet induced obese mice. *Mol. Nutr. Food Res.* **2017**, *61*, 1601104. [[CrossRef](#)]
361. Su, T.; Huang, C.; Yang, C.; Jiang, T.; Su, J.; Chen, M.; Fatima, S.; Gong, R.; Hu, X.; Bian, Z.; et al. Apigenin inhibits STAT3/CD36 signaling axis and reduces visceral obesity. *Pharmacol. Res.* **2020**, *152*, 104586. [[CrossRef](#)]
362. Zhang, J.; Zhao, L.; Cheng, Q.; Ji, B.; Yang, M.; Sanidad, K.Z.; Wang, C.; Zhou, F. Structurally Different Flavonoid Subclasses Attenuate High-Fat and High-Fructose Diet Induced Metabolic Syndrome in Rats. *J. Agric. Food Chem.* **2018**, *66*, 12412–12420. [[CrossRef](#)]
363. Sun, Y.-S.; Qu, W. Dietary Apigenin promotes lipid catabolism, thermogenesis, and browning in adipose tissues of HFD-Fed mice. *Food Chem. Toxicol.* **2019**, *133*, 110780. [[CrossRef](#)]
364. Peng, Y.; Sun, Q.; Xu, W.; He, Y.; Jin, W.; Yuan, L.; Gao, R. Vitexin ameliorates high fat diet-induced obesity in male C57BL/6J mice via the AMPK $\alpha$ -mediated pathway. *Food Funct.* **2019**, *10*, 1940–1947. [[CrossRef](#)]
365. Zhang, L.; Han, Y.-J.; Zhang, X.; Wang, X.; Bao, B.; Qu, W.; Liu, J. Luteolin reduces obesity-associated insulin resistance in mice by activating AMPK $\alpha$ 1 signalling in adipose tissue macrophages. *Diabetologia* **2016**, *59*, 2219–2228. [[CrossRef](#)]
366. Xu, N.; Zhang, L.; Dong, J.; Zhang, X.; Chen, Y.-G.; Bao, B.; Liu, J. Low-dose diet supplement of a natural flavonoid, luteolin, ameliorates diet-induced obesity and insulin resistance in mice. *Mol. Nutr. Food Res.* **2014**, *58*, 1258–1268. [[CrossRef](#)]
367. Sanchez-Gurmaches, J.; Tang, Y.; Jaspersen, N.Z.; Wallace, M.; Martinez Calejman, C.; Gujja, S.; Li, H.; Edwards, Y.J.K.; Wolfrum, C.; Metallo, C.M.; et al. Brown Fat AKT2 Is a Cold-Induced Kinase that Stimulates ChREBP-Mediated De Novo Lipogenesis to Optimize Fuel Storage and Thermogenesis. *Cell Metab.* **2018**, *27*, 195–209. [[CrossRef](#)]
368. Mottillo, E.P.; Balasubramanian, P.; Lee, Y.-H.; Weng, C.; Kershaw, E.E.; Granneman, J.G. Coupling of lipolysis and de novo lipogenesis in brown, beige, and white adipose tissues during chronic  $\beta$ 3-adrenergic receptor activation. *J. Lipid Res.* **2014**, *55*, 2276–2286. [[CrossRef](#)]

369. Zhang, X.; Zhang, Q.-X.; Wang, X.; Zhang, L.; Qu, W.; Bao, B.; Liu, C.-A.; Liu, J. Dietary luteolin activates browning and thermogenesis in mice through an AMPK/PGC1 $\alpha$  pathway-mediated mechanism. *Int. J. Obes.* **2016**, *40*, 1841–1849. [\[CrossRef\]](#)
370. Min, W.; Wu, M.; Fang, P.; Yu, M.; Shi, M.; Zhang, Z.; Bo, P. Effect of Baicalein on GLUT4 Translocation in Adipocytes of Diet-Induced Obese Mice. *Cell. Physiol. Biochem.* **2018**, *50*, 426–436. [\[CrossRef\]](#)
371. Jack, B.U.; Malherbe, C.J.; Mamushi, M.; Muller, C.J.F.; Joubert, E.; Louw, J.; Pfeiffer, C. Adipose tissue as a possible therapeutic target for polyphenols: A case for Cyclopia extracts as anti-obesity nutraceuticals. *Biomed. Pharmacother.* **2019**, *120*, 109439. [\[CrossRef\]](#)
372. Pan, M.-H.; Li, M.-Y.; Tsai, M.-L.; Pan, C.-Y.; Badmaev, V.; Ho, C.-T.; Lai, C.-S. A mixture of citrus polymethoxyflavones, green tea polyphenols and lychee extracts attenuates adipogenesis in 3T3-L1 adipocytes and obesity-induced adipose inflammation in mice. *Food Funct.* **2019**, *10*, 7667–7677. [\[CrossRef\]](#)
373. Liu, Y.; Fu, X.; Lan, N.; Li, S.; Zhang, J.; Wang, S.; Li, C.; Shang, Y.; Huang, T.; Zhang, L. Luteolin protects against high fat diet-induced cognitive deficits in obesity mice. *Behav. Brain Res.* **2014**, *267*, 178–188. [\[CrossRef\]](#)
374. Shanmugasundaram, J.; Subramanian, V.; Nadipelly, J.; Kathirvelu, P.; Sayeli, V.; Cheriyan, B.V. Anxiolytic-like activity of 5-methoxyflavone in mice with involvement of GABAergic and serotonergic systems—In vivo and in silico evidences. *Eur. Neuropsychopharmacol.* **2020**, *36*, 100–110. [\[CrossRef\]](#)
375. Wang, L.; Li, C.; Sreeharsha, N.; Mishra, A.; Shrotriya, V.; Sharma, A. Neuroprotective effect of Wogonin on Rat's brain exposed to gamma irradiation. *J. Photochem. Photobiol. B* **2020**, *204*, 111775. [\[CrossRef\]](#)
376. Wu, C.; Xu, Q.; Chen, X.; Liu, J. Delivery luteolin with folacin-modified nanoparticle for glioma therapy. *Int. J. Nanomed.* **2019**, *14*, 7515–7531. [\[CrossRef\]](#)
377. Guo, Y.; Yu, X.-M.; Chen, S.; Wen, J.-Y.; Chen, Z.-W. Total flavones of *Rhododendron simsii* Planch flower protect rat hippocampal neuron from hypoxia-reoxygenation injury via activation of BK(Ca) channel. *J. Pharm. Pharmacol.* **2020**, *72*, 111–120. [\[CrossRef\]](#)
378. Yu, C.-I.; Cheng, C.-I.; Kang, Y.-F.; Chang, P.-C.; Lin, I.-P.; Kuo, Y.-H.; Jhou, A.-J.; Lin, M.-Y.; Chen, C.-Y.; Lee, C.-H. Hispidulin Inhibits Neuroinflammation in Lipopolysaccharide-Activated BV2 Microglia and Attenuates the Activation of Akt, NF- $\kappa$ B, and STAT3 Pathway. *Neurotox. Res.* **2020**, *38*, 163–174. [\[CrossRef\]](#)
379. Cazarolli, L.H.; Kappel, V.D.; Zanatta, A.P.; Suzuki, D.O.H.; Yunes, R.A.; Nunes, R.J.; Pizzolatti, M.G.; Silva, F.R.M.B. Chapter 2—Natural and Synthetic Chalcones: Tools for the Study of Targets of Action—Insulin Secretagogue or Insulin Mimetic? In *Studies in Natural Products Chemistry*; Atta-ur-Rahman, Ed.; Elsevier: Amsterdam, The Netherlands, 2013; Volume 39, pp. 47–89. ISBN 1572-5995.
380. Bak, E.-J.; Choi, K.-C.; Jang, S.; Woo, G.-H.; Yoon, H.-G.; Na, Y.; Yoo, Y.-J.; Lee, Y.; Jeong, Y.; Cha, J.-H. Licochalcone F alleviates glucose tolerance and chronic inflammation in diet-induced obese mice through Akt and p38 MAPK. *Clin. Nutr.* **2016**, *35*, 414–421. [\[CrossRef\]](#)
381. Karimi-Sales, E.; Mohaddes, G.; Alipour, M.R. Chalcones as putative hepatoprotective agents: Preclinical evidence and molecular mechanisms. *Pharmacol. Res.* **2018**, *129*, 177–187. [\[CrossRef\]](#)
382. Iwasaki, M.; Izuo, N.; Izumi, Y.; Takada-Takatori, Y.; Akaike, A.; Kume, T. Protective Effect of Green Perilla-Derived Chalcone Derivative DDC on Amyloid  $\beta$  Protein-Induced Neurotoxicity in Primary Cortical Neurons. *Biol. Pharm. Bull.* **2019**, *42*, 1942–1946. [\[CrossRef\]](#) [\[PubMed\]](#)
383. Bai, P.; Wang, K.; Zhang, P.; Shi, J.; Cheng, X.; Zhang, Q.; Zheng, C.; Cheng, Y.; Yang, J.; Lu, X.; et al. Development of chalcone-O-alkylamine derivatives as multifunctional agents against Alzheimer's disease. *Eur. J. Med. Chem.* **2019**, *183*, 111737. [\[CrossRef\]](#) [\[PubMed\]](#)
384. Padmavathi, G.; Roy, N.K.; Bordoloi, D.; Arfuso, F.; Mishra, S.; Sethi, G.; Bishayee, A.; Kunnumakkara, A.B. Butein in health and disease: A comprehensive review. *Phytomedicine* **2017**, *25*, 118–127. [\[CrossRef\]](#) [\[PubMed\]](#)
385. Legette, L.L.; Moreno Luna, A.Y.; Reed, R.L.; Miranda, C.L.; Bobe, G.; Proteau, R.R.; Stevens, J.F. Xanthohumol lowers body weight and fasting plasma glucose in obese male Zucker fa/fa rats. *Phytochemistry* **2013**, *91*, 236–241. [\[CrossRef\]](#)
386. Costa, R.; Rodrigues, I.; Guardão, L.; Rocha-Rodrigues, S.; Silva, C.; Magalhães, J.; Ferreira-de-Almeida, M.; Negrão, R.; Soares, R. Xanthohumol and 8-prenylnaringenin ameliorate diabetic-related metabolic dysfunctions in mice. *J. Nutr. Biochem.* **2017**, *45*, 39–47. [\[CrossRef\]](#)
387. Prabhu, D.S.; Rajeswari, V.D. PPAR-Gamma as putative gene target involved in Butein mediated anti-diabetic effect. *Mol. Biol. Rep.* **2020**. [\[CrossRef\]](#)

388. Johnson, R.; de Beer, D.; Dłudla, P.V.; Ferreira, D.; Muller, C.J.; Joubert, E. Aspalathin from Rooibos (*Aspalathus linearis*): A Bioactive C-glucosyl Dihydrochalcone with Potential to Target the Metabolic Syndrome. *Planta Med.* **2018**, *84*, 568–583. [\[CrossRef\]](#)
389. Zhu, X.; Liu, J.; Chen, S.; Xue, J.; Huang, S.; Wang, Y.; Chen, O. Isoliquiritigenin attenuates lipopolysaccharide-induced cognitive impairment through antioxidant and anti-inflammatory activity. *BMC Neurosci.* **2019**, *20*, 41. [\[CrossRef\]](#)
390. Cardozo, C.M.L.; Inada, A.C.; Cardoso, C.A.L.; Filiú, W.F.D.O.; Farias, B.B.D.; Alves, F.M.; Tataru, M.B.; Croda, J.H.R.; Guimarães, R.D.C.A.; Hiane, P.A.; et al. Effect of Supplementation with Hydroethanolic Extract of *Campomanesia xanthocarpa* (Berg.) Leaves and Two Isolated Substances from the Extract on Metabolic Parameters of Mice Fed a High-Fat Diet. *Molecules* **2020**, *25*, 2693. [\[CrossRef\]](#)
391. Hsieh, C.-T.; Chang, F.-R.; Tsai, Y.-H.; Wu, Y.-C.; Hsieh, T.-J. 2-Bromo-4'-methoxychalcone and 2-Iodo-4'-methoxychalcone Prevent Progression of Hyperglycemia and Obesity via 5'-Adenosine-Monophosphate-Activated Protein Kinase in Diet-Induced Obese Mice. *Int. J. Mol. Sci.* **2018**, *19*, 2763. [\[CrossRef\]](#)
392. Iniguez, A.B.; Zhu, M.-J. Hop bioactive compounds in prevention of nutrition-related noncommunicable diseases. *Crit. Rev. Food Sci. Nutr.* **2020**, 1–14. [\[CrossRef\]](#) [\[PubMed\]](#)
393. Liou, C.-J.; Lee, Y.-K.; Ting, N.-C.; Chen, Y.-L.; Shen, S.-C.; Wu, S.-J.; Huang, W.-C. Protective Effects of Licochalcone A Ameliorates Obesity and Non-Alcoholic Fatty Liver Disease Via Promotion of the Sirt-1/AMPK Pathway in Mice Fed a High-Fat Diet. *Cells* **2019**, *8*, 447. [\[CrossRef\]](#) [\[PubMed\]](#)
394. Jalalvand, F.; Amoli, M.M.; Yaghmaei, P.; Kimiagar, M.; Ebrahim-Habibi, A. Acarbose versus trans-chalcone: Comparing the effect of two glycosidase inhibitors on obese mice. *Arch. Endocrinol. Metab.* **2015**, *59*, 202–209. [\[CrossRef\]](#) [\[PubMed\]](#)
395. Dorn, C.; Kraus, B.; Motyl, M.; Weiss, T.S.; Gehrig, M.; Schölmerich, J.; Heilmann, J.; Hellerbrand, C. Xanthohumol, a chalcone derived from hops, inhibits hepatic inflammation and fibrosis. *Mol. Nutr. Food Res.* **2010**, *54*, S205–S213. [\[CrossRef\]](#)
396. Takahashi, K.; Osada, K. Effect of Dietary Purified Xanthohumol from Hop (*Humulus lupulus* L.) Pomace on Adipose Tissue Mass, Fasting Blood Glucose Level, and Lipid Metabolism in KK-Ay Mice. *J. Oleo Sci.* **2017**, *66*, 531–541. [\[CrossRef\]](#)
397. Mahli, A.; Seitz, T.; Freese, K.; Frank, J.; Weiskirchen, R.; Abdel-Tawab, M.; Behnam, D.; Hellerbrand, C. Therapeutic Application of Micellar Solubilized Xanthohumol in a Western-Type Diet-Induced Mouse Model of Obesity, Diabetes and Non-Alcoholic Fatty Liver Disease. *Cells* **2019**, *8*, 359. [\[CrossRef\]](#)
398. Son, M.J.; Minakawa, M.; Miura, Y.; Yagasaki, K. Aspalathin improves hyperglycemia and glucose intolerance in obese diabetic ob/ob mice. *Eur. J. Nutr.* **2013**, *52*, 1607–1619. [\[CrossRef\]](#)
399. Mazibuko-Mbeje, S.E.; Dłudla, P.V.; Roux, C.; Johnson, R.; Ghoor, S.; Joubert, E.; Louw, J.; Opoku, A.R.; Muller, C.J.F. Aspalathin-Enriched Green Rooibos Extract Reduces Hepatic Insulin Resistance by Modulating PI3K/AKT and AMPK Pathways. *Int. J. Mol. Sci.* **2019**, *20*, 633. [\[CrossRef\]](#)
400. Lee, Y.; Kwon, E.-Y.; Choi, M.-S. Dietary Isoliquiritigenin at a Low Dose Ameliorates Insulin Resistance and NAFLD in Diet-Induced Obesity in C57BL/6j Mice. *Int. J. Mol. Sci.* **2018**, *19*, 3281. [\[CrossRef\]](#)
401. Bao, L.D.; Wang, Y.; Ren, X.H.; Ma, R.L.; Lv, H.J.; Agula, B. Hypolipidemic effect of safflower yellow and primary mechanism analysis. *Genet. Mol. Res.* **2015**, *14*, 6270–6278. [\[CrossRef\]](#)
402. Ohnogi, H.; Hayami, S.; Kudo, Y.; Deguchi, S.; Mizutani, S.; Enoki, T.; Tanimura, Y.; Aoi, W.; Naito, Y.; Kato, I.; et al. Angelica keiskei Extract Improves Insulin Resistance and Hypertriglyceridemia in Rats Fed a High-Fructose Drink. *Biosci. Biotechnol. Biochem.* **2012**, *76*, 928–932. [\[CrossRef\]](#) [\[PubMed\]](#)
403. Zhang, T.; Yamashita, Y.; Yasuda, M.; Yamamoto, N.; Ashida, H. Ashitaba (*Angelica keiskei*) extract prevents adiposity in high-fat diet-fed C57BL/6 mice. *Food Funct.* **2015**, *6*, 135–145. [\[CrossRef\]](#) [\[PubMed\]](#)
404. Karkhaneh, L.; Yaghmaei, P.; Parivar, K.; Sadeghizadeh, M.; Ebrahim-Habibi, A. Effect of trans-chalcone on atheroma plaque formation, liver fibrosis and adiponectin gene expression in cholesterol-fed NMRI mice. *Pharmacol. Reports* **2016**, *68*, 720–727. [\[CrossRef\]](#)
405. Nozawa, H. Xanthohumol, the chalcone from beer hops (*Humulus lupulus* L.), is the ligand for farnesoid X receptor and ameliorates lipid and glucose metabolism in KK-Ay mice. *Biochem. Biophys. Res. Commun.* **2005**, *336*, 754–761. [\[CrossRef\]](#) [\[PubMed\]](#)

406. Lee, H.E.; Yang, G.; Han, S.-H.; Lee, J.-H.; An, T.-J.; Jang, J.-K.; Lee, J.Y. Anti-obesity potential of Glycyrrhiza uralensis and licochalcone A through induction of adipocyte browning. *Biochem. Biophys. Res. Commun.* **2018**, *503*, 2117–2123. [[CrossRef](#)]
407. Strycharz, J.; Rygielska, Z.; Swiderska, E.; Drzewoski, J.; Szemraj, J.; Szmigiero, L.; Sliwinska, A. SIRT1 as a Therapeutic Target in Diabetic Complications. *Curr. Med. Chem.* **2018**, *25*, 1002–1035. [[CrossRef](#)]
408. Wang, Z.; Ka, S.-O.; Lee, Y.; Park, B.-H.; Bae, E.J. Butein induction of HO-1 by p38 MAPK/Nrf2 pathway in adipocytes attenuates high-fat diet induced adipose hypertrophy in mice. *Eur. J. Pharmacol.* **2017**, *799*, 201–210. [[CrossRef](#)]
409. Song, N.-J.; Choi, S.; Rajbhandari, P.; Chang, S.-H.; Kim, S.; Vergnes, L.; Kwon, S.-M.; Yoon, J.-H.; Lee, S.; Ku, J.-M.; et al. Prdm4 induction by the small molecule butein promotes white adipose tissue browning. *Nat. Chem. Biol.* **2016**, *12*, 479–481. [[CrossRef](#)]
410. Song, N.-J.; Chang, S.-H.; Kim, S.; Panic, V.; Jang, B.-H.; Yun, U.J.; Choi, J.H.; Li, Z.; Park, K.-M.; Yoon, J.-H.; et al. PI3Ka-Akt1-mediated Prdm4 induction in adipose tissue increases energy expenditure, inhibits weight gain, and improves insulin resistance in diet-induced obese mice. *Cell Death Dis.* **2018**, *9*, 876. [[CrossRef](#)]
411. Hemmerlyckx, B.; Vranckx, C.; Bauters, D.; Lijnen, H.R.; Scroyen, I. Does butein affect adipogenesis? *Adipocyte* **2019**, *8*, 209–222. [[CrossRef](#)]
412. Zhu, H.; Wang, X.; Pan, H.; Dai, Y.; Li, N.; Wang, L.; Yang, H.; Gong, F. The Mechanism by Which Safflower Yellow Decreases Body Fat Mass and Improves Insulin Sensitivity in HFD-Induced Obese Mice. *Front. Pharmacol.* **2016**, *7*, 127. [[CrossRef](#)]
413. Del Rio, D.; Rodriguez-Mateos, A.; Spencer, J.P.E.; Tognolini, M.; Borges, G.; Crozier, A. Dietary (poly)phenolics in human health: Structures, bioavailability, and evidence of protective effects against chronic diseases. *Antioxid. Redox Signal.* **2013**, *18*, 1818–1892. [[CrossRef](#)] [[PubMed](#)]
414. Cory, H.; Passarelli, S.; Szeto, J.; Tamez, M.; Mattei, J. The Role of Polyphenols in Human Health and Food Systems: A Mini-Review. *Front. Nutr.* **2018**, *5*, 1–9. [[CrossRef](#)] [[PubMed](#)]
415. Kim, Y.A.; Keogh, J.B.; Clifton, P.M. Polyphenols and glycémie control. *Nutrients* **2016**, *8*, 17. [[CrossRef](#)] [[PubMed](#)]
416. Schön, C.; Wacker, R.; Micka, A.; Steudle, J.; Lang, S.; Bonnländer, B. Bioavailability study of maqui berry extract in healthy subjects. *Nutrients* **2018**, *10*, 1720. [[CrossRef](#)] [[PubMed](#)]
417. Monagas, M.; Urpi-Sarda, M.; Sánchez-Patán, F.; Llorach, R.; Garrido, I.; Gómez-Cordovés, C.; Andres-Lacueva, C.; Bartolomé, B. Insights into the metabolism and microbial biotransformation of dietary flavan-3-ols and the bioactivity of their metabolites. *Food Funct.* **2010**, *1*, 233–253. [[CrossRef](#)]
418. Cardona, F.; Andr??s-Lacueva, C.; Tulipani, S.; Tinahones, F.J.; Queipo-Ortu??o, M.I. Benefits of polyphenols on gut microbiota and implications in human health. *J. Nutr. Biochem.* **2013**, *24*, 1415–1422. [[CrossRef](#)]
419. Mandalari, G.; Vardakou, M.; Faulks, R.; Bisignano, C.; Martorana, M.; Smeriglio, A.; Trombetta, D. Food Matrix Effects of Polyphenol Bioaccessibility from Almond Skin during Simulated Human Digestion. *Nutrients* **2016**, *8*, 568. [[CrossRef](#)]
420. Pineda-Vadillo, C.; Nau, F.; Dubiard, C.G.; Cheynier, V.; Meudec, E.; Sanz-Buenhombre, M.; Guadarrama, A.; Tóth, T.; Csavajda, É.; Hingyi, H.; et al. In vitro digestion of dairy and egg products enriched with grape extracts: Effect of the food matrix on polyphenol bioaccessibility and antioxidant activity. *Food Res. Int.* **2016**, *88*, 284–292. [[CrossRef](#)]
421. Dufour, C.; Loonis, M.; Delosière, M.; Buffière, C.; Hafnaoui, N.; Santé-Lhoutellier, V.; Rémond, D. The matrix of fruit & vegetables modulates the gastrointestinal bioaccessibility of polyphenols and their impact on dietary protein digestibility. *Food Chem.* **2018**, *240*, 314–322.
422. Wojtunik-Kulesza, K.; Oniszczuk, A.; Oniszczuk, T.; Combrzyński, M.; Nowakowska, D.; Matwijczuk, A. Influence of In Vitro Digestion on Composition, Bioaccessibility and Antioxidant Activity of Food Polyphenols-A Non-Systematic Review. *Nutrients* **2020**, *12*, 1401. [[CrossRef](#)] [[PubMed](#)]
423. Tarko, T.; Duda-Chodak, A. Influence of Food Matrix on the Bioaccessibility of Fruit Polyphenolic Compounds. *J. Agric. Food Chem.* **2020**, *68*, 1315–1325. [[CrossRef](#)] [[PubMed](#)]
424. Rinaldi de Alvarenga, J.F.; Quifer-Rada, P.; Francetto Juliano, F.; Hurtado-Barroso, S.; Illan, M.; Torrado-Prat, X.; Lamuela-Raventós, R.M. Using Extra Virgin Olive Oil to Cook Vegetables Enhances Polyphenol and Carotenoid Extractability: A Study Applying the sofrito Technique. *Molecules* **2019**, *24*, 1555. [[CrossRef](#)] [[PubMed](#)]

425. Beltrán Sanahuja, A.; De Pablo Gallego, S.L.; Maestre Pérez, S.E.; Valdés García, A.; Prats Moya, M.S. Influence of Cooking and Ingredients on the Antioxidant Activity, Phenolic Content and Volatile Profile of Different Variants of the Mediterranean Typical Tomato Sofrito. *Antioxidants* **2019**, *8*, 551. [[CrossRef](#)] [[PubMed](#)]
426. Rinaldi de Alvarenga, J.F.; Quifer-Rada, P.; Westrin, V.; Hurtado-Barroso, S.; Torrado-Prat, X.; Lamuela-Raventós, R.M. Mediterranean soffrito home-cooking technique enhances polyphenol content in tomato sauce. *J. Sci. Food Agric.* **2019**, *99*, 6535–6545. [[CrossRef](#)] [[PubMed](#)]
427. Bouayed, J.; Bohn, T. Exogenous antioxidants—Double-edged swords in cellular redox state: Health beneficial effects at physiologic doses versus deleterious effects at high doses. *Oxid. Med. Cell. Longev.* **2010**, *3*, 228–237. [[CrossRef](#)]
428. Liu, J.; Hao, W.; He, Z.; Kwek, E.; Zhao, Y.; Zhu, H.; Liang, N.; Ma, K.Y.; Lei, L.; He, W.-S.; et al. Beneficial effects of tea water extracts on the body weight and gut microbiota in C57BL/6j mice fed with a high-fat diet. *Food Funct.* **2019**, *10*, 2847–2860. [[CrossRef](#)]
429. Liu, J.; Yue, S.; Yang, Z.; Feng, W.; Meng, X.; Wang, A.; Peng, C.; Wang, C.; Yan, D. Oral hydroxysafflor yellow A reduces obesity in mice by modulating the gut microbiota and serum metabolism. *Pharmacol. Res.* **2018**, *134*, 40–50. [[CrossRef](#)]



© 2020 by the authors. Licensee MDPI, Basel, Switzerland. This article is an open access article distributed under the terms and conditions of the Creative Commons Attribution (CC BY) license (<http://creativecommons.org/licenses/by/4.0/>).



## 7.2. Scientific Article

Sanz-Lamora H, Marrero PF, Haro D, Relat J. A Mixture of Pure, Isolated Polyphenols Worsens the Insulin Resistance and Induces Kidney and Liver Fibrosis Markers in Diet-Induced Obese Mice. Vol. 11, Antioxidants. 2022.







## Article

# A Mixture of Pure, Isolated Polyphenols Worsens the Insulin Resistance and Induces Kidney and Liver Fibrosis Markers in Diet-Induced Obese Mice

Hèctor Sanz-Lamora <sup>1,2</sup>, Pedro F. Marrero <sup>1,3,4</sup>, Diego Haro <sup>1,3,4,\*</sup> and Joana Relat <sup>1,2,4,\*</sup>

<sup>1</sup> Department of Nutrition, Food Sciences and Gastronomy, School of Pharmacy and Food Sciences, Food Torribera Campus, University of Barcelona, E-08921 Santa Coloma de Gramenet, Spain; h.sanz.lamora@ub.edu (H.S.-L.); pedromarrero@ub.edu (P.F.M.)

<sup>2</sup> Institute for Nutrition and Food Safety Research, University of Barcelona (INSA-UB), E-08921 Santa Coloma de Gramenet, Spain

<sup>3</sup> Institute of Biomedicine, University of Barcelona (IBUB), E-08028 Barcelona, Spain

<sup>4</sup> CIBER Physiopathology of Obesity and Nutrition (CIBER-OBN), Instituto de Salud Carlos III, E-28029 Madrid, Spain

\* Correspondence: dharo@ub.edu (D.H.); jrelat@ub.edu (J.R.); Tel.: +34-934-033-790 (D.H.); +34-934-020-862 (J.R.)



**Citation:** Sanz-Lamora, H.; Marrero, P.F.; Haro, D.; Relat, J. A Mixture of Pure, Isolated Polyphenols Worsens the Insulin Resistance and Induces Kidney and Liver Fibrosis Markers in Diet-Induced Obese Mice. *Antioxidants* **2022**, *11*, 120. <https://doi.org/10.3390/antiox11010120>

**Academic Editors:**  
Victoria Cachafeiro and  
Ernesto Martínez-Martínez

Received: 2 November 2021  
Accepted: 1 January 2022  
Published: 5 January 2022

**Publisher's Note:** MDPI stays neutral with regard to jurisdictional claims in published maps and institutional affiliations.



**Copyright:** © 2022 by the authors. Licensee MDPI, Basel, Switzerland. This article is an open access article distributed under the terms and conditions of the Creative Commons Attribution (CC BY) license (<https://creativecommons.org/licenses/by/4.0/>).

**Abstract:** Obesity is a worldwide epidemic with severe metabolic consequences. Polyphenols are secondary metabolites in plants and the most abundant dietary antioxidants, which possess a wide range of health effects. The most relevant food sources are fruit and vegetables, red wine, black and green tea, coffee, virgin olive oil, and chocolate, as well as nuts, seeds, herbs, and spices. The aim of this work was to evaluate the ability of a pure, isolated polyphenol supplementation to counteract the pernicious metabolic effects of a high-fat diet (HFD). Our results indicated that the administration of pure, isolated polyphenols under HFD conditions for 26 weeks worsened the glucose metabolism in diet-induced obese mice. The data showed that the main target organ for these undesirable effects were the kidneys, where we observed fibrotic, oxidative, and kidney-disease markers. This work led us to conclude that the administration of pure polyphenols as a food supplement would not be advisable. Instead, the ingestion of complete “whole” foods would be the best way to get the health effects of bioactive compounds such as polyphenols.

**Keywords:** antioxidants; food matrix; insulin resistance; kidney disease; obesity; polyphenols

## 1. Introduction

Obesity is a worldwide epidemic with severe metabolic consequences. Obesity and its metabolic-related disorders are caused by various complex issues, one of which is an impairment of the adipose tissue functionality and expansion that result in an accumulation of lipids in organs such as liver, heart, pancreas, kidney, out of the white adipose tissue (WAT) [1,2] and an increase in circulating prooxidative, inflammatory adipokines [3,4].

The properties of bioactive compounds and the identification of new therapeutic targets have indicated their potential for the prevention and treatment of metabolic diseases such as obesity and its comorbidities [5]. Polyphenols are secondary metabolites in plants and the most abundant dietary antioxidants, which possess a wide range of health effects [5]. The most relevant food sources are fruit and vegetables, red wine, black and green tea, coffee, virgin olive oil, and chocolate, as well as nuts, seeds, herbs, and spices [6].

Polyphenols have been described as regulators of glucose homeostasis and insulin sensitivity by reducing hepatic glucose output, stimulating insulin secretion, and inhibiting glucose absorption in the intestines [7]. Furthermore, it has been suggested that the antioxidant capacity of polyphenols may protect against the reactive-oxygen-species (ROS)-related diseases such as insulin resistance, mitochondrial dysfunction, type 2 diabetes,

inflammation [8]. Polyphenols have also been shown to induce apoptosis in cancer cells, which interferes with tumor generation and progression [9]. Furthermore, polyphenols' effects have also been observed via lipid profile tests, inducing a hypolipidemic effect that reduced triglycerides as well as total and LDL cholesterol [10].

The bioavailability of polyphenols is low and can be modified by the attachment of additional functional groups onto their basic chemical structures (aglycons). Around 8000 structures of polyphenols have been described; basically, at least one phenolic ring with one or more hydroxyl groups attached can have a diverse physiological impact [11–13]. The absorption of polyphenols depends on the dose and the type, and their effects are associated with their bioavailability and pharmacokinetics [14]. In the intestinal tract, they have shown limited stability and a low absorption rate, likely related to the microbiome which transforms the ingested polyphenols to their active metabolites [15]. Once absorbed, polyphenols are metabolized after their arrival in the liver via portal circulation. This process has been shown to modify their structure and, as a result, their bioavailability and bioactivity [7,16]. Ultimately, the conjugated metabolites reach the bloodstream and the targeted tissues [7,16–18]. Moreover, the inclusion of polyphenols in a food matrix changes its bioavailability, safety, and biological activities [19–21]. Although most digestion assays have been done *in vitro* [22], other research has suggested that food matrices protect the bioactive compounds from intestinal degradation [20,23]. In addition, it has also been reported that exogenous supplementation with isolated bioactive compounds with antioxidant properties may be toxic [24].

Therefore, the aim of this work was to evaluate the ability of a pure, isolated polyphenol supplementation to counteract the pernicious metabolic effects of a high-fat diet (HFD).

For the design of the polyphenol mixture, we included at least one pure isolated compound from each group of the most consumed polyphenols included in the “Mediterranean diet” [25]. Synthetic flavanones, phenolic acids, stilbenes, and tyrosols were included, and a representative compound for each group was selected according to its ease of acquisition and its economic cost. As we were designing a hypothetical-yet-realistic food supplement, we needed to create one that was affordable, safe, and effective.

The total amount of polyphenols added to the diet was calculated according to the polyphenol intake recommended as beneficial by the PREDIMED study, 820 mg in a human diet of 2300 kcal [25,26], and we calculated the dosage for the mice according to our previous research [27,28]. Detailed information about the nutritional intervention used is described below in the materials and methods section.

Our results indicated that the administration of pure, isolated polyphenols within a HFD worsened the glucose metabolism in diet-induced obese mice. The data presented suggest that the main target organ for these undesirable effects were the kidneys, where we observed fibrotic, oxidative, and kidney-disease markers, thus indicating that the administration of pure isolated polyphenols as a food supplement would not be advisable.

## 2. Materials and Methods

### 2.1. Animal Procedures: Dosage Regimen

All the procedures described in this paper were approved by the Animal Ethics Committee at the University of Barcelona (CEEA-UB-137/18P2). Four-week-old normoglycemic C57BL/6J littermate male mice were randomly divided into three groups: mice fed with a standard chow diet (Chow; Envigo 2918) ( $n = 8$ ); mice fed with a 45% fat-derived-calories diet (HFD, D12451, Research Diets) ( $n = 11$ ); and mice fed with a high-fat diet supplemented with pure, isolated polyphenols (HFD + Pol) ( $n = 10$ ) (D12451, Research Diets D18060501). The HFD + Pol was prepared by Research Diets and included a representative mixture of pure, isolated polyphenols acquired from Sigma-Aldrich. This diet contained traces of (S)-2-[(Diphenylphosphino)methyl] pyrrolidine (0.014 mg/g diet). The composition of the polyphenol mixture was designed according to the research of Tresserra-Rimbau et al. [25], and it is detailed in Table 1. The dosage of the compounds included are in a similar and sometimes lower range compared to the dosages previously published for pure, isolated

compounds. The usual range in previous publications goes from 15 mg/kg [29–34]. Considering mice of 35 g and an intake of 4.5 g/day of HFD that means for 15 mg/kg-0.525 mg of polyphenol and for 100 mg/kg-3.5 mg in mice. Cis-stilbene has been just used in cell culture for studying the role of polyphenols in proliferation and apoptosis and dosages are not comparable [35,36]. All of the compounds used, except for the cis-stilbene, have demonstrated previous beneficial effects in obesity and insulin resistance [5].

**Table 1.** Composition of polyphenol mixture.

Family	% Total Polyphenols	Polyphenol (Cas Num)	mg/g Diet
Flavanones	54.4%	Hesperidin (520-26-3)	0.738
		(±)-Naringenin (67604-48-2)	0.234
Phenolic Acids	35.3%	2-Hydroxycinnamic acid (614-60-8)	0.594
		Syringic acid (530-57-4)	0.036
Stilbenes	1.2%	cis-Stilbene (645-49-8)	0.022
Tyrosols	9.1%	Tyrosol (510-94-0)	0.162
Total	100%		1.786

Animals were housed in a temperature-controlled room ( $22 \pm 1$  °C) on a 12 h/12 h light/dark cycle and were fed ad libitum. During the nutritional intervention, animals were weighed weekly, and diets were changed twice per week to prevent the oxidation of polyphenols. At the same time, food and beverage intake were recorded every two days. After 26 weeks of nutritional intervention, the animals were euthanized by cervical dislocation. Blood was extracted by intracardiac puncture, and serum was obtained using centrifugation (1500 rpm, 30 min). Liver; subcutaneous white adipose tissue (scWAT); brown adipose tissue (BAT); and kidneys were isolated, immediately snap-frozen, homogenized with liquid nitrogen, and stored at  $-80$  °C for future analysis.

The antioxidant capacity of the diets was measured at the beginning and the end of the nutritional intervention by the Folin–Ciocalteu method without any significant differences (data not shown). Folin–Ciocalteu is a colorimetric method based on the reduction of a mixture of phosphomolybdic and phosphotungstic acid (Folin–Ciocalteu Reagent 47641 Sigma-Aldrich, St. Louis, MO, USA) produced by polyphenols in an alkaline medium. In this redox reaction, tungsten and molybdenum oxides are formed, developing a blue color (absorbance measured at 765 nm) proportional to the total concentration of polyphenols.

### 2.2. Glucose-Tolerance Test (GTT) and Insulin-Tolerance Test (ITT)

To perform the GTT and ITT assays, the animals were transferred to clean cages and fasted for 6 h from 08:00 h (Zeitgeber Time 0) to 14:00 h (Zeitgeber Time 6) before the tests. A total of 1.5 mg glucose/g body weight (G7021, Sigma-Aldrich, St. Louis, MO, USA) for GTT, and 0.75 UI of insulin/kg body weight (Actrapid, Novo Nordisk, Bagsvaerd, Denmark) were injected intraperitoneally (i.p.) for GTT and ITT, respectively. Blood samples were collected from the tail vein of each mouse by gently massaging fourfold prior the injection (0 min) and at 30-, 60-, and 120-min post-injection. Glucose levels were measured using a glucometer (Glucocard SM, Menarini, Florence, Italy). GTTs were performed at weeks 7, 14, and 21, and ITTs at weeks 8, 15, and 22 of the nutritional intervention.

### 2.3. TBARS Assay

The lipid peroxidation was determined in 25 mg of homogenized kidney and liver, using TBARS kit (KA1381, Abnova, Taipei, Taiwan). This is a fluorometric kit that measures the content of malondialdehyde (MDA) at an excitation wavelength of 530 nm and an emission wavelength of 550 nm. The plates were read twice, and an MDA solution was used as a standard.

#### 2.4. ELISA Assay

Lipocalin-2 serum levels were measured using EMLCN2 solid-phase sandwich enzyme-linked immunosorbent assay kit (ELISA) (EMLCN2 Thermo Fisher Scientific, Waltham, MA, USA). Absorbance was read at 450 nm, and a four-parameter standard curve (4PL) was performed using Graph Pad Prism 9.02.

#### 2.5. Triglycerides Quantification

Liver tissue (100 mg) of each mouse were homogenized in 1 mL solution of Nonidet P40 at 5% (A1694, 0250, Panreac Applichem, Spain). The amount of TG was determined by using the Triglyceride Quantification Colorimetric Kit (MAK266, Sigma Aldrich, St. Louis, MO, USA).

#### 2.6. RNA Isolation and Quantitative Reverse Transcription PCR (qRT-PCR)

Total RNA was extracted from the previously homogenized frozen kidneys using TRI Reagent solution and Phasemaker tubes (A33250, Thermo Fisher Scientific, Waltham, MA, USA), followed by DNase I treatment (K2981, Thermo Fisher Scientific, Waltham, MA, USA) to eliminate genomic DNA contamination. The cDNA was synthesized from 1.5 µg of total RNA using a high-capacity cDNA reverse transcription kit (4368814, Applied Biosystems, Waltham, MA, USA). According to the measurement of the relative mRNA levels, quantitative (q) RT-PCR was performed using SYBR Select Master Mix for CFX (4472942, Applied Biosystems, Waltham, MA, USA) or TaqMan Gene Expression Master Mix (4369514, Applied Biosystems, Waltham, MA, USA). Each mRNA from a single sample was measured in duplicate, using M36b4 and B2m as housekeeping genes. The sequences of the primers used in the qPCR are presented in Supplemental Data (Table S1). Results were obtained by the relative standard curve method and expressed as fold increases, using the chow-diet experimental group as the reference.

#### 2.7. Data Analysis/Statistics

Values were expressed as means  $\pm$  SEM, and a *p*-value  $< 0.05$  was considered statistically significant. Data were studied with statistical analyses using GraphPad Prism, version 9.02 (GraphPad, San Diego, CA, USA). The *p*-values were determined by using a one-way ANOVA with a follow-up Tukey's test. When ANOVA tests presented different variances, Brown-Forsythe, and Welch's corrections with a follow-up Dunnett's T3 tests were applied. For repeated measures the *p*-values were calculated by using a 2-way ANOVA with Geisser-Greenhouse correction. Then a Tukey's multiple comparison tests were performed between groups for each week.

### 3. Results

#### 3.1. Pure, Isolated Polyphenol Mixture Significantly Enhances the HFD-Induced Hyperphagia

HFDs have been shown to induce obesity due to their high energy density from fat and increased food intake, as compared to standard normocaloric diets [37]. In this study, it was observed that, as expected, HFD increased the body weight in both experimental groups (Figure 1). Comparing HFD-only mice with HFD + Pol mice, the dietary supplementation of an HFD with pure, isolated polyphenols had produced a significant increase in kcal intake (Figure 1b) but none in the animal body weight, even an upward trend was observed (*p* = 0.08) (Figure 1a). The weekly body weight and food intake are shown in supplemental figures (Figure S1a,b respectively).

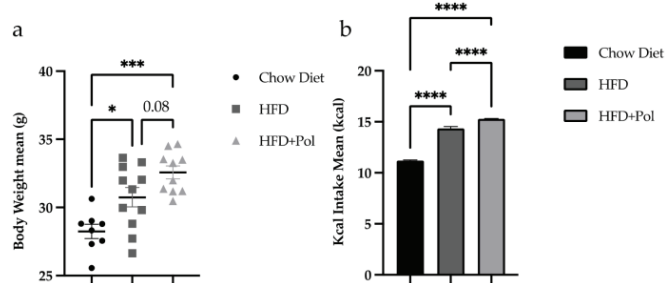


**Figure 1.** Polyphenol dietary supplementation increased the Kcal intake of HFD-only mice. (a) The graph represents the weight-gain mean between the beginning and the end of the dietary intervention (26 weeks). (b) The graph represents the food-intake average (Kcal) during the nutritional intervention. Data are presented as the mean  $\pm$  SEM. \*  $p < 0.05$ ; \*\*\*  $p < 0.001$ ; \*\*\*\*  $p < 0.0001$ . The  $p$ -values were determined by using a one-way ANOVA test and a Tukey’s multiple tests correction. Chow Diet  $n = 8$ ; HFD = 11; HFD + Pol = 10.

Despite there were no differences in the weight gain between HFD-only mice and HFD + Pol mice, we evaluated the tissue weights to determine if there were differences due to the dietary nutritional intervention. As can be seen in Figure 2, subcutaneous (sc) and epididymal (e) WAT, BAT, and kidneys exhibited an upward trend in HFD-only mice compared to control mice and a significant increase in HFD + Pol mice. Moreover, in the case of the kidneys this tendency is also observed in the HFD + Pol when compared to HFD-only mice.

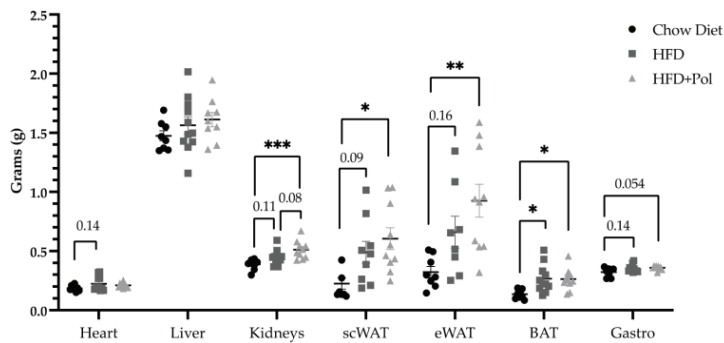


**Figure 2.** The polyphenol supplementation produced extra weight gain in HFD + Pol murine kidneys, as compared to HFD-only murine kidneys. The graph represents the tissue weight (g) of different tissues. Data are presented as the mean  $\pm$  SEM. \*  $p < 0.05$ ; \*\*  $p < 0.01$ ; \*\*\*  $p < 0.001$ . The  $p$ -values were determined by using a one-way ANOVA test and a Tukey’s multiple tests correction. Chow Diet  $n = 8$ ; HFD = 11; HFD + Pol = 10.

**3.2. Mice Supplemented with Polyphenols Show a Worse Response to Glucose and Insulin Bolus than HFD-Only Mice**

As expected, the HFD produced insulin resistance and glucose intolerance. In our experimental model, this impairment in glucose metabolism was observed from week 7

for the GTT and week 8 for the ITT (Figure 3a,b). Our data indicated that the polyphenol supplementation worsened the insulin resistance and glucose intolerance caused by the HFD. The polyphenol-supplemented mice exhibited a worse response to glucose and insulin during the nutritional intervention, as is demonstrated by the GTT and ITT curves (Figures S1 and S2, respectively). This corresponded to a significant increase in the AUCs of both GTT (Figure 3a) and ITT (Figure 3b), indicating a progressive aggravation of the insulin and glucose responses.

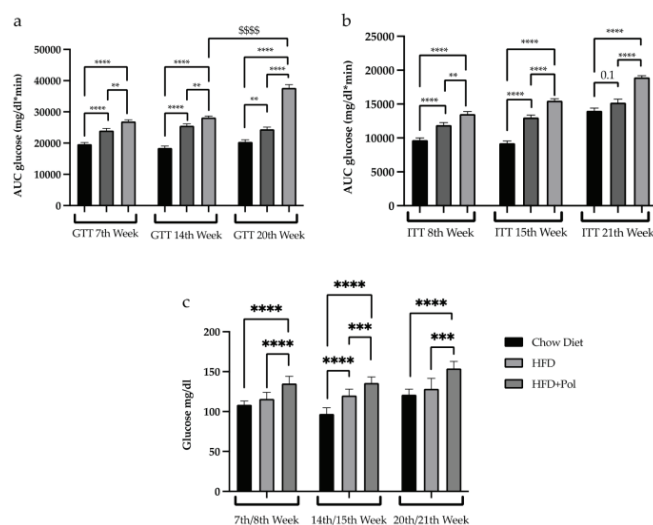


**Figure 3.** Polyphenol dietary supplementation worsened the glucose metabolism caused by an HFD. (a) AUC of the plasma glucose levels after i.p. administration of glucose (1.5 g/kg body weight (b.w.)) in standard-chow-diet, HFD, and HFD + Pol mice groups from the GTTs performed at weeks 7, 14, and 20; (b) AUC of the plasma glucose levels after i.p. administration of insulin (0.75 UI/kg b.w) in standard chow-diet, HFD, and HFD + Pol mice groups from the ITTs performed at weeks 8, 15, and 21; (c) Fasting blood glucose levels after 6 h of fasting. Data are presented as the mean  $\pm$  SEM. \*\*  $p < 0.01$ ; \*\*\*  $p < 0.001$ ; \*\*\*\*  $p < 0.0001$ . \$\$\$\$  $p < 0.0001$ . The  $p$ -values for each week were determined by using a one-way ANOVA test and a Tukey's multiple tests correction. Chow Diet  $n = 8$ ; HFD = 11; HFD + Pol = 10.

This worsened response to glucose and insulin bolus was paired with higher fasting blood glucose in the polyphenol-supplemented animals, as compared to the HFD-only mice (Figure 3c). Contrary to what was expected, our data indicated that the administration of pure, isolated polyphenols added directly to a HFD did not produce healthy benefits but increased the HFD-induced insulin resistance.

### 3.3. Polyphenol-Supplemented HFD Increases the Oxidative Stress Markers in the Kidney

The slight increase in the absolute weight of the kidneys between HFD-only mice and HFD + Pol mice would encourage us to analyze the kidneys of these animals more deeply.

The kidney is one of the tissues targeted by obesity and insulin resistance. Pathologies such as chronic kidney disease (CKD) and diabetic nephropathy are caused not just by high glucose circulating levels but also by lipid accumulation in the renal tissue that contributes

to the development of glomerulitis, chronic inflammation, a high production of ROS, and fibrosis [38]. In this situation, the damaged kidney activates the renin–angiotensin–aldosterone system (RAAS) and secretes specific cytokines that aggravate the systemic symptomatology associated to the CKD and diabetic nephropathy such as hypertension, cardiovascular risk [39,40].

To evaluate the kidney condition, we firstly evaluated the oxidative stress through a thiobarbituric acid reactive substances (TBARS) assay. TBARS quantifies the levels of malondialdehyde (MDA) produced by the decomposition of the unstable peroxides. A TBARS assay can be used as a measurement of damage caused by oxidative stress [41].

Moreover, the expression of antioxidant defense enzymes *glutathione s-reductase* (*Gsr*), *catalase* (*Cat*), and *superoxide dismutase* (*Sod*) was measured to evaluate the kidney response to oxidative stress.

The levels of malondialdehyde (MDA) were increased in the kidneys of the HFD + Pol mice (Figure 4a). Regarding the relative mRNA levels of antioxidant-defense genes, the data showed a significant reduction in the relative mRNA levels of *Gsr* and no significant changes in the expression of *Sod* and *Cat* in HFD-only mice (Figure 4b). No significant changes neither with control mice nor HFD-only mice were detected in HFD + Pol mice.

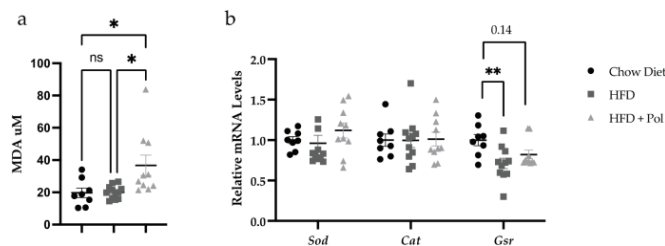


**Figure 4.** Polyphenol-supplemented HFD increased the oxidative stress markers in the kidneys. (a) Malondialdehyde (MDA) levels in the kidneys of standard-chow-fed, HFD-only, and HFD + Pol mice measured by the TBARS assay. (b) Relative mRNA levels of *Sod*, *Cat*, and *Gsr*. Data are presented as the mean  $\pm$  SEM. \*  $p < 0.05$ ; \*\*  $p < 0.01$ . The  $p$ -values were determined by using a one-way ANOVA test and a Tukey's multiple tests correction. Chow Diet  $n = 8$ ; HFD = 11; HFD + Pol = 10.

#### 3.4. Polyphenol-Supplemented HFD Upregulates the Expression of Fibrosis and Kidney Damage Markers

The onset and progression of CKD can be analyzed by the measurement of fibrosis, oxidative stress, and kidney damage markers. Thus, an expression profile of fibrosis and kidney damage markers was conducted. Our results showed an upregulation of *kidney injury molecule-1* (*Kim-1*) [42], and an upregulation in the mRNA levels of the transcription factor *carbohydrate-responsive element-binding protein b* (*ChREBPb*), the increase of which has been related to the progression of diabetic kidneys (Figure 5a) [43]. In addition, an upward trend in the expression of *fibronectin* (*Fn-1*), a protein related to fibrotic processes [44,45] was also detected.

The HFD + Pol mice also showed a significant upregulation of *lipocalin-2* (*lcn2*) (Figure 5a). LCN2 circulating levels increase under different pathological states, particularly kidney injury, bacterial infection, and inflammation as well as in people of advanced age. LCN2 is a biomarker for the development of renal injury, and it is considered an acute phase protein when upregulated in the kidney tubules [46–48]. We also measured the protein levels of LCN2 in the kidneys and despite no significant results a clear upward trend was observed in the kidneys of the HFD + Pol mice (Figure 5b).



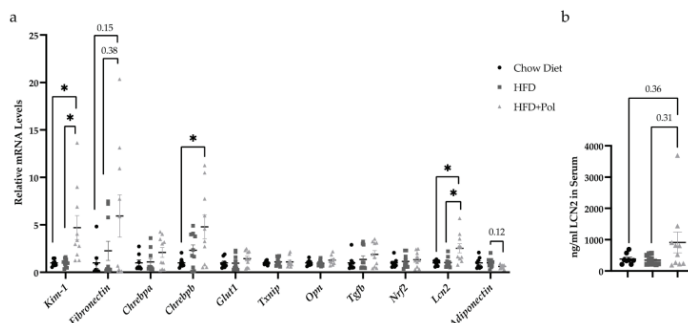


**Figure 5.** HFD + Pol upregulated the expression of fibrosis and kidney-damage markers. **(a)** Relative mRNA levels of several fibrosis, oxidative stress and kidney damage markers, *kidney injury molecule-1 (kim1)*, *fibronectin-1*, *carbohydrate-responsive element-binding protein b (Chrebpb)*, *glucose transporter1 (Glut1)*, *thioredoxin-interacting protein (Txnip)*, *Osteopontin (Opn)*, *Transforming growth factor beta-1 (Tgfb)*, *Nuclear factor erythroid 2-related factor 2 (Nrf2)*, *Lipocalin 2 (Lcn2)* and *Adiponectin*. **(b)** Protein levels of LCN2 measured by ELISA in the kidney. Data are presented as the mean  $\pm$  SEM. \*  $p < 0.05$ . The  $p$ -values for the ELISA assay and *Glut1*, *Txnip*, *Opn*, *Tgfb* and *Nrf2* genes were determined by using a one-way ANOVA test and Tukey's multiple tests correction. For genes showing different variances like *Kim-1*, *Fibronectin-1*, *Chrebpb*, *Chrbpb*, *Lcn2* and *Adiponectin* a one-way ANOVA with Brown-Forsythe and Welch's correction and a Dunnett's comparisons tests were performed. Chow Diet  $n = 8$ ; HFD = 11; HFD + Pol = 10.

### 3.5. Polyphenol-Supplemented HFD Upregulates the Expression of Fibrosis Markers in the Liver and Increases the Hepatic Lipid Content

The liver is a key organ in the maintenance of metabolic homeostasis and is one of the main organs affected by the accumulation of ectopic lipids. The nonalcoholic fatty liver disease (NAFLD) has been strongly associated with obesity and insulin resistance, as well as type 2 diabetes [49,50]. It is well-known that the accumulation of intrahepatic fat leads to liver steatosis that is an important factor for the metabolic complications associated with obesity [51]. To evaluate the impact of dietary polyphenols supplementation in hepatic steatosis, we measured the TG content in the livers of HFD-only mice and HFD + Pol mice the expression of different genes to define the general state of these livers HFD + Pol.

As it is showed in Figure 6a, the hepatic lipid content is higher in both groups of HFD-fed mice compared to control mice and, despite no significance, an upward trend is observed in the HFD + Pol mice compared to HFD-only mice ( $p = 0.07$ ). Regarding the different markers evaluated, our results showed that *fibronectin (Fn-1)* is upregulated in HFD + Pol mice (Figure 6b), thus suggesting a fibrotic process in the livers of polyphenol-supplemented mice.

Besides fibrosis, we also analyzed the expression of genes related to *de novo* lipogenesis (*fatty acid synthase (Fasn)* and *sterol regulatory element binding protein, (Srebp1c)*), and lipid droplets formation (*Cell death activator CIDE-3, (Fsp27b)*), but also markers of the reticulum stress (*Binding immunoglobulin protein (Bip)* and *C/EBP Homologous Protein (Chop)*). No changes in the mRNA levels were detected in any of the genes analyzed (Figure 6b).

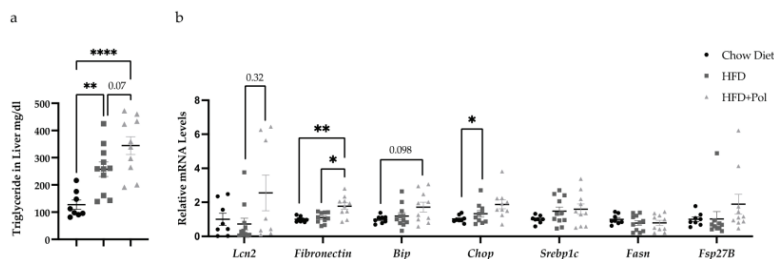


**Figure 6.** HFD + Pol upregulated the expression of fibronectin in the liver. (a) Hepatic TG content. The concentration of TG (ng/uL) was measured in the livers of chow, HFD and HFD + Pol mice. (b) Relative mRNA levels of different genes to evaluate the general state of the livers, *fatty acid synthase (Fasn)*, *sterol regulatory element binding protein, (Srebp1c)*, *Cell death activator CIDE-3, (Fsp27)*, *Binding immunoglobulin protein (Bip)* and *C/EBP Homologous Protein (Chop)*. (b) Protein levels of LCN2 measured by ELISA in the kidney. Data are presented as the mean  $\pm$  SEM. \*  $p < 0.05$ ; \*\*  $p < 0.01$ ; \*\*\*\*  $p < 0.0001$ . The  $p$ -values for the TG assay and *Fasn* gene were determined by using a one-way ANOVA test and a Tukey's multiple tests correction. For genes showing different variances like *Fsp27B*, *Fibronectin-1*, *Srebp1c*, *Chop*, *Lcn2* and *Bip* a one-way ANOVA with Brown-Forsythe and Welch's correction and a Dunnett's comparisons tests were performed. Chow Diet  $n = 8$ ; HFD = 11; HFD + Pol = 10.

#### 4. Discussion

Our data demonstrated that the supplementation of an HFD with pure, isolated polyphenols worsened the effects of the HFD by producing a homeostatic imbalance that resulted in renal and liver fibrosis in mice. We concluded that the HFD + Pol mice exhibited a dysregulation in glucose and insulin metabolism and signs of kidney damage due to their increased levels of MDA, which suggested higher oxidative stress (Figure 4), as well as the results of their gene-expression analyses (Figure 5), where the changes observed in HFD + Pol mice was related to CKD and obesity [52–56], and liver fibrosis.

The kidney damage in HFD + Pol mice was basically defined by the upregulation of *Kim-1* and *Lcn2*.

KIM-1 is a transmembrane glycoprotein with a low expression in kidney but significantly upregulated in damaged kidneys. KIM-1 upregulation in CKD has been associated with an hypoxic environment [57]. A chronic hypoxia due to the structural and functional disorders (alteration of the capillarity, excessive activity of renin-angiotensin system, oxidative stress . . . ) in the kidney is the main pathogenic mechanism of progressive CKD. Hypoxia is a powerful stimulus for KIM-1 expression in the proximal tubular cells. The upregulation of KIM-1 increases the release of cytokines and chemokines, that enhances inflammation, hypoxia and fibrosis, thus aggravating the CKD [58,59].

Based on the literature, one of the possible links between renal damage and the general decline in glucose metabolism could be the iron metabolism. Due to the role of *Lcn2* in the iron metabolism, we also measured the mRNA levels of *transferrin receptor 2 (trf2)*, *hephaestin (heph)*, and *hepcidin (hamp)* in the liver and in the kidney (data not shown), but no differences between the HFD + Pol and HFD-only mice were detected. Similarly, neither the circulating levels of iron were different in supplemented mice versus HFD-fed animals (data not shown). It has been documented that LCN2 is an iron-carrier protein, and its biological activity depends on its iron-load and on where it is produced (renal tubules or macrophages), which defines its dual role in the development of kidney damage [60–62]. Iron-free LCN2 secreted by renal tubular epithelial cells has been associated with renal injury, and the expression and release of macrophage-derived iron-bound LCN2 has been linked to renal recovery [63]. Similarly, it has also been shown that adipose-tissue-derived

LCN2 plays a critical role in causing both chronic and acute renal injury, but it is also essential for the progression of CKD in rodent and human models [46,64]. Viau et al. concluded that LCN2 may act as a growth regulator by mediating the mitogenic effects of epidermal growth factor receptor (EGFR) signaling [46]. The activation of EGFR has been linked to the regulation of several other cellular responses involved in the progression of renal damage, including cell proliferation, inflammatory processes, and extracellular matrix regulation [65]. In our experimental study, the levels of Lcn2 were unaltered in the adipose tissue of the HFD + Pol mice (data not shown).

Fibrosis was evaluated by measuring the mRNA levels of fibronectin both in the kidney and in the liver. Fibrosis is caused by a pathological excess of extracellular matrix deposition that leads to a disruption of tissue structure that at the end should provoke a loss of function. The fibrotic process involves a complex network of signal transduction pathways where the transforming growth factor-beta (TGF $\beta$ ) has a central role [45]. Fibrosis is determined among others by an increase in the expression of collagens, proteoglycans, glycoproteins, and fibronectins [44]. Fibronectin is one of the main players by affecting the TGF $\beta$  release and as responsible protein for the accumulation of collagen and hence the development of fibrosis [66,67].

Altogether, our results suggested that polyphenol-supplementation within a HFD drives to the development of fibrosis in the liver and kidneys that could aggravate the insulin resistance in DIO mice.

#### *The Importance of Food Matrices on the Effects of Polyphenol-Supplementation*

Our results indicated a pernicious effect of pure, isolated polyphenols when administered under HFD conditions. These results may be controversial given current and ongoing research, but we believe that all aspects of polyphenol supplementation should be discussed. In 2010, Bouayed and Torsten published a review suggested the “double-edged sword” of the cellular redox state and exogenous antioxidants [24]. Their report as well as recent research have indicated that it is essential to consider the type, the dosage, the combination, and the consumption matrices involved when using bioactive compounds as the administration of such may alter the physiological balance between oxidation and antioxidant pathways, which may result in either beneficial or deleterious effects [68,69].

The inclusion of complete foods naturally rich in antioxidants (e.g., fruits and vegetables) has been widely recommended by health organizations and has been the basis of many “healthy eating” programs, such as the Mediterranean diet [70,71]. Much research has been focused on the antioxidant effects of phenolic compounds when administered in isolation versus when ingested via their natural source [5], and increasing data has suggested that the beneficial properties of complete foods cannot be attributed to a single compound. Rather, it is the consumption of the food in its whole state (i.e., not extracted, or isolated compounds) that activates the additive, synergistic, and antagonistic effects of the phytochemicals and nutrients. The effects of polyphenols depend on their bioavailability, and it is assumed that just the 5–10% of the total dietary polyphenol intake is absorbed directly through the stomach and/or small intestine [12]. The rest of ingested polyphenols reaches the colon where they are transformed by the microbiota [72,73]. When absorbed, polyphenols undergo phase I and II metabolism (sulfation, glucuronidation, methylation, and glycine conjugation) in the liver [14]. The new-synthesized metabolites may then impact, among others, in the adipose tissue, pancreas, muscle, and liver, where they exert their bioactivity [5].

In addition, it is not only the natural food matrices that are essential [74,75], but also the preparation process and the conditions under which it is ingested (e.g., cooking, juicing, etc.). It has been widely demonstrated that cooking affects the phytochemical content of foods as well as their chemical structures and the bioavailability of their bioactive compounds; in other words, how a food is processed before consumption may be directly related to its health effects [76–81].

## 5. Conclusions

In conclusion, our work demonstrated that the dietary supplementation of an HFD with pure, isolated polyphenols worsened the metabolic disturbances known to be caused by HFDs and directly impacted the kidneys and the liver, increasing oxidative stress, renal damage, and fibrosis. The data presented reinforced the recent trends eschewing pure, isolated antioxidant replacements and instead encouraging the ingestion of complete whole foods, from which the beneficial bioactive compounds originated.

### *Limitations and Follow-Up*

This is an initial work that opens a new research line to study the impact of pure isolated polyphenols in the onset and development of obesity and its metabolic-related pathologies such as insulin resistance and NAFLD. We are aware that the study has limitations, and that further analysis are needed. According to the data presented the next step would be to identify the role of each compound individually on the effects described. A follow-up study is underway to analyze the effects of each compound individually in culture cells to evaluate which compounds or compounds could be the responsible for the deleterious effects observed or if it is the complete mixture. Moreover, a pair-fed study to disassociate the effect of polyphenols from increased caloric intake per se should be a follow-up.

To calculate the power analysis of this experiment our main outcome is the insulin resistance caused by a HFD. Considering the results showed in Figure 2 our experimental approach reaches the significance expected. We have positive results in the kidney and in the liver which means that our experimental approach is well designed, but some variables show a high intragroup variability mainly in the HFD-supplemented animals. This variability is probably due to differences in the polyphenol absorption and bioavailability.

**Supplementary Materials:** The following are available online at <https://www.mdpi.com/article/10.3390/antiox11010120/s1>, Table S1: Sequences of the primers used in SYBR green assays and references for the probes used in TaqMan assays. Figure S1: The curves of GTTs. Figure S2: The curves of ITTs.

**Author Contributions:** Conceptualization: H.S.-L., P.F.M., J.R. and D.H.; data curation: H.S.-L.; formal analysis: H.S.-L. and J.R.; funding acquisition: P.F.M., J.R. and D.H.; investigation: H.S.-L. and J.R.; methodology: H.S.-L., P.F.M., J.R. and D.H.; project administration: P.F.M., J.R. and D.H.; resources: P.F.M., J.R. and D.H.; supervision: P.F.M., J.R. and D.H.; validation: H.S.-L., P.F.M., J.R. and D.H.; visualization, H.S.-L., J.R. and D.H.; writing—original draft: H.S.-L. and J.R.; writing—review and editing: P.F.M., J.R. and D.H. All authors have read and agreed to the published version of the manuscript.

**Funding:** This study was supported by the grant AGL2017-82417-R to P.F.M. and D.H. was funded by MCIN/AEI/ 10.13039/501100011033 and by “ERDF: A way of making Europe”, and the Generalitat de Catalunya (the Government of Catalonia, grant 2017SGR683 to D.H.). APC was funded by the University of Barcelona.

**Institutional Review Board Statement:** The study was conducted according to the guidelines of the Declaration of Helsinki and approved by the Animal Ethics Committee of the University of Barcelona (CEEA-137/18, May 2018).

**Informed Consent Statement:** Not applicable.

**Data Availability Statement:** The data presented in this study are available in this manuscript.

**Acknowledgments:** We would like to thank to the Ministerio de ciencia e innovación (the Ministry of Science of Innovation, Spanish Government), the Generalitat de Catalunya. We would also like to thank the personnel of the animal facilities of the Faculty of Pharmacy and Food Sciences at the University of Barcelona for their support in the animals’ housing and management.

**Conflicts of Interest:** The authors declare no conflict of interest.

## References

1. Peirce, V.; Carobbio, S.; Vidal-Puig, A. The different shades of fat. *Nature* **2014**, *510*, 76–83. [[CrossRef](#)]
2. Carobbio, S.; Pellegrielli, V.; Vidal-Puig, A. Adipose Tissue Function and Expandability as Determinants of Lipotoxicity and the Metabolic Syndrome. *Adv. Exp. Med. Biol.* **2017**, *960*, 161–196.
3. Virtue, S.; Vidal-Puig, A. Adipose tissue expandability, lipotoxicity and the Metabolic Syndrome—An allostatic perspective. *Biochim. Biophys. Acta Mol. Cell Biol. Lipids* **2010**, *1801*, 338–349. [[CrossRef](#)] [[PubMed](#)]
4. Roden, M.; Shulman, G.I. The integrative biology of type 2 diabetes. *Nature* **2019**, *576*, 51–60. [[CrossRef](#)] [[PubMed](#)]
5. Sandoval, V.; Sanz-Lamora, H.; Arias, G.; Marrero, P.F.; Haro, D.; Relat, J. Metabolic Impact of Flavonoids Consumption in Obesity: From Central to Peripheral. *Nutrients* **2020**, *12*, 2393. [[CrossRef](#)] [[PubMed](#)]
6. Tressera-Rimbau, A.; Arranz, S.; Eder, M.; Vallverdú-Queralt, A. Dietary Polyphenols in the Prevention of Stroke. *Oxid. Med. Cell. Longev.* **2017**, *2017*, 7467962. [[CrossRef](#)] [[PubMed](#)]
7. Kim, Y.A.; Keogh, J.B.; Clifton, P.M. Polyphenols and Glycemic Control. *Nutrients* **2016**, *8*, 17. [[CrossRef](#)] [[PubMed](#)]
8. Alfadda, A.A.; Sallam, R.M. Reactive oxygen species in health and disease. *J. Biomed. Biotechnol.* **2012**, *2012*, 936486. [[CrossRef](#)]
9. Sharma, A.; Kaur, M.; Katnoria, J.K.; Nagpal, A.K. Polyphenols in Food: Cancer Prevention and Apoptosis Induction. *Curr. Med. Chem.* **2018**, *25*, 4740–4757. [[CrossRef](#)]
10. Fraga, C.G.; Croft, K.D.; Kennedy, D.O.; Tomás-Barberán, F.A. The effects of polyphenols and other bioactives on human health. *Food Funct.* **2019**, *10*, 514–528. [[CrossRef](#)]
11. Del Rio, D.; Rodríguez-Mateos, A.; Spencer, J.P.E.; Tognolini, M.; Borges, G.; Crozier, A. Dietary (poly)phenolics in human health: Structures, bioavailability, and evidence of protective effects against chronic diseases. *Antioxid. Redox Signal.* **2013**, *18*, 1818–1892. [[CrossRef](#)] [[PubMed](#)]
12. Bohn, T. Dietary factors affecting polyphenol bioavailability. *Nutr. Rev.* **2014**, *72*, 429–452. [[CrossRef](#)]
13. Cory, H.; Passarelli, S.; Szeto, J.; Tamez, M.; Mattei, J. The Role of Polyphenols in Human Health and Food Systems: A Mini-Review. *Front. Nutr.* **2018**, *5*, 1–9. [[CrossRef](#)]
14. Manach, C.; Scalbert, A.; Morand, C.; Rémésy, C.; Jiménez, L. Polyphenols: Food sources and bioavailability. *Am. J. Clin. Nutr.* **2004**, *79*, 727–747. [[CrossRef](#)]
15. Zheng, B.; He, Y.; Zhang, P.; Huo, Y.-X.; Yin, Y. Polyphenol utilization proteins in human gut microbiome. *Appl. Environ. Microbiol.* **2021**, AEM0185121. [[CrossRef](#)]
16. Schön, C.; Wacker, R.; Micka, A.; Steudle, J.; Lang, S.; Bonnländer, B. Bioavailability study of maqui berry extract in healthy subjects. *Nutrients* **2018**, *10*, 1720. [[CrossRef](#)] [[PubMed](#)]
17. Cardona, F.; Andrés-Lacueva, C.; Tulipani, S.; Tinahones, F.J.; Queipo-Ortuño, M.I. Benefits of polyphenols on gut microbiota and implications in human health. *J. Nutr. Biochem.* **2013**, *24*, 1415–1422. [[CrossRef](#)]
18. Monagas, M.; Urpi-Sarda, M.; Sánchez-Patán, F.; Llorach, R.; Garrido, I.; Gómez-Cordovés, C.; Andrés-Lacueva, C.; Bartolomé, B. Insights into the metabolism and microbial biotransformation of dietary flavan-3-ols and the bioactivity of their metabolites. *Food Funct.* **2010**, *1*, 233–253. [[CrossRef](#)]
19. Mandalari, G.; Vardakou, M.; Faulks, R.; Bisignani, C.; Martorana, M.; Smeriglio, A.; Trombetta, D. Food Matrix Effects of Polyphenol Bioaccessibility from Almond Skin during Simulated Human Digestion. *Nutrients* **2016**, *8*, 568. [[CrossRef](#)] [[PubMed](#)]
20. Pineda-Vadillo, C.; Nau, F.; Dubiard, C.G.; Cheynier, V.; Meudec, E.; Sanz-Buenhombre, M.; Guadarrama, A.; Tóth, T.; Csavajda, É.; Hingyi, H.; et al. In vitro digestion of dairy and egg products enriched with grape extracts: Effect of the food matrix on polyphenol bioaccessibility and antioxidant activity. *Food Res. Int.* **2016**, *88*, 284–292. [[CrossRef](#)]
21. Dufour, C.; Loonis, M.; Delosière, M.; Buffière, C.; Hafnaoui, N.; Santé-Lhoutellier, V.; Rémond, D. The matrix of fruit & vegetables modulates the gastrointestinal bioaccessibility of polyphenols and their impact on dietary protein digestibility. *Food Chem.* **2018**, *240*, 314–322.
22. Wojtunik-Kulesza, K.; Oniszczuk, A.; Oniszczuk, T.; Combrzyński, M.; Nowakowska, D.; Matwijczuk, A. Influence of In Vitro Digestion on Composition, Bioaccessibility and Antioxidant Activity of Food Polyphenols—A Non-Systematic Review. *Nutrients* **2020**, *12*, 1401. [[CrossRef](#)]
23. Tarko, T.; Duda-Chodak, A. Influence of Food Matrix on the Bioaccessibility of Fruit Polyphenolic Compounds. *J. Agric. Food Chem.* **2020**, *68*, 1315–1325. [[CrossRef](#)] [[PubMed](#)]
24. Bouayed, J.; Bohn, T. Exogenous antioxidants—Double-edged swords in cellular redox state: Health beneficial effects at physiologic doses versus deleterious effects at high doses. *Oxid. Med. Cell. Longev.* **2010**, *3*, 228–237. [[CrossRef](#)] [[PubMed](#)]
25. Tressera-Rimbau, A.; Medina-Remon, A.; Perez-Jimenez, J.; Martinez-Gonzalez, M.A.; Covas, M.I.; Corella, D.; Salas-Salvado, J.; Gomez-Gracia, E.; Lapetra, J.; Aros, F.; et al. Dietary intake and major food sources of polyphenols in a Spanish population at high cardiovascular risk: The PREDIMED study. *Nutr. Metab. Cardiovasc. Dis.* **2013**, *23*, 953–959. [[CrossRef](#)]
26. Tressera-Rimbau, A.; Guasch-Ferre, M.; Salas-Salvado, J.; Toledo, E.; Corella, D.; Castaner, O.; Guo, X.; Gomez-Gracia, E.; Lapetra, J.; Aros, F.; et al. Intake of Total Polyphenols and Some Classes of Polyphenols Is Inversely Associated with Diabetes in Elderly People at High Cardiovascular Disease Risk. *J. Nutr.* **2016**, *146*, 767–777.
27. Sandoval, V.; Femenias, A.; Martínez-Garza, U.; Sanz-Lamora, H.; Castagnini, J.M.; Quifer-Rada, P.; Lamuela-Raventos, R.M.; Marrero, P.F.; Haro, D.; Relat, J. Lyophilized Maqui (*Aristotelia chilensis*) Berry Induces Browning in the Subcutaneous White Adipose Tissue and Ameliorates the Insulin Resistance in High Fat Diet-Induced Obese Mice. *Antioxidants* **2019**, *8*, 360. [[CrossRef](#)]

28. Sandoval, V.; Sanz-Lamora, H.; Marrero, P.F.P.F.; Relat, J.; Haro, D. Lyophilized Maqui (*Aristotelia chilensis*) Berry Administration Suppresses High-Fat Diet-Induced Liver Lipogenesis through the Induction of the Nuclear Corepressor SMILE. *Antioxidants* **2021**, *10*, 637. [\[CrossRef\]](#) [\[PubMed\]](#)
29. Peng, P.; Jin, J.; Zou, G.; Sui, Y.; Han, Y.; Zhao, D.; Liu, L. Hesperidin prevents hyperglycemia in diabetic rats by activating the insulin receptor pathway. *Exp. Ther. Med.* **2021**, *21*, 53. [\[CrossRef\]](#)
30. Prasatthong, P.; Meeapat, S.; Rattanakankokchai, S.; Bunbupha, S.; Prachaney, P.; Maneesai, P.; Pakdechote, P. Hesperidin ameliorates signs of the metabolic syndrome and cardiac dysfunction via IRS/Akt/GLUT4 signaling pathway in a rat model of diet-induced metabolic syndrome. *Eur. J. Nutr.* **2021**, *60*, 833–848. [\[CrossRef\]](#)
31. Li, S.; Zhang, Y.; Sun, Y.; Zhang, G.; Bai, J.; Guo, J.; Su, X.; Du, H.; Cao, X.; Yang, J.; et al. Naringenin improves insulin sensitivity in gestational diabetes mellitus mice through AMPK. *Nutr. Diabetes* **2019**, *9*, 28. [\[CrossRef\]](#)
32. Hsu, C.L.; Wu, C.H.; Huang, S.L.; Yen, G.C. Phenolic compounds rutin and o-coumaric acid ameliorate obesity induced by high-fat Diet in rats. *J. Agric. Food Chem.* **2009**, *57*, 425–431. [\[CrossRef\]](#) [\[PubMed\]](#)
33. Tanaka, T.; Iwamoto, K.; Wada, M.; Yano, E.; Suzuki, T.; Kawaguchi, N.; Shirasaka, N.; Moriyama, T.; Homma, Y. Dietary syringic acid reduces fat mass in an ovariectomy-induced mouse model of obesity. *Menopause* **2021**, *28*, 1340–1350. [\[CrossRef\]](#)
34. Chandramohan, R.; Pari, L. Antihyperlipidemic effect of tyrosol, a phenolic compound in streptozotocin-induced diabetic rats. *Toxicol. Mech. Methods* **2021**, *31*, 507–516. [\[CrossRef\]](#)
35. Mahbub, A.A.; Le Maitre, C.L.; Haywood-Small, S.L.; Cross, N.A.; Jordan-Mahy, N. Polyphenols act synergistically with doxorubicin and etoposide in leukaemia cell lines. *Cell Death Discov.* **2015**, *1*, 15043. [\[CrossRef\]](#) [\[PubMed\]](#)
36. Mahbub, A.; Le Maitre, C.; Haywood-Small, S.; Cross, N.; Jordan-Mahy, N. Dietary polyphenols influence antimetabolite agents: Methotrexate, 6-mercaptopurine and 5-fluorouracil in leukemia cell lines. *Oncotarget* **2017**, *8*, 104877–104893. [\[CrossRef\]](#)
37. Hariri, N.; Thibault, L. High-fat diet-induced obesity in animal models. *Nutr. Res. Rev.* **2010**, *23*, 270–299. [\[CrossRef\]](#)
38. Mende, C.W.; Einhorn, D. Fatty kidney disease: A new renal and endocrine clinical entity? Describing the role of the kidney in obesity, metabolic syndrome, and type 2 diabetes. *Endocr. Pract.* **2019**, *25*, 854–858. [\[CrossRef\]](#) [\[PubMed\]](#)
39. Yang, P.; Xiao, Y.; Luo, X.; Zhao, Y.; Zhao, L.; Wang, Y.; Wu, T.; Wei, L.; Chen, Y. Inflammatory stress promotes the development of obesity-related chronic kidney disease via CD36 in mice. *J. Lipid Res.* **2017**, *58*, 1417–1427. [\[CrossRef\]](#)
40. Zhu, Q.; Scherer, P.E. Immunologic and endocrine functions of adipose tissue: Implications for kidney disease. *Nat. Rev. Nephrol.* **2018**, *14*, 105–120. [\[CrossRef\]](#)
41. Pryor, W.A. The antioxidant nutrients and disease prevention—what do we know and what do we need to find out? *Am. J. Clin. Nutr.* **1991**, *53*, 391S–393S. [\[CrossRef\]](#)
42. Geng, J.; Qiu, Y.; Qin, Z.; Su, B. The value of kidney injury molecule 1 in predicting acute kidney injury in adult patients: A systematic review and Bayesian meta-analysis. *J. Transl. Med.* **2021**, *19*, 105. [\[CrossRef\]](#)
43. Zhang, W.; Li, X.; Zhou, S.-G. Ablation of carbohydrate-responsive element-binding protein improves kidney injury in streptozotocin-induced diabetic mice. *Eur. Rev. Med. Pharmacol. Sci.* **2017**, *21*, 42–47. [\[PubMed\]](#)
44. Masuzaki, R.; Kanda, T.; Sasaki, R.; Matsumoto, N.; Ogawa, M.; Matsuoka, S.; Karp, S.J.; Moriyama, M. Noninvasive Assessment of Liver Fibrosis: Current and Future Clinical and Molecular Perspectives. *Int. J. Mol. Sci.* **2020**, *21*, 4906. [\[CrossRef\]](#) [\[PubMed\]](#)
45. Jiménez-Urbe, A.P.; Gómez-Sierra, T.; Aparicio-Trejo, O.E.; Orozco-Ibarra, M.; Pedraza-Chaverri, J. Backstage players of fibrosis: NOX4, mTOR, HDAC, and S1P; companions of TGF- $\beta$ . *Cell. Signal.* **2021**, *87*, 110123. [\[CrossRef\]](#)
46. Viau, A.; El Karoui, K.; Laouari, D.; Burtin, M.; Nguyen, C.; Mori, K.; Pillebout, E.; Berger, T.; Mak, T.W.; Knebelmann, B.; et al. Lipocalin 2 is essential for chronic kidney disease progression in mice and humans. *J. Clin. Invest.* **2010**, *120*, 4065–4076. [\[CrossRef\]](#) [\[PubMed\]](#)
47. Kanda, J.; Mori, K.; Kawabata, H.; Kuwabara, T.; Mori, K.P.; Imamaki, H.; Kasahara, M.; Yokoi, H.; Mizumoto, C.; Thoennissen, N.H.; et al. An AKI biomarker lipocalin 2 in the blood derives from the kidney in renal injury but from neutrophils in normal and infected conditions. *Clin. Exp. Nephrol.* **2015**, *19*, 99–106. [\[CrossRef\]](#)
48. Mishra, J.; Ma, Q.; Prada, A.; Mitsnefes, M.; Zahedi, K.; Yang, J.; Barasch, J.; Devarajan, P. Identification of Neutrophil Gelatinase-Associated Lipocalin as a Novel Early Urinary Biomarker for Ischemic Renal Injury. *J. Am. Soc. Nephrol.* **2003**, *14*, 2534–2543. [\[CrossRef\]](#) [\[PubMed\]](#)
49. Browning, J.D.; Horton, J.D. Molecular mediators of hepatic steatosis and liver injury. *J. Clin. Invest.* **2004**, *114*, 147–152. [\[CrossRef\]](#) [\[PubMed\]](#)
50. Sanders, F.W.B.; Acharjee, A.; Walker, C.; Marney, L.; Roberts, L.D.; Imamura, F.; Jenkins, B.; Case, J.; Ray, S.; Virtue, S.; et al. Hepatic steatosis risk is partly driven by increased de novo lipogenesis following carbohydrate consumption. *Genome Biol.* **2018**, *19*, 79. [\[CrossRef\]](#)
51. Unger, R.H.; Clark, G.O.; Scherer, P.E.; Orci, L. Lipid homeostasis, lipotoxicity and the metabolic syndrome. *Biochim. Biophys. Acta* **2010**, *1801*, 209–214. [\[CrossRef\]](#)
52. Jiang, W.; Wang, X.; Geng, X.; Gu, Y.; Guo, M.; Ding, X.; Zhao, S. Novel predictive biomarkers for acute injury superimposed on chronic kidney disease. *Nefrologia* **2021**, *41*, 165–173. [\[CrossRef\]](#) [\[PubMed\]](#)
53. Przybyciński, J.; Dziedziczko, V.; Puchałowicz, K.; Domański, L.; Pawlik, A. Adiponectin in Chronic Kidney Disease. *Int. J. Mol. Sci.* **2020**, *21*, 9375. [\[CrossRef\]](#)
54. Zha, D.; Wu, X.; Gao, P. Adiponectin and Its Receptors in Diabetic Kidney Disease: Molecular Mechanisms and Clinical Potential. *Endocrinology* **2017**, *158*, 2022–2034. [\[CrossRef\]](#)



55. Schena, F.P.; Gesualdo, L. Pathogenetic mechanisms of diabetic nephropathy. *J. Am. Soc. Nephrol.* **2005**, *16* (Suppl. 1), S30–S33. [\[CrossRef\]](#)
56. Lousa, I.; Reis, F.; Beirão, I.; Alves, R.; Belo, L.; Santos-silva, A.; Beir, I.; Alves, R.; Santos-silva, A. New Potential Biomarkers for Chronic Kidney Disease Management — A Review of the Literature. *Int. J. Mol. Sci.* **2021**, *22*, 43. [\[CrossRef\]](#)
57. Lin, Q.; Chen, Y.; Lv, J.; Zhang, H.; Tang, J.; Gunaratnam, L.; Li, X.; Yang, L. Kidney injury molecule-1 expression in IgA nephropathy and its correlation with hypoxia and tubulointerstitial inflammation. *Am. J. Physiol. Renal Physiol.* **2014**, *306*, F885–F895. [\[CrossRef\]](#) [\[PubMed\]](#)
58. Humphreys, B.D.; Xu, F.; Sabbiseti, V.; Grgic, I.; Movahedi Naini, S.; Wang, N.; Chen, G.; Xiao, S.; Patel, D.; Henderson, J.M.; et al. Chronic epithelial kidney injury molecule-1 expression causes murine kidney fibrosis. *J. Clin. Invest.* **2013**, *123*, 4023–4035. [\[CrossRef\]](#)
59. Karmakova, T.A.; Sergeeva, N.S.; Kanukoev, K.Y.; Alekseev, B.Y.; Kaprin, A.D. Kidney Injury Molecule 1 (KIM-1): A Multifunctional Glycoprotein and Biological Marker (Review). *Sovrem. Tekhnologii Meditsine* **2021**, *13*, 64–78. [\[CrossRef\]](#)
60. Mishra, J.; Mori, K.; Ma, Q.; Kelly, C.; Yang, J.; Mitsnefes, M.; Barasch, J.; Devarajan, P. Amelioration of ischemic acute renal injury by neutrophil gelatinase-associated lipocalin. *J. Am. Soc. Nephrol.* **2004**, *15*, 3073–3082. [\[CrossRef\]](#) [\[PubMed\]](#)
61. Mori, K.; Lee, H.T.; Rapoport, D.; Drexler, I.R.; Foster, K.; Yang, J.; Schmidt-Ott, K.M.; Chen, X.; Li, J.Y.; Weiss, S.; et al. Endocytic delivery of lipocalin-siderophore-iron complex rescues the kidney from ischemia-reperfusion injury. *J. Clin. Invest.* **2005**, *115*, 610–621. [\[CrossRef\]](#) [\[PubMed\]](#)
62. Urbschat, A.; Thiems, A.-K.; Mertens, C.; Rehwald, C.; Meier, J.K.; Baer, P.C.; Jung, M. Macrophage-Secreted Lipocalin-2 Promotes Regeneration of Injured Primary Murine Renal Tubular Epithelial Cells. *Int. J. Mol. Sci.* **2020**, *21*, 2038. [\[CrossRef\]](#)
63. Mertens, C.; Kuchler, L.; Sola, A.; Guiteras, R.; Grein, S.; Brüne, B.; von Kneten, A.; Jung, M. Macrophage-Derived Iron-Bound Lipocalin-2 Correlates with Renal Recovery Markers Following Sepsis-Induced Kidney Damage. *Int. J. Mol. Sci.* **2020**, *21*, 7527. [\[CrossRef\]](#)
64. Sun, W.Y.; Bai, B.; Luo, C.; Yang, K.; Li, D.; Wu, D.; Feletou, M.; Villeneuve, N.; Zhou, Y.; Yang, J.; et al. Lipocalin-2 derived from adipose tissue mediates aldosterone-induced renal injury. *JCI Insight* **2018**, *3*, e120196. [\[CrossRef\]](#)
65. Rayego-Mateos, S.; Rodriguez-Diez, R.; Morgado-Pascual, J.L.; Valentijn, F.; Valdivielso, J.M.; Goldschmeding, R.; Ruiz-Ortega, M. Role of Epidermal Growth Factor Receptor (EGFR) and Its Ligands in Kidney Inflammation and Damage. *Mediat. Inflamm.* **2018**, *2018*, 8739473. [\[CrossRef\]](#) [\[PubMed\]](#)
66. Kawelke, N.; Vasel, M.; Sens, C.; von Au, A.; Dooley, S.; Nakchbandi, I.A. Fibronectin protects from excessive liver fibrosis by modulating the availability of and responsiveness of stellate cells to active TGF- $\beta$ . *PLoS ONE* **2011**, *6*, e28181. [\[CrossRef\]](#) [\[PubMed\]](#)
67. Shi, F.; Harman, J.; Fujiwara, K.; Sottile, J. Collagen I matrix turnover is regulated by fibronectin polymerization. *Am. J. Physiol. Cell Physiol.* **2010**, *298*, C1265–C1275. [\[CrossRef\]](#)
68. Pandey, K.B.; Rizvi, S.I. Plant polyphenols as dietary antioxidants in human health and disease. *Oxid. Med. Cell. Longev.* **2009**, *2*, 270–278. [\[CrossRef\]](#)
69. Valko, M.; Leibfritz, D.; Moncol, J.; Cronin, M.T.D.; Mazur, M.; Telser, J. Free radicals and antioxidants in normal physiological functions and human disease. *Int. J. Biochem. Cell Biol.* **2007**, *39*, 44–84. [\[CrossRef\]](#) [\[PubMed\]](#)
70. Santos, L. The impact of nutrition and lifestyle modification on health. *Eur. J. Intern. Med.* **2021**. [\[CrossRef\]](#) [\[PubMed\]](#)
71. Tüccar, T.B.; Akbulut, G. Mediterranean meal favorably effects postprandial oxidative stress response compared with a western meal in healthy women. *Int. J. Vitam. Nutr. Res.* **2021**. [\[CrossRef\]](#)
72. Lavefve, L.; Howard, L.R.; Carbonero, F. Berry polyphenols metabolism and impact on human gut microbiota and health. *Food Funct.* **2020**, *11*, 45–65. [\[CrossRef\]](#)
73. Eker, M.E.; Aaby, K.; Budic-Leto, I.; Brncic, S.R.; El, S.N.; Karakaya, S.; Simsek, S.; Manach, C.; Wiczowski, W.; de Pascual-Teresa, S. A Review of Factors Affecting Anthocyanin Bioavailability: Possible Implications for the Inter-Individual Variability. *Foods* **2019**, *9*, E2.
74. Tang, R.; Yu, H.; Ruan, Z.; Zhang, L.; Xue, Y.; Yuan, X.; Qi, M.; Yao, Y. Effects of food matrix elements (*dietary fibres*) on grapefruit peel flavanone profile and on faecal microbiota during in vitro fermentation. *Food Chem.* **2021**, *371*, 131065. [\[CrossRef\]](#) [\[PubMed\]](#)
75. Jakobeč, L.; Matić, P. Non-covalent dietary fiber - Polyphenol interactions and their influence on polyphenol bioaccessibility. *Trends Food Sci. Technol.* **2019**, *83*, 235–247. [\[CrossRef\]](#)
76. Beltrán Sanahuja, A.; De Pablo Gallego, S.L.; Maestre Pérez, S.E.; Valdés García, A.; Prats Moya, M.S. Influence of Cooking and Ingredients on the Antioxidant Activity, Phenolic Content and Volatile Profile of Different Variants of the Mediterranean Typical Tomato Sofrito. *Antioxidants* **2019**, *8*, 551. [\[CrossRef\]](#) [\[PubMed\]](#)
77. Monari, S.; Ferri, M.; Montecchi, B.; Salinitro, M.; Tassoni, A. Phytochemical characterization of raw and cooked traditionally consumed alimurgic plants. *PLoS ONE* **2021**, *16*, e0256703. [\[CrossRef\]](#)
78. Sun, Q.; Du, M.; Navarre, D.A.; Zhu, M. Effect of Cooking Methods on Bioactivity of Polyphenols in Purple Potatoes. *Antioxidants* **2021**, *10*, 1176. [\[CrossRef\]](#) [\[PubMed\]](#)
79. Samaniego-Sánchez, C.; Martín-del-Campo, S.T.; Castañeda-Saucedo, M.C.; Blanca-Herrera, R.M.; Quesada-Granados, J.J.; Ramirez-Anaya, J.D. Migration of Avocado Virgin Oil Functional Compounds during Domestic Cooking of Eggplant. *Foods* **2021**, *10*, 1790. [\[CrossRef\]](#) [\[PubMed\]](#)

80. Rinaldi de Alvarenga, J.F.; Quifer-Rada, P.; Francetto Juliano, F.; Hurtado-Barroso, S.; Illan, M.; Torrado-Prat, X.; Lamuela-Raventós, R.M. Using Extra Virgin Olive Oil to Cook Vegetables Enhances Polyphenol and Carotenoid Extractability: A Study Applying the sofrito Technique. *Molecules* **2019**, *24*, 1555. [[CrossRef](#)]
81. Rinaldi de Alvarenga, J.F.; Quifer-Rada, P.; Westrin, V.; Hurtado-Barroso, S.; Torrado-Prat, X.; Lamuela-Raventós, R.M. Mediterranean sofrito home-cooking technique enhances polyphenol content in tomato sauce. *J. Sci. Food Agric.* **2019**, *99*, 6535–6545. [[CrossRef](#)] [[PubMed](#)]





### 7.3. Other Scientific Publications

Sandoval V, Femenias A, Martinez-Garza U, Sanz-Lamora H, Castagnini JM, Quifer-Rada P, et al. Lyophilized Maqui (*Aristotelia chilensis*) Berry Induces Browning in the Subcutaneous White Adipose Tissue and Ameliorates the Insulin Resistance in High Fat Diet-Induced Obese Mice. *Antioxidants* (Basel, Switzerland). 2019 Sep;8(9).

Sandoval V, Sanz-Lamora H, Marrero PF, Relat J, Haro D. Lyophilized Maqui (*Aristotelia chilensis*) Berry Administration Suppresses High-Fat Diet-Induced Liver Lipogenesis through the Induction of the Nuclear Corepressor SMILE. *Antioxidants* (Basel, Switzerland). 2021 Apr;10(5).





Article

# Lyophilized Maqui (*Aristotelia chilensis*) Berry Induces Browning in the Subcutaneous White Adipose Tissue and Ameliorates the Insulin Resistance in High Fat Diet-Induced Obese Mice

Viviana Sandoval <sup>1,2</sup>, Antoni Femenias <sup>3</sup>, Úrsula Martínez-Garza <sup>1,2</sup>, Hèctor Sanz-Lamora <sup>1,2</sup>, Juan Manuel Castagnini <sup>4</sup>, Paola Quifer-Rada <sup>5</sup>, Rosa Maria Lamuela-Raventós <sup>1,2,6</sup>, Pedro F. Marrero <sup>1,6,7,\*</sup>, Diego Haro <sup>1,6,7,\*</sup> and Joana Relat <sup>1,2,6,\*</sup>

<sup>1</sup> Department of Nutrition, Food Sciences and Gastronomy, School of Pharmacy and Food Sciences, Food Torribera Campus, University of Barcelona, E-08921 Santa Coloma de Gramenet, Spain

<sup>2</sup> Institute of Nutrition and Food Safety of the University of Barcelona (INSA-UB), E-08921 Santa Coloma de Gramenet, Spain

<sup>3</sup> Applied Mycology Unit, Food Technology Department, University of Lleida, UTPV-XaRTA, Agrotecnio, E-25198 Lleida, Spain

<sup>4</sup> Facultad de Ciencias de la Alimentación, Universidad Nacional de Entre Ríos, Tavella 1450, 3200 Concordia, Argentina

<sup>5</sup> Department of Endocrinology & Nutrition, CIBER of Diabetes and Associated Metabolic Diseases, Biomedical Research Institute Sant Pau, Hospital de la Santa Creu i Sant Pau, E-08041 Barcelona, Spain

<sup>6</sup> CIBER Physiopathology of Obesity and Nutrition (CIBER-OBN), Instituto de Salud Carlos III, E-28029 Madrid, Spain

<sup>7</sup> Institute of Biomedicine of the University of Barcelona (IBUB), E-08028 Barcelona, Spain

\* Correspondence: dhara@ub.edu (D.H.); jrelat@ub.edu (J.R.); Tel.: +34-934-033-790 (D.H.); +34-934-020-862 (J.R.)

Received: 1 July 2019; Accepted: 23 August 2019; Published: 1 September 2019



**Abstract:** Maqui (*Aristotelia Chilensis*) berry features a unique profile of anthocyanidins that includes high amounts of delphinidin-3-O-sambubioside-5-O-glucoside and delphinidin-3-O-sambubioside and has shown positive effects on fasting glucose and insulin levels in humans and murine models of type 2 diabetes and obesity. The molecular mechanisms underlying the impact of maqui on the onset and development of the obese phenotype and insulin resistance was investigated in high fat diet-induced obese mice supplemented with a lyophilized maqui berry. Maqui-dietary supplemented animals showed better insulin response and decreased weight gain but also a differential expression of genes involved in de novo lipogenesis, fatty acid oxidation, multilocular lipid droplet formation and thermogenesis in subcutaneous white adipose tissue (scWAT). These changes correlated with an increased expression of the carbohydrate response element binding protein b (*Chrebpb*), the sterol regulatory binding protein 1c (*Srebp1c*) and Cellular repressor of adenovirus early region 1A-stimulated genes 1 (*Creg1*) and an improvement in the fibroblast growth factor 21 (FGF21) signaling. Our evidence suggests that maqui dietary supplementation activates the induction of fuel storage and thermogenesis characteristic of a brown-like phenotype in scWAT and counteracts the unhealthy metabolic impact of an HFD. This induction constitutes a putative strategy to prevent/treat diet-induced obesity and its associated comorbidities.

**Keywords:** anthocyanins; browning; carbohydrate-responsive element binding protein b; delphinidin; fibroblast growth factor 21; high-fat diet; maqui berry; white adipose tissue

## 1. Introduction

Stimulation of the brown adipose tissue (BAT) and the induction of browning in white adipose tissue (WAT) as a strategy against obesity and its associated metabolic complications has generated growing interest in recent years. This interest is based on the ability of both BAT and browned-WAT to increase energy expenditure (EE) mainly through fatty acid consumption [1,2], and their pivotal role in the control of energy homeostasis in mammals [3,4]. In addition to classical brown adipocytes located in BAT, thermogenic adipocytes with similar characteristics can be found within white adipose tissue (WAT) [3]. These brite/beige adipocytes are metabolically and phenotypically similar to brown adipocytes and can actively contribute to increasing whole-body EE. Specifically, brite/beige adipocytes show a multilocular phenotype and express genes closely related to BAT metabolism (Ucp1 as a marker of its thermogenic capacity in addition to genes implied in de novo lipogenesis (DNL), fatty acid oxidation (FAO), lipolysis, etc.).

Recent evidence shows that the activation of BAT and the induction of browning in WAT can be induced by cold acclimation but also by nutritional inputs under different signaling cascades [2,5–7]. Cold is a classic activator of BAT and of beige adipocyte development and function [5,8]. Regarding nutritional inputs, we recently demonstrated that low-protein diets and the cooked-tomato sauce called “sofrito” are able to induce Ucp1 expression in WAT, thus indicating a browning phenotype [6,7]. In the same way, other authors published that high-fat diets, bioactive compounds and prebiotics can also induce browning in WAT [9–14].

Part of the cold-induced metabolic profile in BAT is regulated by the stimulation of carbohydrate-responsive element binding protein b (ChREBPb) through the Ak strain transforming/protein kinase 2 (AKT2) activity [15]. Besides ChREBP, fibroblast growth factor 21 (FGF21) has shown beneficial effects on glucose/lipid homeostasis and body weight control among other mechanisms by increasing energy expenditure (EE) and inducing browning and UCP1 overexpression in adipose tissues [6,16–19], as well as by promoting the insulin-dependent glucose uptake, mitochondrial biogenesis, and adiponectin secretion in adipocytes [20,21]. In this case, it has been widely demonstrated that FGF21 activity and/or signaling respond to nutritional challenges [22].

Anthocyanidin-rich berries have been proposed for the treatment and prevention of several disorders, including obesity-related metabolic disorders [23–32] but little is known about the molecular mechanisms underlying their beneficial effects. Maqui (*Aristotelia chilensis*) is a native Chilean berry with a unique anthocyanins profile that includes delphinidin-3-O-sambubioside-5-O-glucoside and delphinidin-3-O-sambubioside as the main phenolic compounds [33]. Besides its antioxidant activity, different preparations of maqui have shown positive effects on fasting glucose and insulin levels in humans and murine model of type 2 diabetes and obesity [34–37] and delphinidin-3-sambubioside-5-glucoside has been described as the responsible for hypoglycemic activity in in vivo models [36].

With the global aim of deepening the knowledge of the molecular mechanisms responsible for the metabolic effects of maqui and in some way of the anthocyanidin-rich foods, we investigated the effect of a lyophilized maqui berry preparation on the onset and progression of the diet-induced obesity (DIO) in mice subjected to high-fat diet (HFD) for 16 weeks. We studied the impact of maqui in the metabolic profile of the obese phenotype. We focused on the adipose tissue metabolic phenotype because of its role on the progression of obesity and as a major target to counteract the onset and development of this pathology and its metabolic-associated diseases such as insulin resistance. We analyzed specifically the subcutaneous WAT (scWAT) because growing evidence suggests that this depot is protective to metabolic health while visceral is detrimental [38–43].

Globally, our results highlight the potential role of maqui in the treatment of diet-induced obesity and insulin resistance. Further studies will be needed to identify the effects of maqui on healthy population and the impact of its regular consumption as part of a healthy dietary pattern such as the Mediterranean diet.

## 2. Materials and Methods

### 2.1. Anthocyanins Determinations by UPLC-DAD

For sample preparation, 0.1 g of maqui was extracted with 5 mL of a mixture of water and ethanol 80:20 (*v/v*). The extraction was repeated 3 times to increase extractability of the anthocyanidins. The extract was evaporated under vacuum to remove the ethanol and reconstituted to a final volume of 10 mL with MilliQ water. This procedure was done in triplicate. Finally, the sample was filtered through a 0.22  $\mu\text{m}$  PTFE membrane filter into an amber vial for UPLC analysis.

The quantification and identification of anthocyanins was done using a Waters Acquity Ultra Performance Liquid Chromatography H class (Waters Corp, Milford MA, USA) coupled to Photodiode Array (PDA) detector (Waters Corp, Milford MA, USA). The chromatographic separation was performed by an Acquity BEH C18 column 2.1 mm  $\times$  100 mm, 1.7  $\mu\text{m}$ . The chromatographic method proposed by Andrés-Lacueva et al. (2005) adapted to the UPLC system was used [44]. Briefly, the injection volume was 10  $\mu\text{L}$  and the gradient elution was performed with water/5% formic acid (*v/v*) (A) and 100% acetonitrile (B) at a constant flow rate of 0.75 mL/min. A decreasing linear gradient of solvent A was used. Separation was carried out in 11 min under the following conditions: 0 min, 98% A; 6 min, 95% A; 9 min, 90% A; 9.1 min, 20% A; 9.3 min, 20% A; 9.4 min, 92% A, 11 min, 92% A.

The column was equilibrated for 6 min prior to each analysis. Each maqui anthocyanin was quantified at  $\lambda = 520$  nm using a calibration curves with pure standard purchased in Extrasynthese S. A. (Delphinidin-3-O-sambubioside-5-O-glucoside, delphinidin-3-O-sambubioside, cyanidin-3-O-sambubioside-5-O-glucoside, cyanidin-3-O-glucoside and cyanidin-3-O-sambubioside), and the identification was made by comparing the retention times of the chromatographic peaks with the retention time of the pure phenolic standards. Results were expressed as millimoles of anthocyanins per kilogram of maqui (mmol/kg).

### 2.2. Animal Procedures—Dosage Regimen

Animal procedures were approved by the Animal Ethics Committee of the University of Barcelona (CEEA-173/18). C57BL/6J littermates' male mice ( $n = 23$ ) were housed in a temperature-controlled room ( $22 \pm 1$  °C) on a 12-h/12-h light/dark cycle and were provided free access to commercial rodent chow and tap water prior to the experiments. When animals were four-week-old it was confirmed that all animals were normoglycemic before being randomly assigned into two experimental groups (HFD and HFD supplemented with maqui (HFDM)). Both groups were fed a diet of 45% fat-derived calories (HFD) (D12451, Research Diets) for 16 weeks supplemented or not with lyophilized maqui. HFD group ( $n = 9$ ) had free access to HFD diet and filtered-tap water and HFDM ( $n = 14$ ) group had free access to HFD diet and filtered-tap water supplemented with maqui (20 mg of lyophilized maqui/mL of filtered-tap water). To prepare the supplemented water, 1 g of the lyophilized maqui was added to 50 mL of tap-filtered water. This mixture was prepared extemporaneously every two days to prevent the oxidation of maqui bioactive compounds.

The dosage regimen of maqui was calculated according to the polyphenol intake recommended as beneficial by the Predimed Study (820 mg in a human diet of 2300 kcal) [45,46]. Mice intake is around 10–15 kcal per day, which means 4–5 mg of polyphenols per day scaling-down the recommended beneficial quantity in humans. Table 1 shown that 1g of lyophilized maqui provides 45 mg of anthocyanins. The dose of maqui was adjusted to achieve 4 mg of polyphenols per day, considering that mice take 2–3 mL of water/day. The nutritional composition of the lyophilized maqui used (Maquiberry, Native for Life, Chile) is indicated in the supplemental information (Table S1).

During the 16-week nutritional intervention, food and beverage intake were recorded every two days and body weight twice a week. At the end of the nutritional intervention, the animals were euthanized. Blood was extracted by intracardiac puncture, and serum was obtained by centrifugation (1500 rpm, 20 min). Epididymal WAT (eWAT), scWAT and BAT were isolated, immediately snap-frozen and stored at  $-80$  °C for future analysis.

### 2.3. RNA Isolation and Quantitative RT-PCR

Total RNA was isolated from frozen tissues using TRI Reagent™ Solution (AM9738, Thermo Fisher Scientific, Waltham, USA), followed by DNaseI treatment (K2981, Thermo Fisher Scientific, Waltham, USA). cDNA was synthesized from 1 µg of total RNA using the High-Capacity cDNA Reverse Transcription Kit (4368814, Thermo Fisher Scientific, Waltham, USA). Relative mRNA levels were measured by quantitative PCR (qPCR) using SYBR™ Select Master Mix for CFX (4472942, Thermo Fisher Scientific, Waltham, USA). 18S and B2M were used as housekeeping genes. The sequences of the primers used in qPCR are presented in Table S2. Results were obtained by the relative standard curve method, and values were referred to the HFD group.

### 2.4. Glucose Tolerance Test (GTT) and Insulin Tolerance Test (ITT)

Mice were fasted for 6 h in the morning, and then injected intraperitoneally (i.p.) with 1.5 g of glucose (Sigma)/kg mouse (GTT) or 0.5 UI of insulin solution (Sigma)/kg mouse (ITT). Blood samples were collected from the tail vein, and glucose levels were measured using a glucometer (Glucocard SM, Menarini, Florence, Italy) prior to the i.p. injection and at 30, 60 and 120 min postinjection. GTT was performed 14 weeks after the beginning of maqui supplementation and ITT on week 15th.

### 2.5. Histological Analysis

For the histological analysis, pieces of scWAT of each animal were fixed in 10% formalin (Sigma) and embedded in paraffin. Afterwards, 4 µm-thick sections were cut and stained with hematoxylin and eosin (H&E). Images were acquired using a Digital Upright Microscope BA310 Digital and a Moticom 2500 camera. The selection of the test objects was performed according to color and choosing the same limits for binarization for all images. At least three pictures from different regions of each cut were taken.

### 2.6. Data Analysis/Statistics

GraphPad Prism version 8.02 (GraphPad, San Diego, CA, USA) was used to perform the statistical analyses. Two tailed Student's Test with Welch's correction when not equal SDs can be assumed was used to determine significant differences among experimental groups. The statistical analysis of body weight progression, body weight/calorie intake and curves of GTT and ITT was performed by 2 factor ANOVA with post-hoc test (Bonferroni's). In all cases, *p*-value < 0.05 was considered statistically significant. All data are expressed as the mean ± SEM.

## 3. Results

### 3.1. Maqui Anthocyanin Content

The levels of anthocyanins determined in the lyophilized maqui used in our experimental approach (Maquiberry, Native for Life, Chile) (Table 1) were similar to those reported previously [47–50]. In terms of the total content of anthocyanins, the lyophilized maqui used in this work has an extremely high content (45,052 mg/kg = 4.5%) compared to other similar products like a Freeze-Dried Whole Blueberry (2432 mg/kg = 2.4%) [51] or a dried raspberry solids (750 mg/kg = 0.75%) [52]. The predominant (80%) anthocyanins were delphinidin-3-O-sambubioside-5-O-glucose and delphinidin-3-O-sambubioside, as shown in Table 1 and Figure S1 (Supplemental Materials).

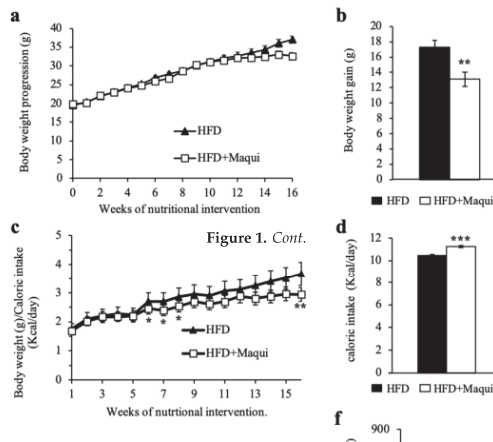
**Table 1.** Anthocyanidin composition of the lyophilized maqui berry. Anthocyanins were determined by UPLC-DAD. The table shows the concentration in mg/g and mmol/kg of the different anthocyanidins detected. The table includes the retention time (min), the limit of detection (LOD) and the limit of quantification (LOQ) for each molecule.

Compound	Conc. (mg/g)	Conc. (mmol/kg)	Retention Time (min)	LOD (mg/L)	LOQ (mg/L)
Delphinidin-3-O-sambubioside-5-O-glucoside	19.645 ± 0.788	24.71 ± 0.99	3.5	1.81	6.02
Delphinidin-3-O-sambubioside	17.770 ± 1.178	28.07 ± 1.86	5.	0.30	1.00
Cyanidin-3-O-sambubioside-5-O-glucoside	2.447 ± 0.063	3.14 ± 0.08	5.5	0.75	2.50
Not identified (quantified as cyd-3-O-glu)	0.402 ± 0.050	0.83 ± 0.10	6.5	-	-
Cyanidin-3-O-glucoside	2.148 ± 0.158	4.43 ± 0.33	7	0.11	0.35
Cyanidin-3-O-sambubioside	2.642 ± 0.201	4.28 ± 0.33	7.3	0.17	0.56
TOTAL	45.052	65.46			

### 3.2. Maqui Dietary Supplementation Reduces HFD-Induced Body Weight Gain and Improves Insulin Sensitivity in Mice

C57BL/6J mice fed an HFD for 16 weeks put on weight (Figure 1a,b) and displayed glucose intolerance (Figure 1e,f) and insulin resistance (Figure 1g,h). Comparing both experimental groups revealed that mice fed HFD supplemented with maqui (HFDM) showed an attenuated progression in body weight (Figure 1a–c), even the animals were hyperphagic, and their daily caloric intake was higher (Figure 1d). Concretely, the HFDM animals put on less weight after the 16 weeks of nutritional intervention (Figure 1b). Even though no statistical differences were observed in the body weight progression (Figure 1a), there were when the ratio between body weight and caloric intake was calculated (Figure 1c). These data indicated that, in some way, there is an increased energy expenditure in these animals.

Regarding the insulin/glucose responsiveness, HFDM mice shown a significant reduction in fasting glucose at Week 15 of the nutritional intervention ( $207.6 \pm 5.5$  vs.  $166.5 \pm 6.1$ ,  $p = 2.7 \times 10^{-5}$ ). It is worth highlighting that, after the glucose injection, the HFDM animals displayed a better glucose curve (Figure 1e) that corresponded to a significant reduction of the area under the curve (AUC) of the GTT (Figure 1f,  $p < 0.05$ ). In the case of the ITT, the curve of glucose after the insulin injection showed significantly lower levels of glucose at the first time-points (Figure 1g). These differences were minimized but maintained over time, even though they did not reach statistical significance (Figure 1g). Finally, the AUC of the ITT showed a clear tendency to a reduction in HFDM (Figure 1h,  $p < 0.08$ ). Although some of the data are not significant individually, altogether they indicate an improvement on glucose tolerance and insulin sensitivity after 16 weeks of maqui dietary supplementation.





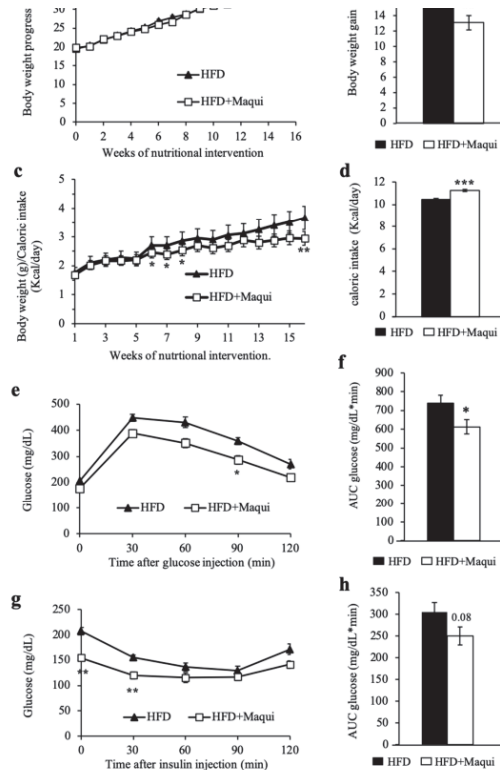


**Figure 1.** Maqui dietary supplementation reduces HFD-induced body weight gain and improves glucose metabolism. (a) Body weight progress (g) for the HFD and HFD+Maqui groups. (b) Total body weight gain (g) for the HFD and HFD+Maqui groups. (c) Body weight gain (g) for the HFD and HFD+Maqui groups. (d) Caloric intake (Kcal/day) for the HFD and HFD+Maqui groups. (e) Glucose (mg/dL) at 0, 30, 60, 90, and 120 min after glucose injection. (f) AUC glucose (mg/dL\*min) for the HFD and HFD+Maqui groups. (g) Glucose (mg/dL) at 0, 30, 60, 90, and 120 min after insulin injection. (h) AUC glucose (mg/dL\*min) for the HFD and HFD+Maqui groups. \*  $p < 0.05$ , \*\*  $p < 0.01$ , \*\*\*  $p < 0.001$  versus the HFD group.

### 3.3. Maqui Dietary Supplementation Induces a Multilocular Phenotype in scWAT

HFD mice were leaner than their littermates (Figures 1a and 2a) and had more BAT and less WAT (Figure 2b,c). Because of the healthier profile observed in HFD mice regarding body weight and insulin resistance, we hypothesized that maqui could be exerting its effects through the induction of browning in scWAT. The H&E staining of scWAT revealed that maqui supplementation induced the transition of unilocular adipocytes to multilocular ones (Figure 2d). No differences in other WAT depots due to maqui supplementation were observed in any analysis performed.

HFD mice were leaner than their littermates (Figures 1a and 2a) and had more BAT and less WAT (Figure 2b,c). Because of the healthier profile observed in HFD mice regarding body weight and insulin resistance, we hypothesized that maqui could be exerting its effects through the induction of browning in scWAT. The H&E staining of scWAT revealed that maqui supplementation induced the transition of unilocular adipocytes to multilocular ones (Figure 2d). No differences in other WAT depots due to maqui supplementation were observed in any analysis performed.

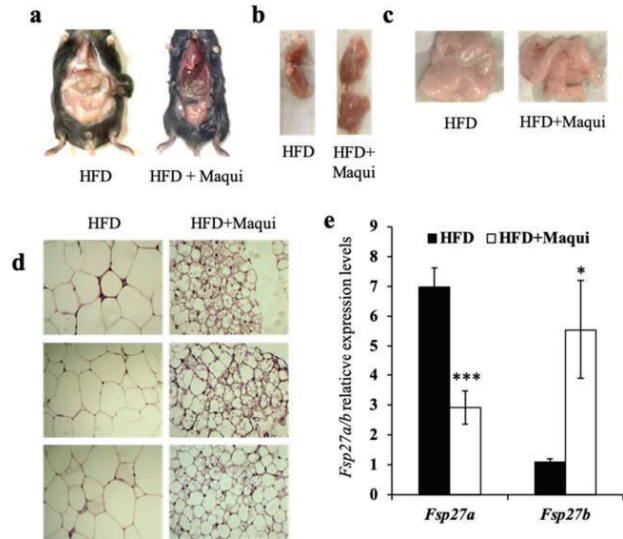


**Figure 2.** Maqui effects on body weight, adiposity, and gene expression. (a) Representative photos of HFD and HFD+Maqui mice. (b) Representative photos of BAT depots. (c) Representative photos of WAT depots. (d) H&E staining of scWAT showing unilocular vs multilocular adipocytes. (e) Bar graph of *Fsp27a/b* relative expression levels. \*\*\* p < 0.001, \* p < 0.05.

In the context of browning, recent publications have shown the relevance of fat-specific protein 27 (*Fsp27*) isoforms in the phenotype of unilocular and multilocular lipid droplets. *Fsp27* is considered to be, at least in part, the protein responsible for the formation and growth of lipid droplets (LDs). Two isoforms can be encoded by both different expression patterns and functions. *Fsp27a* and *Fsp27b* are both involved in the formation of large LDs by targeting and expressing the *Fsp27* isoform to the lipid droplet. The transition of unilocular to multilocular LDs is a key feature of brown-like phenotype of scWAT in HFD mice, the mRNA levels of both *Fsp27* isoforms were measured. The results indicated that the dietary maqui supplementation causes a shift in the expression pattern of *Fsp27*. The scWAT depot of HFD mice showed a significant reduction in the levels of *Fsp27a* and a significant induction of *Fsp27b* expression (Figure 2e), thus reinforcing the idea that maqui causes a brown-like phenotype in the scWAT.

phenotype observed in HFD mice, the mRNA levels of several lipogenic enzymes were measured. The results indicated that the dietary maqui supplementation causes a shift in the expression pattern of *Fsp27*. The scWAT depot of HFD mice showed a significant reduction in the levels of *Fsp27a* and a significant induction of *Fsp27b* expression (Figure 2e), thus reinforcing the idea that maqui causes a brown-like phenotype in the scWAT.

8 of 19

### 3.4. Maqui Induces the Expression of Genes from de Novo Lipogenesis, Fatty Acid Oxidation, Thermogenesis and Browning in scWAT

As shown in Figure 3, in the scWAT of HFD mice, the mRNA levels of genes related to mitochondrial (carnitine palmitoyl transferase 1b (Cpt1b)) and peroxisomal (Acyl-CoA oxidase 3 (Acox3), Enoyl-Coenzyme A, and Hydratase/3-Hydroxyacyl Coenzyme A Dehydrogenase (Ehhadh)) FAO (Figure 3a), DNL (Acetyl-CoA Carboxylase Alpha (Acaca), ATP Citrate Lyase (Acly), Fatty acid synthase (Fasn), Diacylglycerol Acyltransferase 1 (Dgat1), Sterol regulatory binding protein 1c (Srebp1c) and Glycerol Kinase (Glyk)) (Figure 3b) and thermogenesis/browning (Ucp1, Type 2 Iodothyronine Deiodinase (Dio2), Prdm16, Pparg, Creg1, Pgc1a) (Figure 3c) were significantly higher in HFD mice. Maqui treatment significantly reduced the expression of Cpt1b, Acaca, Fasn, Acly, Glyk, Dgat1, Srebp1c, Pgc1a, Prdm16, Pparg, Creg1, and Dio2, and increased the expression of Ucp1. The results suggest that the scWAT of the HFD mice were metabolically closer to the brown-like phenotype (also in the scWAT of the HFD mice) and that the browning did not show a significant difference in the scWAT of the HFD mice. The induction of Ucp1 was observed (data not shown).

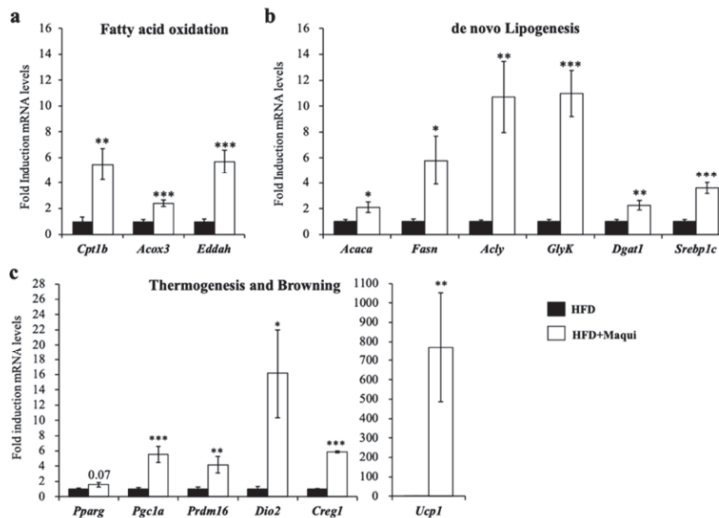


**Figure 3.** Maqui induces the expression of genes from de novo lipogenesis, fatty acid oxidation, and thermogenesis/browning in scWAT. The relative mRNA levels of carnitine palmitoyl transferase 1b (Cpt1b), acyl-CoA oxidase 3 (Acax3), enoyl-Coenzyme A, and Hydratase/3-Hydroxyacyl Coenzyme A Dehydrogenase (Ehhadh), diacylglycerol acyltransferase 1 (Dgat1), sterol regulatory binding protein 1c (Srebp1c), fatty acid synthase (Fasn), acetyl-CoA carboxylase alpha (Acaca), ATP citrate lyase (Acly), glycerol kinase (Glyk), peroxisome proliferator-activated receptor gamma coactivator 1 alpha (Pgc1a), and cellular repressor of adenovirus early region 1 (Creg1) were measured using qRT-PCR in scWAT of HFD and HFD+Maqui mice. Bars represent the fold induction in the mRNA levels versus the HFD animals that are considered the control group, which produces an arbitrary value of 1. Data are presented as the mean  $\pm$  SEM. \*  $p < 0.05$ , \*\*  $p < 0.01$ , \*\*\*  $p < 0.001$  versus the HFD group.



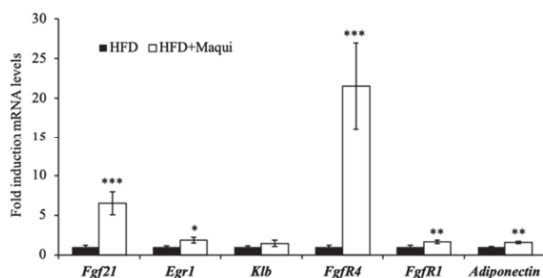


**Figure 5.** Maqui induces the expression of *Fgf21*, *Fgf21* receptors and FGF21 signaling markers in scWAT. The relative mRNA levels of *Fgf21*, *Fgf21R1*, *FgfR4*, *Klf8*, *Adiponectin* and *Egr1* were measured by qRT-PCR in scWAT of HFD and HFD+Maqui mice. Bars represent the fold induction in the HFD animals that are considered the control group and assigned an arbitrary value of 1. Data are presented as the mean  $\pm$  SEM. \*\*\*  $p < 0.001$ , \*\*  $p < 0.01$ , \*  $p < 0.05$ , versus the HFD group.

#### 4. Discussion

Our data show that maqui dietary supplementation ameliorates the unhealthy effects of HFD. By using diet-induced obese mice, the present study demonstrated that supplemented animals displayed better overall responsiveness, decreased weight gain and increased thermogenic activity. The ability to burn calories and increase energy expenditure is a key feature of brown adipocytes. In our study, we demonstrated that supplemented animals displayed increased brown adipocyte markers, decreased weight gain and increased thermogenic activity. These findings are consistent with previous studies showing that scWAT is a key site for the expression of genes involved in brown fat, mitochondrial and peroxisomal FAO, mitochondrial oxidative phosphorylation and energy expenditure.

Obesity is essentially caused by an imbalance between energy intake and energy expenditure. Some evidence indicates that at some point, the white adipose tissue (WAT) fails to adequately keep the surplus of nutrients, which together with an insufficient differentiation of new adipocytes leads to the accumulation of ectopic lipids in non-adipose, relevant organs that may cause the metabolic syndrome. The biomedical relevance of brown and beige adipocytes lies in the ability of these cells to increase EE and burn the excess of energy. The activity of brown/beige or both fat depots is considered a promising strategy for the treatment of metabolic diseases such as obesity or type 2 diabetes [1,2]. Indeed, increasing the activity of brown/beige or both fat depots is considered a promising strategy for the treatment of metabolic diseases [67,68].

Berries are an important source of anthocyanins [27,36,69,70]. Anthocyanins are widely distributed water-soluble polyphenols that have shown important health effects including metabolic effects on glucose metabolism [27,36,69,70]. In this context, maqui berry features a rich profile of anthocyanins and high amounts of delphinidin-3-O-sambubioside, a glucose metabolite and the main anthocyanin in this berry [69,70]. In this context, maqui berry features a rich profile of anthocyanins, which includes higher amounts of delphinidin-3-O-sambubioside [69,70], a glucose metabolite and the main anthocyanin in this berry [69,70].

Our results clearly confirm the previously described effects of maqui regarding glucose metabolism and also describe the capacity of maqui to induce browning in HFD-induced obese mice. Dietary supplemented obese mice showed less weight gain despite their hyperphagic behavior, thus indicating that in some way these animals have a higher metabolic rate, probably due to an increased capacity of maqui to induce browning in HFD-induced obese mice. Dietary supplemented obese mice showed less weight gain despite their hyperphagic behavior, thus indicating that in some way these animals have a higher metabolic rate, probably due to an increased BAT depot and a more energy consuming scWAT. The absence of effects on other WAT depots indicated that scWAT was the target for maqui beneficial effects against diet-induced obesity and



and that at least part of the effects of berries on glucose metabolism and insulin sensitivity go through the improvement of adipose tissue functionality.

BAT thermogenesis is stimulated by adrenergic induction of cAMP production, which activates protein kinase A (PKA) to drive transcription of thermogenic genes (including *Ucp1*), lipolysis and FAO. Although less recognized, the activation of BAT thermogenesis paradoxically induces the anabolic DNL pathway [15,82–84]. Several studies support the important role of ChREBP isoforms in the control of insulin signaling and lipogenesis in adipose tissue and describe the induction of both isoforms' activity under the Glut4-dependent glucose uptake [55,85–88]. In WAT, HFD feeding lowers the expression of *Chrebp* and DNL genes in mice [55]. Moreover, the expression of a constitutively active ChREBP in WAT protects mice against obesity and insulin resistance by among others reducing adiposity and increasing the expression of gene related to adipocyte differentiation and browning [89]. In the same context, an adipose-specific *Chrebp* knockout mice show a decrease in DNL and are insulin resistant with an impaired insulin action in the liver, muscle and fat [85]. Beyond mice, in humans, the expression of *Chrebp* and lipogenic genes in WAT shows a strong correlation with insulin sensitivity, and the improvement of insulin sensitivity in insulin-resistant people restores *Chrebp* and glucose transporter type 4 (*Glut4*) expression in adipose tissue [56].

Our key finding is that this characteristic metabolic feature of BAT also appears in the scWAT of obese mice fed a maqui-supplemented HFD where there is an induction of *Chrebp*, *Chrebpb* and *Glut4* expression and also higher mRNA levels of genes involved in DNL, multilocular LDs formation and thermogenesis/browning. The remaining question is how ChREBP is activated under maqui supplementation. The increased levels of Glut4 in HFD mice indicated that glucose or glucose metabolites could be the major inducers of *Chrebp* expression [90,91]. Moreover, although ChREBP was initially identified as a glucose-responsive factor, recent evidence suggests that it is also essential for fructose-induced lipogenesis both in the small intestine and liver [55,92]. The effects of maqui could, therefore, be attributed to its fructose content. However, the absence of *Chrebpb* induction in liver (data not shown) allows us to rule out this possibility.

SREBP1c is also a key regulator of hepatic DNL [93–98]. It has been demonstrated that, in the liver, SREBP1c and ChREBP are both necessary for the expression of lipogenic and glycolytic genes [88,99]. In adipose tissue, the role of SREBP1c is more controversial. In adipose tissue, the mRNA levels of lipogenic genes did not change in animals using a *Srebp1c* loss of function or gain of function approach, thus indicating that in this tissues *Srebp1c* is not essential for DNL activation [58]. By contrast, mice under caloric restriction (CR) showed an SREBP1c/PGC1a-dependant induction of DNL in adipose tissue giving to *Srebp1c* an role on activating this metabolic pathway under this specific nutritional condition [100]. Finally, CREG1 has been described as an inducer of *Ucp1* and FGF21 expression in an adipocyte P2-Creg1-transgenic (Tg) mice and globally of BAT adipogenesis and browning [101,102]. Our results indicate that maqui supplementation is able to induce the expression of *Chrebp*, *Srebp1c*, *Pgc1a* and *Creg1*, thus we cannot discard any of them as possible contributors to the induction of DNL and thermogenic genes observed.

In addition, in the scWAT of dietary-supplemented obese mice, there was an increase in the expression of peroxisomal FAO enzymes that would make possible the contradiction of having FAO and DNL simultaneously active. Peroxisomal FAO is important in this scenario where, despite an increased expression of *Cpt1b*, the rate-limiting enzyme of mitochondrial FAO, this pathway would be inhibited by the malonyl-CoA produced by DNL.

Apart from the abovementioned mechanisms our data also pointed out the improvement of FGF21 signaling as a way through which maqui could exert its beneficial effects. It has been widely described that FGF21 levels are increased in obesity and diabetes in both animal models and humans [60,103,104]. The downregulation of FGF21 receptors in adipose tissue seems to be the key point to explain the FGF21-resistant state described mainly in obese mice as well as, in some studies, in humans [43,59,60,105–108]. In this context, the restoring of FGF21 signaling can be considered as a potential therapeutic strategy to improve the metabolic parameters of obese individuals and to reduce

the risk of obesity-related diseases and some evidence support this hypothesis [7,109]. In various rodent models of diet-induced obesity a positive correlation between the beneficial effects of polyphenol-rich fruit extracts and FGF21 has been described. This correlation with FGF21 can be due to an induction of FGF21 levels [110,111] or an improvement of the FGF21 signaling [7,112,113]. Finally, FGF21-resistance in adipose tissue has been linked to a decreased production of adiponectin [114]. Adiponectin induces fatty acid oxidation leading to a reduction of ectopic lipids and finally the improvement of insulin sensitivity [115]. In our results, the induction of the mRNA levels of *adiponectin*, *FgfR1*, *FgfR4* and *Egr1* in scWAT of HFDM mice indicates that, in obesity, maqui supplementation increases the sensitivity to FGF21 of scWAT.

Although our results do not allow us to discard that other signaling pathways could stimulate the white to beige/brown transition described, the improvement of FGF21 signaling together with the overexpression of ChREBP, CREG1, PGC1a and SREBP1c are at least key players in the induction of browning described under maqui supplementation. Neuroendocrine signaling or molecules such as leptin or *Bmp8b* will be analyzed in further studies to try to complete the signaling cascade activated by maqui [2,67,116].

To summarize, we demonstrated that a nutritional intervention with maqui partially alleviates the unhealthy effects of HFD in mice. Our results provide evidence that, in mice, a dietary supplementation with maqui added to beverage activates the induction of fuel storage and thermogenesis characteristic of a brown-like phenotype in scWAT. Finally, based on previously published data, our results indicate that maqui could exert its effects, at least in part, through the induction of *Chrebp* expression and the improvement of FGF21 signaling. Finally, it is worth mentioning that in this work the dose of maqui was scaled-down from the polyphenol intake recommended as beneficial in humans by the Predimed Study [45,46]. This is important because several phenolic compounds such as resveratrol, quercetin, cyanidin-3-glucoside (C<sub>3</sub>G), capsaicin, hesperidin have green tea extract have been described as inducers of BAT activity or WAT browning but in most cases the dietary supplementation was performed using high doses and only the active compounds [9–13,117–121].

#### *Limitations of the Present Work and Further Studies*

This work clearly demonstrates that maqui is effective in obese mice. The impact of maqui in healthy individual needs to be evaluated. We do not have data about the effects of maqui on normal chow-fed animals where neither obesity nor insulin resistant is present, but this experimental approach will be included in our further studies. Positive results in this follow-up experiment will allow pointing out the efficacy of the consumption of maqui in the prevention of some metabolic diseases and whether to include its regular consumption as part of a healthy dietary pattern.

On the other hand, despite the observed changes in gene expression, together with the scWAT and BAT appearance and the histological analysis to define properly the browning phenotype, in this study, the translation to protein was assumed. To overcome this limitation, Western blot analyses will be performed to reinforce our results and deepen the mechanism of action of maqui.

#### **5. Conclusions**

In conclusion, our data provide evidence that, in obese mice, a dietary intervention with a regular dose of an anthocyanidin-enriched berry (maqui) can induce a browning phenotype in scWAT and improve partially the insulin sensitivity, thus ameliorating some of the unhealthy effects of HFD. These effects reinforce the anthocyanidin-enriched foods as a potential strategy to prevent or treat type 2 diabetes and obesity-related diseases and point out maqui as a putative functional fruit to counteract at least in part obesity and its metabolic complications. The data presented in this manuscript reinforce the inclusion of maqui in the diet of obese individuals.

**Supplementary Materials:** The following are available online at <http://www.mdpi.com/2076-3921/8/9/360/s1>, Table S1: Maqui extract nutritional composition, Table S2: Sequences of the primers used in SYBR Green assays and references of the probes used in Taqman assays, Figure S1: Chromatogram of the anthocyanins identified in maqui samples. 1: Delphinidin-3-O-sambubioside-5-O-glucoside; 2: Delphinidin-3-O-sambubioside; 3: Cyanidin-3-O-sambubioside-5-O-glucoside; 4: Unknown; 5: Cyanidin-3-O-glucoside; 6: Cyanidin-3-O-sambubioside.

**Author Contributions:** V.S., U.M.-G., H.S.-L. and J.R. performed all the animal procedures (nutritional intervention, ITT, GTT, body weight recording, and food and beverage intake measurements). V.S. and A.F. performed the gene expression analysis and compiled the statistics. V.S. and A.F. analyzed the H&E samples. J.M.C., P.Q.-R. and R.M.L.-R. performed the chromatographic analysis and discussed the anthocyanins results. P.F.M., D.H., J.R. and V.S. designed the experimental approach. R.M.L.-R., P.F.M., D.H. and J.R. supervised the study, analyzed and discussed the results and wrote the paper. All authors read, approved and contributed to the final version of the manuscript.

**Funding:** This study was supported by the Ministerio de Economía y Competitividad (grants AGL2017-82417-R to PFM and DH and AGL2016-75329-R to RML-R), by the Generalitat (grants 2017SGR683 and 2017SGR196), by the Associació Catalana de la Diabetis to JR (grant 600004—Ajut ACD a la recerca en diabetis 2017), Instituto de Salud Carlos III, ISCIII from the Ministerio de Ciencia, Innovación y Universidades (CIBEROBN—AEI/FEDER, UE). VS was supported by Conicyt's fellowship from the Government of Chile. UM-G was supported by Conacyt's fellowship from the Government of México. JMC was supported by BEC.AR fellowship from Ministerio de Educación, Cultura, Ciencia y Tecnología, Argentina. The APC was funded by the University of Barcelona.

**Acknowledgments:** We thank Cambridge Proofreading & Editing LLC.

**Conflicts of Interest:** The authors declare no conflict of interest.

## References

1. Townsend, K.L.; Tseng, Y.-H. Of mice and men: Novel insights regarding constitutive and recruitable brown adipocytes. *Int. J. Obes. Suppl.* **2015**, *5*, S15–S20. [[CrossRef](#)] [[PubMed](#)]
2. Harms, M.; Seale, P. Brown and beige fat: Development, function and therapeutic potential. *Nat. Med.* **2013**, *19*, 1252–1263. [[CrossRef](#)] [[PubMed](#)]
3. Rosenwald, M.; Wolfrum, C. The origin and definition of brite versus white and classical brown adipocytes. *Adipocyte* **2014**, *3*, 4–9. [[CrossRef](#)]
4. Lshibashi, J.; Seale, P. Beige can be slimming. *Science* **2010**, *328*, 1113–1114. [[CrossRef](#)] [[PubMed](#)]
5. Barbatelli, G.; Murano, I.; Madsen, L.; Hao, Q.; Jimenez, M.; Kristiansen, K.; Giacobino, J.P.; De Matteis, R.; Cinti, S. The emergence of cold-induced brown adipocytes in mouse white fat depots is determined predominantly by white to brown adipocyte transdifferentiation. *AJP Endocrinol. Metab.* **2010**, *298*, E1244–E1253. [[CrossRef](#)] [[PubMed](#)]
6. Pérez-Martí, A.; Garcia-Guasch, M.; Tresserra-Rimbau, A.; Carrilho-Do-Rosário, A.; Estruch, R.; Salas-Salvadó, J.; Martínez-González, M.Á.; Lamuela-Raventós, R.; Marrero, P.F.; Haro, D.; et al. A low-protein diet induces body weight loss and browning of subcutaneous white adipose tissue through enhanced expression of hepatic fibroblast growth factor 21 (FGF21). *Mol. Nutr. Food Res.* **2017**, *61*, 1600725. [[CrossRef](#)] [[PubMed](#)]
7. Sandoval, V.; Rodríguez-Rodríguez, R.; Martínez-Garza, Ú.; Rosell-Cardona, C.; Lamuela-Raventós, R.M.; Marrero, P.F.; Haro, D.; Relat, J. Mediterranean Tomato-Based Sofrito Sauce Improves Fibroblast Growth Factor 21 (FGF21) Signaling in White Adipose Tissue of Obese ZUCKER Rats. *Mol. Nutr. Food Res.* **2018**, *62*, 1700606. [[CrossRef](#)]
8. Vitali, A.; Murano, I.; Zingaretti, M.C.; Frontini, A.; Ricquier, D.; Cinti, S. The adipose organ of obesity-prone C57BL/6j mice is composed of mixed white and brown adipocytes. *J. Lipid Res.* **2012**, *53*, 619–629. [[CrossRef](#)]
9. Arias, N.; Picó, C.; Teresa Macarulla, M.; Oliver, P.; Miranda, J.; Palou, A.; Portillo, M.P. A combination of resveratrol and quercetin induces browning in white adipose tissue of rats fed an obesogenic diet. *Obesity* **2017**, *25*, 111–121. [[CrossRef](#)]
10. Serrano, A.; Asnani-Kishnani, M.; Rodríguez, A.M.; Palou, A.; Ribot, J.; Bonet, M.L. Programming of the Beige Phenotype in White Adipose Tissue of Adult Mice by Mild Resveratrol and Nicotinamide Riboside Supplementations in Early Postnatal Life. *Mol. Nutr. Food Res.* **2018**, *62*, e1800463. [[CrossRef](#)]
11. Neyrinck, A.M.; Bindels, L.B.; Geurts, L.; Van Hul, M.; Cani, P.D.; Delzenne, N.M. A polyphenolic extract from green tea leaves activates fat browning in high-fat-diet-induced obese mice. *J. Nutr. Biochem.* **2017**, *49*, 15–21. [[CrossRef](#)] [[PubMed](#)]



12. Mosqueda-Solís, A.; Sánchez, J.; Portillo, M.P.; Palou, A.; Picó, C. Combination of capsaicin and hesperidin reduces the effectiveness of each compound to decrease the adipocyte size and to induce browning features in adipose tissue of western diet fed rats. *J. Agric. Food Chem.* **2018**, *66*, 9679–9689. [[CrossRef](#)] [[PubMed](#)]
13. Reynés, B.; Palou, M.; Rodríguez, A.M.; Palou, A. Regulation of Adaptive Thermogenesis and Browning by Prebiotics and Postbiotics. *Front. Physiol.* **2019**, *9*, 1908. [[CrossRef](#)] [[PubMed](#)]
14. García-Ruiz, E.; Reynes, B.; Diaz-Rua, R.; Ceresi, E.; Oliver, P.; Palou, A. The intake of high-fat diets induces the acquisition of brown adipocyte gene expression features in white adipose tissue. *Int. J. Obes.* **2015**, *39*, 1619–1629. [[CrossRef](#)] [[PubMed](#)]
15. Sanchez-Gurmaches, J.; Tang, Y.; Jespersen, N.Z.; Wallace, M.; Martinez Calejman, C.; Gujja, S.; Li, H.; Edwards, Y.J.K.; Wolfrum, C.; Metallo, C.M.; et al. Brown Fat AKT2 Is a Cold-Induced Kinase that Stimulates ChREBP-Mediated De Novo Lipogenesis to Optimize Fuel Storage and Thermogenesis. *Cell Metab.* **2018**, *27*, 195–209. [[CrossRef](#)] [[PubMed](#)]
16. Fisher, F.M.; Maratos-Flier, E. Understanding the Physiology of FGF21. *Annu. Rev. Physiol.* **2016**, *78*. [[CrossRef](#)] [[PubMed](#)]
17. Gimeno, R.E.; Moller, D.E. FGF21-based pharmacotherapy - potential utility for metabolic disorders. *Trends Endocrinol. Metab.* **2014**, *25*, 303–311. [[CrossRef](#)]
18. De Sousa-Coelho, A.L.; Relat, J.; Hondares, E.; Pérez-Martí, A.; Ribas, F.; Villarroya, F.; Marrero, P.F.; Haro, D. FGF21 mediates the lipid metabolism response to amino acid starvation. *J. Lipid Res.* **2013**, *54*, 1786–1797. [[CrossRef](#)]
19. Fisher, F.F.; Kleiner, S.; Douris, N.; Fox, E.C.; Mepani, R.J.; Verdeguer, F.; Wu, J.; Kharitonkov, A.; Flier, J.S.; Maratos-Flier, E.; et al. FGF21 regulates PGC-1 $\alpha$  and browning of white adipose tissues in adaptive thermogenesis. *Genes Dev.* **2012**, *26*, 271–281. [[CrossRef](#)]
20. Lin, Z.; Tian, H.; Lam, K.S.L.; Lin, S.; Hoo, R.C.L.; Konishi, M.; Itoh, N.; Wang, Y.; Bornstein, S.R.; Xu, A.; et al. Adiponectin mediates the metabolic effects of FGF21 on glucose homeostasis and insulin sensitivity in mice. *Cell Metab.* **2013**, *17*, 779–789. [[CrossRef](#)]
21. Lin, Z.; Pan, X.; Wu, F.; Ye, D.; Zhang, Y.; Wang, Y.; Jin, L.; Lian, Q.; Huang, Y.; Ding, H.; et al. Fibroblast growth factor 21 prevents atherosclerosis by suppression of hepatic sterol regulatory element-binding protein-2 and induction of adiponectin in mice. *Circulation* **2015**, *131*, 1861–1871. [[CrossRef](#)] [[PubMed](#)]
22. Pérez-Martí, A.; Sandoval, V.; Marrero, P.F.; Haro, D.; Relat, J. Nutritional regulation of fibroblast growth factor 21: From macronutrients to bioactive dietary compounds. *Horm. Mol. Biol. Clin. Invest.* **2017**, *30*. [[CrossRef](#)]
23. Tsuda, T. Dietary anthocyanin-rich plants: Biochemical basis and recent progress in health benefits studies. *Mol. Nutr. Food Res.* **2012**, *56*, 159–170. [[CrossRef](#)] [[PubMed](#)]
24. Tsuda, T. Regulation of adipocyte function by anthocyanins; Possibility of preventing the metabolic syndrome. *J. Agric. Food Chem.* **2008**, *56*, 642–646. [[CrossRef](#)] [[PubMed](#)]
25. He, J.; Giusti, M.M. Anthocyanins: Natural Colorants with Health-Promoting Properties. *Annu. Rev. Food Sci. Technol.* **2010**, *1*, 163–187. [[CrossRef](#)] [[PubMed](#)]
26. Guo, H.; Ling, W. The update of anthocyanins on obesity and type 2 diabetes: Experimental evidence and clinical perspectives. *Rev. Endocr. Metab. Disord.* **2015**, *16*, 1–13. [[CrossRef](#)] [[PubMed](#)]
27. Overall, J.; Bonney, S.A.; Wilson, M.; Beermann, A.; Grace, M.H.; Esposito, D.; Lila, M.A.; Komarnytsky, S. Metabolic effects of berries with structurally diverse anthocyanins. *Int. J. Mol. Sci.* **2017**, *18*, 422. [[CrossRef](#)] [[PubMed](#)]
28. Tsuda, T. Recent Progress in Anti-Obesity and Anti-Diabetes Effect of Berries. *Antioxidants* **2016**, *5*, 13. [[CrossRef](#)] [[PubMed](#)]
29. Vendrame, S.; Del Bo', C.; Ciappellano, S.; Riso, P.; Klimis-Zacas, D. Berry Fruit Consumption and Metabolic Syndrome. *Antioxidants* **2016**, *5*, 13. [[CrossRef](#)]
30. Norberto, S.; Silva, S.; Meireles, M.; Faria, A.; Pintado, M.; Calhau, C. Blueberry anthocyanins in health promotion: A metabolic overview. *J. Funct. Foods* **2013**, *5*, 1518–1528. [[CrossRef](#)]
31. Coe, S.; Ryan, L. Impact of polyphenol-rich sources on acute postprandial glycaemia: A systematic review. *J. Nutr. Sci.* **2016**, *5*, e24. [[CrossRef](#)] [[PubMed](#)]
32. Blumberg, J.B.; Basu, A.; Krueger, C.G.; Lila, M.A.; Neto, C.C.; Novotny, J.A.; Reed, J.D.; Rodriguez-Mateos, A.; Toner, C.D. Impact of Cranberries on Gut Microbiota and Cardiometabolic Health: Proceedings of the Cranberry Health Research Conference 2015. *Adv. Nutr.* **2016**, *7*, 759S–770S. [[CrossRef](#)] [[PubMed](#)]

33. Escribano-Bailón, M.T.; Alcalde-Eon, C.; Muñoz, O.; Rivas-Gonzalo, J.C.; Santos-Buelga, C. Anthocyanins in berries of Maqui (*Aristotelia chilensis* (Mol.) Stuntz). *Phytochem. Anal.* **2006**, *17*, 8–14. [[CrossRef](#)] [[PubMed](#)]
34. Miranda-Rottmann, S.; Aspillaga, A.A.; Pérez, D.D.; Vasquez, L.; Martínez, A.L.F.; Leighton, F. Juice and phenolic fractions of the berry *Aristotelia chilensis* inhibit LDL oxidation in vitro and protect human endothelial cells against oxidative stress. *J. Agric. Food Chem.* **2002**, *50*, 7542–7547. [[CrossRef](#)] [[PubMed](#)]
35. Watson, R.R.; Schonlau, F. Nutraceutical and antioxidant effects of a delphinidin-rich maqui berry extract Delphinol (R): A review. *Minerva Cardioangiol.* **2015**, *63*, 1–12. [[PubMed](#)]
36. Rojo, L.E.; Ribnický, D.; Logendra, S.; Poulev, A.; Rojas-Silva, P.; Kuhn, P.; Dorn, R.; Grace, M.H.; Lila, M.A.; Raskin, I. In vitro and in vivo anti-diabetic effects of anthocyanins from Maqui Berry (*Aristotelia chilensis*). *Food Chem.* **2012**, *131*, 387–396. [[CrossRef](#)]
37. Alvarado, J.L.; Leschot, A.; Olivera-Nappa, Á.; Salgado, A.M.; Riaseco, H.; Lyon, C.; Vigil, P. Delphinidin-rich maqui berry extract (Delphinol®) lowers fasting and postprandial glycemia and insulinemia in prediabetic individuals during oral glucose tolerance tests. *Biomed. Res. Inf.* **2016**, *2016*, 9070537. [[CrossRef](#)]
38. Wang, Y.; Kimm, E.B.; Stampfer, M.J.; Willett, W.C.; Hu, F.B. Comparison of abdominal adiposity and overall obesity in predicting risk of type 2 diabetes among men. *Am. J. Clin. Nutr.* **2005**, *81*, 555–563. [[CrossRef](#)]
39. McLaughlin, T.; Lamendola, C.; Liu, A.; Abbasi, F. Preferential fat deposition in subcutaneous versus visceral depots is associated with insulin sensitivity. *J. Clin. Endocrinol. Metab.* **2011**, *96*, E1756–E1760. [[CrossRef](#)]
40. Snijder, M.B.; Dekker, J.M.; Visser, M.; Bouter, L.M.; Stehouwer, C.D.A.; Kostense, P.J.; Yudkin, J.S.; Heine, R.J.; Nijpels, G.; Seidell, J.C. Associations of hip and thigh circumferences independent of waist circumference with the incidence of type 2 diabetes: The Hoorn Study. *Am. J. Clin. Nutr.* **2003**, *77*, 192–197. [[CrossRef](#)]
41. Tran, T.T.; Yamamoto, Y.; Gesta, S.; Kahn, C.R. Beneficial Effects of Subcutaneous Fat Transplantation on Metabolism. *Cell Metab.* **2008**, *7*, 410–420. [[CrossRef](#)] [[PubMed](#)]
42. Stefan, N.; Schick, F.; Häring, H.U. Causes, Characteristics, and Consequences of Metabolically Unhealthy Normal Weight in Humans. *Cell Metab.* **2017**, *26*, 292–300. [[CrossRef](#)] [[PubMed](#)]
43. Li, H.; Wu, G.; Fang, Q.; Zhang, M.; Hui, X.; Sheng, B.; Wu, L.; Bao, Y.; Li, P.; Xu, A.; et al. Fibroblast growth factor 21 increases insulin sensitivity through specific expansion of subcutaneous fat. *Nat. Commun.* **2018**, *8*, 272. [[CrossRef](#)] [[PubMed](#)]
44. Andres-Lacueva, C.; Shukitt-Hale, B.; Galli, R.L.; Jauregui, O.; Lamuela-Raventos, R.M.; Joseph, J.A. Anthocyanins in aged blueberry-fed rats are found centrally and may enhance memory. *Nutr. Neurosci.* **2005**, *8*, 111–120. [[CrossRef](#)] [[PubMed](#)]
45. Tresserra-Rimbau, A.; Medina-Remón, A.; Pérez-Jiménez, J.; Martínez-González, M.A.; Covas, M.I.; Corella, D.; Salas-Salvadó, J.; Gómez-Gracia, E.; Lapetra, J.; Arós, F.; et al. Dietary intake and major food sources of polyphenols in a Spanish population at high cardiovascular risk: The PREDIMED study. *Nutr. Metab. Cardiovasc. Dis.* **2013**, *23*, 953–959. [[CrossRef](#)] [[PubMed](#)]
46. Tresserra-Rimbau, A.; Guasch-Ferre, M.; Salas-Salvadó, J.; Toledo, E.; Corella, D.; Castaner, O.; Guo, X.; Gomez-Gracia, E.; Lapetra, J.; Aros, F.; et al. Intake of Total Polyphenols and Some Classes of Polyphenols Is Inversely Associated with Diabetes in Elderly People at High Cardiovascular Disease Risk. *J. Nutr.* **2016**, *146*, 767–777.
47. Fredes, C.; Osorio, M.J.; Parada, J.; Robert, P. Stability and bioaccessibility of anthocyanins from maqui (*Aristotelia chilensis* [Mol.] Stuntz) juice microparticles. *LWT Food Sci. Technol.* **2018**, *91*, 549–556. [[CrossRef](#)]
48. Brauch, J.E.; Reuter, L.; Conrad, J.; Vogel, H.; Schweiggert, R.M.; Carle, R. Characterization of anthocyanins in novel Chilean maqui berry clones by HPLC–DAD–ESI/MSn and NMR-spectroscopy. *J. Food Compos. Anal.* **2017**, *58*, 16–22. [[CrossRef](#)]
49. Genskowsky, E.; Puente, L.A.; Pérez-Álvarez, J.A.; Fernández-López, J.; Muñoz, L.A.; Viuda-Martos, M. Determination of polyphenolic profile, antioxidant activity and antibacterial properties of maqui [*Aristotelia chilensis* (Molina) Stuntz] a Chilean blackberry. *J. Sci. Food Agric.* **2016**, *96*, 4235–4242. [[CrossRef](#)]
50. Lucas-Gonzalez, R.; Navarro-Coves, S.; Pérez-Álvarez, J.A.; Fernández-López, J.; Muñoz, L.A.; Viuda-Martos, M. Assessment of polyphenolic profile stability and changes in the antioxidant potential of maqui berry (*Aristotelia chilensis* (Molina) Stuntz) during in vitro gastrointestinal digestion. *Ind. Crops Prod.* **2016**, *94*, 774–782. [[CrossRef](#)]
51. Prior, R.L.E.; Wilkes, S.R.; Rogers, T.; Khanal, R.C.; Wu, X.; Howard, L.R. Purified blueberry anthocyanins and blueberry juice alter development of obesity in mice fed an obesogenic high-fat diet. *J. Agric. Food Chem.* **2010**, *58*, 3970–3976. [[CrossRef](#)] [[PubMed](#)]

52. Syamaladevi, R.M.; Sablani, S.S.; Tang, J.; Powers, J.; Swanson, B.G. Stability of Anthocyanins in Frozen and Freeze-Dried Raspberries during Long-Term Storage: In Relation to Glass Transition. *J. Food Sci.* **2011**, *76*, E414–E421. [[CrossRef](#)] [[PubMed](#)]
53. Nishimoto, Y.; Tamori, Y. CIDE Family-Mediated Unique Lipid Droplet Morphology in White Adipose Tissue and Brown Adipose Tissue Determines the Adipocyte Energy Metabolism. *J. Atheroscler. Thromb.* **2017**, *24*, 989–998. [[CrossRef](#)] [[PubMed](#)]
54. Nishimoto, Y.; Nakajima, S.; Tateya, S.; Saito, M.; Ogawa, W.; Tamori, Y. Cell death-inducing DNA fragmentation factor A-like effector A and fat-specific protein 27 $\beta$  coordinately control lipid droplet size in brown adipocytes. *J. Biol. Chem.* **2017**, *292*, 10824–10834. [[CrossRef](#)] [[PubMed](#)]
55. Herman, M.A.; Peroni, O.D.; Villoria, J.; Schön, M.R.; Abumrad, N.A.; Blüher, M.; Klein, S.; Kahn, B.B. A novel ChREBP isoform in adipose tissue regulates systemic glucose metabolism. *Nature* **2012**, *484*, 333–338. [[CrossRef](#)] [[PubMed](#)]
56. Eissing, L.; Scherer, T.; Tödter, K.; Knippschild, U.; Greve, J.W.; Buurman, W.A.; Pinnschmidt, H.O.; Rensen, S.S.; Wolf, A.M.; Bartelt, A.; et al. De novo lipogenesis in human fat and liver is linked to ChREBP- $\beta$  and metabolic health. *Nat. Commun.* **2013**, *4*, 1528. [[CrossRef](#)] [[PubMed](#)]
57. Kursawe, R.; Caprio, S.; Giannini, C.; Narayan, D.; Lin, A.; D'Adamo, E.; Shaw, M.; Pierpont, B.; Cushman, S.W.; Shulman, G.I. Decreased transcription of ChREBP- $\alpha/\beta$  isoforms in abdominal subcutaneous adipose tissue of obese adolescents with prediabetes or early type 2 diabetes: Associations with insulin resistance and hyperglycemia. *Diabetes* **2013**, *62*, 837–844. [[CrossRef](#)] [[PubMed](#)]
58. Song, Z.; Xiaoli, A.; Yang, F.; Song, Z.; Xiaoli, A.M.; Yang, F. Regulation and Metabolic Significance of De Novo Lipogenesis in Adipose Tissues. *Nutrients* **2018**, *10*, 1383. [[CrossRef](#)]
59. Fisher, F.M.; Chui, P.C.; Antonellis, P.J.; Bina, H.A.; Kharitonov, A.; Flier, J.S.; Maratos-Flier, E. Obesity is a fibroblast growth factor 21 (FGF21)-resistant state. *Diabetes* **2010**, *59*, 2781–2789. [[CrossRef](#)]
60. Zhang, X.; Yeung, D.C.Y.; Karpisek, M.; Stejskal, D.; Zhou, Z.; Liu, F.; Wong, R.L.C.; Chow, W.; Tso, A.W.K.; Lam, K.S.L. Serum FGF21 Levels Are Increased in Obesity and Are in Humans. *Diabetes* **2008**, *57*, 1246–1253. [[CrossRef](#)]
61. Montague, C.T.; O'Rahilly, S. The perils of portliness: Causes and consequences of visceral adiposity. *Diabetes* **2000**, *49*, 883–888. [[CrossRef](#)] [[PubMed](#)]
62. Peirce, V.; Carobbio, S.; Vidal-Puig, A. The different shades of fat. *Nature* **2014**, *561*, 124–129. [[CrossRef](#)] [[PubMed](#)]
63. Carobbio, S.; Rodriguez-Cuenca, S.; Vidal-Puig, A. Origins of metabolic complications in obesity: Ectopic fat accumulation. the importance of the qualitative aspect of lipotoxicity. *Curr. Opin. Clin. Nutr. Metab. Care* **2011**, *14*, 520–526. [[CrossRef](#)] [[PubMed](#)]
64. Virtue, S.; Vidal-Puig, A. Adipose tissue expandability, lipotoxicity and the Metabolic Syndrome—An allostatic perspective. *Biochim. Biophys. Acta Mol. Cell Biol. Lipids* **2010**, *1801*, 338–349. [[CrossRef](#)] [[PubMed](#)]
65. Boden, G.; Shulman, G.I. Free fatty acids in obesity and type 2 diabetes: Defining their role in the development of insulin resistance and  $\beta$ -cell dysfunction. *Eur. J. Clin. Investig.* **2002**, *32*, 14–23. [[CrossRef](#)] [[PubMed](#)]
66. Unger, R.H. Lipotoxic Diseases. *Annu. Rev. Med.* **2002**, *53*, 319–336. [[CrossRef](#)] [[PubMed](#)]
67. Whittle, A.; Relat-Pardo, J.; Vidal-Puig, A. Pharmacological strategies for targeting BAT thermogenesis. *Trends Pharmacol. Sci.* **2013**, *34*, 347–355. [[CrossRef](#)]
68. Bartelt, A.; Heeren, J. Adipose tissue browning and metabolic health. *Nat. Rev. Endocrinol.* **2014**, *10*, 24–36. [[CrossRef](#)]
69. Skates, E.; Overall, J.; DeZego, K.; Wilson, M.; Esposito, D.; Lila, M.A.; Komarnytsky, S. Berries containing anthocyanins with enhanced methylation profiles are more effective at ameliorating high fat diet-induced metabolic damage. *Food Chem. Toxicol.* **2018**, *111*, 445–453. [[CrossRef](#)]
70. Skrovankova, S.; Sumczynski, D.; Mlecek, J.; Jurikova, T.; Sochor, J. Bioactive compounds and antioxidant activity in different types of berries. *Int. J. Mol. Sci.* **2015**, *16*, 24673–24703. [[CrossRef](#)]
71. de Pascual-Teresa, S.; Moreno, D.A.; Garcia-Viguera, C. Flavanols and anthocyanins in cardiovascular health: A review of current evidence. *Int. J. Mol. Sci.* **2010**, *11*, 1679–1703. [[CrossRef](#)] [[PubMed](#)]
72. Lee, Y.M.; Yoon, Y.; Yoon, H.; Park, H.M.; Song, S.; Yeum, K.J. Dietary anthocyanins against obesity and inflammation. *Nutrients* **2017**, *9*, 1089. [[CrossRef](#)] [[PubMed](#)]
73. Valenti, L.; Riso, P.; Mazzocchi, A.; Porrini, M.; Fargion, S.; Agostoni, C. Dietary anthocyanins as nutritional therapy for nonalcoholic fatty liver disease. *Oxid. Med. Cell. Longev.* **2013**, *2013*, 145421. [[CrossRef](#)] [[PubMed](#)]

74. Castro-Barquero, S.; Lamuela-Raventós, R.M.; Doménech, M.; Estruch, R. Relationship between mediterranean dietary polyphenol intake and obesity. *Nutrients* **2018**, *10*, 1523. [[CrossRef](#)] [[PubMed](#)]
75. Wu, T.; Yu, Z.; Tang, Q.; Song, H.; Gao, Z.; Chen, W.; Zheng, X. Honeysuckle anthocyanin supplementation prevents diet-induced obesity in C57BL/6 mice. *Food Funct.* **2013**, *4*, 1654–1661. [[CrossRef](#)]
76. Wallace, T.C. Anthocyanins in Cardiovascular Disease. *Adv. Nutr.* **2011**, *2*, 1–7. [[CrossRef](#)]
77. Grace, M.H.; Ribnicky, D.M.; Kuhn, P.; Poulev, A.; Logendra, S.; Yousef, G.G.; Raskin, I.; Lila, M.A. Hypoglycemic activity of a novel anthocyanin-rich formulation from lowbush blueberry, *Vaccinium angustifolium* Aiton. *Phytomedicine* **2009**, *16*, 406–415. [[CrossRef](#)]
78. Fibigr, J.; Šatinský, D.; Solich, P. A UHPLC method for the rapid separation and quantification of anthocyanins in acai berry and dry blueberry extracts. *J. Pharm. Biomed. Anal.* **2017**, *143*, 204–213. [[CrossRef](#)]
79. Schreckinger, M.E.; Wang, J.; Yousef, G.; Lila, M.A.; De Mejía, E.G. Antioxidant capacity and in Vitro inhibition of adipogenesis and inflammation by phenolic extracts of *Vaccinium floribundum* and *Aristotelia chilensis*. *J. Agric. Food Chem.* **2010**, *58*, 8966–8976. [[CrossRef](#)]
80. Milbury, P.E.; Vita, J.A.; Blumberg, J.B. Anthocyanins are Bioavailable in Humans following an Acute Dose of Cranberry Juice. *J. Nutr.* **2010**, *140*, 1099–1104. [[CrossRef](#)]
81. Ruiz, A.; Hermosin-Gutiérrez, I.; Vergara, C.; von Baer, D.; Zapata, M.; Hirschfeld, A.; Obando, L.; Mardones, C. Anthocyanin profiles in south Patagonian wild berries by HPLC-DAD-ESI-MS/MS. *Food Res. Int.* **2013**, *51*, 706–713. [[CrossRef](#)]
82. Motillo, E.P.; Balasubramanian, P.; Lee, Y.-H.; Weng, C.; Kershaw, E.E.; Granneman, J.G. Coupling of lipolysis and de novo lipogenesis in brown, beige, and white adipose tissues during chronic  $\beta$ 3-adrenergic receptor activation. *J. Lipid Res.* **2014**, *55*, 2276–2286. [[CrossRef](#)] [[PubMed](#)]
83. Yu, X.X.; Lewin, D.A.; Forrest, W.; Adams, S.H. Cold elicits the simultaneous induction of fatty acid synthesis and  $\beta$ -oxidation in murine brown adipose tissue: Prediction from differential gene expression and confirmation in vivo. *FASEB J.* **2002**, *16*, 155–168. [[CrossRef](#)] [[PubMed](#)]
84. Bartelt, A.; Weigelt, C.; Cherradi, M.L.; Niemeier, A.; Tödter, K.; Heeren, J.; Scheja, L. Effects of adipocyte lipoprotein lipase on de novo lipogenesis and white adipose tissue browning. *Biochim. Biophys. Acta Mol. Cell Biol. Lipids* **2013**, *1831*, 934–942. [[CrossRef](#)] [[PubMed](#)]
85. Vijayakumar, A.; Aryal, P.; Wen, J.; Syed, I.; Vazirani, R.P.; Moraes-Vieira, P.M.; Camporez, J.P.; Gallop, M.R.; Perry, R.J.; Peroni, O.D.; et al. Absence of Carbohydrate Response Element Binding Protein in Adipocytes Causes Systemic Insulin Resistance and Impairs Glucose Transport. *Cell Rep.* **2017**, *21*, 1021–1035. [[CrossRef](#)] [[PubMed](#)]
86. Katz, L.S.; Xu, S.; Ge, K.; Scott, D.K.; Gershengorn, M.C.  $T_3$  and glucose coordinately stimulate ChREBP-Mediated Ucp1 expression in brown adipocytes from male mice. *Endocrinology* **2018**, *159*, 557–569. [[CrossRef](#)] [[PubMed](#)]
87. Witte, N.; Muenzner, M.; Rietscher, J.; Knauer, M.; Heidenreich, S.; Nuotio-Antar, A.M.; Graef, F.A.; Fedders, R.; Tolkachov, A.; Goehring, I.; et al. The glucose sensor ChREBP links *de-novo* lipogenesis to PPAR $\gamma$  activity and adipocyte differentiation. *Endocrinology* **2015**, *156*, 4008–4401. [[CrossRef](#)]
88. Linden, A.G.; Li, S.; Choi, H.Y.; Fang, F.; Fukasawa, M.; Uyeda, K.; Hammer, R.E.; Horton, J.D.; Engelking, L.J.; Liang, G. Interplay between ChREBP and SREBP-1c coordinates postprandial glycolysis and lipogenesis in livers of mice. *J. Lipid Res.* **2018**, *59*, 475–487. [[CrossRef](#)]
89. Nuotio-Antar, A.M.; Pongvarin, N.; Li, M.; Schupp, M.; Mohammad, M.; Gerard, S.; Zou, F.; Chan, L. FABP4-cre mediated expression of constitutively active ChREBP protects against obesity, fatty liver, and insulin resistance. *Endocrinology* **2015**, *156*, 4020–4032. [[CrossRef](#)]
90. Filhoulaud, G.; Guilmeau, S.; Dentin, R.; Girard, J.; Postic, C. Novel insights into ChREBP regulation and function. *Trends Endocrinol. Metab.* **2013**, *24*, 257–268. [[CrossRef](#)]
91. Baraille, F.; Planchais, J.; Dentin, R.; Guilmeau, S.; Postic, C. Integration of ChREBP-Mediated Glucose Sensing into Whole Body Metabolism. *Physiology* **2015**, *30*, 428–437. [[CrossRef](#)] [[PubMed](#)]
92. Lee, H.J.; Cha, J.Y. Recent insights into the role of ChREBP in intestinal fructose absorption and metabolism. *BMB Rep.* **2018**, *51*, 429–436. [[CrossRef](#)] [[PubMed](#)]
93. Kohjima, M.; Higuchi, N.; Kato, M.; Kotoh, K.; Yoshimoto, T.; Fujino, T.; Yada, M.; Yada, R.; Harada, N.; Enjoji, M.; et al. SREBP-1c, regulated by the insulin and AMPK signaling pathways, plays a role in nonalcoholic fatty liver disease. *Int. J. Mol. Med.* **2008**, *21*, 507–511. [[CrossRef](#)] [[PubMed](#)]

94. Shimomura, I.; Bashmakov, Y.; Horton, J.D. Increased levels of nuclear SREBP-1c associated with fatty livers in two mouse models of diabetes mellitus. *J. Biol. Chem.* **1999**, *274*, 30028–30032. [[CrossRef](#)] [[PubMed](#)]
95. Knebel, B.; Haas, J.; Hartwig, S.; Jacob, S.; Köllmer, C.; Nitzgen, U.; Müller-Wieland, D.; Kotzka, J. Liver-specific expression of transcriptionally active srebp-1c is associated with fatty liver and increased visceral fat mass. *PLoS ONE* **2012**, *7*, e31812. [[CrossRef](#)] [[PubMed](#)]
96. Yahagi, N.; Shimano, H.; Hasty, A.H.; Matsuzaka, T.; Ide, T.; Yoshikawa, T.; Amemiya-Kudo, M.; Tomita, S.; Okazaki, H.; Tamura, Y.; et al. Absence of sterol regulatory element-binding protein-1 (SREBP-1) ameliorates fatty livers but not obesity or insulin resistance in Lepob/Lepob mice. *J. Biol. Chem.* **2002**, *277*, 19353–19357. [[CrossRef](#)] [[PubMed](#)]
97. Moon, Y.A.; Liang, G.; Xie, X.; Frank-Kamenetsky, M.; Fitzgerald, K.; Koteliansky, V.; Brown, M.S.; Goldstein, J.L.; Horton, J.D. The Scap/SREBP pathway is essential for developing diabetic fatty liver and carbohydrate-induced hypertriglyceridemia in animals. *Cell Metab. Cell Metab.* **2012**, *15*, 204–206. [[CrossRef](#)] [[PubMed](#)]
98. Kim, J.B.; Spiegelman, B.M. ADD1/SREBP1 promotes adipocyte differentiation and gene expression linked to fatty acid metabolism. *Genes Dev.* **1996**, *10*, 1096–1107. [[CrossRef](#)]
99. Gnani, A.; Siculella, L.; Paglialonga, G.; Damiano, F.; Giudetti, A.M. 3,5-diiodo-L-thyronine increases de novo lipogenesis in liver from hypothyroid rats by SREBP-1 and ChREBP-mediated transcriptional mechanisms. *IUBMB Life* **2019**. [[CrossRef](#)]
100. Kobayashi, M.; Fujii, N.; Narita, T.; Higami, Y.; Kobayashi, M.; Fujii, N.; Narita, T.; Higami, Y. SREBP-1c-Dependent Metabolic Remodeling of White Adipose Tissue by Caloric Restriction. *Int. J. Mol. Sci.* **2018**, *19*, 3335. [[CrossRef](#)]
101. Kusudo, T.; Hashimoto, M.; Kataoka, N.; Li, Y.; Nozaki, A.; Yamashita, H. CREG1 promotes uncoupling protein 1 expression and brown adipogenesis in vitro. *J. Biochem.* **2019**, *165*, 47–55. [[CrossRef](#)] [[PubMed](#)]
102. Hashimoto, M.; Kusudo, T.; Takeuchi, T.; Kataoka, N.; Mukai, T.; Yamashita, H. CREG1 stimulates brown adipocyte formation and ameliorates diet-induced obesity in mice. *FASEB J.* **2019**, *33*, 8069–8082. [[CrossRef](#)] [[PubMed](#)]
103. Mraz, M.; Bartlova, M.; Lacinova, Z.; Michalsky, D.; Kasalicky, M.; Haluzikova, D.; Matoulek, M.; Dostalova, I.; Humenanska, V.; Haluzik, M. Serum concentrations and tissue expression of a novel endocrine regulator fibroblast growth factor-21 in patients with type 2 diabetes and obesity. *Clin. Endocrinol.* **2009**, *71*, 369–375. [[CrossRef](#)] [[PubMed](#)]
104. Dushay, J.; Chui, P.C.; Gopalakrishnan, G.S.; Varela-Rey, M.; Crawley, M.; Fisher, F.M.; Badman, M.K.; Martinez-Chantar, M.L.; Maratos-Flier, E. Increased fibroblast growth factor 21 in obesity and nonalcoholic fatty liver disease. *Gastroenterology* **2010**, *139*, 456–463. [[CrossRef](#)] [[PubMed](#)]
105. Ge, X.; Chen, C.; Hui, X.; Wang, Y.; Lam, K.S.L.; Xu, A. Fibroblast growth factor 21 induces glucose transporter-1 expression through activation of the serum response factor/Ets-like protein-1 in adipocytes. *J. Biol. Chem.* **2011**, *286*, 34533–34541. [[CrossRef](#)] [[PubMed](#)]
106. Samms, R.J.; Cheng, C.C.; Kharitonov, A.; Gimeno, R.E.; Adams, A.C. Overexpression of  $\beta$ -klotho in adipose tissue sensitizes male mice to endogenous FGF21 and provides protection from diet-induced obesity. *Endocrinology* **2016**, *157*, 1467–1480. [[CrossRef](#)] [[PubMed](#)]
107. Gallego-Escuredo, J.M.; Gómez-Ambrosi, J.; Catalan, V.; Domingo, P.; Giral, M.; Frühbeck, G.; Villarroya, F. Opposite alterations in FGF21 and FGF19 levels and disturbed expression of the receptor machinery for endocrine FGFs in obese patients. *Int. J. Obes.* **2015**, *39*, 121–129. [[CrossRef](#)]
108. Nygaard, E.B.; Møller, C.L.; Kievit, P.; Grove, K.L.; Andersen, B. Increased fibroblast growth factor 21 expression in high-fat diet-sensitive non-human primates (*Macaca mulatta*). *Int. J. Obes.* **2014**, *38*, 183–191. [[CrossRef](#)]
109. Geng, L.; Liao, B.; Jin, L.; Huang, Z.; Triggle, C.R.; Ding, H.; Zhang, J.; Huang, Y.; Lin, Z.; Xu, A. Exercise Alleviates Obesity-Induced Metabolic Dysfunction via Enhancing FGF21 Sensitivity in Adipose Tissues. *Cell Rep.* **2019**, *26*, 2738–2752. [[CrossRef](#)]
110. Monika, P.; Geetha, A. The modulating effect of *Persea americana* fruit extract on the level of expression of fatty acid synthase complex, lipoprotein lipase, fibroblast growth factor-21 and leptin—A biochemical study in rats subjected to experimental hyperlipidemia and obesit. *Phytomedicine* **2015**, *22*, 939–945. [[CrossRef](#)]

111. Tian, L.; Zeng, K.; Shao, W.; Yang, B.B.; Fantus, I.G.; Weng, J.; Jin, T. Short-Term Curcumin Gavage Sensitizes Insulin Signaling in Dexamethasone-Treated C57BL/6 Mice. *J. Nutr.* **2015**, *145*, 2300–2307. [[CrossRef](#)] [[PubMed](#)]
112. Song, H.; Zheng, Z.; Wu, J.; Lai, J.; Chu, Q.; Zheng, X. White Pitaya (*Hylocereus undatus*) Juice Attenuates Insulin Resistance and Hepatic Steatosis in Diet-Induced Obese Mice. *PLoS ONE* **2016**, *11*, e0149670. [[CrossRef](#)] [[PubMed](#)]
113. Yu, Y.; Zhang, X.H.; Ebersole, B.; Ribnicky, D.; Wang, Z.Q. Bitter melon extract attenuating hepatic steatosis may be mediated by FGF21 and AMPK/Sirt1 signaling in mice. *Sci. Rep.* **2013**, *3*, 3142. [[CrossRef](#)] [[PubMed](#)]
114. Hui, X.; Feng, T.; Liu, Q.; Gao, Y.; Xu, A. The FGF21-adiponectin axis in controlling energy and vascular homeostasis. *J. Mol. Cell Biol.* **2016**, *8*, 110–119. [[CrossRef](#)] [[PubMed](#)]
115. Yoon, M.J.; Lee, G.Y.; Chung, J.J.; Ahn, Y.A.; Hong, S.H.; Kim, J.B. Adiponectin increases fatty acid oxidation in skeletal muscle cells by sequential activation of AMP-activated protein kinase, p38 mitogen-activated protein kinase, and peroxisome proliferator-activated receptor  $\alpha$ . *Diabetes* **2006**, *55*, 2562–2570. [[CrossRef](#)]
116. de Cruz Rodrigues, K.C.; Pereira, R.M.; de Campos, T.D.P.; de Moura, R.F.; de Silva, A.S.R.; Cintra, D.E.; Ropelle, E.R.; Pauli, J.R.; de Araújo, M.B.; de Moura, L.P. The Role of Physical Exercise to Improve the Browning of White Adipose Tissue via POMC Neurons. *Front. Cell. Neurosci.* **2018**, *12*, 88. [[CrossRef](#)] [[PubMed](#)]
117. Alberdi, G.; Rodríguez, V.M.; Macarulla, M.T.; Miranda, J.; Churrua, I.; Portillo, M.P. Hepatic lipid metabolic pathways modified by resveratrol in rats fed an obesogenic diet. *Nutrition* **2013**, *29*, 562–567. [[CrossRef](#)]
118. You, Y.; Liang, C.; Han, X.; Guo, J.; Ren, C.; Liu, G.; Huang, W.; Zhan, J. Mulberry anthocyanins, cyanidin 3-glucoside and cyanidin 3-rutinoside, increase the quantity of mitochondria during brown adipogenesis. *J. Funct. Foods* **2017**, *36*, 348–356. [[CrossRef](#)]
119. You, Y.; Yuan, X.; Liu, X.; Liang, C.; Meng, M.; Huang, Y.; Han, X.; Guo, J.; Guo, Y.; Ren, C.; et al. Cyanidin-3-glucoside increases whole body energy metabolism by upregulating brown adipose tissue mitochondrial function. *Mol. Nutr. Food Res.* **2017**, *61*, 1700261. [[CrossRef](#)]
120. You, Y.; Yuan, X.; Lee, H.J.; Huang, W.; Jin, W.; Zhan, J. Mulberry and mulberry wine extract increase the number of mitochondria during brown adipogenesis. *Food Funct.* **2015**, *6*, 401–408. [[CrossRef](#)]
121. Anhé, F.F.; Nachbar, R.T.; Varin, T.V.; Trottier, J.; Dudonné, S.; Le Barz, M.; Feutry, P.; Pilon, G.; Barbier, O.; Desjardins, Y.; et al. Treatment with camu camu (*Myrciaria dubia*) prevents obesity by altering the gut microbiota and increasing energy expenditure in diet-induced obese mice. *Gut* **2019**, *68*, 453–464. [[CrossRef](#)] [[PubMed](#)]



© 2019 by the authors. Licensee MDPI, Basel, Switzerland. This article is an open access article distributed under the terms and conditions of the Creative Commons Attribution (CC BY) license (<http://creativecommons.org/licenses/by/4.0/>).

Article

# Lyophilized Maqui (*Aristotelia chilensis*) Berry Administration Suppresses High-Fat Diet-Induced Liver Lipogenesis through the Induction of the Nuclear Corepressor SMILE

Viviana Sandoval <sup>1,2</sup>, Hèctor Sanz-Lamora <sup>2,3</sup>, Pedro F. Marrero <sup>2,4,5</sup>, Joana Relat <sup>2,3,5,\*</sup>  and Diego Haro <sup>2,4,5,\*</sup> 

- <sup>1</sup> Escuela de Nutrición y Dietética, Facultad de Ciencias para el Cuidado de la Salud, Universidad San Sebastián, Sede De la Patagonia, Puerto-Montt 5501842, Chile; vsandovals@docente.usb.cl
  - <sup>2</sup> Department of Nutrition, Food Sciences and Gastronomy, School of Pharmacy and Food Sciences, Food Torribera Campus, University of Barcelona, E-08921 Santa Coloma de Gramenet, Spain; h.sanz.lamora@ub.edu (H.S.-L.); pedromarrero@ub.edu (P.F.M.)
  - <sup>3</sup> Institute of Nutrition and Food Safety, University of Barcelona (INSA-UB), E-08921 Santa Coloma de Gramenet, Spain
  - <sup>4</sup> Institute of Biomedicine, University of Barcelona (IBUB), E-08028 Barcelona, Spain
  - <sup>5</sup> CIBER Physiopathology of Obesity and Nutrition (CIBER-OBN), Instituto de Salud Carlos III, E-28029 Madrid, Spain
- \* Correspondence: jrelat@ub.edu (J.R.); dharo@ub.edu (D.H.); Tel.: +34-934020862 (J.R.); +34-934033790 (D.H.)

**Abstract:** The liver is one of the first organs affected by accumulated ectopic lipids. Increased de novo lipogenesis and excessive triglyceride accumulation in the liver are hallmarks of nonalcoholic fatty liver disease (NAFLD) and are strongly associated with obesity, insulin resistance, and type 2 diabetes. Maqui dietary supplemented diet-induced obese mice showed better insulin response and decreased weight gain. We previously described that these positive effects of maqui are partially due to an induction of a brown-like phenotype in subcutaneous white adipose tissue that correlated with a differential expression of *Chrebp* target genes. In this work, we aimed to deepen the molecular mechanisms underlying the impact of maqui on the onset and development of the obese phenotype and insulin resistance focusing on liver metabolism. Our results showed that maqui supplementation decreased hepatic steatosis caused by a high-fat diet. Changes in the metabolic profile include a downregulation of the lipogenic liver X receptor (LXR) target genes and of fatty acid oxidation gene expression together with an increase in the expression of *small heterodimer partner interacting leucine zipper protein (Smile)*, a corepressor of the nuclear receptor family. Our data suggest that maqui supplementation regulates lipid handling in liver to counteract the metabolic impact of a high-fat diet.

**Keywords:** anthocyanins; nonalcoholic liver disease; SMILE; high-fat diet; maqui berry; lipogenesis; fatty acid oxidation



**Citation:** Sandoval, V.; Sanz-Lamora, H.; Marrero, P.F.; Relat, J.; Haro, D. Lyophilized Maqui (*Aristotelia chilensis*) Berry Administration Suppresses High-Fat Diet-Induced Liver Lipogenesis through the Induction of the Nuclear Corepressor SMILE. *Antioxidants* **2021**, *10*, 637. <https://doi.org/10.3390/antiox10050637>

Academic Editor: Han Moshage

Received: 17 March 2021

Accepted: 20 April 2021

Published: 21 April 2021

**Publisher's Note:** MDPI stays neutral with regard to jurisdictional claims in published maps and institutional affiliations.



**Copyright:** © 2021 by the authors. Licensee MDPI, Basel, Switzerland. This article is an open access article distributed under the terms and conditions of the Creative Commons Attribution (CC BY) license (<https://creativecommons.org/licenses/by/4.0/>).

## 1. Introduction

The regular consumption of anthocyanins and anthocyanidin-rich berries is considered a potential strategy for the treatment/prevention of obesity-related pathologies, among others [1–9]. The intake of anthocyanins or anthocyanin-rich foods has shown positive effects for bodyweight control both in humans and in rodents. It has also proven effective for reducing fat accumulation, improving glucose tolerance, improving insulin sensitivity, and increasing energy expenditure, inter alia [10–18]. However, there is little information about the molecular mechanisms underlying these effects.

The liver is a key organ in the maintenance of metabolic homeostasis and is one of the first organs affected by accumulated ectopic lipids. Two of the hallmarks of nonalcoholic fatty liver disease (NAFLD) are its higher rate of de novo lipogenesis and its excessive accumulation of triglycerides in the liver. These two parameters are strongly associated



with obesity and insulin resistance, as well as type 2 diabetes [19,20]. The accumulation of intrahepatic fat that leads to liver steatosis is now recognized as the hepatic manifestation of metabolic syndrome and a factor responsible for the metabolic complications associated with obesity [21].

Maqui (*Aristotelia chilensis*) is a berry from Chile with a characteristic profile of anthocyanins, where the main representatives are delphinidin-3-*O*-sambubioside-5-*O*-glucoside and delphinidin-3-*O*-sambubioside [22,23]. The consumption of maqui has shown antioxidant effects and a beneficial impact on fasting glucose and insulin levels both in humans and in rodent models of obesity and type 2 diabetes [24–27]. The hypoglycemic activity of maqui has been linked to delphinidin-3-sambubioside-5-glucoside, which has been pointed out as the molecule responsible for this effect in vivo [25].

In our previous work, we provided evidence that a dietary supplementation with maqui ameliorated part of the unhealthy effects caused by a high-fat diet (HFD) [23]. The published results demonstrated that, in mice, maqui administration induces the expression of fuel storage and thermogenic genes, giving to the subcutaneous white adipose tissue (scWAT) a brown-like phenotype. Our data suggested that maqui could exert its effects, at least in part, through the upregulation of carbohydrate responsive element binding protein b (*Chrebpb*) expression and improved fibroblast growth factor 21 (FGF21) signaling.

With the global aim of describing the molecular mechanisms underlying the metabolic effects of maqui, we evaluated the impact of lyophilized maqui when added to beverages, focusing specifically on the progression of diet-induced obesity (DIO). The liver metabolic profile and hepatic steatosis were analyzed in mice subjected to a HFD for 16 weeks supplemented or not with maqui.

We showed that maqui supplementation decreased hepatic steatosis and the triglyceride accumulation caused by a HFD. This change in liver lipid content observed in maqui-supplemented animals correlates with a downregulation in the expression of fatty acid oxidation genes and an upregulation in the expression of the nuclear receptor family's corepressor SMILE (small heterodimer partner interacting leucine zipper protein), which coincides with a downregulation of the nuclear receptor LXR (lipogenic liver X receptor) target genes. SMILE belongs to the basic leucine zipper family transcription factors and functions as a nuclear corepressor of several members of the nuclear receptor family [28]. Among others, it has been shown that SMILE negatively regulates LXR alpha transcriptional activity by directly interacting with it and competing with its coactivator SRC-1. Moreover, SMILE overexpression inhibits LXR alpha-mediated gene expression of the sterol regulatory binding protein 1c (*Srebp-1c*) and decreased hepatic LXR alpha agonist-induced triglycerides (TG) and lipid accumulation [29].

## 2. Materials and Methods

### 2.1. Animal Procedures: Dosage Regimen

All animal procedures used in this article were approved by the Animal Ethics Committee of the University of Barcelona (CEEA-137/18) and were previously described in Sandoval et al. [23]. Briefly, 4-week-old C57BL/6j male mice ( $n = 23$ ) were housed in a temperature-controlled room ( $22 \pm 1$  °C) under a 12-h/12-h light/dark cycle with free access to filtered tap water and a rodent chow diet. Before the initiation of the nutritional intervention, animals were tested as normoglycemic and randomly assigned into two groups: (1) HFD ( $n = 9$ ) and (2) HFD+M, HFD supplemented with maqui ( $n = 14$ ). Both experimental groups were fed a HFD containing 45% of calories from fat and 4.73 kcal per gram of food (D12451, Research Diets) for 16 weeks with free access to food and water. Moreover, HFD+M mice were supplemented with 4 mg/day of lyophilized maqui (Maqui berry, Native for Life, Chile) added to filtered tap water (20 mg of lyophilized maqui/mL of filtered tap water). To prevent the oxidation of bioactive compounds, the maqui-supplemented water was prepared every two days. The calculation of the maqui's dosage regimen was based on the polyphenol intake recommended as beneficial by the PREDIMED study (820 mg in



a human diet of 2300 kcal) [30,31]. The nutritional information of the lyophilized maqui berry and details of the dosage regimen are detailed in Sandoval et al. [23].

During the nutritional intervention period, the intake of food and beverages was recorded every two days and bodyweight progression was evaluated twice a week. The intake of food and water was measured by the difference between what we put in the cage and what we recovered two days later. The results of the food and liquid intake, including the calorie intake and the bodyweight progression, were published in [23], where it was shown that HFDM mice displayed a lower bodyweight increase after 16 weeks of nutritional intervention, even if they exhibited a higher calorie intake. At week 16, the animals were euthanized. Blood was extracted via an intracardiac puncture, and serum was obtained via centrifugation (1500 rpm, 20 min). The tissues as liver, heart, epididymal, and subcutaneous fat and brown fat were isolated, immediately snap-frozen, and stored at  $-80^{\circ}\text{C}$  for future analysis.

## 2.2. Blood Baseline Glucose Levels

Blood samples were collected from the tail vein and glucose levels were measured using a glucometer (Glucocard SM, Menarini, Florence, Italy). These measurements were performed on week 15, where mice were previously fasted for 6 h in the morning.

## 2.3. Liver Triglyceride Content

Liver tissue (100 mg) of each mouse was homogenized in a 1 mL solution of 5% Nonidet P40 (A1694,0250, PanReac AppliChem, Barcelona, Spain) with ultrapure water. The amount of triglyceride (TG) was determined using the Triglyceride Quantification Colorimetric Kit (MAK266, Sigma Aldrich, St. Louis, MI, USA).

## 2.4. RNA Isolation and Quantitative PCR Analysis

Total RNA was isolated from frozen liver using TRIzol Reagent™ (15609415, Fisher Scientific, Waltham, MA, USA) and genomic DNA traces were removed with the RapidOut DNA Removal Kit™ (13565150, Thermo Scientific, Waltham, MA, USA). Moreover, 1  $\mu\text{g}$  of total RNA was converted to cDNA using the High-Capacity cDNA Reverse Transcription Kit™ (10400745, Applied Biosystems, Foster City, CA, USA). Relative mRNA levels were measured via quantitative PCR (qPCR) using a SYBR™ Select Master Mix for CFX (13206529, Applied Biosystems™, Foster City, CA, USA). The sequences of the primers (Sigma Aldrich, St. Louis, MI, USA) are shown in Table S1. The relative expression of mRNA was normalized using 18S and B2M as housekeeping genes. The 18S gene was used to normalize genes that were analyzed with TaqMan probes and B2M when SYBR green primers were used. The stability of these genes is shown in Supplemental Figure S1. Results were obtained by the relative standard curve method, and values of the HFD group were set to 1.

## 2.5. Histological Analysis

For the histological analysis, pieces of liver from each animal were fixed in 10% formalin (Ref Sigma Aldrich, St. Louis, MI, USA) and embedded in paraffin. Next, 4  $\mu\text{m}$ -thick sections were cut and stained with hematoxylin and eosin (H&E). The images were acquired in a Digital Upright Microscope BA310 Digital and a Moticam 2500 camera. The selection of test objects was performed according to color and choosing the same limits for the binarization of all images. At least three pictures from different regions of each cut were taken.

## 2.6. Data Analysis/Statistics

Values were expressed as means  $\pm$  SEM, and a  $p$ -value of  $<0.05$  was considered statistically significant. Statistical analyses of the data were performed using GraphPad Prism version 8.02 (GraphPad, San Diego, CA, USA). The significance was determined using an unpaired two tailed Student's  $t$  test and with Welch's correction without equal SDs.

### 3. Results

#### 3.1. Maqui Administration Decreases Liver Steatosis and TG Content

Our previous published data showed that maqui dietary supplementation of diet-induced obese mice partially counteracted the unhealthy metabolic impact of a HFD by acting in the subcutaneous white adipose tissue (scWAT) [23]. Since hepatic metabolism is also central to energy homeostasis, in this work, we analyzed the impact of lyophilized maqui berry supplementation in the liver of mice subjected to HFD.

Histological analysis of livers using eosin–hematoxylin staining revealed that mice undergoing HFD, as expected, exhibited a large accumulation of lipids in this organ, and large lipid droplets (LDs) were observed, thus confirming advanced hepatic steatosis (Figure 1a). In contrast, the liver of diet-induced obese mice supplemented with maqui showed fewer and smaller LDs, indicating that maqui supplementation improves hepatic steatosis caused by a HFD (Figure 1a). According to the histology results, the maqui-supplemented group of mice displayed a concomitant decrease in hepatic TG content (Figure 1b).

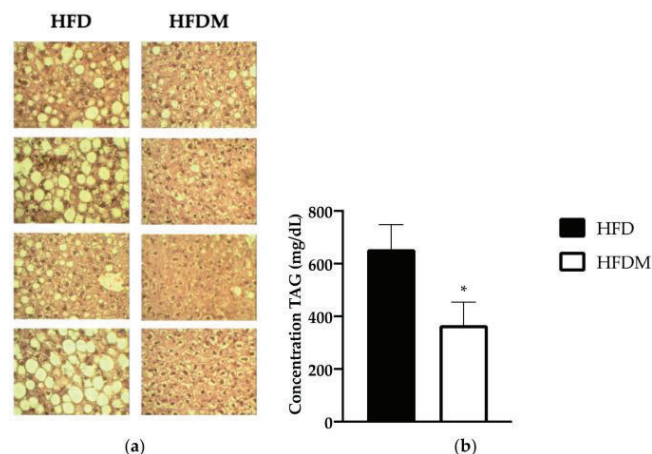


**Figure 1.** Maqui dietary supplementation ameliorates liver steatosis and decreases triglyceride (TG) content. **(a)** Histologic analysis of liver. Representative pictures of the hematoxylin and eosin (H&E)-stained sections of livers from a high-fat diet (HFD) and maqui supplemented HFD (HFDM) (40× magnification). Large lipid droplets (LDs) were observed in HFD images compared to the HFDM group. **(b)** Hepatic TG content. The concentration of TG (ng/uL) was measured in the livers of HFD ( $n = 9$ ) and HFDM ( $n = 14$ ) mice. Data are presented as the mean  $\pm$  SEM. \*  $p < 0.05$ .

Liver is a key organ for maintaining metabolic homeostasis and blood glucose levels through the regulation of fatty acid oxidation and gluconeogenesis. Both pathways are closely related under fasting conditions as fatty acid oxidation is needed to activate gluconeogenesis [32–34]. In order to evaluate the hepatic metabolic profile of HFDM mice, we analyzed the expression levels of fatty acid oxidation and gluconeogenic genes.

#### 3.2. Fatty Acid Oxidation Gene Expression Is Downregulated by Maqui Consumption within a HFD

As hepatic fatty acid oxidation is central to systemic energy balance and liver steatosis susceptibility (associated with peroxisome proliferator-activated receptor alpha (PPAR $\alpha$ ))

dysfunction), we analyzed the mRNA levels of *ppara* and the fatty acid oxidation-related PPAR $\alpha$  target genes. Figure 2 shows the expression of *ppara*, *carnitine palmitoyl transferase 1* (*cpt1a*), the key enzyme in the carnitine-dependent transport of long-chain fatty acids across the mitochondrial inner membrane, and *enoyl-coenzyme A hydratase/3-hydroxyacyl coenzyme A dehydrogenase* (*ehhadh*), one of the key enzymes in the peroxisomal beta-oxidation pathway. The three genes are downregulated in maqui-supplemented HFD-fed mice, indicating a reduction in the oxidative capacity of long and very long chain fatty acids compared to the HFD-fed animals.

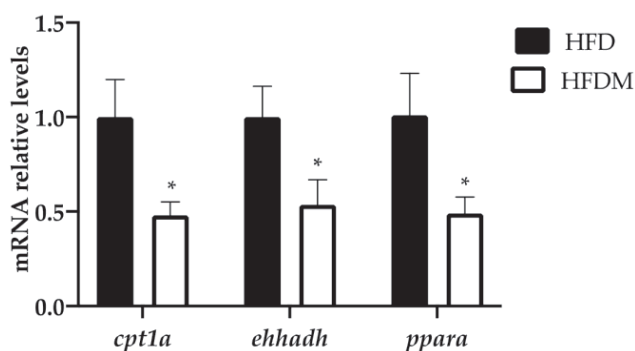


**Figure 2.** Fatty acid oxidation genes are downregulated in the livers of HFD-fed mice supplemented with maqui. Relative hepatic mRNA levels of *carnitine palmitoyltransferase 1a* (*cpt1a*), *enoyl-CoA hydratase, 3-hydroxyacyl-CoA dehydrogenase* (*ehhadh*), and *peroxisome proliferator activated receptor alpha* (*ppara*) were measured via quantitative PCR (qPCR) in HFD ( $n = 9$ ) and HFDM ( $n = 14$ ) animals. Bars represent the relative mRNA levels in the HFD animals, which was the control group and was thus assigned an arbitrary value of 1 in the HFDM. Data are presented as the mean  $\pm$  SEM. \*  $p < 0.05$  versus the HFD group.

### 3.3. The Gluconeogenic Gene *g6Pase* Expression Decreases after Maqui Supplementation

The impairment of hepatic glucose production is considered a hallmark of insulin resistance and a key point for its treatment [35,36]. Moreover, as has been mentioned before, the activation of the gluconeogenic pathway depends on the fatty acid oxidation rate, which is downregulated in HFDM mice (Figure 2).

In order to go deep into the metabolic modifications elicited via maqui supplementation, we analyzed the blood glucose levels in 6 h-fasted mice. The expressions of *phosphoenolpyruvate carboxykinase* (*pepck*) and *glucose-6-phosphatase* (*g6Pase*) were the key enzymes in hepatic glucose production in fed animals. Fasting glucose levels (Figure 3a) and the expression of *g6Pase*, but not *pepck* (Figure 3b), decreased in the maqui-supplemented mice.

The reduction in the fasting glucose levels and in the downregulation of *g6Pase* is in accordance with the previous published data where maqui supplementation improved glucose tolerance in HFD-fed mice [23].

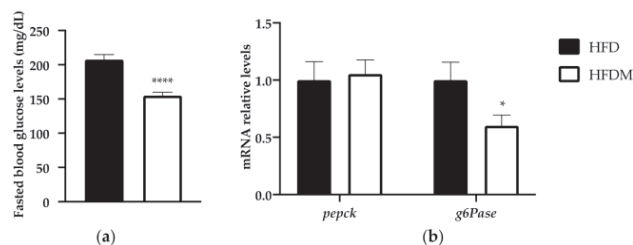


**Figure 3.** Maqui supplementation reduces fasting blood glucose and gluconeogenesis. (a) The fasting blood levels of glucose were measured at week 15 of the nutritional intervention in 6 h-fasted animals. (b) Relative hepatic mRNA levels of *phosphoenolpyruvate carboxykinase (pepck)* and *glucose-6-phosphate (g6Pase)* were measured via qPCR in HFD ( $n = 9$ ) and HFDM ( $n = 14$ ) animals. Bars represent the relative mRNA levels in the HFD animals, which was the control group and was thus assigned an arbitrary value of 1 in the HFDM. Data are presented as the mean  $\pm$  SEM. \*  $p < 0.05$  versus the HFD group; \*\*\*\*  $p < 0.0001$  versus the HFD group.

#### 3.4. The Expression of the Nuclear Receptor Corepressor Smile Increased under Maqui Supplementation

SMILE and peroxisome proliferator-activated receptor gamma coactivator 1 alpha (PGC1a) are both regulators of gluconeogenesis because they control the expression of key gluconeogenic genes. SMILE is an insulin-inducible corepressor that suppresses hepatic gluconeogenesis [37], while PGC1a acts as a coactivator of gluconeogenic genes. Accordingly, with its effect on gluconeogenesis, maqui supplementation induces *smile* gene expression (Figure 3) and diminishes *pgc1a* gene expression (Figure 3). These data correlate with the expression profile of *g6Pase*, as shown in Figure 3b.

#### 3.5. Hepatic Lipogenic Gene Expression Is Downregulated by Maqui Supplementation

SMILE has been described as a corepressor of the nuclear receptor family and has been identified as an inhibitor of the transcriptional activity of LXRa and LXRa-mediated SREBP1c gene expression [29]. To confirm the role of SMILE on the hepatic metabolic effects of maqui, we analyzed the expression of LXR and LXRa target genes, including the key enzymes of the lipogenic pathway.

Although neither the expression of *lxra* nor *lxrb* were changed, the expression of the LXRa target genes *cholesterol 7 alpha-hydroxylase (cyp7a1)* and *phospholipid transfer protein (plt)* was downregulated in HFDM mice (Figure 4). In accordance with these results, which indicated a blockade of LXR transcriptional activity, the mRNA levels of *fatty acid synthase (fasn)*, *stearoyl-CoA desaturase-1 (scd1)*, *fatty acid elongase 6 (elovl6)*, *fatty acid binding protein 1 (fabp1)*, and *sterol regulatory binding protein 1c (sreb1c)* were also downregulated in the maqui-supplemented mice (Figure 4). Furthermore, maqui administration also reduced the expression of *carbohydrate-responsive element-binding protein beta (chrebpb)*, a transcriptional factor that regulates hepatic lipogenesis.

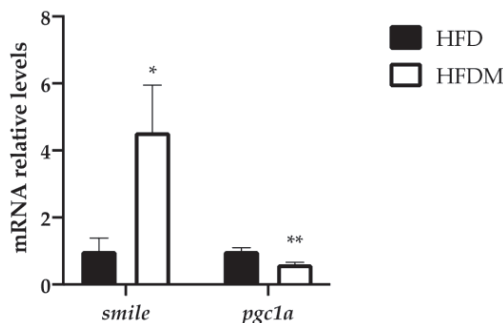


**Figure 4.** Maqui supplementation upregulates the expression of *smile* and downregulates *pgc1a* levels. Relative hepatic mRNA levels of small heterodimer partner interacting leucine zipper protein (*smile*) and peroxisome proliferator-activated receptor gamma coactivator 1 alpha (*pgc1a*) were measured via qPCR in HFD (n = 9) and HFDM (n = 14) animals. Bars represent the relative mRNA levels in the HFD animals, which was the control group and was thus assigned to an arbitrary value of 1 in the HFDM group. Data are presented as the mean ± SEM. \*  $p < 0.05$  versus the HFD group; \*\*  $p < 0.01$  versus the HFD group.

#### 4. Discussion

Our study shows the effect of dietary supplementation with a lyophilized maqui berry preparation on the progression of diet-induced obesity in mice subjected to a HFD for 16 weeks. In the liver, dietary maqui supplementation decreases the amount of TG and ameliorates the hepatic steatosis caused by a HFD. It is well-described that in fatty liver disease there is an increase in hepatic lipid accumulation together with an increase in PPAR $\alpha$  activity, as well as an upregulation of gluconeogenic, beta-oxidative, and ketogenic gene expression [38]. In our experimental model, the dietary maqui supplementation reversed this metabolic profile. The dietary maqui-supplemented animals exhibited an improvement in the hepatic lipid content together with a downregulation of key genes from fatty acid oxidation, gluconeogenesis, and de novo lipogenesis pathways. Moreover, our results point out the upregulation of the SMILE mRNA levels as part of the molecular mechanism underlying the metabolic profile observed in the livers of HFDM mice.

SMILE is a nuclear receptor family corepressor that has been implied in the maintenance of lipid homeostasis by regulating SREBP1c and LXR activities. On one side, it has been described that the activity of the lipogenic transcription factor SREBP-1c is induced by SMILE because it inhibits the insulin-induced gene 1 (Insig) protein and activates SREBP1c maturation [39]. On the other side, SMILE inhibits LXR agonist-induced lipogenic gene expression, thus reducing de novo lipogenesis [29]. Together, SMILE-mediated activation of SREBP-1c and repression of LXR has been proposed as a regulatory mechanism to maintain hepatic lipid synthesis in response to nutrient availability [39]. In our experimental approach, dietary maqui supplementation induces *smile* (Figure 4), which in turn would block LXR transcriptional activity as is shown by the downregulation of the LXR-target genes *cyp7a1* and *pltp*, as well as the mRNA levels of several lipogenic genes including *srebp1c* (Figure 5). Besides the classical lipogenic genes, maqui dietary supplementation also reduces the mRNA levels of *chrebpb*. ChREBPb is a transcriptional factor initially identified as a glucose-responsive factor that has recently been described as essential for fructose-induced lipogenesis both in the small intestine and liver [40–43]. The reduced expression of *chrebpb* in the liver of HFDM (Figure 5b), together with the other genes analyzed, would contribute to diminishing the de novo lipogenesis rate in maqui-supplemented mice. High fructose diets are considered pernicious as they induce lipogenesis, hepatic steatosis,

and, finally, the development of insulin resistance and metabolic syndrome [43–45]. Under maqui supplementation, the lack of induction in the hepatic expression of *chrebbp* suggests that fructose from maqui does not promote the lipogenic pathway. These results reinforce the idea that the metabolic effects of fructose are not the same when fructose is consumed within its natural source or as an added sugar. It is well-described that the overconsumption of sugar-sweetened beverages or foods, or high-fructose diets, leads to adverse effects on health but, on the other hand, it is accepted that fruit intake is protective for human health. Evidence about the effects of consuming natural sources of free sugars, such as fruits, is still scarce [46,47].

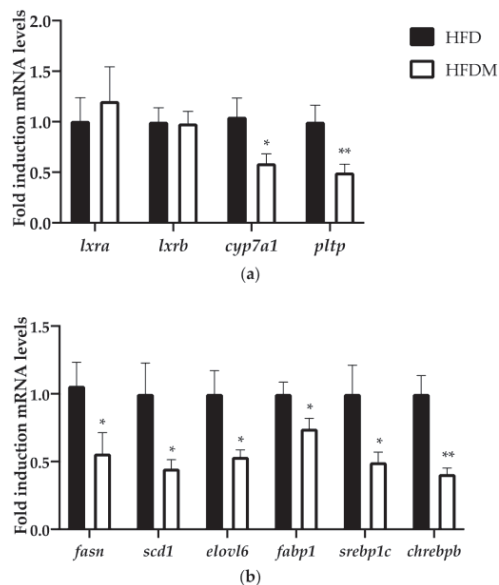


**Figure 5.** Maqui downregulated the LXR-target genes, including the expression of de novo lipogenesis genes. (a) Relative hepatic mRNA levels of *liver x receptor alpha* (*lxra*), *liver x receptor beta* (*lxrb*), *cholesterol 7 alpha-hydroxylase* (*cyp7a1*), and *phospholipid transfer protein* (*pltp*) were measured via qRT-PCR in HFD ( $n = 9$ ) and HFDM ( $n = 14$ ). (b) Relative hepatic mRNA levels of *liver fatty acid synthase* (*fasn*), *stearoyl-CoA desaturase-1* (*scd1*), *fatty acid elongase 6* (*elovl6*), *fatty acid binding protein 1* (*fabp1*), *sterol regulatory binding protein 1c* (*srebp1c*), and *carbohydrate-responsive element-binding protein beta* (*chrebbp*) were measured using qPCR in HFD ( $n = 9$ ) and HFDM ( $n = 14$ ) animals. Bars represent the relative mRNA levels in the HFD animals, which was the control group and was thus assigned to an arbitrary value of 1, and in the HFDM group. Data are presented as the mean  $\pm$  SEM. \*  $p < 0.05$  versus the HFD group; \*\*  $p < 0.01$  versus the HFD group.

Besides de novo lipogenesis, SMILE also regulates the gluconeogenic pathway. Our results showed that blood fasting glucose levels in HFDM mice were lower than in HFD, thus indicating less hepatic glucose production in maqui-supplemented mice. This lower production of glucose in the liver of HFDM mice correlates with the upregulation of *smile*, the downregulation of *pgc1a* and the reduction in *g6pase* expression. A recent study demonstrated that SMILE is an insulin-inducible corepressor that decreases *pgc1a*

expression and the stimulatory effect of PGC1 $\alpha$  on hepatic gluconeogenesis [37]. This effect is produced by the interaction and disruption of the CREB/CRTC2 complex by SMILE that results in a significant inhibition of CRTC2-induced PGC1 $\alpha$  expression [48]. Furthermore, SMILE also inhibited CREB/CRTC2-induced *pepck* and *g6Pase* gene expression by a direct transcriptional repression of these genes [48]. Although no changes were observed in the *pepck* mRNA levels, globally our data suggest that maqui diminishes the gluconeogenic pathway in the livers of diet-induced obese mice.

Another pathway closely related to lipid homeostasis is fatty acid oxidation. It is well-known that a tight regulation of hepatic fatty acid oxidation is essential for maintaining an energy balance. Moreover, liver steatosis susceptibility has been associated with PPAR $\alpha$  dysfunction [49]. Considering that PPAR $\alpha$  is a key regulator of hepatic fatty acid oxidation, we analyzed the expression of PPAR $\alpha$  and the fatty acid oxidation-related PPAR alpha target genes in the liver. Our analysis showed a decrease in fatty acid oxidation gene expression in the maqui-supplemented mice. According to the putative requirement of fatty acid oxidation in gluconeogenesis, these data reinforce the lower gluconeogenic rate detected in the livers of HFDM mice.

Given the role of SMILE as a corepressor of the nuclear receptor family, the inhibition of the PPAR $\alpha$  transcriptional activity could be attributed to SMILE. It has been described that SMILE blocks the activity of several other nuclear receptors such as PPAR gamma, the estrogen receptor, the androgen receptor, or LXR, among others [28,50–52]. Although no experimental data are available about its effect on PPAR $\alpha$  activity, the inhibition of PPAR $\alpha$  transcriptional activity in HFDM mice could be attributed to SMILE. Furthermore, the observed downregulation of PGC1 $\alpha$  may also contribute to the decreased oxidation of fatty acids in HFDM mice.

The remaining question is what component or components of maqui are responsible for its metabolic effects. Ursolic acid is a naturally occurring pentacyclic triterpenoid carboxyl acid with a wide range of biological activities, including hepatoprotective and hypolipidemic effects, both of which have the capacity to reduce hepatic lipid accumulation [50,53]. It has been shown that ursolic acid significantly decreased the mRNA and protein expression of LXR $\alpha$  target lipogenic genes including SREBP1c. The proposed mechanism underlying the effects of ursolic acid is an AMPK-dependent increase in the corepressor SMILE that would antagonize LXR $\alpha$  [50]. Ursolic acid is present in the dichloromethane extract of the leaves of *Aristotelia chilensis* [54], thus suggesting that it may also be present in the lyophilizate maqui used in this work. Besides the anthocyanin profile described in the lyophilizate maqui [23], which surely explains part of the beneficial effects attributed to maqui, ursolic acid, if present, may contribute significantly to the hypolipidemic effects observed in maqui dietary supplemented mice. We aim to test this hypothesis in future work.

## 5. Conclusions

Our data indicated that maqui supplementation transcriptionally regulates lipid handling in the liver in order to counteract the metabolic impact of HFD, resulting in decreased hepatic steatosis (Figure 6). Changes in the hepatic metabolic profile include a downregulation of lipogenic LXR target genes and of fatty acid oxidation gene expression together with an increased expression of SMILE, a corepressor of the nuclear receptor family.

In conclusion, our data reinforce the use of anthocyanidin-enriched foods as a potential strategy to prevent or treat obesity-related diseases and identify maqui as a putative functional fruit to counteract obesity and its metabolic complications. The data presented in this manuscript support the inclusion of maqui in the diet of obese individuals.

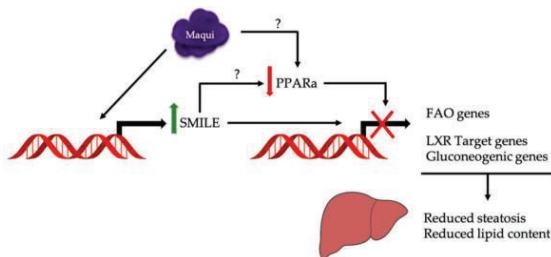


**Figure 6.** Maqui transcriptionally regulates a metabolic response to counteract hepatic steatosis and increased lipid content caused by a HFD. The hepatic metabolic changes observed in maqui-supplemented mice include a downregulation of the lipogenic LXR target gene and fatty acid oxidation and gluconeogenic gene expression together with an increased expression of SMILE, a corepressor of the nuclear receptor family. The upregulation of SMILE may be the mechanism underlying the downregulation of PPARα transcriptional activity but a direct effect of maqui on PPARα expression/activity cannot be discarded.

**Supplementary Materials:** The following are available online at <https://www.mdpi.com/article/10.3390/antiox10050637/s1>, Table S1: Sequences of the primers used in SYBR green assays and references of the probes used in TaqMan assays. Figure S1: Stability of the Housekeeping genes.

**Author Contributions:** Conceptualization: V.S., P.F.M., J.R., and D.H.; data curation: V.S. and H.S.-L.; formal analysis: V.S., H.S.-L., and J.R.; funding acquisition: P.F.M., J.R., and D.H.; investigation: V.S. and H.S.-L.; methodology: V.S., H.S.-L., P.F.M., J.R., and D.H.; project administration: P.F.M., J.R., and D.H.; resources: P.F.M., J.R., and D.H.; supervision: P.F.M., J.R., and D.H.; validation: V.S., H.S.-L., P.F.M., J.R., and D.H.; visualization, V.S., H.S.-L., J.R., and D.H.; writing—original draft: V.S., H.S.-L., P.F.M., J.R., and D.H.; writing—review and editing: P.F.M., J.R., and D.H. All authors have read and agreed to the published version of the manuscript.

**Funding:** This study was supported by the Ministerio de Economía y Competitividad (grant AGL2017-82417-R to P.F.M. and D.H.), the Generalitat de Catalunya (grant 2017SGR683 to D.H.) and the Associació Catalana de la Diabetis (grant 600004 -Ajut ACD a la recerca en diabetis 2017 to J.R.). V.S. was supported by Conicyt's fellowship from the Government of Chile. APC was funded by the University of Barcelona.

**Institutional Review Board Statement:** The study was approved by the Animal Ethics Committee of the University of Barcelona (CEEA-137/18, May 2018).

**Informed Consent Statement:** Not applicable.

**Data Availability Statement:** The data presented in this study are available on request from the corresponding author.

**Acknowledgments:** We would like to thank to the Ministerio de Economía, Industria y Competitividad (Spanish Government), the Generalitat de Catalunya, the Associació Catalana de la Diabetis (ACD), the Government of Chile, and the University of Barcelona for supporting our research. We would also like to thank the personnel of the animal facilities of the Faculty of Pharmacy and Food Sciences at the University of Barcelona for their support in the animals' housing and management.

**Conflicts of Interest:** The authors declare no conflict of interest.



## References

1. Tsuda, T. Dietary anthocyanin-rich plants: Biochemical basis and recent progress in health benefits studies. *Mol. Nutr. Food Res.* **2012**, *56*, 159–170. [\[CrossRef\]](#)
2. Tsuda, T. Regulation of adipocyte function by anthocyanins; Possibility of preventing the metabolic syndrome. *J. Agric. Food Chem.* **2008**, *56*, 642–646. [\[CrossRef\]](#)
3. He, J.; Giusti, M.M. Anthocyanins: Natural Colorants with Health-Promoting Properties. *Annu. Rev. Food Sci. Technol.* **2010**, *1*, 163–187. [\[CrossRef\]](#)
4. Guo, H.; Ling, W. The update of anthocyanins on obesity and type 2 diabetes: Experimental evidence and clinical perspectives. *Rev. Endocr. Metab. Disord.* **2015**, *16*, 1–13. [\[CrossRef\]](#)
5. Overall, J.; Bonney, S.A.; Wilson, M.; Beermann, A.; Grace, M.H.; Esposito, D.; Lila, M.A.; Komarnytsky, S. Metabolic effects of berries with structurally diverse anthocyanins. *Int. J. Mol. Sci.* **2017**, *18*, 422. [\[CrossRef\]](#)
6. Vendrame, S.; Del Bo, C.; Ciappellano, S.; Riso, P.; Klimis-Zacas, D. Berry Fruit Consumption and Metabolic Syndrome. *Antioxidants* **2016**, *5*, 34. [\[CrossRef\]](#)
7. Coe, S.; Ryan, L. Impact of polyphenol-rich sources on acute postprandial glycaemia: A systematic review. *J. Nutr. Sci.* **2016**, *5*, e24. [\[CrossRef\]](#)
8. Blumberg, J.B.; Basu, A.; Krueger, C.G.; Lila, M.A.; Neto, C.C.; Novotny, J.A.; Reed, J.D.; Rodriguez-Mateos, A.; Toner, C.D. Impact of Cranberries on Gut Microbiota and Cardiometabolic Health: Proceedings of the Cranberry Health Research Conference 2015. *Adv. Nutr.* **2016**, *7*, 759S–770S. [\[CrossRef\]](#)
9. Sandoval, V.; Sanz-Lamora, H.; Arias, G.; Marrero, P.F.; Haro, D.; Relat, J. Metabolic Impact of Flavonoids Consumption in Obesity: From Central to Peripheral. *Nutrients* **2020**, *12*, 2393. [\[CrossRef\]](#)
10. Gomes, J.V.P.; Rigolon, T.C.B.; da Silveira Souza, M.S.; Alvarez-Leite, J.I.; Lucia, C.M.D.; Martino, H.S.D.; Rosa, C.D.O.B. Antiobesity effects of anthocyanins on mitochondrial biogenesis, inflammation, and oxidative stress: A systematic review. *Nutrition* **2019**, *66*, 192–202. [\[CrossRef\]](#)
11. Wu, T.; Gao, Y.; Guo, X.; Zhang, M.; Gong, L. Blackberry and blueberry anthocyanin supplementation counteract high-fat-diet-induced obesity by alleviating oxidative stress and inflammation and accelerating energy expenditure. *Oxid. Med. Cell. Longev.* **2018**, *2018*, 4051232. [\[CrossRef\]](#) [\[PubMed\]](#)
12. Calvano, A.; Izuora, K.; Oh, E.C.; Ebersole, J.L.; Lyons, T.J.; Basu, A. Dietary berries, insulin resistance and type 2 diabetes: An overview of human feeding trials. *Food Funct.* **2019**, *10*, 6227–6243. [\[CrossRef\]](#) [\[PubMed\]](#)
13. Esposito, D.; Damsud, T.; Wilson, M.; Grace, M.H.; Strauch, R.; Li, X.; Lila, M.A.; Komarnytsky, S. Black Currant Anthocyanins Attenuate Weight Gain and Improve Glucose Metabolism in Diet-Induced Obese Mice with Intact, but Not Disrupted, Gut Microbiome. *J. Agric. Food Chem.* **2015**, *63*, 6172–6180. [\[CrossRef\]](#) [\[PubMed\]](#)
14. Iizuka, Y.; Ozeki, A.; Tani, T.; Tsuda, T. Blackcurrant extract ameliorates hyperglycemia in type 2 diabetic mice in association with increased basal secretion of glucagon-like peptide-1 and activation of AMP-activated protein kinase. *J. Nutr. Sci. Vitaminol.* **2018**, *64*, 258–264. [\[CrossRef\]](#)
15. Choi, K.H.; Lee, H.A.; Park, M.H.; Han, J.-S. Mulberry (*Morus alba* L.) Fruit Extract Containing Anthocyanins Improves Glycemic Control and Insulin Sensitivity via Activation of AMP-Activated Protein Kinase in Diabetic C57BL/KsJ-db/db Mice. *J. Med. Food* **2016**, *19*, 737–745. [\[CrossRef\]](#)
16. Takikawa, M.; Inoue, S.; Horio, F.; Tsuda, T. Dietary Anthocyanin-Rich Bilberry Extract Ameliorates Hyperglycemia and Insulin Sensitivity via Activation of AMP-Activated Protein Kinase in Diabetic Mice. *J. Nutr.* **2010**, *140*, 527–533. [\[CrossRef\]](#)
17. You, Y.; Yuan, X.; Liu, X.; Liang, C.; Meng, M.; Huang, Y.; Han, X.; Guo, J.; Guo, Y.; Ren, C.; et al. Cyanidin-3-glucoside increases whole body energy metabolism by upregulating brown adipose tissue mitochondrial function. *Mol. Nutr. Food Res.* **2017**, *61*, 1700261. [\[CrossRef\]](#)
18. Solverson, P.M.; Rumpler, W.V.; Leger, J.L.; Redan, B.W.; Ferruzzi, M.G.; Baer, D.J.; Castonguay, T.W.; Novotny, J.A. Blackberry Feeding Increases Fat Oxidation and Improves Insulin Sensitivity in Overweight and Obese Males. *Nutrients* **2018**, *10*, 1048. [\[CrossRef\]](#)
19. Browning, J.D.; Horton, J.D. Molecular mediators of hepatic steatosis and liver injury. *J. Clin. Investig.* **2004**, *114*, 147–152. [\[CrossRef\]](#)
20. Sanders, F.W.B.; Acharjee, A.; Walker, C.; Marney, L.; Roberts, L.D.; Imamura, F.; Jenkins, B.; Case, J.; Ray, S.; Virtue, S.; et al. Hepatic steatosis risk is partly driven by increased de novo lipogenesis following carbohydrate consumption. *Genome Biol.* **2018**, *19*, 79. [\[CrossRef\]](#)
21. Unger, R.H.; Clark, G.O.; Scherer, P.E.; Orci, L. Lipid homeostasis, lipotoxicity and the metabolic syndrome. *Biochim. Biophys. Acta* **2010**, *1801*, 209–214. [\[CrossRef\]](#)
22. Escribano-Bailón, M.T.; Alcalde-Eon, C.; Muñoz, O.; Rivas-Gonzalo, J.C.; Santos-Buelga, C. Anthocyanins in berries of Maqui (*Aristotelia chilensis* (Mol.) Stuntz). *Phytochem. Anal.* **2006**, *17*, 8–14. [\[CrossRef\]](#)
23. Sandoval, V.; Femenias, A.; Martinez-Garza, U.; Sanz-Lamora, H.; Castagnini, J.M.; Quifer-Rada, P.; Lamuela-Raventos, R.M.; Marrero, P.F.; Haro, D.; Relat, J. Lyophilized Maqui (*Aristotelia chilensis*) Berry Induces Browning in the Subcutaneous White Adipose Tissue and Ameliorates the Insulin Resistance in High Fat Diet-Induced Obese Mice. *Antioxidants* **2019**, *8*, 360. [\[CrossRef\]](#)

24. Miranda-Rottmann, S.; Aspillaga, A.A.; Pérez, D.D.; Vasquez, L.; Martínez, A.L.F.; Leighton, F. Juice and phenolic fractions of the berry *Aristotelia chilensis* inhibit LDL oxidation in vitro and protect human endothelial cells against oxidative stress. *J. Agric. Food Chem.* **2002**, *50*, 7542–7547. [[CrossRef](#)]
25. Rojo, L.E.; Ribnicky, D.; Logendra, S.; Poulev, A.; Rojas-Silva, P.; Kuhn, P.; Dorn, R.; Grace, M.H.; Lila, M.A.; Raskin, I. In vitro and in vivo anti-diabetic effects of anthocyanins from Maqui Berry (*Aristotelia chilensis*). *Food Chem.* **2012**, *131*, 387–396. [[CrossRef](#)]
26. Alvarado, J.L.; Leschot, A.; Olivera-Nappa, Á.; Salgado, A.M.; Riosco, H.; Lyon, C.; Vigil, P. Delphinidin-rich maqui berry extract (Delphinol®) lowers fasting and postprandial glycemia and insulinemia in prediabetic individuals during oral glucose tolerance tests. *Biomed Res. Int.* **2016**, 9070537. [[CrossRef](#)] [[PubMed](#)]
27. Watson, R.R.; Schonlau, F. Nutraceutical and antioxidant effects of a delphinidin-rich maqui berry extract Delphinol (R): A review. *Minerva Cardioangiol.* **2015**, *63*, 1–12.
28. Xie, Y.-B.; Nedumaran, B.; Choi, H.-S. Molecular characterization of SMILE as a novel corepressor of nuclear receptors. *Nucleic Acids Res.* **2009**, *37*, 4100–4115. [[CrossRef](#)]
29. Lee, J.-M.; Gang, G.-I.; Kim, D.-K.; Kim, Y.D.; Koo, S.-H.; Lee, C.-H.; Choi, H.-S. Ursodeoxycholic acid inhibits liver X receptor  $\alpha$ -mediated hepatic lipogenesis via induction of the nuclear corepressor SMILE. *J. Biol. Chem.* **2014**, *289*, 1079–1091. [[CrossRef](#)]
30. Tresserra-Rimbau, A.; Medina-Remón, A.; Pérez-Jiménez, J.; Martínez-González, M.A.; Covas, M.I.; Corella, D.; Salas-Salvado, J.; Gómez-Gracia, E.; Lapetra, J.; Arós, F.; et al. Dietary intake and major food sources of polyphenols in a Spanish population at high cardiovascular risk: The PREDIMED study. *Nutr. Metab. Cardiovasc. Dis.* **2013**, *23*, 953–959. [[CrossRef](#)]
31. Tresserra-Rimbau, A.; Guasch-Ferre, M.; Salas-Salvado, J.; Toledo, E.; Corella, D.; Castaner, O.; Guo, X.; Gomez-Gracia, E.; Lapetra, J.; Aros, F.; et al. Intake of Total Polyphenols and Some Classes of Polyphenols Is Inversely Associated with Diabetes in Elderly People at High Cardiovascular Disease Risk. *J. Nutr.* **2016**, *146*, 767–777.
32. Vilá-Brau, A.; De Sousa-Coelho, A.L.; Gonçalves, J.F.; Haro, D.; Marrero, P.F. Fsp27/CIDEa is a CREB target gene induced during early fasting in liver and regulated by FA oxidation rate. *J. Lipid Res.* **2013**, *54*, 592–601. [[CrossRef](#)]
33. Satapati, S.; Sunny, N.E.; Kucejova, B.; Fu, X.; He, T.T.; Méndez-Lucas, A.; Shelton, J.M.; Perales, J.C.; Browning, J.D.; Burgess, S.C. Elevated TCA cycle function in the pathology of diet-induced hepatic insulin resistance and fatty liver. *J. Lipid Res.* **2012**, *53*, 1080–1092. [[CrossRef](#)] [[PubMed](#)]
34. Giménez-Cassina, A.; Garcia-Haro, L.; Choi, C.S.; Osundiji, M.A.; Lane, E.A.; Huang, H.; Yildirim, M.A.; Szlyk, B.; Fisher, J.K.; Polak, K.; et al. Regulation of hepatic energy metabolism and gluconeogenesis by BAD. *Cell Metab.* **2014**, *19*, 272–284. [[CrossRef](#)] [[PubMed](#)]
35. Rizza, R.A. Pathogenesis of fasting and postprandial hyperglycemia in type 2 diabetes: Implications for therapy. *Diabetes* **2010**, *59*, 2697–2707. [[CrossRef](#)] [[PubMed](#)]
36. Lin, H.V.; Accili, D. Hormonal regulation of hepatic glucose production in health and disease. *Cell Metab.* **2011**, *14*, 9–19. [[CrossRef](#)] [[PubMed](#)]
37. Lee, J.-M.; Seo, W.-Y.; Han, H.-S.; Oh, K.-J.; Lee, Y.-S.; Kim, D.-K.; Choi, S.; Choi, B.H.; Harris, R.A.; Lee, C.-H.; et al. Insulin-Inducible SMILE Inhibits Hepatic Gluconeogenesis. *Diabetes* **2016**, *65*, 62–73. [[CrossRef](#)]
38. Geisler, C.E.; Renquist, B.J. Hepatic lipid accumulation: Cause and consequence of dysregulated glucoregulatory hormones. *J. Endocrinol.* **2017**, *234*, R1–R21. [[CrossRef](#)]
39. Zhang, F.; Hu, Z.; Li, G.; Huo, S.; Ma, F.; Cui, A.; Xue, Y.; Han, Y.; Gong, Q.; Gao, J.; et al. Hepatic CREBZF couples insulin to lipogenesis by inhibiting insig activity and contributes to hepatic steatosis in diet-induced insulin-resistant mice. *Hepatology* **2018**, *68*, 1361–1375. [[CrossRef](#)]
40. Iizuka, K. The role of carbohydrate response element binding protein in intestinal and hepatic fructose metabolism. *Nutrients* **2017**, *9*, 181. [[CrossRef](#)]
41. Lee, H.-J.; Cha, J.-Y. Recent insights into the role of ChREBP in intestinal fructose absorption and metabolism. *BMB Rep.* **2018**, *51*, 429–436. [[CrossRef](#)]
42. Ishii, S.; Iizuka, K.; Miller, B.C.; Uyeda, K. Carbohydrate response element binding protein directly promotes lipogenic enzyme gene transcription. *Proc. Natl. Acad. Sci. USA* **2004**, *101*, 15597–15602. [[CrossRef](#)]
43. Geidl-Flueck, B.; Gerber, P.A. Insights into the Hexose Liver Metabolism-Glucose versus Fructose. *Nutrients* **2017**, *9*, 1026. [[CrossRef](#)]
44. Gatineau, E.; Polakof, S.; Dardevet, D.; Mosoni, L. Similarities and interactions between the ageing process and high chronic intake of added sugars. *Nutr. Res. Rev.* **2017**, *30*, 191–207. [[CrossRef](#)]
45. Taskinen, M.-R.; Packard, C.J.; Borén, J. Dietary Fructose and the Metabolic Syndrome. *Nutrients* **2019**, *11*, 1987. [[CrossRef](#)]
46. Pepin, A.; Stanhope, K.L.; Imbeault, P. Are Fruit Juices Healthier Than Sugar-Sweetened Beverages? A Review. *Nutrients* **2019**, *11*, 1006. [[CrossRef](#)]
47. Stanhope, K.L.; Goran, M.I.; Bomy-Westphal, A.; King, J.C.; Schmidt, L.A.; Schwarz, J.-M.; Stice, E.; Sylvetsky, A.C.; Turnbaugh, P.J.; Bray, G.A.; et al. Pathways and mechanisms linking dietary components to cardiometabolic disease: Thinking beyond calories. *Obes. Rev.* **2018**, *19*, 1205–1235. [[CrossRef](#)]
48. Lee, J.-M.; Han, H.-S.; Jung, Y.S.; Harris, R.A.; Koo, S.-H.; Choi, H.-S. The SMILE transcriptional corepressor inhibits cAMP response element-binding protein (CREB)-mediated transactivation of gluconeogenic genes. *J. Biol. Chem.* **2018**, *293*, 13125–13133. [[CrossRef](#)]

49. Kersten, S.; Stienstra, R. The role and regulation of the peroxisome proliferator activated receptor alpha in human liver. *Biochimie* **2017**, *136*, 75–84. [[CrossRef](#)]
50. Lin, Y.-N.; Wang, C.C.N.; Chang, H.-Y.; Chu, F.-Y.; Hsu, Y.-A.; Cheng, W.-K.; Ma, W.-C.; Chen, C.-J.; Wan, L.; Lim, Y.-P. Ursolic Acid, a Novel Liver X Receptor  $\alpha$  (LXR $\alpha$ ) Antagonist Inhibiting Ligand-Induced Nonalcoholic Fatty Liver and Drug-Induced Lipogenesis. *J. Agric. Food Chem.* **2018**, *66*, 11647–11662. [[CrossRef](#)]
51. Jang, H.; Kim, H.-J.; Kim, D.-H.; Park, J.-K.; Sun, W.-S.; Hwang, S.; Oh, K.-B.; Jang, W.-G.; Lee, J.-W. Small heterodimer partner-interacting leucine zipper protein inhibits adipogenesis by regulating peroxisome proliferator-activated receptor  $\gamma$  activity. *Life Sci.* **2015**, *132*, 49–54. [[CrossRef](#)] [[PubMed](#)]
52. Lee, S.-Y.; Song, C.-H.; Xie, Y.-B.; Jung, C.; Choi, H.-S.; Lee, K. SMILE upregulated by metformin inhibits the function of androgen receptor in prostate cancer cells. *Cancer Lett.* **2014**, *354*, 390–397. [[CrossRef](#)] [[PubMed](#)]
53. Mukonowenzou, N.C.; Dangarembizi, R.; Chivandi, E.; Nkomozepi, P.; Erlwanger, K.H. Administration of ursolic acid to new-born pups prevents dietary fructose induced non-alcoholic fatty liver disease in Sprague Dawley rats. *J. Dev. Orig. Health Dis.* **2021**, *12*, 101–112. [[CrossRef](#)] [[PubMed](#)]
54. Muñoz, O.; Christen, P.; Cretton, S.; Backhouse, N.; Torres, V.; Correa, O.; Costa, E.; Miranda, H.; Delporte, C. Chemical study and anti-inflammatory, analgesic and antioxidant activities of the leaves of *Aristolelia chilensis* (Mol.) Stuntz, Elaeocarpaceae. *J. Pharm. Pharmacol.* **2011**, *63*, 849–859. [[CrossRef](#)]

